x 97

Journal of Polymer Science

PART A-1: POLYMER CHEMISTRY

Volume 7, 1969

Board of Editors: H. MARK · C. G. OVERBERGER · T. G FOX

Advisory Editors: R. M. FUOSS · J. J. HERMANS · H. W. MELVILLE · G. SMETS

Editor: C. G. OVERBERGER · **Associate Editor:** E. M. PEARCE

Advisory Board:

T. ALFREY, JR.
Midland, Mich.

W. J. BAILEY
Baltimore, Md.

D. S. BALLANTINE
Washington, D. C.

M. B. BIRENBAUM
Trenton, N. J.

F. A. BOVEY
Murray Hill, N. J.

J. W. BREITENBACH
Wien

W. J. BURLANT
Dearborn, Mich.

G. B. BUTLER
Gainesville, Fla.

S. BYWATER
Ottawa

T. W. CAMPBELL
Waynesboro, Va.

W. L. CARRICK
Bound Brook, N. J.

H. W. COOVER, JR.
Kingsport, Tenn.

F. DANUSSO
Milano

F. R. EIRICH
Brooklyn, N. Y.

E. M. FETTES
Monroeville, Pa.

N. D. FIELD
Easton, Pa.

F. C. FOSTER
Rolling Meadows, Ill.

H. N. FRIEDLANDER
Durham, N. C.

K. C. FRISCH
Wyandotte, Mich.

N. G. GAYLORD
New Providence, N. J.

W. E. GIBBS
Dayton, Ohio

A. R. GILBERT
Schenectady, N. Y.

J. E. GUILLET
Toronto

H. C. HAAS
Cambridge, Mass.

J. P. KENNEDY
Linden, N. J.

W. KERN
Mainz

J. LAL
Akron, Ohio

R. W. LENZ
Amherst, Mass.

C. S. MARVEL
Tucson, Ariz.

F. R. MAYO
Menlo Park, Calif.

R. B. MESROBIAN
Chicago, Ill.

H. MORAWETZ
Brooklyn, N. Y.

M. MORTON
Akron, Ohio

S. MURAHASHI
Osaka

G. NATTA
Milano

K. F. O'DRISCOLL
Villanova, Pa.

S. OKAMURA
Kyoto

P. PINO
Pisa

C. C. PRICE
Philadelphia, Pa.

B. RÅNBY
Stockholm

J. H. SAUNDERS
New Martensville, West Va.

C. SCHUERCH
Syracuse, N. Y.

W. H. SHARKEY
Wilmington, Del.

W. R. SORENSON
Ponca City, Okla.

V. T. STANNETT
Raleigh, N. C.

J. K. STILLE
Iowa City, Iowa

M. SZWARC
Syracuse, N. Y.

A. V. TOBOLSKY
Princeton, N. J.

E. J. VANDENBERG
Wilmington, Del.

L. A. WALL
Washington, D. C.

F. X. WERBER
Garfield, N. J.

O. WICHTERLE
Prague

F. H. WINSLOW
Murray Hill, N. J.

M. WISMER
Springdale, Pa.

E. A. YOUNGMAN
Emeryville, Calif.

INTERSCIENCE PUBLISHERS

Copyright © 1969, by John Wiley & Sons, Inc.

Statement of ownership, management, and circulation (Act of October 23, 1962: Section 4369, Title 39 United States Code)

1. Date of filing: October 24, 1969
2. Title of Publication: JOURNAL OF POLYMER SCIENCE
3. Frequency of issue: monthly
4. Location of known office of publication: 20th and Northampton Streets, Easton, Pennsylvania 18042
5. Location of headquarters of general business offices of publisher: 605 Third Avenue, New York, New York 10016
6. The names and addresses of publisher, editor, and managing editor:

Publisher: John Wiley & Sons, Inc., 605 Third Avenue, New York, New York 10016

Editor: Herman Mark, Polytechnic Institute of Brooklyn, 333 Jay Street, Brooklyn, New York 11201, C. G. Overberger, Univ. of Michigan, Ann Arbor, Mich., and T. G Fox, Mellon Institute, Pittsburgh, Pennsylvania 15213

Managing Editor: None

7. Owner: John Wiley & Sons, Inc., 605 Third Avenue, New York, New York 10016
The following is a list of stockholders owning or holding 1% or more of John Wiley and Sons, Inc. stock as of August 31, 1969:
Cynthia W. Darby, Box 651, Bridgehampton, New York 11932, Edward P. Hamilton, 605 Third Avenue, New York, New York, 10016, W. Bradford Wiley & Francis Lobdell, Trustees Elizabeth W. Hamilton Trust, 605 Third Avenue, New York, New York 10016, Edward P. Hamilton as Trustee under the Will of Elizabeth Wiley Hamilton, % Gifford, Woody, Carter & Hays. 1 Wall Street, New York, New York 10005, I. M. Kolthoff, University of Minnesota, School of Chemistry, Minneapolis, Minnesota, Willy Levinger, 336 Central Park West, New York, New York, Eric S. Proskauer & Charles H. Lieb as Trustees U-A dated 11/27/62 made by Jenny R. Proskauer, 220 Central Park South, New York, New York 10019, Francis Lobdell & William J. Seawright, Trustees F-B-O Deborah Elizabeth Wiley, U-A dated 6/2/58, % John Wiley & Sons, Inc., 605 Third Avenue, New York, New York, Cynthia W. Darby & Julia W. Gilbert as Trustees U-W Kate R. Q. Wiley, % Gifford, Woody, Carter & Hays, 1 Wall Street, New York, New York, Francis Lobdell and William J. Seawright Trustees F-B-O Peter Book Wiley, U-A dated 6/2/58, % John Wiley & Sons, Inc., 605 Third Avenue, New York, New York, Francis Lobdell & William J. Seawright, Trustees F-B-O William Bradford Wiley II, U-A dated 6/2/58, % John Wiley & Sons, Inc. 605 Third Avenue, New York, New York, Edward P. Hamilton & Cynthia Wiley Darby as Trustees under the will of William O. Wiley, % Gifford, Woody, Carter & Hays, 1 Wall Street, New York, New York, Adele E. Windheim, 8 Dundee Road, Larchmont, New York, Dif & Company, Post Office Box 1447, 135 Devonshire Street, Boston, Massachusetts, W. Bradford Wiley & E. P. Hamilton, Trustees for Edward P. Hamilton Foundation, U-A dated 12/23/57, % John Wiley & Sons, Inc., 605 Third Avenue, New York, New York, Pitt & Company, P. O. Box 2444, Church Street Station, New York, New York 10008, Reing & Company, P. O. Box 491, Church Street Station, New York, New York 10015, and Shaw & Company, P. O. Box 491, Church Street Station, New York, New York 10015

8. Known bondholders, mortagees, and other security holders owning or holding 1 per cent or more of total amount of bonds, mortgages, or other securities: None

9. Paragraphs 7 and 8 include, in cases where the stockholder or security holder appears upon the books of the company as trustee or in any other fiduciary relation, the name of the person or corporation for whom such trustee is acting, also the statements in the two paragraphs show the affiant's full knowledge and belief as to the circumstances and conditions under which stockholders and security holders who do not appear upon the books of the company as trustees, hold stock and securities in a capacity other than that of a bona fide owner. Name and addresses of individuals who are stockholders of a corporation which itself is a stockholder or holder of bonds, mortgages or other securities of the publishing corporation have been included in paragraphs 7 and 8 when the interests of such individuals are equivalent to 1 per cent or more of the total amount of the stock or securities of the publishing corporation.

	10. Extent and nature of circulation	Average no. copies each issue during preceding 12 months	Single issue nearest to filing date
A.	Total no. copies printed (*net press run*)	2900	2900
B.	Paid circulation		
	1. Sales through dealers and carriers, street vendors and counter sales	—	—
	2. Mail subscriptions	2424	2424
C.	Total paid circulation	2424	2424
D.	Free distribution (*including samples*) by mail, carrier or other means	104	104
E.	Total distribution (*Sum of C and D*)	2528	2528
F.	Office use, left-over, unaccounted, spiled after printing	372	372
G.	Total (*Sum of E & F—should equal net press run shown in A*)	2900	2900

(Signature of editor, business manager, or owner)

I certify that the statements made by me above are correct and complete.

J. Barnes Jr.

CONTENTS

Vol. 7, Issue Nos. 1–12

Journal of Polymer Science
Part A-1: Polymer Chemistry

ISSUE NO. 1, JANUARY

Note

ISSUE NO. 2, FEBRUARY

Notes

Book Reviews

Errata

Issue No. 3, March

Notes

Book Reviews

Erratum

ISSUE NO. 4, APRIL

Issue No. 5, May

Notes

Issue No. 6, June

Notes

Issue No. 7, July

Note

ISSUE NO. 8, AUGUST

Notes

Book Reviews

Errata

Issue No. 9, September

Notes

Issue No. 10, October

Notes

Issue No. 11, November

Notes

Book Reviews

Erratum

ISSUE NO. 12, DECEMBER

Notes

Editorial Policy

At a number of meetings of the *Journal's* Editorial Board the Editors have reviewed and discussed the overall editorial policy that guides them in evaluating manuscripts submitted for publication. It will undoubtedly be helpful to prospective authors to reiterate that policy here.

Naturally, the *Journal of Polymer Science* will at all times be selective in accepting contributions on the basis of merit and originality. The *Journal* is not intended as a repository for unevaluated data. Preference will be given to papers that contribute new concepts, new or more comprehensive interpretations, or novel experimental approaches and results.

When preparing a manuscript, please consider critically the following questions for they embody the criteria by which the editors and referees will judge contributions.

Referees are chosen on the basis of competence and activity in the area embodied by the manuscripts. Authors may submit their recommendations for referees they feel may be particularly qualified to evaluate their manuscripts, however, the editors are in no way bound by these recommendations and are free to accept or reject these recommendations. In either case, the identity of the referee will remain anonymous.

Are the scientific problems clearly stated; are they significant?

Is the development of theoretical ideas logical and lucid? Are all quantities and symbols defined explicitly? Are all assumptions explicitly identified?

Are experimental data of an accuracy commensurate with the present development of technique, and do they elucidate the scientific problem? Are the experimental procedures and data given in sufficient detail to permit the reader to form a judgment of the work?

Are interpretations sound, and are the conclusions borne out by the evidence? Are tentative or speculative interpretations clearly labelled as such? Has full account been taken of pertinent earlier investigations?

Is the presentation clear, concise, and grammatical? Is the synopsis adequate; does it emphasize the important aspects of the problem, results, and conclusions?

Referees are chosen on the basis of competence and activity in the area embodied by the manuscripts. Authors may submit their recommendations for referees they feel may be particularly qualified to evaluate their manuscripts, however, the editors are in no way bound by these recommendations and are free to accept or reject these recommendations. In either case, the identity of the referee will remain anonymous.

In addition to meeting standards for excellence and significance, manuscripts for Part B (*Polymer Letters*) should exhibit a degree of novelty and timeliness that warrants speedy publication, even in preliminary form. Short communications, however meritorious, that do not meet this test can be considered for "Notes" in Part A. The Notes are generally to be regarded as complete publications of limited scope, while Letters may sometimes deal with important material to be elaborated later in a full-length paper.

JOURNAL OF POLYMER SCIENCE: PART A-1 VOL. 7, 3-14 (1969)

Anionic Graft Copolymerization of Diene Polymers with Vinyl Monomers

YUJI MINOURA and HIROSHI HARADA, *Department of Applied Chemistry, Faculty of Engineering, Osaka City University, Kita-ku, Osaka, Japan*

Synopsis

A mixture of homopolymer and graft copolymer was obtained by adding the monomer at 0°C to the polylithiodiene solution. Styrene, methyl methacrylate, and acrylonitrile were used as the monomers. Polylithiodienes were prepared by the metalation of diene polymers, i.e., polybutadiene or polyisoprene, with the use of *n*-butyllithium in the presence of a tertiary amine (*N*,*N*,*N'*,*N'*-tetramethylethylenediamine) in *n*-heptane. The graft copolymers were separated by solvent extraction and were confirmed by turbidimetric titration and elementary analysis. Oxidation of the polybutadiene–styrene grafts revealed that the molecular weight of the side chains was the same as the molecular weight of the free polystyrene formed. The grafting efficiency and grafting percentage were studied for polybutadiene–styrene graft copolymers prepared under various conditions.

INTRODUCTION

As described in a previous report,[1] diene polymers in *n*-heptane solution are metalated by *n*-butyllithium (BuLi) in the presence of a tertiary amine, i.e., *N*,*N*,*N'*,*N'*-tetramethylethylenediamine (TMEDA), and thus lithiated polymers are produced. If a suitable monomer which can be polymerized by an anionic mechanism is added to the lithiated diene polymer solution, the polymerization can start at the macromolecular organolithium and the monomer can be grafted on to the diene polymer. There are not many examples of the synthesis of graft copolymers by an anionic mechanism. Among these, there is a series of studies[2] by Greber and Egle on formation of graft copolymers by polymerizing monomers using polymer anions or radical anions produced by the reaction between various polymers and organometallic compounds. Also, graft copolymers have been obtained by reacting "living" polystyrene with poly(methyl methacrylate)[3] and poly(vinyl chloride).[4] As regards the graft copolymerization of diene polymers, research has been done mainly on the radical mechanism, as seen in the method[5] in which chain transfer to the polymer is used; kinetic investigations have also been made in detail. However no example of the graft copolymerization of diene polymers by an anionic mechanism is known so far.

EXPERIMENTAL

Materials

The polybutadiene (PB), polyisoprene (PI), BuLi, TMEDA, and the solvent, *n*-heptane, used were as described in the previous report.[1] Styrene (St), methyl methacrylate (MMA), and acrylonitrile (AN) were purified by distillation.

Lithiation of Diene Polymer and Graft Copolymerization with Vinyl Monomers

The lithiated polymer solution was synthesized by the method described in the previous report.[1] A mixture of homopolymer and graft copolymer was obtained by adding a solution of the monomer in benzene at 0°C to the lithiated diene polymer solution.

Separation of Graft Polymers

Polymer mixtures of PB–St and PI–St types, obtained from the polymerization of styrene with the lithiated polymer and BuLi, were subjected to boiling acetone extraction and separated into free polystyrene (soluble in acetone) and the graft polymers (insoluble in acetone). Polymer mixtures of the PB–MMA and PI–MMA types were subjected to continuous extraction by petroleum ether, acetone, and benzene, with the result that free rubber, free poly(methylmethacrylate) and the graft polymers were successively separated. Graft polymers of the PB–AN and PI–AN types were subjected to extraction with dimethylformamide with the resultant separation of the graft polymers, which were insoluble. Separation of the graft polymers was confirmed by turbidimetric titration, elemental analysis and infrared spectrometry.

Measurement Values

The percentage grafting and grafting efficiency were defined by the equations:

$$\text{Grafting percentage} = \frac{\text{Wt of grafted vinyl polymer}}{\text{Wt of polymer of main chain}} \times 100$$

$$\text{Grafting efficiency} = \frac{\text{Wt of grafted vinyl polymer}}{\text{Wt of total vinyl polymer polymerized}} \times 100$$

The intrinsic viscosity of benzene solutions of the polymer were obtained with an Ubbelohde viscometer at 30°C.

The degree of polymerization for polystyrene was calculated from Tobolsky's equation:[6]

$$\bar{P}_v = 1770 \times [\eta]\, 1.40$$

RESULTS AND DISCUSSION

Polybutadiene–Styrene Graft Copolymers

Synthesis and Separation of Graft Copolymers. Graft copolymerization was carried out under various conditions to obtain graft copolymers having varying numbers and lengths of side chains. The polymer mixtures obtained were separated into two parts by extraction with boiling acetone: the soluble polymer consisted of free polystyrene, which was polymerized by the residual BuLi; the acetone-insoluble residue was the graft polymer, which was readily soluble in benzene The result of this separation and the result of the turbidimetric titration, carried out on the polymer mixture, agreed well with each other, as shown in Figure 1. Extraction with boiling acetone was found to be a suitable method for the separation of the graft polymer.

Also, it was found from Figure 1 that there was no free PB. The result of the polybutadiene–styrene graft polymerization is shown in Table I.

Effects of the Concentrations of BuLi and Monomer on the Percentage Grafting and Grafting Efficiency. The grafting percentage and grafting efficiency may be dependent on the concentrations of BuLi and styrene used in the lithiation and polymerization at a constant concentration of PB. Considering results from anionic polymerization, the following may be expected: (*1*) if the BuLi concentration used in the lithiation is constant, the grafting percentage should be proportional to the monomer

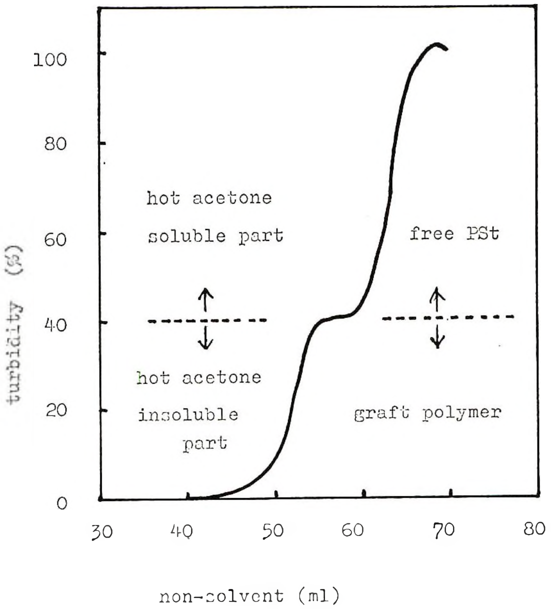

Fig. 1. Turbidimetric titration curve for the mixture of free polystyrene and PB–St graft polymer (sample 7). Solvent, benzene, 100 ml; nonsolvent, 10:1 mixture of methanol and acetone; polymer, 0.7 g.

TABLE I
Styrene Polymerization by Lithiated PB[a]

No.	$[PB]_0$, mole $\times 10^{2}$[b]	$[BuLi]_0$, mole $\times 10^{2}$[c]	Lithiation of PB, mole-%	$\frac{[PBLi]^{d}}{[BuLi]_0}$	Styrene, mole $\times 10^2$	Conversion of styrene, %	Graft mixture obtained, g	Mixture polymer, g	Graft polystyrene, g	Grafting percentage, %	Grafting efficiency, %
1	1	0.1	5.7	0.57	0.44	60	0.81	0.73	0.08	37	72
2	1	0.1	5.7	0.57	1.3	100	1.89	1.36	0.53	150	60
3	1	0.1	5.7	0.57	2.6	100	3.38	2.17	1.21	298	57
4	1	0.1	5.7	0.57	4.4	97	4.98	3.20	1.78	494	60
5	1	0.2	9.5	0.47	0.44	71	0.86	0.67	0.19	24	41
6	1	0.2	9.5	0.47	1.3	58	1.32	0.78	0.54	44	38
7	1	0.2	9.5	0.47	2.6	100	3.47	1.36	2.11	157	29
8	1	0.2	9.5	0.47	4.4	100	5.22	2.46	2.76	350	41
9	1	0.3	11.7	0.39	0.44	44	0.74	—	—	—	—
10	1	0.3	11.7	0.39	1.3	66	1.43	0.73	0.70	34	21
11	1	0.3	11.7	0.39	2.6	80	2.71	0.92	1.79	100	25
12	1	0.3	11.7	0.39	4.4	100	5.48	3.10	2.38	474	51

[a] Lithiation of PB, 80°C, 40 min; polymerization of styrene, 0°C, 10 hr.

[b] 0.54 g of PB corresponds to 0.01 mole of monomer units.

[c] Equimolar amount of TMEDA with BuLi was used.

[d] Concentration of lithiated PB.

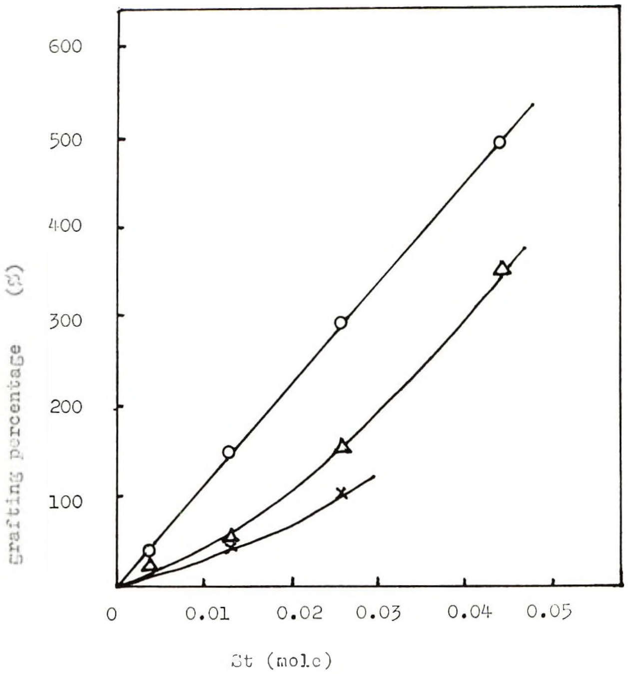

Fig. 2. Relationship between the grafting percentage and amount of styrene monomer used: (○) $[\mathrm{BuLi}]_0 = 1 \times 10^{-3}$ mole; (△) $[\mathrm{BuLi}]_0 = 2 \times 10^{-3}$ mole; (×) $[\mathrm{BuLi}]_0 = 3 \times 10^{-3}$ mole. PB, 0.01 mole.

concentration, and the grafting efficiency should not be dependent on the monomer concentration; (*2*) if the monomer concentration is constant, the grafting percentage and grafting efficiency should be dependent on $[\mathrm{PBLi}]/[\mathrm{BuLi}]_0$, where PBLi is the concentration of lithiated PB; thus, the larger the value of $[\mathrm{PBLi}]/[\mathrm{BuLi}]_0$ (from Table I, the smaller $[\mathrm{BuLi}]_0$), the higher the grafting percentage and grafting efficiency.

The actual results, shown in Figures 2 and 3, indicate that the above expectations are realized generally, i.e., the grafting percentage and grafting efficiency decreased as $[\mathrm{BuLi}]_0$ increased, and the grafting percentage was proportional to the monomer concentration at low concentrations of BuLi. The grafting efficiency had no relation to the monomer concentration at a given BuLi concentration. However as the BuLi concentration increased, the overall deviation became wide, which seems to be due to the problem of the solubility of the lithiated polymer in *n*-heptane. With an increase in the lithiation, the solubility of the lithiated polymer in *n*-heptane decreases, and a dark red precipitate gradually deposits on the wall of the reaction vessel. It is considered that compared with the case where $[\mathrm{BuLi}]_0$ was 0.067 mole/l., the level at which the polymerization was carried out in a homogeneous system, in the case of high BuLi concentrations, a more complex polymerization system was formed, including a heterogeneous system.

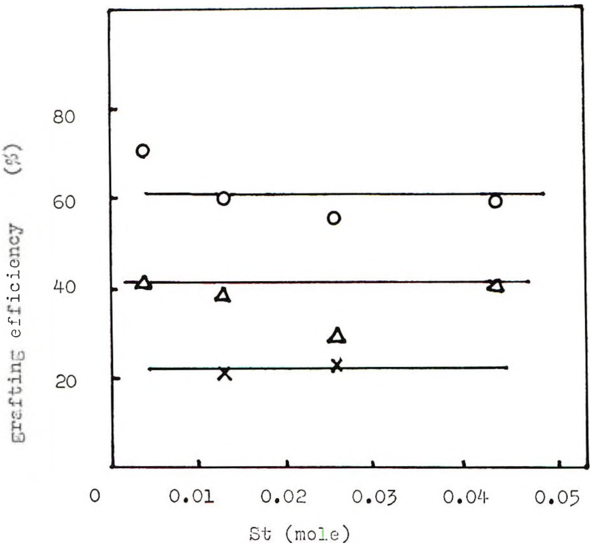

Fig. 3. Relationship between the grafting efficiency and amount of styrene monomer used. PB, 0.01 mole. Symbols as in Fig. 2.

Comparison between Grafted Polystyrene on Side Chain and Free Polystyrene. Graft polymers of the PB–St type were subjected to oxidative treatment with perbenzoic acid and periodic acid, and the grafted polystyrene obtained by cutting the PB of the main chain of the graft polymer and the free polystyrene initiated by the BuLi remaining in the reaction mixture, were compared with each other. The operation used here is shown in Figure 4. From the result of the infrared spectra, it was found that PSt-C, which was obtained from the oxidative treatment of the graft polymer, showed no absorption due to PB, and the results of the elemental analysis were identical with those of polystyrene.

ANAL. Calcd for polystyrene-C; C, 92.3%; H, 7.7%. Found: C, 92.1%; H, 7.8%.

Therefore, PSt-C contained no PB. PSt-A is the polystyrene polymerized freely in the reaction mixture and PSt-B is the polystyrene which was subjected to the same oxidative treatment as the graft polymer.

The results of the intrinsic viscosity studies of PSt-A, PSt-B, and PSt-C (Table I) are shown in Figures 5 and 6. The three polymers all have the same intrinsic viscosity. Therefore, it can be concluded that the polystyrene grafted to PB and the polystyrene initiated by the remaining BuLi have the same molecular weight.

Intrinsic Viscosity of Graft Polymers. The intrinsic viscosity of the PB in the main chain, the graft polymer, and the grafted polystyrene were measured. The main chain PB was obtained by directly hydrogenating the lithiated PB with ethanol. From these results, the length and numbers

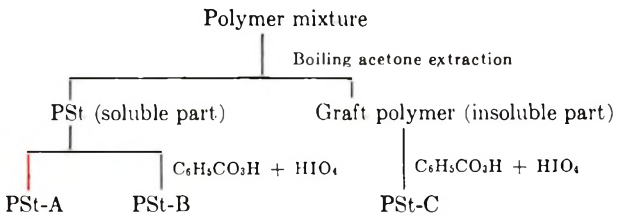

Fig. 4. Oxidative treatment of PB–St graft polymer.

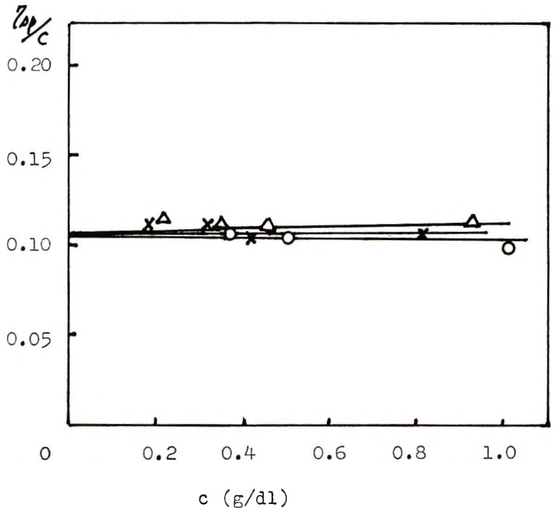

Fig. 5. Solution viscosity of grafted polystyrene and free polystyrene (sample 7): (○) PSt-A; (×) PSt-B; (△) PSt-C.

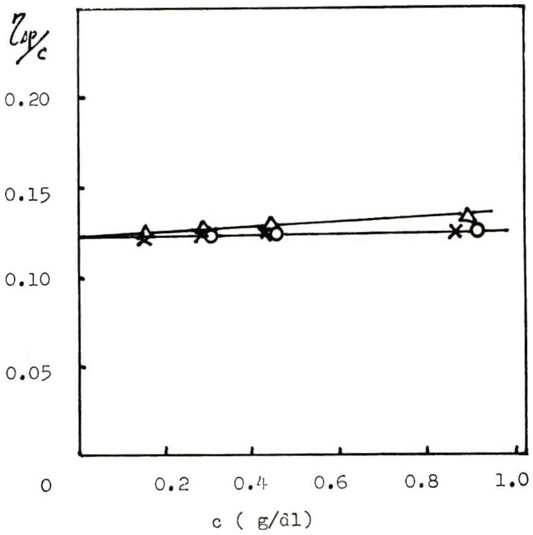

Fig. 6. Solution viscosity of grafted polystyrene and free polystyrene (sample 8): (○) PSt-A; (△) PSt-B; (△) PSt-C.

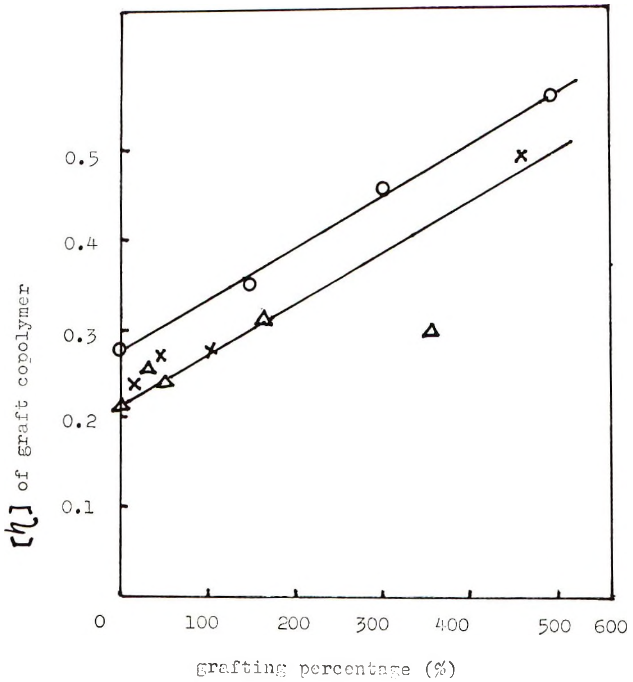

Fig. 7. Relationship between intrinsic viscosity of graft polymers and grafting percentage: (○) $[\mathrm{BuLi}]_0 = 1 \times 10^{-3}$ mole; (△) $[\mathrm{BuLi}]_0 = 2 \times 10^{-3}$ mole; (×) $[\mathrm{BuLi}]_0 = 3 \times 10^{-3}$ mole. PB_0, 0.01 mole.

TABLE II
Intrinsic Viscosity and the Length and Number of Side Chains for PB–St Graft Polymers

	[η] (benzene, 30°C)				
No.	PB of main chain	Graft polymer	PSt of side chain	$\bar{P}_n$ of side chain	Number of side chains per 100 monomer unit of PB
1	0.28	—	0.12	91	0.21
2	0.28	0.35	0.13	105	0.74
3	0.28	0.46	0.17	161	0.96
4	0.28	0.56	0.22	213	1.2
5	0.21	0.26	0.08	55	0.23
6	0.21	0.24	0.10	71	0.32
7	0.21	0.31	0.11	81	1.01
8	0.21	0.28	0.13	105	1.74
9	0.20	0.24	0.04	19	—
10	0.20	0.28	0.07	46	0.29
11	0.20	0.29	0.10	71	0.73
12	0.20	0.51	0.12	91	2.7

of polystyrene chains grafted on PB were calculated; the results are shown in Table II.

Figure 7 shows the relationship between the intrinsic viscosity of the

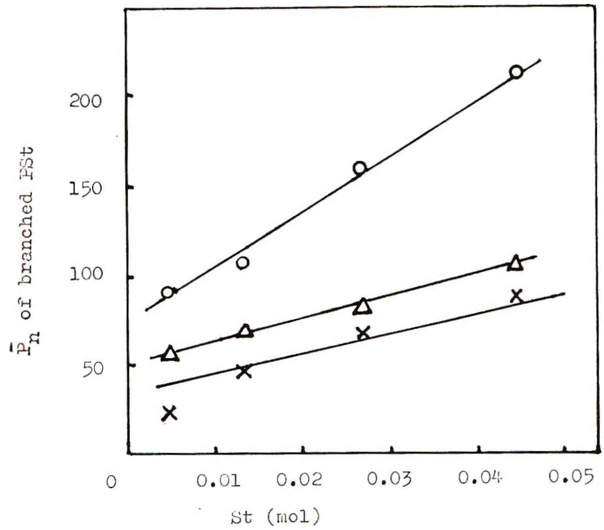

Fig. 8. Relationship between the degree of polymerization of grafted polystyrene and initial styrene content. Symbols as in Fig. 7.

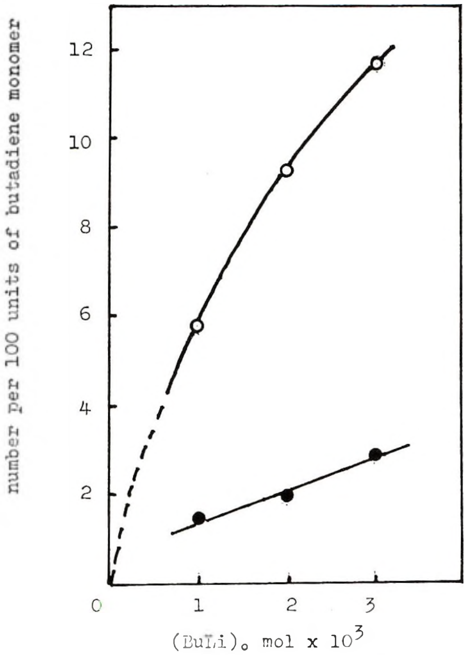

Fig. 9. Comparison of the degree of litiation of PB with the number of side chains in the graft copolymer: (○) degree of lithiation of PB; (●) number of side chains in graft copolymer.

graft polymers and the grafting percentage; the intrinsic viscosity increased almost linearly with the increase in grafting percentage.

Figure 8 shows the relationship between the degree of polymerization of the polystyrene grafted and the quantity of styrene monomer added. The degree of polymerization increased proportionally to the increase in the quantity of the monomer.

Figure 9 shows the degree of lithiation of PB and the number of branches along the main chains in relation to the quantity of BuLi used with a constant quantity of styrene monomer.

TABLE III

Graft Copolymerization of PB and Vinyl Monomers[a]

<table>
<tr><th rowspan="2">No.</th><th rowspan="2">PB, mole</th><th rowspan="2">BuLi, mole</th><th rowspan="2">Monomer, mole</th><th rowspan="2">Conversion of monomer, %</th><th colspan="3">Selective extraction, wt-%</th></tr>
<tr><th>Free PB</th><th>Graft polymer</th><th>Vinyl polymer</th></tr>
<tr><td>13</td><td>0.04</td><td>0.008</td><td>MMA 0.11</td><td>92</td><td>1.3</td><td>57.3</td><td>41.2</td></tr>
<tr><td>14</td><td>0.018</td><td>0.0036</td><td>AN 0.17</td><td>85</td><td colspan="2">65</td><td>35</td></tr>
</table>

[a] Lithiation of PB: 80°C, 60 min; polymerization of monomer: 0°C.

TABLE IV

Properties of Graft Polymers

	Analysis			Grafting percentage, %	Grafting efficiency, %	[η] (benzene, 30°C)	
No.	C, %	H, %	N, %			Graft polymer	Vinyl polymer (PMMA)
13	67.8	6.7	—	230	50	1.21	0.91
14	79.3	7.7	11.52	77[a]	11	—	—

[a] Calculated from nitrogen content.

TABLE V

Graft Copolymerization of I and Vinyl Monomers[a]

<table>
<tr><th rowspan="2">No.</th><th rowspan="2">PI, mole</th><th rowspan="2">BuLi, mole</th><th rowspan="2">Monomer mole</th><th rowspan="2">Conversion of monomer, %</th><th colspan="3">Selective extraction, wt-%</th></tr>
<tr><th>Free PI</th><th>Graft polymer</th><th>Vinyl polymer</th></tr>
<tr><td>15</td><td>0.05</td><td>0.005</td><td>St 0.1</td><td>95</td><td colspan="2">49.5</td><td>50.5</td></tr>
<tr><td>16</td><td>0.03</td><td>0.01</td><td>MMA 0.2</td><td>30</td><td>13.1</td><td>35.6</td><td>51.3</td></tr>
<tr><td>17</td><td>0.03</td><td>0.004</td><td>AN 0.18</td><td>43</td><td colspan="2">38.5</td><td>61.5</td></tr>
</table>

[a] Lithiation of PI: 80°C, 60 min; polymerization of monomer: 0°C.

TABLE VI
Properties of Graft Polymers

No.	Analysis			Grafting percentage, %	Grafting efficiency, %	[η] (benzene, 30°C)		
	C, %	H, %	N, %			Free PI	Graft polymer	Vinyl polymer
15	89.7	10.1	—	89	31.6	0.72		Pst 0.054
16	69.55	6.65	—	63	18.5	1.34	2.8	PMMA 0.57
17	83.7	9.9	4.75	22[a]	11.0	—	—	—

[a] Calculated from nitrogen content.

Graft Copolymerization of PB and Other Monomers

After PB was lithiated, graft polymers were obtained by initiating methyl methacrylate and acrylonitrile with the lithiated PB.

The reaction conditions and the results of the selective extraction of the graft polymers are shown in Table III, and the properties of the graft polymers obtained are shown in Table IV.

Graft Copolymerization of PI and Various Monomers

Graft polymers were obtained by polymerizing styrene, methyl methacrylate, and acrylonitrile in the presence of lithiated PI.

Table V shows the results of the experiments, and Table VI the properties of the graft polymers.

References

1. Y. Minoura, K. Shiina, and H. Harada, *J. Polym. Sci.*, A-1, **6**, 559 (1968).
2. G. Greber and G. Egle, *Makromol. Chem.*, **53**, 206 (1962); *ibid.*, **53**, 208 (1962); *ibid.*, **54**, 136 (1962); *ibid.*, **59**, 174 (1963); *ibid.*, **64**, 68 (1963); *ibid.*, **64**, 207 (1963); *ibid.*, **67**, 196 (1963); *ibid.*, **71**, 47 (1964).
3. G. Finaz, Y. Gallot, J. Parrod, and R. Rempp, *J. Polym. Sci.*, **58**, 1363 (1962).
4. Y. Gallot, R. Rempp, and J. Parrod, *J. Polym. Sci.* B, **1**, 329 (1963).
5. Y. Minoura, Y. Mori, and M. Imoto, *Makromol. Chem.*, **24**, 205 (1957).
6. A. V. Tobolsky, *J. Amer. Chem. Soc.*, **74**, 938 (1952).

Received August 28, 1967
Revised April 19, 1968

JOURNAL OF POLYMER SCIENCE: PART A-1 VOL. 7, 15–22 (1969)

Thermostable Organic Polymers Devoid of Hydrogen and Other Pendent Groups*

STEPHEN S. HIRSCH, *Chemstrand Research Center, Inc., Durham, North Carolina 27702*

Synopsis

Aromatic hydrogen atoms in thermostable polymers can be surprisingly labile at relatively low temperatures and may participate extensively in degradative reactions. If hydrogen were eliminated from the polymer chain, a number of degradative pathways would be excluded. Replacement of hydrogen with other pendent groups such as fluoride or trifluoromethyl still leaves a potential "handle" to enter into unwanted reactions, therefore, all bonds not required to create the chain were eliminated. The polyimide devoid of hydrogen from pyrazinetetracarboxylic dianhydride and 2,5-diamino-1,3,4-thiadiazole was synthesized. This polymer exhibits extraordinary high temperature oxidation stability. Films of this composition support weight in air up to 592°C, and rupture at this temperature is accompanied by no charring whatever. By comparison, the corresponding polymer from pyromellitic dianhydride, with two hydrogen atoms per repeating unit begins to char at 320°C.

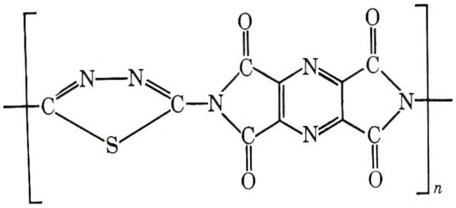

INTRODUCTION

Users of thermally stable organic materials are becoming increasingly aware that oxidative failure, rather than thermal decomposition alone, is responsible for the initial product breakdown during the majority of applications. It becomes necessary, therefore, to design the maximum of oxidation resistance as well as thermal stability into high performance polymers.

Earlier work[1] has revealed that aromatic hydrogen atoms, ordinarily considered quite unreactive, can be surprisingly labile and participate extensively in degradative and cross-linking reactions even in inert atmospheres. The presence of oxygen would be expected to render C—H bonds

---

* Paper presented at the 154th National Meeting, American Chemical Society, Chicago, Ill., September 10–15, 1967.

even more susceptible to attack. It is not the strength of the phenyl-H bond which determines aromatic hydrogen reactivity in these instances, but rather, the availability of suitable reaction pathways and the overall energy changes accompanying the processes.

Additional evidence became available which made aromatic carbon–hydrogen bonds suspect. Of eighteen model compounds tested, representing structures used in thermostable polymer systems, the poorest thermal stability by far was that of 2,5-diphenyl-1,3,4-oxadiazole (I).[2]

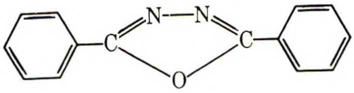

I

Nonetheless, certain fibers and films containing oxadiazole rings in their structures (along with other hydrogen-containing groups) exhibit excellent long-term stability in air at 200–400°C.[3,4] While pyrolysis studies and weight loss measurements (TGA) provide a picture of gross bond failure, loss of physical properties of fibers and films begins with more subtle changes such as oxidation, crosslinking and disorientation. This is particularly true when long-term stability is considered at temperatures considerably below the TGA inflection.

Since oxadiazole-containing structures possess resistance to the subtle changes just described when they are used below the temperature of gross bond failure, it is not surprising that the utility of such structures in air is not predicted from pyrolysis studies conducted in inert media. To account for the fact, then, that structures such as alt. poly[1,3,-1,4-phenylene-2,5-(1,3,4-oxadiazole)],[4] II

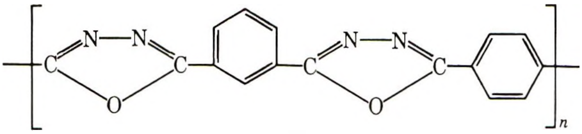

II

have considerable value at high temperatures in air, we hypothesized that the absence of hydrogen on the oxadiazole rings was responsible, at least in part, for minimizing property-destroying reactions.

DISCUSSION

To test the above thinking, a program was undertaken to prepare an aromatic polymer totally devoid of hydrogen and to evaluate it for thermo-oxidative stability. It was not desired to replace hydrogen by another group such as fluoride or trifluoromethyl. Such an approach appears to result in diminution of thermal properties as often as improvement. Rather, it was intended to do away with the available valency altogether. For example, =CH— groups can be replaced with nitrogen atoms (=N—)

and —CH_2— groups with oxygen (—O—) or sulfur (—S—). Such modifications lead to a series of heterocyclic polymers which, in a sense, bridge the gap between organic and inorganic polymers and which contain no bonds whatever other than those necessary to create the chain. Thus, no pendent "handles" of any type would be present to enter into unwanted, degradative reactions.

Polyimides were chosen, as a class, for initial investigation. The reasons were threefold: (1) polyimides have been shown to possess excellent thermal properties; (2) aromatic dianhydrides, with four points of attachment to the center ring have few remaining positions which must be deprived of hydrogen and (3) synthesis and polymer-forming reactions did not appear formidable.

The polyimide composition chosen for investigation was the product resulting from the reaction of pyrazinetetracarboxylic dianhydride (PTDA) with 2,5-diamino-1,3,4-thiadiazole (DATD).

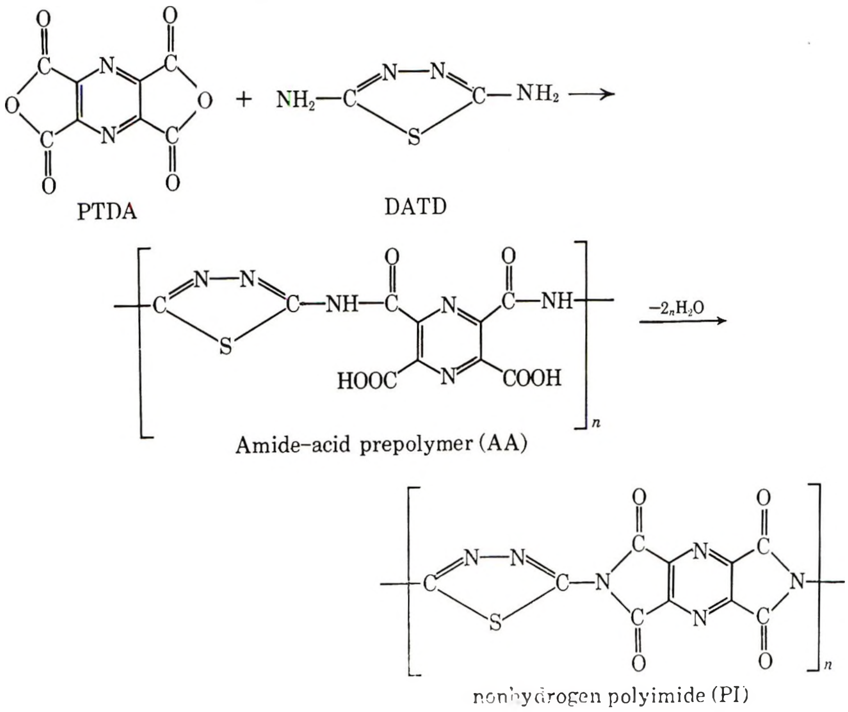

DATD and pyrazinetetracarboxylic acid (PTCA) were prepared by adaptations of methods described in the literature.[5,6] Preparation of the corresponding dianhydride has not, however, been reported. Treatment of the acid with acetic anhydride under very mild conditions followed by sublimation afforded the desired dianhydride.

Polymerization with equimolar quantities of these starting materials in dimethylacetamide or *N*-methylpyrrolidone proceeded very rapidly at room temperature to give a viscous, castable, 7% solids dope in 1.5 hr.

The polymer solubility was found to be very dependent on reaction conditions, and rather sudden gelation occurred if the reaction were allowed to proceed too far. If a lower per cent solids was used, gelation set in at lower viscosity build-ups, and the amide-acid gel, once formed, would not redissolve in any solvent. The limited solubility of the amide-acid necessitated casting of films well before maximum molecular weight was attained. While the films were sufficiently strong to permit easy handling, strength and high temperature utility of the corresponding polyimide apparently suffered from molecular weight limitations.

Conversion of the amide-acid to polyimide was accomplished by slow heating to 375°C and maintenance at this temperature for 2 hr in air or nitrogen. A very deep red transparent, smooth film resulted which, as predicted for such a composition, exhibited outstanding oxidation resistance at elevated temperatures. If the AA film were placed into a hot oven rather than heated slowly, decomposition rather than conversion to polyimide resulted. This was doubtlessly due to the facile decarboxylation which pyrazinecarboxylic acids undergo.

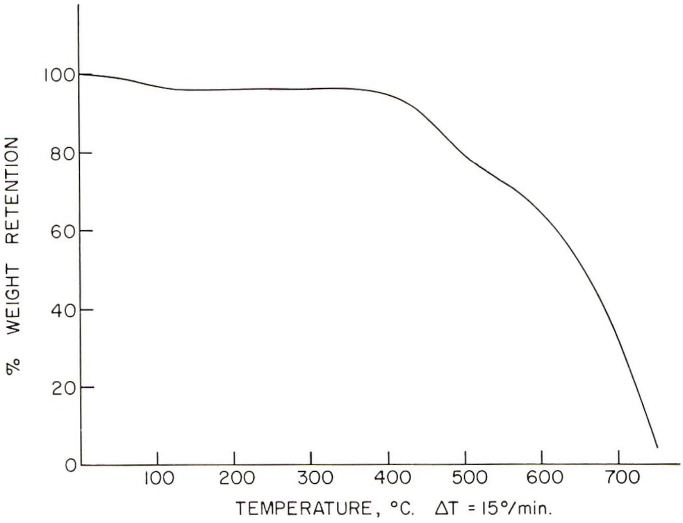

Fig. 1. TGA plot of PTDA–DATD PI in air.

Testing of the new polyimide film was conducted with two chief goals in mind: (1) comparison of high-temperature resistance in air with that of a well known, hydrogen-containing polyimide and (2) demonstrating that the thermal resistance in air was similar to that in nitrogen, which would indicate oxidation resistance. In the first test, samples of PTDA-DATD PI film were compared with specimen films of the polypyromellitimide of oxydianiline. The films were maintained at 400°C in air for 25 hr and were inspected periodically. The PTDA–DATD PI appeared to undergo no changes other than a very slow diminution in size, while the hydrogen-containing reference sample suffered charring, bubbling, wrinkling, em-

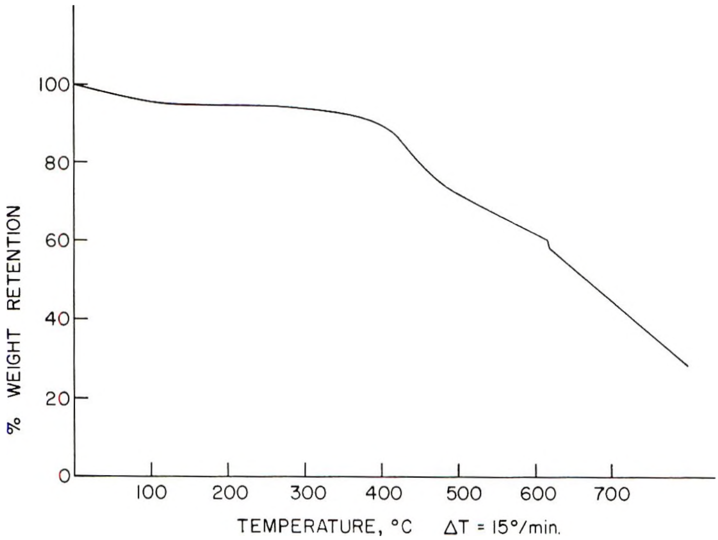

Fig. 2. TGA plot of PTDA–DATD PI in nitrogen.

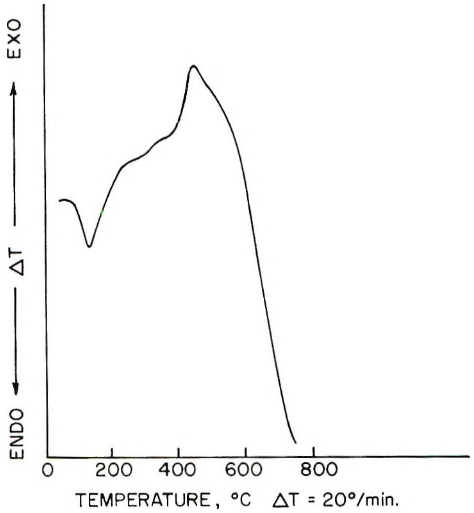

Fig. 3. DTA thermogram of PTDA–DATD PI in air.

brittlement and cracking during the test period. The recovered PTDA–DATD PI was transparent, smooth, and no less flexible than at the start.

To determine whether resistance to high temperatures in air was equivalent to that in nitrogen (a measure of oxidation resistance), thermogravimetric analyses (TGA), differential thermal analyses (DTA), and zero strength measurements were made in both media. The TGA curves in nitrogen and air were almost superimposable up to 600°C (Figs. 1 and 2). The DTA curves were also almost identical in both media (Figs. 3 and 4), again showing no difference due to air oxidation. Zero strength tempera-

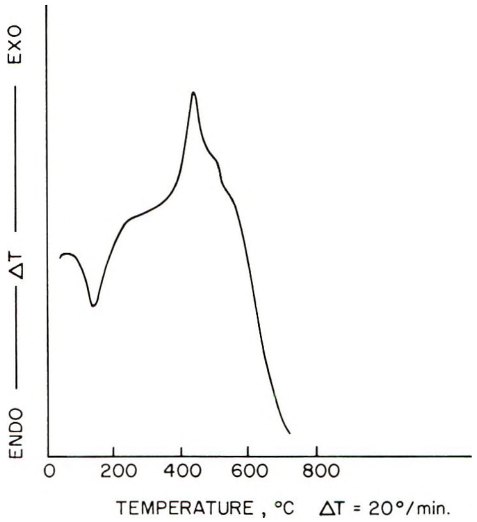

Fig. 4. DTA thermogram of PTDA–DATD PI in nitrogen.

tures (20 psi load) similarly were alike in both air and nitrogen (579°C in nitrogen; 592°C in air) reflecting no difference due to air. Special mention must be made that upon rupture at nearly 600°C in air, it was transparent flexible film, *not a charred form,* which had been supporting the weight. In fact, we have not been able to cause this polymer to char under any conditions.

It may be seen that the TGA inflection for this polymer is not particularly high (425°C in air), however, the slope after "break" is not steep. The relatively low inflection is likely due to three factors: (1) less than optimum molecular weight; (2) the fact that achievement of well-oriented films was not a goal of this project; and (3) the absence of charring hinders weight retention. However, the polymer is decidedly more inert chemically than many compositions with higher TGA inflections.

To obtain a direct comparison of the PTDA–DATD PI with an analogous structure containing some hydrogen, the corresponding polymer from pyromellitic dianhydride (PMDA) was prepared. This composition contains two hydrogen atoms per repeating unit.

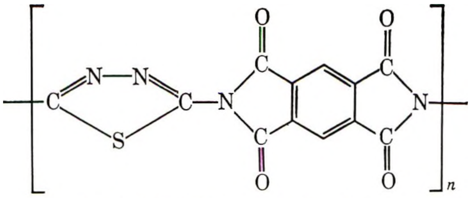

PMDA–DATD polyimide (PI)

In striking contrast to the behavior of the wholly nonhydrogen analog, fibers and films from PMDA–DATD PI char extensively at 320°C in air or nitrogen. The difference between zero and two hydrogen atoms per repeating unit thus has a major effect on the thermo-oxidative stability of this type of polyimide.

EXPERIMENTAL

Pyrazinetetracarboxylic Dianhydride

Recrystallized (from constant boiling HCl) PTCA (16 g) was stirred under nitrogen with 400 ml of acetic anhydride (bp 139–140°C). The mixture was heated slowly to 80–85°C (not higher!), whereupon the PTCA dissolved with apparent concomitant reaction. The solution was maintained at 80°C for $^1/_2$ hr after solution was completed and then concentrated to a slush under water aspirator vacuum. (If the reaction mixture is heated under reflux at atmospheric pressure, a brown solid is obtained upon evaporation of acetic anhydride from which no PTDA can be sublimed.) The flask containing the slush was placed in a vacuum oven maintained at 80°C and evacuated under full oil pump vacuum overnight to afford a quantitative yield of PTDA. The product was sublimed under vacuum* and after discarding a forecut, very pale green crystals of high purity were collected. No melting point was observed for this material, but gradual decomposition (darkening) set in at 180°C. After reaction with water, the sole product was PTCA, as evidenced by infrared spectrum.

ANAL. Calcd for $C_8N_2O_6$: C, 43.66%; H, 00.00%; N, 12.73%. Found: C, 43.61%; H, none; N, 12.84%.

Polyimide Formation

A typical polymerization was run as follows: PTDA (0.4624 g) was weighed into a thoroughly dried 1-oz screw cap bottle having a polyethylene-lined cap. Dimethylacetamide (10 ml, dried over 5A molecular sieves) was added from a syringe and the bottle swirled until solution occurred. Then DATD (0.2440 g) was added, and the mixture was shaken vigorously by hand. Solution with concomitant reaction and darkening occurred rapidly followed by gradual lightening to a yellow color. The mixture was tumbled end over end at room temperature for approximately 1.5 hours until it appeared that gelation was imminent. Films were then cast with the aid of a Gardner knife. The amide-acid films were cured to the PTDA-DATD polyimide by the following gradual heat treatment: heating from room temperature to 250°C at a rate of 4°C/min; heating from 250°C to 300°C at 1.1°C/min; 300°C isothermal for 1 hr; heating from 300°C to 350°C at 1.1°C/min; 350°C isothermal for $1^1/_4$ hr; heating from 350°C to 375°C at 1.1°C/min; finally 375°C isothermal for 2 hr. In this way it was found that decarboxylation and formation of bubbly film was avoided and that smooth conversion to polyimide was achieved.

---

* It is well to sublime from a loosely covered dish; otherwise black, diaphanous specks will contaminate the sublimate. Sublimation proceeds above 180°C.

Zero Strength Temperature

Strips of PTDA–DATD PI film approximately $^1/_3 \times 1^1/_4$ in. were cut and measured accurately in width and thickness. Sufficient weight was hung from the sample to correspond to a load of 20 psi of cross-section. The sample was suspended in a quartz tube in a vertical tube furnace and the temperature was raised from ambient to break at 4°C/min. The procedure was repeated in air and nitrogen atmospheres, and the temperature required for film rupture was noted in each case.

CONCLUDING REMARKS

PTDA–DATD PI polymer, although of only moderate molecular weight and strength, exhibits outstanding thermal and oxidative resistance. However, the PTDA–DATD AA and PI are regarded largely as models for nonhydrogen polymer systems. They were chosen for preliminary investigation because of relative ease of synthesis of starting materials and to prove the hypothesis that elimination of hydrogen leads to oxidative stability. Other compositions which are expected to be of greater strength and thermal stability are currently under consideration. Continued application of this approach should lead to new levels of thermo-oxidative stability of organic materials.

This work was performed under Air Force Contract Number AF33(657)11163 administered by the Air Force Materials Laboratory, Wright-Patterson Air Force Base, Ohio.

The technical assistance of Messrs. G. K. Ragep and M. T. Bryant is acknowledged with thanks. Dr. Jack Preston's advice concerning preparation of the manuscript is appreciated.

References

1. S. S. Hirsch, *J. Org. Chem.*, **32,** 2433 (1967).
2. S. S. Hirsch and M. R. Lilyquist, *J. Appl. Polym. Sci.*, **11,** 305 (1967).
3. A. H. Frazer and F. T. Wallenberger, *J. Polym. Sci.*, **A2,** 1171 (1964).
4. J. Preston and W. B. Black, *J. Polym. Sci. B*, **4,** 267 (1966).
5. H. Beyer, *Chem. Ber.*, **82,** 143 (1949).
6. H. I. X. Mager and W. Berends, *Rec. Trav. Chim.*, **76,** 28 (1957).

Received April 18, 1968

JOURNAL OF POLYMER SCIENCE: PART A-1 VOL. 7, 23-33 (1969)

Microstructure of Ethylene–Vinyl Chloride Copolymers. I. Direct Verification of Terminal Radical Effects on Copolymerization by a Simplified NMR Approach

CHARLES E. WILKES, J. C. WESTFAHL, and RICHARD H. BACKDERF, *The B. F. Goodrich Company Research Center, Brecksville, Ohio 44141*

Synopsis

The sequence distributions of monomer units in a series of high-pressure, bulk ethylene–vinyl chloride copolymers have been determined by high-resolution NMR spectroscopy. The concentrations of EE, VV, and EV (VE) monomer pairs or diads were used with NMR-determined compositions to calculate, in addition to the sequence distribution parameters, the reactivity ratio product for the system. Inclusion of feed data allowed the calculation of individual reactivity ratios. Well within experimental error, the reactivity ratio product (r_1r_2 = 0.7) determined from microstructure analysis—independent of monomer feed data—was equal to that determined by the standard Fineman-Ross technique. Terminal monomer unit effects on the copolymerization were observed. The nonrandom structures result from a copolymerization described by first-order Markoffian statistics.

Introduction

The copolymerization of ethylene and vinyl chloride has been described as a random or zeroth-order Markoffian process. From the feed and composition data of high-pressure bulk copolymerizations, Burkhart and Zutty[1] found the reactivity ratio product (r_1r_2) equal to 0.85 ± 0.26. This they considered equivalent to unity, thus representative of an ideal or random copolymerization. Schaefer[2] described the emulsion copolymerization of ethylene and vinyl chloride as random ($r_1r_2 \cong 1.0$) from a detailed high-resolution, multiple-resonance NMR study.

We have completed a microstructure analysis of both bulk and emulsion ethylene–vinyl chloride copolymers by high-resolution NMR spectroscopy. Use of the run-number concept[3] simplifies the calculation of monomer sequence distribution and reactivity ratios from the distribution of monomer sequence distribution and reactivity ratios from the distribution of monomer diads. In part I of this study we shall describe the analytical procedure and, for the bulk copolymers, compare the NMR observed microstructures with those calculated from copolymerization theory (reactivity ratios.) We have found r_1r_2 to be 0.68 ± 0.11 by microstructure analysis and 0.71 ± 0.10 from feed and composition data. The process thus tends slightly toward alternation, and terminal radical effects are indicated.

Experimental

Bulk ethylene–vinyl chloride copolymers were prepared at 50°C and 28000 psi with the use of diisopropylperoxydicarbonate (IPP) as an initiator. Copolymer compositions were determined by NMR and by chlorine analysis. Calculation of feed ratios in preliminary experiments involved weighing in the vinyl chloride at 5°C and pressuring with ethylene to 21000 psi. (Total pressure at 50°C was approximately 28000 psi.) From pressure–density–temperature curves and known volumes the weights of ethylene were determined. In later copolymerizations we weighed both the vinyl chloride and the ethylene after introducing each into the bomb.

Although some conversions went as high as 16%, reactivity ratios calculated from the integrated form of the copolymerization equation[4] were equivalent, within experimental error, to those calculated by the Fineman-Ross technique[5] (Table I). In addition, NMR spectra of 50 mol-% ethylene bulk copolymers run to conversions of 3.1, 12.6, and 14.9% were essentially identical. (Similar results were obtained for 46 mol-% ethylene emulsion copolymers run to conversions of 3.5 and 6.5%.)

TABLE I
Experimentally Determined Reactivity Ratios

r_1	r_2	r_1r_2	Method
0.18 ± 0.04	3.35 ± 0.30	0.60 ± 0.14	Integrated copolymerization equation
0.22 ± 0.02	3.21 ± 0.30	0.71 ± 0.10	Fineman-Ross technique
0.21 ± 0.02	3.21 ± 0.22	0.68 ± 0.11	NMR microstructure analysis

Interpretation of NMR Spectra

In Figure 1 are shown NMR spectra of (*a*) 50 mol-% ethylene and (*b*) 72 mol-% ethylene copolymers. The spectra were taken at 140°C in *o*-dichlorobenzene. The peak (or multiplet) assignments, chemical shifts (relative to hexamethyldisiloxane) and corresponding structures are given in Table II. Our results (at 60 MHz) for the chemical shifts of methylenes with CHCl nearest and next-nearest neighbors are comparable to those of Schaefer,[2] who experimented at 100 MHz. Relative to the chemical shift of a methylene in a polyethylene-type sequence, a methylene with a CHCl nearest neighbor is 24 Hz farther downfield. A methylene with a CHCl next-nearest neighbor is approximately 11 Hz farther downfield. With two next-nearest neighbor CHCl's, the methylene proton resonance is 22 Hz downfield.

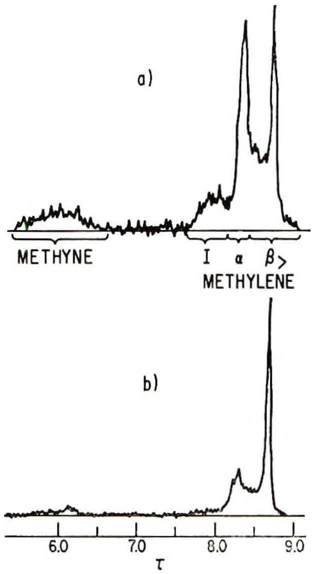

Fig. 1. NMR spectra of ethylene–vinyl chloride copolymers (60 MHz, 140°C, *o*-dichlorobenzene): (*a*) 50 mol-% ethylene; (*b*) 72 mol-% ethylene.

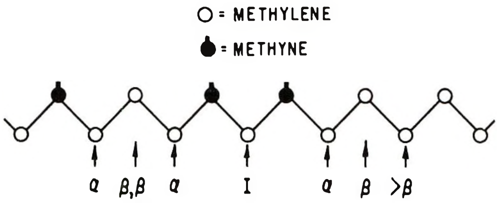

Fig. 2. Description of methylene protons in an ethylene–vinyl chloride copolymer.

We refer to the methylene situated between two CHCl's (i.e., in a vinyl chloride–vinyl chloride pair sequence) as I or "inner" (see Fig. 2). A methylene adjacent to a CHCl and also to another methylene is labeled α and a methylene with no CHCl nearest neighbors and two or less CHCl

TABLE II
Nuclear Magnetic Resonance Chemical Shift Assignments

Structure	Shift downfield from HMDS, Hz	
$—CH_2—CH_2—CH_2^*—CH_2^*—CH_2—CH_2$	74	High % E copolymers of E–VCl
$—CHCl—CH_2—CH_2^*—CH_2—CHCl$	96	2,6-Dichloroheptane
$—CHCl—CH_2^*—CH_2—CH_2$	98	E–VCl copolymers
$—CHCl—CH_2^*—CH_2^*—CHCl$	108	2,5-Dichlorohexane
$—CHCl—CH_2^*—CHCl$	113-*d,l* 134-*meso*	2,4-Dichloropentane
$—CHCl—CH_2^*—CHCl$	124	High % VCl copolymers of E–VCl

next-nearest neighbors we call $\beta>$. The $\beta>$ ("beta or greater") methylenes are lumped into one class, since the structure calculations allow this simplification (see below). Methylenes with one CHCl nearest neighbor and one CHCl next-nearest neighbor (as in 2,5-dichlorohexane) were not observed in our NMR spectra. These would correspond to tail-to-tail vinyl chloride sequences or triads containing an ethylene between two head-to-head vinyl chlorides.

The copolymer composition was determined from the NMR spectra as follows. Let X = methyne proton area, Y = methylene proton area; then

$$E = (Y - 2X)/4$$

where E is proportional to mole per cent ethylene,

$$V = X$$

where V is proportional to mole per cent vinyl chloride,

$$\text{Mol-\% ethylene} = E/(E + V) \times 100$$

$$\text{Mol-\% vinyl chloride} = V/(E + V) \times 100$$

Characterization of Monomer Sequence Distribution

Since each ethylene contains two methylenes and each vinyl chloride contains one, the total number of methylenes per 100 monomer units is:

$$\text{Total CH}_2 = 2\,(\%\ \text{E}) + \%\ \text{V} = T$$

Each VV pair contains one I-type methylene, therefore the fraction of I-type methylenes is:

$$f(\text{CH}_2)_\text{I} = \%\ \text{VV}/T$$

where % VV equals 100 × the number of VV pairs divided by the total number of VV, EE, EV, and VE pairs. Similarly:

$$f(\text{CH}_2)\alpha = \frac{(\%\ \text{EV} + \%\ \text{VE})}{T}$$

$$f(\text{CH}_2)\beta> = \frac{2\,(\%\ \text{EE}) + {}^1/_2\,(\%\ \text{EV} + \%\ \text{VE})}{T}$$

Thus, the monomer pair or diad distribution is:

$$(\%\ \text{EV} + \%\ \text{VE}) = T\,f(\text{CH}_2)\alpha$$

$$\%\ \text{VV} = T\,f(\text{CH}_2)_\text{I}$$

$$\%\ \text{EE} = ({}^1/_2)\ T\,f(\text{CH}_2)\beta> - ({}^1/_4)\ T\,F(\text{CH}_2)\alpha$$

In order to simplify the mathematical treatment of the diad distribution and the calculation of monomer sequence distribution parameters, we shall use the run-number concept, coined and derived by Harwood and Ritchey.[3]

The run number R equals the average number of monomer sequences (of both monomers 1 and 2) per 100 monomer units. (A sequence is a run of monomers of one type bounded on both ends by monomer of the second type.) The formulae relating R to diad concentrations and monomer sequence distribution are summarized here.

$$R\ (\mathrm{EV, VE}) = (\%\ \mathrm{EV} + \%\mathrm{VE})\ \text{pairs}$$

$$R\ (\mathrm{VV}) = 2\ (\%\ \mathrm{V}\text{-}\%\ \mathrm{VV})$$

where $\%\ \mathrm{V}$ = mole $\%$ V in copolymer; $\%\ \mathrm{VV} = \%\ \mathrm{VV}$ pairs.

$$R\ (\mathrm{EE}) = 2\ (\%\ \mathrm{E}\text{-}\%\ \mathrm{EE})$$

where $\%\ \mathrm{E}$ = mole $\%$ E in copolymer; $\%\ \mathrm{EE} = \%\ \mathrm{EE}$ pairs.

$$P_{\mathrm{VE}} = R/2\ (\%\ \mathrm{V})$$

$$P_{\mathrm{EV}} = R/2\ (\%\ \mathrm{E})$$

$$P_{\mathrm{VV}} = \frac{(\%\ \mathrm{V}\text{-}R/2)}{\%\ \mathrm{V}} = 1\text{-}P_{\mathrm{VE}}$$

$$P_{\mathrm{EE}} = \frac{(\%\ \mathrm{E}\text{-}R/2)}{\%\ \mathrm{E}} = 1\text{-}P_{\mathrm{EV}}$$

where P_{VE} = probability that a given V unit has an E unit on its right (or left); also, P_{VE} = probability that a growing polymer chain ending in V will add an E unit. P_{EV}, P_{VV}, and P_{EE} are defined in like manner. The number-average sequence lengths of both monomers are:

$$N_{\mathrm{E}} = \%\ \mathrm{E}/(R/2) = 1/P_{\mathrm{EV}}$$

$$N_{\mathrm{V}} = \%\ \mathrm{V}/(R/2) = 1/P_{\mathrm{VE}}$$

Invoking the accepted copolymerization theory formulae, one may relate reactivity ratios to the parameters derived above.

$$P_{\mathrm{EV}} = \frac{K_{\mathrm{EV}}M_{\mathrm{V}}}{K_{\mathrm{EV}}M_{\mathrm{V}} + K_{\mathrm{EE}}M_{\mathrm{E}}} = \frac{1}{r_1 F + 1}$$

where $r_1 = K_{\mathrm{EE}}/K_{\mathrm{EV}}$ (subscript 1 refers to ethylene), F = mole ratio E/V in feed, and

$$P_{\mathrm{VE}} = \frac{K_{\mathrm{VE}}M_{\mathrm{E}}}{K_{\mathrm{VE}}M_{\mathrm{E}} + K_{\mathrm{VV}}M_{\mathrm{V}}} = \frac{1}{1 + r_2/F}$$

where $r_2 = K_{\mathrm{VV}}/K_{\mathrm{VE}}$ (subscript 2 refers to vinyl chloride). Therefore,

$$r_1 F + 1 = 1/P_{\mathrm{EV}} = N_{\mathrm{E}}$$

$$(r_2/F) + 1 = 1/P_{\mathrm{VE}} = N_{\mathrm{V}}$$

Thus, the number-average sequence length of each monomer in the copolymer is a simple function of reactivity ratio and feed. Since

$$\begin{aligned} r_1 r_2 &= r_1 F\ (r_2/F) \\ &= (N_{\mathrm{E}} - 1)\ (N_{\mathrm{V}} - 1) \\ &= \left(\frac{\%\ \mathrm{E}}{R/2} - 1\right)\left(\frac{\%\ \mathrm{V}}{R/2} - 1\right) \end{aligned}$$

the reactivity ratio product can be determined from the copolymer composition and run number, independent of feed ratio. Thus, analysis of one copolymer, without knowledge of monomer feeds, allows one to determine whether that series of copolymers will be characterized as random or tending either toward alternation or toward blockiness.

For this specific analysis, much of the value of the run number approach lies in the three methods for calculating R. Since R (EV, VE) must equal R (EE) must equal R (VV), we have a criterion of internal consistency in determining the fraction of I, α, and $\beta>$ methylenes from the NMR spectra. The overlap of peaks, especially those corresponding to α methylenes and methylenes β to two CHCl's, initially caused problems in the calculations. However, refinement of the data (peak areas) until the three R values were reasonably consistent was easily accomplished. Another source of internal consistency in the area assignments occurs for copolymers of 50/50 mol composition. One may easily prove that for these copolymers the % EE pairs must equal the % VV pairs. Coupled with the refinement of R values, this check provides a good deal of confidence in the final structural parameters.

Results

In Table III we have listed the compositions and percentages of I, α, and $\beta >$ methylenes for the bulk copolymers. Table IV shows the results of the sequence distribution calculations. R (avg) = the average of R (EV, VE), R (EE), and R (VV). $\Delta R = |R\text{ (avg)} - R\text{ (EE)}| = |R\text{ (avg)} - R\text{ (VV)}|$.

TABLE III
Copolymer Compositions and Methylene Proton Distributions

		Methylene proton distribution		
Sample	E, mol-%	I, %	α, %	$\beta>$, %
A	38.5	25.6	37.7	36.7
B	51.0	14.5	36.7	48.8
C	51.0	14.7	36.1	49.2
D	64.3	7.0	30.5	62.5
E	29.3	37.5	34.3	28.2
F	50.0	15.0	36.2	48.8
G	60.9	8.0	31.9	60.1
H	50.0	14.8	36.3	48.9
I	72.0	5.3	24.6	70.1

TABLE IV

Results of Monomer Sequence Distribution Calculations

Sample[a]	R (avg)	ΔR	r_1F	r_2/F	r_1r_2	P_{EV}	P_{EE}	P_{VE}	P_{VV}
A	52.2	0.1	0.48	1.36	0.65	0.68	0.32	0.42	0.58
B	55.3	0.9	0.85	0.77	0.66	0.54	0.46	0.56	0.44
C	54.4	0.7	0.88	0.80	0.70	0.53	0.47	0.55	0.45
D	49.9	1.4	1.58	0.43	0.68	0.39	0.61	0.70	0.30
E	44.4	0.1	0.32	2.19	0.70	0.76	0.24	0.31	0.69
F	54.4	0.5	0.84	0.84	0.70	0.54	0.46	0.54	0.46
G	51.5	0.9	1.37	0.52	0.71	0.42	0.58	0.66	0.34
H	54.6	0.9	0.83	0.69	0.83	0.55	0.45	0.55	0.45
I[b]	41.8	3.9	2.44	0.34	0.83	0.29	0.71	0.75	0.25

[a] The samples correspond to those shown in Table III.

[b] The difficulty in measuring the very small absorption due to I-type methylene protons makes the calculated parameters for this sample less reliable.

TABLE V
Reactivity Ratios Calculated from Monomer Sequence Distribution Parameters

Sample	E, mol-%	E/VCl, in feed, mol/mol	r_1	r_2
A	38.5	2.11	0.22	2.86
B	51.0	3.90	0.22	3.02
C	51.0	3.90	0.22	3.13
D	64.3	7.68	0.20	3.31
E	29.3	1.62	0.20	3.55
F	50.0	3.90	0.21	3.27
G	60.9	5.52	0.25	2.86
H	50.0	3.90	0.21	3.25
I	72.0	10.70	0.23	3.63

By virtue of the derivation of run number, R (avg) = R (EV, VE). In order to include only data from the copolymer analysis in this table, we have listed the values of r_1F and r_2/F (where F is mole ratio E/V in feed). The parameters r_1F and r_2/F are directly calculable from sequence distribution data. F must be known in order to extract values of r_1 and r_2. The composition and feed data and individual reactivity ratios calculated from sequence distribution parameters are given in Table V. The Harwood-Ritchey plot relating run number, monomer feed ratios and reactivity ratios is shown in Figure 3. The slope of the straight line, r_1, equals 0.21 and the intercept, r_2, equals 3.2.

The reactivity ratios calculated from feed and composition data and from the monomer sequence distribution analysis are summarized in Table I. The deviations for the reactivity ratios determined from the integrated copolymerization equation were estimated from the Mayo-Lewis plot of r_1 versus r_2.[6] The values of the reactivity ratios and their standard deviations from the Fineman-Ross technique were calculated by least squares. The standard deviation σ in r_1r_2 is calculated as:

$$\sigma\ (r_1r_2) = r_1r_2 \left[\left(\frac{\sigma\ (r_1)}{r_1} \right)^2 + \left(\frac{\sigma\ (r_2)}{r_2} \right)^2 \right]^{1/2}$$

From microstructure analysis, the reported values of $\sigma(r_1r_2)$, $\sigma(r_1)$, and $\sigma(r_2)$ are the standard deviations from the mean of eight values. Based on the estimated errors in composition and in measuring the methylene areas, the error in r_1r_2 for each sample was calculated. The average value of this error was 0.12, similar to the standard deviation from the mean (0.11).

The errors in P_{EV}, P_{EE}, P_{VE}, and P_{VV} were also calculated from estimates of experimental errors. For example,

$$\Delta P_{VE} = P_{EV}\ [(\Delta R/R)^2 + (\Delta\%E/\%\ E)^2]^{1/2}$$

was derived from the formula $P_{EV} = R/2(\%E)$. The estimated error in the experimental value of mol per cent ethylene (i.e., $\Delta\%E$) is the average deviation of two to four measurements. ΔR was found as outlined

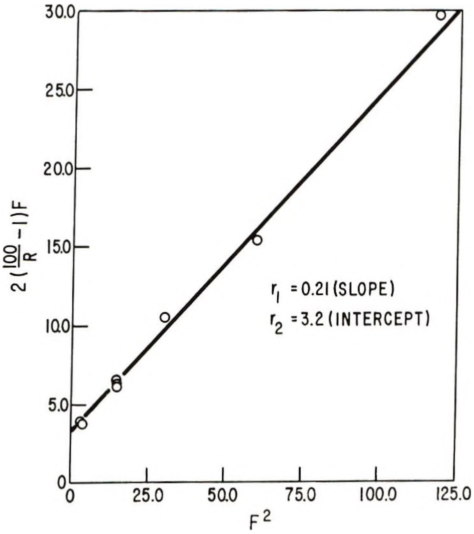

Fig. 3. Harwood-Ritchey plot: $2[(100/R) - 1] F = r_1F^2 + r_2$, where R = run number, F = moles E/moles VCl in feed.

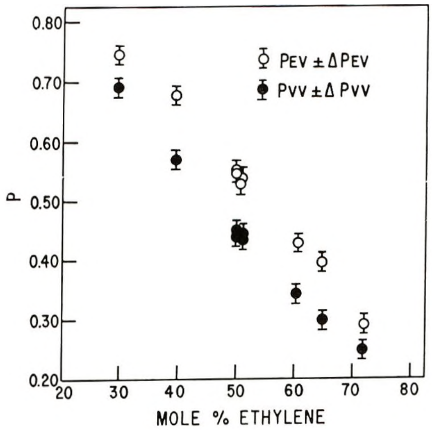

Fig. 4. Plot of P_{EV} and P_{VV} vs. mol-% ethylene.

above. This parameter reflects errors in measuring the NMR absorption areas for the I, α and $\beta >$ methylene protons as well as errors in composition. A plot of $P_{EV} \pm \Delta P_{EV}$ and $P_{VV} \pm \Delta P_{VV}$ versus mole per cent E is shown in Figure 4. Observe that, over the composition range from 29 to 72 mol-% ethylene, P_{EV} does not equal P_{VV}. If the copolymerization were independent of terminal monomer unit effects, P_{EV} would equal P_{VV}, and r_1r_2 ($r_e\ r_v$) would equal 1.0. Our results definitely show that these conditions are not met. The copolymerization is not random; rather, it follows first-order Markoffian statistics.

Determination of the monomer triad distribution would be necessary to study the penultimate effects described by second-order Markoffian statis-

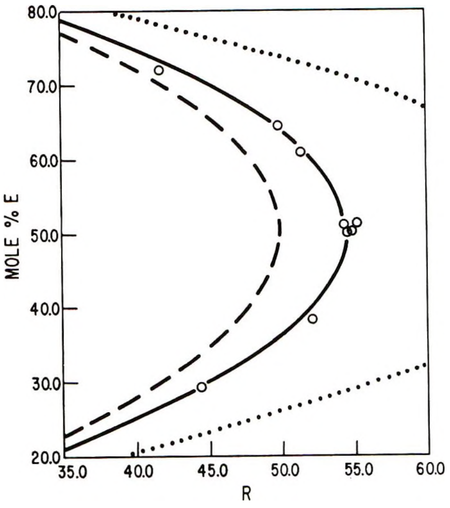

Fig. 5. Plot of mol-% ethylene in copolymer vs. run number: (○) observed for bulk E–VCl copolymers; (- -) calculated, $r_1r_2 = 1.0$; (——) calculated, $r_1r_2 = 0.7$; (. . .) calculated, $r_1r_2 = 0.1$.

tics. The excellent agreement we obtained between observed and calculated structure for first-order statistics precluded the more complex study. Schaefer's results[2] from such a study indicate that the copolymerization reaction is lower than second-order Markoffian.

The run number of a copolymer is a very descriptive structural parameter since from it (and composition) can be calculated all the other common structural parameters. We have plotted mol per cent E versus *R* (run number) for the bulk ethylene–vinyl chloride copolymers (Fig. 5). Theoretical curves for $r_1r_2 = 1.0$, 0.7, and 0.1 have been included to provide perspective. The observed points fall on the curve for $r_1r_2 = 0.7$, the reactivity ratio product determined from feed and product composition data. This vividly demonstrates that the structures observed by NMR analysis of the monomer diad distributions are indeed identical to those predicted by copolymerization theory.

As pointed out in the experimental section, the bulk copolymers were made at conversions as high as 16% (the average being 10–12%). For a feed consisting of 20 mol-% vinyl chloride, the instantaneous copolymer composition is calculated ($r_1 = 0.22$, $r_2 = 3.2$) as 48.9% vinyl chloride. At 10% conversion, the integrated copolymer composition is 46.7% and, at that point, the instantaneous copolymer composition is 44.4%. Thus, the maximum difference from the mean composition is approximately 2.2 mol-% vinyl chloride. The structural features observed by NMR (or infrared, x-ray, DTA, etc.) methods for this "average" copolymer should, in all likelihood, be experimentally indistinguishable from those of a "pure" copolymer of the same overall composition. To test this point, we performed the following experiment. Equal weights of two copolymers, of

51.0 and 64.3 mol-% ethylene, were dissolved in *o*-dichlorobenzene and the NMR spectrum was taken of the mixture. The percentages of I, α, and $\beta >$ methylenes and compositions for the two copolymers, in addition to the similar values calculated and observed for the mixture, are listed in Table VI. Within experimental error, the values observed for the mixture are equal to those calculated from the average of the two initial copolymers. Also listed in Table VI are the theoretical values calculated for a 57.5 mol-% ethylene copolymer for which $r_1r_2 = 0.7$. Thus, the structure of the average 57.7 mol-% E copolymer, in which % E deviates by ±6.6, is experimentally equivalent to that of a "pure" copolymer of the same composition. This range corresponds to a copolymer run to approximately 25% conversion. The close agreement was surprising, in view of the wide composition variation, and may be fortuitous. One should not assume that all other copolymers with such a wide variation in composition will yield similar results. When the composition in a copolymer is extremely inhomogeneous, one will observe features corresponding to blocks of both monomers. In the ethylene-vinyl chloride analysis, the I and $\beta >$ methylene areas and correspondingly the VV and EE pair concentrations would be too high for the given composition and reactivity ratio product. This is, in fact, a technique which can be developed to gauge the compositional heterogeneity of copolymers without fractionation and analysis of each fraction.

TABLE VI
NMR Analysis of Copolymer Mixture

Sample	E, mol-%	I, %	α, %	β, %
Copolymer 1 (0.1 g)	51.0	14.7	36.1	49.2
Copolymer 2 (0.1 g)	64.3	7.0	30.5	62.5
Mixture (0.2 g) (observed)	57.4	11.7	33.6	54.7
Mixture (0.2 g) (calculated)	57.7	10.9	33.3	55.9
Calculated ($r_1r_2 = 0.7$)	57.5	10.1	33.7	56.1

In a forthcoming paper,[6] we shall compare the microstructures of a series of bulk and emulsion ethylene-vinyl chloride copolymers which are predicted to be quite different from reactivity ratio data.

We gratefully acknowledge the assistance of A. Schreiber Di Caprio and E. J. Sehm in preparation of the ethylene-vinyl chloride copolymers.

References

1. T. D. Burkhart and N. L. Zutty, *J. Polym. Sci. A*, **1**, 1137 (1963).
2. J. Schaefer, *J. Phys. Chem.*, **70**, 1975 (1966).
3. H. J. Harwood and W. M. Ritchey, *J. Polym. Sci.*, **2**, 601 (1964).
4. F. R. Mayo and F. M. Lewis, *J. Amer. Chem. Soc.*, **66**, 1594 (1944).
5. M. Fineman and S. D. Ross, *J. Polym. Sci.*, **5**, 259 (1950).
6. C. E. Wilkes, R. H. Backderf, and J. C. Westfahl, in preparation.

Received March 18, 1968

JOURNAL OF POLYMER SCIENCE: PART A-1 VOL. 7, 35-46 (1969)

Synthesis, Reactivity, and Polymerization of Vinylureas

C. G. OVERBERGER,* G. MONTAUDO,† and S. ISHIDA,
Departments of Chemistry, Polytechnic Institute of Brooklyn, Brooklyn, New York 11201, and *The University of Michigan, Ann Arbor, Michigan 48104*

Synopsis

The syntheses of N,N'-divinylureas and some related compounds are reported. Polymerization of these monomers and determination of the structures of the resulting polymers are described. Evidence is presented which supports the tendency of vinylureas to react through their tautomeric form.

INTRODUCTION

N-Vinylureas (I, R = alkyl) are particularly interesting compounds because of their potential ability to form polymers with functional groups which would allow these polymers to undergo additional reactions that would result in structure modifications. Moreover, N,N'-divinylureas might cyclopolymerize to give polymers containing active hydrogen atoms.

N-Vinylureas were first synthesized by Jones and Mason[1] and have been studied during the last decade.[2,3] The synthesis of polymers derived from N-vinylureas has also been reported,[2] and the structure of these polymers was assumed to be only of the pendent type (II); no other structures were considered.

$CH_2{=}CH{-}NH{-}CO{-}NH{-}R$

I

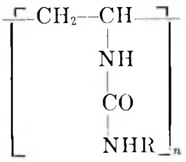

$$\left[\begin{array}{c} CH_2{-}CH \\ | \\ NH \\ | \\ CO \\ | \\ NHR \end{array}\right]_n$$

II

The possibility that these ureas can react either in their vinyl form (III) or in their tautomeric form (IV) has received

$$\underset{\text{III}}{{-}CO{-}NH{-}CH{=}CH_2} \rightleftharpoons \underset{\text{IV}}{{-}CO{-}N{=}CH{-}CH_3}$$

little consideration to date.

---

* Present address: The University of Michigan, Ann Arbor, Mich. 48104.

† On leave from the Institute of Industrial Chemistry, University of Catania, Italy.

We have obtained evidence that vinylureas react only through their tautomeric form (IV) under certain reaction conditions. This paper is concerned with the synthesis and polymerization of some *N*-vinyl- and *N*,*N'*-divinylureas. On the basis of experimental data, the structures of the isolated polymeric materials have been shown to be of type V rather than type II for the cases involving *N*-vinylureas. Furthermore, the data support structure V (R = vinyl) for the cases concerned with *N*,*N'*-divinylurea rather than structures II and VI.

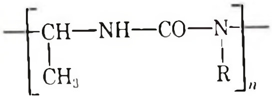

$$\left[-\underset{\displaystyle CH_3}{CH}-NH-CO-\underset{\displaystyle R}{N}-\right]_n$$

V

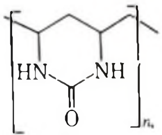

VI

RESULTS AND DISCUSSION

Evidence for Tautomerization

The vinylureas studied (Table I) were found to exist in the vinyl form (III) on the basis of NMR analysis. No tautomerization could be detected at room temperature. When the temperature was increased to 80–100°C, a considerable decrease in vinyl absorption occurred after 1 hr. Within 24 hr vinyl absorption disappeared completely and could not be regenerated on standing at room temperature. Molecular weight measurements of the materials isolated from the NMR tubes indicated that low molecular weight polymers had formed.

The preponderance of an electron distribution (VII), which contains a high electron density at the terminal carbon atom, was also indicated by the fact that hydrogens 1 and 2 (see Table I for numbering system) absorb at a relatively higher field than would have been anticipated. It is conceivable that electron distribution such as VII enhances the formation of tautomeric form IV which could not be detected but which would certainly account for the ease of hydrolysis of *N*-vinylureas to the corresponding aldehydes and ureas. This behavior would be similar to that of vinylamine, which tautomerizes easily.

$$-CO-NH-CH{=}CH_2 \leftrightarrow -CO-\overset{\oplus}{N}H{=}CH-\overset{\ominus}{C}H_2$$

VII

Other reactions leading to products which could be rationalized by the intermediacy of tautomeric forms were investigated. When *N*-vinyl-*N'*-ethylurea was heated with ethylurea, an addition product (VIII) was formed which could be accounted for by the following reaction sequence. The reaction was also found to be strongly acid catalyzed; the presence of small amounts of acid caused immediate reaction at room temperature. The structure of VIII was assigned on the basis of elemental analysis, molecular weight determination, and NMR analysis. The formation of

TABLE I

Chemical Shifts[a] and Spin Coupling Constants of Vinylureas in DMSO-d_6 at 30°C

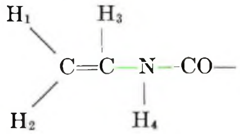	Chemical shifts, τ				Spin coupling constants, cps			
	H_1^b	H_2^b	H_3^c	H_4^b	J_{12}	J_{23}	J_{13}	J_{34}
N-Vinylurea	5.97	5.70	3.30	1.60	0.0	15.5	9.0	10.0
N-Vinyl-*N*′-ethylurea	6.02	5.75	3.26	1.70	0.0	16.0	9.0	11.0
N-Vinyl-*N*′,*N*′-diethylurea	6.03	5.48	3.35	1.65	0.0	16.0	9.0	10.0
N,*N*′-Divinylurea	6.05	5.73	3.56	1.65	0.0	14.0	8.5	10.2
N,*N*′-Di-*trans*-propenylurea	8.39[d]	5.15	3.53	1.97	7.0	15.0	1.5	11.0

[a] Measured from TMS internal standard, using a Varian A-60 analytical spectrometer.

[b] Doublet.

[c] Octet.

[d] Methyl group.

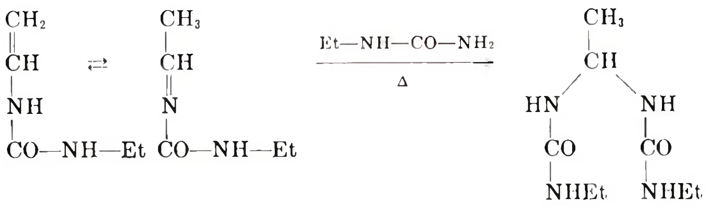
$$\mathrm{CH_2{=}CH{-}NH{-}CO{-}NH{-}Et} \rightleftarrows \mathrm{CH_3{-}CH{=}N{-}CO{-}NH{-}Et} \xrightarrow[\Delta]{\mathrm{Et{-}NH{-}CO{-}NH_2}} \mathrm{CH_3{-}CH(NH{-}CO{-}NHEt)_2}$$

VIII

isomeric compound IX was ruled out because an authentic sample of IX prepared by a separate route (see Experimental Section) exhibited different properties and spectra.

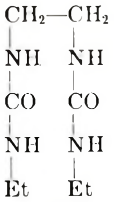
$$\mathrm{Et{-}NH{-}CO{-}NH{-}CH_2{-}CH_2{-}NH{-}CO{-}NH{-}Et}$$

IX

For the studies concerned with divinylureas, the intermediacy of a tautomeric form was strongly suggested by the results of the attempted preparation of one of the three desired divinylureas. While *N*,*N*′-divinylurea (X) and *N*,*N*′-di-*trans*-propenylurea (XI) could be prepared from the reactions of vinylisocyanate and *trans*-propenylisocyanate, respectively, with hexamethyldisilazane, the reaction of isopropenylisocyanate with hexamethyldisilazane failed to yield the expected *N*,*N*′-diisopropenylurea (XII). Instead, an *s*-triazine derivative (XIII) was obtained. The formation of

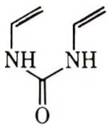
X

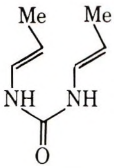

XI

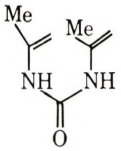

XII

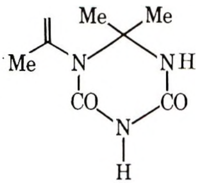

XIII

compound XIII can be accounted for by assuming that *N*,*N*′-diisopropenylbiuret (XIV) was formed first. *N*,*N*′-Disubstituted biurets[4–7] have been found to form in preference to *N*,*N*′-disubstituted ureas, depending on the structure of the isocyanate employed in the initial reaction with

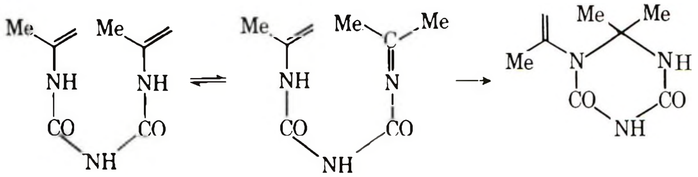

XIV XII

hexamethyldisilazane. Intermediate XIV could then cyclize to yield XIII via tautomerization and subsequent self-addition.

The structure of XIII was assigned on the basis of elemental analysis, molecular weight determination, and NMR analysis. The NMR spectrum possessed six peaks in the ratio of 6:3:1:1:1:1, the order being that of decreasing field strength. The two peaks at high field (τ = 8.56 and 8.13) were attributed to two kinds of methyl groups. The two peaks at low field (τ = 2.09 and 0.47), which disappear in deuterated water, were assigned to the amide hydrogens. The two middle peaks (τ = 5.07 and 4.79) were assigned to the vinylidene protons. These results appear to rule out a dimeric structure which was previously considered.[8]

Polymerization Results

Polymerization studies were undertaken for *N*-vinylurea, *N*-vinyl-*N'*-ethylurea, *N*-vinyl-*N,N'*-diethylurea and *N,N'*-divinylurea. Heating of *N*-vinylurea and *N*-vinyl-*N'*-ethylurea was sufficient to generate polymeric materials. Radical-initiated reactions and photopolymerization resulted in the same products. Acidic catalysis was effective for polymerization of *N*-vinylurea but not for *N*-vinyl-*N'*-ethylurea. For the polymers studied, NMR analysis supports the self-addition structure V rather than the pendent structure II. Studies of model compounds of each of these structures indicate that main chain methylene hydrogens should absorb at 8.1–8.5 τ, but the polymers obtained in this work exhibit peaks at 8.8–9.0 τ corresponding to three hydrogens. This observation is indicative of the presence of methyl groups and hence in favor of structure V.

Low molecular weight polymers (DP = 4–6) were formed in the cases studied. The NMR spectrum of the *N*-vinylurea polymer possesses four broad peaks at 8.8, 4.9, 4.2, and 3.5 τ in the ratio of approximately 3:1:1:2. The two peaks with the lowest τ values disappear in deuterated water and are assigned to the amide hydrogens. The NMR spectrum of the *N*-vinyl-*N'*-ethylurea polymer shows broad peaks at 9.0, 6.9, and 4.0 τ in the ratio of approximately 6:5:1.5.

The —C—CH_2—C— methylene hydrogens of a model compound (XV) (see Experimental Section) for the pendent structure (II) absorb at 8.45 τ. Compound VIII, a model for a structure of type VI,

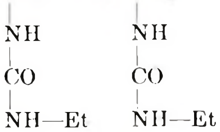

$$\begin{array}{lll} CH_2\text{—}CH_2\text{—}CH_2 \\ | & & | \\ NH & & NH \\ | & & | \\ CO & & CO \\ | & & | \\ NH\text{—}Et & & NH\text{—}Et \end{array}$$

XV

exhibits a —CH—CH_3 methyl peak doublet in its NMR spectrum at 8.75 τ. The latter result suggests a structure of type V, rather than II for the *N*-vinylurea polymer. The NMR peak intensities and chemical shifts for the *N*-vinylurea polymer are in agreement with those calculated for a polymer of DP = 4–5 with a structure of type V, assuming that the terminal vinyl group has been hydrolyzed. For the *N*-vinyl-*N*′-ethylurea polymer, the ratio of 6:2 for the two peaks at 9.0 and 6.9 τ is also in favor of structure V because a pendent structure should have exhibited a $-C-CH_2-C$-methylene peak at 8.4–8.5 τ.

N-Vinyl-*N*′,*N*′-diethylurea could not be polymerized by any of the methods employed. This result is comparable to the work of Hart,[2] who was unable to polymerize *N*-vinyl-*N*′,*N*′-methylphenyl-urea. It is quite possible that this is due to the fact that disubstitution on the nonvinylic nitrogen atom, while not affecting vinyl polymerization, inhibits the self-addition process leading to polymer of structure V.

In the case of *N*,*N*′-divinylurea, radical-initiated polymerization afforded insoluble polymers.[8] However, heating of *N*,*N*′-divinylurea resulted in soluble polymers which exhibited the same composition and infrared spectra as the insoluble polymers. Essentially the same soluble materials were obtained by acid catalyzed polymerization of *N*,*N*′-divinylurea. Molecular weights of these polymers are consistent with a DP of about 10. The NMR spectra of the thermally formed polymers possessed a very intense, broad peak at 8.9 τ and some residual vinyl absorption at lower τ values. Model compounds (XVII, XVIII) (see Experimental Section) for the cyclic structure (VI) exhibit $-C-CH_2-C-$ methylene absorptions at 8.30 and 8.10 τ, respectively. These results favor a self-addition polymer of structure V for the polymers mentioned above.

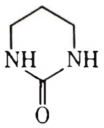
XVII

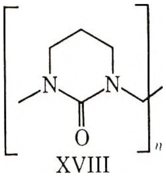
XVIII

However, there are some indications that the polymers obtained from the photopolymerization reactions of *N*,*N*′-divinylurea possessed partially cyclic structures. NMR spectra of these materials exhibited not only the peak at 8.9 τ observed for the thermally formed polymers but also a peak of almost equal intensity at 8.3 τ.

It is interesting to note that the polymer formed from the thermal polymerization of *N*,*N*′-divinylurea could also be obtained by hydrolyzing vinyl isocyanate in neutral media. Normally, the product of hydrolysis of an isocyanate in neutral media is a urea derivative, as indicated in the reaction sequence (1).

$$R{-}N{=}C{=}O \xrightarrow{H_2O} RNH{-}COOH \xrightarrow{-CO_2} RNH_2 \xrightarrow{R-N=C=O} RNH{-}CO{-}NHR \qquad (1)$$

However, *N*,*N*′-divinylurea was not isolated when vinyl isocyanate was hydrolyzed in this fashion. Instead, a white solid identical to the product obtained from the thermal polymerization of *N,N'*-divinylurea was formed. Failure to obtain *N,N'*-divinylurea by this route has been reported.[9,10] It appears plausible that *N,N'*-divinylurea is first formed during the hydrolysis reaction and then quickly polymerized by a water-catalyzed reaction.

EXPERIMENTAL SECTION

N-Vinylurea and *N*-Vinyl-*N'*-ethylurea

Both of these ureas were prepared by the method of Hart.[2]

N,N'-Divinylurea (X)

Vinyl isocyanate (0.21 mole) was added, with stirring, to a solution of hexamethyldisilazane (0.1 mole) in anhydrous tetrahydrofuran (100 ml), and the mixture was heated to gentle reflux for 4 hr. The solvent and volatile components were evaporated under vacuum at room temperature, and the remaining solid was dissolved in a mixture of benzene (200 ml) and methanol (5 ml). The colorless material which precipitated was filtered, washed with benzene, and dried (yield 65%). Recrystallization from ethyl acetate afforded the divinylurea which decomposed at 155–157°C. When no solvent was used for this reaction, the volatile components were evaporated under vacuum and trimethylsilylisocyanate was isolated in 80% yield. The infrared spectrum showed vinyl bands at 1665, 967, and 828 cm^{-1}; NMR in (DMSO-d_6) showed peaks at 1.65(1), 3.53(1), 5.73(1) and 6.05(1) τ; τ values from TMS as an internal standard and numbers in parenthesis refer to relative intensities (for all other NMR data as well).

ANAL. Calcd for $C_5H_8N_2O$: C, 53.56%; H, 7.19%; N, 24.99%. Found: C, 53.68%; H, 7.46%; N, 25.16%.

N,N'-Di-*trans*-propenylurea (XI)

trans-Propenylisocyanate (0.42 mole) was added, with stirring, to a solution of hexamethyldisilazane (0.2 mole) in benzene (200 ml), and the mixture was heated under reflux for 5 hr. The solvent and any volatile material were evaporated under vacuum at room temperature. The solid residue was dissolved in a mixture of benzene (250 ml) and methanol (10 ml). The methanolysis product was filtered, washed with benzene, and dried (yield 51.6%). Recrystallization from methanol gave a white solid which decomposed at 196–197°C. Infrared spectra showed vinyl bands at 1690 and 935 cm^{-1}. The NMR study (DMSO-d_6) gave peaks at 1.97(1), 3.53(1), 5.15(1) and 8.39(3) τ.

ANAL. Calcd for $C_7H_{12}N_2O$: C, 59.97%; H, 8.63%; N, 19.99%. Found: C, 60.05%; H, 8.62%; N, 19.90%.

2,4-Dioxo-5-isopropenyl-6,6-dimethylhexahydro-*s*-triazine (XIII)

Isopropenylisocyanate (0.5 mole) was added with stirring to a solution of hexamethyldisilazane (0.25 mole) in benzene (250 ml), and the mixture was refluxed for 6 hr. The solvent and any volatile material were evaporated under vacuum at room temperature; the residue was redissolved in a mixture of benzene (100 ml) and methanol (20 ml). The precipitated white solid was filtered, washed with ethyl acetate and dried (yield 30.4%). Recrystallization from tetrahydrofuran yielded a white solid which decomposed at 220°C. Infrared studies showed vinyl bands at 1650 and 915 cm^{-1}; NMR peaks (DMSO-d_6) were observed at 0.47(1), 2.09(1), 4.79(1), 5.07(1), 8.13(3), and 8.56(6) τ.

ANAL. Calcd for $C_8H_{13}N_3O$: C, 52.44%; H, 7.15%; N, 22.44%; molecular weight, 183. Found: C, 52.40%; H, 7.14%; N, 22.86%; molecular weight, 190 (acetone), 180 (methanol).

N-Vinyl-*N*,*N*′-diethylurea

Vinyl isocyanate (0.1 mole), dissolved in ethyl ether (200 ml), was slowly added to a stirred solution of diethylamine (0.1 mole) in ethyl ether (300 ml) at −30°C. The mixture was stirred for an additional hour at the same temperature. The white precipitate which formed was filtered, washed with ethyl ether and dried (yield 62%). Recrystallization from cyclohexane yielded needles, mp 76–77°C. Vinyl bands appeared in the infrared at 970 and 850 cm^{-1}; NMR (DMSO-d_6) peaks were at 1.65(1), 3.35(1), 5.48(1), 6.03(1), 6.70(4), and 8.95(6) τ.

ANAL. Calcd for $C_7H_{14}N_2O$: C, 59.13%; H, 9.92%; N, 19.70%. Found: C, 59.50%; H, 9.98%; N, 19.94%.

N-Ethylene-bis-*N*′-ethylurea (IX)

Ethyl isocyanate (0.2 mole), dissolved in ethyl ether (250 ml), was slowly added to a stirred solution of ethylenediamine (0.1 mole) in ethyl ether (300 ml) at −30°C. The mixture was stirred for an additional hour at the same temperature. The resulting white precipitate was filtered, washed with acetone, and dried (yield 95%). Recrystallization from methanol afforded a white solid, mp 219°C (lit.[11] 201°C). The infrared studies showed amide bands at 1625 and 1585 cm^{-1}; NMR peaks (DMSO-d_6) were at 4.02(2), 6.98(4), and 8.99(3) τ.

ANAL. Calcd for $C_8H_{18}N_4O_2$: C, 47.51%; H, 8.97%; N, 27.70%. Found: C, 47.62%; H, 8.85%; N, 27.54%.

N-Propyl-1,3-bis-*N*′-ethylurea (XV)

Ethyl isocyanate (0.2 mole), dissolved in ether (250 ml), was slowly added to a stirred solution of 1,3-diaminopropane (0.1 mole) in ethyl ether (300 ml) at −30°C. The mixture was allowed to reach room temperature, and the resulting white precipitate was filtered, washed with acetone and dried (yield 92%). Recrystallization from methanol gave a solid of mp 201°C. The infrared spectrum showed amide bands at 1610 and 1530 cm^{-1}; NMR studies (DMSO-d_6) showed peaks at 4.20(2), 6.90(4), 8.45(2), and 8.95(3) τ.

ANAL. Calcd for $C_9H_{20}N_4O_2$: C, 49.98%; H, 9.32%; N, 25.90%. Found: C, 49.62%; H, 9.12%; N, 26.15%.

N-Ethylidene-bis-*N*′-ethylideneurea (VIII)

N-Vinyl-*N*′-ethylurea (0.03 mole) and ethylurea (0.035 mole) were dissolved in benzene (10 ml), and the solution was heated at 80°C for 2 hr. The white precipitate which formed was filtered, washed with benzene, and dried (yield 81%). The material melted at 176°C after recrystallization from methanol–acetone. Infrared studies showed amide bands at 1635 and 1555 cm^{-1}; NMR (DMSO-d_6) peaks were at 3.99 (2, doublet), 4.91 (1, multiplet), 7.01 (4, multiplet), 8.75 (3, doublet) and 9.00 (6, triplet) τ.

ANAL. Calcd for $C_8H_{18}N_4O_2$: C, 47.51%; H, 8.97%; N, 27.71%; molecular weight, 202. Found: C, 47.50%; H, 9.15%; N, 27.91%; molecular weight, 198 (dimethylformamide).

The reaction was repeated with acetone as the solvent at 65°C. A white precipitate slowly formed; after 90 hr the reaction was stopped and VIII was recovered in 55% yield.

The addition of AIBN as radical initiator has no effect on the reaction. Addition of catalytic amounts of concentrated sulfuric acid to a solution of *N*-vinyl-*N*′-ethylurea and ethylurea in acetone at room temperature resulted in immediate formation of VIII which was recovered in 45% yield.

Poly(1-methylenetetrahydro-2-pyrimidinone) (XVIII)

Tetrahydro-2-pyrimidinone (0.025 mole) was added to an alkaline solution (pH 12) of trioxymethylene (0.05 mole) in water (10 ml). The mixture was stirred until the solid dissolved and then was neutralized to pH 7 by using 0.1*N* HCl. In this way an aqueous solution of 1,3-bishydroxymethyltetrahydro-2-pyrimidinone was obtained.[12] To this solution was added tetrahydro-2-pyrimidinone (0.025 mole), the pH was adjusted to 1 and gentle heating (45°C) was applied for 10 min. After cooling, the white solid which precipitated was filtered, washed with water and dried (yield 68%). After repeated dissolving in chloroform and reprecipitation with acetone, the product melted at 285–290°C. Infrared spectra showed an amide band at 1635 cm^{-1}; NMR peaks ($CDCl_3$) were at 5.00(2), 6.60(4) and 8.10(2) τ.

ANAL. Calcd for $(C_5H_8N_2O)_n$: C, 53.56%; H, 7.19%; N, 24.98%. Found: C, 52.39%; H, 7.14%; N, 24.64%; molecular weight, 2260 (chloroform).

Polymerization of *N*-Vinylurea

A solution of *N*-vinylurea (0.03 mole) in acetone was heated at 70°C for 36 hr in a sealed tube. The solvent was evaporated, the solid residue washed with ethyl ether, redissolved in acetone, filtered, and precipitated by cooling at Dry-Ice temperature (yield 58%), mp 167–170°C (dec.). Infrared spectra showed amide bands at 1650 and 1540 cm^{-1}; NMR (DMSO-d_6) peaks were at 3.50(2), 4.20(1), 4.90(1), and 8.80(3) τ.

ANAL. Calcd for $(C_3H_6N_2O)_n$: C, 41.85%; H, 7.02%; N, 32.54%. Found: C, 40.11%; H, 7.53%; N, 30.52%; molecular weight, 350 (dimethylformamide).

The reaction was repeated in the presence of AIBN (5 mg). A white precipitate formed, and after 3 hr the reaction was stopped. A solid material was obtained (33% yield) which was insoluble in methanol and acetone but soluble in water. It decomposed at 175°C. This material showed the same infrared spectrum as the material described above. With benzene as the solvent, yields were as high as 81%.

ANAL. Found: C, 48.31%; H, 7.06%; N, 28.06%.

Addition of catalytic amounts of concentrated H_2SO_4 (96.4%) to a solution of *N*-vinylurea in acetone at room temperature resulted in immediate formation of a product which was recovered in 40% yield. This compound was soluble in methanol and was shown to be identical with the product obtained from the thermal reaction.

In another experiment, a solution of *N*-vinylurea (0.2 mole) in methanol (50 ml) was irradiated with a Hg lamp (250 watts) for 48 hr at −20°C. After evaporation of the solvent, a white solid was recovered, redissolved in acetone, filtered, and precipitated by cooling at Dry-Ice temperature (yield 80%). This material decomposed at about 160°C and was found to be identical to the product obtained from the thermal reaction. The molecular weight was 455 (methanol).

Polymerization of *N*-Vinyl-*N′*-ethylurea

N-Vinyl-*N′*-ethylurea (0.02 mole) was dissolved in acetone (5 ml) and heated at 70°C for 24 hr in a sealed tube. A white solid formed, which was filtered, washed with ethyl ether, and dried (yield 62%). The product was dissolved in methanol, filtered, the solvent evaporated and the residue washed with ethyl ether. After drying, it decomposed at 160–165°C. The sample was then suspended in acetone, refluxed for several minutes and filtered while the solution was warm. The white product obtained had a decomposition point of 176–180°C. The infrared spectrum showed amide bands at 1640 and 1560 cm^{-1}; NMR (DMSO-d_6) peaks were at 4.00 (1.5), 6.90(2), and 9.00(6) τ.

ANAL. Calcd for $(C_5H_{10}N_2O)_n$: C, 52.61%; H, 8.83%; N, 24.54%. Found: C, 52.49%; H, 8.79%; N, 24.55%; molecular weight, 555 (methanol); $[\eta]$ = 0.08 dl/g (methanol, 25°C).

The reaction was repeated in the presence of AIBN (5 mg), and the same compound was recovered. If benzene was used as the solvent, yields increased to 95%. The molecular weight was 465 (methanol).

Photopolymerization of *N*-vinyl-*N′*-ethylurea at −20°C for 48 hr afforded the same material obtained from the thermal reaction.

N-Vinyl-*N′*-ethylurea was easily hydrolyzed by dissolving in water. Ethylurea and acetaldehyde were identified as the hydrolysis products.

Attempted Polymerization of *N*-Vinyl-*N'N'*-diethylurea

All attempts to polymerize *N*-vinyl-*N'*,*N'*-diethylurea by the same methods as those used for the other vinylureas failed.

Polymerization of *N*,*N'*-Divinylurea

N,*N'*-Divinylurea (0.05 mole) was dissolved in acetone (25 ml) and heated at 65°C for 30 hr. A white precipitate formed, was filtered, washed with acetone, and dried (yield 25%). The sample decomposed at 180–200°C and was soluble in methanol. The infrared spectrum showed amide bands at 1635 and 1540 cm^{-1}; NMR (DMSO-d_6) showed clearly only a very broad and intense peak at 8.90 τ; other, less defined peaks were downfield.

ANAL. Calcd for $(C_5H_8N_2O)_n$: C, 53.56%; H, 7.19%; N, 24.99%. Found: C, 49.74%; H, 7.74%; N, 25.05%; molecular weight, 1100 (methanol).

Radical-initiated polymerization (AIBN) resulted in insoluble materials (yield 52%) decomposing at 232–240°C. The infrared spectrum was identical to that of the material obtained by thermal polymerization.

ANAL. Found: C, 49.60%; H, 7.73%; N, 23.03%.

Other experiments carried out with different initiators (benzoyl peroxide, persulfate, γ-rays) or solvents (methanol, dimethylformamide, tetrahydrofuran) yielded essentially the same insoluble materials. Addition of catalytic amounts of concentrated H_2SO_4 (96.4%) to a solution of *N*,*N'*-divinylurea in acetone at room temperature resulted in immediate formation of a product which was recovered in 62% yield. This compound was soluble in methanol and was shown to be identical to the material obtained from the thermal reaction. When it was allowed to stand under vacuum overnight in the presence of P_2O_5, it became insoluble in methanol.

Photopolymerization of *N*,*N'*-divinylurea in tetrahydrofuran ($1:10^3$) at -20°C for 48 hr afforded in 15% yield a material with mp 170°C (dec.). This solid gave the same elemental analysis and infrared spectrum as the products obtained from the thermal reaction, but the NMR spectrum (DMSO-d_6) showed two peaks at 8.30 and 8.90 τ.

Hydrolysis of Vinyl Isocyanate

Vinyl isocyanate cooled to Dry-Ice temperature was injected in a 100 ml flask stoppered with a serum cap, and a calculated amount of water was then injected. The water immediately solidified and the mixture was allowed to reach room temperature in 2 hr, after which time a steady reaction was observed. A white solid product was formed and some gas was evolved. Any liquid remaining was then removed under vacuum at room temperature, and the solid material obtained was found to decompose at 85°C with gas evolution. After drying under vacuum overnight at 65°C, the decomposition point was raised to 180°C.

ANAL. Found: C, 48.14%; H, 7.27%; N, 24.56%; molecular weight, 403 (methanol).

The material was washed twice with boiling acetone, dissolved in methanol, and filtered to remove impurities; the remaining solid after being dried under vacuum at 65°C exhibited a mp of 178–181°C (dec.). Infrared spectra showed amide bands at 1635 and 1540 cm^{-1}; the NMR (DMSO-d_6) spectrum was identical to that obtained from the thermal polymerization products of *N*,*N*′-divinylurea.

ANAL. Found: C, 48.23%; H, 7.69%; N, 22.01%.

The above experiments were carried out using the following proportions of vinyl isocyanate to water: 5:1, 1:1, and 1:5. Yields, based on vinyl isocyanate, were in all cases about 60%, and the products obtained in all experiments were identical.

Acidic hydrolysis of vinyl isocyanate affords a mixture of acetaldehyde, ammonia, and carbon dioxide.[2]

Thermal polymerization of vinyl isocyanate is known to yield only insoluble material.[13]

A fellowship of the Italian National Council of Research to G. Montaudo for the academic year 1966–67, is gratefully acknowledged.

This paper comprises a portion of the dissertation submitted by S. Ishida in partial fulfillment of the requirements for the degree of Doctor of Philosophy at the Polytechnic Institute of Brooklyn.

References

1. L. W. Jones and J. P. Mason, *J. Amer. Chem. Soc.*, **49**, 2528 (1927).
2. R. Hart, *Bull. Soc. Chim. Belg.*, **66**, 229 (1957).
3. M. Sato, *J. Org. Chem.*, **26**, 770 (1961).
4. U. Wannagut, H. Burger, C. Kruger, and J. Pump, *Z. Anorg. Chem.*, **321**, 208 (1963).
5. W. Fink, *Ber.*, **97**, 1433 (1964).
6. G. Ortel, H. Malz, H. Holtzschmidt, and E. Degener, German Pat. 1,154,475 (1963).
7. J. F. Klebe, J. B. Bunsh, and J. E. Lyons, *J. Amer. Chem. Soc.*, **86**, 4400 (1964).
8. C. G. Overberger and S. Ishida, *J. Polym. Sci. B*, **3**, 789 (1965).
9. G. Welzel, Ph.D. Dissertation, Freiburg (1960).
10. A. Crashaw, personal communication.
11. J. Volhard, *Ann.*, **119**, 357 (1867).
12. R. L. Wayland, U. S. Pat. 3,158,501 (1964).
13. C. G. Overberger, S. Osaki, and H. Mukamal, *J. Polym. Sci. B*, **2**, 627 (1964).

Received March 20, 1968

JOURNAL OF POLYMER SCIENCE: PART A-1 VOL. 7, 47–54 (1969)

Studies in Some New Initiator Systems for Vinyl Polymerization. III. Amine–Halogen Systems as Redox Initiators

DINABANDHU PRAMANICK and SANTI R. PALIT,
Department of Physical Chemistry, Indian Association for the Cultivation of Science, Jadavpur, Calcutta, India

Synopsis

Amine–halogen redox systems are very efficient initiators of polymerization of a number of vinyl monomers in benzene media and are rather inefficient initiators in aqueous media. A large number of aliphatic amines and a few aromatic amines have been used. Among the halogens, chlorine and bromine are very effective. Iodine initiates with a few amines only. Endgroups incorporated are halogen and amine totalling an average of nearly one per chain in the case of polymerization in benzene media and 0.5–0.7 per chain in polymerization in aqueous media. In the light of endgroup results, a mechanism of initiation through halogen and amine radicals has been suggested.

INTRODUCTION

Although amines are in many cases retarders or even inhibitors[1] of polymerization, they have been used several times as activators in redox vinyl polymerization[2,3] and in dye-sensitized photopolymerization.[4,5] Our search for new initiators[6] revealed that amines are also capable of forming very efficient redox initiators in conjunction with halogen. The present paper deals with polymerization by halogen–amine initiator with particular reference to endgroups.

EXPERIMENTAL

Materials

Purified methyl methacrylate (MMA) and other mononers were used. Br_2 reagent was prepared by dissolving liquid Br_2 (E. Merck) in distilled benzene and Cl_2 reagent by bubbling the dried gas in the same solvent. A dilute solution of I_2 in benzene served as the I_2 reagent. Aqueous chlorine, bromine, and iodine were prepared as described previously.[7] Strength was determined in each case iodometrically. The amines used were all analytical reagent-grade reagents.

Polymerization Procedure

Polymerization in benzene medium was carried out in Pyrex ampules sealed under vacuum and allowed to continue for 3 hr at 60°C. Aqueous polymerization was carried out as before,[7] and the polymers purified in the usual way[8] and then dried under vacuum.

Endgroup Analysis

The purified polymers, after proper treatment, were subjected to the appropriate dye-partition test for the expected amine[9,10] and halogen[11] endgroups and also for the hydroxyl[12] endgroup for the polymers prepared in aqueous media. Optical density measurement was carried out spectrophotometrically and halogen endgroups determined by the method of difference as before.[7]

Molecular Weight Determination

Number-average molecular weight of the poly-MMA samples was determined viscometrically in benzene solution at 35 ± 0.1°C with the help of the equation:[13]

$$\bar{M}_n = 2.81 \times 10^5 [\eta]^{1.32}$$

RESULTS

General Features and Relative Efficiencies

Benzene Medium. A large number of amines, both aliphatic and aromatic, were employed with halogens (Cl_2, Br_2, and I_2) to initiate the poly-

TABLE I
Initiator Systems Involving Halogens in Combination with Various Amines for the Polymerization of MMA in Benzene under Vacuum[a]

	Chlorine			Bromine			Iodine		
Amine	Induction period, min	Yield in 3 hr, %	[η]	Induction period, min	Yield in 3 hr, %	[η]	Induction period, min	Yield in 3 hr, %	[η]
Dimethylamine	b	—	—	b	—	—	b	—	—
n-Propylamine	b	—	—	b	—	—	b	—	—
n-Butylamine	120	51	1.05	145	20	0.88	b	—	—
Methylbutylamine	112	57	—	130	31	—	b	—	—
tert-Butylamine	200	55	0.89	185	33	0.73	b	—	—
n-Hexylamine	110	56	0.77	130	23	0.42	b	—	—
Di-*n*-heptylamine	110	58	—	150	26	—	b	—	—
n-Dodecylamine	50	63	0.72	60	40	0.51	b	—	—
Dodecyldimethylamine	40	65	0.70	45	42	0.52	b	—	—
Cetyldimethylamine	36	66	0.82	56	41	0.65	240	7	1.76
Ethylenediamine	50	60	1.98	65	62	2.15	280	11	2.32
Hexamethylenetetramine	200	15	—	b	—	—	b	—	—
Dimethylaniline	90	58	1.46	110	60	1.52	280	8	1.80
Diphenylamine	160	12	—	200	7	—	b	—	—

[a] Conditions: [MMA] = 5.58M; [Halogen] = 1 × $10^{-4}M$; [Amine] = 1 × $10^{-2}M$; 60°C.

[b] No initiation.

merization of MMA in benzene medium. Table I compares the initiating efficiences and the polymerization rate. The induction period decreases roughly in the order *n*-butyl- > *n*-hexyl- > *n*-dodecyl- > dodecyldimethylamine. The per cent conversion also follows a more or less regular relationship: dodecyldimethyl- > *n*-dodecyl- > *n*-hexyl- > *n*-butylamine. Amines lower than butylamine cannot initiate the polymerization, as also is the case with aniline and pyridine. Dimethylaniline, however, forms an efficient initiator. Diphenylamine is only slightly active, presumably because of steric factors and its very weak basicity.

Compared with Br_2 initiation, Cl_2 initiation in most cases is associated with a slightly shorter induction period and higher yield of polymer having comparatively higher $[\eta]$. I_2 fails to initiate except in three systems, where it acts only as a poor initiator. This fact is important in view of the strong inhibitive property of I_2.

Aqueous Medium. Amine–halogen combinations can initiate polymerization also in aqueous phase, but with much less efficiency as shown in Table II. In aqueous solution iodine does not initiate, probably due to its inhibitive property. However, it has been shown earlier[6] that the Fe^{+2}–I_2 system is a good initiator in aqueous phase incorporating about 0.5 iodine endgroup per polymer chain.

TABLE II
Initiator Systems Involving Halogens in Combination with Various Amines for the Aqueous Polymerization of MMA under Nitrogen[a]

	Chlorine			Bromine		
Amine	Induction period, min	Yield in 3 hr, %	$[\eta]$	Induction period, min	Yield in 3 hr, %	$[\eta]$
Diethylamine	180	11	1.78	b	—	—
Triethylamine	156	15	—	b	—	—
n-Butylamine	60	30	1.80	85	8	0.82
n-Hexylamine	70	28	1.48	104	12	0.81
n-Dodecylamine	66	26	1.22	72	15	0.71

[a] Conditions: [MMA] = $0.094M$; [Halogen] = $1 \times 10^{-3}M$; [Amine] = $1 \times 10^{-3}M$; 25–30°C.

[b] No initiation.

Monomer Selectivity

Amine–halogen initiators were found very effective for the polymerization of MMA and ethyl methacrylate in benzene and to some extent in aqueous media. But in case of styrene, only *n*-dodecylamine and di-*n*-heptylamine in combination with Cl_2 or Br_2 could act as initiator in benzene, the yield of polymer being very low. The ethylenediamine–Br_2 system alone was able to initiate the polymerization of vinyl acetate in benzene medium. The product, obtained in low yield, was a semi solid polymer.

Endgroup Analysis

For endgroup analysis some suitable and typical initiator systems were selected, and the endgroup results of the polymers obtained are shown in Tables III and IV, respectively, for polymerization in benzene and in aqueous media. Depending upon the initiator concentrations, fair to good re-

TABLE III
Endgroup Results of PMMA Obtained by Initiation with Amine–Halogen Initiators in Benzene Media[a]

Halogen	[Halogen], $M \times 10^4$	Amine	[Amine], M	$[\eta]$	Endgroup per chain Amine	Halogen	Total
Chlorine	1.371	Dodecylamine	0.051	0.59	0.61	0.43	1.04
	1.371		0.182	0.43	0.66	0.32	0.98
	1.371		0.399	0.34	0.67	0.27	0.94
	2.592		0.182	0.38	0.64	0.34	0.98
	4.004		0.182	0.36	0.63	0.41	1.04
	6.655		0.182	0.33	0.59	0.45	1.04
Bromine	6.23	Dodecylamine	0.049	0.42	0.60	0.52	1.12
	6.23		0.167	0.40	0.69	0.45	1.14
	31.15		0.167	0.27	0.58	0.49	1.07
Chlorine	1.371	*n*-Hexylamine	0.057	0.63	0.52	0.56	1.08
	1.371		0.201	0.49	0.58	0.44	1.02
	6.655		0.201	0.33	0.44	0.42	0.86
Bromine	8.98	*n*-Butylamine	0.132	0.66	0.45	0.63	1.08
	8.98		0.514	0.44	0.48	0.41	0.89
Chlorine	1.371	Cetyldimethylamine	0.084	0.73	0.73	0.42	1.15
	1.371		0.320	0.51	0.79	0.28	1.07
Bromine	8.98	Ethylenediamine	0.260	1.75	1.82	0.31	2.13
	8.98		0.435	1.47	1.96	0.28	2.24
	8.98		1.392	1.24	2.03	0.19	2.22
Bromine	8.98	Dimethylaniline	0.089	1.09	—	0.29	0.29
	8.98		0.241	0.71	—	0.16	0.16
	8.98		0.358	0.59	—	0.25	0.25

[a] Conditions: [MMA] = 5.58M; 60°C.

TABLE IV
Endgroup Results of PMMA Obtained by Initiation with *n*-Butylamine–Chlorine Initiator System in Aqueous Phase[a]

[*n*-Butylamine], $M \times 10^3$	[Chlorine], $M \times 10^3$	$[\eta]$	Endgroup, per chain Amine	Halogen	Total
2.630	1.327	1.71	0.27	0.21	0.48
2.630	2.654	1.53	0.31	0.27	0.58
2.630	3.981	1.29	0.32	0.30	0.62
2.630	6.635	0.98	0.39	0.32	0.71
5.260	2.654	1.31	0.28	0.26	0.54
10.520	2.654	0.92	0.26	0.28	0.54

[a] Conditions: [MMA] = 0.094M; 25–30°C.

sponse to the dye-partition test for amine and halogen endgroups was exhibited by all of the polymer samples.

In case of polymerization in benzene (Table III), for any system, say *n*-dodecylamine–Cl_2, it is seen that at a fixed Cl_2 concentration ($1.37 \times 10^{-4}M$) the amine endgroup content per chain increases very slightly from 0.61 to 0.67 with increase in amine concentration. Again, at a fixed amine concentration ($0.182M$), chlorine incorporation increases from 0.32 to 0.45 per chain with increasing Cl_2 concentration. The total average endgroup per chain is in the vicinity of unity in almost all cases. With Br_2 as the halogen, the result practically remains unaltered, the only change being that halogen incorporation is slightly higher and the molecular weight of the polymer is somewhat less.

Again as one goes from *n*-dodecylamine to *n*-hexylamine and down to *n*-butylamine, it is seen that amine incorporation per polymer molecule is lowered from 0.7 to 0.4. On the other hand, the order of the amines remaining the same, the intrinsic viscosity of the resulting polymer samples exhibits a tendency to increase.

As to the substituted amines, cetyldimethylamine incorporates a slightly higher amount of amine endgroups per chain (0.79) compared with *n*-dodecylamine (0.66). In case of ethylenediamine, about 1.8–2.0 amino endgroups per chain are incorporated, and the intrinsic viscosity of the resulting polymers is comparatively higher. On the other hand, polymer obtained by initiation with dimethylaniline–Br_2 system did not respond to the dye test for amino endgroup. This is not unexpected, because polymers containing an aromatic amine endgroup do not, in general, give a color with disulfine blue[9,10] dye reagent. So in this case, detection and estimation of amino endgroups in the polymer could not be carried out by the dye test. Only the halogen endgroup (0.16 to 0.29 per chain) has been detected and estimated.

In the case of polymerization in aqueous media (Table IV) the amino endgroup incorporation was somewhat less, between 0.27–0.39 per chain, and increased with increasing chlorine concentration. Halogen endgroups were incorporated to the extent of 0.21–0.32 per chain and increased with increasing amine incorporation. The polymer samples were subjected to the dye test for hydroxyl[12] endgroups, but no positive response was found. The average total endgroup per chain was always found in the region of 0.5–0.7.

DISCUSSION

Mechanism

Complete inhibition of polymerization by hydroquinone and DPPH and the linear relationship between $1/\bar{M}_n$ and square root of initiator (chlorine) concentration (Fig. 1) clearly indicates the radical nature of the polymerization reaction.

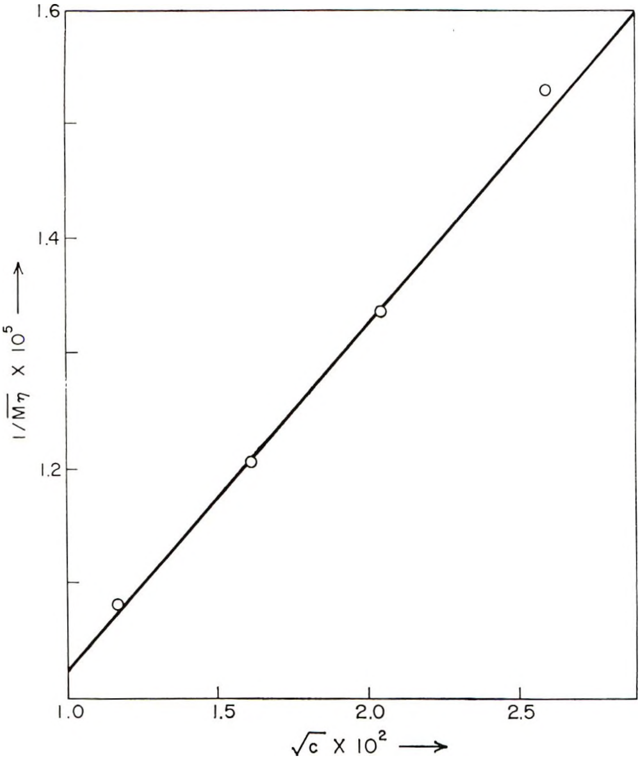

Fig. 1. Reciprocal of $\overline{M}_n$ vs. square root of chlorine concentration in dodecylamine–chlorine-initiated polymerization of MMA. [MMA] = 5.58M; Amine = 0.182M.

Earlier Fueno and co-workers[14] observed that either a binary mixture of $C_6H_5N(CH_3)_2$ and $C_6H_5CH_2Cl$ or the corresponding quaternary salt could polymerize MMA and suggested the generation of initiating radicals by decomposition of the quaternary salt. Saxena[15] detected halogen end-groups in PMMA prepared by aqueous initiation with quaternary ammonium halide in the presence of sunlight. It appears likely that quaternary ammonium compounds in aqueous and nonaqueous media are capable of producing initiating free radicals by some type of self-decomposition.

Recently, formation of a quaternary compound as an intermediate in the halogen–tertiary amine reaction has been demonstrated by the work of Bhome and Krause,[16] who were able to isolate chlorotrimethylammonium chloride, in the reaction of chlorine and trimethylamine in CCl_4 solution [eq. (1)].

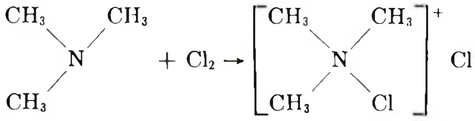

(1)

Considering the above facts, it seems plausible that all the three classes of amines, primary, secondary, and tertiary, react with halogens to produce an intermediate quaternary ammonium derivative through a nucleophilic displacement on the halogen by the amine [eq. (2)].

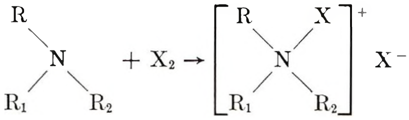

(2)

The intermediate decomposes as shown in eq. (3) to generate the initiating ammonium and halogen radicals.

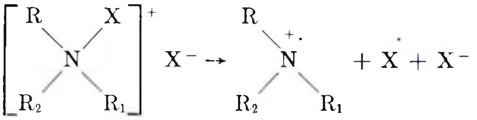

(3)

Such decomposition of *N*-haloammonium salts is well-known.[17,18] In fact, the free-radical addition of *N*-haloammonium compounds to substituted olefins (under nitrogen atmosphere and at ambient temperature) has proved a potential synthetic route to prepare halogenated amines from substituted olefins.[19] A further example of quaternary nitrogen compounds producing $^+\dot{N}R_3$ ion radicals on decomposition is found in the quaternary hydroxylamine derivative postulated to be an intermediate, e.g., the reaction of benzoyl peroxide and dimethylaniline.[20]

Amine Endgroups

The extent of amine incorporation is found to increase with increasing chain length of the amine. The higher incorporation of amine endgroups with ethylenediamine probably occurs because the initiator fragment contains two amino groups.

The fate of the dimethylaniline radical, i.e., whether incorporated or not, could not be determined by the dye test. Earlier, Imoto[21] failed to detect any amine fragment in the polymer initiated by the benzoyl peroxide–dimethylaniline system and concluded that only benzoate radicals acted as initiators, whereas the dimethylaniline radicals (stabilized by resonance) would favor their recombination. But since only 0.3 halogen endgroup per chain has been found, it appears that dimethylaniline radicals have probably been incorporated in the polymer, though no conclusive experimental evidence was obtained.

Halogen Endgroups

The amount of bromine incorporation in the polymer is always somewhat higher than that of chlorine, and it is accompanied by a decrease in yield and $[\eta]$. This is probably attributable to the occurrence of some substitution, addition as well as termination by bromine radical may be taking place.[7] Incorporation of iodine endgroups could not be tested because of the very low yield of polymer produced by I_2–amine initiator.

In almost all cases the average total endgroups incorporated is about one per chain which once more indicates that termination of poly(methyl methacrylate) radicals in a homogeneous medium takes place mostly by disproportionation.

In aqueous polymerization initiated by the *n*-butylamine–Cl_2 system, both amine and halogen incorporation is comparatively less than in nonaqueous polymerization, and the total endgroups per chain is 0.5–0.7 (Table IV). Besides, the polymers did not contain any hydroxyl endgroups, although in most aqueous polymerizations hydroxyl endgroups are generally present. These experimental results are in agreement with our previous observation[7] on ammonia–halogen initiator in aqueous phase.

One of the authors (D.P.) wishes to acknowledge gratefulness to the Government of India for affording him of a Man-power Fellowship during the tenure of the present work.

References

1. W. R. Yates and J. L. Ihrig, *J. Amer. Chem. Soc.*, **87**, 711 (1965).
2. V. H. Longemann and W. Becker, *Makromol. Chem.*, **3**, 49 (1949).
3. L. Horner, *Angew. Chem.*, **61**, 411 (1949).
4. G. K. Oster, G. Oster, and G. Prati, *J. Amer. Chem. Soc.*, **79**, 595 (1957).
5. N. Uri, *J. Amer. Chem. Soc.*, **74**, 5808 (1952).
6. M. K. Saha, M. Sen, and D. Pramanick, *J. Polym. Sci., A-1*, **4**, 2137 (1966).
7. D. Pramanick and S. R. Palit, *J. Polym. Sci.*, in press,
8. S. R. Palit and P. Ghosh, *J. Polym. Sci.*, **58**, 1225 (1962).
9. S. Maiti and M. K. Saha, *Sci. Culture*, **32**, 242 (1966).
10. S. Maiti and M. K. Saha, *J. Polym. Sci. A-1*, **5**, 151 (1967).
11. M. K. Saha, P. Ghosh, and S. R. Palit, *J. Polym. Sci. A*, **2**, 1365 (1964).
12. P. Ghosh, P. K. Sengupta, and A. Pramanick, *J. Polym. Sci. A*, **3**, 1725 (1965).
13. J. H. Baxendale, S. Bywater, and M. G. Evans, *J. Polym. Sci.*, **1**, 237 (1946).
14. T. Fueno, T. Tsuruta, and J. Furukawa, *J. Polym. Sci.*, **15**, 594 (1955).
15. G. K. Saxena, *Sci. Culture*, **31**, 483 (1965).
16. H. Bhome and W. Krause, *Chem. Ber.*, **84**, 170 (1951).
17. M. E. Wolff, *Chem. Rev.*, **63**, 55 (1963).
18. R. S. Neale and R. L. Hinman, *J. Amer. Chem. Soc.*, **85**, 2666 (1963).
19. R. S. Neale, *Tetrahedron Letters*, **1966**, 483.
20. G. Walling and N. Indictor, *J. Amer. Chem. Soc.*, **80**, 5814 (1958).
21. M. Imoto, T. Otsu, and K. Kimura, *J. Polym. Sci.*, **15**, 475 (1955).

Received March 25, 1968

JOURNAL OF POLYMER SCIENCE: PART A-1 VOL. 7, 55–72 (1969)

Triptycene Polymers

E. HOFFMEISTER,* J. E. KROPP,† T. L. McDOWELL,‡
R. H. MICHEL and W. L. RIPPIE,** *Yerkes Research and Development Laboratory, E. I. du Pont de Nemours & Company, Film Department, Buffalo, New York 14207*

Synopsis

New, bifunctional, bridgehead-substituted triptycenes were synthesized and used to prepare a series of triptycene polymers, including polyesters, polyamides, polyurethanes, and a polyoxadiazole. Certain of these partially aliphatic polymers were thermally stable. Clear and colorless films were obtained in some instances.

INTRODUCTION

Many oxidation- and heat-stable polymers are highly conjugated aromatic structures.[1] These are frequently colored. By interrupting the conjugation with stable aliphatic units such as 9,10-triptycyl groups,[2] it should be possible to obtain colorless, thermally stable polymers. Consequently bifunctional, bridgehead-substituted triptycenes (R-Tr-R, I) were synthesized by the benzyne–anthracene route[3] and a wide variety of polymers prepared from them (Table I).

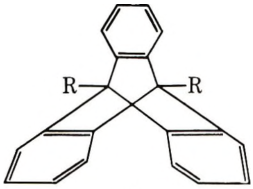

I

Ia, R = CH_2OH
Ib, R = CH_2CH_2OH
Ic, R = CH_2OCOCl
Id, R = $COCl$
Ie, R = $COOCH_3$
If, R = $CONHNH_2$
Ig, R = $COOH$
Ih, R = NH_2
Ii, R = NCO
Ij, R = $CH_2COOCH_2CH_3$

---

* Present address: Eastman Kodak Co., Rochester, N. Y.
** Present address: Joseph Seagram & Sons, Louisville, Ky.
† Present address: 3M Co, St. Paul, Minn.
‡ Present address: Iowa State University, Ames, Iowa.

TABLE I
Polymer Properties

Polymer	Structure	η_{inh}	PMT, °C[a]	Thermogravimetric analysis Decomposition Temp, °C[b] In air	Thermogravimetric analysis Decomposition Temp, °C[b] In N$_2$
II	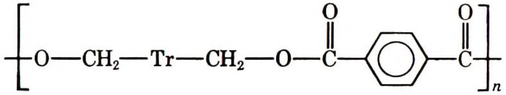	0.1[c]	350–380	420	
III	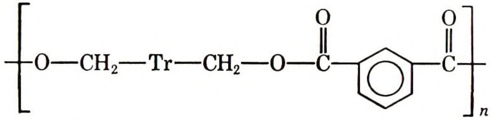	0.1[c] 0.2 0.51	270 370 370	 460 430	 465
IV	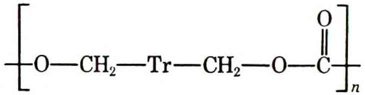 $\left[\mathrm{O{-}CH_2{-}Tr{-}CH_2{-}O{-}\overset{O}{\overset{\|}{C}}}\right]_n$	0.28[c]	385	440	
V	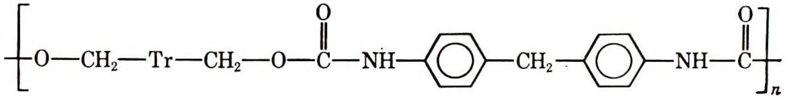	0.46[d] 0.59	 320	310	
VI	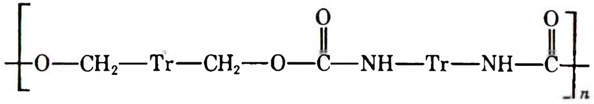 $\left[\mathrm{O{-}CH_2{-}Tr{-}CH_2{-}O{-}\overset{O}{\overset{\|}{C}}{-}NH{-}Tr{-}NH{-}\overset{O}{\overset{\|}{C}}}\right]_n$	0.09[e]	311		

VII	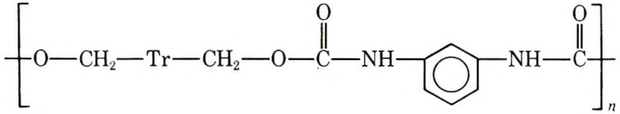	0.47[d]	320	350	
VIII	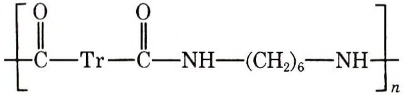	1.13[f]		365	
IX	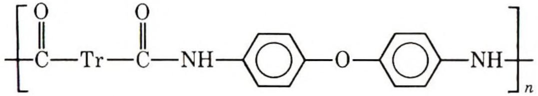	1.63[f]	>500	440	445
X	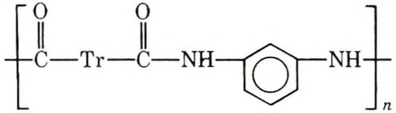	0.94[f]	>500	385	
XI	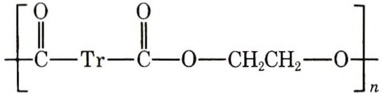	0.05[f]			
XII	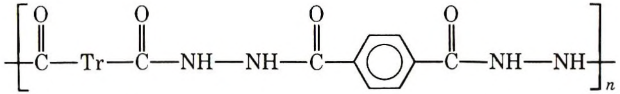	1.27[g]	>500	430	
XIII	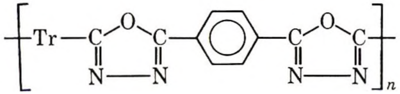	Intractable	>500	440	408

TABLE I *continued*
Polymer Properties

Polymer	Structure	η_{inh}	PMT, °C[a]	Thermogravimetric analysis Decomposition Temp, °C[b] In air	In N_2
XIV	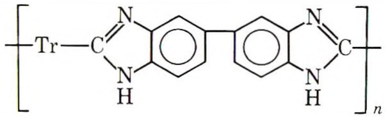	Intractable	>500		
XV	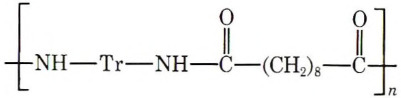 $\left[NH—Tr—NH—\overset{O}{\overset{\|}{C}}—(CH_2)_8—\overset{O}{\overset{\|}{C}} \right]_n$	0.08[e]	140		
XVI	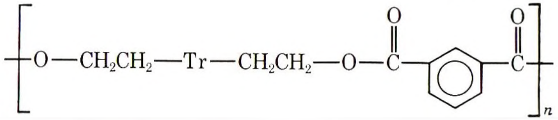	0.1[c]	220–225	370	

---

[a] Polymer melt temperature is the temperature at which a piece of polymer leaves a molten trail on a heated block (stick temperature) or a powder becomes clearly liquid.

[b] 10% weight loss, heating rate 6°C/min.

[c] 0.5% in nitrobenzene at 30°C.

[d] 0.5% in s-tetrachloroethane at 30°C.

[e] In dimethylacetamide at 30°C.

[f] 0.5% in methane sulfonic acid at 30°C.

[g] 0.5% solution in 4% lithium chloride, 3:7 pyridine/hexamethylphosphoramide.

Only the polyesters and polyurethanes of Ia and the polyamides of Id were obtained in moderate to high molecular weight. The polyesters and polyamides were thermally stable and colorless.

DISCUSSION

Polymers from 9,10-Bis(hydroxymethyl)triptycene (Ia)

Melt polyesterification was first carried out with the diol Ia and diphenyl terephthalate. This polymer (II) solidified at 350–380°C at an inherent viscosity of ~0.1 (see Table I for viscosity solvents), which made it impossible to obtain high polymer by melt condensation. When diphenyl isophthalate was used in place of terephthalate, the stick temperature of the polyester (III) was 270°C at an inherent viscosity of 0.1, and melt condensation could be carried to a higher molecular weight. The highest inherent viscosity obtained was 0.51. The stick temperature of this polymer was 370°C.

The polycarbonate IV was prepared from diol Ia and diphenyl carbonate by essentially the same melt techniques used for the isophthalate. This polymerization also gave a very high melting polymer at relatively low inherent viscosities (stick temperature of 380°C at $\eta = 0.28$).

The condensation of diol Ia with diisocyanates was very slow, even when the reactive methylenebis(4-phenyl isocyanate) was used. While ethylene glycol gave high polymer with this diisocyanate in less than 2 hr at 115°C,[4] the above dihydroxy compound (Ia) yielded low polymer ($\eta = 0.23$) after 2 days at ~145°C and moderate polymer ($\eta = 0.41$) after 4 days at this temperature. Dibutyltin dilaurate and Dabco(triethylenediamine) had only a small catalytic effect, probably because catalysis involves crowding of the transition state by complexation of the dihydroxy compound.[5] However, *n*-butyllithium reduced the time required to form high polymer to less than 1 hr because it converts hydroxyls to the more reactive, less bulky alkoxide ions. There was some indication that prolonged reaction times with butyllithium, as well as excessive quantities of catalyst, resulted in product degradation.

1,3-Phenylene diisocyanate and 2,4-tolyl diisocyanate were also reacted with Ia in the presence of butyllithium.

The possibility of homopolymerization of the diisocyanates under anionic conditions was disproved by the infrared spectra which left little doubt that the products were urethanes, and not ureas. Furthermore, the spectra were identical to those of polyurethanes prepared from chloroformate Ic and the corresponding diamine.

Polymerization of diol Ia with the diisocyanate Ii in refluxing *s*-tetrachloroethane led only to very low molecular weight polymer VI. Ethylene glycol and diisocyanate Ii gave also low polymer which demonstrates this diisocyanate's poor reactivity.

Polymers from 9,10-Bis(methylenechloroformyl)triptycene (Ic)

Because the slow reaction of diol Ia with diisocyanates was attributed to steric hindrance, 9,10-bis(methylenechloroformyl)triptycene (Ic) was synthesized and reacted with 1,3-phenylenediamine to form the polyurethane VII. An inherent viscosity of 0.47 was attained in 6 hr at 145°C, which was a considerable improvement over the uncatalyzed diol-diisocyanate reaction.

Polymers from 9,10-Triptycenedicarbonyl Chloride (Id)

Interfacial polymerization of diacid chloride Id with hexamethylenediamine, gave polyamide VIII, (η = 1.13) melting at 315°C. The solution polymerization of this acid chloride with 4,4′-diaminodiphenyl ether (IX) and 1,3-phenylenediamine (X) showed a large dependence of molecular weight upon the polymerization medium (see Table II). High yields of high molecular weight polymer were obtained by the proper choice of solvent.

TABLE II
Solvent Effect on Polyamidation

	Inherent viscosity[a]	
Reaction solvent	Polyamide IX	Polyamide X
Ethyl acetate	1.63	
Isopropyl acetate	1.54	
Ethyl acetate–chloroform (1:1)	1.50	0.18
Chloroform	0.93	0.08
Tetrahydrofuran	0.79	
Isopropyl acetate–chloroform (1:1)	0.60	
Nitrobenzene	0.42	
Dioxane	0.37	0.94
Dimethylacetamide	0.22	0.20
Ethyl acetate–dioxane (1:1)		0.35

[a] Inherent viscosity, 0.5% in methanesulfonic acid at 30°C.

The solubility of these polyamides is unusual. Most polyamides are soluble in highly polar hydrogen bonding solvents. The triptycene polyamides are insoluble in these but are soluble in solvents of intermediate polarity such as chloroform and ethyl acetate. We attribute this solubility difference to the shielding of the amide linkage by the bulky triptycene structure. Thus, the only groups available for solvation are the hydrocarbon portions of the molecules or the ether portion, for polymer IX. These are more compatible with less polar solvents and would lead to the observed solubilities.

The reaction of diacid chloride Id with ethylene glycol gave only low molecular weight polymers (η_{inh} = 0.05). The diglycolate technique of Eareckson[6] was used to produce polyester XI, but again only low polymer

(η_{inh} = 0.1) was obtained. The inherent viscosity did increase slightly when the method of Whinfield[7,8] was used to split off the ethylene glycol endgroups.

The interfacial reaction between 9,10-triptycenedicarbonyl chloride and aqueous hydrazine gave only low polymer. When the diacid chloride was reacted with terephthalic acid dihydrazide in hexamethylphosphoramide a high molecular weight polyhydrazide (η = 1.27) was obtained. This polyhydrazide was found to be soluble in 4% lithium chloride in 3:7 pyridine–hexamethylphosphoramide and insoluble in other solvent systems.

The polyhydrazide was partially converted thermally to an intractable polyoxadiazole (XIII) (73% conversion by oxygen analysis, and 78% conversion by thermogravimetric analysis).

Other Polymers from Triptycene Intermediates

The melt condensation of the dimethyl ester Ie with 3,3′-diaminobenzidine resulted in a low molecular weight polybenzimidazole (XIV). Better results would be expected with diphenyl ester but no further study was made of this polymerization.

The interfacial polymerization of the diamine Ih with sebacyl chloride only led to low molecular weight polyamide XV. The poor reactivity of the diamine Ih was confirmed by its failure to react with acetic anhydride after 24 hr.

Preparation of the polyester from 9,10-bis(hydroxyethyl)triptycene (Ib) and diphenyl isophthalate under conditions similar to those used for polymer III led only to low polymer (XVI) due to product pyrolysis.

Thermal Stability of Polymers

Since tough films could not be prepared from most of the polymers, their thermal stabilities had to be compared by thermogravimetric studies on the powder. The decomposition was usually sharp and a 10% weight loss was used for comparison of relative thermal stabilities (see Table I).

We observed a thermal stability limit (440–460°C) which was surprisingly constant for the structurally different polyester III, polyamide IX, and polyoxadiazole XIII. This result suggests that the triptycene nucleus or its α bond may be the stability limiting structural unit. The mechanism of decomposition in air is probably thermal, rather than oxidative because both decomposition in air and in nitrogen occur at 440–450°C.

The apparent lack of oxidative decomposition in these polymers is of particular interest. The partially aliphatic nucleus of triptycene and the methylene portion of the bis(hydroxymethyl) polymers should have rendered these polymers oxidatively unstable. However, the triptycene structure must shield these aliphatic portions from oxidation. This protection may be due to steric hindrance or to the electronic interactions of the triptycene system.[9]

In contrast to the above mentioned polymers, the weaker urethane linkage of polymer VII and the unprotected methylene groups of polymer VIII limit their thermal stability.

Film Properties

Solution casting produced clear and colorless films, except where prolonged drying at elevated temperatures was required and decomposition occurred. Generally, the films were weak or brittle which, in part, may be attributed to their high crystallinity as demonstrated by powder x-ray crystallographs (VIII = 80%, IX = 50% crystalline), and in part to the stiffness of the polymer chains. A further description of the film properties is given in Table III.

TABLE III
Film Properties

	Polyamide IX[a]	Polyurethane V[b]
Inherent viscosity	1.61	0.55
Modulus, kpsi	338	470
Tenacity, kpsi	11	17
Elongation, %	5	5
Pneumatic impact, kg-cm	—	0.26 (0.77 Mils)
Tear, g	3.3	—
Dielectric strength, V/mil at 25°C	3677	5300
Dielectric constant 10^3, cps at 25°C	3.80	3.68
Dissipation factor 10^3, cps at 25°C	0.0114	0.0070
Resistivity (125 V), ohm-cm	—	3.0×10^{17}
Water vapor permeability, g/100 m^2-hr (mil basis)	976	560
Gas permeability, cc/100 $in.^2$-24 hr-atm (mil basis)		
O_2	135	960
N_2	19	830
CO_2	40	670

[a] Films cast from 1:1 chloroform–ethyl acetate and dried under vacuum at 60°C overnight indicated no detectable residual solvent in the infrared spectrum.

[b] Films cast from 10% solution in tetrahydrofuran, dried at 60–70°C under vacuum overnight and then at 150–160°C under vacuum overnight. Such films contained <0.1% solvent.

Bifunctional Triptycene Derivatives

Although an extensive list of 9-substituted triptycenes had been synthesized,[10-13] only a few examples of 9,10-disubstituted triptycene derivatives are on record.[13,14]

The Diels-Alder addition of benzyne from benzene-diazonium-2-carboxylate to 9,10-disubstituted anthracenes furnished a convenient route to bifunctional triptycenes. Employing a modified version of Friedman and Logullo's procedure for benzyne addition to anthracenes,[3,13] we have synthesized 9,10-bis(acetoxymethyl)triptycene and its hydrolysis product, 9,10-bis(hydroxymethyl)triptycene (Ia), in greater than 90% yields. The hydroxymethyl functionality provided a key intermediate, since simple chemical transformations could readily convert this group into other substituents.

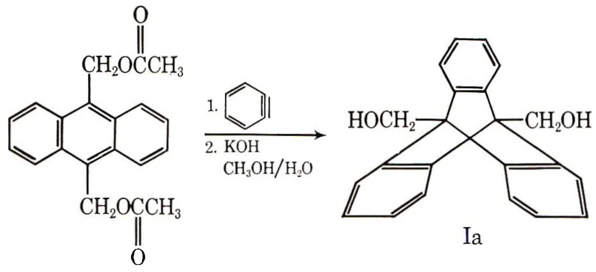

When benzyne was generated from the diazonium salt *in situ*, a 72% yield of Ia was obtained. In contrast, when benzenediazonium 2-carboxylate

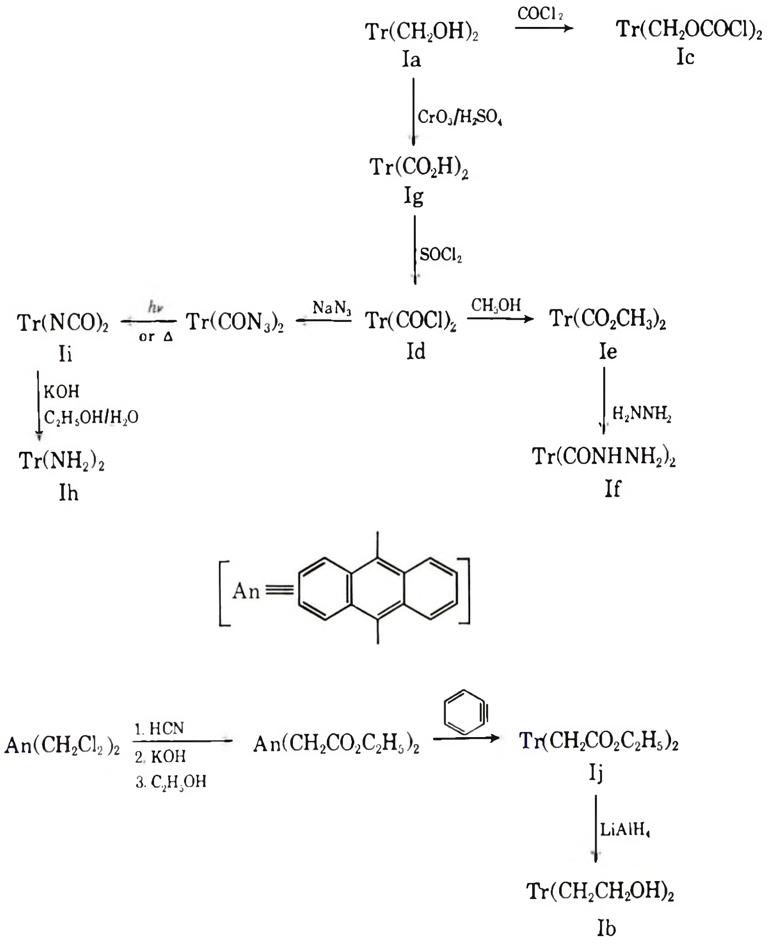

Fig. 1. Synthesis of disubstituted triptycenes.

TABLE IV
9,10-Disubstituted Triptycenes

Compound no.	R	Mp, °C	Yield, %	Formula	C, % Calcd	C, % Found	H, % Calcd	H, % Found	Cl, % Calcd	Cl, % Found	N, % Calcd	N, % Found
Ia	CH_2OH	310–311	96	$C_{22}H_{16}O_2$	84.05	84.73	5.77	5.82				
Ib	CH_2CH_2OH	Broad range >145	—	$C_{24}H_{22}O_2$	84.17	84.11	6.47	6.51				
Ic	CH_2OCOCl	267–268	77	$C_{24}H_{18}O_4Cl_2$	65.61	65.60	3.76	3.74	16.14	15.79		
Id	$COCl$	322–323	90	$C_{22}H_{12}O_2Cl_2$	69.67	69.69	3.19	3.11	18.70	18.86		
Ie	CO_2CH_3	269	96 (crude)	$C_{24}H_{18}O_4$	77.82	78.10	4.90	4.94				
If	$CONHNH_2$	350	25 (crude)	$C_{22}H_{18}N_4O_2$								
Ig	CO_2H	>325 (dec)	90	$C_{22}H_{14}O_4$	77.18	77.12	4.12	4.60				
Ih	NH_2	290–292	83	$C_{20}H_{16}N_2$	84.48	84.28	5.67	5.74			9.85	9.70
Ii	NCO	171–172	73	$C_{22}H_{12}N_2O_2$	78.56	78.63	3.60	3.54			8.33	8.47
Ij	$CH_2CO_2C_2H_5$	255–255.5	64	$C_{28}H_{26}O_4$	78.85	78.90	6.14	6.20				

was isolated, washed free of its mother liquor, cautiously kept moistened with the reaction solvents, and subsequently decomposed in the presence of 9,10-bis(acetoxymethyl) anthracene,[15] a 96% yield of pure diol Ia was achieved.

For modification of the 9,10-substituent groups, conventional reaction schemes were utilized, as outlined in Figure 1; data characterizing the derivatives prepared are listed in Table IV. Infrared and NMR spectral assignments support the structure indicated.

The diethyl ester of 9,10-triptycenediacetic acid (Ij) and its reduction product, 9,10-bis(β-hydroxyethyl)triptycene (Ib), were prepared by the addition of benzyne to the diethyl ester of 9,10-anthracenediacetic acid (Fig. 1). The latter had been synthesized previously[16-18] and reacted smoothly with benzyne to furnish the desired triptycene ester in 64% yield.

The synthetic steps depicted in Figure 1 proceeded without serious complications. Side reactions occurring in the thermal rearrangement of 9,10-triptycenedicarbonyl azide (an explosive compound) to the isocyanate (Ii) precluded high yields. It was found that photolytic conversion of azide to isocyanate in benzene solution was decidedly more convenient than the customary thermal decomposition. The diisocyanate Ii and diamine Ih were moderately volatile compounds and were best purified by sublimation.

EXPERIMENTAL

Preparation of Polymers

Polyester III from 9,10-Bis(hydroxymethyl)triptycene and Diphenyl Isophthalate by Melt Condensation

Into a polymer tube equipped with a side arm (directed slightly downward) were charged 3.1436 g (10.00 mmole) Ia, 3.1831 g (10.00 mmole) diphenyl isophthalate, and 0.001 g zinc acetate. A small amount of benzene was used to wash the reagents down into the tube and was removed by vacuum. The tube was deaerated by alternately flushing with nitrogen and evacuating. Both openings were then sealed and the tube was heated to 280°C in a dimethyl phthalate vapor bath. Phenol condensed in the side arm and was returned periodically to the reaction mixture during the initial $2^1/_4$ hr to avoid the loss of diphenyl isophthalate. During the next $1^3/_4$ hr, phenol was collected continuously. During the final hour of heating, the polymer foamed up and became so viscous that it did not flow back to the bottom of the tube. A sample of this polymer had an inherent viscosity of 0.07 in nitrobenzene (0.5% solution at 30°C) and a stick temperature of 275°C. The polymer was now transferred to a small stirred vessel and was heated to 330–340°C at 0.75 mm for 2 hr. A sample was taken and found to have a viscosity of 0.26 and a stick temperature of 370°C. The apparatus walls were cleaned of condensate which contained both carbonyl and hydroxyl groups (probably diol Ia). The polymer was returned to the apparatus and reheated to 330–340°C at 0.3–0.75 mm for an additional 2 hr. The melt was not well stirred throughout this last cycle, since it had become too viscous. The inherent viscosity of the final polymer was 0.51 and the stick temperature 370°C.

Polyurethanes from 9,10-Bis(hydroxymethyl)Triptycene and Diisocyanates

Methylenebis(4-phenyl Isocyanate) Polyurethane V. In a flame-dried, 100-ml three-necked flask equipped with condenser, drying tube, magnetic stirrer, and nitrogen inlet were charged 3.1436 g (10.00 mmol) Ia (redried at 100°C under vacuum just before use), 35 ml dioxane (distilled from sodium) and 2.5026 g (10.00 mmol) methylenebis(4-phenyl isocyanate) (vacuum-distilled and stored at −16°C). The diisocyanate was washed in with 5 ml dioxane. The mixture was heated to reflux and 0.01–0.02 ml of a 15% butyllithium solution in hexane was injected. The viscous solution was cooled after 20 min. The polymer was precipitated and washed with methanol in a blender and dried at 100°C under vacuum. The colorless product (yield ~95%) had an inherent viscosity of 0.59 in tetrachloroethane (0.5% solution at 30°C). Self-supporting film could be cast from tetrahydrofuran. The infrared spectrum of the film was typical of polyurethane with NH absorption at 3330 cm^{-1}. The polymer's stick temperature was 320°C.

1,3-Phenylene Diisocyanate and 2,4-Tolyl Diisocyanate. 1,3-Phenylene diisocyanate (as received from Ott Chemical Company) and 2,4-tolyl diisocyanate (vacuum-distilled) were reacted separately with Ia as above 1 hr reaction time being allowed. The data obtained for the polymeric products are given in Table V.

TABLE V

Diisocyanate	Inherent viscosity in tetrachloroethane (0.5% solution at 30°C)	Stick temp, °C
1,3-Phenylene[a]	0.20	315
2,4-Tolyl	0.42	310

[a] Reaction was initiated with ~0.04 ml butyllithium solution.

Polyurethane VII from 9,10-Bis(methylenechloroformyl)triptycene and 1,3-Phenylenediamine

In a 100-ml three-necked flask equipped with condenser and drying tube, nitrogen bubbler, Glascol mantle, and magnetic stirrer were charged 40 ml dry *sym*-tetrachloroethane, 1.0814 g (10.00 mmole) 1,3-phenylenediamine, and 4.393 g (10.0 mmole) Ic. The reaction mixture was heated to the boiling point with stirring and nitrogen bubbling for 6 hr. The polymer precipitated from this solution with methanol had an inherent viscosity of 0.47 in tetrachloroethane (0.5% solution at 30°C). A self-supporting, but brittle film could be cast from the polymerization mixture. The stick temperature was about 320°C. The infrared spectrum of this polymer was identical to that from Ia and 1,3-phenylene diisocyanate.

Polyamide VIII-X from 9,10-Triptycenedicarbonyl Chloride and Diamines

1,6-Hexamethylenediamine. A solution of 2.5 g (6.6 mmole) acid chloride Id in 50 ml chloroform was placed in a 250-ml beaker and a solution of 1.92 g (16.5 mmole) 1,6-hexamethylenediamine in 25 ml water was carefully poured on top. Polymerization occurred at the interface, but no rope could be pulled. Instead, a flaky solid was obtained. The mixture was rapidly stirred for 15 min to complete polymerization. Methanol was added to break the emulsion, and the solids were filtered off, washed twice with 100 ml methanol, and dried to give 2.60 g, 76% yield, of polymer with an inherent viscosity of 1.13 in methanesulfonic acid (0.5% solution at 30°C). Polymer cast from a dimethyl sulfoxide organosol at 160°C yielded a clear but brittle film.

4,4′-Diaminodiphenyl Ether. This polymerization was carried out in a range of solvents and mixed solvents. Depending on polymerization medium, the following general procedure led to inherent viscosities in methanesulfonic acid in the range 0.22–1.66 (0.5% solution at 30°C) (see Table II). The higher viscosities correspond to osmotic pressure molecular weights of 30,000–40,000.

A suspension of 1.3224 g (6.596 mmole) powdered 4,4′-diaminodiphenyl ether in 25 ml ethyl acetate was stirred at room temperature with 1.90 ml (13.70 mmole) freshly distilled triethylamine. To this was added 2.500 g (6.596 mmole) acid chloride Id along with 50 ml solvent over a period of 3 hr. The mixture was allowed to react for 1$^1/_2$ days before pouring into 500 ml methanol. The methanolic suspension was stirred for 2 hr, filtered, and dried to give 3.31 g, 98% yield, of polymer with an inherent viscosity in methanesulfonic acid of 1.11 (0.5% in solution at 30°C). The infrared showed absorption (in Nujol) at $\nu_{\max} = 1685, 1492, 1217\ \mathrm{cm}^{-1}$. Clear, colorless films were cast from ethyl acetate–chloroform.

1,3-Phenylenediamine. A suspension of 0.7133 g (6.596 mmole) 1,3-phenylenediamine and 1.90 ml triethylamine in 50 ml of 1:1 ethyl acetate–chloroform was stirred at room temperature. Diacid chloride Id was added as a solid in three batches with the addition of some rinse solvent. Total acid chloride was 2.500 g (6.596 mmol) in a total volume of 50 ml of solvent. The suspension was stirred for 1$^1/_2$ days and poured into 500 ml methanol. The solids were stirred in methanol for 2 hr, filtered, and dried in a vacuum oven at 100°C to give 3.75 g of polymer with an inherent viscosity of 0.18 in methanesulfonic acid (0.5% solution at 30°C). The infrared showed absorption in Nujol at $\nu_{\max} = 3422, 1698, 1600, 1519\ \mathrm{cm}^{-1}$.

This reaction was repeated in a range of solvents and mixed solvents to give polymer with inherent viscosities of 0.13–0.94 (see Table II).

Polyhydrazide XII from 9,10-Triptycenedicarbonyl Chloride and Terephthalic Acid Dihydrazide

Terephthalic acid dihydrazide was prepared by refluxing dimethyl terephthalate with an excess of hydrazine hydrate in benzene for 24 hr. The product which was recrystallized from water decomposed at 340°C.

A suspension of 1.2809 g (6.596 mmole) terephthalic acid dihydrazide in 50 ml of dry hexamethylphosphoramide was stirred at room temperature. A sample of 1.2500 g Id was added, dissolving the suspended material; the resulting solution became noticeably viscous. After 1 hr stirring, another 1.2500 g chloride was added (total 2.500 g, 6.596 mmole) and the flask rinsed with an additional 50 ml solvent. After 30 min, a precipitate appeared. This mixture was stirred overnight under nitrogen and then poured into 500 ml water. The solids were collected and washed in a blender with 500 ml water, then with 100 ml methanol. The solids were collected and dried to give 3.46 g, 98% yield of polymer with an inherent viscosity of 1.27 (0.5% solution in 4% LiCl 3:7 pyridine–hexamethylphosphoramide at 30°C), $\nu_{\max} = 1618, 1310, 1250 \text{ cm}^{-1}$ in Nujol.

Polyoxadiazole XIII from Poly(terephthalyl-9,10-triptycenehydrazide) XII

A sample of poly(terephthalyl-9,10-triptycenehydrazide) was placed in a polymerization tube and flushed with nitrogen. This tube was heated to 270–285°C at 0.1 mm pressure for 100 hr to give the darkened polyoxadiazole. Oxygen analysis indicated 73% conversion, calcd: O, 6.82%; found: O, 8.51%.

Preparation of Polymer Intermediates

9,10-Bis(hydroxymethyl)triptycene (Ia)

To a solution of 13.7 g (100 mmole) of anthranilic acid and 0.15 g of trichloroacetic acid in 150 ml of tetrahydrofuran (THF) at 0°C was added slowly with stirring 25 ml of redistilled amyl nitrite. A tan-orange precipitate separated and was allowed to warm to room temperature over 1 hr. The solid was collected on a polyethylene filter and washed with cold THF until the washings were colorless. (*Caution:* Benzenediazonium 2-carboxylate should be kept moist at all times, since it presents serious danger of explosion if allowed to dry). The solid was then washed quickly with cold methylene chloride and transferred to a refluxing suspension of 24.5 g (75.5 mmole) of 9,10-bis(acetoxymethyl) anthracene[15] by use of a polyethylene policeman and a stream of methylene chloride. The resulting suspension was refluxed for 2 hr, and the solvent was removed at reduced pressure, leaving a brown paste. This was dissolved in 100 ml of diglyme, 8 g of maleic anhydride was added, and the brown solution was refluxed for 1 hr. The mixture was then poured into a solution of 40 g of potassium hydroxide in 120 ml water/240 ml methanol, and the suspension was boiled for 30 min with stirring. Water was added until crystallization was complete, and the product was filtered. The ivory solid was washed with water until the washings were neutral and dried, affording 22.2 g (70.6 mmole, 93.7%) of 9,10-bis(hydroxymethyl)triptycene (Ia), mp 310–311°C. The mother liquors yielded a second crop of tan solid, which after recrystallization had mp 304–305°C, for a total yield of 22.8 g (72.6 mmole, 96.2%).

The infrared spectrum showed absorption in Nujol at ν_{max} = 3580–3500, (2940, 2850, 1450, 1370), 1300 (w), 1270 (w), 1220 (w), 1150, 1060 (s), 1025, 913 (w), 758–750 (broad, s) cm^{-1}.

9,10-Triptycenedicarboxylic Acid (Ig)

A paste consisting of 4.46 g of chromium trioxide and 4.0 ml of concentrated sulfuric acid was carefully diluted to 15 ml with water and allowed to cool to room temperature. This solution was added to a suspension of 5.0 (15.9 mmole) of Ia in 190 ml of acetone at a rate such that the temperature did not exceed 35°C. The green mixture was then stirred overnight at room temperature. The volume was reduced to one-half, and an equal volume of water was added. Most of the acetone was then removed on a rotary evaporator, and the suspended green powder was filtered and washed with water until colorless. The moist filter cake was dissolved in 75 ml of 10% potassium hydroxide solution, the solution filtered and acidified with 10% hydrochloric acid. The resulting precipitate was digested on the steam bath for 15 min, filtered, and dried in a vacuum oven at 100°C for 4 hr, affording 4.88 g (14.2 mmole, 90%) of 9,10-triptycenedicarboxylic acid (Ig), mp >325°C (dec). The infrared spectrum showed absorption in Nujol at ν_{max} = 1695 and 1266 cm^{-1}.

9,10-Triptycenedicarbonyl Chloride (Id)

A solution of 5.7 g (16.6 mmole) of Ig in 110 ml of dioxane was added dropwise over 3 hr to 40 ml of purified thionyl chloride at reflux under nitrogen. The pale yellow solution was refluxed with stirring for an additional 6 hr and allowed to cool to room temperature overnight. The solvent was removed on a rotary evaporator, and the residue was recrystallized from carbon tetrachloride, furnishing three crops of diacid chloride Id with a total weight of 5.68 g (15.0 mmole, 90%). An analytical sample had mp 322–323°C. The infrared spectrum showed absorption in Nujol at ν_{max} = 1785, 1058, and 1042 cm^{-1}.

9,10-Triptycenedicarbonyl Azide and 9,10-Triptycene Diisocyanate (Ii)

To a stirred suspension of 4.8 g (12.5 mmole) of Id in 55 ml dry hexamethylphosphoramide was added 2.01 g (31 mmole) of sodium azide, and the mixture was stirred in a drybox for 16 hr. The reaction mixture was poured into 500 ml of water with stirring, and the 5.21 g of white precipitate was filtered and dried in a vacuum desiccator under aspirator pressure. Recrystallization from 30 ml dimethylformamide (DMF)/150 ml water afforded 4.33 g (11 mmole, 88%) of white solid, whose infrared spectrum showed characteristic azide absorption at 2130 cm^{-1}. (*Caution:* The crude 9,10-triptycenedicarbonyl azide is explosive and should not be heated or subjected to low-pressure evacuation in the solid state.)

The azide was suspended in 50 ml of dry xylene and refluxed under nitrogen for 16 hr. Repeated concentration of the xylene mixture and treatment with low-boiling petroleum ether gave three successive fractions of crude product containing 9,10-triptycene diisocyanate (Ii) and 9,10-triptycenedicarboxylic acid (Ig), the latter fractions being enriched in the desired diisocyanate. Each fraction was sublimed separately at 170–230°C/0.5–1.5 mm, and the sublimates were combined and resublimed to yield 1.81 g (5.38 mmole, 43%, based on diacid chloride Id) of diisocyanate Ii, mp 171–172°C. The infrared spectrum showed absorption in Nujol at ν_{max} = 3070, 2270, 1190, 1003, 890, 758–745 (broad) cm^{-1}.

An alternative, more convenient, photochemical synthesis was accomplished as follows.

A solution of 1.0 g (25.5 mmole) of dicarbonyl azide and 0.5 ml of acetophenone in 75 ml of dry benzene was placed in a quartz, cylindrical cell of 100 ml capacity, equipped with a condenser, drying tube, magnetic stirrer, and nitrogen sparger. The cell was fastened in a Rayonet Srinivasan-Griffin photochemical reactor chamber, equipped with low pressure mercury lamps, emitting principally light of 2537 Å. The solution was sparged with nitrogen for 15 min and was then photolyzed at 35°C, under nitrogen, for 1 hr. The solution had become pale brown. The total volume of photolyzate was reduced to 20 ml and was passed through a 2 × 20 cm column of Florisil, 150 ml of benzene being used as eluent. The solvent was evaporated, leaving 0.80 g of oily solid. This was sublimed at 0.4 mm and 150–170°C to give 0.335 g (39.2%) of Ii, mp 170–173°C, whose infrared spectrum matched that of an analytical sample.

The use of a photosensitizer does not seem to be required for this transformation, since product yields of 33% were achieved in the absence of acetophenone.

9,10-Triptycenediamine (Ih)

A 2.11 g (5.8 mmole) sample of diisocyanate Ii was suspended in 30 ml of 5% potassium hydroxide solution. Ethanol (10 ml) was added to this, and the mixture was refluxed for 8 hr. The reaction mixture was colorless and contained suspended, white solid. Addition of 25 ml of water, filtration, and washing with 10 ml of water afforded 1.79 g of ivory solid. This was sublimed twice at 0.6 mm and 220°C to give 1.37 g (4.81 mmole, 83%) of 9,10-triptycenediamine (Ih). An analytical sample had mp 290–292°C. The infrared spectrum in Nujol showed absorption at ν_{max} = 3350, 1590 (broad), 1300, 928 (broad), 890, 798 (broad), 752 (broad) cm^{-1}. The NMR spectrum in fully deuterated dimethyl sulfoxide displayed signals at 2.72 τ (quartet), 3.22 τ (quartet), and 6.82 τ (singlet) with the area ratios 3:3:2.

9,10-Triptycenediacetic Acid, Diethyl Ester (Ij)

The procedure of benzyne addition, described for the preparation of diol Ia was repeated, 27.5 g (78.6 mmole) of 9,10-anthracenediacetic acid, diethyl ester[16–18] being used as the substrate. The reflux mixture was poured into a solution of 25 g of potassium hydroxide in 120 ml water/240 ml methanol and stirred for a few minutes. Water was added until the total volume was about 750 ml. The mixture was filtered, and the ivory solid was washed with water, until the washings were neutral, furnishing 23.9 g of crude ester (Ij), mp 253.5–255.5°C. This was dissolved in 200 ml of DMF, treated with charcoal, and filtered. The solution was concentrated to about 180 ml, and 40 ml of water was added, causing incipient crystallization. The mixture was cooled in ice, filtered, and the product washed with methanol, yielding 21.5 g (60.2 mmole, 64%) of white crystals, mp 255–255.5°C. The infrared spectrum in Nujol showed maxima at 1724, 1445, 1188, 1141, and 745 cm^{-1}.

9,10-Bis(β-hydroxyethyl)triptycene (Ib)

Lithium aluminum hydride (2.7 g, 80% excess) was dissolved in 1 liter of dry THF in a 2-liter flask, equipped with a Soxhlet extractor, condenser, and drying tube. In the extractor thimble was placed 16.8 g (39.4 mmole) of diester Ij. After a 23-hr reflux, the THF solution was decanted from the solid to decompose any excess lithium aluminum hydride. After hydrogen evolution had stopped, about 200 ml of water and enough 5% hydrochloric acid solution to dissolve all the solid were added. The acidic solution was then extracted twice with ether, and the extracts were combined and dried over anhydrous sodium sulfate. The ether was evaporated, leaving a white foamy solid. This was recrystallized from ether to give a glassy solid, which still contained a small amount of impurity whose infrared spectrum evidenced carbonyl absorption. The contaminant was sublimed away from the diol Ib, leaving an analytical sample which melted broadly above 145°C. The infrared spectrum in Nujol showed maxima at 3265, 1150, 1015, 742 cm^{-1}.

9,10-Triptycenedicarboxylic Acid, Dimethyl Ester (Ie)

A suspension of 3.30 g (8.6 mmole) of 9,10-triptycenedicarbonyl chloride (Id) was refluxed in 50 ml of methanol for 2 hr. The suspended solid was displaced by a precipitate of different texture. The mixture was cooled and filtered to give 3.16 g (8.3 mmole, 96%) of crude dimethyl ester. A chloroform solution of the crude product was passed over alumina, and the residue was recrystallized from dioxane to give a product with mp 260–262°C; the melting point of the analytical sample was 269°C. The infrared spectrum in Nujol showed maxima at 1719, 1252, 1019 cm^{-1}.

9,10-Triptycenedicarbonylhydrazide (If)

A suspension of 1.00 g (2.64 mmole) of 9,10-triptycenedicarboxylic acid, dimethyl ester (Ie) in 50 ml of methanol was refluxed with 40 ml of 64% hydrazine solution for 8 hr, until the system became homogeneous. Heating was continued for 2 hr, the excess solvent was distilled off, and the residue filtered and dried to give 0.25 g (0.675 mmole, 25%) of crude hydrazide (If), mp 350°C. The infrared spectrum in Nujol showed maxima at 3468, 3193, 1662, 1618, 1044, and 968 cm^{-1}.

9,10-Bis(methylenechloroformyl)triptycene (Ic)

Phosgene (200 ml) was condensed at 0°C in a three-necked flask, equipped with a Dry Ice condenser, calcium chloride–protected outlet, gas inlet tube, magnetic stirrer, and water bath. The gas inlet tube was replaced by a stopper, and 400 ml of chilled glyme, distilled from sodium, was added, followed by 10.0 g (36 mmole) of 9,10-bis(hydroxymethyl)triptycene (Ia). The reaction mixture was warmed to 41°C and stirred for 6.25 hr. The reaction was cooled, stirred overnight at room temperature, then reheated to 41°C and stirred for 7.5 hr. After another overnight stirring period at room temperature, the phosgene was evaporated and destroyed by passage through alcoholic potassium hydroxide solution. Removal of the glyme on a rotary evaporator left a colorless residue. Crystallization from carbon tetrachloride and drying at vacuum pump pressure over phosphorus pentoxide afforded 11.1 g of colorless, crystalline product, mp 266–267°C whose infrared spectrum in Nujol exhibited a characteristic band at 1755 cm^{-1}. Concentration of mother liquors gave 1.0 g of colorless product, mp 267–268°C, for a total yield of 12.1 g (27.6 mmole, 76.5%).

All melting points are corrected. The melting behavior of polymer was characterized either by determining the temperature at which a lump leaves a molten trail on a heated block (stick temperature) or a powder becomes obviously liquid. Infrared spectra were scanned on a Perkin-Elmer Infracord, and NMR spectra were run with a Varian Associated HR-60 dual-purpose spectrometer, TMS being used as internal standard. The x-ray crystallinities were estimated from the areas of crystalline peaks and amorphous background in goniometer traces.

References

1. C. S. Marvel, paper presented at American Chemical Society 147th Meeting, Philadelphia, Pa., April 1964, *Polymer Preprints* **5,** No. 1, 167 (1964).
2. P. D. Bartlett and F. D. Greene, *J. Amer. Chem. Soc.*, **76,** 1088 (1954).
3. L. Friedman and F. M. Logullo, *J. Amer. Chem. Soc.*, **85,** 1549 (1963).
4. W. R. Sorenson and T. W. Campbell, *Preparative Methods of Polymer Chemistry,* Interscience, New York, 1961; p. 111.
5. K. C. Frisch, S. L. Reegen, W. V. Floutz, and J. P. Oliver, *J. Polym. Sci. A-1,* **5,** 35 (1967).
6. W. M. Eareckson, III, *J. Polym. Sci.*, **40,** 399 (1959).
7. J. R. Whinfield, *Nature,* **158,** 930 (1946).
8. J. R. Whinfield and J. T. Dickson, Brit. Pat. 578,079 (June 14, 1946).
9. P. H. Heller and D. H. Geske, *J. Org. Chem.*, **31,** 4249 (1966).
10. P. D. Bartlett and F. D. Greene, *J. Amer. Chem. Soc.*, **76,** 1088 (1954).
11. W. Theilacker and K. H. Beyer, *Chem. Ber.*, **94,** 2968 (1961).
12. E. C. Kornfeld, P. Barney, J. Blankley, and W. Faul, *J. Med. Chem.*, **8,** 342 (1965).
13. F. W. Logullo, Ph.D. Thesis, Case Institute of Technology (1965).
14. B. H. Klanderman, *J. Amer. Chem. Soc.*, **87,** 4649 (1965).
15. G. M. Badger and J. W. Cook, *J. Chem. Soc.*, **1939,** 802.
16. A. Kretov and V. V. Litvinov, *Zh. Prikl. Khim.*, **35,** 464 (1962).
17. G. Rio, *Ann. Chim.*, **9,** 182 (1954).
18. M. W. Miller, R. W. Amidon, and P. O. Tawney, *J. Amer. Chem. Soc.*, **77,** 2845 (1965).

Received February 8, 1968
Revised April 19, 1968

JOURNAL OF POLYMER SCIENCE: PART A-1 VOL. 7, 73-81 (1969)

Synthesis of 4-Vinylbiphenyl–Isoprene Block Copolymers and Their Characterization by Gel-Permeation Chromatography

J. HELLER, J. F. SCHIMSCHEIMER,
R. A. PASTERNAK, C. B. KINGSLEY, *Polymer Chemistry Department, Stanford Research Institute, Menlo Park, California 94025*
and J. MOACANIN, *Jet-Propulsion Laboratory, California Institute of Technology, Pasadena, California 91103*

Synopsis

4-Vinylbiphenyl–isoprene ABA block copolymers were prepared by initiating 4-vinylbiphenyl with *n*-butyllithium in benzene, adding isoprene, and coupling the resulting AB anion with phosgene. Preliminary coupling experiments with a polyisoprene anion have shown that virtually quantitative coupling could be achieved provided the phosgene was added extremely slowly. The block copolymers could be quantitatively analyzed by gel-permeation chromatography from a knowledge of the ratio of the refractive index increments of the two homopolymers and the overall composition.

INTRODUCTION

ABA block copolymers, where A represents polystyrene and B polybutadiene or polyisoprene, are now well known. These materials behave as vulcanized elastomers below the glass transition temperature of the A segment, but above this temperature they can be processed as any other thermoplastic material. A great deal of attention has been given to materials where A represents polystyrene,[1] but only passing mention is made of materials where A represents a higher melting vinylaromatic monomer.[2]

This paper reports the synthesis of 4-vinylbiphenyl–isoprene ABA block copolymers and the detailed characterization of these materials by gel-permeation chromatography. A study of the mechanical properties of these materials is now in progress and will be reported at a later date.

EXPERIMENTAL

Purification of Materials

4-Vinylbiphenyl. The monomer (Aldrich Chemical Company) was first dissolved in benzene and passed through a column containing successive layers of silicic acid and alumina. It was then recrystallized to a sharp

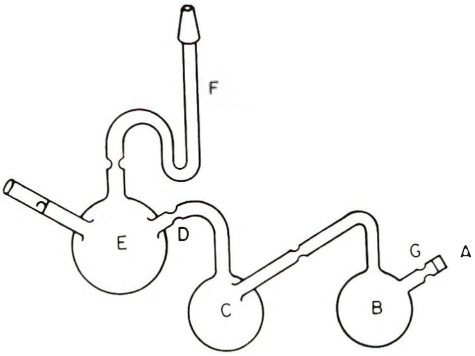

Fig. 1. Apparatus for purification of 4-vinylbiphenyl.

melting point from methanol and dried. The monomer was next dissolved in pure benzene to a known concentration, and a measured amount of this solution was injected through a neoprene serum cap (A) into bulb B, which contained calcium hydride (Fig. 1). Next, the solution in bulb B was frozen, the apparatus evacuated, and the tube sealed off at G. The mixture was allowed to melt and then left standing at room temperature until all evolution of hydrogen ceased (about 18 hr). The solvent was stripped off and the monomer carefully sublimed into bulb C. Bulb B was then sealed off and the monomer sublimed into bulb E. After sealing off at D, purified benzene was distilled into the bulb and the contents were frozen and degassed. The bulb was then sealed off at F and stored in a freezer until ready for use.

Isoprene. The monomer (Phillips Petroleum, Research Grade) was placed over calcium hydride on a vacuum system, degassed, and allowed to stand for 24 hr. It was then distilled into a bulb containing a sodium mirror, allowed to react for 2–3 hr, distilled into another bulb with a sodium mirror, allowed to react again for 2–3 hr, and finally distilled into a tube with a breakseal. This tube was stored in a freezer until ready for use.

Benzene. The reagent-grade material was stored in a 1-liter bulb attached to a vacuum system with polystyryllithium as scavenger. A red color of the solution was taken as evidence of purity.

***n*-Butyllithium.** *n*-Butyllithium (Foote Mineral Co., 1.6M in *n*-hexane) was taken directly from the bottle with the use a of hypodermic syringe and transferred in an argon-filled polyethylene bag through a serum cap into a tube equipped with a breakseal on one end and a constriction and a neoprene serum cap on the other end. The contents of the tube were then frozen, and the tube was evacuated through the serum cap with a hypodermic needle. The contents were allowed to melt and again evacuated and frozen. The tube was next sealed off at the constriction and stored in a freezer until ready for use.

Phosgene. The gas was admitted up to atmospheric pressure into a small evacuated tube equipped with a breakseal and a capillary tube having an extremely fine orifice (about 0.001 mm diameter). The construction

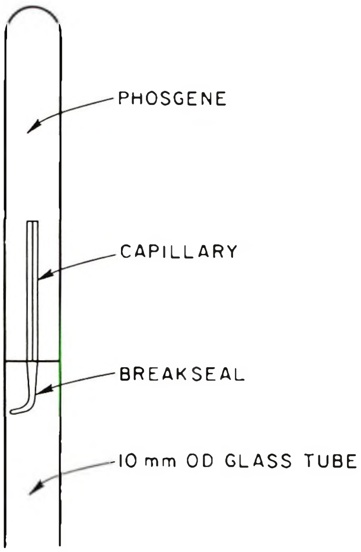

Fig. 2. Construction of phosgene tube.

of this tube is shown in Figure 2. The phosgene is then liquified and the tube sealed off.

Polymerizations

Polymerizations were carried out in the apparatus shown in Figure 3. An initiator bulb E, an isoprene bulb F, a 4-vinylbiphenyl benzene solution bulb G, and a phosgene bulb H were sealed onto the reactor B. The whole assembly was then evacuated to 10^{-5} torr and flamed. After cooling the

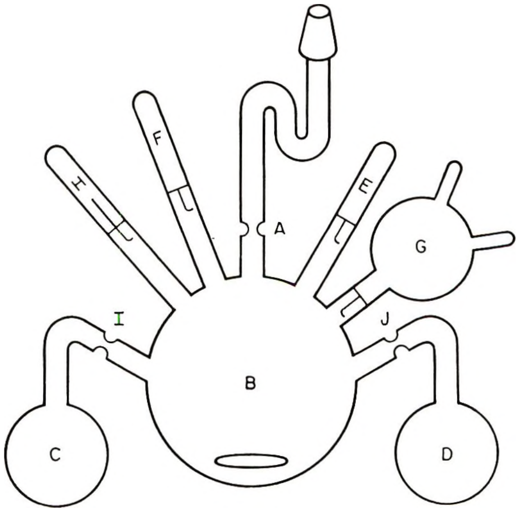

Fig. 3. Polymerization apparatus.

assembly, benzene was condensed into bulb B and degassed, and the reactor was sealed off at A. The initiator ampoule E was broken and the whole apparatus thoroughly rinsed with the benzene–initiator solution. The 4-vinylbiphenyl bulb G was next broken and the polymerization allowed to proceed about 4–5 hr, during which time the solution gradually developed a deep red color. A portion of the solution in B was then transferred to bulb C which was sealed off at I. Then the isoprene ampoule F was broken. Depending on the relative amounts of isoprene and 4-vinylbiphenyl, the color changes either abruptly or gradually to yellow. The polymerization was usually allowed to proceed overnight, and a portion of this solution was then transferred to bulb D, which is sealed off at J. The phosgene ampoule H was next broken, and the gas was allowed to diffuse very slowly into the polymer solution which was vigorously agitated until the solution became colorless. The reactor was opened, the material was poured into an excess of methanol, and based on the amount of polymer, about 1% of β-phenylnaphthylamine antioxidant was added. The coagulated polymer was filtered and dried overnight in a vacuum oven. The contents of bulbs C and D were also worked up and the contents used for characterization of the A and AB segments.

Polymer Characterization

The block copolymers were characterized by gel-permeation chromatography (GPC) and osmometry. Gel-permeation chromatography measurements were carried out on a Waters Associates unit using a combination of four columns filled with a crosslinked polystyrene gel having the following pore sizes: one 1×10^6, one 1.5×10^5, one 3×10^4, and one 8×10^3 Å. The operating conditions were toluene solvent at 70°C, pumped at 1 cc/min. Number-average molecular weight measurements were determined on a Mechrolab high-speed osmometer, and differential refractive indices were measured with a Brice-Phoenix instrument.

RESULTS AND DISCUSSION

The primary prerequisite to the synthesis of pure block copolymers is rigorous purity of the monomers. Isoprene is relatively easy to purify to a very high degree by distillation from sodium mirrors,[3] but the solid nature of 4-vinylbiphenyl makes its rigorous purification prohibitively difficult. Thus it was not possible to obtain a monomer which was entirely free of reactive impurities. Although styrene can be purified by distillation from small amounts of initiator,[4] this method could not be applied to 4-vinylbiphenyl.

Thus, a synthetic method had to be selected where the purity of the A monomer is not crucial for the attainment of homogeneous materials. A coupling technique, whereby the A monomer is polymerized first, the B monomer is then added, and the AB anion is next coupled with a reactive dihalide, provides such an approach, if a quantitative degree of coupling can be achieved. Using this technique the residual impurities in the A monomer will only destroy some initiator but will not lead to AB segment formation. By estimating the degree of purity of the A monomer, it is not difficult to use a slight excess of *n*-butyllithium to compensate for the amount of initiator destroyed.

The coupling of a polymer–lithium chain with reactive halides has been described in some detail in connection with the synthesis of branched polystyrenes.[5] However, to ensure complete reaction, an excess as large as 20% of polymer–lithium chains was used and the linear polymer later removed by fractionation. Furthermore, to ensure that proper stoichiometry was being used, the polymer–lithium species was first sampled and the molecular weight determined. Thus, this method was not considered satisfactory for the preparation of pure materials, and other techniques for achieving quantitative coupling were investigated.

It was considered that very slow addition of a highly reactive dihalide to a dilute polymer–lithium solution should result in a quantitative coupling reaction. A survey of the literature[6] indicated that phosgene would be an excellent candidate. Preliminary coupling studies with a 40,000 molecular weight polyisoprene–lithium with the use of gel-permeation chromatography as the analytical method showed that a virtually quantitative coupling could be achieved without concern for the stoichiometry of the reaction if the phosgene gas is added very slowly. Because very slow addition is so critical, a special tube with a very narrow capillary was constructed so that phosgene could only diffuse slowly into the vigorously agitated polymer-lithium solution. The construction of this tube is shown in Figure 2.

A particularly attractive aspect of preparing ABA block copolymers by a

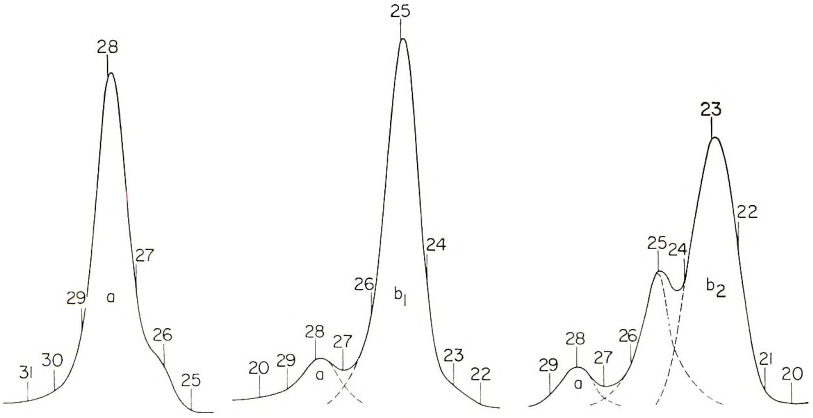

(a) (b) (c)

Fig. 4. Gel-permeation chromatograph of run 8871-13: (*a*) poly-4-vinylbiphenyl A segment; (*b*) poly-4-vinylbiphenyl–polyisoprene AB segment; (*c*) coupled AB segment. Composition of final product: homopolymer A, 4.7%; AB block, 26%; ABBA block, 69%.

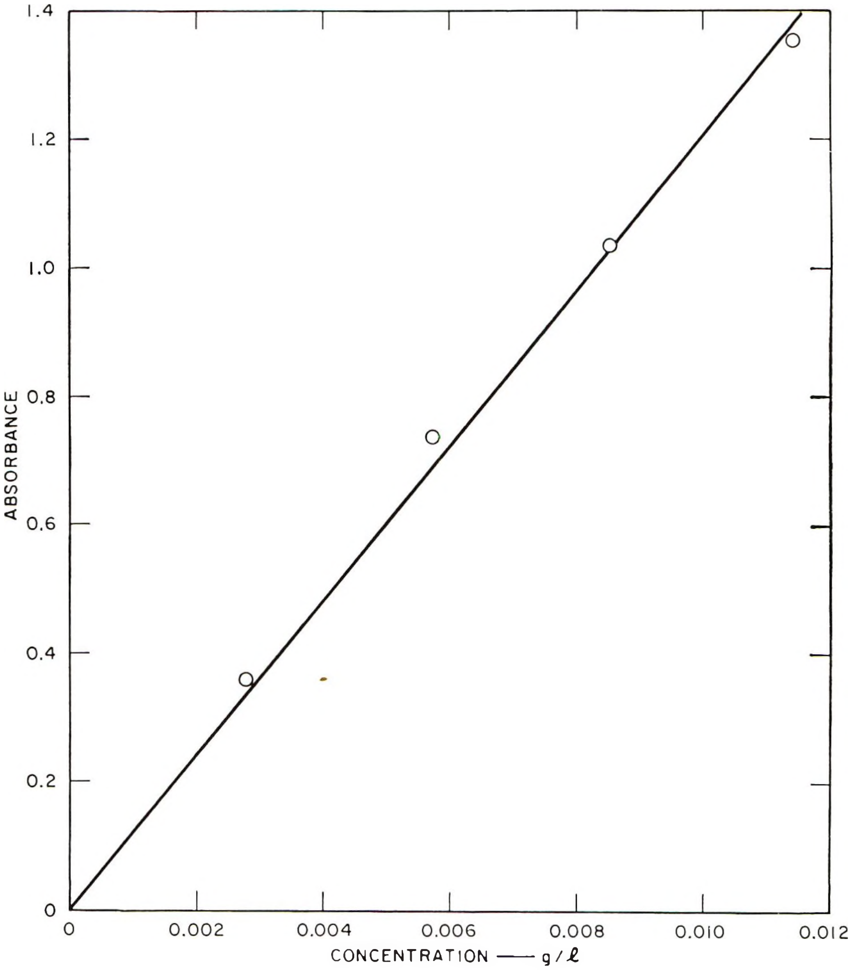

Fig. 5. Ultraviolet absorption at 2575 Å of poly-4-vinylbiphenyl in tetrahydrofuran as a function of concentration.

coupling technique is that the molecular weight of the ABA block is double that of the AB segment so that gel-permeation chromatography can easily resolve the polymer components. This is not always possible with polymers prepared by sequential addition, particularly materials which have an A segment of relatively low molecular weight. Figure 4 shows GPC traces of an A segment, an AB segment, and the coupled ABBA product, where the A and AB segments represent materials sampled from the actual run (bulbs C and D, Fig. 3).

Since GPC uses a differential refractometer as a detector, the peak area is proportional to the amount and to the refractive index increment of sample eluted. If the ratio of refractive index increments of the two homopolymers and the overall composition of the injected material are known, the constituent polymers in the sample can be quantitatively determined.

The overall composition of the sample can be calculated from the monomer feed, provided the conversion is quantitative, but it is better determined from the ultraviolet maximum of 4-vinylbiphenyl at 2575 Å using the calibration plot shown in Figure 5. In Figure 6 is shown a plot of re-

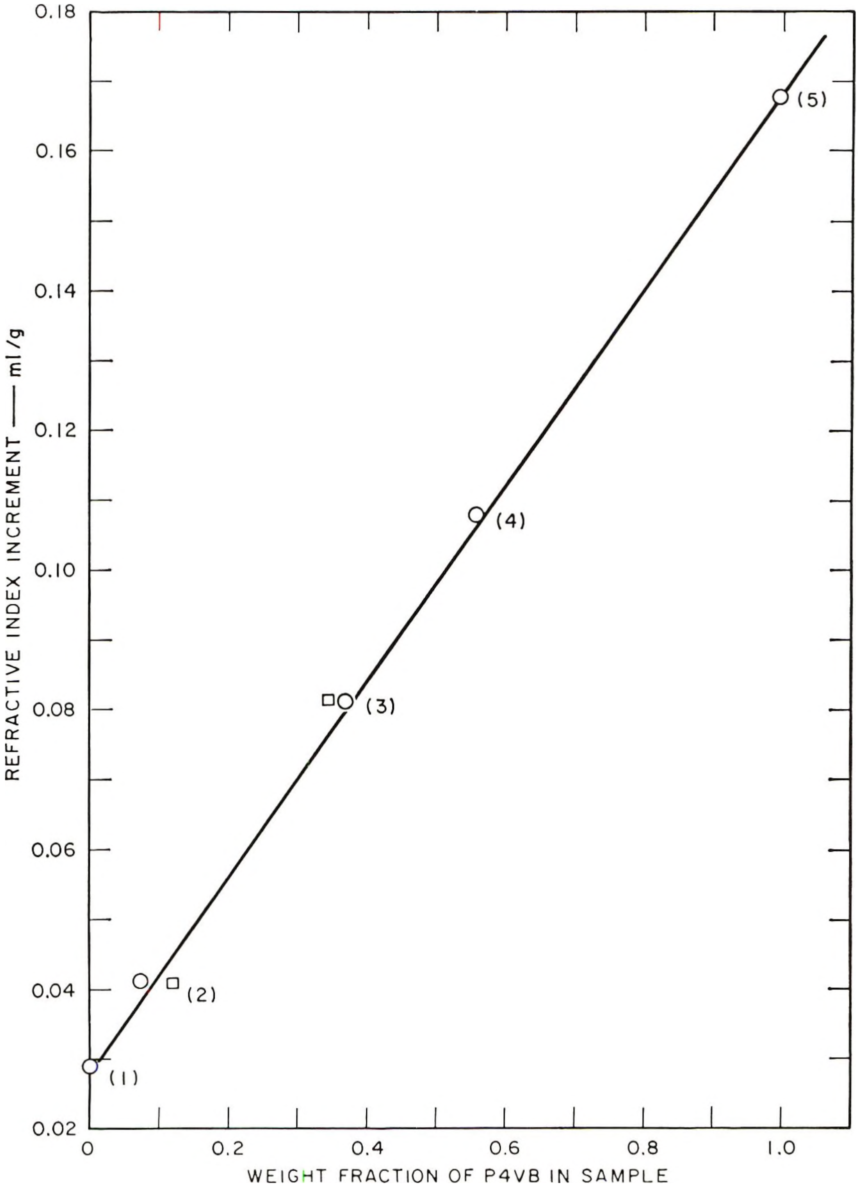

Fig. 6. Refractive index increment in toluene of 4-vinylbiphenyl (A)–isoprene (B) block copolymers as a function of weight fraction of 4-vinylbiphenyl. Samples and molecular weights are: (*1*) B (91,000), (*2*) ABBA (117,000), (*3*) AB (97,000), (*4*) AB (97,000) + ABA (124,000), (*5*) A (130,000); Weight fraction A calculated from (○) weight or (□) ultraviolet data.

fractive index increments ($\Delta n/C = \dot{n}$) at 5460 Å of various 4-vinylbiphenyl–isoprene block copolymers versus the weight fraction of poly-4-vinylbiphenyl. The linearity of the plot verifies that the contributions of the two homogeneous segments to the overall refractive index are additive. A similar additivity has also been noted for a poly(methyl methacrylate)–polystyrene system.[7]

In view of the linear relationship, the refractive index increment of the polymer can be expressed as follows:

$$\dot{n}_{\mathrm{A+B}} = \dot{n}_{\mathrm{B}} + W_{\mathrm{A}}(\dot{n}_{\mathrm{A}} - \dot{n}_{\mathrm{B}}) \tag{1}$$

where $\dot{n}_{\mathrm{A}}$ and $\dot{n}_{\mathrm{B}}$ are the refractive index increments of homopolymers A and B and W_{A} is the weight fraction of A in the sample. If the GPC trace shows a single peak of area a corresponding to homopolymer A and a single or double peak of total area b for the block (ABBA and/or AB), then the following relationships will hold:

$$W_{\mathrm{A}}^{a} = k(a/\dot{n}_{\mathrm{A}}) \tag{2a}$$

$$W_{\mathrm{AB}}^{b} = k(b/\dot{n}_{\mathrm{AB}}) \tag{2b}$$

$$W_{\mathrm{A}}^{a} + W_{\mathrm{AB}}^{b} = 1 = k(a + b)/\dot{n}_{\mathrm{A+B}} \tag{2c}$$

where W_{A}^{a} and W_{AB}^{b} are the weight fractions associated with the peak areas, k is a proportionality factor, and $\dot{n}_{\mathrm{A+B}}$ is the refractive index increment of the injected sample.

By dividing eq. (2a) by eq. (2c) and substituting for $\dot{n}_{\mathrm{A+B}}$ by eq. (1), one obtains:

$$W_{\mathrm{A}}^{a} = a/(a + b)\ (\dot{n}_{\mathrm{A+B}}/\dot{n}_{\mathrm{A}}) = a/(a + b)[(\dot{n}_{\mathrm{B}}/\dot{n}_{\mathrm{A}}) + W_{\mathrm{A}}\ (1 - \dot{n}_{\mathrm{B}}/\dot{n}_{\mathrm{A}})] \tag{3}$$

The weight fraction of A in the original material W_{A} can be determined, as already mentioned, from the ultraviolet spectrum and the ratio $\dot{n}_{\mathrm{B}}/\dot{n}_{\mathrm{A}}$ can be determined with a differential refractometer. Alternatively, a solution of known composition can be injected in a GPC unit, and, provided the two peaks are clearly resolved, $\dot{n}_{\mathrm{B}}/\dot{n}_{\mathrm{A}}$ evaluated as follows:

$$\dot{n}_{\mathrm{B}}/\dot{n}_{\mathrm{A}} = a_{\mathrm{B}}w_{\mathrm{A}}/a_{\mathrm{A}}w_{\mathrm{B}} \tag{4}$$

where a_i and w_i represent the respective peak areas and homopolymer weights.

Thus, with a knowledge of W_{A} and $\dot{n}_{\mathrm{B}}/\dot{n}_{\mathrm{A}}$, W_{A}^{a} can be calculated from eq. (3) and the weight fraction W_{AB}^{b} can be determined by simple arithmetic. Since in the case treated here the composition of AB and ABBA is the same, their relative amounts are equal to the respective areas

$$W_{\mathrm{AB}}^{b} = W_{\mathrm{AB}}^{\mathrm{tot}}\ b_1/(b_1 + b_2) \tag{5a}$$

$$W_{\mathrm{ABBA}}^{b} = W_{\mathrm{AB}}^{\mathrm{tot}}\ b_2/(b_1 + b_2) \tag{5b}$$

where b_1 and b_2 are the respective GPC areas of the AB and ABBA segments.

The results of a few representative runs are presented in Table I. Further synthetic work and mechanical evaluations are now in progress and will be reported at a later date.

TABLE I
Characterization of 4-Vinylbiphenyl-Isoprene ABBA Block Copolymers

	Molecular weight		Weight fraction of	Composition of block[4]		
Run no.	Total[1]	A Segment[2]	A, W_A[3]	$W_A{}^a$	$W_{AB}{}^{b_1}$	$W_{ABBA}{}^{b_2}$
8871-13	280,000	69,000	0.450	0.047	0.260	0.690
8871-15	112,000	4,000	0.075	0	0	1.000
8871-16	138,000	10,000	0.150	0.020	0.130	0.850

[1] By membrane osmometry.

[2] From eq. (1) and ultraviolet composition as follows: $\bar{M}_n$ (A) = %4VB × $\bar{M}_n$ total/2.

[3] From ultraviolet at 2575 Å.

[4] From GPC.

This work was performed for the Jet Propulsion Laboratory, California Institute of Technology, sponsored by the National Aeronautics and Space Administration under Contract NAS 7-523.

References

1. G. Holden, E. T. Bishop, and N. R. Legge, *J. Polym. Sci. C.*, **26**, 37 (1968)
2. E. Franta and P. Rempp, *Compt. Rend.*, **254**, 674 (1962).
3. M. Morton, E. E. Bostick, and R. G. Clarke, *J. Polym. Sci. A*, **1**, 475 (1963).
4. M. Morton, A. Rembaum, and J. L. Hall, *J. Polym. Sci. A*, **1**, 461 (1963).
5. J. A. Gervasi and A. B. Gosnell, *J. Polym. Sci. A-1*, **4**, 1391 (1966).
6. G. Finaz, Y. Gallot, J. Parrod, and P. Rempp, *J. Polym. Sci.*, **58**, 1363 (1962).
7. S. Krause, *J. Phys. Chem.*, **65**, 1618 (1961).

Received April 21, 1968

JOURNAL OF POLYMER SCIENCE: PART A-1 VOL. 7, 83-99 (1969)

La Luminescence différée du Styrène en Solution vitreuse dans le Méthylcyclohexane

K. HAYASHI,* *Centre d'Etudes Nucléaires, Saclay, France,*
A. DÉROULÈDE, et F. KIEFFER,
Laboratoire de Physico-chimie des Rayonnements,
Faculté des Sciences, Orsay, France

Synopsis

The trapping of electrons and styrene cations and anions has been studied in a methylcyclohexane glass by the techniques of deferred luminescence. *Radiothermoluminescence* curves consist of two peaks, at 90 and 95°K, in this matrix. The second peak increases linearly with styrene concentration up to $2 \times 10^{-2}M$ when it reaches a constant value, whereas the first peak increases from 10^{-4} to $10^{-3}M$ and then decreases at higher concentrations and is not discernible at concentrations above $10^{-2}M$. We propose two mechanisms which are qualitatively consistent with this behavior and are based essentially on the recombination of styrene cations with thermally detrapped electrons in the first peak and with anions in the second peak. *Photothermoluminescence* (i.e., thermoluminescence after photoionization with ultraviolet light) similarly consists of the 90 and 95°K peaks for a $10^{-3}M$ solution and of the 95° peak alone for a 10^{-d} M solution.

Radiophotoluminescence excitation spectra at 77°K, corresponding to absorption spectra of trapped electrons and styrene anions, show that anions are the predominant negative species in 10^{-2} molar solution, and trapped electrons in 10^{-3} molar solution. *Spectral analysis* of radiothermoluminescence shows the presence of two emission bands, one of which is identical with styrene fluorescence excited by the 254 Nm mercury line (λ_{max} = 292, 302, 307, and 317 Nm). The other band has three fairly poorly resolved maxima at 474, 486 and 496 nm and seems to correspond to the fluorescence of $C_6H_5\dot{C}H$-CH_3 radicals formed during radiolysis.

Il a été montré récemment[1–5] qu'en phase liquide la polymérisation du styrène sous rayonnement s'effectue par un mécanisme ionique lorsque le styrène est soigneusement purifié et lorsqu'il est débarrassé notamment de traces d'eau, d'anhydride carbonique et d'oxygène. Rappelons que des études cinétiques ont donné les valeurs suivantes pour les constantes de vitesse de polymérisation par les trois mécanismes possibles: cationique $3{,}5 \times 10^6$,[3,5] anionique $6{,}5 \times 10^4$,[6] et radicalaire 35[7] mole^{-1} sec^{-1} à 20°C. L'étude de la conductivité[4] a confirmé l'intervention des ions. En présence des impuretés déjà énumérées, les mécanismes ioniques sont supprimés.

Les centres actifs responsables de la polymérisation ionique du styrène ont été identifiés par d'autres techniques. Ainsi, Metz et coll.[8] ont observé

---

* Adresse permanente: Department of Polymer Chemistry, Kyoto University, Kyoto, Japan.

l'anion styrène en phase liquide par radiolyse pulsée. Son maximum d'absorption se situe à 370 nm et sa durée de vie est 4×10^{-6} sec. La présence d'eau inhibe sa formation. Le cation styrène n'a pas été observé par ces auteurs.

Les anions et les cations de styrène piégés dans des matrices vitreuses ont été mis en évidence par RPE.[9] Les spectres RPE constituent des singulets de 15 gauss pour l'anion et de 23 gauss pour le cation. La distinction entre les deux est basée sur la nature de la matrice piégeante et sur le blanchiment par la lumière visible. Ainsi, dans le méthyl-2 tétrahydrofuranne (capteur de charges positives), l'ion observé est l'anion, tandis que dans le chlorure de *n*-butyle (capteur d'électrons), c'est le cation. L'anion disparaît par blanchiment optique, mais pas le cation.

Les spectres d'absorption ont été étudiés dans des matrices vitreuses.[10,11] Les valeurs de λ_{max} sont 350, 460, et 640 nm pour le cation, 400 et 590 nm pour l'anion.

D'autre part, l'étude de la luminescence différée d'hydrocarbures aromatiques dans un verre de méthylcyclohexane[12] permet de distinguer deux mécanismes de recombinaison des cations aromatiques A^+ piégés: la courbe de radiothermoluminescence d'un tel verre comporte deux pics, à 90 et à 95°K, dont le premier correspond à la libération thermique des électrons piégés, à leur diffusion et à la recombinaison

$$e^- + A^+ \rightarrow A^* \rightarrow A + h\nu$$

et le deuxième correspond à la diffusion des espèces moléculaires et à la recombinaison anion-cation:

$$A^- + A^+ \rightarrow A + A^* \rightarrow A + h\nu$$

Lorsque le dépiégeage est effectué optiquement à 77°K, l'électron libéré qui se recombinera avec le cation provient, selon l'énergie de la lumière excitatrice, du dépiégeage d'un électron piégé ou du détachement à partir d'un anion.[12,13]

Il nous a semblé intéressant d'étudier le piégeage d'espèces chargées dans des solutions vitreuses de styrène dans le méthylcyclohexane, par les techniques de la luminescence différée.

METHODES EXPERIMENTALES

Purification des produits

Le méthylcyclohexane (Eastman-Kodak, spectro grade) était purifié par chromatographie gazeuse.

Le styrène était lavé par la soude, puis par l'eau, séché sur tamis moléculaire et distillé deux fois sous vide. Il était redistillé immédiatement avant la préparation des solutions, par évaporation à la température ambiante et condensation à 77°K.

Le méthyltétrahydrofuranne (Serlabo) et le chlorure de *n*-butyle (Prolabo) étaient séchés sur tamis moléculaire et distillés.

Radiothermoluminescence (RTL)

Des échantillons de 0,5 cm^3 de solution de styrène dans le méthylcyclohexane étaient dégazés par des cycles de congélation, pompage et fusion, dans une cellule en cuivre décrite précédemment.[14] La pression résiduelle était 10^{-4} mm de mercure environ. Pour éviter une cristallisation partielle, il est nécessaire de refroidir les solutions le plus rapidement possible: nous avons atteint ce résultat en posant la cellule dans l'azote liquide sur un bloc de cuivre préalablement refroidi.[15] L'absence de zones cristallisées était vérifiée à la fin de l'enregistrement de la courbe de thermoluminescence par l'absence d'un troisième pic situé vers 120°K.

L'irradiation était faite à l'aide d'une source de cobalt 60 de 120 curies. Des échantillons de différentes concentrations étaient irradiés avec une même dose de 4800 rad, le débit de dose étant 80 rad/min.

Après l'ouverture de la cellule sous azote liquide, celle-ci était transférée dans un cryostat rempli d'azote liquide, et reliée à un photomultiplicateur (Radiotechnique 51 UVP) par un guide de lumière en silice Suprasil. Un thermocouple était placé entre l'échantillon et le guide de lumière. Le courant anodique, proportionnel à la quantité de lumière émise, et la température étaient enregistrés simultanément, ce qui nous permettait de construire la courbe de thermoluminescence (intensité lumineuse en fonction de la température, pendant une montée linéaire de celle-ci). La vitesse de réchauffement était d'environ 2°C/min.

Blanchiment optique

Des courbes de RTL ont été enregistrées après blanchiment par la lumière d'une lampe quartz-iode à filament de tungstène, de 600 W, sans filtre et à travers un filtre en silicium transmettant seulement l'infra-rouge de longueur d'onde supérieure à $1{,}1\mu$.

Analyse spectrale de la RTL

Afin de disposer d'une plus grande quantité de lumière pour l'analyse spectrale, nous avons effectué cette analyse sur des échantillons $10^{-2}M$ irradiés à l'aide d'une source de ^{60}Co de 2000 curies: dose 1,5 Mrad, avec un débit de dose de 0,7 Mrad/heure. Les cellules en cuivre utilisées pour ces expériences étaient profondes de quelques millimètres seulement et s'adaptaient dans un cryostat spécial muni de deux guides de lumière placés à angle droit l'un par rapport à l'autre. Ce dispositif a été décrit antérieurement.[12]

Par un photomultiplicateur (Radiotechnique 150 UVP) en contact avec l'un des guides de lumière on enregistrait la courbe de thermoluminescence globale. L'autre guide de lumière conduisait à un monochromateur à la sortie duquel on enregistrait le spectre de l'émission au cours du réchauffement, à l'aide d'un deuxième photo multiplicateur (E.M.I. 9558 BQ). Un moteur à deux sens de rotation, monté sur le mono chromateur (Jobin-Yvon), faisait tourner le prisme de manière à balayer le domaine spectral compris entre 280 et 600 nm en deux minutes, alternativement dans un sens et dans l'autre. Ce montage était analogue à celui décrit antérieurement,[16] mais le balayage plus lent et la vitesse de réchauffement moindre (environ 1°C/min) permettaient d'enregistrer le spectre sur un enregistreur galvanométrique (Sefram Graphispot VAC).

L'étalonnage des longeurs d'onde était fait avec les raies d'une lampe à vapeur de mercure basse pression. Le spectre de photoluminescence des mêmes solutions vitreuses, servant de référence, était pris dans le même cryostat contenant un échantillon non irradié, placé à 45° par rapport aux deux guides de lumière; l'excitation se faisait par la raie 253,7 nm du mercure, isolée par un deuxième monochromateur.

Spectres d'Excitation de la Radiophotoluminescence (RPL)

La technique utilisée était celle décrite antérieurement;[12,13] le cryostat et les cellules contenant les échantillons étaient les mêmes que pour l'analyse spectrale de la RTL. Après l'irradiation (dose d'environ 100 krad), l'échantillon, conservé à 77°K, était éclairé, à travers l'un des deux guides de lumière par des éclairs de 0,25 sec d'une lumière dont on faisait varier la longueur d'onde entre 350 et 2500 nm. Par le jeu de deux obturateurs électromécaniques synchronisés, un photomultiplicateur (E.M.I. 9558 BQ) en contact avec le deuxième guide de lumière était découvert 0,2 sec après la fin de l'excitation. Le signal anodique était photographié sur l'écran d'un oscilloscope. En portant l'intensité de ce signal au temps zéro en fonction du nombre d'onde de la lumière excitatrice, on obtient le spectre d'excitation de la RPL.

Photothermoluminescence (PTL)

Le mode opératoire était identique à celui employé en RTL, mais l'ionisation était produite par irradiation avec la raie 253,7 nm d'une lampe à mercure basse pression, munie d'un filtre Corning 7.54.

RÉSULTATS EXPÉRIMENTAUX ET INTERPRÉTATION

Étude des Courbes de RTL des Verres de Méthylcyclohexane en Fonction de la Concentration de Styrène

Une étude en fonction de la dose faite antérieurement[15] a montré que, aux faibles doses utilisées dans le présent travail, la quantité de lumière émise par des solutions de durène dans le méthylcyclohexane variait linéairement avec la dose, quelles que soient les concentrations utilisées. Nous étions donc très nettement en-dessous des doses de saturation où toutes les molécules de soluté risqueraient d'être ionisées dans les solutions les plus diluées. Dans le présent travail, les conditions étaient par conséquent comparables pour toutes les solutions utilisées. Après irradiation, une faible proportion seulement des molécules de styrène dispersées dans le verre étaient ionisées: au maximum 15% pour la solution la plus diluée ($10^{-4}M$), en admettant que $G = 3$ paires d'ions par 100 eV et en négligeant le fait qu'une partie de ces ions se recombinent avant d'être piégés.

Avant d'enregistrer les courbes de RTL, nous laissions décroître pendant environ une demi-heure la luminescence émise "spontanément" à 77°K. Nous obtenions ainsi des courbes de déclin qu'on pouvait décomposer en une succession de deux ou trois exponentielles, comme cela avait déjà été signalé par ailleurs.[17,18] La quantité de lumière émise à 77°K augmente avec la concentration en styrène: si l'on prend comme unité la quantité émise par une solution $10^{-3}M$, on trouve 4,7 pour une solution $10^{-2}M$ et 6,5 pour une solution $10^{-1}M$.

La courbe de RTL comporte deux pics, situés à 90 ± 1 et à 95 ± 1°K, comme dans le cas d'autres solutés étudiés antérieurement en solution dans le méthylcyclohexane.[19] La Figure 1 montre des courbes de RTL

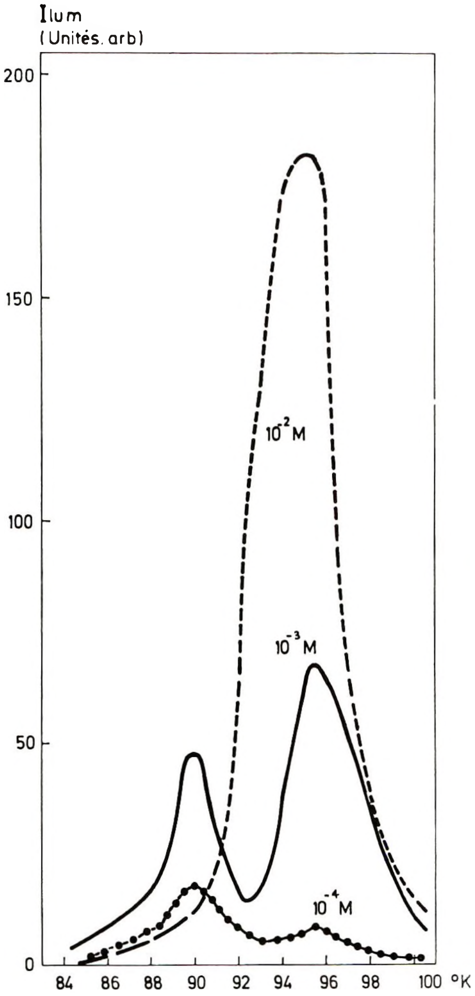

Fig. 1. Courbes de RTL de solutions vitreuses de styrène dans le méthylcyclohexane.

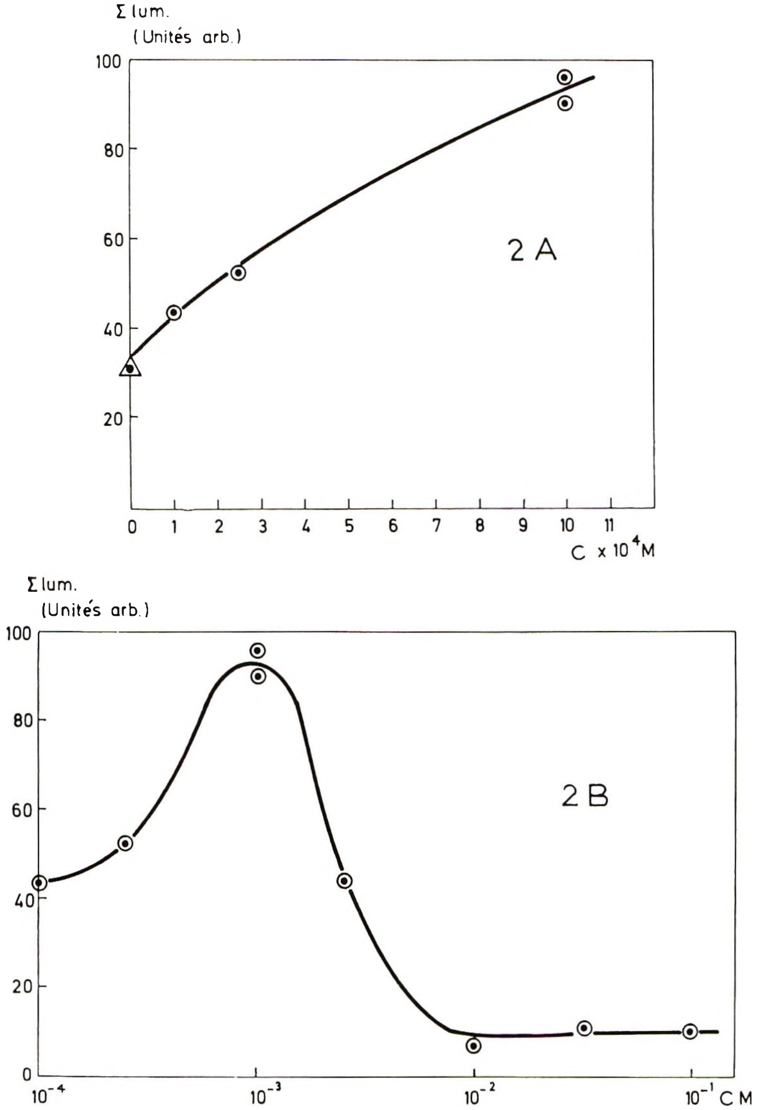

Fig. 2. Evolution de la quantité de lumière émise au cours du premier pic de RTL avec la concentration de styrène: (*A*) faibles concentrations (échelle linéaire) (*B*) ensemble des concentrations étudiées (échelle logarithmique).

typiques obtenues à 3 concentrations différentes. Il apparaît que le deuxième pic augmente régulièrement avec la concentration, tandis que le premier pic augmente lorsqu'on passe d'une solution $10^{-4}M$ à une solution $10^{-3}M$, mais n'est plus discernable pour la solution $10^{-2}M$. Pour suivre cette évolution de manière plus détaillée, nous avons tracé des courbes donnant, en fonction de la concentration, la quantité de lumière émise au cours de chaque pic, c'est-à-dire la surface intégrée comprise sous chaque pic. Les courbes de la Figure 2 montrent l'évolution du premier pic avec la concentration. On voit que la quantité de lumière émise croît en passant du solvant pur à une solution $10^{-3}M$ de styrène (courbe A, échelle linéaire des concentrations) et qu'elle décroît aux concentrations supérieures à $10^{-3}M$ (courbe B, échelle logarithmique des concentrations). Comme le montre la Figure 3 (courbe A), le deuxième pic croît linéairement avec la concentration jusqu'à une concentration comprise entre $10^{-3}M$ et $10^{-2}M$, pour atteindre un palier à $2 \times 10^{-2}M$. La partie linéaire apparait plus clairement, pour les concentrations inférieures à $10^{-3}M$, sur la courbe B où l'échelle des concentrations est dilatée d'un facteur 100.

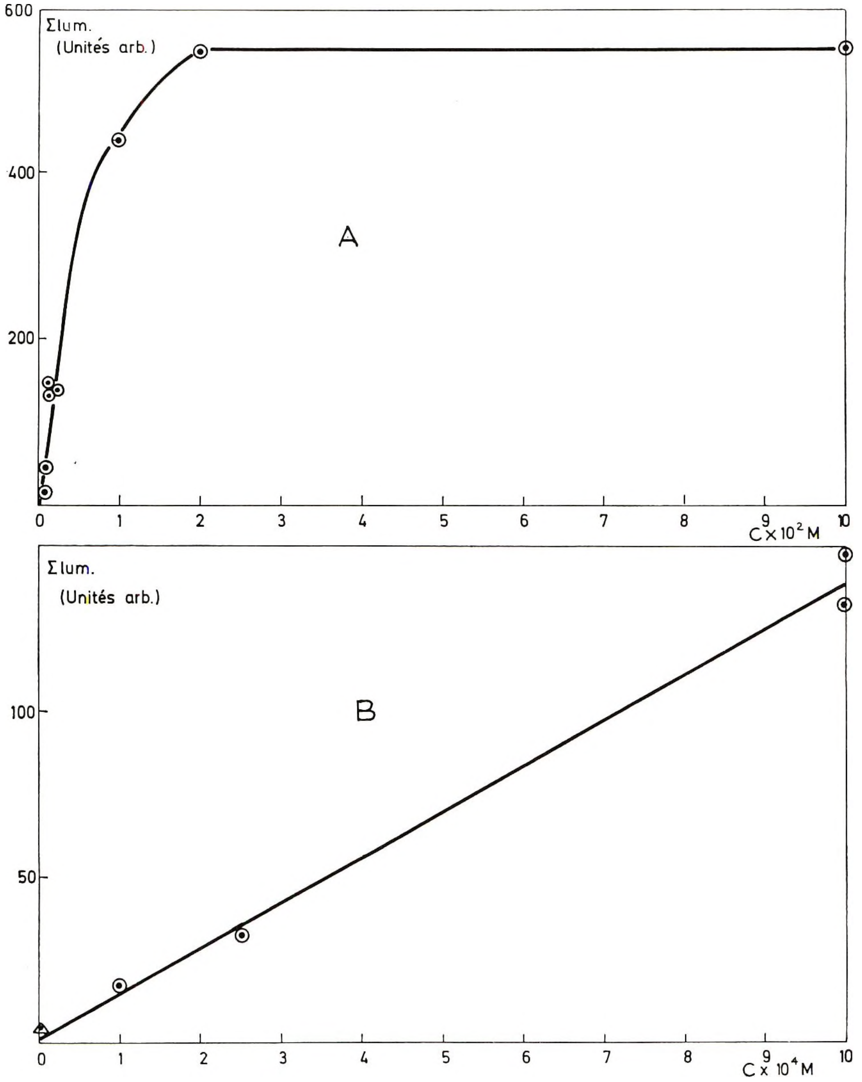

Fig. 3. Evolution de la quantité de lumière émise au cours du deuxième pic de RTL avec la concentration de styrène: (A) ensemble des concentrations utilisées; (B) faibles concentrations (échelle dilatée 100×).

Pour interpréter ces résultats, rappelons les différentes réactions qui peuvent avoir lieu au cours de l'irradiation et au cours du réchauffement, en omettant les réactions purement radicalaires qui ne semblent pas intervenir dans la RTL.[18] Les symboles utilisés sont: S pour les molécules de solvant, A pour les molécules de soluté aromatique, P pour les pièges physiques, R pour les radicaux.

*Pendant l'irradiation:**

$$\mathrm{S} \rightsquigarrow \mathrm{S}^{+} + e^{-} \tag{1}$$

$$\mathrm{S} \rightsquigarrow \mathrm{R}\cdot + \mathrm{R}'\cdot \tag{2}$$

$$e^{-} + \mathrm{P} \rightarrow e_{\mathrm{p}}^{-} \text{ (électron piégé)} \tag{3}$$

$$e^{-} + \mathrm{A} \rightarrow \mathrm{A}^{-} \tag{4}$$

$$e^{-} + \mathrm{R}\cdot \rightarrow \mathrm{R}^{-} \tag{5}$$

$$\mathrm{S}^{+} + \mathrm{A} \rightarrow \mathrm{S} + \mathrm{A}^{+} \tag{6}$$

Vu les concentrations, on peut négliger l'effet direct du rayonnement sur les molécules de soluté.

Au cours du premier pic de RTL (où la diffusion des espèces moléculaires n'est pas possible):

$$e_{p}^{-} \rightarrow e^{-} \text{ (électron mobile)} \tag{7}$$

$$e^{-} + \mathrm{S}^{+} \rightarrow \mathrm{S}^{*} \tag{8}$$

suivi d'une désexcitation non radiative, sauf si un transfert d'excitation sur une molécule A pas trop éloignée est possible.

$$e^{-} + \mathrm{A}^{+} \rightarrow \mathrm{A}^{*} \rightarrow \mathrm{A} + h\nu \tag{9}$$

$$e^{-} + \mathrm{A} \rightarrow \mathrm{A}^{-} \tag{10}$$

Au cours du deuxième pic de RTL (où la diffusion des espèces moléculaires peut avoir lieu)

$$\mathrm{A}^{-} + \mathrm{A}^{+} \rightarrow \mathrm{A} + \mathrm{A}^{*} \rightarrow \mathrm{A} + h\nu \tag{11}$$

$$\mathrm{A}^{-} + \mathrm{S}^{+} \rightarrow \mathrm{A} + \mathrm{S}^{*} \xrightarrow[\text{d'excitation}]{\text{Transfert}} \mathrm{S} + \mathrm{A}^{*} \rightarrow \mathrm{A} + h\nu \tag{12}$$

$$\mathrm{R}^{-} + \mathrm{A}^{+} \rightarrow \mathrm{R}\cdot + \mathrm{A}^{*} \rightarrow \mathrm{A} + h\nu \tag{13}$$

$$\mathrm{R}^{-} + \mathrm{S}^{+} \rightarrow \mathrm{R}\cdot + \mathrm{S}^{*} \xrightarrow{+\mathrm{A}} \mathrm{R}\cdot + \mathrm{A}^{*} \rightarrow \mathrm{A} + h\nu \tag{14}$$

Voyons comment change l'importance relative de ces réactions lorsque la concentration de A augmente. D'abord, pendant l'irradiation, par compétition entre les pièges P et les molécules A,[21-24] les réactions (3) et (5) sont défavorisées à l'avantage de (4); d'autre part la réaction (6) est

---

* Pour une discussion détaillée du sort des électrons éjectés par les photons γ, voir Magat.[20]

favorisée. Donc, parmi les espèces piégées, la concentration de S^+, e_p^-, et R^- diminue, tandis que celle de A^+ et A^- augmente.

Au cours du premier pic, la réaction (7) fournira moins d'électrons disponibles pour les diverses recombinaisons. La réaction (8) perdra en importance parce que le nombre de S^+ a diminué tandis que l'importance relative de (9) et de (10) sera augmentée. Comme seule la réaction (9) peut conduire à une émission de lumière, la quantité de lumière émise tendra à diminuer parce que le nombre d'électrons piégés sera moindre et elle tendra, d'autre part, à augmenter parce que, après leur dépiégeage, ces électrons réagiront en plus forte proportion selon (9). Nous pouvons donc expliquer qualitativement la courbe de la Figure *2B:* jusqu'à une concentration $10^{-3}M$, le nombre d'électrons piégés n'a pas été réduit trop considérablement par suite de la compétition du styrène pour les électrons résultant de (1). C'est l'augmentation du nombre de cations styrène qui l'emporte et la quantité de lumière émise croît. Au contraire, lorsque la concentration atteint $10^{-2}M$, le nombre d'électrons piégés a été réduit à un tel point que la réaction (9) n'a pratiquement plus lieu, faute d'électrons disponibles. Nous verrons plus loin que les spectres d'excitation de la RPL confirment cette hypothèse: dans la solution $10^{-3}M$ de styrène, le spectre des électrons piégés est beaucoup plus intense que celui des anions styrène, tandis que c'est l'inverse dans la solution $10^{-2}M$.

Au cours du deuxième pic, les quatre réactions envisagées peuvent conduire à l'émission de lumière. La réaction (11) sera doublement favorisée par une concentration accrue de A [réactions (4) et (6)], tandis que (12) et (13) seront à la fois favorisées [réactions (4), respectivement (6)] et défavorisées [réactions (6), respectivement (5)]. Enfin, la réaction (14) sera doublement défavorisée [réactions [5] et (6)]. Malgré la grande affinité électronique des radicaux, qui peut en faire des pièges à électrons,[25–28] les réactions (13) et (14) sont négligeables dans les expériences de RTL décrites ici, à cause de la faible dose employée. Si le transfert de charge (6) se fait à d'assez grandes distances, ce que nous ne pouvons pas affirmer pour le moment, la réaction (12) sera peu importante en comparaison avec (11). Si (11) est ainsi la réaction prédominante qui donne naissance au deuxième pic, il est normal de trouver pour ce pic une relation linéaire avec la concentration de styrène. Le palier observé aux concentrations supérieures à $2 \times 10^{-2}M$ est vraisemblablement dû à la limite de solubilité du styrène dans le MCH à basse température: l'augmentation de la quantité de styrène présente n'a alors pour seul effet que l'augmentation du nombre ou de la taille des cristallites de styrène qui se forment lors du refroidissement, la concentration des molécules dispersées dans le verre restant constante.

Comme nous l'avons vu, la quantité de lumière émise pendant la décroissance isotherme à 77°K augmente encore avec la concentration, lorsque le premier pic de RTL est déjà fortement réduit par suite de la diminution du nombre d'électrons piégés, entre $10^{-3}M$ et $10^{-2}M$ et même jusqu'à $10^{-1}M$. Il faut admettre que la luminescence observée à 77°K est due seulement à des électrons piégés assez près des cations de styrène pour qu'ils aient une forte probabilité de se recombiner avec eux lors des dépiégeages et repiégeages successifs postulés par Debye et Edwards.[29] Il semble que le nombre d'électrons piégés à proximité des cations de styrène augmente avec la concentration de styrène, bien que le nombre total d'électrons piégés diminue.

Effet du Blanchiment optique et d'Additifs sur la RTL

Les expériences de blanchiment optique à 77°K ont donné des résultats qui sont en accord avec les mécanismes que nous venons d'exposer. Ces résultats sont représentés dans la Figure 4. Ils ont tous été obtenus avec une solution de styrène $10^{-3}M$ dans le MCH. Le courbe A représente la RTL normale d'un tel échantillon. La courbe B montre que le premier pic a complètement disparu après un éclairement de 30 minutes dans l'infrarouge ($\lambda > 1{,}1\mu$). On sait que, dans les matrices d'hydrocarbures, l'électron piégé absorbe dans ce domaine spectral[30] et qu'un éclairement prolongé aboutit au dépiégeage complet des électrons.[12] La disparition du premier pic confirme donc que ce pic est dû aux électrons piégés [réactions (7) et (9)].

Si l'éclairement est effectué sans filtre, c'est-à-dire avec une lumière qui comporte, outre l'infra-rouge, le visible et du proche ultra-violet, il ne subsiste aucune RTL (courbe *C*). L'anion styrène absorbe à 400 et à 590 nm (25000 et 17000 cm^{-1})[11] et l'éclairement dans les bandes d'absorption des anions conduit au photodétachement d'un électron à partir de ces anions.[12,23,31] En éclairant dans un vaste domaine spectral couvrant à la fois les bandes d'absorption des électrons piégés et des anions styrène, nous avons fait disparaître les deux, et les réactions (11) et (12), comme la réaction (7) ne peuvent plus avoir lieu.

Après irradiation d'une solution $10^{-3}M$ de styrène contenant en outre du méthyl-2 tétrahydrofuranne ($10^{-1}M$) qui est un capteur de charges positives,[9,24] nous avons obtenu la courbe 4D. On voit que les deux pics ont diminué considérablement, mais que leur rapport reste sensiblement le même. On peut attribuer cet effet à une réaction compétitive avec la réaction (6):

$$\text{S}^+ + \text{MTHF} \rightarrow \text{S} + \text{MTHF}^+$$

La recombinaison de MTHF^+ avec les espèces négatives conduirait à une molécule excitée de MTHF^* dont la désactivation serait non radiative.

De même, pour une solution $10^{-3}M$ de styrène contenant du chlorure de *n*-butyle ($10^{-1}M$), on obtient la courbe 4*E*. L'efficacité des composés halogénés comme capteurs d'électrons par attachement dissociatif est bien connue.[11] Il n'est donc pas surprenant que les réactions (3), (4), et (5) soient pratiquement supprimées au bénéfice de la formation de Cl^-. La suppression du premier pic est donc normale. La recombinaison de Cl^- avec A^+ a apparement un rendement lumineux très faible ou même nul,

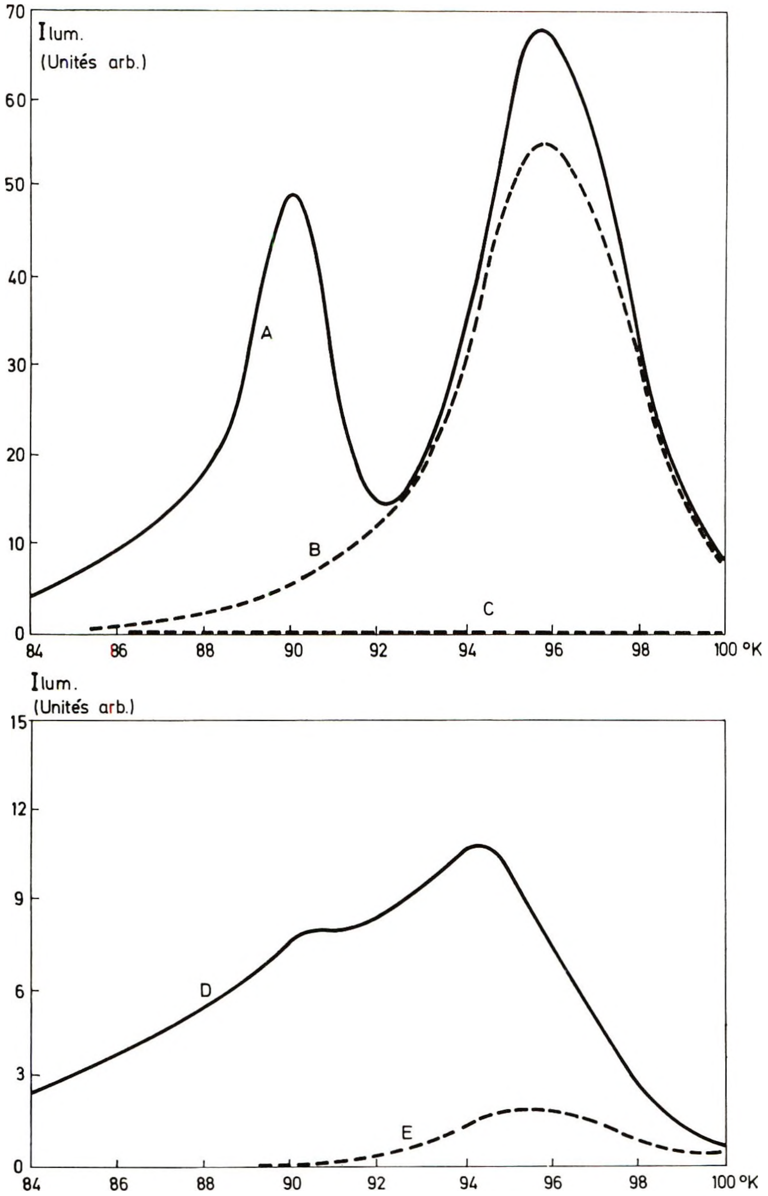

Fig. 4. Influence du blanchiment optique et de la présence d'additifs sur la courbe de RTL d'une solution de styrene $10^{-3}M$: (A) courbe normale; (B) courbe obtenue après blanchiment par l'infra-rouge ($\lambda > 1{,}1\mu$); (C) courbe obtenue après blanchiment par la lumière totale d'une lampe à filament de tungsténe; (D) courbe obtenue en présence de méthyl-2 tétrahydrofuranne ($10^{-1}M$); (E) courbe obtenue en présence de chlorure de n-butyle ($10^{-1}M$).

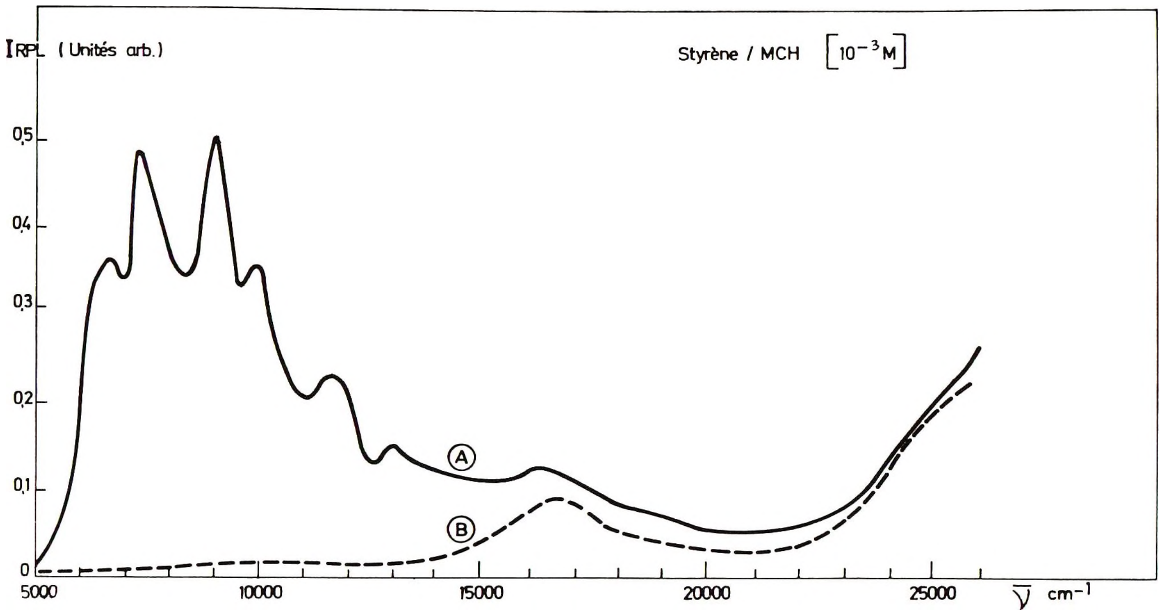

Fig. 5. Spectre d'excitation de la RPL d'une solution de styrène $10^{-3}M$: (*A*) non blanchie; (*B*) après blanchiment par l'infra-rouge.

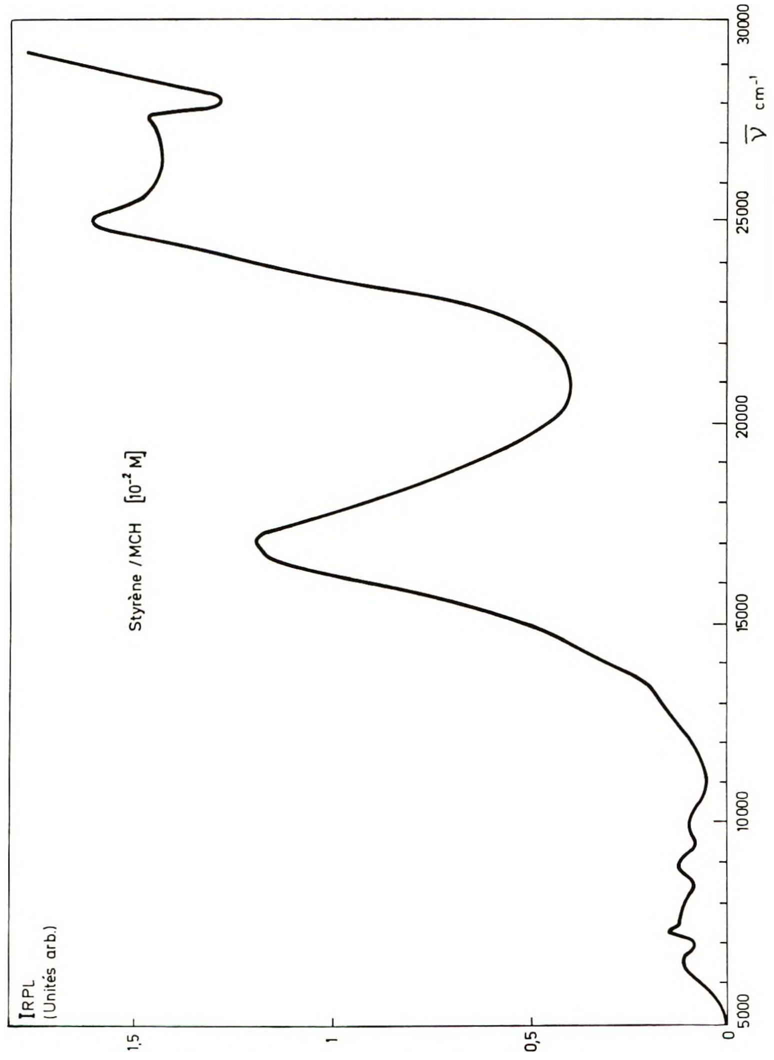

Fig. 6. Spectre d'excitation de la RPL d'une solution de styrène $10^{-2}M$.

le deuxième pic extrêmement réduit qui est encore observé pouvant être dû aux anions de styrène peu nombreux qui auraient quand même été formés selon la réaction (4).

Spectres d'Excitation de la RPL

Les spectres d'excitation de RPL des Figures 5 et 6 font apparaître une réponse à l'excitation dans trois domaines de fréquences. La bande située entre 5000 et 12000 cm^{-1} correspond à l'absorption des électrons piégés[30,31] et les deux bandes situées à 17000 et 25000 cm^{-1} correspondent à l'absorption des anions de styrène.[11] La structure apparaissant dans la région où les électrons piégés absorbent n'est pas due à l'absorption des électrons piégés, mais à celle du solvant.[12]

On voit que, dans la solution $10^{-3}M$ (Fig. 5), les électrons piégés prédominent, tandis que dans la solution $10^{-2}M$ (Fig. 6), on observe surtout la réponse due aux anions styrène. Cela démontre clairement l'augmentation du nombre d'anions styrène et la diminution du nombre d'électrons piégés lorsqu'on passe d'une solution $10^{-3}M$ à une solution $10^{-2}M$.

Le blanchiment optique dans l'infra-rouge fait disparaître la réponse dans le domaine d'absorption des électrons piégés (Fig. 5, courbe *B*), comme cela a été signalé pour d'autres solutés.[12]

Analyse spectrale de la RTL

Pour pouvoir comparer les spectres de photoluminescence et de RTL du styrène dans le MCH, nous avons enregistré ces deux spectres avec le même appareillage. Dans le spectre de photoluminescence nous avons trouvé seulement la fluorescence avec des maximums à 292, 302, 307, et 317 nm (Fig. 7, courbe *A*). Dans le spectre de RTL (courbe *B*), on observe les

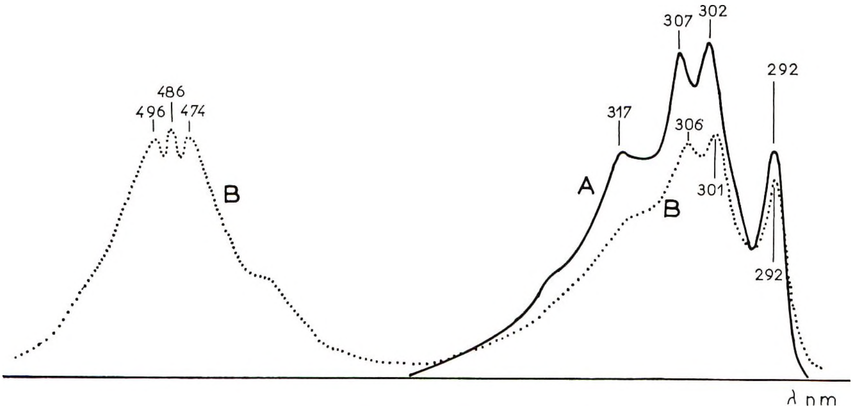

Fig. 7. Analyses spectrales de solutions de styrène $10^{-2}M$: (*A*) spectre de photoluminescence (λ_{exc} = 253.7 nm); (*B*) spectre de RTL (spectre corrigé en tenant compte de la variation de l'intensité de luminescence).

mêmes bandes d'émission et en outre une bande assez mal résolue comportant des maximums à 474, 486, et 496 nm et qui correspond vraisemblablement à la fluorescence du radical $C_6H_5—\dot{C}H—CH_3$ formé[32] au cours de la radiolyse et dont l'émission pourrait être due à un transfert d'énergie à partir des molécules de styrène excitées, soit à partir du mécanisme "trivial" d'émission et de réabsorption, soit par transfert résonnant.[33]

Photothermoluminescence du Styrène dans le Méthylcyclohexane

L'irradiation du styrène en solution vitreuse dans le MCH par la lumière ultra-violette ($\lambda = 253{,}7$ nm) conduit également à son ionisation, comme le montrent les courbes de photothermoluminescence de la Figure 8. Comme dans la RTL, la courbe de PTL comporte les deux pics pour la solution $10^{-3}M$ et seulement le deuxième pic pour la solution $10^{-2}M$. On peut donc admettre que, dans la solution $10^{-2}M$, pratiquement tous les électrons libérés dans le processus de photoionisation sont capturés par des molécules de styrène. Le mécanisme, beaucoup plus simple ici que dans le cas de la RTL, a été étudié en détail récemment pour des solutions de durène dans le MCH.[34] Le solvant n'absorbe pas le rayonnement utilisé, et seul le soluté s'ionise:

$$A \xrightarrow{h\nu} A^+ + e^-$$

Les seules réactions possibles ensuite pendant l'irradiation sont les réactions (3) et (4) du schéma que nous avons donné plus haut pour l'irradiation γ. Par conséquent, la formation d'un anion A^- implique que l'électron peut parcourir toute la distance qui sépare son ion-parent A^+ de la molécule A la plus proche sans être piégé dans la matrice.

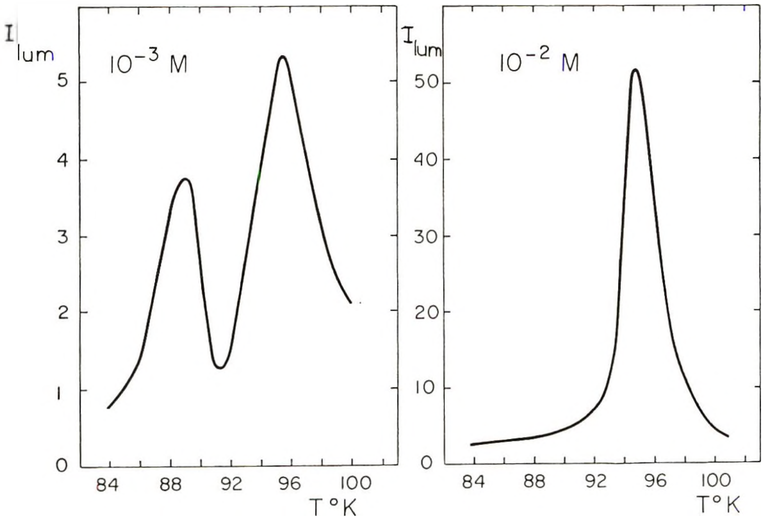

Fig. 8. Courbes de PTL de solutions de styrène dans le méthylcyclohexane.

Si nous admettons en première approximation que tous les électrons libérés sont capturés par des molécules de styrène dans la solution $10^{-2}M$, il s'ensuit que les électrons peuvent parcourir 55 Å sans être piégés dans le verre. L'observation d'un premier pic assez important pour la solution $10^{-3}M$ indique qu'une fraction importante des électrons sont piégés dans le verre lorsque la distance à parcourir est comprise entre 55 et 120 Å.

CONCLUSION

Nous avons montré que les phénomènes observés dans l'étude de la RTL pouvaient être expliqués, du moins qualitativement, par des mécanismes mettant en jeu les cations et les anions du styrène et des électrons piégés dans la matrice de méthylcyclohexane. La présence des électrons et des anions styrène piégés dans ce verre, après irradiation γ, a été prouvée par les spectres d'excitation de RPL. Alors qu'il serait possible, à la rigueur, d'interpréter la RTL sans faire intervenir les cations styrène [par la réaction (8), suivie de transfert d'excitation sur une molécule de styrène, pour le 1er pic, et par les réactions (12) et (14) pour le deuxième pic], l'obtention des mêmes courbes en PTL ne peut s'expliquer que par l'intervention des cations styrène parce que, dans ce cas, les molécules du solvant ne peuvent s'ioniser. Nous pouvons donc affirmer que l'ensemble de nos résultats expérimentaux démontre la formation de cations et d'anions du styrène lorsque celui-ci est irradié dans un verre de MCH à 77°K par les rayons γ du ^{60}Co.

Références

1. R. C. Potter, C. L. Johnson, D. J. Metz, et R. H. Bretton, *J. Polym. Sci. A-1*, **4**, 419 (1966).
2. R. C. Potter, R. H. Bretton, et D. J. Metz, *J. Polym. Sci. A-1*, **14**, 2295 (1966).
3. K. Ueno, F. Williams, K. Hayashi, et S. Okamura, *Trans. Faraday Soc.*, **63**, 1478, (1967).
4. K. Hayashi, Y. Yamazawa, T. Takagaki, F. Williams, K. Hayashi, et S. Okamura, *Trans. Faraday Soc.*, **63**, 1489 (1967).
5. F. Williams, K. Hayashi, K. Ueno, K. Hayashi, et S. Okamura, *Trans. Faraday Soc.*, **63**, 1501 (1967).
6. D. N. Bhattacharrya, C. L. Lee, J. Smid, et M. Szwarc, *J. Phys. Chem.*, **69**, 612 (1965).
7. M. S. Matheson, E. E. Auer, E. B. Bevilacqua, et E. J. Hart, *J. Amer. Chem. Soc.*, **73**, 1700 (1951).
8. D. J. Metz, R. C. Potter et J. K. Thomas, *J. Polym. Sci. A-1*, **5**, 877 (1967).
9. T. Iwamoto, K. Hayashi, S. Okamura, et H. Yoshida, *Int. J. Rad. Phys. Chem.*, sous presse.
10. J. P. Guarino et W. H. Hamill, *J. Amer. Chem. Soc.*, **86**, 777 (1964).
11. T. Shida et W. H. Hamill, *J. Chem. Phys.*, **44**, 4372 (1966).
12. A. Déroulède, F. Kieffer, et M. Magat, "*International Conference on Radiation Chemistry*," Argonne 1968; *Advan. Chem. Ser.*, **82**, 401 (1968).
13. A. Déroulède et F. Kieffer, *Nature*, **215**, 1475 (1967).
14. J. Bullot, A. Déroulède et F. Kieffer, *J. Chim. Phys.*, **1966**, 150.
15. M.-J. Caperan, Diplôme d'Etudes Supérieures, Faculté des Sciences, Orsay, France, 1967.

16. J. Bullot, A. Déroulède et F. Kieffer, *Internationales Lumineszenz-Symposium, Munich,* **1965**, p. 173.
17. A. Déroulède, Thèse de doctorat 3ème cycle, Paris 1964.
18. A. Déroulède, F. Kieffer, et M. Magat, *Israel J. Chem.* **1**, 509 (1963).
19. M. J. Caperan, J. Bullot, A. Déroulède, et F. Kieffer, *Compt. Rend.* **264**, 1013 (1967).
20. M. Magat, *J. Chim. Phys. (Paris)*, **1966**, 142.
21. J. P. Guarino, M. R. Ronayne et W. H. Hamill, *Rad. Res.*, **17**, 379 (1962).
22. M. R. Ronayne, J. P. Guarino, et W. H. Hamill, *J. Amer. Chem. Soc.*, **84**, 4230 (1962).
23. P. J. Dyne et O. A. Miller, *Can. J. Chem.*, **43**, 2696 (1965).
24. D. R. Smith et J. J. Pieroni, *Can. J. Chem.*, **43**, 2141 (1965).
25. V. G. Nikol'skii, V. A. Tochin et N. Ya. Buben, *Fiz. Tverd. Tela*, **5**, 2248 (1963).
26. M. V. Alfimov, V. G. Nikol'skii, et N. Ya. Buben, *Kin. Kataliz*, **5**, 268 (1964).
27. V. A. Tochin, V. G. Nikol'skii et N. Ya. Buben, *Khim. Vysok. Energ.*, **1**, 71 (1967).
28. V. A. Tochin et N. Ya. Buben, *Khim. Vysok. Energ.*, **1**, 78 (1967).
29. P. Debye et J. O. Edwards, *J. Chem. Phys.*, **20**, 236 (1952).
30. J. B. Gallivan et W. H. Hamill, *J. Chem. Phys.*, **44**, 2378 (1966).
31. J. B. Gallivan et W. H. Hamill, *J. Chem. Phys.*, **44**, 1279 (1966).
32. A. Déroulède, F. Kieffer, et E. Migirdicyan, *J. Chim. Phys.* (Paris), à paraître.
33. Th. Förster, *Discussions Faraday Soc.*, **27**, 7 (1959).
34. M. Gauthier-Bodard et J. Bullot, communication à la Conférence Internationale sur la luminescence, Munich, Septembre 1967, *J. Chim. Phys.* (Paris), sous presse.

Received May 8, 1968

JOURNAL OF POLYMER SCIENCE: PART A-1 VOL. 7, 101-109 (1969)

Steady-State Distribution of Water in Cellulose Acetate Membrane

S. ROSENBAUM* and O. COTTON, *Western Division Research Laboratories, The Dow Chemical Company, Walnut Creek, California 94598*

Synopsis

The effect of hydrostatic pressure applied to a solution on one side of a membrane on the steady-state concentration distribution of permeating solvent inside the membrane has been examined with a view to distinguishing between different mechanisms of permeation in reverse osmosis. The concentration gradients found experimentally in stacks of cellulose acetate films support the view that permeation takes place by diffusion in a nonporous membrane.

In a preceding paper[1] it was shown that the permeation of solvent through a semipermeable membrane from a solution of higher solute concentration under hydrostatic pressure to the dilute side can be understood by a simple mechanism of diffusion down a concentration gradient in a nonporous membrane. Application of pressure can reverse the direction of the gradient prevailing in osmosis by modifying the concentration distributions at the membrane-solution interfaces. The experimental results on water and cellulose acetate membranes[2-5] agree well with a permeation equation derived on that basis, especially if the concentration dependence of diffusion and partition coefficients is taken into account.[6] Most of this evidence, predominantly from measurements of rates of permeation, cannot provide positive confirmation, however, since it is possible to derive a similar relation[1] without recourse to a specific mechanism. The possibility that a continuous pressure gradient inside the membrane provides a driving force which transports the permeant in the absence of or against an adverse concentration gradient through static channels connecting the two solutions could then be regarded as a valid alternative. One of the few experiments which could provide a clear differentiation between these alternatives is the actual measurement of the steady-state concentration distribution of permeant along the direction of net transport.

One reason for the lack of reported work on this may be the experimental difficulty involved in measurements inside the usually thin membrane while it is operating. The experiment reported here was an attempt to

---

* Present address: Western Regional Research Laboratory, U. S. Department of Agriculture, Albany, California 94710.

avoid the difficulties by using a stack of membranes as a model for a single membrane. After steady state was indicated by constancy of permeation rate, the aim was to retrieve the individual membranes before reequilibration after release of pressure could change substantially any concentration gradient established in the steady state. The work was confined to water in cellulose acetate membranes.

Experimental and Results

The membranes were clamped in a Monel cell which was provided with magnetic stirring on the high-pressure side (I)[6] and was kept in a constant temperature bath at 25.0 ± 0.1°C. Water or aqueous sodium chloride solution was pumped through the high-pressure side and the permeation rate measured by the volume of permeant emerging on the other. After the permeation rate had become constant, the cell was quickly drained of liquid and taken apart. The membranes were then separated, blotted free of surface water, placed in tared test tubes covered with polyethylene stoppers, and weighed. The basic validity of the blotting method had been confirmed earlier.[7] In addition to the use of maximum speed (2.5–3 min total time) in all operations from draining to stoppering, the inside membranes were made relatively thick to minimize redistribution of water between membranes. At the end of all experiments with a given stack, the membranes were dried to constant weight in a vacuum oven at 80°C. The concentrations were expressed in molal units (moles of water per gram of dry membrane). This involves a change in dimension from the common form of Fick's law, but the experimental scatter, considerable in any case, is reduced by the elimination of volume or density measurements. The outer membranes were regarded as providing less reliable results, e.g., because of their easier redistribution with the liquid side they contact. These were cast thinner than the rest, since they were not to be used in the evaluation of the results, and since there were practical limitations on the total thickness of the stack. Cellulose triacetate membranes were cast from dichloromethane, those of lower acetyl content from acetone, all from 10% solutions onto glass plates, followed by air drying for at least 2 hr and heat-setting in water for 1 hr at 90°C. All polymers were supplied by the Eastman Chemical Company.

The results of the first experiment, with cellulose triacetate (acetyl content 43.6%), are shown in Figure 1; the molal concentration of water in each membrane C_m is plotted against the distance x_c of its central plane from the outer membrane surface in contact with the high-pressure solution (left), 0.5 molal aqueous NaCl. With the exception of one point the plot is fairly linear. The straight line drawn through the four other points indicates a concentration gradient somewhat higher than, but of the order of magnitude and direction expected. The broken vertical lines show the membrane interfaces in the stack. In a more systematic series, similar indications were obtained with excessive scatter. Much of the latter appears unavoidable in a method requiring quick and reproducible execution of a large number of operations leading to a measurement of very small weight differences. A major part of the scatter was attributed, however, on the basis of previous experience, to differences in the properties of the consitituent membranes. These differences are reduced but not eliminated by using membranes from the same casting. In order to avoid this membrane scatter, it was decided to repeat the experiment four times and switch the four internal membranes so that each would occupy each position once; the average concentration should then have the membrane scatter cancelled out. Since the salt on the high-pressure side (I) is not essential for

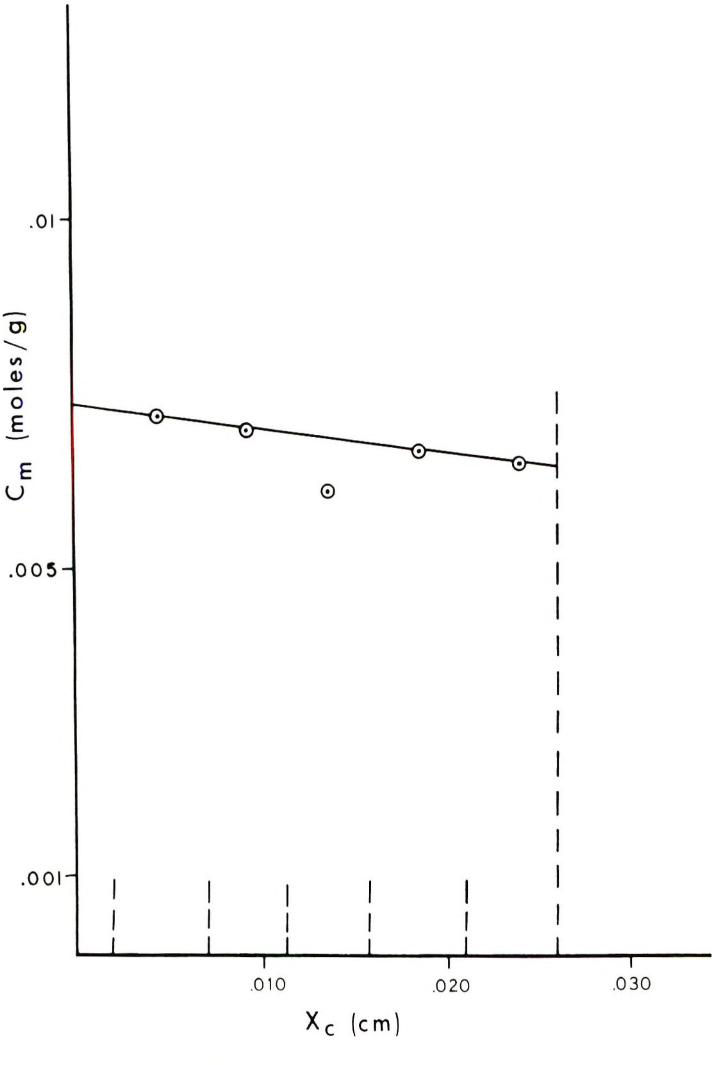

Fig. 1. Variation of concentration of water in membrane with distance x_c from pressure interface; acetyl content 43.6%.

the basic question posed, the effect of pressure on the water gradient, but introduces a number of experimental limitations, the following experiments were carried out with deionized water on both sides. Also, the total water content, hence the magnitude of the effect to be expected, was increased by use of a cellulose acetate membrane of 38.4% acetyl content.

The results are shown in Table I. In most cases the total weight W_m of membrane and water decreased consistently with x_c even for any one individual membrane at a given pressure. Figure 2 shows a plot of average molal concentration $\bar{C}_m$ against the average distance $\bar{x}_c$ from the high pressure surface for the two pressures examined. (It should be noted that a close interpretation of results based on $\bar{x}_c$ would have exact validity only if the concentration gradient is linear or if all internal membranes are of the same thickness. This does not seem to place any serious limitations on the discussion here.) The lines as drawn are based on a least square fit. The slope at 136 atm was twice that at 68 atm. The water content of the stack equilibrated with water at atmospheric pressure was 0.0108 mol/g.

TABLE I
Variation of Weight W_m of Membrane with Distance X_c from Pressure Interface (Acetyl Content 38.4%)

	Membrane				W_m, g	
No.	Thickness, cm	Dry wt, g	Position	x_c, cm	$p = 68$ atm	$p = 136$ atm
2	0.0106	0.7319	II	0.0094	0.8586	0.8508
			III	0.0218	0.8392	0.8525
			IV	0.0305	0.8378	0.8423
			V	0.0429	0.8377	0.8337
3	0.0124	0.7626	II	0.0103	0.9995	1.0034
			III	0.0209	0.9959	1.0039
			IV	0.0314	0.9897	0.9891
			V	0.0420	0.9816	0.9898
4	0.0106	0.7178	II	0.0094	0.8279	0.8316
			III	0.0199	0.8271	0.8281
			IV	0.0324	0.8290	0.8365
			V	0.0429	0.8189	0.8339
5	0.0105	0.7198	II	0.0094	0.8277	0.8311
			III	0.0200	0.8260	0.8294
			IV	0.0324	0.8235	0.8344
			V	0.0430	0.8259	0.8365

Discussion

The discussion will be facilitated by reference to Figure 3, in which concentration profiles in the membrane for different pressure profiles are represented diagrammatically. The abscissa is the (positive) distance from the surface in contact with the solution in the high-pressure side I, and the ordinate is activity a_s in solution(s), concentration C_m in the membrane (m), or the product $p\bar{V}$ of pressure and partial molar volume.

In permeation through a nonporous membrane, the permeant experiences well defined phase changes as it enters and leaves the membrane. If surface equilibrium can be assumed in the steady state, the concentration just inside the membrane can be obtained by the methods of equilibrium thermodynamics. At each interface[1]

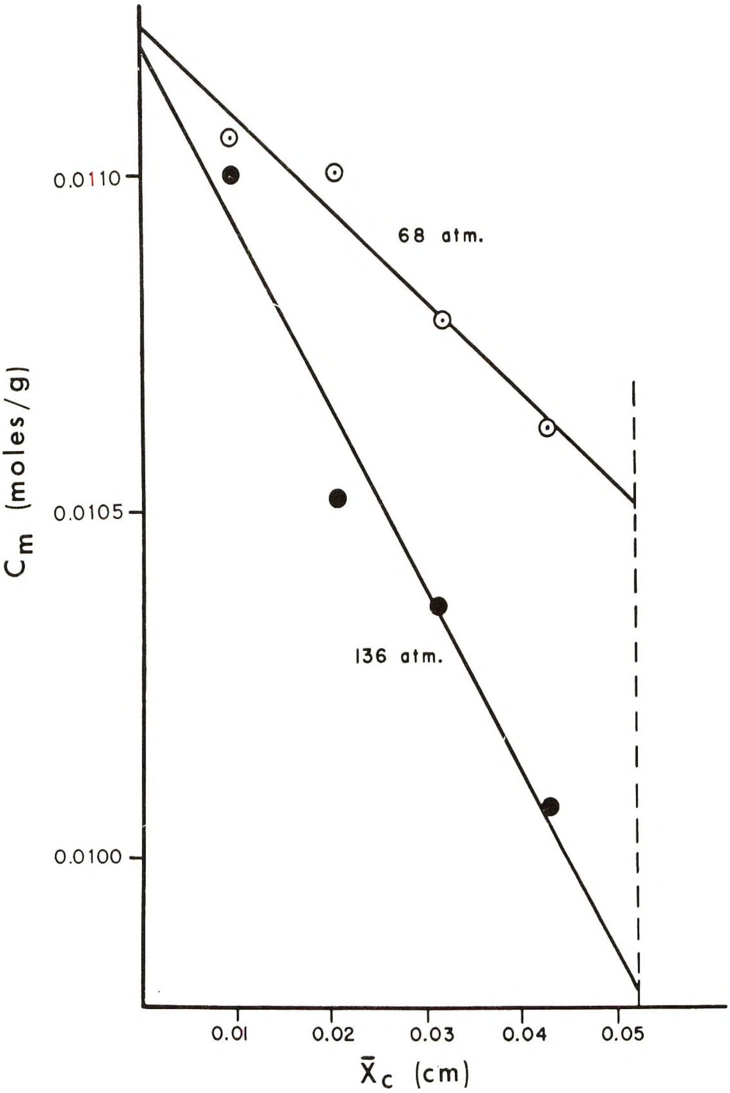

Fig. 2. Variation of average concentration $\bar{C}_m$ in membrane with average distance $\bar{X}_c$ from pressure interface; acetyl content 38.4%.

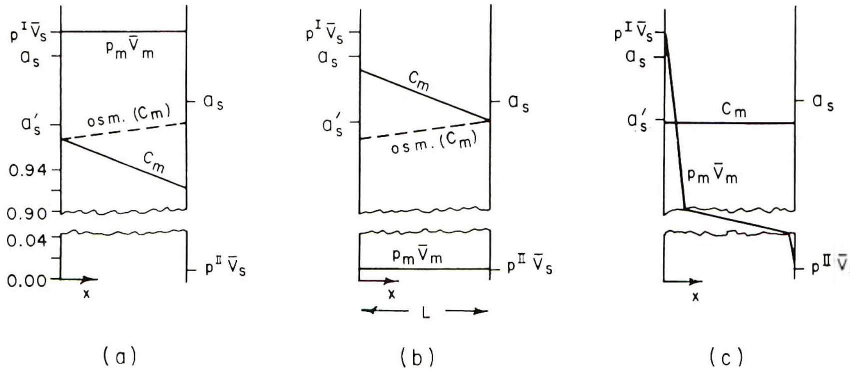

Fig. 3. Relation of concentration and pressure in membrane to activity and pressure in solution: (*a*) nonporous membrane, $p_m = p^I$; (*b*) nonporous membrane, $p_m = p^{II}$; (*c*) porous membrane. Ordinate scale for activity in solution.

$$C_m = Ka_s' \exp\left\{\frac{\int_1^{p_s} \bar{V}_s dp_s - \int_1^{p_m} \bar{V}_m dp_m}{RT}\right\} \tag{1}$$

a_s' is the activity in solution at 1 atm and $K = K_N/\gamma_m'$ where K_N is the Nernst distribution constant and γ_m' is the activity coefficient in the membrane at concentration C_m and at atmospheric pressure. When $\bar{V}$ is independent of p and the exponent small enough,

$$C_m = Ka_s' \{1 + [(p_s\bar{V}_s - p_m\bar{V}_m)/RT]\} \tag{2}$$

The contribution $p\bar{V}$ to the chemical potential in each phase represents the energy required to introduce a mole of the permeant from the same phase at atmospheric pressure. The second term in eq. (2) shows the change in the distribution resulting from the application of pressure by comparison to the atmospheric pressure distribution given by the first term. For a given pressure p_s imposed on the solution the sign and magnitude of the change depends on the magnitude of the pressure p_m in the membrane.

Attention will at first be confined to flat membranes clamped tightly on a very fine fritted filter where the stresses on the membrane polymer should be the same in all directions and equal to the force per unit area exerted by the filter plate to counter the hydrostatic pressure applied to the solution. The pressure on the permeant will, in a free-volume treatment[7] be equal or lower than that on the polymer depending on the relative sizes of permeant and free volume cage. Differences between $p\bar{V}$ terms will be discussed as differences in p.

Figures 3*a* and 3*b* have been drawn for two special cases. In Figure 3*b* the permeant unit, e.g. a single molecule, is much smaller than the free volume unit, so that p_m is equal to the atmospheric pressure. In Figure

3*a* the permeant is in contact with the walls of the cage equivalent to that of the polymeric constituents. In the latter case the pressure on the permeant p_m is equal to that in the solution under high-pressure p_s^I. By comparison with an experiment at atmospheric pressure there is therefore no change in the equilibrium distribution at the interface with solution I. At the low-pressure side II, however, $p_m > p_s$ and, as seen from eq. (2), the concentration just inside the membrane is lowered by comparison to the atmospheric pressure distribution. Conversely, when $p_m = p_s^{II}$ (Fig. 3*b*) the distribution at the low-pressure side II is unchanged, but the concentration in the membrane just inside the high-pressure interface I is increased by comparison to the atmospheric pressure equilibrium. Either case results in a concentration gradient in the same direction.

In a self-supported tubular membrane the radial and axial stresses individually vary in the direction (x) of permeation, but the mean normal stress is independent of x. The effect on the permeant should then be similar in principle to that in a supported membrane, but stresses outside the limits of p_m discussed above may be feasible.

From eq. (1), if K and diffusion coefficient D are constant, and confining exponential expansion to the first two terms, the concentration gradient in a membrane of thickness L is

$$\frac{C_m^I - C_m^{II}}{L} = \frac{K\bar{V}_s}{LRT}\left(1 - \frac{p_m\bar{V}_m}{RT}\right)\left[\left(p_s^I - p_s^{II}\right) - \left(\pi^I - \pi^{II}\right)\right] \quad (3)$$

where $\pi = -(RT/\bar{V}_s)\ \ln a_s'$ is the osmotic pressure in solution.

The magnitude of the gradient at moderate pressures thus depends little on the magnitude of p_m, and the lines in Figures 3*a* and 3*b* are almost parallel. If K is concentration-dependent but D is not, the lines should still be straight but different in slope from that calculated from eq. (3). If K is constant but D is concentration dependent, the gradients are curved and equation (3) gives the average gradient.

If permeation takes place through pores extending from one side of the membrane to the other, there should be a continuous pressure gradient inside the membrane. There appears to be no basis then for expecting a concentration gradient in the direction discussed. This case is illustrated in Figure 3*c*.

The experimental results reported in the previous section show a concentration gradient in the same direction as in Figures 3*a* and 3*b*. This is inconsistent with pore flow and supports the view that permeation takes place by diffusion.

The straight solid line drawn through the first results, at 68 atm pressure difference, in Figure 2 give an experimental gradient of 0.016 mol/cm^4. With $\bar{V}_s$ = 18 cc, L = 0.0524 cm, and K = 0.013 mol/cc (from the experimental equilibrium C_m at atmospheric pressure) the gradient expected from eq. (3) is 0.012 mol/cm^4, 25% lower than that found experimentally. To convert concentrations from the experimental molal to molar units a common factor of 1.2 (in grams dry membrane per cubic centimeter of wet membrane) was used. The exact value is not critical for the comparison since it enters into both calculations.

Considering the experimental difficulties, the agreement with eq. (3) is regarded as close, but in view of similar deviations found in related experiments,[6] it seems worthwhile to accept the residual discrepancy as real. It cannot be interpreted by resort to further mechanisms in addition to molecular diffusion, since the experimental gradient is actually higher than the predicted one. The data show no clear departure from linearity. The simplest explanation would be that the activity coefficient γ_m' is not independent of C_m. All equilibrium isotherms reported[6] for sorption of water vapor by cellulose acetate show curvature convex to the relative humidity axis.

The concentration gradient was exactly twice as high when the pressure difference was doubled to 136 atm (Fig. 2). While this was gratifying, it is obvious from the nature of the data that this is to some extent fortuitous. We have even greater reservations about the convergence of the two gradients near $\bar{x}_c = 0$, which gives the appearance of close adherence to Figure 3*a*. During the extended series of experiments on the same membranes, with repeated application and release of pressure, there was a gradual downward drift in the total water content of the membrane. Due to the use of the experimental averaging procedure, this should not have had an appreciable effect on the gradients, but the absolute magnitude of the concentrations is thought to be less reliable. Also in other experiments, specifically designed to measure the effect of pressure variation on equilibrium and steady-state water content, ambiguous results were obtained. It is therefore thought preferable to leave open for a more thorough study whether the model illustrated by Figure 3*a* provides an adequate description.

It may be argued that the use of a membrane stack places doubt on the validity of the results for single membranes. While this procedure could readily have resulted in a masking of an existing concentration gradient, however, it is hard to see how it can lead to the appearance of a gradient not present in a single membrane. Such a method was used by Garvie and Neale[8] to study substantive dye distribution in cellophane films. Peters et al.[9] have recently shown that the results, as reanalyzed by Crank,[10] are in line with those they obtained by microdensitometric measurements on a single film.

The author would like to acknowledge the contributions of Turner Alfrey, Jr. Thanks are also due to H. I. Mahon, W. E. Skiens, and D. E. DuBocq.

References

1. S. Rosenbaum, *J. Polym. Sci. B*, **6**, 307 (1968).
2. A. S. Michaels, H. J. Bixler, and R. M. Hodges, *J. Colloid Sci.*, **20**, 1034 (1965).
3. H. K. Lonsdale, U. Merten, and R. L. Riley, *J. Appl. Polym. Sci.*, **9**, 1341 (1965).
4. W. E. Skiens and H. I. Mahon, *J. Appl. Polym. Sci.* **7**, 1549 (1963).

5. S. Loeb and S. Sourirajan, *Adv. Chem. Ser.*, **38**, 117 (1963).
6. S. Rosenbaum and W. E. Skiens, *J. Appl. Polym. Sci.*, **12**, 2169 (1968).
7. S. Rosenbaum, H. I. Mahon, and O. Cotton, *J. Appl. Polym. Sci.*, **11**, 2041 (1967).
8. W. M. Garvie and S. M. Neale, *Trans. Faraday Soc.*, **34**, 335 (1938).
9. R. H. Peters, J. H. Petropoulos, and R. McGregor, *J. Soc. Dyers Colourists*, **77**, 704 (1961).
10. J. Crank, *Phil. Mag.*, **39**, 362 (1948).

Received January 9,1968
Revised May 22, 1968

JOURNAL OF POLYMER SCIENCE: PART A-1 VOL. 7, 111–125 (1969)

Polymerization of Aromatic Nuclei. XIV. Polymerization of Toluene with Aluminum Chloride–Cupric Chloride

PETER KOVACIC* and J. S. RAMSEY, *Department of Chemistry, Case Western Reserve University, Cleveland, Ohio 44106*

Synopsis

The polymerization of toluene with aluminum chloride and cupric chloride was performed in carbon disulfide and in a neat system. The solvent reaction produced an insoluble, light-brown product which did not melt below 350°C. In the neat system, polymerization was much more vigorous, yielding a dark, purple-brown solid with mp ~250°C and molecular weight of 634. Infrared, NMR, and ultraviolet spectroscopy, along with elemental analysis and oxidative degradation, indicated that the backbone chain contains *o*-polyphenylene units with the methyl group situated in the 4-position. Some *p*-polyphenylene structures may also be present. Evidence for small amounts of benzyl and polynuclear moieties was obtained. The mechanistic aspects are discussed. Our principal conclusions concerning oligomer structure are in disagreement with those of Kuwata.

INTRODUCTION

Aromatic nuclei are known to undergo polymerization in catalyst–oxidant systems,[1] e.g., aluminum chloride–cupric chloride. Since the initial discovery involving benzene,[2] nuclear coupling has been effected with various other parent hydrocarbons, such as biphenyl[3] and naphthalene.[4] Several reports have been made of studies with substituted aromatic compounds. In the case of chlorobenzene,[5] the product structure consisted mainly of *o*-polyphenylene chains with chlorine atoms in the 4-positions. Lawson et al. polymerized the isomeric xylenes using ferric chloride or molybdenum pentachloride.[6] They concluded that reaction involved the nucleus exclusively in the case of *o*-xylene, but that some methylene structures are formed with the *meta* and *para* isomers.

The purpose of the present work was to investigate the polymerization of toluene by aluminum chloride–cupric chloride with principal emphasis on elucidation of the polymer structure. After our investigations were under way, Kuwata published his results from this system together with the conclusion that the product is polybenzyl.[7] Using a modification in the oxidant component, De Vries converted toluene to oligomers containing about ten

---

* Present address: Department of Chemistry, University of Wisconsin, Milwaukee, Milwaukee, Wisconsin 53201.

monomer units.[8] In earlier work from our laboratory the behavior of toluene on exposure to ferric chloride[9] or aluminum chloride–molybdenum pentachloride[10] was determined. In addition to higher molecular weight materials, diarylmethane hydrocarbons were isolated in both cases. A few publications treat the polymerization of toluene under other conditions. Pyrolysis of alkylbenzenes, including toluene, at about 800°C yielded polymers and oligomers.[11] Infrared spectra of the polymers pointed to the presence of polyethylene chains with pendant aryl groups. Hoigne and Gauemann observed polymer formation on irradiation of toluene with γ-rays.[12] The dimer type fraction consisted of components containing bibenzyl, biphenyl, and diarymethane structures.

RESULTS AND DISCUSSION

During this work two systems were used for the polymerization of toluene. In carbon disulfide, a molar ratio of monomer/$AlCl_3$/$CuCl_2$ = 1/4/2 was found to give polymer with the best appearance and highest yield. In the neat system, a ratio of $AlCl_3/CuCl_2 = 2/1$ was employed with a large excess of monomer. Hereafter, the polymer prepared in carbon disulfide will be referred to as polymer A and that prepared in a neat system as polymer B.

In carbon disulfide the polymerization proceeded smoothly with evolution of acid gas. On the assumption that two molecules of hydrogen chloride were formed per monomer unit, the yield of acid gas was 91% of the theoretical. The hydrogen chloride evolved during polymerization in the absence of solvent came off so vigorously that an accurate determination was difficult (80% of theory was collected in one experiment with perhaps some loss).

By analogy with the oxidative cationic mechanism postulated for benzene[2] and chlorobenzene[5] and on the basis of experimental evidence, the reaction is thought to proceed as shown in eqs. (1) and (2).

$$H_2O + AlCl_3 \rightleftharpoons H_2O \longrightarrow AlCl_3 \rightleftharpoons H^+AlCl_3(OH)^- \quad (1)$$

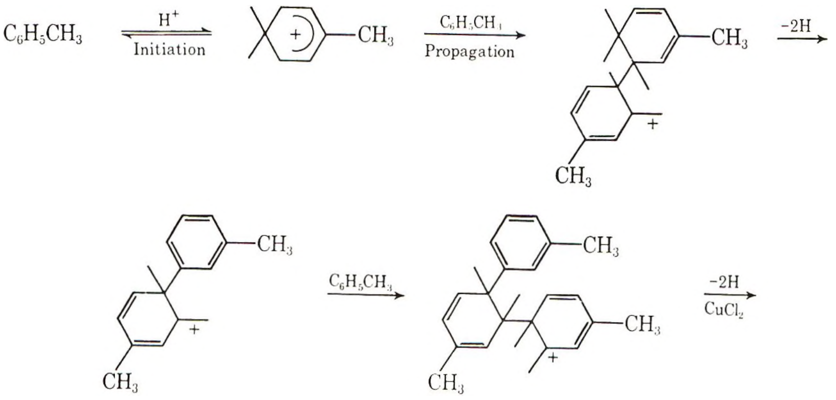

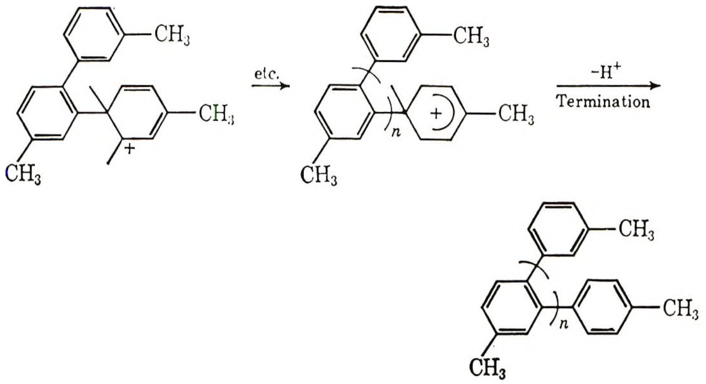

(2)

I

As in the case of chlorobenzene,[5] this scheme uses the *para* position for initiation and propagation. It appears possible for attack also to occur at the *ortho* position. For comparison, isopropylation of toluene gives[13] rise to an *ortho*/*para* ratio of 1.1. The *ortho* participation would most likely result in the formation of substituted *p*-polyphenylene entities (II). Any *meta* attack could conceivably generate the same types of repeating units as in I and II.

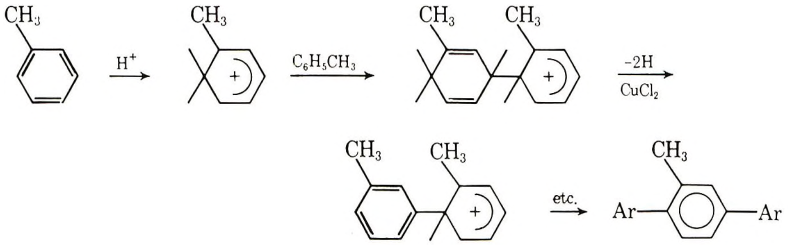

(3)

II

One should also consider the possibility of methyl group participation[7] by hydride abstraction leading to the formation of polybenzyl type entities (III).

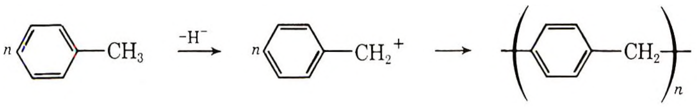

(4)

III

Elemental Analysis and Physical Properties

The analytical data (Table I) for polymer A fitted in reasonably well for a nuclear coupled polymer having the repeating unit I. Only a small amount of chlorine was detected, indicating that chlorination by the metal halide was not an important reaction. The C/H ratio for polymer A was 1.23 as compared with a value of 1.17 for I. This loss of hydrogen (~7%) can be rationalized by postulating the formation of polynuclear structures,

TABLE I
Elemental Analysis of Toluene Polymers

Polymer	C, %	H, %	Cl, %	C/H, atom ratio
A	92.7	6.2	0.4	1.23
B	91.2	5.6	0.8	1.36
I[a]	93.2	6.7	0	1.17

[a] Calculated.

e.g., IV, by intramolecular cyclization at certain points along the polymer chain.

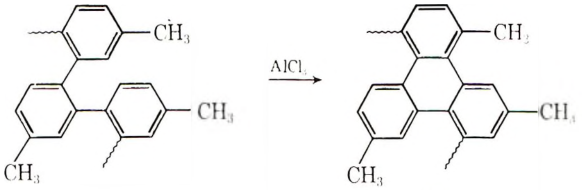

IV (5)

Polymer A was a fine, light brown powder. If, however, polymerization was continued for a longer period of time, i.e., greater than 2 hr, the color became markedly darker. Since the polynuclear entity is a much more powerful chromophoric group than *o*-polyphenylene (I), the color is probably due in large part to these moieties. Kovacic et al. noticed a similar color change with the chlorobenzene oligomers[5] prepared under various conditions, i.e., at 30°C the oligomer possessed a yellow color in contrast with the darker hue characteristic of the 60°C product. Polymer B was much darker in color, possessing a deep purple tinge. The C/H ratio (1.36) deviated quite significantly from the theoretical figure of 1.17, representing a net loss of hydrogen of 16%. If this decrease in hydrogen is due to the formation of polynuclear entities, the darker color of polymer B compared with polymer A is nicely rationalized. Kuwata reported[7] the toluene polymer to be a brown powder. In accord with the earlier observation,[7] both polymers A and B displayed strong fluorescence in organic solvents, which also suggests the presence of polynuclear structures.

Polymer A remained essentially unchanged even when heated to 350°C while crude polymer B usually melted at about 230–250°C with softening at lower temperatures. Whereas polymer B exhibited a molecular weight of 634, corresponding to the presence of seven monomer units, polymer A was too insoluble to permit a determination. In the prior study,[7] a molecular weight of 3200 was observed for the product from the neat system, with a softening point of about 330°C (after some purification). Various lines of evidence, e.g., NMR data (*vide infra*), indicate that polymer B has a more irregular structure than the solution polymer. Hence, these properties of polymer A might well be a reflection of a high degree of regularity. On the other hand, the presence of a small number of crosslinks cannot be discounted.

NMR Spectra

The nuclear magnetic resonance spectrum (Fig. 1, Table II) of polymer A showed two singlets, one at 2.3 δ due to aliphatic protons and the other at 7.15 δ resulting from aromatic proton signals. Integration revealed the two types to be present in equal amounts. Several model compounds were examined for comparison, namely, toluene and 2,5-dimethylbiphenyl, both of which gave aliphatic signals at 2.2–2.3 δ. Structures I and II correlate satisfactorily with these data.

The NMR spectrum of polymer B (Fig. 2, Table II) consisted of broad,

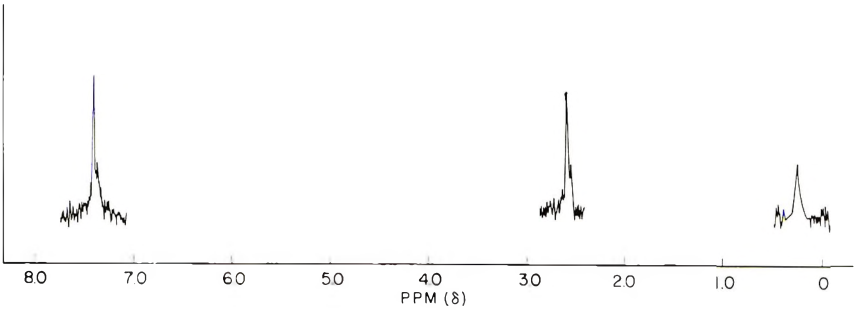

Fig. 1. NMR spectrum of polymer A.

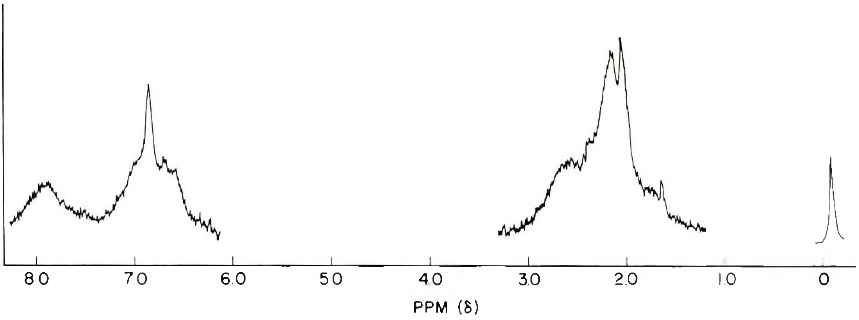

Fig. 2. NMR spectrum of polymer B.

TABLE II
NMR Data

Material	Aromatic protons, δ	Aliphatic protons, δ	
		Methylene	Methyl
Polymer A	7.15–7.2		2.3–2.35
Polymer B	6.5–8.2		1.9–2.9
Polymer C[a]	6.2–8.0		1.5–3.7
Polybenzyl	6.2–7.3	3.3–3.9	
2,5-Dimethylbiphenyl	7.0–7.3		2.2–2.3
Toluene	7.2		2.2–2.3

[a] Toluene polymer prepared and isolated according to Kuwata's procedure[7] (Fig. 3).

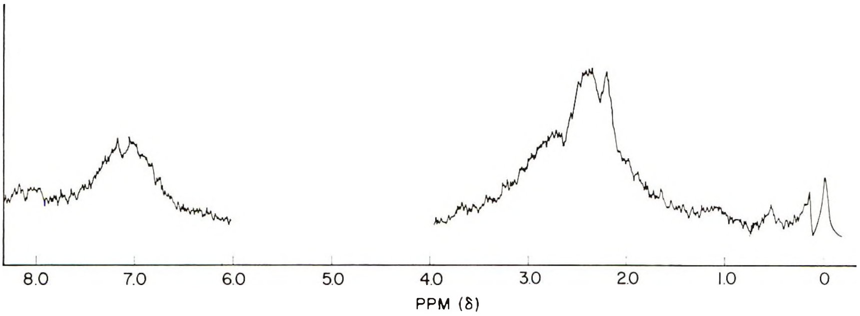

Fig. 3. NMR spectrum of polymer C.

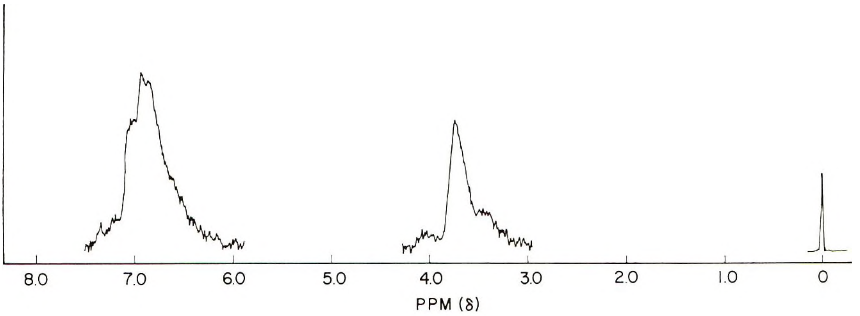

Fig. 4. NMR spectrum of polybenzyl.

irregular peaks in the regions, 1.9–2.9 δ (aliphatic) and 6.5–8.2 δ (aromatic) in the ratio of 0.8–0.9. The value of somewhat less than one from integration is consistent with the low analysis for hydrogen. From the spectrum one can conclude that polymer B possesses a structure somewhat more complicated and irregular than that of polymer A.

Kuwata, on limited evidence, postulated[7] a polybenzyl structure for the polymer. An authentic sample[14] of polybenzyl was prepared by treatment of benzyl alcohol with concentrated sulfuric acid. In the NMR analysis (Fig. 4, Table II) the signal arising from methylene protons fell at 3.3–3.9 δ with an integration of 2:1 for aromatic to aliphatic protons. Thus, both the position of the aliphatic protons and the integrated value of aliphatic: aromatic for the toluene polymer are in disagreement with the corresponding data for polybenzyl. Furthermore, there was no indication of aliphatic protons of the type Ar_3CH in the toluene product in the characteristic region 5.5 δ.

Since no signal was evident in the methylene region for our toluene polymers, experiments with model compounds (diphenylmethane and 2,5-dimethylbiphenyl) were carried out in order to ascertain the limits for detection experimentally. At the concentrations used, we found that methylene protons were barely visible at a ratio of 1:9 for the models. Hence, this suggests that benzyl structures can comprise no more than about 10% of the total make-up of the toluene product.

Oxidative Degradation

Oxidation studies were performed with the aim of further elucidating the chemical nature of the polymer. In accord with Kuwata's experience,[7] much difficulty was encountered in attempts to locate a suitable oxidizing agent. For example, the chromic acid–acetic acid method, which functioned well with *p*-polyphenylene[2] and the chlorobenzene oligomers,[5] failed to give satisfactory results in the present case. Fortunately, aqueous sodium dichromate[15] at high temperatures and pressure was found to degrade the toluene polymer to low molecular weight fragments which could be characterized.

Oxidation of polymer A with this reagent gave a mixture of acids in 5–10% yield. Esterification of the crude product with methanol, followed by gas chromatographic analysis, gave the following esters: methyl benzoate, methyl 4-methylbenzoate, dimethyl phthalate, dimethyl terephthalate, dimethyl 4-methylphthalate, and trimethyl trimellitate. The dimethyl ester of benzophenone-4,4′-dicarboxylic acid was isolated by column chromatography. These compounds were identified by comparison of their infrared and NMR spectra with those for the authentic esters.

The repeating unit in I can be designated as the precursor of trimellitic acid and 4-methylphthalic acid. That portion of I arising from termination would serve as the forerunner for terephthalic acid and 4-methylbenzoic acid. Trimellitic acid might also be derived from II. During work-up of the oxidation mixture, carbon dioxide was liberated in copious amounts, presumably originating from gross oxidation and decarboxylation. One can visualize decarboxylation reactions giving rise to benzoic acid, phthalic acid, and terephthalic acid. In fact, conversion of trimellitic acid to terephthalic acid was observed under simulated oxidation conditions. A reasonable interpretation for the presence of benzophenone-4,4′-dicarboxylic acid is the existence of some benzyl moieties in the polymer chains, which could also produce terephthalic and phthalic acids. However, according to the NMR studies these groups would be present in no more than minor quantities.

Oxidation of polymer B and esterification in a similar manner gave the following products: methyl benzoate, dimethyl isophthalate, dimethyl terephthalate, trimethyl trimellitate, and benzophenone-4,4′-dimethylcarboxylate. Also present were trace amounts of other compounds thought to be methyl 4-methylbenzoate and dimethyl 4-methylisophthalate on the basis of retention times in gas chromatography. The results were similar to those from polymer A except that dimethyl isophthalate was isolated with ease. In the case of polymer A, although this compound was not detected, it may be present in small amounts as a contaminant of dimethyl terephthalate. Isophthalic acid might be generated *via* decarboxylation or by oxidation of the endgroup formed in initiation or through termination by *meta* substitution. The presence of larger amounts of this component from polymer B oxidation suggests that this polymer possesses a lower molecular weight than polymer A and hence a higher percentage of the requisite end group units. However, alternative interpretations are also possible.

In relation to the isolated components from oxidation of both polymers, trimellitic and terephthalic acids were the chief products, whereas 4,4'-dicarboxybenzophenone was obtained only in minute quantities.

Kuwata reported[7] that oxidation of the polymer with potassium permanganate in acetone yielded a crude product which exhibited ketone, but not carboxyl, functionality according to the infrared spectrum. No individual components were isolated from the degradation.

Infrared Spectra

Although the infrared spectrum (Fig. 5) was not of high quality, 1,2,4-substitution was indicated by absorption maxima in the aromatic region at 815–820 cm^{-1} (s), (lit.[16] for two adjacent hydrogens, 800–860 cm^{-1}) and at 870 cm^{-1} (w), (lit.[16] for an isolated hydrogen, 860–900 cm^{-1}). The repeating units in I and structure II are consistent with these findings. Kuwata observed strong absorption at 820 cm^{-1} for his material.

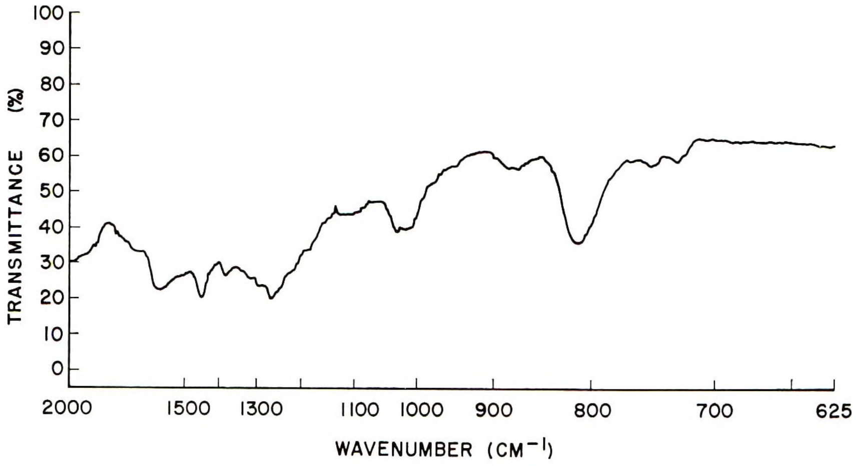

Fig. 5. Infrared spectrum of polymer A.

Ultraviolet and Visible Spectra

In the ultraviolet spectra (Figs. 6 and 7) strong absorption occurred at 250–255 mμ for both polymers. In addition, polymer B exhibited peaks, including fine structure, in the 330–430 mμ region. For comparison toluene is characterized by absorption at 261 mμ,[17] and the chlorobenzene oligomer shows λ_{max} = 255 mμ.[5] Jones has pointed out that when steric effects repress conjugation, the spectrum approximates that of the parent aromatic compound.[18] In the case of the toluene polymer, as with chlorobenzene oligomers, *o*-polyphenylene linkages allow for little conjugative interaction because of adverse steric effects.

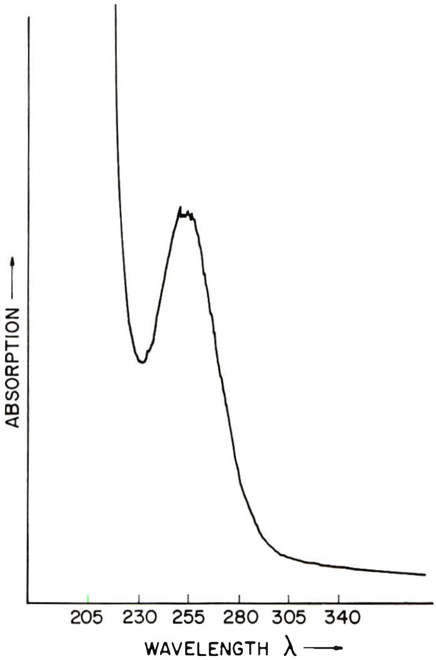

Fig. 6. Ultraviolet spectrum of polymer A.

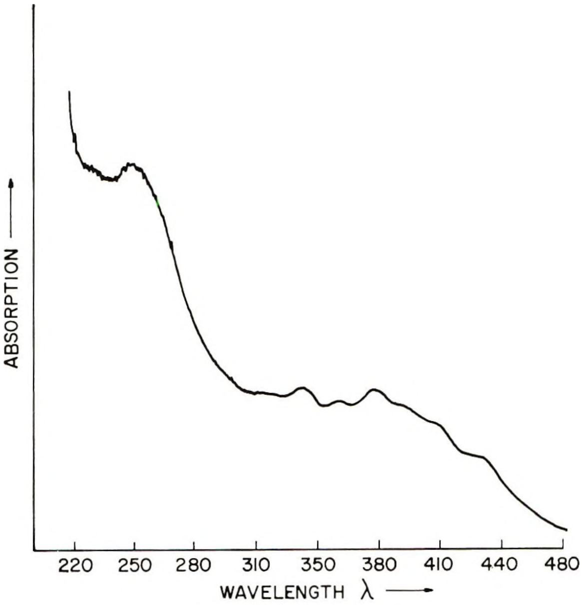

Fig. 7. Ultraviolet spectrum of polymer B.

Relative Rates of Polymerization

The polymerization of toluene in the neat system proceeded at a very much faster rate than in the presence of carbon disulfide. Several factors should be considered in relation to rationalization of the results: (*1*) the solvent may coordinate with the propagating species thus reducing its activity; (*2*) the carbon disulfide may complex with the aluminum chloride catalyst rendering it less effective. The relative rates of polymerization of benzene, toluene, and chlorobenzene were in the order, toluene ≫ benzene > chlorobenzene (Fig. 8). These results are in keeping with the known relative reactivities of these aromatic compounds in electrophilic substitution reactions.

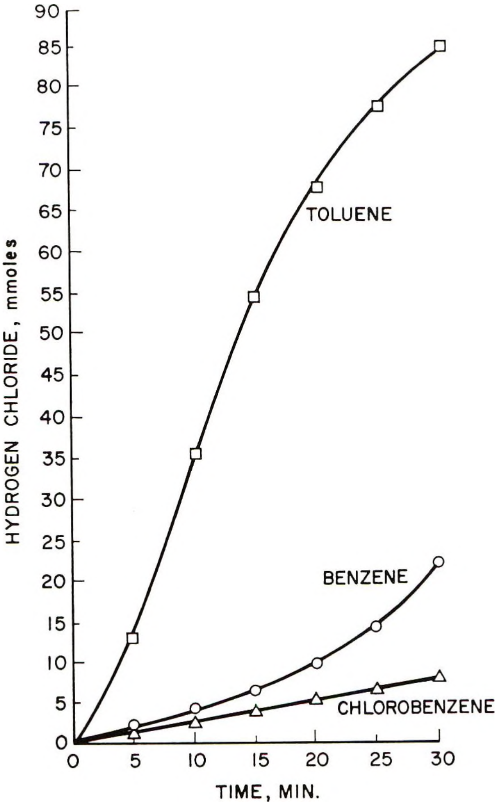

Fig. 8. Relative rates of polymerization of toluene, benzene, and chlorobenzene.

EXPERIMENTAL

Materials

The chemicals used in this research were obtained from the following sources: toluene (spectrograde), Matheson, Coleman and Bell Co.; aluminum chloride (anhydrous), J. T. Baker Chemical Co.; cupric chloride, Allied Chemical Co.

Analytical Procedures and Apparatus

Spectra were obtained on a Beckman IR8 infrared spectrophotometer, a Beckman DB ultraviolet spectrophotometer, or a Varian Associates A-60 nuclear magnetic resonance unit. The infrared spectra of polymers were obtained with potassium bromide disks. Cyclohexane solutions were used for ultraviolet analysis, and carbon disulfide solutions for NMR determinations (suspension with polymer A). Melting points were determined on a Thomas Hoover capillary melting point apparatus. An Aerograph gas chromatograph manual temperature programmer with a 27 in. SF96/Chromosorb P column was used for all separations. Elemental analyses and molecular weight determinations (vapor-pressure osmometry) were carried out by Galbraith Laboratories, Knoxville, Tennessee.

Polymerization of Toluene with Aluminum Chloride–Cupric Chloride

General Procedures

The reaction was carried out under nitrogen in a three-necked flask equipped with a paddle stirrer and a nitrogen inlet. A mixture of aluminum chloride (33 g, 0.25 mole) and cupric chloride (17.5 g, 0.125 mole) was added in one portion to a stirred solution of toluene (previously purged with nitrogen) (5.75 g, 0.0625 mole) in carbon disulfide (100–150 ml) at 0°C. The light-brown reaction mixture became dark almost immediately, but no acid gas was evolved at this stage. After the ice bath was removed, the temperature gradually rose, whereupon at 15–20°C, acid gas appeared and was emitted continuously for the duration of the experiment. As time passed the amount of acid gas given off decreased. The reaction was allowed to proceed for 90 min. Excess carbon disulfide was then decanted from the reaction mixture, and the remaining solvent was removed by passing a brisk flow of nitrogen through the reaction vessel. The hard cake was then broken up and added slowly, with vigorous stirring, to 1 liter of ice-cold, dilute hydrochloric acid. Filtration yielded a dark-brown solid which was triturated with hot, dilute hydrochloric acid and then washed thoroughly with hot, deionized water until a negative test for chloride ion was obtained. After being dried at 110°C for 12 hr, the brown product (4.6 g, ~80% yield based on monomer) was in the form of a fine powder. The acid gas evolved during the polymerization was collected in a trap containing 150 ml of 1*N* sodium hydroxide, 91% yield (based on cupric chloride).

In an alternate procedure, to a stirred suspension of aluminum chloride (32.2 g, 0.25 mole) in 100 ml toluene (first purged with nitrogen) at 0°C. was added cupric chloride (16.8 g, ~0.125 mole). Removal of the ice bath resulted in a moderately fast rise in temperature, and after 4 min at 18–20°C a vigorous evolution of gas occurred. The rate of generation of acid gas slackened considerably after a few minutes, but continued to be evolved for the duration of the experiment. After 1 hr, the reaction mixture was poured into ice-cold, dilute hydrochloric acid (500 ml) and steam-distilled.

The solid remaining in the pot was washed well with hot deionized water, filtered, blended, and dried, yielding 3.72 g (66% yield based on cupric chloride). The product was a dark, purple solid.

Polymerization was also carried out according to the method of Kuwata.[7]

Oxidation of Toluene Polymer with Aqueous Sodium Dichromate[15]

Toluene Polymer (Carbon Disulfide System). The polymer (16 g, 0.18 mole), sodium dichromate (75 g, 0.25 mole, 40% excess) and water (300 ml) were shaken in an autoclave for 48 hr at 250°C. The cooled mixture was filtered to remove insoluble chromium compounds. Because of the difficulty in dissolving the inorganic material with acid, the amount of unchanged polymer was not determined. The residue was washed several times with distilled water to remove water soluble products. Acidification of the aqueous filtrate with 50% hydrochloric acid resulted in vigorous evolution of carbon dioxide accompanied by foaming. On standing overnight a fine, light brown, powdery solid deposited which was collected by filtration, 0.5 g. The filtrate, on extraction with 1.5 liter of ether and subsequent removal of solvent, yielded a white solid, 1.5 g.

The brown solid was esterified by refluxing for 12 hr with a mixture of methanol (200 ml)-sulfuric acid (2 ml) saturated with hydrogen chloride. The mixture was diluted with water (100 ml) and extracted with ether. Removal of the ether gave a yellow-white solid which on column chromatography (activated alumina and chloroform) yielded dimethyl terephthalate, mp 140°C, and the dimethyl ester of benzophenone-4,4′-dicarboxylic acid (mp 225°C, lit.[19] mp 225°C.).

Similar esterification of the white solid gave a small amount of yellow liquid which contained the indicated components by gas chromatographic analysis: methyl benzoate, methyl 4-methylbenzoate, dimethyl phthalate, dimethyl terephthalate, dimethyl 4-methylphthalate, and trimethyl trimellitate. The esters were identified by comparison of their infrared and NMR spectra with those of the authentic materials and by mixture melting points whenever possible.

In an alternate procedure after oxidation in the autoclave for 48 hr at 250°C, the reaction mixture was filtered. Acidification of the alkaline filtrate was followed by extraction (without filtration) with 2 liters of ether. Removal of the ether yielded a brown-white solid (~2 g) which was triturated with dry ether (30 ml) and filtered from a small amount of cream colored solid. Recrystallization from ether gave white needles of the dimethyl ester of benzophenone-4,4′-dicarboxylic acid, mp 225°C.

Gas chromatography of the ether filtrate showed that all of the esters mentioned in the alternate procedure were present.

Toluene Polymer (Neat System). A mixture of the polymer (12 g, 0.13 mole), sodium dichromate (53.6 g, 0.18 mole, 40% excess) and water (300 ml) was maintained at 250°C for 24 hr with shaking. After filtration, acidification of the filtrate with 50% hydrochloric acid evolved much carbon dioxide. A fine, brown solid deposited on standing overnight, which was filtered and dried, 2.7 g. Esterification in the usual manner followed by filtration gave a dark brown solid, 1.4 g. Since this product appeared to be relatively high molecular weight material, it was not further investigated. The methanol filtrate was diluted with water and extracted with ether, yielding on removal of solvent, an orange colored solid. Chromatography through activated alumina (chloroform elution) gave a white solid (mp 130–135°C; mp 140–141°C on recrystallization from ether) and an off-white solid, mp 200–215°C. The compounds were shown to be dimethy terephthalate and the dimethyl ester of benzophenone-4,4′-dicarboxylic acid by comparison of their infrared spectra with those of the authentic esters.

The original acid filtrate yielded a white solid (0.7 g) on extensive extraction with ether. Esterification and gas chromatography of the resulting product showed the following esters to be present: methyl benzoate, dimethyl isophthalate, and trimethyl trimellitate. The dimethylisophthalate, mp 62–65°C (gas chromatography collection) was probably contaminated with dimethyl terephthalate. Recrystallization from ether raised the melting point to 67–68°C.

Oxidation of Toluene Polymer with Potassium Permanganate

The polymer (3 g), suspended in acetone (50 g) at 56°C. was treated dropwise with potassium permanganate (11 g) suspended in hot acetone (300 ml) over a period of 16 hr. After 30 hr of stirring and heating, the reaction mixture was filtered, and the brown solid was triturated with 18% hydrochloric acid. Filtration yielded a brown solid (2.75 g) which was extracted with ether. However, no residue resulted from removal of the solvent. An infrared spectrum of the solid indicated the presence of both carbonyl and carboxyl groups. Distillation of the acetone filtrate yielded a negligible amount of residue.

By means of a different work-up procedure, the brown solid from filtration of the reaction mixture was extracted with sodium hydroxide. Acidification of the extract with dilute acid produced a few milligrams of fine, brown solid which did not melt below 250°C. The infrared spectrum of this product showed the presence of both carbonyl and carboxyl groups. This type of oxidation was carried out several times with similar results on polymer prepared both in carbon disulfide and in a neat system.

Oxidation of Toluene Polymer with Chromic Anhydride

By analogy with the procedure[2] used for oxidative degradation of *p*-polyphenylene, the toluene polymer (10 g), chromic anhydride (120 g), glacial acetic acid (610 ml), and water (100 ml) were placed in a round-bottomed flask and heated at the reflux temperature for 1–10 hr. The cooled reaction mixture was stirred with dilute hydrochloric acid and filtered. No degradation products were obtained in any of the oxidations, even when the acid filtrate was extracted thoroughly with ether. Many oxidations with chromic anhydride–acetic acid-water were performed under various conditions with no apparent success.

Preparation of Authentic Esters

Methyl benzoate, dimethyl phthalate, dimethyl isophthalate, dimethyl terephthalate, and methyl 4-methylbenzoate were prepared by refluxing the parent acid (2 g) for 12 hr with a methanol (200 ml)–sulfuric acid (2 ml) solution saturated with hydrogen chloride. Pure samples of the esters for infrared and NMR analyses were obtained by collection from the gas chromatograph.

Benzophenone-4,4′-dicarboxylic acid was obtained by oxidation of 4,4′-dimethylbenzophenone with potassium permanganate according to Vogel.[20] The diacid (mp 300°C) was esterified with methanol and sulfuric acid. The dimethyl ester, recrystallized from chloroform, was obtained as fine, white needles, mp 225°C (lit.[19] mp 225°C).

Dimethyl 4-methylphthalate was prepared in the following manner: The conditions employed for the Diels-Alder reaction in the first step were similar to those used by Frank et al.[21] to prepare 3-methyl-1,2,3,6-tetrahydrophthalic anhydride. From maleic anhydride (37.5 g), picric acid (50 mg) in benzene (125 ml), and freshly distilled isoprene (26 g), 4-methyl-1,2,3,6-tetrahydrophthalic anhydride was obtained in ~70% yield, mp 64–65°C(lit.[22] mp 64–65°C). This material was dehydrogenated to 4-methylphthalic anhydride in about 70% yield by the procedure[23] of Newman and McCleary for the synthesis of 3-methylphthalic anhydride. The desired material, purified by distillation under reduced pressure, melted at 89–93°C (lit.[22] mp 88–94°C). The dimethyl ester was prepared in the usual way.

Decarboxylation of Trimellitic Acid

A mixture of trimellitic acid (10 g), sodium dichromate (14 g), and water (300 ml) was placed in an autoclave and maintained at 250°C for 24 hr with shaking. After filtration of the reaction mixture, acidification of the filtrate with 20% hydrochloric acid yielded a white solid. Additional solid was obtained by ether extraction of the aqueous solution. Esterification by our standard procedure revealed the presence of dimethyl terephthalate and trimethyl trimellitate (gas chromatographic and infrared analyses).

Preparation of Polybenzyl

Polybenzyl was prepared according to the procedure of Shriner and Berger[14] by the addition of benzyl alcohol to well-stirred, concentrated sulfuric acid at 0°C. With slow addition of the alcohol a salmon-red, stringy solid which floats on the acid was formed, as reported. Care was taken to avoid any local concentration of benzyl alcohol as this results in the formation of a green, insoluble product. The reaction mixture was then poured over crushed ice. After standing overnight, the polymer was isolated by filtration and purified by several washings with water. After being dried over phosphorus pentoxide in a desiccator, the product was a cream-colored solid, mp 80–90°C. Shriner and Berger found that the polybenzyl contained units resulting from propagation by both *para* and *ortho* attack, the former apparently predominating.

Relative Rates of Polymerization of Aromatic Monomers

A mixture of the aromatic monomer (3 mole) (benzene, chlorobenzene, toluene) and anhydrous aluminum chloride (0.25 mole) was adjusted to 29 ± 1°C with vigorous stirring under dry nitrogen (flow rate, 200 ml/min). Anhydrous cupric chloride (0.125 mole) was added in a single portion and the reaction was followed by titration of the evolved acid gas with standard base. The rate data for benzene, toluene, and chlorobenzene are summarized in Figure 8. The polymer yields were found to be in the following ratio: toluene/benzene/chlorobenzene = 69/20/3.[24]

This work was performed for the Jet Propulsion Laboratory, California Institute of Technology, sponsored by the National Aeronautics and Space Administration under contract NAS7-100. We are grateful to Mr. David D. Lawson for helpful discussions, and to Dr. Li-Chen Hsu for some of the preliminary experiments.[24]

References

1. P. Kovacic and J. Oziomek, *J. Org. Chem.*, **29**, 100 (1964).
2. P. Kovacic and A. Kyriakis, *J. Amer. Chem. Soc.*, **85**, 454 (1963).
3. P. Kovacic and R. M. Lange, *J. Org. Chem.*, **29**, 2416 (1964).
4. P. Kovacic and F. W. Koch, *J. Org. Chem.*, **30**, 3176 (1965).
5. P. Kovacic, J. T. Uchic, and L. Hsu, *J. Polym. Sci., A-1*, **5**, 945 (1967).
6. D. D. Lawson, R. F. Haack and J. D. Ingham, *Jet Propulsion Laboratory Space Programs Summary*, **4**, No. 37-30, 94 (1964).
7. H. Kuwata, *Mem. Proc. Fac. Eng. Hiroshima Univ.*, **2**, No. 3, 55 (1965).
8. L. De Vries, U. S. Pat. 3,367,986 (1968).
9. P. Kovacic, C. Wu, and R. W. Stewart, *J. Amer. Chem. Soc.*, **82**, 1917 (1960).
10. P. Kovacic and R. M. Lange, *J. Org. Chem.*, **30**, 4251 (1965).
11. V. V. Korshak, S. V. Rogozhin, T. A. Sidorov, J. Chao, and L. I. Komarova, *Izv. Akad. Nauk SSSR, Otd. Khim. Nauk*, **1963**, 912.
12. J. Hoigne and T. Gauemann, *Helv. Chim. Acta*, **47**, 260 (1964).
13. S. H. Patinkin and B. S. Friedman, in *Friedel-Crafts and Related Reactions*, G. A. Olah, Ed., Vol. II, Interscience, New York, 1964, p. 9.
14. R. L. Shriner and A. Berger, *J. Org. Chem.*, **6**, 305 (1941).
15. L. Friedman, D. L. Fishel, and H. Shechter, *J. Org. Chem.*, **30**, 1453 (1965).
16. L. J. Bellamy, *The Infra-Red Spectra of Complex Molecules*, Wiley, New York, 1964, p. 65.
17. R. A. Friedel and M. Orchin, *Ultraviolet Spectra of Aromatic Compounds*, Wiley, New York, 1951, Spectrum No. 8.
18. R. N. Jones, *J. Amer. Chem. Soc.*, **67**, 2127 (1945).
19. N. R. Campbell and J. H. Hunt, *J. Chem. Soc.*, **1951**, 960.
20. A. I. Vogel, *Practical Organic Chemistry*, Wiley, New York, 3rd ed., 1962, p. 520.
21. R. L. Frank, R. D. Emmick, and R. S. Johnson, *J. Amer. Chem. Soc.*, **69**, 2313 (1947).
22. N. Rabjohn, M. F. Drumm, and R. L. Elliott, *J. Amer. Chem. Soc.*, **78**, 1631 (1956).
23. M. S. Newman and C. D. McCleary, *J. Amer. Chem. Soc.*, **63**, 1542, (1941).
24. L. C. Hsu, Ph.D. Thesis, Case Institute of Technology, 1965.

Received May 15, 1968

JOURNAL OF POLYMER SCIENCE: PART A-1 VOL. 7, 127–138 (1969)

Polymerization of Aromatic Nuclei. XV. Polymerization of 2,5-Di- and 2,3,5-Trichlorothiophenes with Aluminum Chloride–Cupric Chloride

J. S. RAMSEY and PETER KOVACIC,* *Department of Chemistry, Case Western Reserve University, Cleveland, Ohio 44106*

Synopsis

2,5-Dichlorothiophene was polymerized to a solid in 93% yield on treatment with aluminum chloride–cupric chloride in carbon disulfide under mild conditions. The product is believed to be poly-5-chloro-2,3-thienylene on the basis of elemental analysis and infrared and NMR spectral data. Hydrogen chloride was collected in 90% of the theoretical amount. Dimer- and tetramer-type fractions were isolated from the polymer. 2,3,5-Trichlorothiophene underwent an analogous transformation in trichlorobenzene at 90–100°C. Polythienylenes coupled through the 2,3-positions have not been reported previously. The net effect of the reaction is nuclear coupling by dehydrohalogenation. We believe that the mechanism involves cationic polymerization accompanied by loss of hydrogen chloride. 2-Chlorothiophene and thiophene gave products of complex make-up.

INTRODUCTION

Most of the prior investigations on polymerization of simple thiophenes have been carried out with the parent compound. Although Victor Meyer noted in 1883 that sulfuric acid transformed thiophene to an amorphous solid,[1] little work was done in the following years to identify this type of resin. Klages and Liecke reported[2] that hydriodic acid at 140°C. gave a cokelike solid, hydrogen sulfide, and sulfur. Several investigators[3,4] observed that this aromatic nucleus and hydrogen fluoride reacted to give an amorphous, red solid. Thiophene has also been converted to noncrystalline substances by the action of ferric chloride[5] or aluminum chloride.[6a] Topchiev and collaborators[7,8] performed the polymerization in the presence of Ziegler catalysts. Safarov and Proskurnin obtained high molecular weight material by irradiation of aqueous solutions with γ rays.[9] More recently, oligomers have been isolated from treatment of thiophene with silica–alumina gel or orthophosphoric acid.[6b] The trimer type entity was found to contain both aromatic and reduced nuclei.

In the benzenoid series, the combination of aluminum chloride and cupric chloride has been used for nuclear coupling.[10–13] The aim of the present

---

* To whom correspondence should be addressed; Department of Chemistry, University of Wisconsin at Milwaukee, Milwaukee, Wisc. 53201.

study was to investigate the behavior of several chlorinated thiophenes in the aluminum chloride–cupric chloride system. Our attention was centered principally on structure elucidation and mechanistic aspects.

RESULTS AND DISCUSSION

Polymerization of 2,5-Dichlorothiophene

Reaction Variables

From studies on the polymerization of 2,5-dichlorothiophene with various amounts of catalyst and cupric chloride, a monomer/catalyst/cupric chloride ratio of 1/4/2 appeared to give the smoothest reaction, as well as product of highest yield (93% based on monomer) and best appearance (light brown powder melting at about 115–150°C). Addition of the metal halides to the monomer in carbon disulfide resulted in a darkening of the reaction mixture after a few moments, but no gas was evolved at temperatures below 12°C. A vigorous evolution of acid fumes commenced at 12–15°C and continued, though at an ever decreasing pace, during the 2 hr reaction span at 0–29°C. Hydrogen chloride was collected in 90% of the theoretical yield (based on one mole of gas per mole of monomer). With lesser amounts of the metal halides, e.g, 1/2/1 ratio, the reaction proceeded at a slower rate, on the basis of gas evolution, and produced a lower yield of polymer. Continuation of the polymerization for periods of time longer than 2 hr resulted in brown-black material possessing a gritty texture. When the amount of cupric chloride was reduced to a catalytic level, a lowered yield (~55%) of gas resulted and the product was a black tar. Similarly, with only small quantities of aluminum chloride, gas evolution was at a low value (~35%) and the product, originally a brown solid, turned purple and took on a cokelike appearance on standing. Therefore, for optimum results an excess of both aluminum chloride and cupric chloride was required.

Polymer Characterization

The evidence indicates that polymerization proceeds as shown in eq. (1).

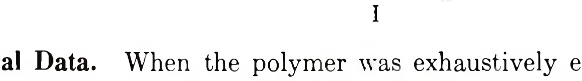

I

(1)

Analytical Data. When the polymer was exhaustively extracted with hexane to remove impurities and lower molecular weight fractions, analytical figures were obtained for the elemental constituents which were in good agreement with theory for structure I. The repeating unit in the chain is a 2,3,5-tri-substituted thiophene. Infrared data for the polymer (Fig. 1) are in good accord[6c] with the spectral characteristics of a number of

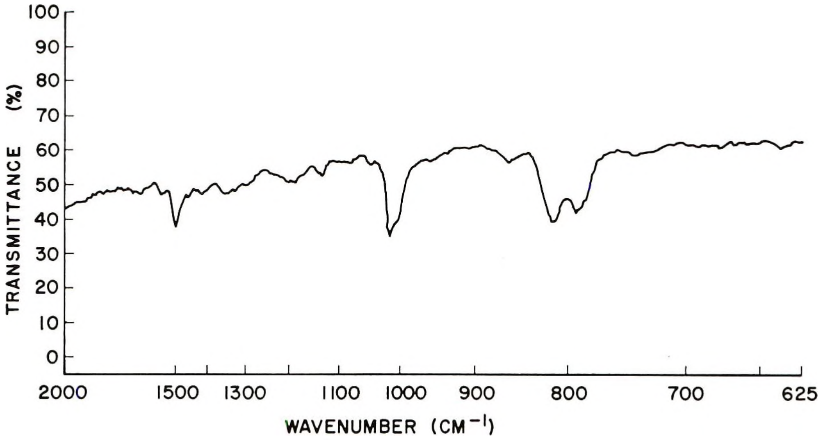

Fig. 1. Infrared spectrum of 2,5-dichlorothiophene polymer (I).

simple model compounds bearing this same substitution pattern(Table I). The NMR spectrum showed a broad, irregular signal in the 6.7–7.5 δ region. Since the product was insoluble in common solvents at room temperature, we did not obtain molecular weight information. The material was observed to dissolve in hot trichlorobenzene. X-ray analysis revealed an amorphous character.

TABLE I
Infrared Spectral Data

Material	Characteristic infrared bands, cm^{-1}		
Polymer (I)	790	815	860
$C_8H_3Cl_3S_2$ (II)	790	819	860
$C_{16}H_6Cl_4S_4$ (III)	778	814	858
2,3,5-Trichlorothiophene	773	813	862
2,5-Dichlorothiophene	784		864

Low Molecular Weight Products. Fortunately, we were able to isolate and investigate several low molecular weight fractions of the polymer. The ether-soluble portion yielded a pale yellow liquid which was made up of at least three substances. Difficulty was encountered in isolating the major component from gas chromatography. Although the material has not been completely characterized, the available evidence indicates a dimer-type entity, possibly of structure II.

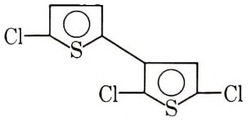

II

This proposal is in excellent agreement with the elemental analysis. In addition, the molecular weight of 273 compares quite favorably with the

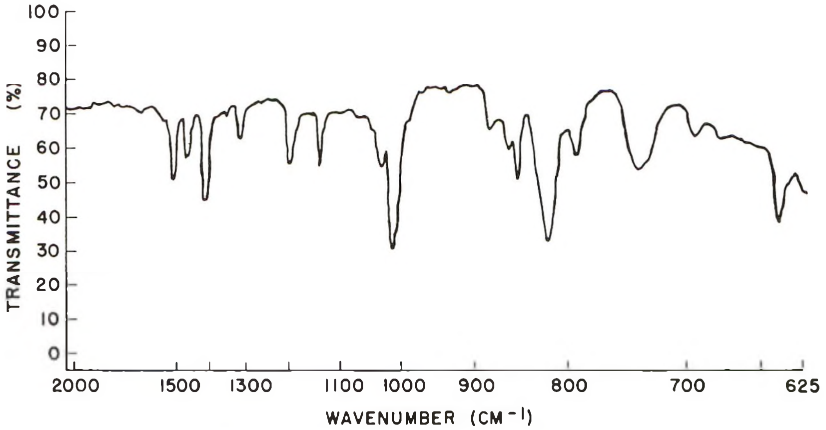

Fig. 2. Infrared spectrum of $C_8H_3Cl_3S_2$ (II).

theoretical value of 270. Satisfactory correlations were observed between the infrared absorption maxima (Fig. 2) and peaks characteristic[6c] of 2,5-di- and 2,3,5-trisubstituted thiophenes (Table I). In the NMR spectrum two doublets and a singlet appeared in the aromatic region (doublet:singlet ratio of 2:1), in keeping with prediction for II. A study[14] of many mono- and disubstituted thiophenes revealed that the coupling constants fall in four distinct regions: $J_{3,5}$ = 1.25–1.70 cps, $J_{2,5}$ = 3.20–3.65 cps, $J_{3,4}$ = 3.45–4.35 cps, and $J_{4,5}$ = 4.90–5.80 cps. A J value of 3.45 cps for our compound lends further credence to the structural assignment since a representation with hydrogens in the 2,5-positions seems highly unlikely.

The ether-soluble portion of the polymer also provided a higher molecular weight fraction (yellow solid, mp 197–199°C) on application of sublimation or column chromatography. The information suggests a tetrameric structure, for which structure III is tentatively advanced as a possibility based on the limited experimental data.

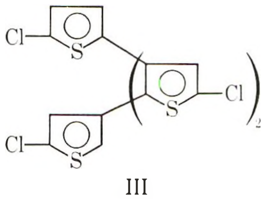

III

The formula for III accords quite nicely with the elemental analysis, and the recorded figure of 454 for the molecular weight fits well with theory (465). In the infrared spectrum we observed the expected substitution pattern (Fig. 3).

Attempted Degradation. Many unsuccessful attempts, entailing oxidation, desulfurization, and dechlorination, were made to obtain chemical evidence concerning the nature of the polymer. Since this gap exists

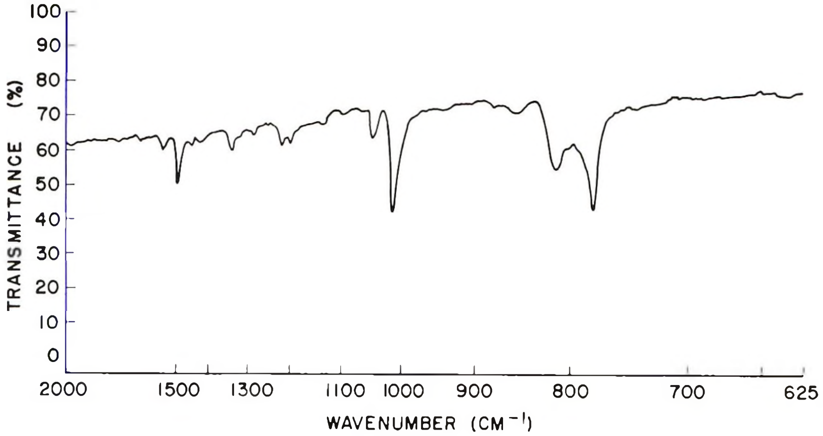

Fig. 3. Infrared spectrum of $C_{16}H_6Cl_4S_4$ (III).

in the characterization picture, the structural assignment should be regarded as tentative.

Polymerization Mechanism

Our conditions are quite similar to those used previously for the polymerization of various aromatic monomers.[10–13] Data[10,15] from the earlier studies support the notion of an oxidative cationic mechanism in the benzenoid studies. Furthermore, the stoichiometry indicates loss of two hydrogens per monomer unit, as in the conversion of benzene to *p*-polyphenylene[10] [eq. (2)].

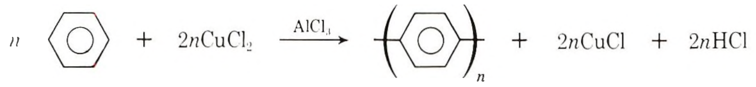

(2)

It is clear from the evidence that a similar scheme is not operative in the present studies, perhaps because of adverse steric factors. Our observations indicate that polymerization of the chlorinated thiophenes involves nuclear coupling with a mole of hydrogen chloride being evolved per monomer nucleus. Several pathways can be envisioned in relation to the detailed aspects. Although the nature of the repeating unit is the same in both cases, there is a difference in the terminal structure.

Scheme A:

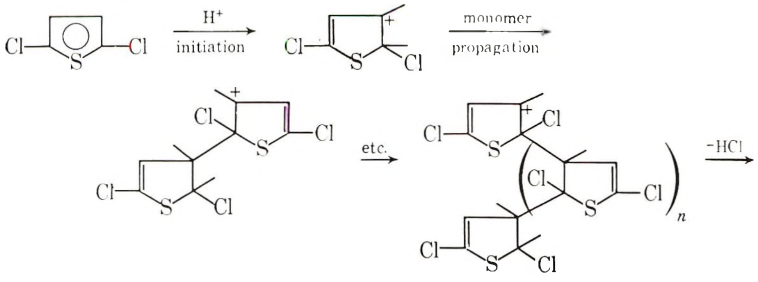

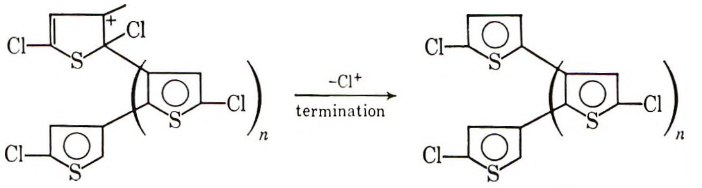

(3)

IV

Scheme B:

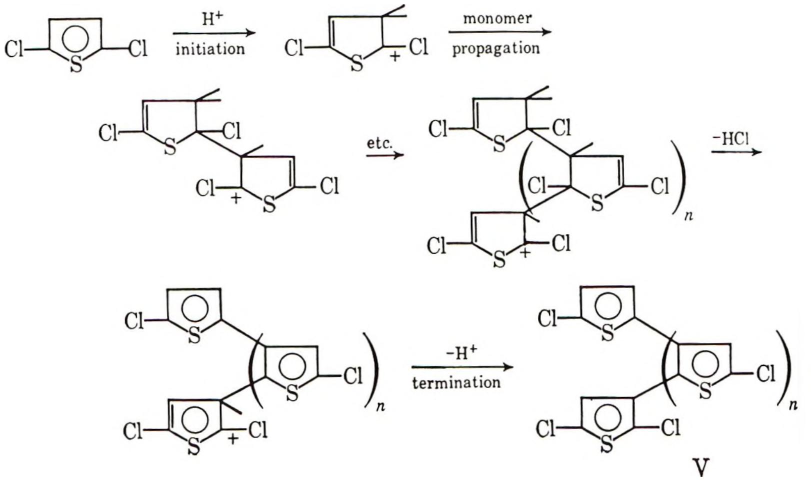

(4)

V

As in the benzene case,[10,15] we propose initiation by a proton derived from a catalyst–cocatalyst (aluminum chloride–Brönsted acid) complex.

$$H_2O + AlCl_3 \rightleftharpoons H_2O\text{-----}AlCl_3 \rightleftharpoons H^{\delta+}AlCl_3(OH)^{\delta-} \qquad (5)$$

Propagation entails attack on the aromatic monomer nucleus by a growing σ-complex carbonium ion. Conceivably, initiation might occur by protonation either at the 2- or 3-position [eqs. (3) and (4)]. By analogy, attack by an electrophile at the 3-position of 2,5-disubstituted thiophenes is well known,[16] as well as fixation in the 2-position of an appropriate 2-substituted thiophene with eventual displacement of the resident group.[17] Scheme A serves to rationalize formation of III, whereas B is in accord with the presence of II. A third possibility for termination might involve intramolecular nuclear attack by the growing end. There may be minor amounts of reduced structures[6b] present in the polymer chains.

According to the general hypothesis, rearomatization is achieved by loss of hydrogen chloride. Since aluminum chloride is known[18] to function as a catalyst for dehydrohalogenation, one might suppose that this metal halide alone would suffice. However, the data reveal best results when appreciable amounts of cupric chloride are included. Copper salt may act to decrease the activity of aluminum chloride in a favorable manner. Alternatively, perhaps copper chlorides participate efficiently to effect dehydrohalogenation in a redox capacity [eq. (6)].

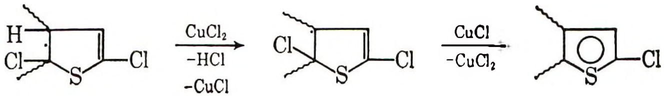

(6)

The mechanistic route postulates the existence of aliphatic sulfide moieties during reaction. The known complexing ability[19,20] of sulfides with metal halides may explain the need for relatively large amounts of the inorganic components. There is uncertainty concerning the stage at which loss of hydrogen chloride occurs.

Part of the polymer color is apparently derived from the 2,3-polythienylene backbone. In fact, the dimer and tetramer-type components exhibited a yellow hue. However, a model of the polymer indicates steric hindrance to coplanarity. Thiophene nuclei linked in chains through the 2- and 5-positions give rise to potent chromophores.[21] One should also consider color contribution by small amounts of impurities and polynuclear structures.

The net effect then is nuclear coupling of a haloaromatic by dehydrohalogenation. Polythienylenes coupled through the 2-3-positions appear to be unique. To our knowledge this represents a novel type of polymerization. A somewhat related transformation was reported recently, namely, conversion of hydroquinone to VI by treatment with zinc chloride at high temperatures.[22]

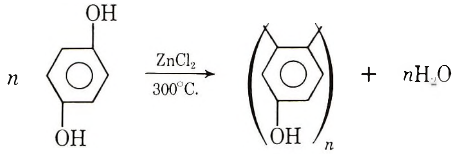

VI

(7)

Paushkin and co-workers[22] advanced a benzyne mechanism for the reaction. We feel that an alternative pathway merits consideration, one analogous to the scheme for 2,5-dichlorothiophene except that water is eliminated. There is also a certain degree of similarity to the conversion of bromophenol to polyphenylene oxide by exposure to copper in basic solution[23].

Polymerization of 2,3,5-Trichlorothiophene

Using the aluminum chloride–cupric chloride system, we found that higher temperatures (90–100°C) were required for polymerization of 2,3,5-trichlorothiophene with trichlorobenzene as solvent. A brick-red, insoluble solid was formed which melted at about 180°C. Evolution of hydrogen chloride amounted to 88% of theory. The reaction, which was also carried out in the neat system, apparently proceeds as illustrated in eq. (8).

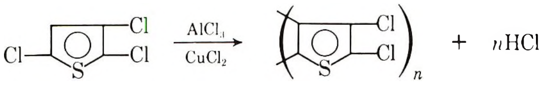

(8)

Analytical data for the elements are in reasonable agreement with the proposition. Sublimation of the product afforded a bright yellow solid which had a tetramer-type structure on the basis of elemental analysis and molecular weight determination. Structure VII serves as a tentative designation based on the limited evidence.

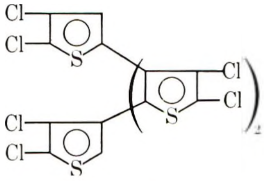

VII

The theoretical considerations advanced for 2,5-dichlorothiophene would appear to apply in this case also. Requirement of more drastic conditions for 2,3,5-trichlorothiophene can be rationalized on the basis if enhanced steric factors and a more deactivated aromatic nucleus.

Polymerization of 2-Chlorothiophene and Thiophene

Under the standard conditions these monomers gave products which appear to possess complicated structures. From the elemental analyses, the chains presumably contain both aromatic and reduced moieties. Relatively small amounts of hydrogen chloride were generated.

EXPERIMENTAL

Materials

Thiophene, Matheson, Coleman and Bell, was used directly. 2-Chlorothiophene, K&K Laboratories, and 2,5-dichlorothiophene, Aldrich Chemical Co., were purified by distillation. 2,3,5-Trichlorothiophene[24] was obtained by pyrolysis of 2,2,3,4,5-pentachlorothiolane which was synthesized from 2-chlorothiophene. Anhydrous aluminum chloride was from the J. T. Baker Chemical Co. and cupric chloride from Allied Chemical Co.

Analytical Procedures and Apparatus

Spectra were obtained with a Becknan IR8 infrared spectrophotometer (potassium bromide disks for the polymer and tetramer-type products, and neat for the dimer-type product). A Varian Associates A-60 nuclear magnetic resonance unit was used (polymer in tetrachloroethylene at 80–90°C, external TMS, and the dimer-type product in carbon disulfide). Gas–liquid partition chromatography (GLPC) investigations were carried out with a 6-ft column of 20% SF96 on Chromosorb P at 180°C. Melting points were determined on a Thomas-Hoover melting point apparatus. Elemental analysis and molecular weight determinations (vapor pressure osmometry) were performed by Galbraith Laboratories, Knoxville, Tennessee.

General Procedures for Polymerization

2,5-Dichlorothiophene. (a) To a stirred solution of 2,5-dichlorothiophene (20 g, 0.13 mole) in carbon disulfide (120 ml), previously purged with dry nitrogen, was added a mixture of aluminum chloride (69.2 g, 0.52 mole) and cupric chloride (35 g, 0.26 mole) at 0°C. At 12°C a vigorous evolution of acid gas commenced and continued at a brisk rate for about 1 hr. After 2 hr at 0–29°C, the rate of gas evolution had subsided considerably. Excess carbon disulfide was decanted from the blue-black reaction mixture, and the remaining sludge was washed with carbon disulfide (100 ml) to extract any unchanged monomer. The last traces of solvent were removed by passing a stream of nitrogen through the reaction flask for 1 hr. The dry mass was broken up and slowly added to ice-cold 20% hydrochloric acid (400 ml) with stirring. Filtration yielded a brown lumpy solid which was triturated with hot dilute hydrochloric acid (200 ml). This was followed by trituration with hot, deionized water until a negative test (silver nitrate) for chloride was obtained. The polymer, after being blended and dried, was a fine, light brown powder, 14 g. (~90% yield based on monomer). The solid darkened at 105–110°C, softened at 110–115°C, turned to a red-black viscous form at 115–118°C, and became a red mobile oil at 140–150°C.

ANAL. Calcd for $\text{-(}C_4HClS\text{)-}_n$: C, 41.2%; H, 0.9%; Cl, 30.4%; S, 27.5%. Found: C, 40.2%; H, 0.8%; Cl, 31.8%; S, 27.2%.

The residue, after extraction (about 20% dissolved) of the product with ether in a Sohxlet apparatus for 24 hr, darkened at 136°C, softened at 145°C, assumed a dark viscous appearance at 150–160°C, and then changed to a red mobile oil at 180°C. After extraction of the polymer with hexane for 120 hr in a Soxhlet apparatus, the residue (50%) gave the following data.

ANAL. Calcd for $\text{-(}C_4HClS\text{)-}_n$: C, 41.2%; H, 0.9%; Cl, 30.4%; S, 27.5%. Found: C, 41.44%; H, 0.93%; Cl, 30.12%; S, 27.3%.

The evolved acid gas was collected in a trap containing standardized sodium hydroxide and then back titrated with acid. On the basis of one mole of gas being liberated per mole of monomer, the yield of hydrogen chloride was 86–90% of the theoretical.

(b) Monomer (20 g, 0.13 mole) in carbon disulfide (120 ml) was treated with aluminum chloride (69.2 g, 0.52 mole) as described in (a) with only little evolution of acid gas. After 2 hr, a sample of the reaction mixture was drawn off and worked up on the usual way yielding an oil. The remainder of the reaction mixture was then treated with cupric chloride (35 g, 0.26 mole) at −10°C and warmed to 20°C for 0.5 hr. A dark brown liquid with a foul odor was obtained on work-up.

(c) 2,5-Dichlorothiophene (20 g, 0.13 mole) in carbon disulfide was treated with aluminum chloride (34.6 g, 0.26 mole) and cupric chloride (5 g, 0.037 mole) as in (a). After the usual work-up, a sticky brown mass was obtained which turned to a black tar when dried under reduced pressure.

(d) 2,5-Dichlorothiophene (20 g, 0.13 mole) in carbon disulfide (120 ml), when treated with aluminum chloride (5 g, 0.037 mole) and cupric chloride (17.5 g, 0.13 mole) as in (a), yielded a coarse purple solid (10.8 g).

2,3,5-Trichlorothiophene. (a) A mixture of the monomer (4 g, 0.021 mole) dissolved in trichlorobenzene (60 ml), previously purged with dry nitrogen, aluminum chloride (11.2 g, 0.084 mole), and cupric chloride (5.6 g, 0.042 mole) was heated at 90–100°C for 2 hr with stirring. After the cooled reaction mixture was filtered, the brown-black sludge gave an orange solid on stirring with cold 18% hydrochloric acid. Purification was accomplished by repeated washings with hot dilute hydrochloric acid followed by trituration with hot, deionized water. The brick red solid, mp ~180°C, was obtained in approximately 63% yield.

ANAL. Calcd for $-\!\!(C_4Cl_2S)\!\!-_n$: C, 31.8%; Cl, 46.9%; S, 21.2%. Found: C, 31.12%; Cl, 49.2%; S, 18.87%.

Hydrogen chloride was evolved in 88% of the theoretical amount.

(b) A mixture of aluminum chloride (14.4 g, 0.108 mole), cupric chloride (7.2 g, 0.053 mole), and 2,3,5-trichlorothiophene (10.9 g, 0.058 mole) in carbon disulfide (10 ml) was heated at 90–100°C for 1 hr. On cooling, filtration afforded a yellow-brown solid in quantitative yield.

ANAL. Calcd for $-\!\!(C_4Cl_2S)\!\!-_n$: 31.8%; Cl, 46.9%; S, 21.2%. Found: C, 30.95%; Cl, 48.56%; S, 19.77%.

2-Chlorothiophene. 2-Chlorothiophene (10 g, 0.084 mole) in carbon disulfide (60 ml) was treated at −10°C with a mixture of aluminum chloride (44.7 g, 0.336 mole) and cupric chloride (22.5 g, 0.168 mole). Removal of the ice-salt bath resulted in a gradual rise in temperature to about 20°C, at which temperature acid gas began to evolve. After 2 hr, the mixture was worked up in the usual manner. The product, a light brown solid, weighed 5.8 g. On the assumption that one molecule of hydrogen chloride is formed per monomer unit, the yield of acid gas was 21%. Analytical data are given in Table II.

TABLE II

		C, %	H, %	Cl, %	S, %
Calcd for	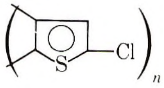	41.2	0.9	30.4	27.5
Calcd for	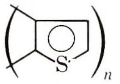	58.5	2.4	—	39.1
Calcd for	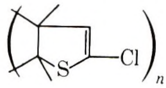	40.5	2.5	29.9	27.0
Found		43.9	1.9	22.4	28.0

Thiophene. To a stirred solution of thiophene (10 g, 0.12 mole) in carbon disulfide (120 ml), previously purged with nitrogen, was added a mixture of aluminum chloride (63 g, 0.47 mole) and cupric chloride (32 g, 0.23 mole) at 0°C. After removal of the cooling bath, stirring was continued for 2 hr as the mixture came to room temperature. No evolution of acid gas was detected from the brown reaction mixture. Carbon disulfide was decanted, and the brown residue, dried by a stream of nitrogen, was triturated first with hot 18% hydrochloric acid and then with hot deionized water. Drying yielded a mustard-colored solid, about 7 g. Analytical data are given in Table III.

TABLE III

		C, %	H, %	S, %	Cl, %
Calcd for	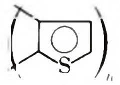	58.5	2.4	39.1	—
Calcd for	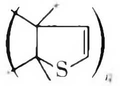	57.1	4.8	38.1	—
Found		54.1	4.3	33.9	2.3

Low Molecular Weight Products

2,5-Dichlorothiophene Polymer. 2,5-Dichlorothiophene polymer (15 g) was placed in a Soxhlet apparatus and extracted for 0.5 hr with ethyl ether. Removal of solvent yielded a red oil which deposited a yellow solid on standing. After the solid was separated from the liquid portion, chromatography through alumina (elution with hexane) gave a bright yellow solid, mp 197–199°C (single entity?). The same material could also be obtained by sublimation of the crude solid.

ANAL. Calcd for $C_{16}H_6Cl_4S_4$: C, 41.3%; H, 1.2%; Cl, 30.1%; S, 27.5%; MW 465. Found: C, 41.2%; H, 0.84%; Cl, 30.4%; S, 27.5%; MW 454.

Distillation of the liquid fraction under reduced pressure gave a pale yellow oil, bp 100–113°C at about 0.4 mm, 1.35 g. Gas chromatographic analysis showed the presence of three peaks, two minor and one major. The major fraction was collected from the gas chromatograph.

ANAL. Calcd for $C_8H_3Cl_3S_2$: C, 35.6%; H, 1.1%; Cl, 39.5%; S, 23.8%; MW 269. Found: C, 35.9%; H, 1.4%; Cl, 39.4%; S, 23.8%; MW 273.

2,3,5-Trichlorothiophene Polymer. Sublimation of the crude polymer with a vacuum pump at 200–230°C yielded a yellow solid. Sublimation prevented a determination of melting point.

ANAL. Calcd for $C_{16}H_2Cl_8S_4$: C, 31.7%; H, 0.33%; Cl, 46.7%; MW 606. Found: C, 32.6%; H, 0.64%; Cl, 47.21%; MW 618.

A preliminary communication of these data has been published.[25]

This work was performed for the Jet Propulsion Laboratory, California Institute of Technology, sponsored by the National Aeronautics and Space Administration under contract NAS7-100 We are grateful to Dr. Herbert C. Brown and Mr. David D. Lawson for helpful discussions, to Dr. Jerome B. Lando for the x-ray experiment, and to Mr. Anthony P. Manzara and Dr. Li-chen Hsu for assistance with the thiophene work.

References

1. V. Meyer, *Ber.*, **16,** 1465 (1883).

2. A. Klages and C. Liecke, *J. Prakt. Chem.*, **61,** 307 (1900).

3. W. Klatt, *Z. Anorg. Allgem. Chem.*, **232,** 393 (1937).

4. K. Fredenhagen, *Z. Physik. Chem.*, **164,** 176 (1933).

5. J. Bruce, F. Challenger, H. B. Gibson, and W. E. Allenby, *J. Inst. Petrol.*, **34,** 226 (1948).

6. H. D. Hartough, *Thiophene and Its Derivatives,* Interscience, New York, 1952, (a) p. 165, (b) p. 166, (c) p. 106 ff.

7. A. V. Topchiev, Y. Y. Gol'dfarb, and B. A. Krentsel, *Vysokomol. Soedin.*, **3,** 870 (1961).

8. A. V. Topchiev, B. A. Krentsel, and Y. A. Gol'dfarb, *Izv. Akad. Nauk SSSR, Otd. Khim. Nauk*, **1959,** 369.

9. S. A. Safarov and M. A. Proskurnin, *USSR Pat.* 142,648 (1961).

10. P. Kovacic and A. Kyriakis, *J. Amer. Chem. Soc.*, **85,** 454 (1963).

11. P. Kovacic and F. W. Koch, *J. Org. Chem.*, **30,** 3176 (1965).

12. P. Kovacic, J. T. Uchic, and L. C. Hsu, *J. Polym. Sci. A-1*, **5,** 945 (1967).

13. P. Kovacic and J. S. Ramsey, *J. Polym. Sci. A-1*, in press.

14. S. Gronowitz, *Advances in Heterocyclic Chemistry*, Vol. 1, A. R. Katritzky, ed., Academic Press, New York, 1963, p. 8.

15. P. Kovacic, F. W. Koch, and C. E. Stephan, *J. Polym. Sci. A*, **2,** 1193 (1964).

16. H. D. Hartough and L. G. Conley, *J. Amer. Chem. Soc.*, **69,** 3096 (1947).

17. H. D. Hartough and A. I. Kosak, *J. Amer. Chem. Soc.*, **69,** 3093 (1947).

18. C. A. Thomas, *Anhydrous Aluminum Chloride in Organic Chemistry,* Reinhold, New York, 1941, pp. 94, 103, 104.

19. N. N. Greenwood and K. Wade, *Friedel-Crafts and Related Reactions,* G. A. Olah, ed., Vol. I, Interscience, New York, 1963, p. 587.

20. H. J. Worth and H. M. Haendler, *J. Amer. Chem. Soc.*, **64,** 1232 (1942).

21. J. W. Sease and L. Zechmeister, *J. Amer. Chem. Soc.*, **69,** 270 (1947).

22. Y. M. Paushkin, L. S. Polak, O. Y. Omarov, and I. I. Patalakh, in *International Symposium on Macromolecular Chemistry* (*J. Polym. Sci. C*, **16**), O. Wichterle and B. Sedláček, Eds., Interscience, New York, 1967, p. 2215.

23. R. W. Lenz, *Organic Chemistry of Synthetic High Polymers,* Interscience, New York, 1967, p. 170.

24. H. L. Coonradt and H. D. Hartough, *J. Amer. Chem. Soc.*, **70,** 1158 (1948).

25. J. S. Ramsey and P. Kovacic, *Chem. Commun.*, in press.

Received June 14, 1968

JOURNAL OF POLYMER SCIENCE: PART A-1 VOL. 7, 139-155 (1969)

Molecular Structure Parameters in Certain Semiconducting Polymers

J. H. T. KHO and HERBERT A. POHL,* *School of Engineering, Princeton University, Princeton, New Jersey*

Synopsis

The condensation polymers formed by condensing aromatic hydrocarbons or their derivatives with aromatic acids are quite conductive. The room temperature resistivities of 42 polymers studied here range from 10^2 to 10^{12} ohm-cm. It is found that the resistivities are inversely related to the number of fused rings in the hydrocarbon portion of the monomer for either the homopolymers or copolymers. The resistivities are strongly dependent, inversely, upon the acid strength of the acid monomer reactants. For all the polymers studied, the conductivity σ depended upon the pressure P as $\ln(\sigma/\sigma_0) = (b^*/k)P^{1/2}$ where b^* is seen to be an inverse function of the number of fused rings in the monomer in accord with theory. The resistivity ρ varied with absolute temperature T, as $\ln \rho \propto (1/T)$ for all polymers. Thermoelectric powers were determined, and the various relationships established among energy interval, resistivity at "infinite temperature," carrier concentrations and mobility ratios, number of fused rings, and pressure coefficients are discussed. The polymers are p-type. Doping by Be^{++} or Cu^{++} has a small effect, increasing the conductivity slightly. Electron spin concentrations and carrier concentrations are directly related among the polymers, being found nearly equal for the most conductive but differing by up to nine orders of magnitude in the least conductive polymers.

INTRODUCTION

The interesting family of polymers known as the polyacene quinone radical polymers (PAQR polymers) have been shown to exhibit enhanced electronic behavior such as semiconduction, piezo-conductivity, and extremely high dielectric constants.[1-10]

PAQR polymers are condensation polymers obtained by condensation of aromatic hydrocarbons derivatives with acids or their derivatives such as amhydrides, amides and imides. Such polymers are highly conjugated. Conjugation in a certain superlative degree, i.e., ekaconjugation,[10] is considered to be a key characteristic in polymers exhibiting enhanced electric properties, such as semiconduction, and a high concentration of unpaired spins. The extent of potential ekaconjugation is proportional to the number of consecutive π-electron orbitals in the molecular structure; the degree of potential ekaconjugation is proportional to the coupling between succes-

---

* Present address: Department of Physics, Oklahoma State University, Stillwater, Oklahoma 74074.

sive π-electron orbitals. In comparison to most other known types of polymers, the PAQR polymers exhibit especially high σ_∞ values, relatively high mobilities, and therefore, probably possess such long-range orbital symmetry. The factor σ_∞ is obtained from the experimentally observed relation

$$\sigma = \sigma_\infty \exp \{-E_a/kT\} \tag{1}$$

where σ is specific conductivity, E_a is activation energy, k is the Boltzmann constant, T is absolute temperature, and σ_∞ is the extrapolated conductivity at infinite temperature and pressure, $P = 0$.

The purpose of the present study is to examine specifically the effects of the following variables on the electrical properties of the PAQR polymers: (a) hydrocarbon portion of the polymer; (b) acidic portion of the polymer; (c) copolymerization; (d) metallic complexing; (e) pressure and temperature.

EXPERIMENTAL

The PAQR polymers synthesized for this present study may be roughly classified into four main groups: (A) those formed with pyromellitic diahydride (PMA) as the "fixed" aromatic acid derivative, and with variously substituted aromatic hydrocarbon derivatives; (B) those formed with pyrene as the "fixed" hydrocarbon, and with various aromatic acids or anhydrides; (C) copolymers, with pyrene as a comonomer with some other hydrocarbon derivative and with PMA as the "fixed" acid; (D) metal-doped polymers formed by metal ions held by ligands on group (A) polymers.

Synthesis of PAQR Polymers

Purified reactants were ground together with anhydrous $ZnCl_2$ catalyst. The mole ratios were: for group A, hydrocarbon derivative/PMA/$ZnCl_2$ = 1:1:1; for group B, pyrene/aromatic acid/$ZnCl_2$ = 1:1:1; for group C, the copolymers, pyrene/substituted aromatic hydrocarbon/PMA/$ZnCl_2$ = 1:1:1:1.5. The mixed components, in a lightly stoppered 150 × 20 mm Pyrex test tube were then heated for 20 hr at 306°C in a benzophenone vapor bath, cooled, ground fine, and leached with 0.1*M* HCl three times to extract $ZnCl_2$. The powders were then purified by exhaustive extraction with H_2O (12 hr), ethanol (24 hr), then toluene (24 hr) in Soxhlet extractors, then dried at 60°C in air for 6 hr, cooled, and stored over a desiccant.

Synthesis of Metal-Doped PAQR Polymers

Portions of four polymers (Nos. 30, 31, 34, 35) were selected for doping. Approximately 0.1 g of each was weighed, then steeped in 10 ml of either 1*N* $Be(NO_3)_2$ or 1*N* $CuSO_4$ at 60°C for 24 hr, held at 25°C for 24 hr, filtered, washed several times with distilled H_2O, dried, and stored over a desiccant for one week before conductivity measurements.

Measurements

Resistance–pressure–temperature measurements were made as described earlier[1,2,5] at ten temperatures between 25 and 120°C. Thermoelectric power (Seebeck coefficient) measurements were made as described earlier[1,2] at 100 kg/cm^2, ten readings for each sample, with temperature intervals up to 30°C. Spin concentrations were determined with the use of doubly recrystallized diphenylpicryl hydrazyl (DPPH) as reference standard, by a resonance method with the equipment and considerable assistance of Dr. Robert Pressley at the Palmer Physical Laboratory. The spectra of the samples and of the DPPH were produced with finely divided Li metal as internal reference.

RESULTS AND DISCUSSION

Conductivity and Chemical Structure

We may consider the behavior of macromolecular semiconduction from either physical or chemical aspects. Much has been written and studied about the physical aspects. The movement of the carriers and the type of carriers have been discussed elsewhere,[1–8,10–16] especially by Pohl et al.[7,10]

TABLE I
Room Temperature Resistivity of PAQR Polymers[a]

Sample no.	Substituted aromatic hydrocarbon	Room temperature resistivity at 1800 kg/cm^2, ohm-cm
26	Violanthrone	5.9×10^3
4	Phenanthrene	2.9×10^5
1	Pyrene	3.9×10^5
30	Quinizarin	8.2×10^5
24	Alizarin	1.5×10^6
6	Anthracene	2.4×10^6
18	Indigo	3.9×10^6
31	Quinoxaline	5.6×10^6
22	Congo Red	2.1×10^7
14	Benzoazurine C	3.1×10^7
10	Aniline Black	5.2×10^7
20	Meldola Blue	1.7×10^8
8	p-Naphtholbenzein	3.3×10^8
34	2-5 Dihydroxy-*p*-benzoquinone	5.4×10^8
16	Amaranth	5.8×10^8
35	2,5-Dichloro-3,6-dihydroxy-*p*-Benzoquinone	7.2×10^8
12	Eosin Y	1.3×10^9
3	Fluorescein	7.7×10^{10}

[a] Group A: PMA vs. various substituted aromatic hydrocarbons (SAHC:PMA:-$ZnCl_2$ = 1:1:1).

The possible effects of grain boundaries was discussed previously[16] and was examined in much detail by Hartman and Pohl.[18] Extrinsic effects were also discussed[6,10,16,17] in previous reports. Localized states and trapping were considered by Pohl et al.[5,10,17] and Eley et al.[12–15]

With regard to the chemical aspects, the conductivity of macromolecular solids depends strongly on the molecular length[5,7,10,11,19] and upon the specific chemical structure parameters.

We shall consider first the effects of chemical structure parameters. The compositions and room temperature resistivity at 1800 kg/cm² of 42 PAQR polymers are tabulated in Tables I–III.

TABLE II

Room Temperature Resistivity of PAQR Polymers[a]

Sample no.	K_a	Aromatic acid or anhydride	Room temperature resistivity at 1800 kg/cm², ohm-cm
64	1.25×10^{-3}	*o*-Iodobenzoic acid	2.7×10^{2}
68	1.40×10^{-3}	Chloroacetic acid	5.9×10^{2}
55	1.29×10^{-3}	*o*-Chlorobenzoic acid	7.3×10^{2}
59	1.51×10^{-4}	*m*-Chlorobenzoic acid	1.3×10^{3}
62	3.98×10^{-4}	*p*-Nitrobenzoic acid	2.7×10^{3}
70		1,12-Benzoperylene dicarboxyl anhydride	2.8×10^{4}
63	7.22×10^{-5}	*p*-Fluorobenzoic acid	7.8×10^{4}
58	3.98×10^{-5}	Gallic acid	1.3×10^{7}
72		Xanthene-10-carboxylic acid	1.5×10^{7}
57		Syringic acid	2.2×10^{7}
71		9-Fluorenecarboxylic acid	9.8×10^{11}
60	1.51×10^{-5}	*m*-Aminobenzoic acid	4.7×10^{12}

[a] Group B: pyrene vs. various aromatic acids (pyrene:AA:$ZnCl_2$ = 1:1:1).

It has been shown earlier that the structure of the monomer is an important factor in the resistivity of the polymer.[1,2,4,5,9] The number of fused aromatic rings in the monomer is indicative of its degree of conjugation extent, and is a useful parameter in studying the effect of structure on the conductivity of the polymer. The conductivity σ is proportional to the size of the unit charge transported $|e|$, to the number of carriers n, and to the mean mobility μ of the carriers.

$$\sigma = |e|n\mu \tag{2}$$

Increased ekaconjugation should strongly increase the concentration of available carriers—which might be holes or electrons or both—and moderately increase the ease of electron transport or mobility. A prime factor in the transport will be the electron transfer from molecule to molecule. It is

TABLE III
Room Temperature Resistivity of PAQR Copolymers[a]

Sample no.	Substituted aromatic hydrocarbon	Room temperature resistivity at 1800 kg/cm^2, ohm-cm
27	Violanthrone	2.8×10^3
40	Pyrene	5.6×10^3
25	Alizarin	1.3×10^4
19	Indigo	1.5×10^5
7	*p*-Naphtholbenzein	7.5×10^5
13	Eosin Y	1.0×10^6
9	Aniline Black	1.4×10^6
21	Meldola Blue	6.8×10^6
2	Fluorescein	7.1×10^7
17	Amaranth	1.0×10^8
23	Congo Red	7.4×10^9
15	Benzoazurine G	2.4×10^{10}

[a] Group C: pyrene, PMA vs. various substituted aromatic hydrocarbons (pyrene:-SAHC:PMA:$ZnCl_2$ = 1:1:1:1.5).

presently thought that where the mobilities are less than 1–10 cm^2/V-sec that transport is mainly by "hopping," rather than by a grander-scale process describable as "wave-packet drifting" through a crystal lattice. Measurements to date on the PAQR polymers indicate the mobilities to be of the "hopping" class. To the extent that this involves electrons "hopping over" or tunnelling through intermolecular potential barriers, we shall expect mobility to be greatly aided by any means which diminishes intermolecular distances, in particular, distances between π orbital centers on neighboring molecules. To the extent that orbitals on molecules separated by van der Waals-type distances (ca. 3–4 Å) can be mixed, we would expect a (lesser) effect on the ease of carrier formation when intermolecular distances are diminished. Among the ways one may expect to vary intermolecular distances are: pressure, hydrogen bonding, donor–acceptor complexing, and intermolecular ionic attraction. The latter three would appear favorable only in the event that they specifically act to increase intermolecular electron orbital overlap between the π systems (i.e., orthogonality conditions). Pressure effects are expected to be general and always increase orbital overlap and hence conductivity between ekaconjugated molecules. With these thoughts in mind, we have examined the effect of pressure and of incorporating into the polymer such chemical structures as might conceivably reduce intermolecular distances as by having internal salt structures, hydrogen bonding, or intermolecular complexing.

We see from Figure 1 that the resistivity of the polymers with the hydrocarbon portion varied does decrease strongly as the number of fused rings of the monomer increases. A similar behavior is observed in the copolymer series (Fig. 2). Here also is compared the behavior of the homopolymer

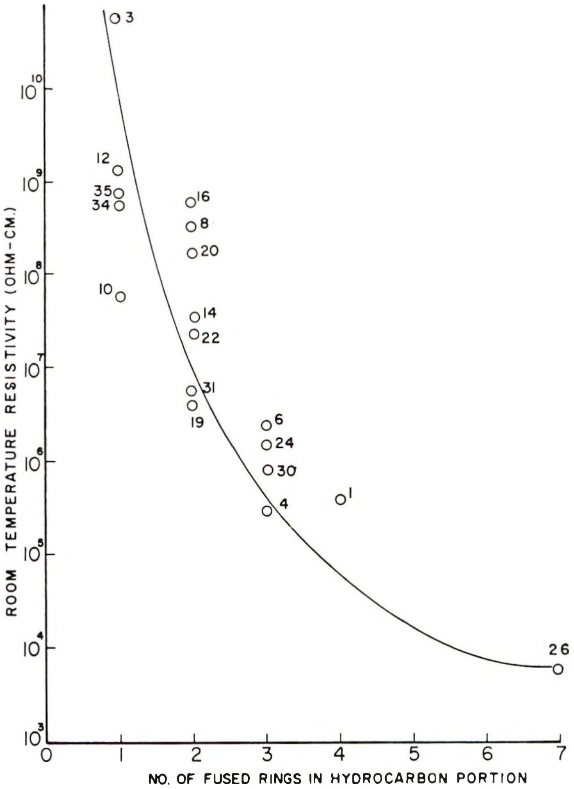

Fig. 1. Room temperature resistivity as a function of the number of fused rings in the hydrocarbon portion of the homopolymers.

series with that of the copolymer series. The series[1] obtained from the starting compositions 2:1:1 (hydrocarbon:acid:catalyst mole ratio) having two to four fused rings have rather lower resistivities than for the 1:1:1 mole ratio.

Evidence for the probable importance of internal salt-like structure in increasing the polymer conductivity is to be seen in Figure 3, in which the resistivity of the polymer is observed to be remarkably lowered (through nine orders of magnitude) in proportion to the ionization constant K_a of the acid used in the synthesis. Increased content of ionic states can be expected to accentuate both carrier formation and mobility by foreshortening intermolecular distance.

An attempt to further diminish inter molecular distances by complexing was made by using metal ion chelation. PAQR polymers prepared from pyromellitic anhydride and quinizarine (no. 30), quinoxaline (no. 31), 2,5-dihydroxy-*p*-benzoquinone (no. 34), or 2,5-dichloro-3,6-dihydroxy-*p*-benzoquinone (no. 35) can contain potential metal chelation structures:

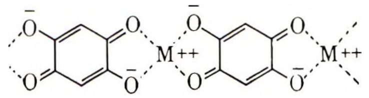

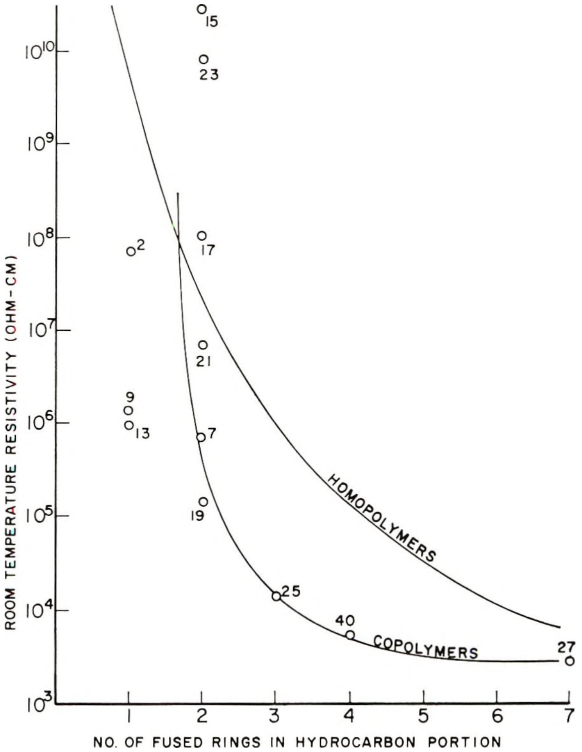

Fig. 2. Room temperature resistivity as a function of the number of fused rings in the hydrocarbon portion of homopolymers and copolymers.

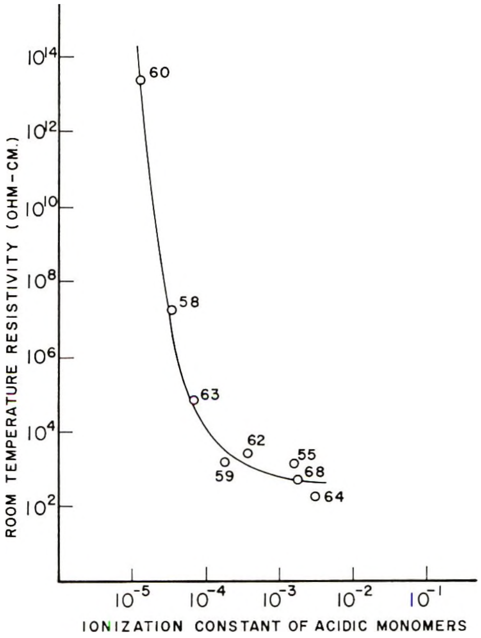

Fig. 3. Room temperature resistivity of the homopolymers as a function of the acidic monomer portion.

Treatment of these polymers with aqueous Cu^{++} or Be^{++} salts gave material containing small (1–2% by weight) amounts of metal, presumably reacted as above. As Table IV shows, the metal-doped dry polymers were only slightly more conductive (1.4–61%) than the precursor polymers. That only small effects are noted can mean either that the interatomic distances and electron transport were not much affected by replacing the hydrogen bonds with chelation, or that the expected effect has very specific spatial requirements which the above combinations did not happen to meet.

TABLE IV
Room Temperature Resistivity of Metal-Doped PAQR Polymers

Sample no.	Doping metal	Ions	Resistivity, ohm-cm	Decrease in resistivity due to doping, %
30		None	8.2×10^5	
31		None	5.6×10^6	
34		None	5.4×10^8	
35		None	7.2×10^8	
30A	Beryllium		7.9×10^5	3.7
31A	Beryllium		5.4×10^6	3.6
34A	Beryllium		4.0×10^8	25.9
35A	Beryllium		7.1×10^8	1.4
30B	Copper		7.6×10^5	7.3
31B	Copper		4.6×10^6	17.0
34B	Copper		2.1×10^8	61.1
35B	Copper		6.7×10^8	7.0

From the point of view that one might seek to enhance ekaconjugation by having the orbitals of the ligand groups increase their overlap through the intermediation of the metal ion, one would expect tetrahedral coordination to cause two bifunctional ligand groups to become attached at planes at right angles to each other (as in Be^{++}, for example) and would thereby quite thoroughly minimize intermediated π–π overlap between. On the other hand, those ions which were capable of square planar or octahedral coordination, for example, could offer a $d\pi$–$p\pi$ bonding through the ion for the pair of bifunctional ligands. In such a case, ekaconjugation may be enhanced. Cu^{++} ion, which presumably would coordinate octahedrally here, can coordinate in either a planar or nonplanar fashion with the two bifunctional ligands. Planar coordination would be expected to increase orbital interaction of the organic ligands and increase ekaconjugation and conductivity. Nonplanar coordination would be expected to cause little increase in ekaconjugation. The data can be taken to suggest that Cu^{++} ion is indeed more effective than the Be^{++} ion.

Piezo-Conductivity, and Thermal Effects

The effect of extreme pressures on the resistivity of a number of polymers has been examined earlier.[1–3,8,9] It was shown that large piezo-conductiv-

TABLE V
Pressure Coefficient of Resistivity for PAQR Polymers

Group A polymers		Group B polymers	
Sample no.	Pressure coefficient $b^* \times 10^6$, eV/atm$^{1/2}$ °K	Sample no.	Pressure coefficient $b^* \times 10^6$, eV/atm-$^{1/2}$°K
1	3.93	70	2.25
26	4.52	65	3.02
24	4.66	62	3.15
31	5.44	57	3.47
3	5.61	55	4.05
30	5.82	59	4.99
20	6.21	72	5.39
10	6.83	58	6.29
35	7.90	68	7.12
12	8.92	63	7.57

ity coefficients were observable at pressures up to 100,000 atm. An interpretative relation has been derived by Pohl[3] by using an absolute reaction rate formalism

$$\ln (\sigma/\sigma_0) = P^{1/2} [(b_0/kT) + (b''/k)] = (b^*/k)P^{1/2} \tag{3}$$

where P is pressure applied, σ is specific conductivity at P, T, σ_0 is specific conductivity at $P = 0$, $T = T$, and k is the Boltzmann constant; b^*, b'', b_0 are pressure coefficients of resistivity, being the total, the entropy, and the enthalpy factors, respectively.

The results for 20 polymers, at pressures up to 2200 kg/cm², are indicated in Table V. The conductivity for each followed eq. (3), to within experimental error. A typical result is shown in Figure 4 for the PAQR polymer prepared from *m*-chlorobenzoic acid and pyrene.

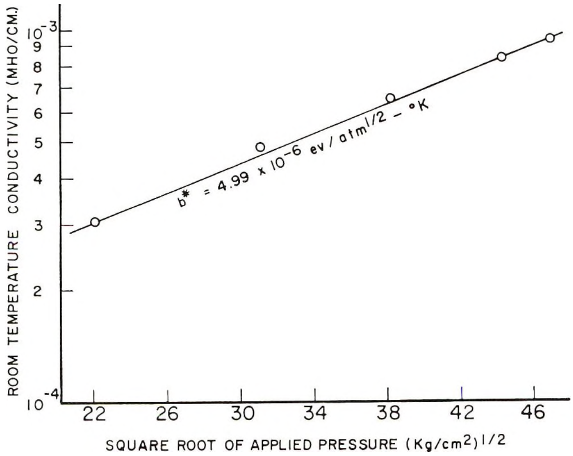

Fig. 4. Room temperature conductivity as a function of the square root of the applied hydrostatic pressure for polymer 59.

The piezo-conductivity coefficient at constant temperature b^* may be regarded as a structural parameter relating the effective area of contact or tunneling cross section for intermolecular electron transfer to the pressure. Alternatively, it relates the ease of tunneling between molecules to the intermolecular geometric overlap of orbitals as affected by pressure. As noted previously,[3] it was expected that the thermal activation energy, E_{a0} would be proportional to b^*. This expectation again appears to be borne out, as can be seen by reference to Figure 5. For rather similar reasons, we expect

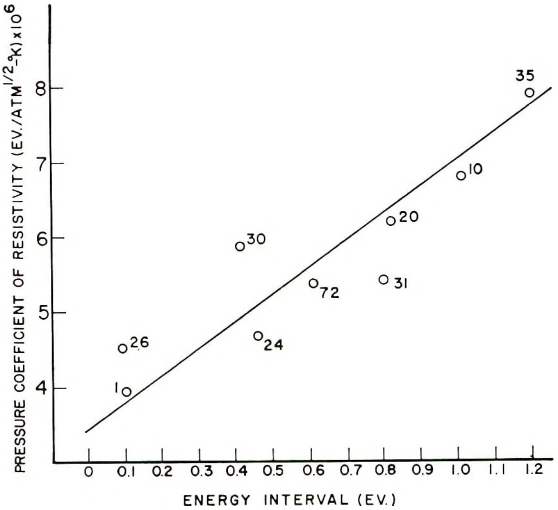

Fig. 5. Pressure coefficient of resistivity as a function of energy interval.

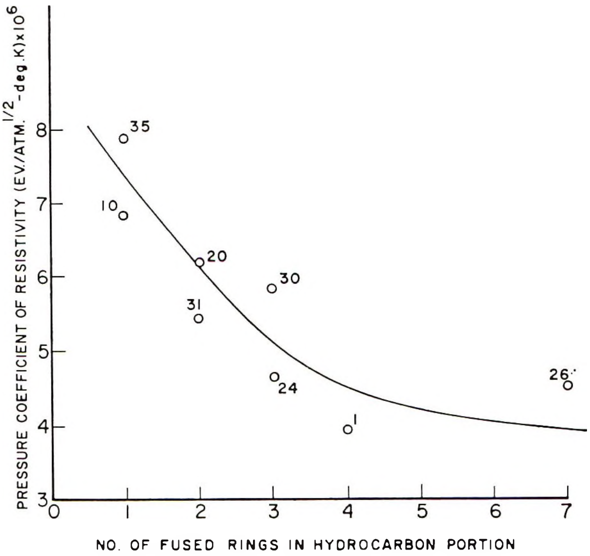

Fig. 6. Pressure coefficient of resistivity as a function of the number of fused rings in the hydrocarbon portion of the PAQR homopolymers.

b^* to decrease as the number of fused rings in the monomer increases. This, too, is observable in Figure 6.

The temperature dependence of these materials is in accord with the Arrhenius plot to within experimental error [eq. (1)]. The activation energies, as ΔE, range from 0.09 to 1.2 eV. Values of the energy interval ΔE and σ_∞, expressed as its reciprocal ρ_∞, are given for 16 PAQR polymers in Table VI.

TABLE VI
Values of Energy Interval and Resistivity at Infinite Temperature for PAQR Polymers

Sample no.	ΔE, eV	ρ_0, ohm-cm
35	1.20	5.1×10^{-2}
34	0.95	4.8×10^{0}
31	0.80	9.2×10^{-1}
4	0.47	3.0×10^{1}
24	0.46	1.9×10^{2}
30	0.41	5.2×10^{2}
8	1.02	7.8×10^{-1}
20	0.82	1.9×10^{1}
9	0.11	1.5×10^{-1}
2	0.38	2.7×10^{1}
10	1.01	1.4×10^{-1}
1	0.10	5.6×10^{4}
26	0.09	1.0×10^{3}
27	0.10	3.7×10^{2}
72	0.61	7.6×10^{-1}
13	0.11	8.9×10^{1}

As discussed earlier, it is reasonable to consider that in the ekaconjugated organic solids, the formations of unpaired spins and of ionization occur in sequential steps, e.g.,

$$\mathrm{R} \leftrightharpoons \cdot\mathrm{R}\cdot \tag{4}$$

$$2\mathrm{R} \leftrightharpoons \mathrm{R}\cdot^{+} + \mathrm{R}\cdot^{-} \tag{5}$$

where R denotes the original ekaconjugated ground state molecules, $\cdot\mathrm{R}\cdot$ are biradial exicted state molecules, and $\mathrm{R}\cdot^{+}$, $\mathrm{R}\cdot^{-}$ are fully ionized molecules, also carrying unpaired spins. The equilibria can be written

$$[\cdot\mathrm{R}\cdot]/[\mathrm{R}] = K_1 = \exp\{-\Delta F_1/kT\} \tag{6}$$

$$[\mathrm{R}\cdot^{+}][\mathrm{R}\cdot^{-}]/[\mathrm{R}]^2 = K_3 = \exp\{-\Delta F_3/kT\} \tag{7}$$

In an intrinsic semiconductor, $[\mathrm{R}\cdot^{+}] = [\mathrm{R}\cdot^{-}]$, i.e., the concentration of negative equals the concentration of positive carriers. The ratio of total unpaired spin concentration to positive carrier concentration is then:

$$\begin{aligned}[\mathrm{F.R.}]/[\mathrm{R}\cdot^{+}] &= 2\,[K_1\,K_3^{-1/2} + 1]\\ &= \exp\left\{\frac{1}{kT}\left(-\Delta F_1 + \frac{\Delta F_3}{2}\right)\right\} + 1 \end{aligned} \tag{8}$$

where $[\mathrm{F.R.}] = 2\,[\cdot\mathrm{R}\cdot] + [\mathrm{R}\cdot^{-}] + [\mathrm{R}\cdot^{+}]$

The ratio approaches 2 if all molecules are very easily excited, and approaches the ratio of the two dissociation constants if they are not. Such behavior is indeed implied, as may be seen in Figure 7, which compares the observed spin concentrations with the suggestive "carrier concentrations" calculated by using simple band theory. Only for easily excited molecular systems are the spin and carrier concentrations nearly equal. Where excitation is difficult, the concentration ratio may apparently approach 10^9.

The magnitude of the thermal activation energy for the production of carriers, expressed as $\Delta E = 2E_a$, is seen to be directly proportional to the reciprocal of the number of fused rings in the monomer segments. This confirms earlier observations[1,2] (Fig. 8) and is in accord with expectation based upon quantum mechanical arguments using the "metallic" model for calculating energy levels in cyclic π-electron systems.[1,10,12,13]

In a manner developed by Eley and Parfitt[13] for a series of organic monomers, a plot here of log σ_∞ versus the ΔE values shows the values to be somewhat related for the semiconducting polymers examined here, as may be seen in Figure 9. Just how this is to be interpreted is still something of a problem.[14] The experimental observation is that eq. (1) is closely followed in each instance. This implies that σ_∞ is not a strong function of temperature (i.e., not exp $\{E/kT\}$ but rather as $T^{\pm M}$, perhaps, where M is small, for example).

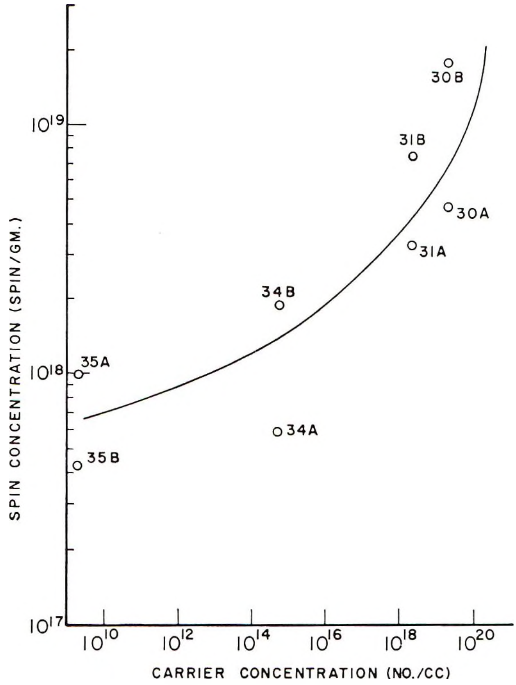

Fig. 7. Spin concentration versus carrier concentration.

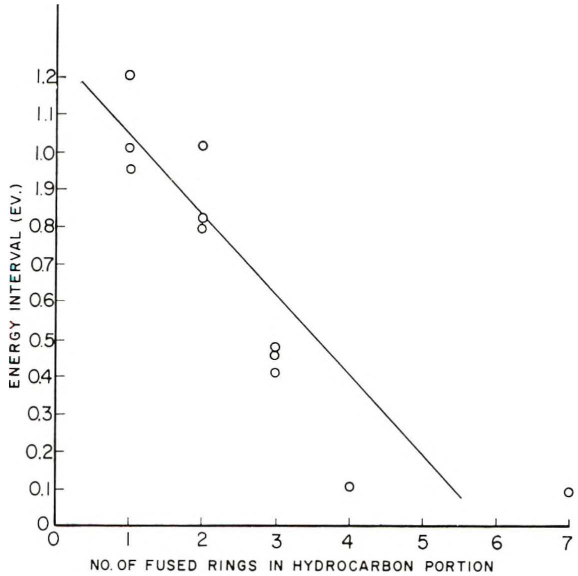

Fig. 8. Energy interval as a function of the number of fused rings in the hydrocarbon portion of the PAQR homopolymers.

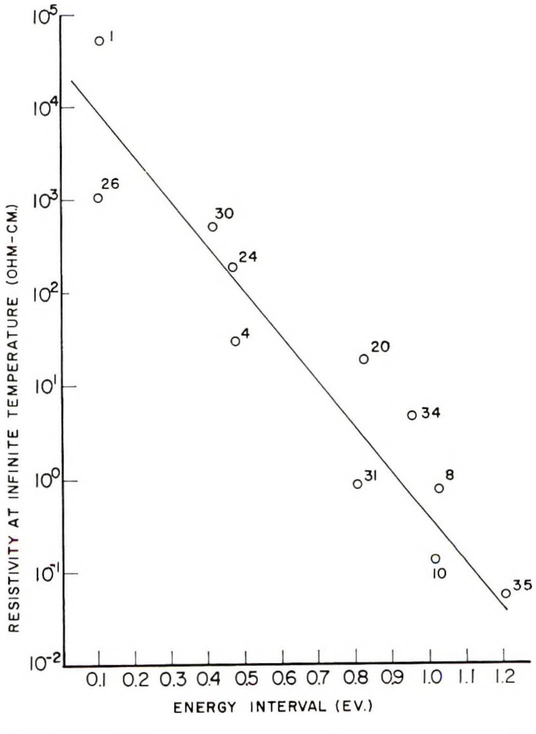

Fig. 9. Resistivity at "infinite" temperature as a function of energy interval for PAQR homopolymers.

If one applied the band theory equation, for example,

$$\sigma_\infty = \frac{|e|\ 2(2\pi mkT)^{3/2}}{h^2} \cdot \mu \cong 4\mu \text{ (at 25°C)}$$

then the observed values of σ_∞ imply mobilities of 10^4–10^{-2} cm^2/V sec, which appear to range unreasonably high. The problem is more acute in data for the proteins, etc., of Eley and Spivey,[15], where mobilities of up to 10^{15} cm^2/V-sec. would be so interpretable. It is interesting to note that this implied mobility, or better, the σ_∞ term, is generally observed to be larger, the lower the conductivity of the organic solid.

It would seem more satisfactory to regard σ_∞ as made up of preexponential terms describing limiting behaviors of both the concentration carriers and their mobility, and to assume therefore an exponential temperature dependence of both carrier concentration and mobility. This implies, as is now generally accepted, that carrier movement in such substances as we are discussing is by "hopping" or thermally sensitive tunneling processes. Then

$$\sigma = \sigma_\infty \exp\{-\Delta E/2kT\} \tag{9}$$

$$\mu = \mu_0 \exp\{-E_s/kT\} \tag{10}$$

$$n = N_0 \exp\{-E_g/2kT\} \tag{11}$$

$$\Delta E = E_g + 2E_s \tag{12}$$

$$\sigma_\infty = |e| N_0\, \mu_0 \tag{13}$$

where E_s is the saddle-height energy of the thermally activated mobility process and is probably of a magnitude $0 \leq E_s \leq 1.0$ eV for the systems discussed. A theoretical estimate of E_s as ≈ 0.1 eV was made by Pohl[16] from polarizability considerations. Here, the carrier density pre-exponential term N_0 can be considered as ranging from about 10^{19} cm^{-3} (as for parabolic state density distribution calculated in band theory) to about 10^{21} cm^{-3} (as for narrowly populated excitation bands). This reinterpretation of σ_∞ and hence of the implied mobility as μ_0 and not μ perhaps helps in removing some of the embarassment over the large values observed.

In terms of the absolute reaction rate formalism developed earlier[3]

$$\mu = |e|\ (Ld/3h) \exp\{\Delta S\ddagger/k\} \exp\{-\Delta H\ddagger/kT\} \tag{14}$$

where L is molecular length, d is the hop half-width between molecules, h is Planck's constant, and $\Delta S\ddagger$, and $\Delta H\ddagger$ are the entropy and heat of activation, respectively, for the activated state. In the approximation there discussed where the transfer of the electron is treated as roughly equivalent (quantum mechanically) to a particle in a box comprised of the "overlapped" segments of the two molecules,

$$\exp\{\Delta S\ddagger/k\} = f\ddagger/f = \{h/(2\pi mkT)^{1/2}\}(a\ddagger/V) \tag{15}$$

where $f\ddagger$ and f are the partition functions of the activated and precursor systems, m is the effective mass of the electron (or holes), $a\ddagger$ is the area of contact of the two molecules, and V is the volume of the originating molecule.

For planar ekaconjugated molecules, which can be regarded as thin disks of thickness t = constant,

$$V \cong t\, L^2 \tag{16}$$

leading to the expectation that

$$\sigma_\infty \propto 1/L \tag{17}$$

This expectation is at least partially confirmed experimentally on noting the trend shown in Figure 10 between the values of σ_∞ and FR, the number of fused rings in the hydrocarbon portion of the monomer.

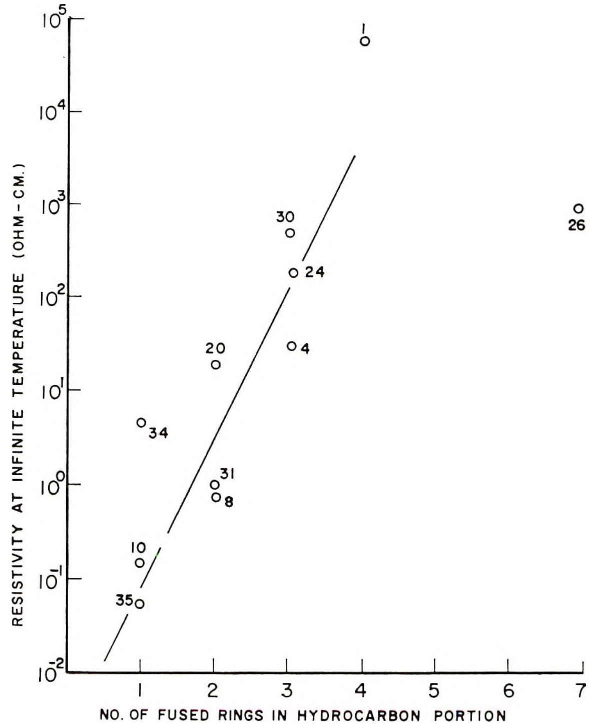

Fig. 10. Resistivity at "infinite" temperature as a function of the number of fused rings in the hydrocarbon portion of the PAQR homopolymers.

The thermoelectric power, corrected for the absolute thermoelectric power of Pt contacts was determined as described earlier.[1,2,17,20] The voltage difference across the hot and cold junctions, ΔV, was linear with temperature difference ΔT up to 30°C. The values of the Seebeck coeffi-

TABLE VII
Values of Seebeck Coefficient, Mobility Ratio, and Figures of Merit for PAQR Polymers

Polymer no.	Q, $\mu V/°C$	ΔE, eV	$C = \mu_e/\mu_h$	ρ_{25}, ohm-cm	Z, $°C^{-1}$[a]
63	0.05			7.8×10^4	7.7×10^{-18}
30	8.1	0.41	0.96	8.2×10^5	1.9×10^{-14}
24	12.0	0.46	0.97	1.5×10^6	2.3×10^{-14}
55	52.8			7.3×10^2	9.2×10^{-10}
68	56.0			5.9×10^2	1.3×10^{-9}
70	59.3			2.8×10^4	3.0×10^{-11}
62	60.1			2.7×10^3	3.2×10^{-10}
26	61.0	0.09	0.68	5.9×10^3	1.5×10^{-10}
64	64.5			2.7×10^2	3.7×10^{-9}
59	66.1			1.3×10^3	8.0×10^{-10}

[a] Z = figure of merit, calculated from $Z = Q^2/\rho K$, where K = thermal conductivity assumed as 1×10^{-3} cal/cm-sec-°C.

cient $Q = \Delta V/\Delta T$ ranged from 0.05 to 66.1 $\mu V/°C$. (Table VII). Because of equipment and noise limitations, only samples with room temperature resistivities ranging from 100 to 10^6 ohm-cm were measured. The mobility ratio, $C = \mu_e/\mu_h$ for the three polymers for which both $\Delta E \cong E_g$ and @ were determined, was calculated by using eq. (18)[20]:

$$C = \frac{(E_g/2) + 2kT - QT}{(E_g/2) + 2kT + QT} \tag{18}$$

The polymers examined were all p-type, with indicated mobility ratios of 0.68 to 0.97. This implies fit of the observed data to the assumptions that the polymeric semiconductors here are indeed intrinsic semicondictors with equal populations of electron and hole-type carriers, but with the mobility of the electrons slightly less than that of the holes. This is in agreement with prior studies.[1,2,19]

Finally, we note that in these organic molecular solid semiconductors, that the electronic conductivity is simple function of the major chemical structure present. Where the hydrocarbon portion was held fixed and the acid portion varied, conduction depended rather cleanly and quite sharply on the strength of the acid. (Fig. 3). Where the acidic portion was held fixed and the hydrocarbon portion varied, the conduction depended rather cleanly and strongly on the number of contiguous fused rings of the hydrocarbon (See Fig. 1). Thirdly, we note that upon copolymerizing, even massive concentrations of second components cause but little change in the conductivity of a given polymeric molecular solid (Fig. 2). For these reasons we conclude that electronic conduction in ekaconjugated macromolecules is dependent mainly on the major chemical constituents of ekaconjugated type, and rather little upon impurities having ekaconjugation of a lower order than that of the host. This agrees with theoretical expectation for impurity effects in conjugated macromolecular solids.[6]

The authors express their sincere appreciation to Dr. Robert Pressley, Palmer Physical Laboratory, Princeton University for his assistance in making ESR determinations.

A portion of the work reported here was supported jointly by the Army, Navy, and Air Force under Signal Corps Contract DA-036-039ac 78105; DA Project 3-99-15-105; WADD Project 7371 at the Plastics Laboratory, Princeton University, and a portion at Oklahoma State University on NASA Contract NAS 5-10323.

References

1. H. A. Pohl and E. H. Engelhardt, *J. Phys. Chem.*, **66,** 2085 (1962).

2. H. A. Pohl and D. A. Opp, *J. Phys. Chem.*, **66,** 2121 (1962).

3. H. A. Pohl, A. Rembaum, and A. W. Henry, *J. Amer. Chem. Soc.*, **84,** 2699 (1962).

4. H. A. Pohl, C. Cappas, and C. Gogos, *J. Polym. Sci. A*, **1,** 2207 (1963).

5. H. A. Pohl and R. P. Chartoff, *J. Polym. Sci. A*, **2,** 2787 (1964).

6. H. A. Pohl, in *Electronic Aspects of Biochemistry*, B. Pullman, Ed., Academic Press, New York, 1964, p. 121.

7. A. Rembaum, J. Moacanin, and H. A. Pohl, (a) *Progr. in Dielectrics*, **6,** 41 (1965); (*b*) *ibid.*, **6,** 94 (1965).

8. R. Rosen and H. A. Pohl, *J. Polym. Sci. A-1*, **4,** 1135 (1966).

9. J. W. Mason, R. D. Hartman, and H. A. Pohl, in *Electrical Conduction Properties of Polymers* (*J. Polym. Sci. C*, **17**), A. Rembaum and R. F. Landel, Eds., Interscience, New York, 1967, p. 187.

10. H. A. Pohl, in *Electrical Conduction Properties of Polymers* (*J. Polym. Sci. C*, **17**), A. Rembaum and R. L. Landel, Eds., Interscience, New York, 1967, p. 13.

11. H. A. Pohl, in *Solid State Chemistry*, Vol. 1, H. Reiss, Ed., MacMillan, New York, 1964, Chap. 8, especially p. 319.

12. D. D. Eley, G. D. Parfitt, M. J. Perry, and D. H. Taysum, *Trans. Faraday Soc.*, **49,** 79 (1953).

13. D. D. Eley and G. D. Parfitt, *Trans. Faraday Soc.*, **51,** 1529 (1955).

14. D. D. Eley and G. D. Parfitt, *Horizons in Biochemistry*, by B. Pullman and M. Kasha, Eds., Academic Press, New York, 1962, p. 348.

15. D. D. Eley and D. I. Spivey, *Trans. Faraday Soc.*, **56,** 1432 (1960).

16. H. A. Pohl and J. P. Laherrere, *Proceedings of the Fourth Conference on Carbon*, S. Mrozowski, Ed., Pergamon Press, New York, 1960, p. 259.

17. H. A. Pohl and S. A. Rosen, in *Proceedings of the Fifth Conference on Carbon*, Vol. 2, Pergamon Press, New York, 1963, p. 113.

18. R. D. Hartman and H. A. Pohl, *J. Polym. Sci.*, **6**, 1135 (1968).

19. H. A. Pohl, J. A. Bornmann, and W. Ito, in *Organic Semiconductors*, J. J. Brophy and J. W. Buttrey, Eds., MacMillan New York, 1962.

20. A. Winterstein, H. Vetter, and K. Schoen, *Ber.*, **68,** 1079 (1953).

Received October 6, 1967
Revised April 4, 1968

JOURNAL OF POLYMER SCIENCE: PART A-1 VOL. 7, 157–172 (1969)

Synthesis and Properties of Self-Protecting Polyarylates

V. V. KORSHAK, S. V. VINOGRADOVA, S. A. SILING, S. R. RAFIKOV, Z. YA. FOMINA, and V. V. RODE, *Institute of Element-Organic Compounds, Academy of Sciences of the USSR, Moscow, USSR*

Synopsis

Self-protective polyesters were synthesized in two ways: by polymer analog transformations on polymers obtained and by introduction of inhibiting groups into the polymer during synthesis. It is shown that the Fries rearrangement takes place in the aromatic polyesters in the presence of the Friedel-Crafts catalysts and on ultraviolet irradiation as well. Thermogravimetric analysis of the rearranged polymers and investigations of the influence of the ultraviolet irradiation on their properties show that the rearrangement markedly increases the photochemical and thermal stability of the polymers. Photostabilization may also be accomplished by the introduction of inhibiting groups, such as hydroxyl, sulfur, or phosphorus into the polymer molecule.

DISCUSSION

The problem of stabilizing polymers against various destructive forces becomes important as a result of the increasing use of polymeric materials in industry. Thermal and light stabilization of heat-stable polymers, worked up and used at high temperatures, is one of the most significant aspects of this question.

The purpose of the present study was to form self-protecting thermostable polymers on the basis of well-known heterochain aromatic polyesters, the polyarylates.[1]

Many studies on stabilization mechanism and principles of stabilizer selection have appeared recently. A number of requirements are imposed upon substances used as stabilizers; they must be well compatible with the polymer, should not impair the mechanical properties of the polymers, should not be washed out by solvents, must be stable to ultraviolet irradiation, and must be stable at elevated temperatures. The choice of stabilizers with such properties is often a difficult problem.

Taking this into account, the synthesis of polymers capable of self-stabilization due to some structural features or to stabilizing groups included in the molecule has considerable promise.

Inhibiting groups may be introduced into polyarylates both by a polycondensation process and by polymer analog transformations directly on the polymer.

Application of the Fries Rearrangement to the Synthesis of Self-Protecting Polyacrylates

As the polyarylates are polyesters of bisphenols, the Fries rearrangement was found to be possible both by heating the polymer with Friedel-Crafts catalysts[2–4] and by ultraviolet irradiation.[3–5]

Before studying the Fries rearrangement on polyarylates we investigated the pattern of this process with model compounds for the polyarylates. Dibenzoates of 3,3′-bis(4-hydroxyphenyl)phthalide (phenolphthalein), of 2,2′-bis(4-hydroxyphenyl)propane, and of 9,9′-bis(4-hydroxyphenyl)fluorene were synthesized and used as model compounds.

Suitable dibenzoyl bisphenols were obtained by heating bisphenol dibenzoates both in *p*-ditolylmethane and nitrobenzene solutions in the presence of $AlCl_3$, as well as by ultraviolet irradiation of 1% solution of dibenzoates in chloroform. The structures of these dibenzoyl bisphenols are confirmed by the infrared spectra, elemental analysis data, and by the presence of HO groups in the compounds. The fact that under certain conditions the Fries rearrangement takes place in all the bis-phenol dibenzoates studied encouraged us to study this reaction with polymers too.

The polyarylate of isophthalic acid and phenolphthalein (polyarylate Ph-1) formed by polycondensation in a high-boiling solvent[6] was taken as starting substance for the Fries rearrangement investigation.

The reaction in polymers was carried out in *p*-ditolylmethane in the presence of $AlCl_3$, $TiCl_4$, $SnCl_4$, or $ZnCl_2$ and by ultraviolet irradiation of 1% solution of polymers in chloroform. One may assume that the Fries rearrangement in polyarylates proceeds as the idealized scheme shown in eq. (1).

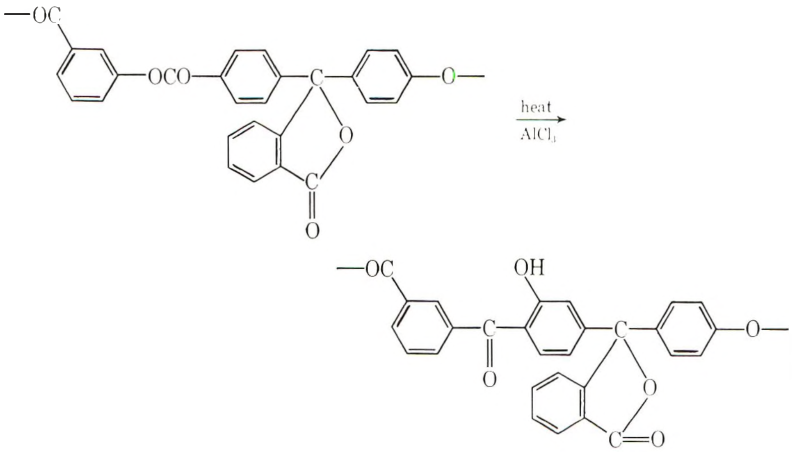

(1)

Polyarylate Ph–I

Figure 1 shows the infrared spectra for polyarylate Ph-1 before and after rearrangement. It is seen that a carbonyl-stretching absorption band at 1630–1640 cm^{-1} appears in the infrared spectrum of a rearranged polyarylate. A slight shift of the absorption towards a lower frequency may be explained by a hydrogen bond between the carbonyl group and the hydroxyl group in the *ortho* position. The formation of an *o*-hydroxycarbonyl structure is confirmed by the ultraviolet spectra of the polyarylates studied (Figs. 2 and 3), which have an absorption band at 310–360 mμ after irradiation. On determination of hydroxyl groups in the polyarylate by acetylating the polymer by acetic anhydride in pyridine,[7] the polymer conversion as calculated from the increasing content of hydroxyl groups, was found to be from 5 to 35%, depending on the nature of the polymer and reaction conditions (Table I).

TABLE I
Dependence of the Degree of Conversion of Polyarylate Ph–I from Isophthalic Acid and Phenolphthalein on Reaction Conditions[a]

No.	Catalyst	Polyarylate structural unit catalyst ratio, mole	Reaction temperature, °C	Reaction time, hr	Polyarylate conversion, %
1	$AlCl_3$	1:0.3	120	1	5
2	"	1:03	120	2–3	10
3	"	1:03	160	1	30
4	"	1:03	160	2	35
5	"	1:0.1	160	2	15
6	"	1:0.1	160	3	30
7	$TiCl_4$	1:0.3	160	2	22
8	$SnCl_4$	1:0.3	160	2	12
9	$ZnCl_2$	1:0.3	160	2	0

[a] The reaction was carried out in *p*-ditolylmethane.

Photostability. After the Fries rearrangement the polyarylates contain carbonyl and hydroxyl groups *ortho* to one another which can form cyclic structures similar to that involved in known light absorbers of the hydroxybenzophenone type. They are responsible for a strong absorption in the ultraviolet with a wave-length of 340 mμ which may lead to the ester bond cleavage.

Thus, by reactions on polyarylates, polymers containing inhibiting groups in the chain were obtained. This fact favored their light stability. For instance, after irradiation of polyarylate Ph-1 films with a PRK-2 mercury vapor lamp at a residual pressure of 10^{-4} of Hg for 75 hr the strength of films from transformed polyarylate is almost the same as that of the corre-spooding unirradiated films (Table II).

In this case it should be taken into account that, as shown by Rodè et al.[8] the films from polyarylate Ph-1 become more brittle after irradiation and their mechanical strength diminishes sharply in comparison with the corresponding values for unirradiated films.

TABLE II

Dependence on Irradiation Time of Mechanical Properties of Unoriented Films from Polyarylate Ph-1 from Isophthalic Acid and Phenolphthalein Subjected to the Rearrangement

Irradiation time, hr	Temperature, °C	Tensile strength σ of film, kg/cm^2	Elongation to break ϵ, %
0	20	1000	5
	100	660	25
	200	300	5
10	20	1250	7
35	20	1000	5
75	20	950	5
	100	600	5
	200	300	5

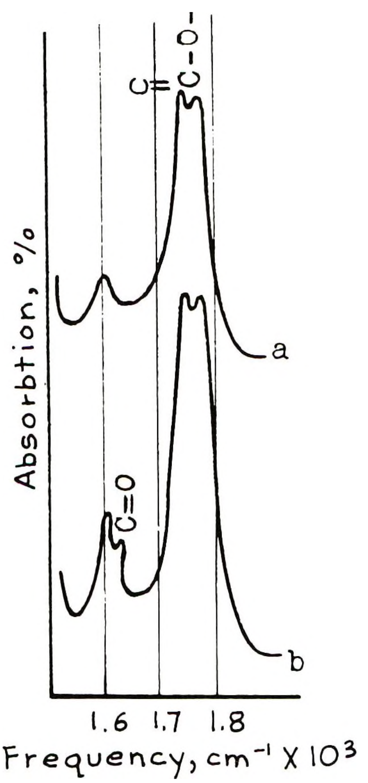

Fig. 1. Infrared spectra of polyarylate Ph-1: (*a*) before and (*b*) after the Fries rearrangement.

The weight loss during irradiation of films from polyarylate subjected to the Fries rearrangement is approximately one tenth of that of the starting polyarylate (Fig. 4).

The data for the increased photostability of polyarylate with oxyketone groups formed in the Fries reaction are confirmed by the results obtained on studying irradiated polyarylate solutions.

Thus, the irradiation of a 1% solution of the polyarylate from terephthalic acid and phenolphthalein (Ph-1) in cyclohexanone for 10 hr results in a 90% reduction in viscosity while the viscosity of 1% solution of the polymer

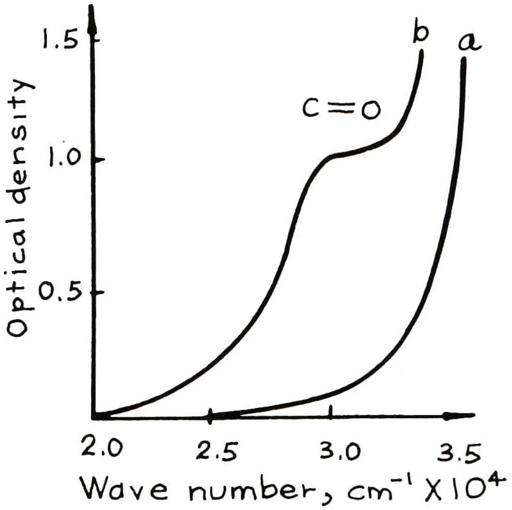

Fig. 2. Ultraviolet spectra of polyarylate Ph-1: (*a*) before and (*b*) after the Fries rearrangement.

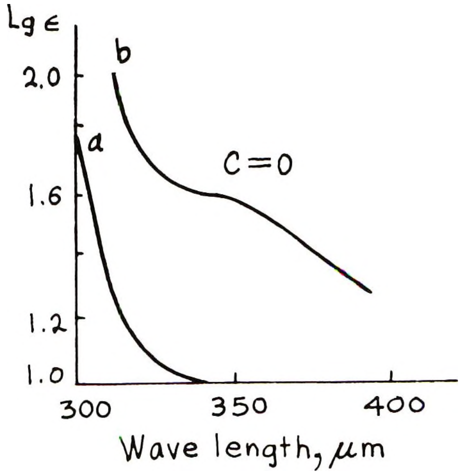

Fig. 3. Ultraviolet spectra of polyarylate D-I: (*a*) before and (*b*) after the Fries rearrangement.

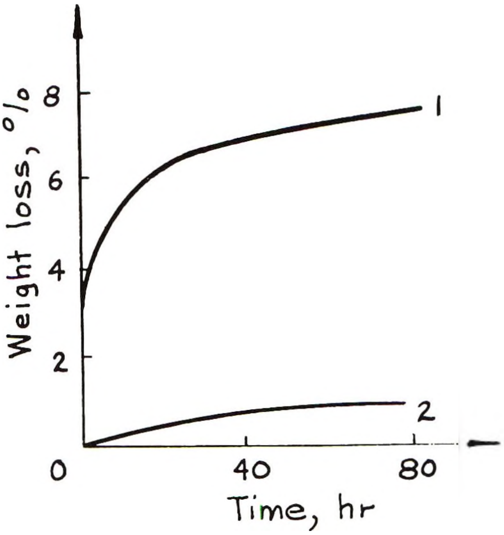

Fig. 4. Dependence of weight loss on the time of irradiation with PRK-2 lamp under residual pressure of 10^{-4} mm Hg for films from (*1*) polyarylate Ph-I (I) and (*2*) its transformation product.

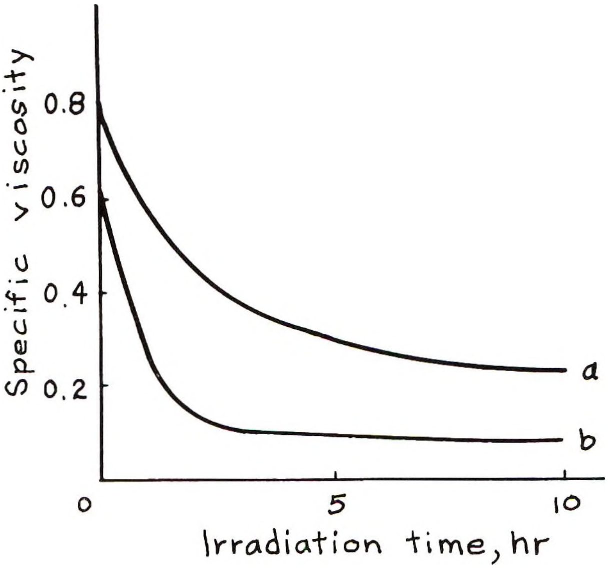

Fig. 5. Change of specific viscosity on irradiation of 1% solution of polyarylate Ph-2: (*a*) in chloroform and (*b*) in cyclohexanone.

in chloroform on the same exposure is reduced by 70% (Fig. 5). Infrared and ultraviolet spectra of polyarylate Ph-2 irradiated in chloroform are similar to those given in Figures 2 and 3; this allows us to conclude that the irradiation of polyarylate solutions in chloroform causes the Fries rearrangement, which stabilizes the polyarylates. The spectra of polyarylates irradiated in cyclohexanone are similar to that of the starting polymer, however, which indicates that there is no Fries rearrangement in this case.

At the same time, on irradiation of a 1% solution of phenolphthalein dibenzoate in cyclohexanone, phenolphthalein and a small amount of benzaldehyde were obtained. This may be apparently explained by the reaction of aroyl and phenoxide radicals with the solvent [eq. (2)].

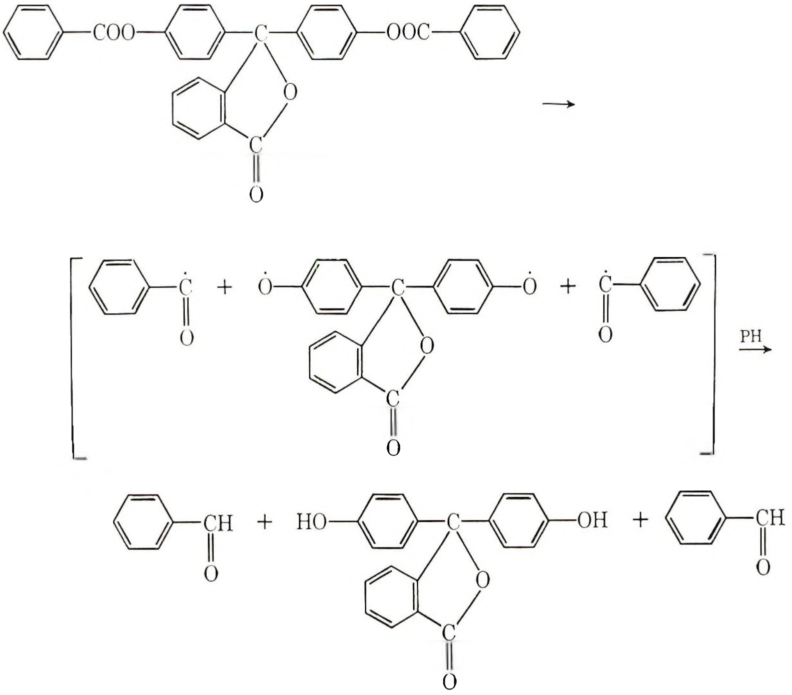

(2)

Thermostability. We have studied the thermostability of polyarylates undergoing Fries rearrangement by the thermogravimetric method.

The correlation of curves (Fig. 6) representing the temperature dependence of weight loss in polyarylate shows that the decomposition of polyarylate Ph-1 subjected to the Fries rearrangement begins 40°C higher and that of polyarylate D-1 20°C higher than in the case of unirradiated polymers.

The decomposition rate of rearranged polyarylates is considerably lower than that of the starting ones.

We have calculated the apparent activation energy of thermal destruction of polymers from the thermogravimetric analysis data by the method suggested by Reich and Levy.[9] This was 23 and 36 kcal/mole for polyarylate Ph-I and the product of its rearrangement, and 17 and 24 kcal/mole for polyarylate D-I and the product of its rearrangement, respectively.

Thus, we have reason to suggest that the Fries rearrangement carried out on polyarylates makes them more thermostable. This may be apparently attributed to new groups formed in polymeric chains.

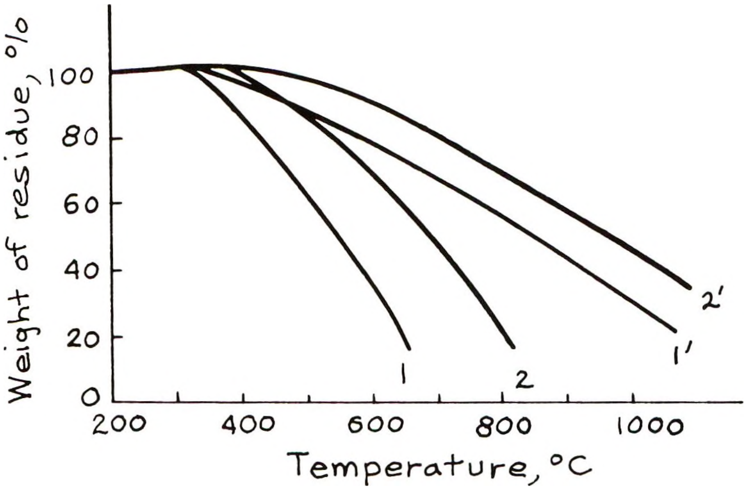

Fig. 6. Dependence of weight loss on temperature: (*1*) for polyarylate D-I and (*1'*) its transformation product (I); (*2*) for polyarylate Ph-I and (*2'*) its transformtion product.

Photostability of Polyarylates Containing Sulfur, Phosphorus, and Hydroxyl Groups

As mentioned above, self-protecting polymers can be also produced by using a substance containing some inhibiting groups in the molecule as one of the starting compounds. We have studied the possibility of forming polyarylates internally protected against light aging by introducing phosphorus and sulfur atoms or free phenolic groups into polymer molecules. For this purpose, mixed polyarylates based on phenolphthalein were synthesized. The amount of modifying agent was so chosen that the element of the polymer structure and reactive groups did not exceed 1-1.5%.

Phosphorus- and Sulfur-Containing Polyarylates. To synthesize sulfur-containing polyarylates, terephthalic and isophthalic acid chlorides, phenolphthalein, as well as phenol sulfophthalein and 4,4'-dioxydiphenyl sulfone were used.[10]

Phosphorus-containing polymers were synthesized from phenolphthalein and chlorides of bis(p-carboxyphenyl)methylphosphine of methylphosphinic and terephthalic acid.[11]

Properties of the polyarylates are represented in Table III.

Figure 7*a* shows a curve of viscosity change of 1% solution of these polyarylates in chloroform after irradiation for 10 hours. It is seen that the viscosity of polyarylates 2,3,5 (Table III) is reduced only slightly, while that of polyarylate Ph-1 (polymer 1 of Table III) is about 70% lower.

As shown in Figure 7*b*, the irradiation of a 20% solution of polyarylates 3,5 (Table III) in chloroform did not lead to viscosity reduction at all. The molecular weight and hydroxyl group equivalent change in the process only slightly. At the same time the molecular weight of polyarylate 1 increases by 40% after irradiation under similar conditions. It can be assumed that the crosslinking rate is higher than the macromolecule scission one.

We have also studied the ultraviolet irradiation of films from polyarylated 1, 3, 4, and 6 of Table III. Figure 8 gives the curves of tensile strength change for films during irradiation.

Thus, the investigation of polyarylates in the irradiation process indicates that the introduction of sulfur and phosphorus atoms into polyarylate increases the light stability.

Hydroxyl-Containing Polyarylates. To synthesize hydroxyl-containing polyarylates, phloroglucinol was used as one of the components.[12] It was

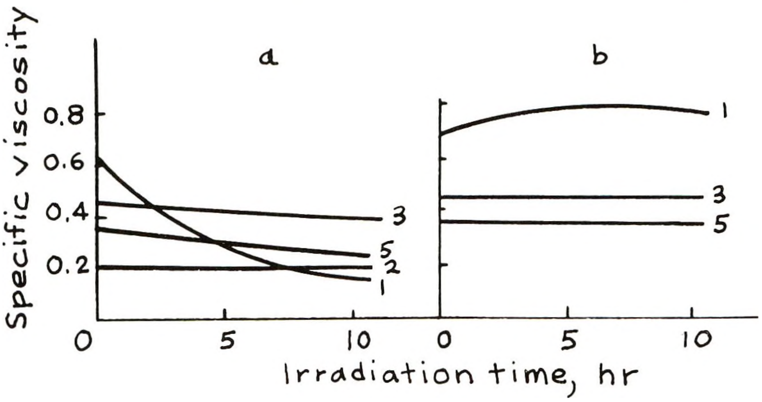

Fig. 7. Change of specific viscosity on irradiation of (*a*) 1% and (*b*) 20% solutions of polyarylates in chloroform for 10 hr. Figures at curves correspond to polymer numbers from Table III.

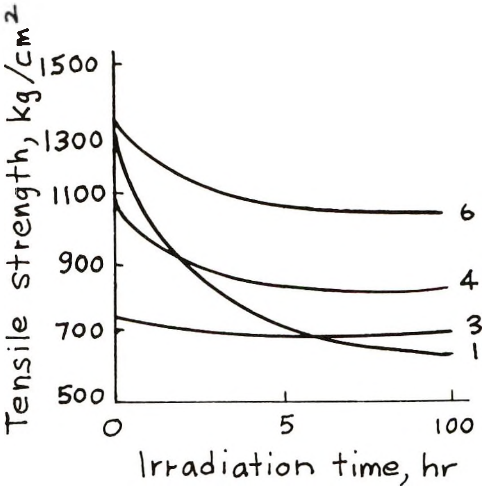

Fig. 8. Dependence of tensile strength of polyarylate films on the irradiation time in the air.

TABLE III
Structure and Properties of Phosphorus- and Sulfur-Containing Polyarylates

No.	Mole ratio of starting substance	Structural unit of polyarylate	η_{red} dl/g in chloroform	Softening temperature, °C[a]
1	Phenolphthalein/terephthalic acid chloride, 1:1	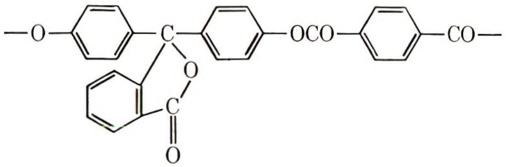	0.65	320
2	Phenolsulfophthalein/terephthalic acid chloride, 1:1	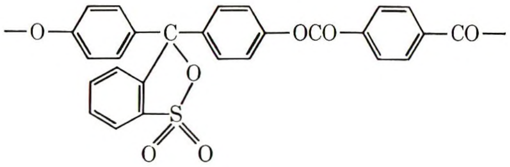	0.20	265
3	Phenolphthalein/-phenolsulfophthalein/terephthalic acid chloride, 0.9:0.1:1	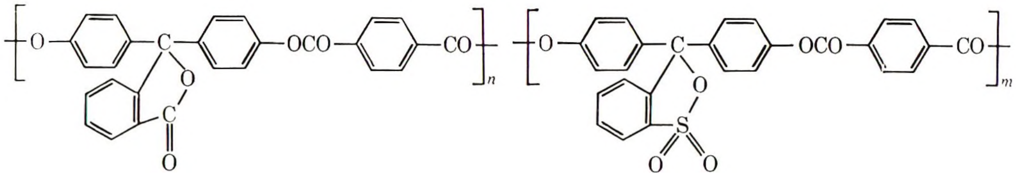	0.47	296

4	Phenolphthalein/4,4′-dihydroxydiphenyl sulfone/terephthalic acid chloride, 0.9:0.1:1	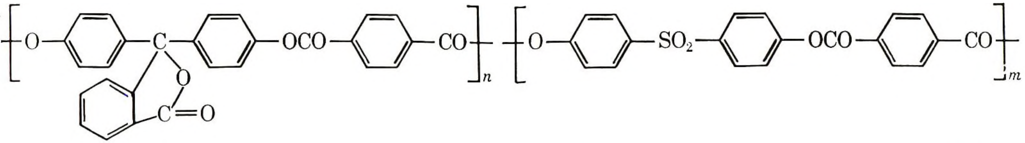	0.56	310
5	Phenolphthalein/terephthalic and methylphosphinic acid chlorides, 1:0.9:0.1	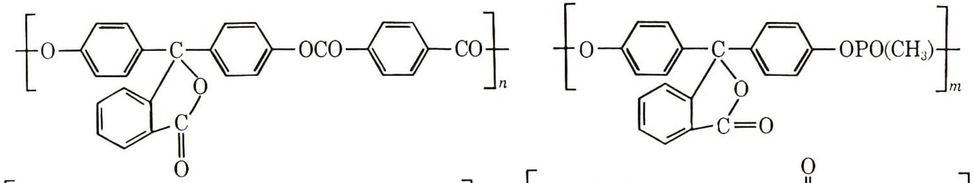	0.37	270
6	Phenolphthalein/chlorides of terephthalic acid and of bis(*p*-carboxyphenyl)-methylphosphine oxide, 1:0.9:0.1	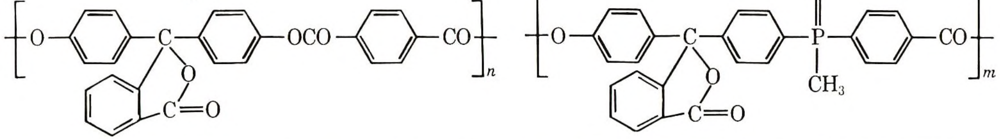	0.57	320

---

[a] Capillary melting point at heating rate of 3–4°C/min (1–2°C/min near mp).

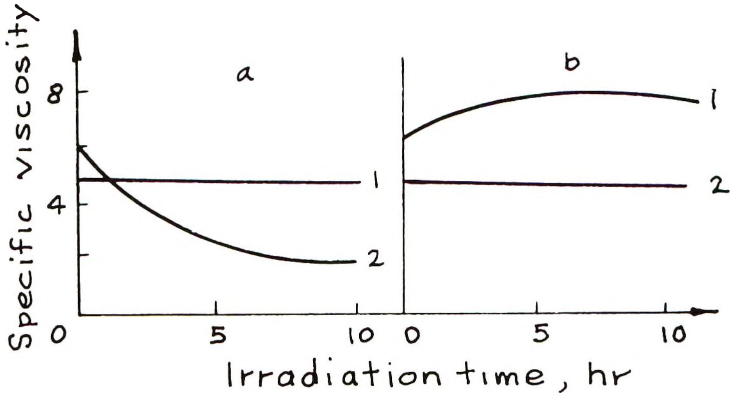

Fig. 9. Change of specific viscosity on irradiation of (*a*) 1% and (*b*) 20% solutions of (*1*) a hydroxyl-containing polyacrylate and (*2*) polyacrylate Ph-2 in chloroform.

thought that the presence of a hydroxyl group directly on the benzene ring in such polyarylates would favor their thermo- and photostability.

Hydroxyl-containing polyarylates based on terephthalic acid, phenolphthalein, and phloroglucinol were synthesized by high-temperature polycondensation in chlorinated diphenyl. The mole ratio of starting substances was 1:0.9:0.1, respectively. The idealized structure of polyarylates obtained is shown as (3).

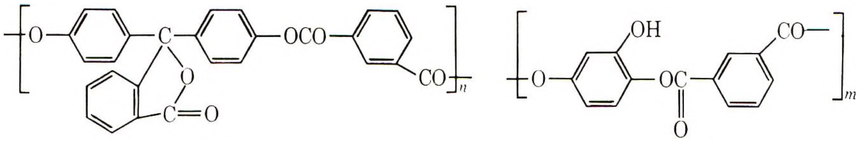

We have studied the destruction of 1% and 20% solution of the polyarylate in chloroform by ultraviolet irradiation. It is seen from the curves given in Figure 9 that the introduction of phloroglucinol residues, hydroxyl groups, to polyarylate results in a considerable increase in photostability of polyarylate solutions.

Similar results were obtained on ultraviolet irradiation of films from hydroxyl-containing polyarylates. Thus, after 10 hr irradiation at 40 ± 2°C the tensile strength of polyarylate 1 (Fig. 8) becomes 50% lower, while that of hydroxyl-containing polyarylates practically do not change.

EXPERIMENTAL

Terephthalic acid chloride was obtained by the reaction of terephthalic acid with thionyl chloride,[10] recrystallized from petroleum ether, and distilled in vacuum; BP 115°C/2 mm Hg, mp 82–82.5°C*. The yield is 90% of the theory.

Isophthalic acid chloride was synthesized by the above method; bp

---

* Herein and below the melting point was determined in a capillary, the temperature being increased at a rate of 3–4°C/min and 1–2°C/min near the melting point.

119–121/6 mm Hg, mp 41–42°C (lit.[13] mp 41–42°C). The yield is 95% of the theory.

To prepare the chloride of bis(p-carboxyphenyl)methylphosphine oxide, 10.8 g of bis(p-carboxyphenyl)methylphosphine oxide and 100 ml of freshly distilled thionyl chloride were placed in a pear-shaped flask and heated on the water bath at 40°C for 3 hr. Thionyl chloride was removed by distillation, and the residue was dissolved in dry benzene. The acid chloride was isolated by pouring the benzene solution into petroleum ether, filtering off, and drying in a desiccator over P_2O_5 and paraffin. The yield is 90% of the theory; mp 114–115°C which agrees with the reported value.

Methylphosphinic acid chloride was obtained by the method described[10] in the literature.

Phenolphthalein dibenzoate was produced by the reaction of an alkali solution of phenolphthalein with benzoyl chloride. The phenolphthalein dibenzoate obtained was recrystallized from a benzene–petroleum ether mixture (6:1 by volume) and dried *in vacuo* at 80°C. The yield is 70% of the theory; mp 166.5–167.5°C (lit.[14] mp 169°C).

Diphenylolpropane dibenzoate and 9,9-bis(4-oxyphenyl)fluorene dibenzoate were synthesized by the above method, the yield of each compound being 65–70%; mp of the diphenylolpropane dibenzoate 157.5–158°C; mp of the fluorene compound 204–205°C.

In preparation of 3,3′-bis(4-hydroxy-3-benzoylphenyl)phthalide, 0.006 mole of $AlCl_3$ was added to 0.002 mole of phenolphthalein dibenzoate at 0°C with stirring, and the mixture was heated at 170°C for 40 min, cooled, washed with 30 ml of 6*N* solution of HCl with ice, then with water, and extracted from 15–20 ml of boiled benzene. The extract was treated with 20–30 ml of 2*N* NaOH solution to isolate reaction products. The alkali solution was neutralized with 6*N* HCl solution and kept in the refrigerator for 12 hr. The precipitate was reprecipitated with water from an ice acetic acid solution and recrystallized from aqueous ethyl alcohol.

In the synthesis of 3,3′-bis(4-hydroxy-3-benzoylphenyl)phthalide in solution, $AlCl_3$ (3 mole per mole of dibenzoate) was added to 20–25% dibenzoate solution in ditolylmethane or in nitrobenzene at 0°C on stirring, and the reaction mixture was then heated at 150°C for 20–40 min.

After the reaction was completed, the mixture was cooled, washed in a separatory funnel with 6*N* HCl solution, and extracted with 2*N* NaOH solution. Further treatment was as described above.

2,2′-Bis(4-hydroxy-3-benzoylphenyl)propane and 9,9-bis(4-hydroxy-3-benzoylphenyl)fluorene were synthesized by a method similar to that described above.

In the synthesis of 3,3′-bis(4-hydroxy-3-benzoylphenyl)phthalide by ultraviolet irradiation, a 1% solution of phenolphthalein dibenzoate in chloroform was subjected to ultraviolet irradiation for 10 hr.

Phenolsulfophthalein was obtained by condensation of phenol with dry *o*-sulfonbenzoic acid.[15] Phenolsulfophthalein dried at 120–140°C decomposes at 200°C without melting according to the data reported.[15]

TABLE IV
Characteristics of Dibenzoyl Bisphenols

Dibenzoyl bisphenol	Formula	Elemental analysis				OH content, %		Melting point, °C
		C, %		H, %				
		Found	Calcd	Found	Calcd	Found	Calcd	
3,3′-Bis(4-hydroxy-3-benzoylphenyl)phthalide	$C_{34}H_{22}O_6$	77.13	77.56	4.11	4.27	6.75	6.50	170–171
2,2′-Bis(4-hydroxy-3-benzoylphenyl)propane	$C_{29}H_{24}O_4$	79.27	79.80	5.42	5.50	7.70	7.26	160–161
9,9-Bis(4-hydroxy-3-benzoylphenyl)fluorene	$C_{39}H_{26}O_4$	83.36	83.87	4.56	4.56	6.50	6.10	204–205

Dihydroxy diphenylsulfone was obtained by condensation of phenol with sulfuric acid,[16] recrystallization from aqueous alcohol, washing with water and drying at 80°C of 2–3 mm Hg; mp 250°C (lit.[16] mp 249°C).

For the synthesis of polyarylates of Table III, the polycondensation of dicarboxylic acid chlorides with bisphenols was carried out in chlorinated diphenyl at a concentration of 0.6 mole/l (per one of the components).[6] The polymer yield was about 90% of the theory; η_{red} of 0.5% solution of the polymer in tricresol at 20°C was 0.8 dl/g.

The synthesis of mixed polyarylates containing free hydroxyl groups[12] was carried out in chlorinated diphenyl in two stages.

At the first stage the interaction of terephthalic acid chloride with phenolphthalein yields a prepolymer having acid chloride endgroups. The reaction was carried out at 175–180°C for 2 hr and at 210°C for 3 hr.

At the second stage the interaction of the prepolymer with polyatomic phenols takes place giving a mixed polyarylate containing free hydroxyl groups. To do this, the reaction mixture was cooled to 110°C, the phloroglucinol was gradually introduced and the reaction carried out at 180°C over a period of 3–5 hr, and at 200°C for 3 hours, an aliquot being taken every 10–15 min to verify the solubility. After completing the reaction, the reaction mixture was dissolved in chloroform, the polymer was precipitated by pouring the solution into methanol, then filtered off, washed thoroughly with methanol, hot water, methanol again, and dried at 40°C/2–3 mm Hg. The polymer yield was 90% of the theory, η_{red} of 0.5% solution in tricresol at 20°C 0.48 dl/g.

The Fries rearrangement was carried out by heating a polyarylate suspension in *p*-ditolylmethane with 10% of a catalyst (from polymer weight) at 160°C for 2 hr. The reaction product was poured in to a hydrochloric acid–ice mixture (1:1), filtered, washed with water to neutrality, twice reprecipitated from chloroform with methanol, extracted with methanol in a Soxhlet apparatus for 40 hr, and dried *in vacuo* at 80°C. The yield of the modified polyarylate is nearly quantitative.

η_{red} of a 0.5% solution of the polyarylate in tricresol at 20°C was 0.8 dl/g before rearrangement and 0.76 dl/g after rearrangement.

Elemental analysis data for the rearranged polyarylate are given in Table V.

Photodestruction of polyarylate solutions was carried out in flat-bottomed quartz flasks immersed in a quartz bath with water to remove the heat and to absorb the infrared rays. Ubbelohde viscometers were attached to determine the intrinsic viscosity before and after irradiation and the specific viscosity during irradiation.

TABLE V

	Found		Calculated	
	C, %	H, %	C, %	H, %
Before rearrangement	74.73	3.21	75.0	3.51
After rearrangement	74.51	3.36	75.0	3.51

A 400-W mercury vapor lamp of the PRK-type was used as an ultraviolet irradiation source The light beam of this lamp had the following wavelength distribution: 2000–2800 Å, 15-15.5%; 2800–3200 Å, 25–25.5%; 3200–3800 Å, 19.5%; visible spectrum, 40%.

The lamp capacity was regulated by a voltameter and controlled by a transformer.

The films of 40 ± 5 $m\mu$ thickness were irradiated at 40–42°C in air at a residual pressure of 1×10^{-4} mm Hg; the distance between the lamp and the quartz flask was 90 mm, from that to the film 100 mm.

The softening temperature is assumed to be a temperature corresponding to the point of intersection of tangents to thermomechanical curves at the point where the polymer begins to flow at a load of 100 g; the sample diameter was 4 mm.

The strength of the film was measured with the dynamometer. The film samples 40–50 $m\mu$ thick and 2 mm wide were placed between a fixed and a movable (0.0684 mm/sec) clamp.

References

1. V. V. Korshak and S. V. Vinogradova, *Polyarylates*, Moscow, 1964.

2. V. V. Korshak, S. V. Vinogradova, and S. A. Siling, USSR Pat. 171,555 (October 15, 1963); *Byul. Izobretenii* **1965**, No. 11, 76.

3. D. Bellus, Z. Manasek, P. Hrdlovič, and P. Slama, in *International Symposium on Macromolecular Chemistry, Prague* (*J. Polym. Sci. C*, **16**), O. Wichterle and B. Sedláček, Eds., Interscience, New York, 1967, p. 287.

4. M. Okaware, S. Tani, and E. Imoto, *Kogyo Kagaku Zasshi*, **68**, 223 (1965).

5. C. B. Maerov, *J. Polym. Sci.*, *3A*, 487 (1965).

6. V. V. Korshak, S. V. Vinogradova, and S. A. Siling, *Zh. Org. Khim.*, **2**, 1441 (1966).

7. Houben-Weyl, *Methoden der organischen Chemie, II, Analytische Methoden*, Verlag Georg Tieme, Stuttgart, 1953.

8. V. V. Rodě, Ya. S. Yarov, and S. R. Rafikov, *Vysokomol. Soedin.*, **6**, 2168 (1964).

9. L. Reich and D. W. Levi, *Makromol. Chem.*, **66**, 104 (1963).

10. V. V. Korshak, S. V. Vinogradova, and Z. Ya. Fomina, USSR Pat. 170,667. (July 8, 1964); *Byul. Izobretenii*, **1965**, No. 9, 68.

11. V. V. Korshak, S. V. Vinogradova, and Z. Ya. Fomina, USSR Pat. 172,038 (June 12, 1964); *Byul. Izobretenii* **1965**, No. 12, 65.

12. V. V. Korshak, S. V. Vinogradova, and Z. Ya. Fomina, USSR Pat. 175,656 (May 29, 1964); *Byul. Izobretenii* **1965**, No. 20, 66.

13. C. Lieberman and M. Cardos, *Ber.* **46**, 211 (1913).

14. F. Reinel and F. Siegel, *Ber.*, **56**, 1554 (1923).

15. R. Morgan and B. Horr. *J. Amer. Chem. Soc.*, **74**, 4528 (1952).

16. A. M. Kinear and E. A. Perren, *J. Chem. Soc.*, **1952**, 3437.

17. A. Bistryski and K. Nencki, *Ber.*, **29**, 1321 (1886).

18. Sbernood, *J. Amer. Chem. Soc.*, **45**, 486 (1923).

19. J. Annaheim, *Ann.*, **172**, 36 (1874).

20. V. V. Korshak, S. V. Vinogradova, and S. N. Salazkin, *Vysokomol. Soedin.*, **3**, 72 (1961).

Received February 13, 1968
Revised June 5, 1968

JOURNAL OF POLYMER SCIENCE: PART A-1 VOL. 7, 173–181 (1969)

Free-Radical Copolymerizations of 1,2-Dichloroethylenes. Evidence for Chain Transfer by Chlorine Atom Elimination

T. L. DAWSON, R. D. LUNDBERG, and F. J. WELCH,
Research and Development Department, Union Carbide Corporation,
Chemicals and Plastics, South Charleston, West Virginia

Synopsis

Trialkylboron–oxygen, an active, low-temperature free-radical initiator, has been employed to investigate the effects of very low temperatures on the copolymerizations of vinyl acetate with *cis* and *trans*-1,2-dichloroethylenes. The low temperatures favor the propagation rate relative to the transfer rate, such that high molecular weight copolymers containing substantial quantities of 1,2-dichloroethylene can be prepared. The molecular weights of the copolymers depend only on the amounts of 1,2-dichloroethylene in the copolymers, regardless of the isomer which takes part in the copolymerization. Since the double bond of the *trans* isomer is about six times as reactive as that of the *cis* isomer, this indicates that the dominating chain transfer reaction occurs by chlorine atom elimination subsequent to the addition of the dichloroethylene unit to the growing free radical chain. It is suggested that a similar chain-transfer mechanism occurs in the polymerization of vinyl chloride, wherein an infrequent head-to-head placement of monomer unit is followed by ejection of a chlorine atom to form an olefinic bond and termination of that growing chain. The presence of the 1,2-dichloroethylene unit in the copolymer increases the glass transition temperature approximately 1°C per weight per cent copolymerized with the vinyl acetate.

INTRODUCTION

The 1,2-dichloroethylenes are very reluctant to homopolymerize.[1,2] Only low yields of low molecular weight homopolymers have been reported. Copolymerization studies have been performed,[3,4] but the preponderance of chain transfer which occurs at ambient or higher temperatures limits even the ability to produce high molecular weight copolymers containing large quantities of these comonomers. It has been suggested that the somewhat balanced electrical charge on the double bond and the increased steric hindrance caused by substituents in both 1 and 2 positions contribute to the lack of activity.[3] The inherent chain-transfer property, giving very low molecular weight products, makes it difficult to obtain mechanical properties of the copolymers and representative compositional analyses which are essentially free of endgroup effects.

To prepare high molecular weight copolymers containing substantial amounts of 1,2-dichloroethylene, for study of the effect of the 1,2-dichloroethylene group on molecular weight and physical properties, a low-temperature copolymerization study was undertaken. Vinyl acetate was chosen as the comonomer because its double bond and resultant free radical are of approximately the same reactivity as those of the 1,2-dichloroethylenes, and it can be homopolymerized readily at low temperatures. The resultant copolymers were analyzed to obtain accurate reactivity ratios, chain-transfer molecular weight effects, and physical properties.

EXPERIMENTAL

The vinyl acetate and *cis* and *trans*-1,2-dichloroethylenes were fractionally distilled to greater than 99% purity and then stored at −78°C prior to use.

To obtain quantitative results with the trialkylboron–oxygen initiator, the control of oxygen content in catalytic concentrations is required. High-vacuum techniques were, therefore, employed throughout.

The monomers and tributylboron were degassed thoroughly prior to their distillation *in vacuo* into the polymerization flasks. The volumes of the liquids were measured by distillation from graduated tubes or by employing a cathetometer to measure the vertical distance on a tube of known inside diameter. After melting and mixing the liquid components thoroughly, a small measured quantity of oxygen was then added by condensation of the oxygen from the manifold into the polymerization tube cooled in liquid nitrogen. From the known volume of the manifold, the measured pressure drop in the manifold, and the temperature, the exact weight of condensed oxygen was controlled and measured. After adding the oxygen, the contents were again melted, mixed thoroughly, and then warmed to the desired polymerization temperature. The concentrations of tributylboron and oxygen were 0.041 and 0.012 mole/l., respectively, in the +30°C experiments and 0.082 and 0.012 mole/l., respectively, in the −45 to −50°C experiments.

To control accurately the low polymerization temperatures, an automatic low-temperature controller was constructed. This apparatus operated unattended over long time intervals at temperatures down to −150°C. The controller consisted of a safety valve, a solenoid valve, a liquid nitrogen tank which maintained a pressure of 25 psi, a Dewar flask containing a liquid with a low freezing point in which a copper coil was immersed, and a relay temperature controller with copper–Constantan thermocouple actuation. When the temperature of the coolant warmed to the set point, the controller transmitted current through the solenoid causing it to open and allow passage of cold nitrogen through the coil in the bath. As the temperature cooled below the set point, the current was broken and the valve closed. The accuracy of control depended upon the temperature. At −50 to −90°C, control within about ±0.5°C was maintained, while at −142°C control was possible only within about ±3°C.

The possibility of post-polymerization was minimized by mixing a precooled acetone solution of a free-radical inhibitor, monomethyl ether of hydroquinone, into the cold polymerizations prior to their precipitation. Subsequently the polymers were repeatedly precipitated into hexane from acetone to remove the remaining monomer. The samples were dried *in vacuo* and then analyzed for monomer composition by chlorine analyses. Only relative values of molecular weights were required for interpretation of the results. The molecular weights were, therefore, estimated from reduced viscosity measurements at 30°C in acetone at 0.2% concentration by using the approximation:[5] $\eta_{\text{red}} \cong [\eta] \cong 1.76 \times 10^{-4} M^{0.68}$

To minimize the effects of drifts in composition with increasing conversion, the low-temperature copolymerizations were stopped at conversions below 10%. The 30°C copolymerizations were stopped in the range of 10–40% conversion.

RESULTS AND DISCUSSION

Copolymers containing various quantities of the 1,2-dichloroethylenes were prepared at +30°C and −45 or −50°C by varying the initial monomer ratios of vinyl acetate/1,2-dichloroethylene. Considerably higher molecular weight copolymers were formed at the lower temperatures, even though higher catalyst concentrations were employed. Viscosity-average molecular weights of the order of 10,000 to 50,000 were obtained at −45 to −50°C for copolymers containing 10–40 mole-% 1,2-dichloroethylene, while copolymers of similar compositions prepared at +30°C had molecular weights of the order of 10,000 and less. The decrease in rate of transfer relative to rate of propagation occurred at the lower polymerization temperatures without altering substantially the compositions of the copolymers.

Reactivity Ratios

The relative reactivities of the double bonds of the *cis* and *trans* isomers play an important role in the interpretation of the chain transfer mechanism. Although the monomer reactivity ratios for this system have been reported in the literature, a slight discrepancy exists (Table I). These values were, therefore, calculated for the higher molecular weight copolymers which were prepared at the lower temperatures.

Figure 1 illustrates a plot, according to the method of Fineman and Ross,[6] for determining the reactivity ratios for the vinyl acetate (M_1)/*trans*-1,2-dichloroethylene (M_2) copolymerizations. These data were generated from the highest molecular weight copolymers which were prepared at −45°C. Low conversion experiments were employed even though the composition of this system does not drift markedly with increasing conversion. It was not necessary to use the integrated form of the copolymer equation. The line on Figure 1 and the resultant reactivity ratios were calculated by the method of least squares.

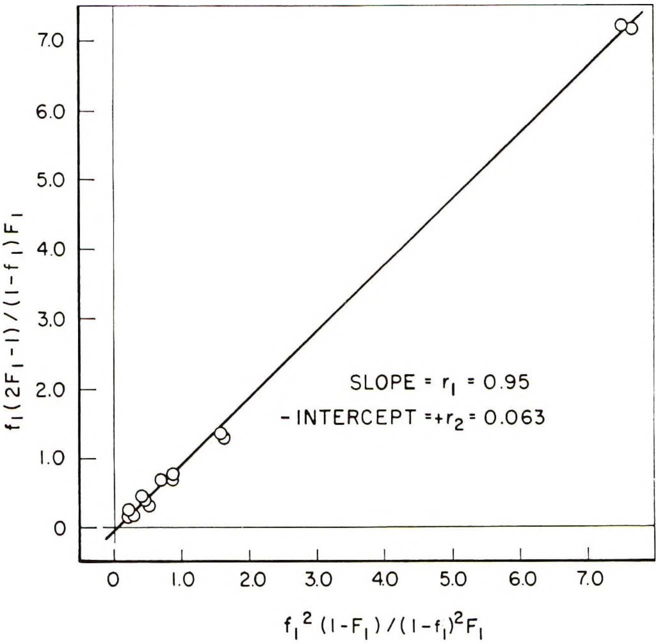

Fig. 1. Fineman and Ross monomer reactivity ratio plot[6] for the copolymerization of vinyl acetate (M_1) with *trans*-1,2-dichloroethylene (M_2) at −45°C.

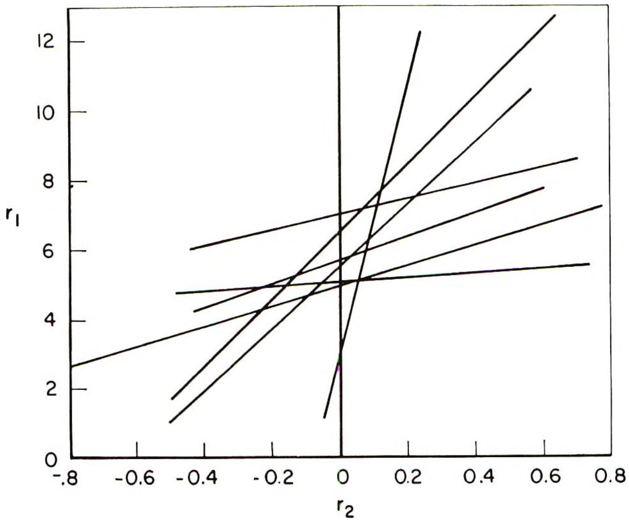

Fig. 2. Monomer reactivity ratio plot from the integrated form of the copolymerization equation[7] for the copolymerization of vinyl acetate (M_1) with *cis*-1,2-dichloroethylene (M_2) at −50°C.

Figure 2 illustrates a plot, obtained by using the integrated form of the copolymer equation,[7] for determining the reactivity ratios for vinyl acetate (M_1)/*cis*-1,2-dichloroethylene (M_2). These data were also generated from high molecular weight copolymers prepared at −50°C. Even though low conversion experiments were employed with this system, the integrated form of the copolymer equation was utilized for additional accuracy because in this case the composition drifts rapidly with increasing conversion.

The data from the +30°C copolymerizations were treated by the same methods used for the low-temperature copolymerizations. The lower molecular weights of these copolymers and the higher conversion experiments would, however, both be expected to render the resultant reactivity ratios somewhat less accurate than those from the low temperature experiments.

The reactivity ratios from the low temperature copolymerizations are summarized in Table I, where they are compared to the values from the +30°C copolymerizations and the previously reported values from higher-temperature copolymerizations.

TABLE I
Monomer Reactivity Ratios for
Vinyl Acetate (M_1)–1,2-Dichloroethylene (M_2)

Polymerization temperature, °C	Reactivity ratios			
	trans isomer		*cis* isomer	
	r_1	r_2	r_1	r_2
68[a]	0.85	0	2.8	0
60[b]	0.99 ± 0.02	0.086 ± 0.01	6.3 ± 0.2	0.018 ± 0.003
30	0.95	0.05	3–4	~0
−45	0.95	0.06	—	—
−50	—	—	5–7	~0

[a] Data of Alfrey and Greenberg.[3]
[b] Data of Lewis and Mayo.[4]

The identical reactivity ratios of 0.95 obtained for vinyl acetate monomer at +30 and −45°C with the *trans* isomer compare closely to the previously reported values obtained at 60°C[4] and 68°C.[3] These results demonstrate the expected near constant temperature dependence and a slight drift in accuracy with the lower molecular weight analogs.

The reactivity ratio of 5–7 obtained for vinyl acetate at −50°C with the *cis* isomer also compares closely to the earlier work of Lewis and Mayo at 60°C.[4] The similar set of experiments with the *cis* isomer at +30°C gave a reactivity ratio for the vinyl acetate of only 3–4. Although this later result is in the same range as the value reported by Alfrey and Greenberg[3] for 68°C copolymerization, the value obtained with the highest molecular weight copolymers is considered to be the most accurate since end group structures would not alter substantially the compositional analyses.

We conclude, therefore, that the vinyl acetate radical reacts at about equal rates with the double bonds of vinyl acetate and *trans*-1,2-dichloroethylene and that the rates of these reactions are about six times the rate of the reaction of the vinyl acetate radical with the double bond of the *cis* isomer.

Chain-Transfer Effects

In these studies the 1,2-dichloroethylenes participated as both comonomer and chain-transfer agent. Accurate chain-transfer constants could not, therefore, be calculated from these data.

The data on Figure 3 illustrate that the molecular weights of the copolymers depend only on the amounts of 1,2-dichloroethylene in the copolymer, regardless of the isomer which takes part in the copolymerization. This effect was observed both at +30°C and at −45 to −50°C. Since the double bond of the *trans* isomer is about six times more reactive than that of the *cis* isomer this indicates that either: (1) the radical abstraction reactions parallel the reactivities of the double bonds toward radical addition, and that the temperature dependence of these reactions is the same, or (2) the dominating chain transfer reaction occurs by elimination of the chlorine atom subsequent to the addition of the 1,2-dichloroethylene unit to the growing free-radical chain.

The latter hypothesis, which we believe is more logical, was suggested by Ewald and co-workers for the peroxide-initiated isomerization and polymerization of 1,2-dichloroethylene.[8] It is now well known that 2-chloroalkyl radicals, of the structure produced by the addition of radicals to 1,2-

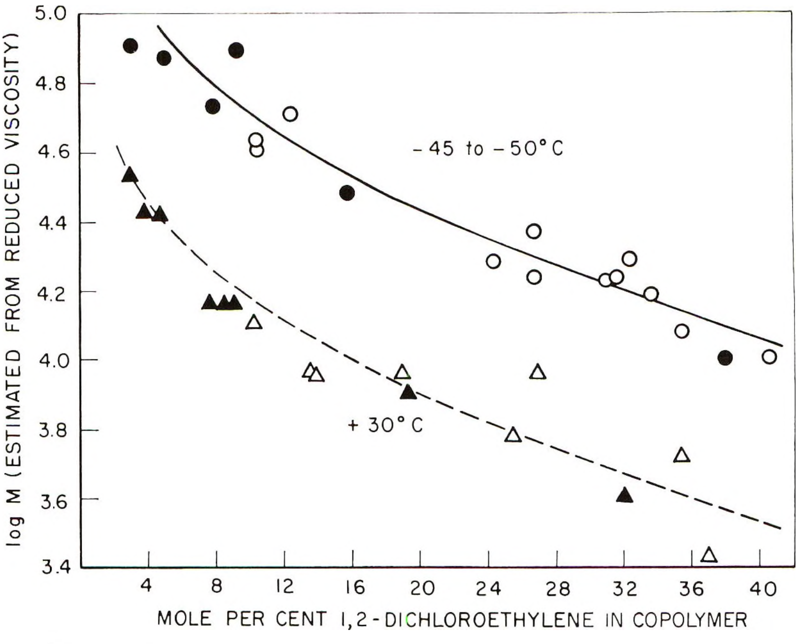

Fig. 3. Effect on the molecular weight of the percentage of 1,2-dichloroethylene in vinyl acetate copolymers: (●,▲) *cis* isomer; (○,△) *trans* isomer.

dichloroethylene double bonds, readily eject the chlorine atom forming an olefinic double bond.[9,10]

Extension of the Transfer Mechanism to the Polymerization of Vinyl Chloride

The molecular weight of poly(vinyl chloride) also is limited by chain transfer to monomer in both bulk[11] and solution[12] polymerization processes. Burnett and Wright proposed that transfer to vinyl chloride involves abstraction of the chlorine atom by the polymer radical forming a vinyl radical.[12] More recent data suggest, however, that chlorine atoms are not much more susceptible to abstraction by radicals than are hydrogen atoms.[13] For example, chlorobenzene, which has a carbon–chlorine bond similar to that in vinyl chloride,[14] does not differ appreciably from benzene in chain transfer activity in radical polymerization. In the polymerization of vinyl acetate, transfer constants for chlorobenzene[15] and benzene[16] are comparable, being 0.00026 and 0.00024, respectively.

However, vinyl chloride[17] and other vinyl monomers[18,19] undergo some reverse addition to the polymer radical (that is head-to-head addition). In the case of vinyl chloride polymerization, when head-to-head addition occurs, it gives a 2-chloro primary alkyl radical [eq. (1)] which could, like the 1,2-dichloroethylene radical, readily eject the β-chlorine atom forming an olefinic double bond [eq. (2)].

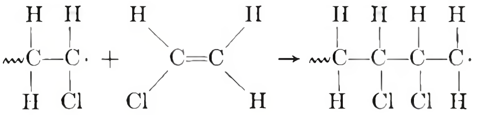

$$\sim\!\sim CH_2{-}\dot{C}HCl + ClHC{=}CH_2 \rightarrow \sim\!\sim CH_2{-}CHCl{-}CHCl{-}\dot{C}H_2 \qquad (1)$$

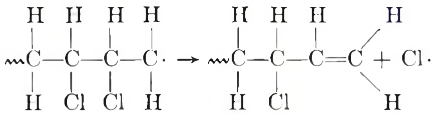

$$\sim\!\sim CH_2{-}CHCl{-}CHCl{-}\dot{C}H_2 \rightarrow \sim\!\sim CH_2{-}CHCl{-}CH{=}CH_2 + Cl\cdot \qquad (2)$$

Since vinyl chloride is a reasonably reactive monomer, the reactive 2-chloro primary alkyl radicals formed by reverse addition would in some cases, again like the 1,2-dichloroethylenes, add to monomer before they could decompose so that the polymer would continue to grow.

To extend our data to vinyl chloride polymerization we must assume, as an approximation, that the rate of β-chlorine atom elimination relative to further monomer addition is of the same order for the pendant 2-chloro and 1,2-dichloro primary alkyl radicals. Since the data on Figure 3 indicate that the dominating chain-transfer reaction occurs by chlorine atom elimination, calculations from these data further illustrate that at +30°C about 1 out of every 17 1,2-dichloroethylene units which copolymerize will eject a chlorine atom before adding monomer. At −45 to −50°C this relative rate of radical elimination to monomer addition is reduced to only about 1 to 60. The recent data of Sobue and Kubota[20] show that a $\overline{DP}$ of about 1420

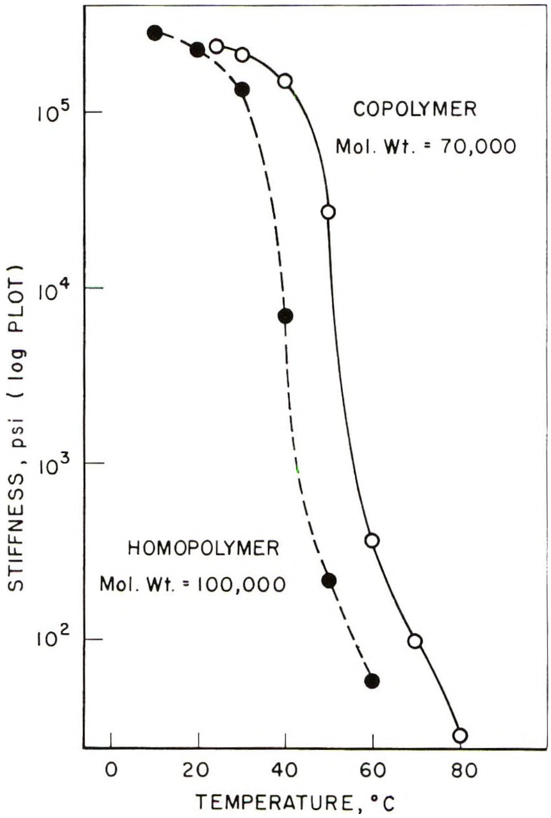

Fig. 4. Comparison of temperature–stiffness curves for poly(vinyl acetate) and a copolymer of vinyl acetate containing 13 wt-% of copolymerized 1,2-dichloroethylene: (●) homopolymer; (○) copolymer.

is obtained when poly(vinyl chloride) is prepared at low conversion in bulk at +30°C by γ-radiation initiation. Further calculations from these data illustrate, therefore, that if the rate of chlorine atom elimination relative to monomer addition is the same for the 2-chloro primary alkyl radical formed by head-to-head addition of vinyl chloride units, and if this is the predominant chain-transfer mechanism in the polymerization of vinyl chloride, then the amount of head-to-head units in poly(vinyl chloride) prepared at +30°C would be about 1.2 mole-%. It has been reported that poly(vinyl chloride) prepared at 60°C contains 1.5 mole-% of head-to-head units.[17] This is about the same percentage which has been reported for head-to-head units in poly(vinyl acetate) prepared at that temperature.[19] At lower polymerization temperatures the amount of head-to-head addition is smaller. In the case of poly(vinyl acetate) it is approximately 1 mole-% when the polymerization is conducted at +30°C,[19] and it should be about the same for poly(vinyl chloride) prepared at +30°C. The calculated value for the amount of head-to-head units in poly(vinyl chloride) is by no means conclusive, but it is strikingly close to the measured value. We suggest, therefore, that the dominant molecular weight controlling process in the polymerization of vinyl chloride proceeds by this β-chloro elimination mechanism rather than by direct atom abstraction from monomer.

Glass Transition Temperatures of Copolymers

The near unity value of the reactivity ratio for vinyl acetate with *trans*-1,2-dichloroethylene demonstrates that the vinyl acetate radical reacts at about equal rates with the double bonds of vinyl acetate and *trans*-1,2-dichloroethylene. The compositions of the copolymers are, therefore, roughly equal to the compositions of the monomer charges, so this system was employed to prepare a moderately uniform copolymer for use in thermal property measurements. At −78°C, a copolymer with a molecular weight of about 70,000 containing 13 wt-% 1,2-dichloroethylene was prepared. The temperature–stiffness curve obtained for this copolymer is illustrated with Figure 4. The increase in T_g of about 12°C over that for poly(vinyl acetate) demonstrates the high glass transition temperature of 1,2-dichloroethylene homopolymer. Extrapolation indicates the T_g of the homopolymer is well above 100°C. A possible advantage of 1,2-dichloroethylene as a comonomer is, therefore, to increase the softening point of a resin.

References

1. J. W. Breitenbach, A. Schindler, and C. Pflug, *Monatsh.*, **81**, 21 (1950).
2. C. E. Frank and A. U. Blackman, *J. Amer. Chem. Soc.*, **72**, 3283 (1950).
3. T. Alfrey, Jr., and S. Greenberg, *J. Polym. Sci.*, **3**, 297 (1948).
4. F. M. Lewis and F. R. Mayo, *J. Amer. Chem. Soc.*, **70**, 1533 (1948).
5. R. H. Wagner, *J. Polym. Sci.*, **2**, 21 (1947).
6. M. Fineman and S. D. Ross, *J. Polym. Sci.*, **5**, 259 (1950).
7. F. R. Mayo and F. M. Lewis, *J. Amer. Chem. Soc.*, **66**, 1594 (1944).
8. A. H. Ewald, S. D. Hamann, and J. E. Stutchbury, *Trans. Faraday Soc.*, **53**, 991 (1957).
9. C. Steel, *J. Phys. Chem.*, **64**, 1588 (1960).
10. J. M. Tedder, *Quart. Revs.*, **14**, 354 (1960).
11. W. I. Bengough and R. G. W. Norrish, *Proc. Roy. Soc.* (London), **A200**, 301 (1950).
12. G. M. Burnett and W. W. Wright, *Proc. Roy. Soc.* (London), A221, 28 (1954).
13. F. W. Evans, R. J. Fox, and M. Szwarc, *J. Amer. Chem. Soc.*, **82**, 6414 (1960).
14. W. A. Waters, *Physical Aspects of Organic Chemistry*, Van Nostrand, New York, 1950, p. 68.
15. A. A. Vansheidt and G. Hardy, *Acta Chim. Hung.*, **20**, 261 (1959); *Resins, Rubbers, Plastics*, **14**, 303 (1960).
16. R. N. Chadha and G. S. Misra, *Trans. Faraday Soc.*, **54**, 1227 (1958).
17. T. Ohtsu and T. Nakata, *Enka Biniiru to Porima*, **5**, 18 (1965); translation in *Studies on Polyvinyl Chloride*, Book No. 1, Institute of Polymer Industry, Tokyo, Japan.
18. C. W. Wilson, III, and E. R. Santee, Jr., in *Analysis and Fractionation of Polymers* (*J. Polym. Sci. C*, **8**), J. J. Mitchell, Jr. and F. W. Billmeyer, Jr., Eds., Interscience, New York, 1965, p. 97.
19. P. J. Flory and F. S. Leutner, *J. Polym. Sci.*, **3**, 880 (1948); *ibid.*, **5**, 267 (1950).
20. H. Sobue and H. Kubota, *Makromol. Chem.*, **90**, 276 (1966).

Received April 10, 1968
Revised June 3, 1968

JOURNAL OF POLYMER SCIENCE: PART A-1 VOL. 7, 183-199 (1969)

γ-Ray-Induced Copolymerization of Carbon Monoxide with Cyclic Ethers*

TSUTOMU KAGIYA, MASATSUNE KONDO,
KENICHI FUKUI, *Faculty of Engineering, Kyoto University, Kyoto, Japan*, and HISAO YOKOTA, *Takarazuka Radiation Laboratory, Sumitomo Atomic Energy Industries, Ltd., Takarazuka, Japan*

Synopsis

The γ-ray copolymerization of carbon monoxide with cyclic ethers, such as ethylene oxide, phenyl glycidyl ether, 1,3-dioxolane, 2-vinyl-1,3-dioxolane, terahydrofuran, 1,4-dioxane, and acetaldehyde was studied. A yellowish or brownish powdery copolymer was obtained in most of the cases examined. The infrared spectra showed that copolymers containing the ester structural unit were produced in the copolymerization with cyclic ethers which have no vinyl groups, and that a copolymer containing a ketone structure was produced from cyclic ether having vinyl group. It was found that the copolymer with ethylene oxide also had a β-propiolactone ring structure at the chain end or the side chain. The copolymers were confirmed to be partially crystalline from the x-ray diffraction diagrams. Further, a ring-opening polymerizability of the cyclic ether by γ-radiation was discussed. And it was found that as the bond dissociation energy between the carbon-oxygen linkage of the cyclic ether is small, the polymer yield both in the homopolymerization and copolymerization with carbon monoxide is high. A mechanism for the copolymerization is proposed on the basis of the results.

INTRODUCTION

In recent years, copolymerizations of carbon monoxide and olefins or vinyl monomers by γ-ray irradiation or by radical initiators have been reported by several groups of workers.[1-6] It has been also reported that carbon monoxide is copolymerized with epoxides[7] or with formaldehyde[8,9] by ionic catalyst to produce polyester. On the other hand, it has been reported that cyclic ethers polymerize by γ-ray irradiation to produce only a viscous liquid except in the polymerization of cyclohexene oxide.[10,11]

The authors carried out a study on the copolymerization of carbon monoxide and cyclic compounds, and have previously reported the alternating copolymerization[12,13] of carbon monoxide and aziridines and the terpolymerization[14-16] of carbon monoxide, aziridines, and olefins by radical initiator or by γ-ray irradiation.

The present paper is concerned with the copolymerization of carbon monoxide with cyclic ethers, such as ethylene oxide, propylene oxide, phenyl glycidyl ether, 1,3-dioxolane, 2-vinyl-1,3-dioxolane, tetrahydrofuan, 1,4-dioxane, and acetaldehyde by γ-ray irradiation.

EXPERIMENTAL

Materials and Procedure

Carbon monoxide (99.2% purity) was obtained commercially. Commercial ethylene oxide, propylene oxide, and phenyl glycidyl ether were dried over calcium hydride and then purified by distillation before use (ethylene oxide, bp 9.5–10°C; propylene oxide, bp 34–35°C; phenyl glycidyl ether, bp 87–88°C/4.5 mm Hg). Commercial tetrahydrofuran and 1,4-dioxane were dried over metallic sodium and then fractionated before use (tetrahydrofuran, bp 65–66°C; 1,4-dioxane, bp 100–101°C). 1,3-Dioxolane,[17] 2-vinyl-1,3-dioxolane,[18] and acetaldehyde[19] were prepared according to the literature (1,3-dixolane, bp 74–76°C; 2-vinyl-1,3-dioxolane, bp 115–116°C; acetaldehyde, bp 20.5–21°C).

The radiation copolymerization was carried out as follows. A measured amount of cyclic ether was charged into a stainless steel autoclave of 30 ml capacity. The vessel was degassed twice *in vacuo* under cooling with liquid nitrogen. Then, a measured amount of carbon monoxide was fed into the vessel from a reservoir. The vessel was exposed to γ-rays from a 5000-Ci^{60}Co source at a dose rate of 3.0×10^5r/hr and temperature of 10–15°C. After the irradiation, the vessel was opened to purge the unreacted monomer by evaporating under reduced pressure or by precipitating with diethyl ether; it was then dried *in vacuo* and weighed.

Analysis of the Copolymer

The composition of the copolymer was determined by elementary analysis with a Yanagimoto CHN Corder, Model MT-1, apparatus. The melting point of the copolymer was determined visually in air with the use of a Yanagimoto melting point measuring apparatus, Model MP-32. The reduced viscosity of a 0.5% solution in acetone at 30°C was measured with an Ostwald viscometer. The infrared spectrum was obtained by using the potassium bromide pellet technique with a Hitachi double-beam infrared spectrometer, Model EPI-2. The x-ray diffraction diagram was recorded with a powder method with a Rigaku Denki x-ray diffractometer, Model D-3F, employing Ni-filtered CuKα radiation by means of standard techniques. The NMR spectrum was measured at 60°C with a Japan Electron high-resolution NMR spectrometer, Model 4H-100, at 100 Mcps in trifluoroacetic acid. The differential thermogram was obtained by using sandwiches with α-alumina powder as a diluent in platinum cell with a Shimadzu differential thermal apparatus, Model DT-10.

Experimental Related to the Copolymerization

The following experiments were carried out in order to elucidate the properties and the structure of the carbon monoxide–ethylene oxide copolymer, and the mechanism of the copolymerization.

Preparation of Homopolymers. Poly(ethylene oxide) was prepared by the polymerization of ethylene oxide (4.5 g) with $Al(C_2H_5)_3$ catalyst (0.15 g) in 50 vol-% benzene solution at 25°C for 48 hr. The polymer yield was 10.0 wt-%; MW, 2.4×10^4). Poly-β-propiolactone[20] was prepared by the polymerization of β-propiolactone (2.3 g) with pyridine catalyst (10 mg) in bulk at 0°C for 7 days (polymer yield, 90.4 wt-%; MW, 4.52×10^4). Poly-β-vinyl-β-propiolactone was prepared by essentially the same method as that described by Smith[21] (bp 45°C/2.5 mm Hg; specific gravity at 25°C 1.048, n_D^{10} 1.4423). The polymerization of β-vinyl-β-propiolactone (0.4 ml) was carried out with $BF_3O(C_2H_5)$ catalyst (0.1 ml) in 10 vol-% chloroform solution in a sealed glass tube at 15°C for 1.5 hr (polymer yield, 17 wt-%).

Irradiation of Carbon Monoxide. The irradiation of carbon monoxide (3.0 g) was carried out as the same method described above. The solid product formed was dried *in vacuo.*

Reaction of Carbon Monoxide–Ethylene Oxide Copolymer with Ethylenimine. A 1.0 g portion of the carbon monoxide–ethylene oxide copolymer obtained in the present study was dissolved in 3 ml of acetone, and then 1.0 g of ethylenimine as 50 vol-% acetone solution was added. The mixture was held at 20°C for 20 hr. After the reaction, the copolymer reacted was washed thoroughly with diethyl ether, dried *in vacuo* and weighed (yield, 0.115 g).

Irradiation of Poly(ethylene Oxide) with β-Propiolactone or with Carbon Monoxide. A mixture of poly(ethylene oxide) (0.5 g) obtained above and β-propiolactone (2.0 g) was irradiated in a sealed glass ampule at 3.0×10^5 r/hr and 15°C for 190 hr. Also, a mixture of poly(ethylene oxide) (0.5 g) and carbon monoxide (3.0 g) was irradiated in a stainless steel autoclave of 30 ml capacity under the same conditions as described above. The polymer irradiated was washed thoroughly with a large amount of diethyl ether and dried *in vacuo.*

Content of Ester Groups in the Carbon Monoxide–Ethylene Oxide Copolymer. The contents of ester and β-propiolactone ring in the resulting copolymer were estimated by means of infrared spectrometry. The following relation between the ratio of absorption intensity of two ester C=O groups ($D_{C=O}$) and its mole ratio was obtained in chloroform with various concentrations of the mixture of β-propiolactone and the esters, such as methyl acetate, propyl acetate, and poly-β-propiolactone:

$$\frac{D_{C=O} \text{ of } \beta\text{-propiolactone}}{D_{C=O} \text{ of ester}} = 0.60 \frac{\text{Moles of } \beta\text{-propiolactone}}{\text{Moles of ester}}$$

Copolymerization of Carbon Monoxide and Ethylene Oxide by Radical Initiators. The copolymerization (carbon monoxide, 3.0 g; ethylene oxide, 4.4 g) was carried out according to the procedure described above by the use of radical initiators, such as benzoyl peroxide and α,α′-azobisisobutyronitrile (0.5 mole-% added to ethyleneoxide) at 60°C for 42 hr.

TABLE I

Copolymerization of Carbon Monoxide and Cyclic Ethers by γ-Ray Irradiation[a]

Cyclic ether		Carbon monoxide, g	Polymer yield, g	Reduced viscosity, dl/g[b]	Melting point, °C	Polymer composition (mole ratio)		Elementary analysis (found)		Appearance of polymer
Type	Wt, g					CO	Cyclic ether	C, %	H, %	
	—	3.0	0.032	—	—	—	—	—	—	Brown powder
Ethylene oxide	4.4	3.1	0.211	0.062	76–87	0.82	1.00	49.78	5.99	Yellowish powder
"	4.4	—	0.075	—	—	—	—	—	—	Yellowish liquid
Propylene oxide	5.3	2.8	0.262	0.027	110–130	0.73	1.00	55.92	7.69	Yellowish, powdery
"	5.0	—	0.071	—	—	—	—	—	—	Yellowish liquid
Phenyl glycidyl ether	15.2	3.1	0.845	0.034	50–60	0.33	1.00	70.97	6.23	Brownish, pasty
"	15.2	—	0.105	—	—	—	—	—	—	Brownish liquid

1,3-Dioxolane	5.5	3.2	0.493	0.030	—	1.39	1.00	44.75	5.55	Brownish, pasty
"	5.0	—	0.032	—	—	—	—	—	—	Yellowish liquid
2-Vinyl-1,3-dioxolane	7.9	3.2	1.931	—	70–77	0.38	1.00	56.88	7.10	Yellowish, powdery
Tetrahydrofuran	7.0	3.0	0.252	0.044	95–115	2.24	1.00	49.86	6.46	Brownish, powdery
"	5.5	—	0.035	—	—	—	—	—	—	Yellowish liquid
1,4-Dioxane	8.9	3.1	0.577	0.042	120–140	1.91	1.00	47.41	3.95	Yellowish, powdery
"	5.0	—	0.086	—	—	—	—	—	—	Yellowish liquid
Acetaldehyde	4.5	3.0	0.139	—	—	0.62	1.00	50.85	6.56	Yellowish, pasty
"	6.7	—	0.029	—	—	—	—	—	—	Yellowish liquid

[a] Reaction conditions: temperature, 10–15°C; dose rate, 3.0×10^5 r/hr; total dose, 5.7×10^7 r; reaction vessel, 30 ml capacity.

[b] Measured with 0.5% solution in acetone at 30°C.

RESULTS AND DISCUSSION

Characterization of the Copolymer of Carbon Monoxide and Cyclic Ethers

Results of the Copolymerization. The results of the γ-ray copolymerization of carbon monoxide with cyclic ethers are shown in Table I in comparison with the data for homopolymerization of the cyclic ethers.

In the homopolymerization of cyclic ethers, only viscous products were obtained by γ-ray irradiation. Contrary to this, in the copolymerization of carbon monoxide with cyclic ethers a yellowish or brownish powdery product was obtained in most cases. The products produced were insoluble in diethyl ether but soluble in acetone or chloroform. From the viscosity measurement, the irradiation products were found to be polymeric. The results of elementary analysis showed that the polymers were composed of carbon monoxide and cyclic ethers. In addition, the copolymer of carbon monoxide with ethylene oxide gradually became insoluble in acetone and chloroform during storage at room temperature and also solidified on heating around 120°C and did not remelt. On the other hand, carbon monoxide gave a brown, powdery product with low yield by γ-ray irradiation as reported by Colombo et al.[6] and Lind.[22] Accordingly, the polymers produced from carbon monoxide with cyclic ethers may contain a small amount of the irradiation product of carbon monoxide as a mixture. A great part of the product was soluble in acetone but insoluble in diethyl ether and chloroform and did not melt on heating up to 300°C.

Infrared Spectra of the Copolymer. Figure 1 shows the infrared spectra of the copolymers obtained by the γ-ray copolymerization of carbon monoxide with cyclic ethers. The irradiation product of carbon monoxide displayed a broad absorption band at 1800–1400 cm^{-1} which is probably due to a carbonyl group. Obviously, the infrared spectra of the copolymers of carbon monoxide with cyclic ethers are different from the spectrum of the irradiation product of carbon monoxide. Most of the copolymers exhibited characteristic absorption bands at near 1730 and 1200–1000 cm^{-1} which were assignable to stretching vibrations of ester $C{=}O$ and of ester and ether $C{-}O{-}C$ groups, respectively. The copolymer of carbon monoxide and ethylene oxide also exhibited an absorption peak at 1815 cm^{-1}, which is probably assignable to the ester $C{=}O$ group of the four-membered lactone ring. It was also found that the infrared spectrum of the carbon monoxide–ethylene oxide copolymer was different from that of the copolymer of carbon monoxide with ethylene oxide produced by $Al(i\text{-}C_4H_9)_3$–H_2O–$Co(CH_3COCH_2COCH_3)_3$ catalytic systems[7] and poly-β-propiolactone produced by pyridine catalyst,[20] especially regarding the absorption at 1815 cm^{-1}. On the other hand, the copolymer of carbon monoxide and 2-vinyl-1,3-dioxolane exhibited characteristic absorption peaks attributed to the ketone group at 1710 cm^{-1} and to the ether group of the dioxolane ring at 1140 and 1040 cm^{-1}.

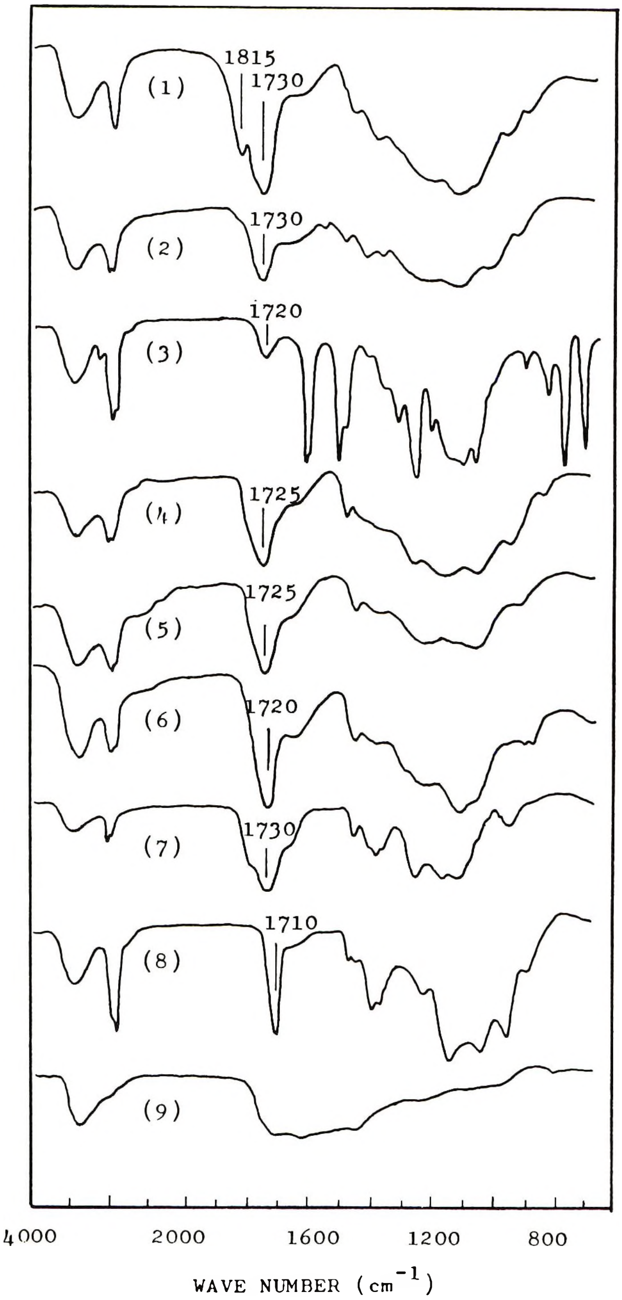

Fig. 1. Infrared spectra of copolymer of carbon monoxide with: (*1*) ethylene oxide; (*2*) propylene oxide; (*3*) phenyl glycidyl ether; (*4*) 1,3-dioxolane; (*4*) tetrahydrofuran; (*6*) 1,4-dioxane; (*7*) acetaldehyde; (*8*) 2-vinyl-,3-dioxolane; (*9*) irradiation product of carbon monoxide.

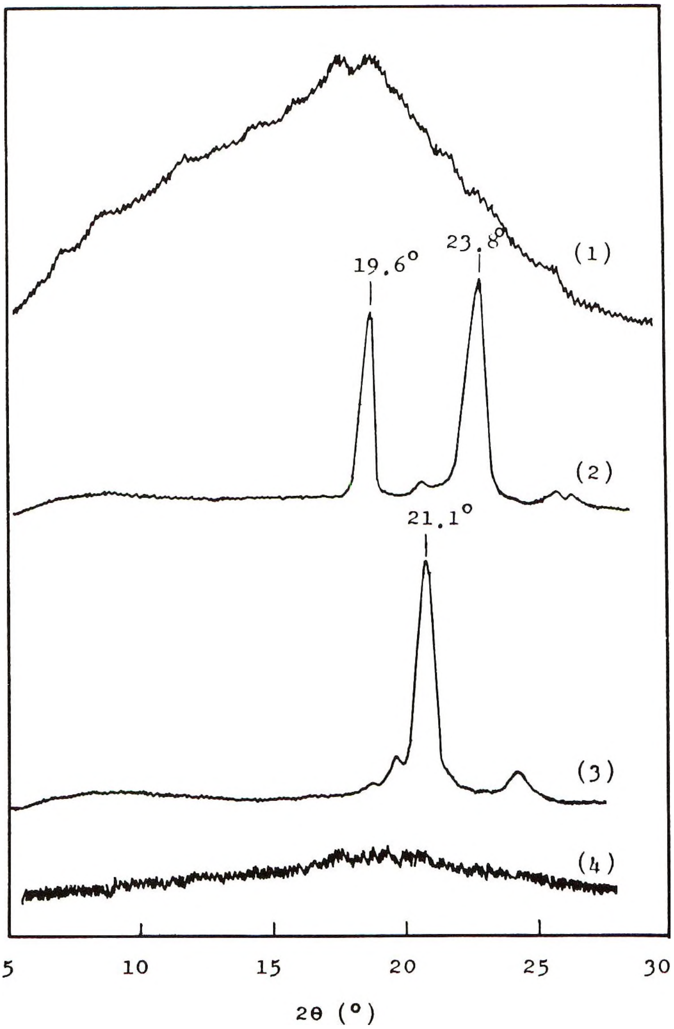

Fig. 2. X-ray diffraction diagrams of: *(1)* carbon monoxide–ethylene oxide copolymer; *(2)* poly(ethylene oxide); *(3)* poly-β-propiolactone; *(4)* irradiation product of carbon monoxide.

These results show that copolymers containing the ester structure are produced in the copolymerization with cyclic ethers which have no vinyl groups, while the copolymer containing ketone structure is produced from cyclic ether having vinyl group, not through the ring-scission but through the vinyl polymerization.

X-Ray Diffraction Diagrams of the Copolymers. Figure 2 shows the x-ray diffraction diagram of the carbon monoxide–ethylene oxide copolymer in comparison with the diagrams of the irradiation product of carbon monoxide, poly(ethylene oxide), and poly-β-propiolactone, which were obtained in the present study. The diagram of the carbon monoxide–ethylene oxide copolymer is quite different from that of crystalline poly(ethylene oxide) and poly-β-propiolactone and that of the irradiation product of carbon monoxide which shows no crystallinity. The copolymer showed some crystallinity, which suggests that the copolymer is not a mixture of polymers, such as poly(ethylene oxide) and poly-β-propiolactone. The x-ray diffraction of the copolymers of carbon monoxide with other cyclic ethers are shown in Figure 3. The copolymers were also confirmed to be partially crystalline.

NMR Spectrum of the Copolymer of Carbon Monoxide with Ethylene Oxide. The NMR spectrum of carbon monoxide–ethylene oxide copolymer

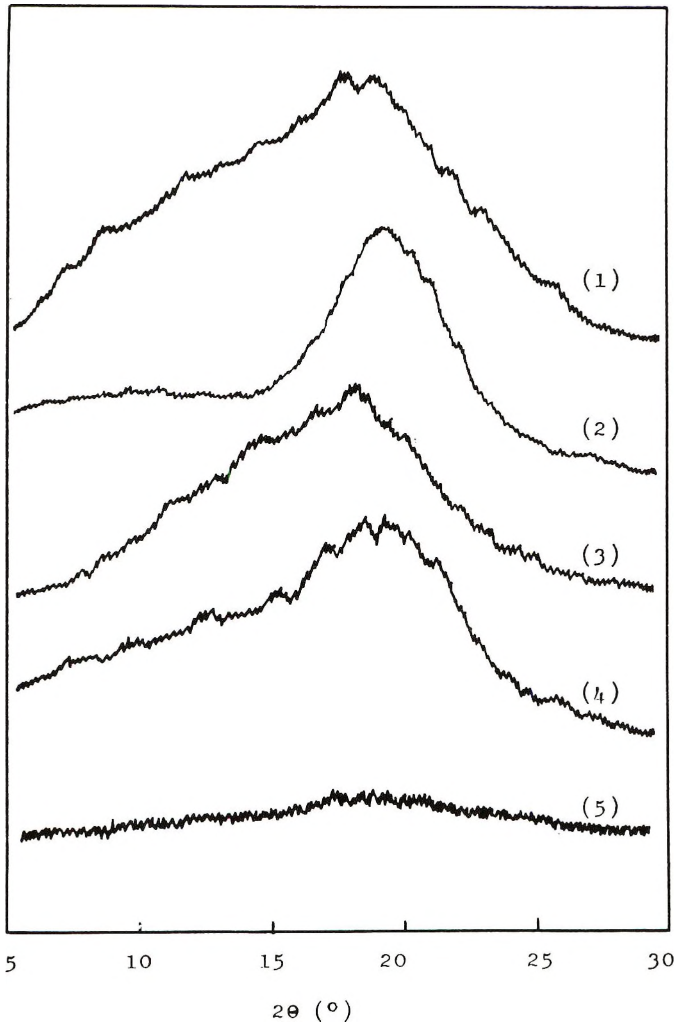

Fig. 3. X-ray diffraction diagrams of copolymers of carbon monoxide with: (*1*) ethylene oxide; (*2*) 2-vinyl-1,3-dioxolane; (*3*) tetrahydrofuran; (*4*) 1,4-dioxane; (*5*) irradiation product of carbon monoxide.

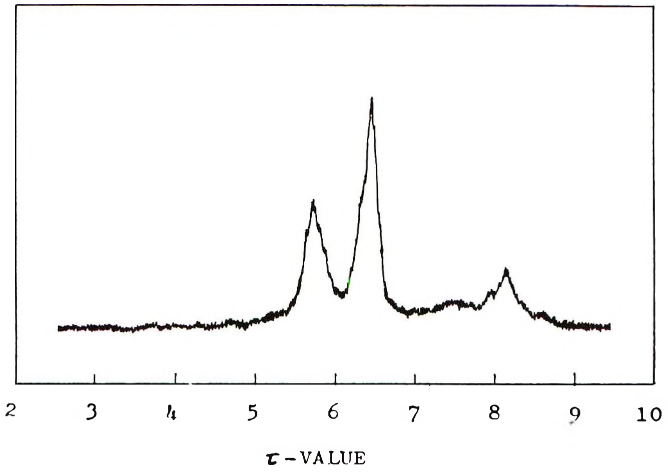

Fig. 4. NMR spectrum of carbon monoxide–ethylene oxide copolymer.

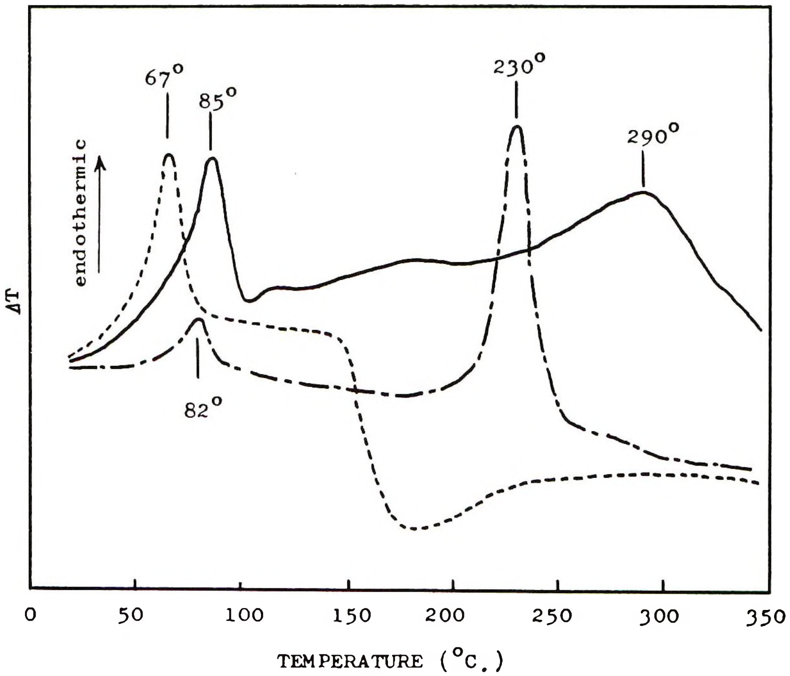

Fig. 5. Comparison of differential thermograms of: (——) carbon monoxide–ethylene oxide copolymer; (–·–) poly-β-propiolactone; (--) poly(ethylene oxide).

is shown in Figure 4. The spectrum shows main peaks at τ values of 5.75 (A) and 6.46 (B), which are assignable to an $+O\text{-}CH_2(A)\text{-}CH_2(B)\text{-}\overset{O}{\overset{\|}{C}}+$ unit or $+O\text{-}CH_2(B)\text{-}CH_2+$ unit. The broad peak at τ 7–8 and the peak at τ 8.16

may probably be attributable to the proton of a cyclic compound and the methyl group of the polymer chain end, respectively. The result is in accord with that from the infrared analysis and thus, verifies that the copolymer consists mainly of ester structures.

Differential Thermogram of the Copolymer of Carbon Monoxide with Ethylene Oxide. The differential thermogram of the carbon monoxide–ethylene oxide copolymer is shown in Figure 5 in comparison with poly(ethylene oxide) and poly-β-propiolactone obtained in the present study with triethylaluminum and pyridine catalyst, respectively. The differential thermogram of the carbon monoxide–ethylene oxide copolymer was different from that of poly(ethylene oxide) and poly-β-propiolactone, and the copolymer showed endothermic peaks at 85 and 290°C which corresponded to the melt and thermal decomposition, respectively. It was found that the decomposing point of the carbon monoxide–ethylene oxide copolymer was higher than that of poly-β-propiolactone.

Structure of the Copolymer of Carbon Monoxide with Ethylene Oxide

The following study was devoted to determining the structure of the carbon monoxide–ethylene oxide copolymer and the mechanism of the copolymerization. As described above, it was inferred from the infrared and NMR spectra that the carbon monoxide–ethylene oxide copolymer contained a four-membered lactone structure. In order to confirm this structure, the copolymer was compared with poly-β-vinyl-β-propiolactone which was prepared by $BF_3O(C_2H_5)_2$ catalyst.[23] It was found from the infrared spectrum that the poly-β-vinyl-β-propiolactone mainly consisted of the two structural units I and II, which were formed by ring scission and vinyl polymerization of the monomer.

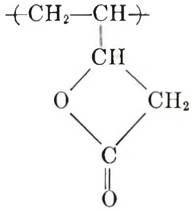

I

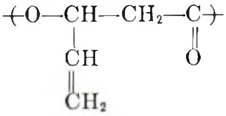

$$-\!\!(O-\underset{\substack{|\\CH\\\|\\CH_2}}{CH}-CH_2-\underset{\substack{\|\\O}}{C}\!\!)-$$

II

Poly-β-vinyl-β-propiolactone exhibited characteristic absorption peaks at 1820 and 1730 cm^{-1} which were assignable to ester $C=O$ groups of polymer I and II, respectively, as shown in Figure 6. The absorption peaks at 1815 and 1730 cm^{-1} of the carbon monoxide–ethylene oxide copolymer are similar to those of this poly-β-vinyl-β-propiolactone. It was previously reported that β-propiolactone and ethylenimine easily copolymerize with and without cationic catalysts to produce polyamide.[24] Futher, to confirm the existence of the β-propiolactone structure in the carbon monoxide–ethylene oxide copolymer, the reaction of the copolymer with ethylenimine was examined without catalyst in acetone solution as described in the

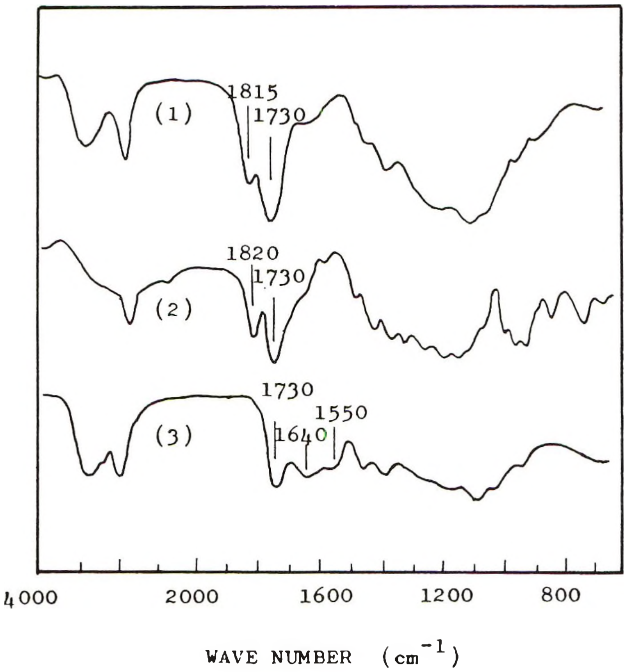

Fig. 6. Infrared spectra of: (*1*) carbon monoxide–ethylene oxide copolymer; (*2*) poly-β-vinyl-β-propiolactone, measured in chloroform solution; (*3*) reacted polymer of carbon monoxide–ethylene oxide copolymer with ethylenimine.

experimental section. The reacted polymer became a brownish powder and insoluble in acetone and did not melt on heating to 300°C. As shown in Figure 4, the infrared spectrum of the reacted polymer showed that the absorption peak at 1815 cm^{-1} in the carbon monoxide–ethylene oxide copolymer disappeared and new characteristic absorption bands assigned to secondary amide groups appeared near 1640 and 1550 cm^{-1}. This reaction of carbon monoxide–ethylene oxide copolymer with ethylenimine, probably produced a crosslinked polymer, as shown in eq. (1).

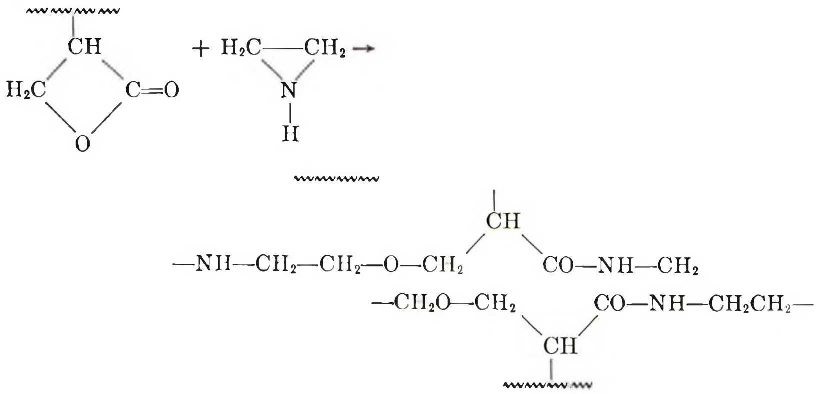

(1)

These results show that the carbon monoxide–ethylene oxide copolymer possesses a β-propiolactone structure at the chain end or on the side chain. According to these results, it may be concluded that the reaction of carbon monoxide with ethylene oxide by γ-irradiation gives copolymer which composed of the structural units III–VI.

$$-\!\!(CH_2-CH_2-O)\!\!-$$

III

(Ether unit)

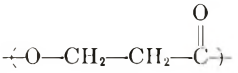

$$-\!\!(O-CH_2-CH_2-\overset{\overset{O}{\|}}{C})\!\!-$$

IV

(Ester unit)

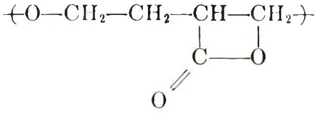

V

(Lactone-ended unit)

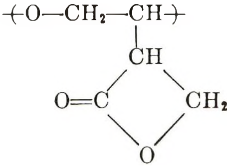

VI

(Pendant unit)

As described above, the molar ratio of carbon monoxide to ethylene oxide in the copolymer was calculated to be 0.82:1 from the elementary analysis. This shows that the content of polymer III is comparatively lower than that of polymers IV–VI. The mole ratio of polymer IV to polymers V and VI was also estimated to be 6.5:1 from infrared spectrometery. Further, the formation of the polymer having β-propiolactone structure was studied in the following way. If it is assumed that β-propiolactone is produced by the reaction of carbon monoxide and ethylene oxide on γ-irradiation, polymer V or VI may be produced by dehydrogenation of the lactone with polymer produced during the polymerization. It is also assumed that polyester is produced by a insert reaction of carbon monoxide to the poly(ethylene oxide) formed in the polymerization. For some information on this process, the γ-irradiated products of the mixtures of carbon monoxide and ethylene oxide, and of poly(ethylene oxide) and β-propiolactone were analyzed by infrared spectrometry. β-Propiolactone monomer and the polymer having the β-propiolactone structure, were not detected in the irradiated products of the both mixtures, respectively.

In addition, the irradiated poly(ethylene oxide) with carbon monoxide showed almost the same infrared spectrum as the nonirradiated polymer, and no absorption band assigned to the carbonyl group was observed. The mechanism of the copolymerization will be discussed in a latter section.

Ring-Opening Polymerization of Cyclic Ethers

It has been reported that the basicity or the stress of the ring of the cyclic monomer is a factor in the copolymerization of cyclic ethers, formals, and esters[25] or in the polymerization of cyclic hydrocarbons.[26,27] For this reason the γ-ray polymerization of cyclic ethers and copolymerization with carbon monoxide were briefly studed in connection with the basicity or the bond-dissociation energy for the carbon–oxygen linkage of the monomer (D_{C-O}).

No correlation between the polymer yield and the basicity of the cyclic monomer was obtained. On the other hand, in the homopolymerization of cyclic ethers and the copolymerization with carbon monoxide the polymer yield (based on cyclic ether) in Table I increased with the use of a cyclic ether having a small D_{C-O} value as shown in Figure 7. This fact indicate that the D_{C-O} of the cyclic ethers contributes greatly to both polymerizations. Thus, the result suggests that the ring scission of cyclic ethers caused by radical reaction predominates in the γ-ray polymerizations. Accordingly, the increase in the polymer yield with the use of cyclic ether

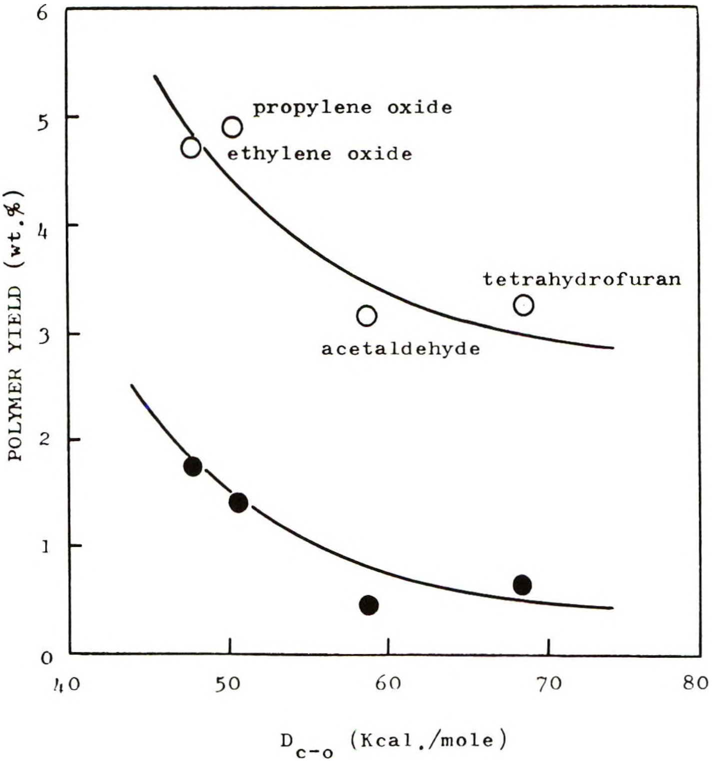

Fig. 7. Polymer yield versus bond dissociation energy of cyclic ether (Dc-o) plotted by using the data given in Table I: (○) copolymerization with carbon monoxide; (●) homopolymerization.

having small D_{C-O} may be ascribed to the increase of the propagation by γ-ray irradiation ring cleavage of cyclic monomer.

Mechanism of the γ-Ray Copolymerization of Carbon Monoxide with Ethylene Oxide

The reaction mechanism of the γ-ray copolymerization of carbon monoxide with ethylene oxide is discussed as follows on the basis of the results described above.

Formation of the Initiating Species by γ-Radiation. From the relation between the polymer yield and D_{C-O} as described above, it was considered that a carbonyl radical as the initiating species could be produced by the reaction of a radical formed by the radiolysis of ethylene oxide with carbon monoxide, as eqs. (2) and (3) show.

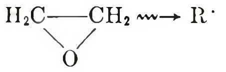

(2)

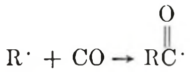

$$R\cdot + CO \rightarrow R\overset{\overset{O}{\|}}{C}\cdot \qquad (3)$$

Initiation. Since the radical produced is electrophilic, the addition of ethylene oxide, which is nucleophilic, to the cationic radical is considered to occur exclusively. The initiation reaction proposed is, therefore, as shown in eq. (4).

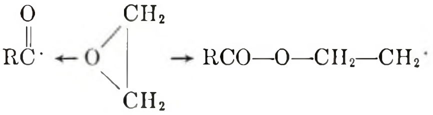

(4)

Propagation. In the propagation reaction, when the addition of ethylene oxide to the growing polymer chain follows alternatively the addition of carbon monoxide, a polymer having an ester structure is produced, as shown in eq. (5).

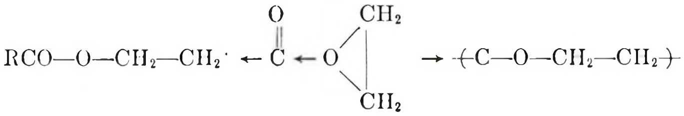

(5)

The addition of ethylene oxide only to the growing polymer chain gives a polymer having an ether structure, as shown in eq. (6).

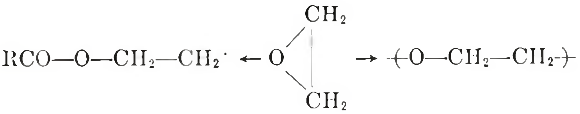

(6)

Unlike reactions (5) and (6), polymers having a β-propiolactone structure are believed to be produced when a ring structure is formed at the chain end by the tail-to-tail reaction of the growing polymer chain with ethylene oxide and the subsequent addition of carbon monoxide, and futher when the intramolecular chain transfer or termination reaction occurs with the hydrogen extraction reaction. That is, the polymer having a β-propiolactone structure is formed at the chain end by the α-hydrogen-extraction reaction of the lactone with the carbonyl radical as shown in eq. (7). The pendant-type polymer is also formed through the same reaction as eq. (6) and further by the hydrogen-extraction reaction of the neighboring hydrogen atom next to the lactone with the hydrogen radical extracted in eq. (7), as shown in eq. (8).

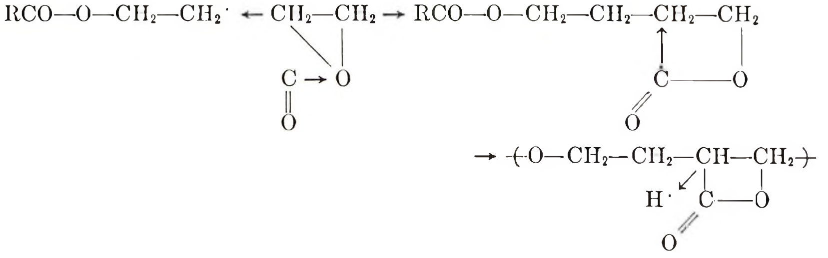

(7)

or

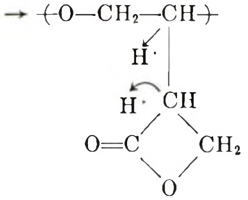

(8)

In addition, the copolymerization of carbon monoxide with ethylene oxide by radical catalysts, such as benzoyl peroxide and α,α'-azobisisobutyronitrile, was studied to confirm the reaction mechanism described above at 60°C for 42 hr, but only a trace amount of liquid homopolymer of ethylene oxide was obtained and no copolymer could be obtained by these catalysts. This result is in accord with the mechanism that the polymer chain grows by the γ-ray ring cleavage of cyclic monomer.

A quantitative study of the copolymerization of carbon monoxide and cyclic ethers by γ-ray irradiation will be reported in a subsequent paper.

References

1. M. M. Brubaker, D. D. Coffman, and H. H. Hoehen, *J. Amer. Chem. Soc.*, **74,** 1509 (1952).
2. D. D. Coffman, P. S. Pinkney, F. T. Wall, W. H. Hood, and H. S. Young, *J. Amer. Chem. Soc.*, **75,** 3391 (1952).
3. Y. Chatani, T. Takizawa, S. Murahashi, Y. Sakata, and Y. Nishimura, *J. Polym. Sci.*, **55,** 811 (1961).
4. P. Colombo, M. Steinberg, and J. Fontana, *J. Polym. Sci. B*, **1,** 447 (1963).
5. P. Colombo, M. Steinberg, and D. Macchia, *J. Polym. Sci. B*, **1,** 483 (1963).
6. P. Colombo, L. E. Kukacka, J. Fontana, R. N. Chapman, and M. Steinberg, *J. Polym. Sci. A-1*, **4,** 29 (1966).

7. J. Furukawa, Y. Iseda, T. Saegusa, and H. Fujii, *Makromol. Chem.*, **89**, 263 (1965).

8. M. Modena, M. Ragazzini, and E. Gallinella, *J. Polym. Sci. B*, **1**, 567 (1963).

9. M. Ragazzini, M. Modena, E. Gallinella, and G. Cevidalli, *J. Polym. Sci. A*, **2**, 5203 (1964).

10. S. Peneczek, J. Wieteszka, and P. Kubisa, *Makromol. Chem.*, **97**, 225 (1966).

11. D. Cordischi, M. Lenzi, and M. Mele, *J. Polym. Sci. A*, **3**, 3421 (1965).

12. T. Kagiya, S. Narisawa, T. Ichida, K. Fukui, H. Yokota, and M. Kondo, *J. Polym. Sci. A-1*, **4**, 293 (1966).

13. T. Kagiya, S. Narisawa, T. Ichida, N. Ohta, and K. Fukui, *Kogyo Kagaku Zasshi*, **69**, 2220 (1966).

14. T. Kagiya, S. Narisawa, T. Ichida, K. Fukui, and H. Yokota, *J. Polym. Sci. A-1*, **4**, 2171 (1966).

15. T. Kagiya, I. Maruta, T. Ichida, S. Narisawa, and K. Fukui, *J. Polym. Sci. A-1*, **5**, 1645 (1967).

16. T. Kagiya, T. Ichida, S. Narisawa, and K. Fukui, *J. Polym. Sci. A-1*, **5**, 2031 (1967).

17. M. J. Astle, A. Zaslowsky, and P. G. Lafyatis, *Ind. Eng. Chem.*, **46**, 787 (1954).

18. T. Kagiya, T. Nakayama, Y. Nakai, and K. Fukui: *J. Polym. Sci. A-1*, **5**, 2351 (1967).

19. A. Umezawa, *Experimental Methods in Organic Chemistry* (*Zikken Yukikagaku*), Maruzen, Tokyo, 1964, p. 250.

20. T. Kagiya, T. Sano, and K. Fukui, *Kogyo Kagaku Zasshi*, **67**, 951 (1965).

21. C. W. Smith, *Acrolein*, Wiley, New York, 1962, p. 142.

22. S. C. Lind, *Radiation Chemistry of Gases*, Reinhold, New York, 1961, p. 112ff.

23. T. Kagiya, S. Asai, and K. Fukui, unpublished data.

24. T. Kagiya, S. Narisawa, K. Manabe, and K. Fukui, *J. Polym. Sci. B*, **3**, 617 (1965).

25. Y. Yamashita, T. Tsuda, M. Okada, and S. Iwatsuki, *J. Polym. Sci. A-1*, **4**, 2121 (1966).

26. F. S. Dainton, T. R. E. Devlin, and P. A. Small, *Trans. Faraday Soc.*, **51**, 1710 (1955).

27. P. A. Small, *Trans. Faraday Soc.*, **51**, 1717 (1955).

Received March 23, 1968
Revised June 20, 1968

JOURNAL OF POLYMER SCIENCE: PART A-1 VOL. 7, 201-208 (1969)

Unit Cell Dimensions of Isotactic Polyvinylcyclopropane

H. D. NOETHER, *Celanese Research Company, Summit, New Jersey 07901,*
C. G. OVERBERGER* and G. HALEK,† *Polytechnic Institute of Brooklyn, Brooklyn, New York 11201*

Synopsis

The unit cell dimensions of isotactic polyvinylcyclopropane were determined, based on crystalline, oriented fiber and film samples. Two structures were found: (*1*) a hexagonal structure with $a = 13.6$ Å, $c = 6.48$ Å, 3_1 helix, space group $P3_1$ and $P3_2$, $\rho(\text{calc}) = 0.9805$ g/cm^3, $\rho(\text{obs}) = 0.975$ g/cm^3; (*2*) a tetragonal structure with $a = 15.21$ Å, $c = 20.85$ Å, 10_3 helix, space group $I\bar{4}$, $\rho(\text{calc}) = 0.926$ g/cm^3.

In a previous publication[1] a synthesis of vinylcyclopropane and its polymerization to polyvinylcyclopropane has been described. An x-ray diffraction pattern of the polymer was recorded, indicating a crystalline and, therefore, probably a stereospecific, polymeric material. More recently, Natta et al.[2] showed that an oriented sample of such a polymer had a fiber repeat length of 6.50 Å and appeared to be isotactic, possessing a helical chain arrangement of the 3_1 type. He also reported that heating the polymer for a certain time at 180°C seemed to produce a second crystalline modification.

In connection with x-ray diffraction investigations of vinyl and allyl cycloaliphatic, isotactic polymers to establish trends in the types of helices and their packing in the unit cell as a function of the size of the cycloaliphatic side group,[3] the behavior of the first member of such a series was of obvious interest.

This paper will describe the x-ray diffraction data and the unit cell dimensions derived from the measurements of oriented samples of this polymer. The synthesis of the monomer, details of its polymerization, and chemical evaluation will be described elsewhere.[4]

Experimental

Vinylcyclopropane, after polymerization with a Ziegler-Natta type catalyst at room temperature,[4] was extracted with a series of solvents to remove atactic material.

The x-ray diffraction photographs were obtained from the polymer pow-

---

* Present address: The University of Michigan, Ann Arbor, Michigan 48104.

† Present address: Celanese Plastics Co., Clark, New Jersey 07066.

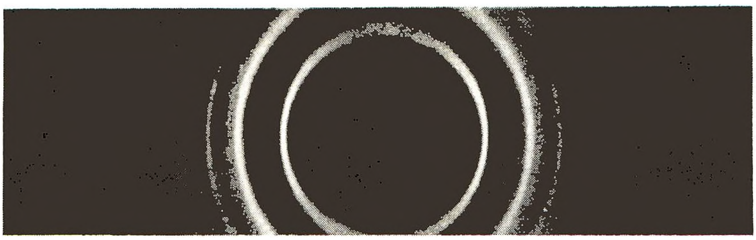

Fig. 1. Polyvinylcyclopropane powder, heptane-insoluble fraction, heat-treated $^1/_2$ hr at 175–180°C. Powder camera, 114.6 mm diameter.

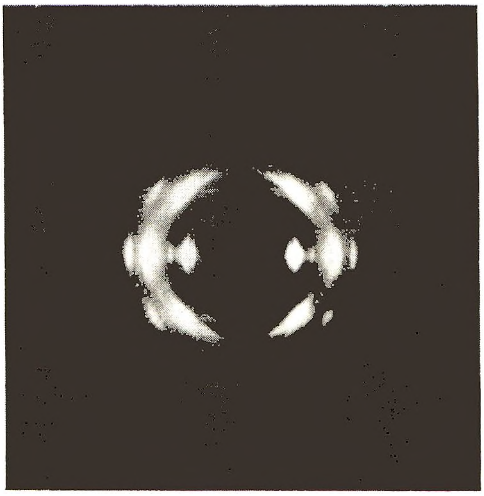

Fig. 2. Fiber pattern of PVCP, fiber drawn, 170–175°C. Unicam cylindrical camera, 30 mm. radius.

der as isolated after polymerization and after extraction and heat-treatment procedures. The polymer, especially the heptane-insoluble fraction (which in the case of polypropylene[5,6] is highly stereospecific and crystalline), did not crystallize too readily. Perhaps the tendency to form a smectic structure also exists, as it does in the case of polypropylene.[7,8]

However, fibers could be meltspun by hand and then drawn and oriented in a wide range of temperatures (80–180°C). They were annealed up to 6 hr at constant length in the range 160–195°C to yield highly crystalline, well oriented samples.

The x-ray patterns were obtained with Ni-filtered CuKα radiation. Powder cameras were used for both powder and fiber samples; flat plate cameras for preliminary studies; cylindrical cameras with 28.7 mm, 30 mm, and 57.3 mm radii were used with the fiber bundles either perpendicular to the x-ray beam or in an inclined position to determine the helix and monomer repeat lengths. Some representative photographs, obtained with powder and cylindrical cameras are shown in Figures 1–4. The ξ spacings of the diffraction spots on the various layer lines, as obtained from Bernal charts, as well as their intensities are listed in Table I.

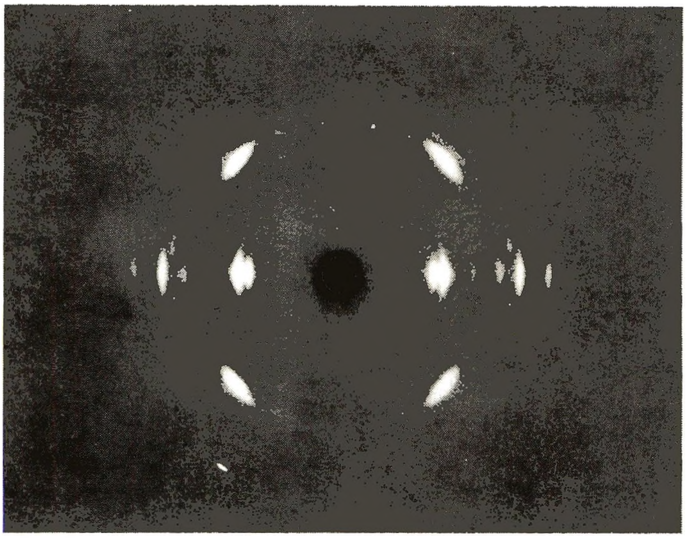

Fig. 3. Fiber pattern of PVCP, manually melt-spun, drawn at 160°C, annealed at 190°C for 6 hr. Unicam cylindrical camera, 57.3 mm radius.

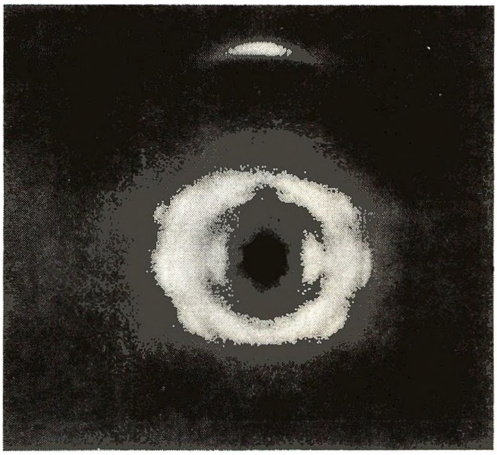

Fig. 4. Fiber pattern of PVCP, same sample as in Fig. 2. Unicam cylindrical camera 30 mm radius. Fiber inclination 22°.

TABLE IA
Observed Spacings and Their Indexing in the Tetragonal and Hexagonal Systems

Observed				Tetragonal		Hexagonal	
Layer	Intensity	ξ		*hkl*	Calcd	*hkl*	Calcd
Equator	vs	0.204		200	0.203		
	vs	0.227				110	0.227
	m	0.286		220	0.287		
	m	0.350				210	0.346
	s	0.395				300	0.393
	s	0.457		240	0.454	220	0.453
	vw	0.572		440	0.574		
	vw	0.600	hex?	600?	0.608	410	0.600
	vw	0.821		800	0.810	520	0.816
1st	w	0.220		211	0.227		
	m+	0.369		321	0.366		
	w	0.422		411	0.418		
2nd	w	merid.		002			
	vvw	0.204		202	0.203		
	w	0.288		222	0.287		
	w+	0.321		312	0.321		
	vvw	0.358?		?			
	vvw	0.405?		402	0.405		
3rd	m	0.127				101	0.131
1st hex	vvs dbl.	0.227		213	0.227	111	0.227
	w	0.263				201	0.262
	m	0.348				211	0.346
	vw?	0.393				301?	0.393
	w	0.454	hex?	423?	0.454	221	0.453
	w?	0.560				321	0.570
	vw	0.605	hex?	613	0.608	411	0.599
	w	0.680		633	0.680	331?	0.680
4th	s	0.145		114	0.144		
	s	0.202		204	0.203		
6th	w	0.143		116	0.144		
2nd hex	m	merid.				002	
		or 0.130				102	0.131
	w	0.225				112	0.227
7th	w	0.227		217	0.227		
9th	w	merid.		009			
3rd hex	w	merid.				003	
10th	vw	merid.		00,10			

TABLE IB
Unit Cell Data

	Tetragonal	Hexagonal
a^*	0.1014	—
a, Å	15.21	13.6
d_{100}^*	—	0.1313
d_{100}, Å	—	11.74
c^*	0.0740	0.238
c, Å	20.85	6.48
ρ, g/cm³ Calcd	0.926	0.9805
Obsd	—	0.975 g/cm³
Helix	10_3	3_1
Monomer length, Å	2.09	2.16
Space group	$I\bar{4}$	$P3_1$, $P3_2$

Results and Discussion

Attempts to produce the structure modification observed by Natta[2] on annealing above 180°C were unsuccessful. No new diffraction lines could be observed. However, a detailed examination of the relative intensities of various diffraction spots for samples drawn and annealed under a wide range of conditions showed considerable variations in intensities. This comparison and the analogous observations for other isotactic cycloaliphatic polymers[3] indicated that the observed pattern had their origin in more than one type of crystal structure. Most noticeable was this effect for samples drawn at 170–175°C.

Indexing of the diffraction spots was started by considering those layers which seemed to belong to only one of the structures. This procedure allowed the determination of the base of one of the unit cells as being tetragonal: $a = b = 15.21$ Å (Table II). It also allowed the indexing of the diffraction spots on the equator and near the strongest layer line (3rd) where major interference with the other structure would have to occur.

The observed layer intensities (absence of 5th and 8th layers and the relative intensities of the others) agree with those calculated according to Cochran et al.[9] for a 10_3 helix. This was confirmed by inclined photographs showing an intense meridional spot on the 10th layer. The structure is very similar to other tetragonal structures of the polyvinylcycloaliphatics:[3] tetragonal system, $a = b = 15.21$ Å, $c(10_3) = 20.85$ Å, four helices of 10 monomers each per cell; space group $I\bar{4}$; $\rho(\text{calc}) = 0.926$ g/cm³; the length in the fiber direction is 2.09 Å per monomer unit.

The more important of the two structures of polyvinylcyclopropane is based on the data given in Table III. They represent the spots of major intensity on both the equator and that layer which in this arrangement corresponds to one turn of the helix. A detailed study of the photographs and measurement of the individual layers (Table IV) reveals that the bunching together of some of the layers is due to the fact that the pitch of

TABLE II
Polyvinylcyclopropane II (Tetragonal)

Observed data				Calcd from a^*_{avg}
Layer	Intensity	ξ	*hkl*	
Equator	vs	0.204	200	0.203
	m	0.286	220	0.287
	s	0.457	240	0.454
	vw	0.572	440	0.574
	vw	0.600	hex.? 600?	0.608
	vw	0.821	800	0.810
1st	w	0.220	211	0.227
	m+	0.369	321	0.366
	w	0.422	411	0.418
2nd	w	merid.	002	—
	vvw	0.204	202	0.203
	w	0.288	222	0.287
	w+	0.321	312	0.321
	vvw	0.358?	?	—
	vvw	0.405?	402	0.405
3rd	vvs dbl.	0.227	213	0.227
	w	0.454	hex.? 423?	0.454
	vw	0.605	hex.? 613	0.608
	w	0.680	633	0.680
4th	s	0.145	114	0.144
	s	0.202	204	0.203
6th	w	0.143	116	0.144
7th	w	0.227	217	0.227
9th	w	merid.?		?
10th	vw	merid.	00,10	—

the helices in the two structures in not quite the same. Thus, the 3rd and 4th, and 6th and 7th, and the 9th and 10th layers of the tetragonal structure straddle the 1st, 2nd and 3rd layers, repectively, of the major structure. This is quite apparent from cylindrical photographs (see Figs. 2 and 3).

This major structure crystallizes in the hexagonal system and when indexed has the axes: $a = 13.6$ Å; $c = 6.48$ Å. The helix type is 3_1; there are three helices or nine monomer units per unit cell. The arrangement must be quite similar to the one reported by Natta[10] for *tert*-butyl acrylate and also found for one of the structures of polyallylcyclohexane.[3]* The calculated density is $\rho(\text{calc}) = 0.9805$ g/cm^3 which checks the observed value $\rho(\text{obs}) = 0.975$ g/cm^3 (density-gradient method). The monomer repeat distance in the axis direction is $6.48/3 = 2.16$ Å.

The helix should, therefore, be quite similar to that of other isotactic polymers with 3_1 helices such as polypropylene, polystyrene, etc.

---

* The presence of only three helices per unit cell could indicate that on crystallization a separation into crystallites containing either right- or left-handed helices takes place; thus space groups $P3_1$ and $P3_2$ are possible. The three monomer units of each helix cannot be in completely equivalent positions, since the requirements for $R\bar{3}$, all (hkl) absent for $(h - k + l \neq 3n)$, is not fulfilled.

TABLE III
Polyvinylcyclopropane I (Hexagonal)

Observed data				Calcd from
Layer	Intensity	ξ	hkl	$d^*_{100\ \mathrm{avg}}$
Equator	vs	0.227	110	0.227
	m	0.350	210	0.346
	s	0.395	300	0.393
	s	0.457	220	0.453
	vw	0.600	410	0.600
	vw	0.821	520	0.816
1st	m	0.127	101	0.131
	vvs dbl.	0.227	111	0.227
	w	0.263	201	0.262
	m	0.348	211	0.346
	vw?	0.393?	301?	0.393
	w	0.454	221	0.453
	w?	0.560	321	0.570
	vw	0.605	411	0.599
	w	0.680	331?	0.680
2nd	m	merid.	002	—
		or 0.130	102	0.131
	w	0.225	112	0.227
3rd	w	merid.	003	—

TABLE IV
Layer Line Spacings for Polyvinylcyclopropane I and II

Intensity	ζ	00l (tetragonal)[a]	00l (hexagonal)[b]
m	0.070	001	
w	0.161	002	
m+	0.222[c]	003	
vs	0.241		001
s	0.288	004	
m−	0.446	006	
m	0.479		002
m−	0.514	007	
w	0.678	009	
m	0.699		003
w	0.727	00,10	

[a] c^* (tetrag.) = 0.0740; c_t = 20.85 Å.

[b] c^* (hexag.) = 0.238; c_h = 6.48 Å.

[c] 003 (tetragonal) is calculated from average of tetragonal layer spacings.

In previous comparisons[3] it had been established that the space requirements of the substituting group determine the pitch of a helix. The cyclopropane group is relatively small and requires less space than the isopropyl group in poly-3-methylbutene. The latter provides for this space by a 4_1 helix. 1-Butene is also most stable in a 3_1 helical arrangement, though other more expanded helical structures have been found.[11,12] The fact that polyvinylcyclopropane crystallizes in both the 3_1 and 10_3 helical arrangement suggests that the space requirements of the cyclopropyl group can barely be accommodated in a 3_1 type of arrangement and that a slight expansion of the helical diameters and a change of pitch (possibly due to change in space requirements at elevated temperature) provides enough room for 10 monomer units. This change is accompanied by a very minor change in the conformation of the central C-helix and slightly reduces the length for one monomer unit in the *c*-axis direction.

On the other hand, the change from the 3_1 to the 10_3 helix destroys the exact alignment of the substitutents at 120° angles from each other and places them at directions 108° apart. However, this modification in angle between adjacent cyclopropyl groups is enough to require the packing of the helices in the much more open type of arrangement available in the tetragonal system.[3]

This paper comprises a portion of the dissertation submitted by G. Halek in partial fulfillment of the requirements for the degree of Doctor of Philosophy in the Graduate School of the Polytechnic Institute of Brooklyn.

References

1. C. G. Overberger, A. E. Borchart, and A. Katchman, *J. Polym. Sci.*, **44**, 491 (1960).
2. G. Natta, D. Sianesi, D. Morero, I. W. Bassi, and G. Caporiccio, *Atti Acad. Nazl. Lincei, Rend. Class Sci. Fis., Mat. Nat.*, [8] **28**, 551 (1960).
3. H. D. Noether, *International Symposium on Macromolecular Chemistry, Prague* 1965 (*J. Polym. Sci. C*, **16**), O. Wichterle and B. Sedláček, Eds., Interscience, New York, 1967, p. 725.
4. C. G. Overberger and G. Halek, to be published.
5. G. Natta and P. Corradini, *Nuovo Cimento* (*Suppl. 1*), **15**, 40 (1960).
6. R. G. Quynn, J. L. Riley, D. A. Young, and H. D. Noether, *J. Appl. Polym. Sci.*, **2**, 166 (1959).
7. G. Natta, *Makromol. Chem.*, **35**, 94 (1960).
8. R. L. Miller, *Polymer*, **1**, 135 (1960).
9. W. Cochran, F. M. C. Crick, and V. Vand, *Acta Cryst.*, **5**, 581 (1952).
10. G. Natta, *Makromol. Chem.*, **35**, 94 (1960).
11. A. Turner-Jones, *J. Polym. Sci. B*, **1**, 455 (1963).
12. R. L. Miller and V. F. Holland, *J. Polym. Sci. B*, **2**, 519 (1964).

Received April 21, 1968
Revised June 19, 1968

JOURNAL OF POLYMER SCIENCE: PART A-1 VOL. 7, 209-216 (1969)

Polymerization by Crystallization of Trioxane from Cyclohexane Solutions in Presence of 1,3-Dioxolane

M. BACCAREDDA, M. GIORGINI, A. LUCCHESI, F. MORELLI, and R. TARTARELLI, *Centro Nazionale di Chimica delle Macromolecole del C.N.R., Sezione VI; Istituto di Chimica Industriale ed Applicata dell'Università di Pisa, Italy*

Synopsis

Trioxane–1,3-dioxolane copolymers of high molecular weights and good thermal stability are obtained with high yields by a crystallization-polymerization method. The feed consists of concentrated solutions of trioxane in cyclohexane in the presence of dissolved 1,3-dioxolane. The 1,3-dioxolane/trioxane molar ratio in the feed lies in the range 2 to 10%. The results are compared with those obtained from isothermal copolymerizations.

Suitably high molecular weight and thermal stability are required for polyoxymethylene for practical applications. A high degree of polymerization can be achieved by purification of the monomer (mainly by removal of water, which is a strongly active chain-transfer agent[1,2]). Thermal stability can be improved either by esterifying the unstable terminal groups or by introducing into the chain a small number of C-C sequences, capable of blocking the degradation initiated at chain ends or internal points by destructive agents.

Several comonomers, including cyclic acetals, cyclic ethers, lactones, and vinyl compounds[3–14] have been proposed.

Weissermel et al.,[5] studying the trioxane–ethylene oxide system, obtained during the induction period a copolymer rich in ethylene oxide; it was postulated that this prepolymer successively reacted with growing polyoxymethylene chains by inter- or intramolecular transacetylation, giving rise to a copolymer characterized by randomly distributed C-C sequences. The transacetylation mechanism may be extended to copolymerizations with other comonomers.

Kučera and Pichler,[7,8] studying the trioxane–1,3-dioxolane system, found that 1,3-dioxolane disappeared from the monomer phase at a faster rate than trioxane and that a nearly statistical distribution of monomers in the copolymer was obtained. In addition to the above polymerization experiments carried out in bulk or in solution, a product of good thermal stability can be obtained by applying the crystallization-polymerization method to molten trioxane suspended in an inert medium in the presence of ethylene oxide.[15] The crystallization polymerization of trioxane, extensively described in previous papers,[16-21] consists in starting either from concentrated solutions or from undiluted molten monomer, initiated by a suitable catalyst, above room temperature and successively inducing crystallization of trioxane by cooling the system from the initial to room temperature. The highest conversions and molecular weights are obtained if the cooling is started at the point where a sudden temperature rise of the reaction mixture, due to an increase in polymerization rate, is observed. The most probable mechanism for this crystallization-polymerization process is the precipitation of trioxane, during the cooling stage, from the solution or from the melt on active crystalline seeds (growing chains) formed during the first stage of the reaction (between the initial temperature and the temperature of incipient precipitation). The final product is a mixture of two polymers: one, of relatively low molecular weight, formed in solution, the other, comprising most of the sample, of much higher molecular weight, obtained during the cooling. A peculiarity of this method is that higher yields and higher molecular weights are obtained, compared with conventional polymerizations initiated under the same conditions.

In the present paper, the crystallization-polymerization method is employed in order to obtain trioxane–1,3-dioxolane copolymers from concentrated solutions of trioxane in the presence of dissolved comonomer.

EXPERIMENTAL

Trioxane and 1,3-dioxolane (Schuchardt), diphenylamine, sodium acetate, and cobalt sulfate RP (Carlo Erba) were employed without purification; cyclohexane RP (Carlo Erba) was purified by the usual methods; BF_3 etherate (Eastman) was twice distilled under vacuum, the middle fraction of the second distillation being used.

Polymerization experiments were carried out in the same equipment and under the same conditions as previously described.[17] The cooling was started at the point marked by a sudden temperature rise of the reaction mixture. Initial and final temperatures were 56 and 26°C, respectively.

The final product was repeatedly washed with boiling acetone to eliminate polydioxolane which might have been present.

Inherent viscosity ($\ln \eta_{rel}/c$) measurements were made at 60°C in *p*-chlorophenol (containing 2% α-pinene) solutions and at 0.5 g/dl polymer concentration.

Thermal stability was determined in samples containing an antioxidant (diphenylamine, 2%). The antioxidant, in acetone solution, was added to the polymer in powder and the solvent was eliminated under vacuum at 60°C. The samples, 300 mg, were placed in small glass test tubes (8 mm diameter, 100 mm height) in a oven at 220°C in a nitrogen (free of oxygen) atmosphere. The test tube was hung on a scale pan. The thermally unstable fractions of the products were determined at 220°C in samples to which were added 2% diphenylamine and 0.5% sodium acetate.

Chromatographic analysis of the thermal decomposition products was carried out on samples containing 3% cobalt sulfate. After treatment with cobalt sulfate in water–acetone solutions, the samples were dried under vacuum. Experiments were made with a Carlo Erba pyrolysis unit. The degradation products were separated on a column 4 m in length and 5 mm in diameter, filled with 20% poly(ethylene glycole) supported on Teflon. Analyses were performed with a Carlo Erba, Model G. V. gas-chromatographic apparatus equipped with a flame ionization detector. The temperature of the column was set at 118°C; helium was employed as carrier gas with a flow rate of 67 ml/min. The duration of the pyrolysis was 18 sec.

RESULTS

Copolymerization experiments were performed in cyclohexane solutions (trioxane concentration = 5.3 mole/l.) with BF_3 etherate (1.5×10^{-3} mole/l.) as catalyst. 1.3-Dioxolane/trioxane molar ratios (D/T), varying from 2 to 10%, were employed in the feed.

Two sets of experiments were carried out: (I) isothermal copolymerizations at 56°C with comonomers in solution; (II) copolymerizations started at 56°C and followed by cooling at a constant rate of 30°C/hr from 56 to 26°C.

The results, obtained from copolymerizations I and II, stopped 1 hr after the increase of the reaction rate, are compared.

Yields and inherent viscosities of the products obtained from the two sets of experiments as functions of the molar ratio in the feed, D/T, are reported in Figure 1. It is clear from this figure that the crystallization-polymerization method gives higher yields and products of much higher molecular weights than the solution polymerization. For low D/T values (3–4%), yields are not much different from those obtained in the trioxane homopolymerization;[18] with further increase of D/T, the yields decrease. In copoly-

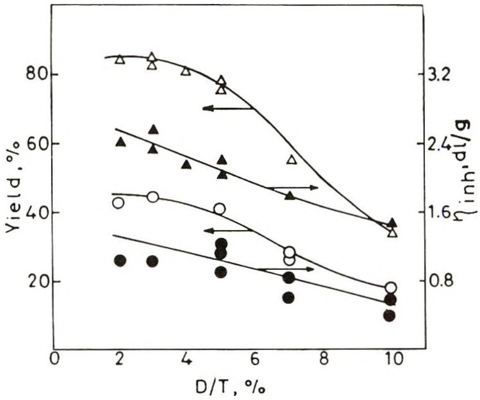

Fig. 1. Plots of (○,△) yield and (●,▲) inherent viscosity for copolymers I and II vs. 1,3-dioxolane/trioxane molar ratio, D/T in the feed: (○,●) copolymer I; (△,▲) copolymer II.

merization II, this effect can be attributed, in addition to the decrease of the polymerization rate, to the subsequent spontaneous nucleation of trioxane on crystallization from the solution.[18] By increasing the D/T ratio, copolymers with lower inherent viscosities are obtained. Crude copolymers I and II show different melting behaviors; while the melting point of copolymer I regularly decreases as D/T increases, that of copolymer II has a practically constant value, coincident with the fusion temperature of the homopolymer. A similar behavior was also previously noted in trioxane–ethylene oxide copolymer prepared by the crystallization-polymerization method (15).

Elementary analysis of the products gives qualitative evidence of the presence of 1,3-dioxolane units in the polymeric chain.

Thermal Stability

While trioxane homopolymer subjected to high temperature decomposes at a very high rate, the products obtained in the presence of 1,3-dioxolane either by the crystallization-polymerization method or by polymerization in solution, are characterized by two decomposition stages: the first at a rather high decomposition rate, the second at a much lower rate. The increase of the thermal stability of the products is due to the 1,3-dioxolane units present in the polymer backbone. Chain ends in the copolymer or homopolymer molecules are responsible for the initial high rate loss; successive decomposition at lower rate follows approximately first-order kinetics [-ln(% undecomposed polymer) = K(time)]. Values of K calculated for copolymers I and II at 220°C are reported versus D/T in Figure 2. Higher D/T molar ratios produce a better thermal stability of the products and lower the amount of unstable fractions (Fig. 3). Unstable fractions have been determined at the end of the first stage of decomposition on subjecting the sample to thermal degradation at 220°C after addition of a small quantity (0.5%) of sodium acetate.[22]

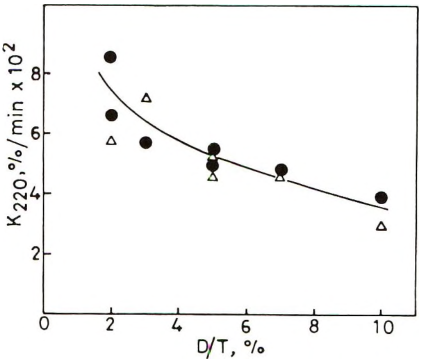

Fig. 2. Degradation rate constant K_{220}, for copolymers I and II vs. 1,3-dioxolane/trioxane molar ratio D/T in the feed: (●) copolymer I; (△) copolymer II.

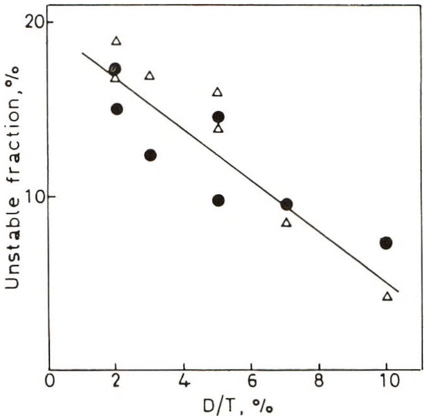

Fig. 3. Unstable fraction in copolymers I and II vs. 1,3-dioxolane/trioxane molar ratio D/T in the feed: (●) copolymer I; (△) copolymer II.

Pyrolysis

Characterization of the copolymers, in addition to the elementary analysis, has been performed by pyrolysis and gas-chromatography of the degra-

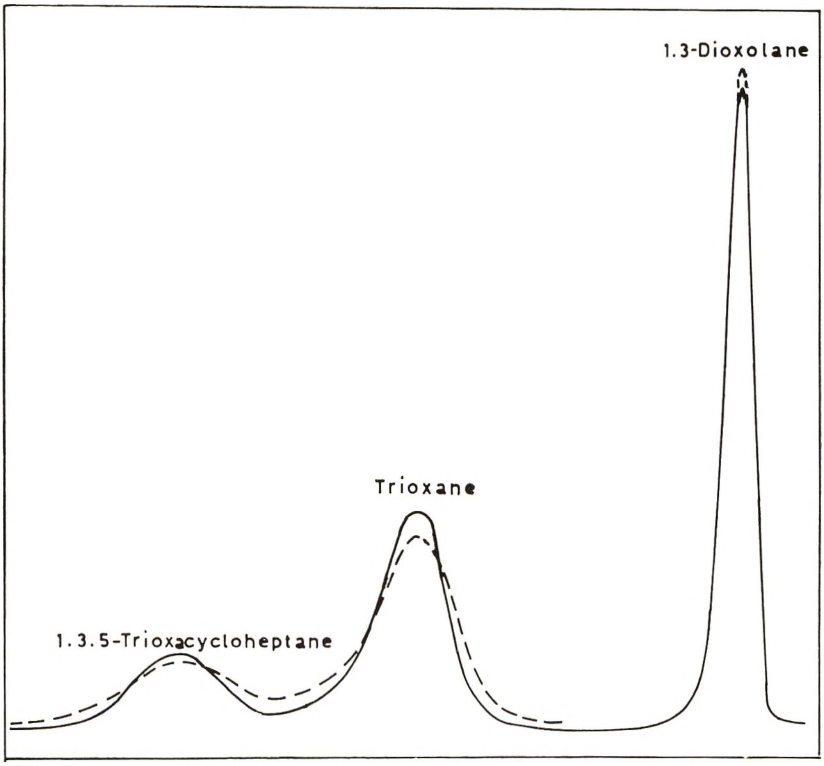

Fig. 4. Pyrograms obtained from 1.5-g samples of copolymers I and II: (——) copolymer I, D/T = 3%; (- -) copolymer II, D/T = 4%.

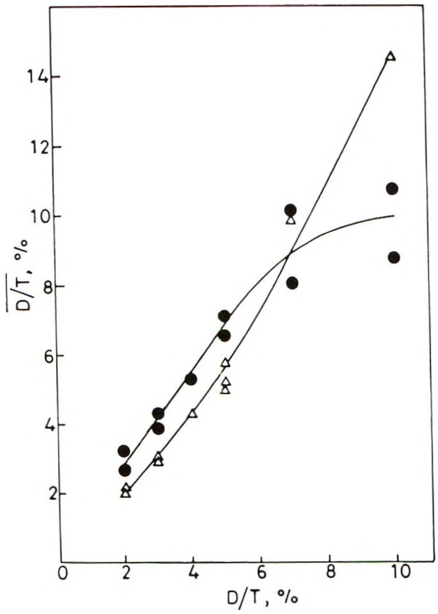

Fig. 5. 1,3-Dioxolane/trioxane molar ratio $\overline{D/T}$ in the copolymers I and II vs. molar ratio D/T in the feed: (●) copolymer I; (△) copolymer II.

dation products. Pyrolysis was carried out with an electrically heated Ni–Cr filament in the carrier gas collected with the gas-chromatographic apparatus. The identification of the degradation products was facilitated by the presence of cobalt sulfate catalyst.[23] Typical fragments of the components were identified by a flame-ionization detector; 1,3-dioxolane, trioxane, 1,3,5-trioxacycloheptane and tetraoxane were found. Figure 4 shows pyrograms obtained for copolymers I and II; peaks characteristic of tetraoxane (because of its long retention time) and of fragments formed by noncatalytic pyrolysis have not been carried in the figure. The sum of the areas of 1,3-dioxolane and 1,3,5-trioxacycloheptane (relative to 1,3-dioxolane) peaks is a linear function of the sample amount pyrolyzed in the range 0.9–2 mg and is independent of the current intensity of the filament in the range 1.3–1.7 A. Thus, the ratio between the above sum and the sample weight is a quantity which is related to the percentage of 1,3-dioxolane units present in the copolymer chain; its quantitative determination is possible by calibration against standard samples.[23]

The 1,3-dioxolane/trioxane molar ratios, $\overline{D/T}$, in the copolymers I and II, determined by gas chromatography of the degradation products, are plotted against D/T in Figure 5.

CONCLUSIONS

The method of polymerization of trioxane by crystallization from its solutions can be extended also to obtain copolymers by using mixtures of comonomers.

Copolymers of good thermal stability and high molecular weight are obtained in high yields from concentrated solutions of trioxane and 1,3-dioxolane in cyclohexane with BF_3 etherate as catalyst. In copolymerizations by crystallization, carried out with undiluted molten comonomer mixtures, the catalyst amount is very critical (a slight excess of catalyst causes an abrupt decrease of the molecular weight[19]); however in the same type of polymerization, if comonomer solutions are used, the degree of polymerization can be more easily controlled, even if relatively high contents of water are present.[20]

At a D/T value in the feed equal to 5%, at the start of precipitation a 25% yield of trioxane and 6.5% $\overline{\mathrm{D/T}}$ in the copolymer were obtained; at the end of the polymerization yields and $\overline{\mathrm{D/T}}$ values were 77% and 5.5%, respectively. From this it is quite evident that further copolymerization of 1,3-dioxolane occurs during the crystallization of trioxane.

Thus, it can be postulated that the growing chains induce polymerization of the precipitating trioxane and 1,3-dioxolane, which enters into the crystal as an impurity. Owing to the high crystallinity of the polymers obtained by crystallization,[16] the introduction of 1,3-dioxolane units into the polymeric chains by transacetalization reactions may be considered unlikely.

References

1. M. Kučera and E. Spousta, *Makromol. Chem.*, **82,** 60 (1965).
2. H. Baader, V. Jaacks, and W. Kern, *Makromol. Chem.*, **82,** 213 (1965).
3. W. Kern, H. Cherdron, V. Jaacks, H. Baader, H. Deibig, A. Giefer, L. Höhr, and A. Wildenau, *Angew. Chem.*, **73,** 177 (1961).
4. L. Höhr, H. Cherdron, and W. Kern, *Makromol. Chem.*, **52,** 59 (1962).
5. K. Weissermel, E. Fisher, K. Gutweiler, and H. D. Herman, *Kunststoffe,* **54,** 410 (1964).
6. W. Kern, *Chemiker-Ztg.*, **88,** 623 (1964).
7. M. Kučera and J. Pichler, *Polymer*, **5,** 371 (1964).
8. J. Pichler and M. Kučera, *Coll. Czechoslov. Chem. Commun.*, **30,** 991 (1965).
9. Z. Starčuk, M. Kučera, M. Cupák, and E. Hladký, paper presented at International Symposium on Macromolecular Chemistry, Prague 1965, Preprint P58.
10. S. Rösinger, H. Hermann, and K. Weissermel, paper presented at International Symposium on Macromolecular Chemistry, Prague 1965, Preprint P547.
11. W. Kern, H. Deibig, A. Giefer and V. Jaacks, *Pure Appl. Chem.*, **12,** 371 (1966).
12. V. Jaacks, *Makromol. Chem.*, **101,** 33 (1967).
13. W. Kern and V. Jaacks, *Kolloid-Z.*, **216–217,** 286 (1967).
14. T. Higashimura, A. Tanaka, T. Miki, and S. Okamura, *J. Polym. Sci. A-1,* **5,** 1927 (1967).
15. M. Baccaredda, E. Butta, F. Morelli, and G. Masetti, *Makromol. Chem.*, **93,** 137 (1966).
16. M. Baccaredda, E. Butta, P. Giusti, and F. Morelli, *Macromolecular Chemistry, Paris 1963* (*J. Polym. Sci. C*, **4**), M. Magat, Ed., Interscience, New York, 1964, p. 953.
17. F. Morelli, G. Masetti, E. Butta and M. Baccaredda, *J. Polym. Sci.*, *A*, **3,** 2441 (1965).
18. F. Morelli and R. Tartarelli, *Chim. Ind.* (Milan), **49,** 30 (1966).
19. F. Morelli, G. Masetti and R. Tartarelli, *Chim. Ind.* (Milan), **49,** 1037 (1967).
20. F. Morelli and R. Tartarelli, *Chim. Ind.* (Milan), **50,** 547 (1968).

21. F. Morelli, G. Verri, and R. Tartarelli, *Chim. Ind.* (*Milan*), in press.
22. I. Mejzlík and J. Pác, *Makromol. Chem.*, **82**, 226 (1965).
23. K. H. Burg, E. Fisher and K. Weissermel, *Makromol. Chem.*, **103**, 268 (1967).

Received June 19, 1968

JOURNAL OF POLYMER SCIENCE: PART A-1 VOL. 7, 217-235 (1969)

Effect of a Trifluoromethyl Group on the Polymerizability of α-Olefins by Transition Metal Catalysts

C. G. OVERBERGER* and G. KHATTAB, *Department of Chemistry, Institute of Polymer Research, Polytechnic Institute of Brooklyn, Brooklyn, New York 11201*

Synopsis

Several α-olefins containing the trifluoromethyl group were prepared and characterized. 4,4,4-Trifluoro-1-butene, 3-trifluoromethyl-1-butene, 5,5,5-trifluoro-1-pentene, and 4-trifluoromethyl-1-pentene were homopolymerized with VCl_3–$Al(i\text{-}Bu)_3$ catalyst. The trifluorobutenes gave low-melting polymers with low fluorine contents. Polymers obtained from the trifluoropentenes were soluble having moderately high intrinsic viscosities. Copolymerizations of these monomers with their nonfluorinated homologs by the same catalyst system indicated low reactivities of the fluoromonomers. Nuclear magnetic resonance spectra of the fluorinated and nonfluorinated monomers and their respective spectroscopic studies with the catalyst $(C_5H_5)_2TiCl_2$–$Al(CH_3)_3$ indicated an electron deficiency of the vinyl group of the fluorobutenes. This was related to the inductive effect of the trifluoromethyl group. The inductive effect of this group was absent in the fluoropentenes and the nonfluorinated monomers. The electron-deficient vinyl group of the fluorobutenes apparently did not allow these monomers to coordinate with the active sites of the catalyst. Polymerization studies of the nonfluorinated monomers, 1-butene, 3-methyl-1-butene, 1-pentane, and 4-methyl-1-pentene, with the catalyst VCl_3–$Al(Bu)_3$, were performed in the presence of compounds containing the trifluoromethyl group. Results indicated that this group did not retard the rate of polymerization of these monomers. Evidence is presented to show that a catalytic amount of benzotrifluoride enhanced the rate of polymerization of α-olefins, particularly that of sterically hindered monomers such as 3-methyl-1-butene.

INTRODUCTION

The mechanism of polymerization of α-olefins by transition metal catalyst systems has attracted the attention of many investigators.[1–12] Comprehensive reviews of the subject have recently appeared.[13,14]

In general there is agreement that a coordination process between the α-olefin and the *d*-orbitals of the transition metal is a primary step in most of these types of polymerization. However, differences in the nature of this coordination are not completely resolved. The use of fluoroolefins to test this generality seemed appropriate, since the carbon–fluorine dipole withdraws electrons from the double bond and should prevent the coordina-

---

* Present address: Department of Chemistry, The University of Michigan, Ann Arbor, Michigan 48104.

tion step. In addition, the question of whether fluorocarbons would react as other carbon–halogen bonds are reported to do or coordinate with transition metal systems via the fluorine electrons, and thus function as a catalyst inhibitor, had not been satisfactorily answered.

Accordingly, the syntheses of fluoroolefins was projected in such a way as to systematically remove the carbon–fluorine dipole from the double bond.

α-Olefins containing the trifluoromethyl group have previously been prepared and described.[15] Monomers containing fluorine atoms or a trifluoromethyl group attached directly to the double bond failed to polymerize with transition metal catalysts. When the trifluoromethyl group was insulated from the vinyl double bond by one or more methylene groups, alleged polymers resulted upon treatment of the monomer with a VCl_3–$Al(i\text{-}Bu)_3$ catalyst. However, these polymers were obtained only in low yield and as insoluble, noncharacterizable materials.

In this paper we describe improvements in the preparations of 4,4,4-trifluoro-1-butene, 3-trifluoromethyl-1-butene, 5,5,5-trifluoro-1-pentene, and 4-trifluoromethyl-1-pentene, as well as a study of their polymerizabilities to test the above proposals.

EXPERIMENTAL

All melting and boiling points are uncorrected. The analyses were done at the laboratories of Schwarzkopf, N.Y., and at the laboratories of Alfred Bernhardt, Mülheim, West Germany.

Materials

4,4,4-Trifluorobutyl Acetate. A solution of 33.8 g (0.36 mole) of *N*,*N*-dimethylaniline (44.8 g, 0.35 mole) of 4,4,4-trifluoro-1-butanol (prepared according to the procedure of Walborsky et al.[16]), and approximately 100 ml of anhydrous ether was prepared. It was heated to reflux and 27.5 g (0.35 mole) of acetyl chloride was added at a rate such that the reaction mixture refluxed without external heating. The mixture was cooled to room temperature, and 100 ml of water was added to dissolve dimethylaniline hydrochloride. The ether solution was washed with water and dried over anhydrous magnesium sulfate. Ether was removed by distillation and the product was purified by two distillations at atmospheric pressure yielding 36.7 g (83.3%) of 4,4,4-trifluorobutylacetate, bp 138°C, n_D^{25} 1.3559 (bp 141°C, n_D^{25} 1.3590 prepared by a different acetylation procedure.[15]

ANAL. Calcd for $C_6H_9F_3O_2$: C, 42.36%; H, 5.29%; F, 33.53%. Found: C. 42.42%; H, 5.44%; F, 33.74%.

4,4,4-Trifluoro-1-butene. 4,4,4-Trifluoro-1-butene was obtained by pyrolyzing the acetate according to the procedure of Overberger and Davidson.[15]

1-Chloro-3-trifluoromethylbutane. The general procedure of Bunnett was employed.[17] To a mixture of 130.5 g (0.9 mole) of 3-trifluoro-1-

butanol and 121 g (1.0 mole) of *N*,*N*-dimethylaniline was added dropwise 118 g (1.0 mole) of thionyl chloride at a rate such that the temperature of the mixture was maintained between 35–55°C. 1-Chloro-3-trifluoromethylbutane (113 g, 70.3%) was obtained, bp 103°C, n_D^{25} 1.3632.

ANAL. Calcd for $C_5H_8F_3Cl$: C, 37.40%; H, 5.02%; F, 35.49%; Cl, 22.08% Found: C, 37.45%; H, 5.06%; F, 35.67%; Cl, 22.06%.

4-Trifluoromethyl-1-pentanol. 1-Chloro-3-trifluoromethylbutane (106.5 g, 1.0 mole) was allowed to react with 26.7 g (1.1 g-at) of magnesium in 500 ml of anhydrous ether. Paraformaldehyde (50 g, 1.66 mole), which was dried previously for 2 days over phosphorus pentoxide in a vacuum desiccator, was depolymerized by heating in an oil bath at 180–200°C and was passed into the Grignard reagent with the aid of a slow stream of dry nitrogen according to the procedure of Gilman.[18] 4-Trifluoromethyl-1-pentanol (103.9 g, 66.4%) was obtained, bp 158–159°C, n_D^{25} 1.3717.

ANAL. Calcd for $C_6H_{11}F_3O$: C, 46.15%; H, 7.10%; F, 36.50%. Found: C, 45.90%; H, 7.42%; F, 36.27%.

4-(Trifluoromethyl)pentyl Acetate. 4-Trifluoromethyl-1-pentanol (101.5 g, 0.65 mole) was dissolved in 150 ml of anhydrous ether and to the resulting solution was added 84.7 g (0.7 mole) of *N*,*N*-dimethylaniline. Acetyl chloride (54.9 g, 0.7 mole) was added, and the product was worked up according to Hauser.[19] 4-(Trifluoromethyl)pentyl acetate, 114.4 g (89.2%) was obtained, bp 171–174°, n_D^{25} 1.3756.

ANAL. Calcd for $C_8H_{13}F_3O_2$: C, 48.48%; H, 6.61%; F, 28.76%. Found: C, 48.43%; H, 6.70%; F, 28.91%.

4-Trifluoromethyl-1-pentene. The procedure of Overberger and Davidson[15] was employed. 4-(Trifluoromethyl)pentyl acetate, 114 g (0.57 mole) was pyrolyzed at 5.25 ± 10°C under dry nitrogen introduced into the system at a slow rate. 4-Trifluoromethyl-1-pentene (40.2 g, 50.4%) was obtained, bp 63°C, n_D^{25} 1.3410. The product was found to be pure when examined on silver nitrate and polyglycol columns of a Perkin-Elmer Model 154D Vapor Fractometer (bp 55–56°C, n_D^{25} 1.3403 by the synthesis of Boord[15]).

ANAL. Calcd for $C_6H_9F_3$: C, 52.17%; H, 6.57%; F, 41.26%. Found: C, 52.05%; H, 6.68%; F, 41.17%.

1-Chloro-4,4,4-trifluorobutane. Thionyl chloride (82.6 g, 0.7 mole) was allowed to react with a mixture of 80 g (0.62 mole) of 4,4,4-trifluoro-1-butanol and 84.6 g (0.7 mole) of *N*,*N*-dimethylaniline, following the procedure of Bunnett.[17] 1-Chloro-4,4,4-trifluorobutane (70.5 g, 76.9%) was obtained, bp 85°C, n_D^{20} 1.3510 (bp 86.6°C, n_D^{20} 1.3505 by chlorination of 1,1,1-trifluorobutane)[20].

ANAL. Calcd for $C_4H_6F_3Cl$: C, 32.78%; H, 4.13%; F, 38.89%; Cl, 24.19%. Found: C, 32.95%; H, 4.11%; F, 38.87%; Cl, 24.11%.

5,5,5-Trifluoro-1-pentanol. 1-Chloro-4,4,4-trifluorobutane, (75.3 g, 0.51 mole) was reacted with 14.0 g (0.6 g-atm) of magnesium turnings in approximately 500 ml of ether. Paraformaldehyde (24.0 g, 0.8 mole), which had been dried previously for 2 days over phosphorus pentoxide in a vacuum desiccator, was depolymerized by heating in an oil bath and led into contact with the solution containing the Grignard reagent with the aid of a current of dry nitrogen. The reaction mixture was allowed to cool to room temperature, and 300 g of crushed ice was added all at once. A sufficient amount of 30% sulfuric acid was then added to dissolve the magnesium hydroxide, and the mixture was steam-distilled. The distillate was saturated with sodium chloride and the ether layer was separated. The ether solution was dried over anhydrous magnesium sulfate, filtered and the ether was distilled. The product was purified by distillation at atmospheric pressure yielding 53.7 g (72.7%) of 5,5,5-trifluoro-1-pentanol, bp 146°C, n_D^{20} 1.3596.

ANAL. Calcd for $C_5H_9F_3O$: C, 42.25%; H, 6.31%; F, 40.10%. Found: C 42.47%; H, 6.59%; F, 40.09%.

5,5,5-Trifluoropentyl Acetate. The general procedure of Hauser et al. for the preparation of acetate esters was employed.[19] 5,5,5-Trifluoro-1-pentanol (64 g, 0.45 mole), was dissolved in 150 ml of anhydrous ether and to the resulting solution was added 66.6 g (0.55 mole) of *N*,*N*-dimethylaniline. The mixture was heated to reflux, the external heat source was removed, and acetyl chloride (43.2 g, 0.55 mole), was added at a rate such that the ether refluxed gently. 5,5,5-Trifluoropentyl acetate (69.5 g, 84%) was obtained, bp 161–162°C, n_D^{20} 1.3674.

ANAL. Calcd for $C_7H_{11}F_3O_2$: C, 45.65%; H, 6.02%; F, 30.95%. Found: C, 45.80%; H, 6.19%; F, 30.85%.

5,5,5-Trifluoro-1-pentene. The general method for the pyrolysis of esters was used.[15] 5,5,5-Trifluoropentyl acetate (66.3 g, 0.36 mole) was pyrolyzed at 520 ± 10°C under a current of dry nitrogen. 5,5,5-Trifluoro-1-pentene (22.9 g, 51.2%), was obtained, bp 40°C, n_D^{25} 1.3232. This was found pure by injection on silver nitrate and polyglycol columns of a Perkin-Elmer Model 154D Vapor Fractometer (bp 39–40°C, n_D^{25} 1.3230 by Boord olefin synthesis[15]).

ANAL. Calcd for $C_5H_7F_3$: C, 48.39%; H, 5.70%; F, 45.92%. Found: C, 48.63%; H, 5.92%; F, 45.53%.

Polymerization

A high-pressure 40-ml capacity glass tube, to which was attached a device carrying two stainless steel valves and a Quick Connect connection (Fig. 1), was used for all polymerization reactions. This system was tested and found to withstand 400 psi or 2×10^{-2} mm at room temperature. The system was charged with materials as follows.

A known weight of the solid part of the catalyst, VCl_3, $TiCl_3$, etc., was transferred into the glass tube. It was screwed into the steel regulators and cooled in a Dry Ice–acetone mixture. Through the Quick Connect with the lower valve opened, the tube was evacuated to 2×10^{-2} mm pressure. The valve was closed and the evacuating tube was disconnected. The system was flushed with prepurified, dried nitrogen through the Quick Connect by opening the lower valve. This process of evacuation and flushing was repeated twice. A self-sealing serum cap was then inserted on the outer end of the upper valve. Monomers were injected by means of a hypodermic syringe having a long needle which was inserted into the serum cap and through the opened valves. Similarly, a known volume of the standard aluminum alkyl solution was introduced. Finally, the required amount of the solvent was added. The valves were closed and the serum cap was removed. The contents of the tube were frozen by immersing it in liquid nitrogen, evacuated to 2×10^{-2} mm, as described earlier, and thawed. It was immersed again in liquid nitrogen and flushed with nitrogen. The degassing process was repeated twice, after which the tube was warmed to room temperature. Polymerization was effected by heating the tube in a constant-temperature oil bath with rocking for the desired period of time at the chosen temperature. The tube was cooled in a Dry Ice–acetone bath, the valves were opened, and the regulating device was disconnected from the glass tube. The contents of the tube were added to 200 ml of a stirred

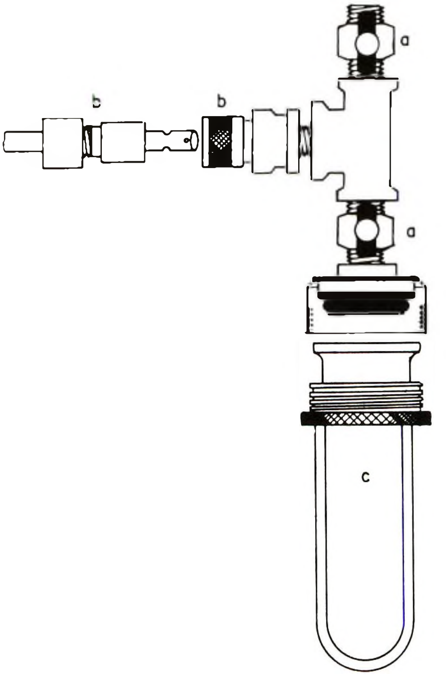

Fig. 1. Polymerization apparatus: (*a*) valves; (*b*) Quick-connect; (*c*) polymerization tube.

10% solution of hydrochloric acid in methanol. When all the catalyst had dissolved, the methanol-insoluble polymer was filtered and dissolved, whenever possible, in an appropriate solvent and precipitated into methanol. It was filtered in a tared sintered-glass funnel, washed with methanol thoroughly, dried in a vacuum oven at 100°C and a pressure of 100 mm, and the weight of dry polymer was determined.

Special procedures were developed for handling the gaseous monomers. 1-Butene and 4,4,4-trifluoro-1-butene, being gases at room temperature, were withdrawn from their reservoirs by means of a calibrated 0.5-liter capacity gas syringe. The polymerization tube, while immersed in a Dry Ice–acetone mixture, was partially evacuated. Through a serum cap, a known volume of the gaseous monomer was condensed into the tube and the resultant pressure difference was equalized with nitrogen.

Melting point ranges of the fluorinated polymers were determined on a Kofler hot-stage polarizing microscope. Those of the nonfluorinated polymers were determined on a Fisher-Johns hot-stage melting point apparatus.

Spectroscopic Studies of the Coordination between the Soluble Catalyst and the Monomers

The possibilities of coordination between the homogeneous catalyst $(C_5H_5)_2$ $TiCl_2$–$Al(CH_3)_3$ and the fluorinated and nonfluorinated monomers were studied on a Perkin-Elmer Model 202 Ultraviolet–Visible spectrophotometer. Quartz reaction and reference cells of 1 cm path length were used. The catalyst solution was prepared at room temperature using the following concentrations: $[(C_5H_5)_2TiCl_2]$ = 0.25 mmole in 25 ml of benzene; $[Al(CH_3)_3]$ = 1.15 mmoles in 25 ml of benzene.

The catalyst solution was prepared according to the polymerization scheme previously described. The reaction cell was stoppered with a serum cap of a proper size thereby rendering it air-tight. It was rinsed three times with the catalyst solution and finally filled to four-fifths of its capacity. Monomer was injected into the cell by means of a hypodermic syringe. The spectra were obtained in the range 390–750 mμ in a scanning time of about 1 min.

Nuclear Magnetic Resonance (NMR) Spectra of the Monomers

All data were obtained using a Varian Model-60 HR NMR spectrometer for 50% solutions of monomer in spectrograde carbon tetrachloride. Tetramethylsilane was used as an internal reference at 25°C.

RESULTS AND DISCUSSION

Homopolymerization reactions of the fluoromonomers with a variety of catalysts are summarized in Table I. Under the same polymerization conditions, the trifluorobutenes were reluctant to polymerize, while the trifluoropentenes gave polymers of relatively high viscosities and melting

TABLE I. Homopolymerization Reactions of the Fluoromonomers[a]

No.	Monomer	Amt. monomer, mmole	MX_n	AlR_3	Time, hr	Temp, °C	Conversion, %
1	4,4,4-Trifluoro-1-butene	10	VCl_3	$Al(i\text{-}Bu)_3$	72	70	1.0[b]
2	3-Trifluoromethyl-1-butene	10	"	"	72	70	1.0
3	4-Trifluoromethyl-1-pentene	10	"	"	72	70	37.0[c]
4	5,5,5-Trifluoro-1-pentene	10	"	"	72	70	61.0[d]
5	4,4,4-Trifluoro-1-butene	12	"	$AlEt_2Cl$	48	90	Trace
6	3-Trifluoromethyl-1-butene	11.3	"	"	48	90	Trace
7	3-Trifluoromethyl-1-butene	9	TiF_3	$Al(i\text{-}Bu)_3$	48	70	0.0[e]
8	4-Trifluoromethyl-1-pentene	8	"	"	48	70	0.0[e]
9	3-Trifluoromethyl-1-butene	9	$TiCl_3$	"	72	70	0.0[f]
10	4-Trifluoromethyl-1-pentene	8	"	"	72	70	0.0[f]
11	4,4,4-Trifluoro-1-butene	10	$TiCl_3A,A$	$AlEt_2Cl$	48	70	Trace
12	3-Trifluoromethyl-1-butene	10	"	"	48	70	Trace
13	4-Trifluoromethyl-1-pentene	10	"	"	48	70	10.0[g]
14	5,5,5-Trifluoro-1-pentene	10	"	"	48	70	49.0[h]
15	4,4,4-Trifluoro-1-butene	10	VAc[i]	"	72	70	0.0
16	3-Trifluoromethyl-1-butene	10	"	"	72	70	0.0
17	4-Trifluoromethyl-1-pentene	8	"	"	72	70	0.0
18	5,5,5-Trifluoro-1-pentene	5	"	"	72	70	0.0
19	4,4,4-Trifluoro-1-butene	10	$NbCl_5$	$Al(i\text{-}Bu)_3$	96	70	0.0
20	3-Trifluoromethyl-1-butene	10	"	"	96	70	0.0
21	4,4,4-Trifluoro-1-butene	10	$ZrCl_4$	"	96	70	0.0
22	3-Trifluoromethyl-1-butene	10	"	"	96	70	0.0

[a] Unless otherwise specified, the following conditions were applied: MX_n = 1 mmole; AlR_3 = 2.5 mmole; solvent = n-heptane, 4 ml.

[b] Low melting polymer (110–120°C). ANAL. Calcd for $(C_4H_5F_3)_n$: C, 43.64%; H, 4.58%; F, 51.77%. Found: C, 64.01%; H, 9.40%; F, 27.09%.

[c] Mp 260°C, has a very limited solubility (approximately 0.01 g/100 ml of hexamethylphosphoramide or perfluorokerosene at 130°C.). ANAL. Calcd for $(C_6H_9F_3)_n$: C, 52.17%; H, 6.57%; F, 41.26%. Found: C, 52.31%; H, 6.68%; F, 41.08%.

[d] Mp 225°C, $[\eta]$ = 0.684 in hexamethylphosphoramide at 25°C. ANAL. Calcd for $(C_5H_7F_3)_n$: C, 48.39%; H, 5.70%; F, 45.92%. Found: C, 48.22%; H, 6.34%; F, 45.53%.

[e] Pyridine was added in a 1:1 mole ratio to Ti. [f] Pyridine was added in a 1:1 mole ratio to Ti. $TiCl_3$ = 0.5 mole; $AlEt_2Cl$ = 1.25 mmole.

[g] This polymer is slightly colored, mp 132–7°C; it resembles run 3 in being sparingly soluble.

[h] Mp = 162–168°C, $[\eta]$ = 0.585 in hexamethylphosphoramide at 25°C. [i] VAc is vanadium triacetylacetonate.

points (runs 1–4, 11–14). Poly-4-trifluoromethyl-1-pentene, obtained in run 3, has a higher melting point and limited solubility compared to poly-5,5,5-trifluoro-1-pentene, obtained in runs 4 and 14. Determination of the intrinsic viscosity of poly-4-trifluoromethyl-1-pentene was not possible because of the limited solubility of this polymer; those of poly-5,5,5-trifluoro-1-pentenes, prepared with different catalysts, were determined in hexamethylphosphoramide. Poly-5,5,5-trifluoro-1-pentene obtained from VCl_3–$Al(i\text{-}Bu)_3$ has a higher molecular weight (intrinsic viscosity of 0.684) than that obtained from $TiCl_3$–$AlEt_2Cl$ (intrinsic viscosity of 0.585). In actuality, the intrinsic viscosity graphs for polymers prepared from these catalysts showed a difference in the slopes of the plots of reduced viscosity versus concentration, the polymer prepared by the former catalyst showing a greater slope. This behavior has not been investigated further, but could possibly be accounted for by the different degrees of tacticities of the polymers.

The trifluorobutenes could not be polymerized to high molecular weight, soluble polymers. The analysis of poly-4,4,4-trifluoro-1-butene (run 1, Table I) indicates the presence of one fluorine atom per monomer unit. Since this polymer was practically insoluble in a variety of solvents, the probability exists that it had crosslinked through the pendent functional groups.

A similar decrease in the fluorine contents of polymers containing the trifluoromethyl group, but to a lesser degree, has been previously reported.[15] These polymers, namely, poly-4,4,4-trifluoro-1-butene, poly-3-trifluoromethyl-1-butene, poly-5,5,5-trifluoro-1-pentene, and poly-4-trifluoromethyl-1-pentene, were insoluble in a variety of solvents. In the present work, the polytrifluoropentenes were found soluble in hexamethylphosphoramide. Table I shows that only two catalysts were effective in polymerizing the fluoropentenes. These were VCl_3–$Al(i\text{-}Bu)_3$ and $TiCl_3$–$Al(C_2H_5)_2Cl$. The former catalyst polymerized 5,5,5-trifluoro-1-pentene to a polymer of a higher melting point and intrinsic viscosity than did $TiCl_3$–$Al(C_2H_5)_2Cl$. Also, poly-4-trifluoromethyl-1-pentene, prepared with the vanadium catalyst, had a much higher melting point than that prepared with the titanium catalyst. In fact, among a number of catalysts employed, VCl_3–$Al(i\text{-}Bu)_3$ was reported the only effective catalyst for the polymerization of these fluoromonomers.[15]

The reluctance of the trifluorobutene monomers to polymerize was further confirmed by copolymerizing these monomers with their nonfluorinated homologs. Table II summarizes the results of these reactions which were carried out under the same conditions, i.e., time, temperature, and monomer and catalyst concentrations. There is a common feature in these results, namely, that the per cent conversions to polymers decrease with increase of mole fraction of the fluoromonomers in the feed, while their fluorine contents rise.

The quantitative determination of monomer reactivity ratios in heterogeneous transition metal catalyst systems in not possible due to diffusion

TABLE II

Copolymerization Reactions of the Fluorinated and Nonfluorinated Monomers with VCl_3–$Al(i\text{-}Bu)_3$ in *n*-Heptane for 8 Hr[a]

			Conversion, %[b]				
Run no.	X_H	X_F	A, a[c]	B, d[d]	B, b[e]	C, c[f]	D, d[g]
1	0.2	0.8	2.5	0.9	0.2	11.4	3.0
2	0.4	0.6	7.0	5.7	0.6	14.0	6.7
3	0.6	0.4	17.6	26.3	19.9	49.0	7.6
4	0.8	0.2	32.0	38.6	35.3	47.0	16.4

[a] Conditions: total monomer = 20 mmole; *n*-heptane = 4 ml; VCl_3 = 1 mmole; $Al(i\text{-}Bu)_3$ = 2.5 mmole; 70°C; 1 hr.

[b] Monomers: A = $CF_3CH_2CH{=}CH_2$; a = $CH_3CH_2CH{=}CH_2$; B = $CF_3CH(CH_3)$$-CH{=}CH_2$; b = $CH_3CH(CH_3)CH{=}CH_2$; C = $CF_3CH(CH_3)CH_2CH{=}CH_2$; c = $CH_3CH(CH_3)CH_2CH{=}CH_2$; D = $CF_3CH_2CH_2CH{=}CH_2$; d = $CH_3CH_2CH_2CH{=}CH_2$.

[c] ANAL. Run 1: C, 76.21%; H, 12.24%; F, 11.55%. Run 2: C, 81.75%; H, 13.58%; F, 4.55%. Run 3: C, 83.57%; H, 14.01%; F, 2.73%. Run 4: C, 83.59%; H, 13.83%; F, 2.70%.

[d] ANAL. Run 1: C, 83.42%; H, 13.71%; F, 2.95%. Run 2: C, 86.04%; H, 14.21%; F, 0.00%. Run 3: C, 85.91%; H, 14.34%; F, 0.00%. Run 4: C, 86.01%; H, 14.22%; F, 0.00%.

[e] Analyses for these polymers are not available.

[f] ANAL. Run 1: C, 62.75%; H, 8.89%; F, 28.35%. Run 2: C, 69.32%; H, 10.88%; F, 19.75%. Run 3: C, 74.09%; H, 11.77%; F, 14.11%. Run 4: C, 79.55%; H, 12.90%; F, 7.63%.

[g] ANAL. Run 1: C, 59.85%; H, 8.80%; F, 32.41%. Run 2: C, 66.80%; H, 9.81%; F, 22.94%. Run 3: C, 72.34%; H, 11.26%; F, 16.98%.

problems. Qualitatively, however, the homopolymerization and copolymerization data revealed that the trifluorobutenes are less reactive toward the heterogeneous Ziegler-type catalysis than are the trifluoropentenes. Furthermore, all fluoromonomers are less reactive than the corresponding nonfluorinated monomers. The following possibilities may be considered to explain these results: (*1*) low electron density in the double bond of the fluoromonomers (because of the inductive effect of the polar group) decreases the tendency of these monomers to coordinate with the catalyst, or (*2*) strong tendency of the fluoromonomers to coordinate with the catalyst not only via double bond, but also via the trifluoromethyl group. The effect of such coordination may deactivate the active sites of the catalyst.[23]

Nuclear magnetic resonance spectra of 4,4,4-trifluoro-1-butene and of 3-trifluoromethyl-1-butene indicate that the spectra of protons (b) and (c) were shifted to a lower field by approximately 0.25τ, compared to the spectra of the nonfluorinated homologs (Figs. 2 and 3). Those of proton (a) remained unchanged. Such a behavior could result from the inductive effect of the polar group along the chain. A strong inductive effect would most probably deshield protons (b) and (c) by decreasing the electron density in the double bond. Proton (a) was unaffected probably because the loss of electrons from the vinyl group is compensated by a gain of electrons

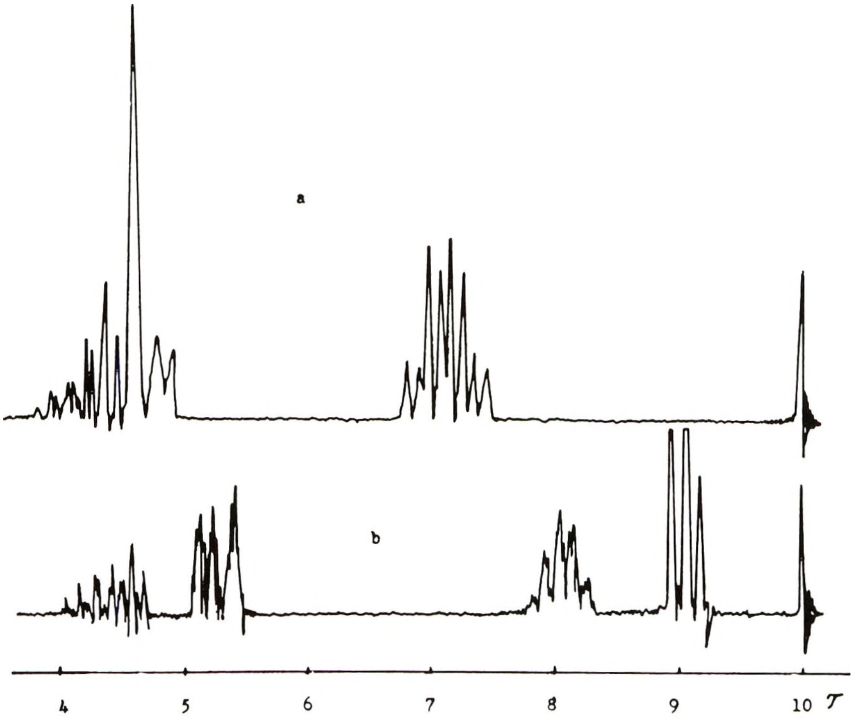

Fig. 2. NMR spectra: (*a*) 4,4,4-trifluoro-1-butene; (*b*) 1-butene.

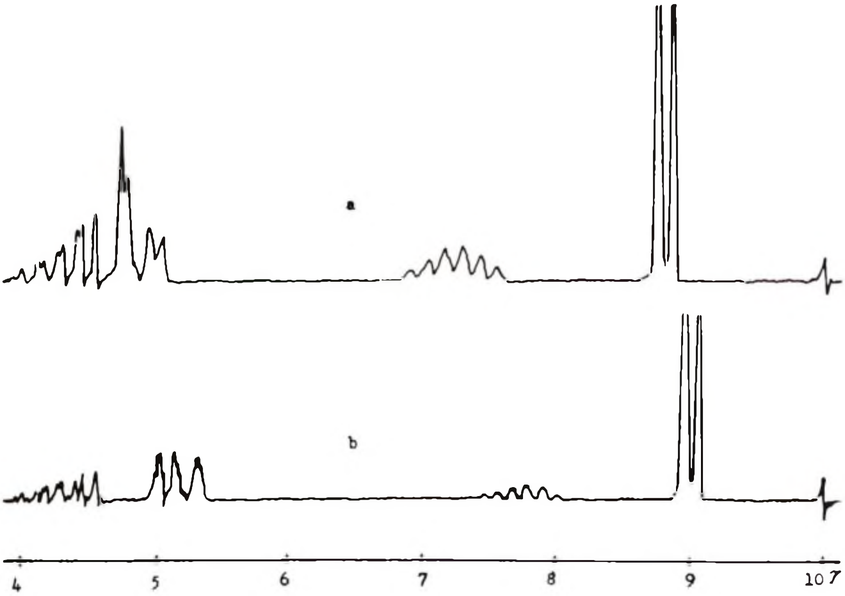

Fig. 3. NMR spectra: (*a*) 3-trifluoromethyl-1-butene; (*b*) 3-methyl-1-butene.

between carbon atoms 2 and 3. The electronic environment of proton (a) thus remained virtually unchanged.

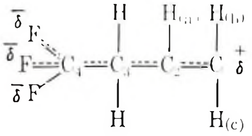

Contrary to the fluorobutenes, in the fluoropentenes all three protons of the vinyl group appeared at lower field than in the nonfluorinated monomers (Figs. 4 and 5). In this case, some cyclic interaction between the fluorine atoms and the vinyl electrons may be possible.

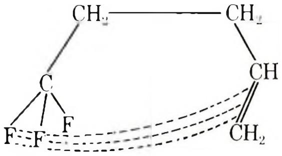

Such electronic interactions, if they exist, are relatively weak and would be diminished at the polymerization temperatures employed, thereby restoring the reactivity to the vinyl double bond. Perhaps this explains why the fluoropentenes are more reactive than the fluorobutenes. In the latter cases there is a permanent deficiency of the electron density of the vinyl

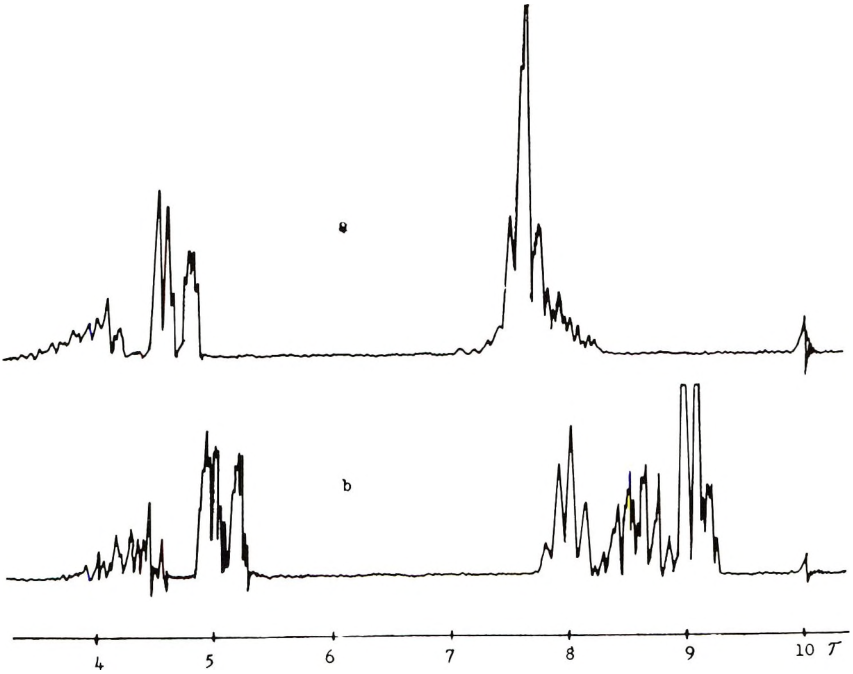

Fig. 4. NMR spectra: (*a*) 5,5,5-trifluoro-1-pentene; (*b*) 1-pentene.

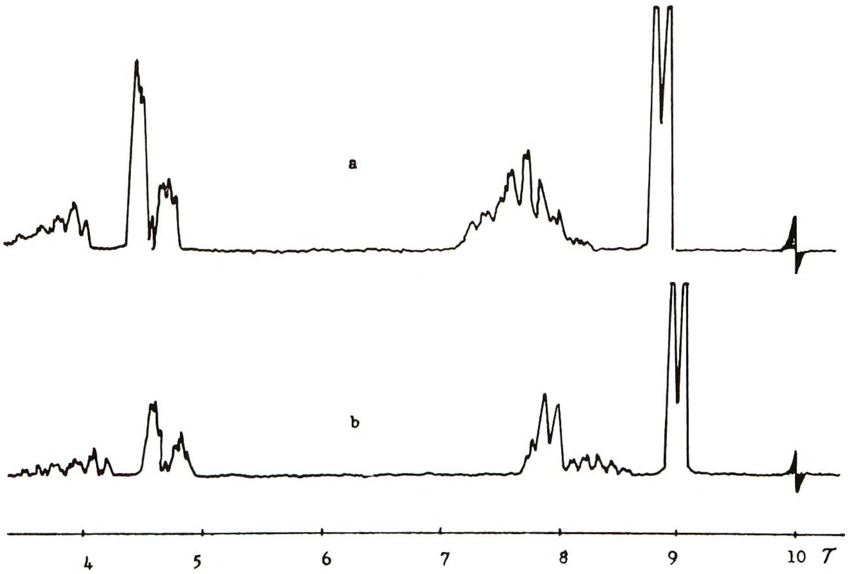

Fig. 5. NMR spectra: (*a*) 4-trifluoromethyl-1-pentene; (*b*) 4-methyl-1-pentene.

group. It is, therefore, expected that the trifluorobutenes do not coordinate (or if they do, they do so to a very small extent) with the active catalyst. This conclusion supports the suggestions of Carrick,[9] Uelzmann,[11] and Chatt[22] that coordination of the olefin with the transition metal is a primary step in the polymerization process.

Spectroscopic Studies of the Catalyst–Monomer Interactions

Dicyclopentadienyltitanium dichloride, $(C_5H_5)_2TiCl_2$, is soluble in benzene. Addition of aluminum alkyls to this compound results in the formation of a homogeneous catalyst capable of polymerizing ethylene[23] and styrene.[12] Aluminum alkyls whose alkyl groups contain β-hydrogens, such as $Al(C_2H_5)_3$ and $Al(C_2H_5)_2Cl$, can form a catalyst with $(C_5H_5)_2TiCl_2$ but undergo spontaneous decomposition into an inactive species after a short time. On the other hand, $Al(CH_3)_3$ gives stable catalysts in the absence of monomers.[24] For the purposes of this research, the system $(C_5H_5)_2TiCl_2$–$Al(CH_3)_3$ was chosen. A solution of $(C_5H_5)_2TiCl_2$ in benzene has an absorption maximum at 520 mμ. Addition of trimethylaluminum caused the absorption maximum to shift to 450 mμ.

If the electronic configuration of the ground state of this catalyst is perturbed, one would expect a shift in the wavelength of the absorption maximum (λ_{max}). A coordination process between the π-electrons of a vinyl group and the empty *d*-orbitals of the catalyst will produce a ground state with different electronic configurations. The new system should, therefore, show an absorption maximum at a different wavelength. One may conclude that a coordination process takes place between the olefin and the catalyst if a shift in the absorption maximum is observed. A series of experiments was carried out to verify which of the monomers used was capable of coordinating with the catalyst. The time required for the change in absorption maximum was 5–15 min after injecting the monomer. The change is faster for reactive monomers such as 1-butene than for monomers such as 3-methyl-1-butene. The results of these experiments are listed in Table III.

TABLE III
Absorption Maxima of the Catalyst $(C_5H_5)_2TiCl_2$–$Al(CH_3)_3$ in Presence of Monomers

Monomer	Absorption maximum, mμ
1-Butene	440
4,4,4-Trifluoro-1-butene	450
1-Pentene	435
5,5,5-Trifluoro-1-pentene	440
3-Methyl-1-butene	443
3-Trifluoromethyl-1-butene	450
4-Methyl-1-pentene	440
4-Trifluoromethyl-1-pentene	442

Unlike the rest of the monomers, which showed definite changes in the absorption maxima of the systems after adding the monomers, the trifluorobutenes did not do so. If one assumes a correlation between these changes in absorption maxima and polymerizabilities, it implies that the fluorobutenes are unable to coordinate with the catalyst, compared to the fluoropentenes and the nonfluorinated monomers. The results also seem to rule out the possibility that fluorobutene coordinates with the catalyst through the polar group as well as through the vinyl group.

Polymerization of α-Olefins in the Presence of a Trifluoromethyl Group

If the trifluoromethyl group alone deactivates the catalyst, then it should do so regardless of the nature of the compound to which it is attached. For example, monomers such as 1-butene and 1-pentene (otherwise known to polymerize by the Ziegler-type catalyst) might be less reactive toward these catalysts in the presence of compounds such as CF_3-R or CF_3-Ar. To investigate this possibility, a series of experiments was conducted to determine the polymerizability of α-olefins in the presence of CF_3 groups.

The results (Table IV) indicate that the presence of a trifluoromethyl group in the system does not deactivate the catalyst. This leaves no alternative but to conclude that the trifluoromethyl groups in the butene monomers deactivate the double bond by electron withdrawal.

A second result from Table IV was the increased conversion of monomer to polymer in the presence of an aromatic nucleus carrying a trifluoromethyl group. A trifluoroalkyl compound, with the same dipole moment as the

TABLE IVA

Polymerization of α-Olefins in Presence of Cosolvents for 3 Hr[a]

Run no.	Monomer	Conversion, %[b]				
		n-Heptane only	(1) *n*-Heptane + 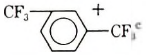 [c]	(2) *n*-Heptane + 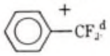 [d]	(3) *n*-Heptane + 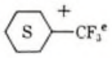 [e]	*n*-Heptane + 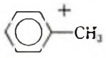
A	$CH_3CH_2CH=CH_2$	65	67	91	61	50
B	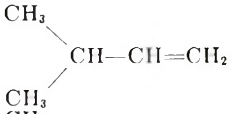 $(CH_3)_2CH-CH=CH_2$	42	91	100	40	35
C	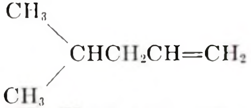 $(CH_3)_2CHCH_2CH=CH_2$	52	82	100	52	35
D	$CH_3CH_2CH_2CH=CH_2$	73	71	88	71	63

[a] Conditions: monomers = 10 mmole; solvent, *n*-heptane = 4 ml; cosolvent = 10 mmole of CF_3 (or CH_3) group; VCl_3 = 1 mmole; Al(*i*-Bu)$_3$ = 2.5 mmole; 70°C.

[b] The error in reproducibility of the conversions is approximately 5–10%.

[c] Dipole moment = 2.43 D.[25]

[d] Dipole moment = 2.60 D.[26]

[e] Dipole moment = 2.40 D.[26]

TABLE IVB

Analytical Data (Found)[a]

	A			B			C			D		
	1	2	3	1	2	3	1	2	3	1	2	3
C, %	85.85	85.77	85.73	85.81	85.96	85.78	85.47	85.30	85.93	85.55	85.42	85.89
H, %	14.43	14.29	14.46	14.69	14.29	14.41	14.11	14.37	14.34	14.32	14.38	14.41

trifluoroaromatic solvents, did not change the rate of polymerization. Thus, the dipole moment alone is unlikely to be the reason for the increase in rate of polymer formation. There are few examples in the literature describing enhancements in the rates of polymerization of α-olefins in the presence of aromatic solvents.

Minsker[27] found an increase in the rate of polymerization of propylene by $TiCl_3$–$Al(C_2H_5)_3$ in the presence of aromatic solvents. The rate reached a maximum at 3.4 mole/l. concentration of the aromatic solvents in *n*-heptane. Such a rate enhancement was also reported by Berslaw[23] for the polymerization of ethylene by $(C_5H_5)_2$–$Al(C_2H_5)_2Cl$ in toluene. No such effect was observed when toluene was replaced by heptane.

In the present work, toluene was chosen to determine whether or not the aromatic nucleus was solely responsible for this phenomenon. Contrary to what has been reported, toluene decreases the rate of polymerization of α-olefins in the VCl_3–$Al(i\text{-}Bu)_3$ system. Benzotrifluoride showed a more dramatic effect, particularly on 3-methyl-1-butene, whereas toluene exerted an opposite effect on this monomer and gave a slower rate. Based on these findings, one may draw the following conclusions.

(*1*) The decrease in the per cent conversion to polymers in the presence of toluene might be attributed to a competitive loss of monomers through a Friedel-Crafts type alkylation of the aromatic solvent. The rate of such alkylation is faster for aromatic compounds with electron-releasing groups. Alkylation of toluene with sterically hindered monomers such as 3-methyl-1-butene is probably faster than the polymerization of these monomers. On the other hand, benzotrifluoride does not undergo a Friedel-Crafts-type reaction, since the trifluoromethyl group deactivates the ring. Unfortunately we have not as yet verified this experimentally.

(*2*) There is a combined effect of both the aromatic nucleus and trifluoromethyl group on the increase of conversion of polymers. None of these groups alone causes such effects as has been shown by the experiments with toluene and (trifluoromethyl)cyclohexane.

(*3*) Sterically hindered monomers such as 3-methyl-1-butene exhibit low reactivity towards Ziegler-type catalysis. The fact that conversions of polymer in the presence of benzotrifluoride have increased may suggest that either the growing chain ends were stabilized and did not decompose to inactive sites, and/or that a larger number of active sites on the catalyst was created.

Stabilization of the growing chain ends may be explained in terms of the ionic contributions to the catalyst by the cosolvent. Benzotrifluoride may act to solvate the organometallic bond, thereby making active areas on the catalytic sites for the polymerization of α-olefins.

Attempts to homopolymerize the trifluorobutenes in the presence of benzotrifluoride were unsuccessful. The results, which are listed in Table V, further confirm the earlier findings about these monomers.

The optimum conditions for the polymerization of α-olefins by VCl_3–$Al(i\text{-}Bu)_3$ in the presence of benzotrifluoride have been investigated. 3-

TABLE V
Polymerization of Fluorobutenes in Presence of Benzotrifluoride

Monomer	Monomer, mmole	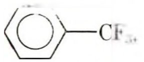 mmole	UCl_3, mmole	Al(*i*-Bu)$_3$, mmole	Time, hr	Temp, °C	Conversion, %
$CF_3CH_2CH{=}CH_2$	10	10	1.0	2.5	24	70	0.0
 $CF_3\underset{\displaystyle CH_3}{\underset{\vert}{C}}HCH{=}CH_2$	10	10	1.0	2.5	24	70	0.0

Methyl-1-butene was selected as the monomer. The results of these investigations are listed in Table VI.

TABLE VI
Polymerization of 3-Methyl-1-butene in the Presence of Benzotrifluoride for 1 Hr[a]

Run no.	Monomer, mmole	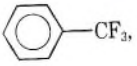 mmole	Conversion, %	Mp, °C
1	10	0.0	16	260
2	10	0.25	62	250–253
3	10	0.50	77	248–250
4	10	0.75	80	247–250
5	10	1.00	85	247–249
6	10	1.50	88	
7	10	1.50	96	
8	10	1.75	96	
9	10	2.00	96	247–249

[a] Conditions: VCl_3 = 1 mmole; Al(*i*-Bu)$_3$ = 2.5 mmole; *n*-heptane = 4 ml; 70°C.

These data are plotted as per cent conversion versus concentration of benzotrifluoride in Figure 6. The results indicate that only small amounts of benzotrifluoride, equivalent to about 25 mole-% of that of VCl_3, are sufficient to cause an appreciable enhancement of the conversion to polymer.

While the vanadium trichloride catalyst seems to be activated by benzotrifluoride, titanium trichloride is adversely affected. The activity of this

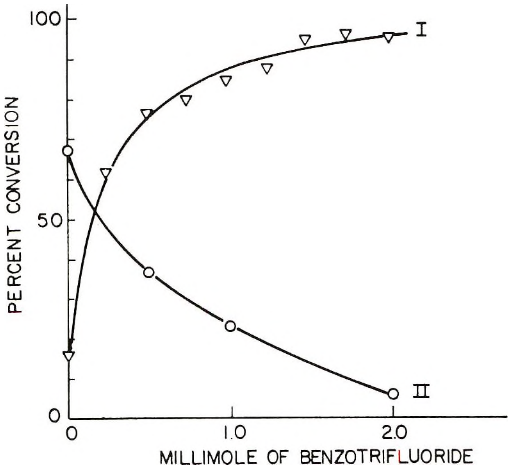

Fig. 6. Homopolymerization of 3-methyl-1-butene in presence of benzotrifluoride: (*I*) with VCl_3 and Al(*i*-Bu)$_3$; (II) with $TiCl_3$ and Al(*i*-Bu)$_3$. Polymerization: 1 hr at 70°C.

catalyst (as measured by conversion to polymer) decreased upon addition of benzotrifluoride. The experimental results obtained by polymerizing 3-methyl-1-butene with $TiCl_3$–Al(*i*-Bu)$_3$ are summarized in Table VII.

TABLE VII
Polymerization of 3-Methyl-1-butene with $TiCl_3$–Al(*i*-Bu)$_3$ in the Presence of Benzotrifluoride for 1 Hr[a]

Run no.	Monomer, mmole	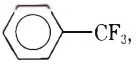 mmole	$TiCl_3$, mmole	Al(*i*-Bu)$_3$, mmole	Conversion, %
1	20	0.0	1.0	2.5	68
2	20	0.5	1.0	2.5	36
3	20	1.0	1.0	2.5	25
4	20	2.0	1.0	2.5	5

[a] Conditions: *n*-heptane, solvent = 8 ml; Temperature = 70°.

These data are plotted in Figure 6 as per cent conversion versus concentration of benzotrifluoride. There is no apparent explanation for this phenomenon. Benzotrifluoride may have reacted with aluminum chloride which is present in this catalyst (but not in vanadium trichloride), thereby destroying the active sites of the catalyst.

This paper comprises a portion of the dissertation submitted by G. Khattab in partial fulfillment of the requirements for the Degree of Doctor of Philosophy in the Graduate School of the Polytechnic Institute of Brooklyn.

References

1. K. Ziegler, E. Holzkamp, H. Breily and H. Martin, *Angew. Chem.*, **67**, 541 (1955).
2. K. Ziegler, *Angew. Chem.*, **71**, 623 (1959).
3. G. Natta, *J. Polym. Sci.*, **16**, 143 (1955); *Angew. Chem.*, **68**, 393 (1959).
4. G. Natta, P. Pino, G. Mazzanti, U. Gianini, E. Mantica, and M. Peraldo, *J. Polym. Sci.*, **26**, 120 (1957).
5. G. Natta and G. Mazzanti, *Tetrahedron*, **8**, 86 (1960).
6. D. B. Ludlum, A. W. Anderson, and C. E. Ashby, *J. Amer. Chem. Soc.*, **80**, 1380 (1958).
7. W. L. Carrick and G. L. Karapinka, *J. Polym. Sci.*, **55**, 145 (1961).
8. W. L. Carrick, F. J. Karol, G. L. Karapinka, and J. J. Smith, *J. Amer. Chem. Soc.*, **82**, 1502 (1960).
9. W. L. Carrick, A. G. Chasar, and J. J. Smith, *J. Amer. Chem. Soc.*, **82**, 5319 (1960).
10. P. Cossee, *Trans. Faraday Soc.*, **58**, 1226 (1962).
11. H. Uelzmann, *J. Polym. Sci.*, **32**, 457 (1958); *J. Org. Chem.*, **25**, 671 (1960); *J. Polym. Sci.*, **37**, 561 (1959).
12. C. G. Overberger and P. A. Jarovitzky, *J. Polym. Sci. A*, **3**, 1438 (1965).
13. L. Reich and A. Schindler, *Polymerization by Organometallic Compounds*, Interscience, New York, 1966, Chaps. III and IV.
14. J. Boor, Jr., in *Macromolecular Reviews*, Vol. 2, Interscience, New York, 1967, pp. 115-268.
15. C. G. Overberger and E. B. Davidson, *J. Polym. Sci.*, **62**, 23 (1962).

16. H. M. Walborsky, M. Baum, and D. F. Lonerini, *J. Amer. Chem. Soc.*, **77**, 3637 (1955).
17. G. M. Bunnett and A. L. Hock, *J. Chem. Soc.*, **1927**, 472.
18. H. Gilman and W. E. Catlin, *Organic Synthesis, Coll. Vol. I*, A. H. Blatt, Ed., Wiley, New York, 2nd ed., 1961, p. 188.
19. C. R. Hauser, B. E. Hudson, B. Abramovitch, and J. C. Shivers, *Organic Synthesis, Coll. Vol. III*, E. C. Horning, Ed., Wiley, New York, 1955, p. 142.
20. A. Henne and J. Hinkamp, *J. Amer. Chem. Soc.*, **67**, 1197 (1945).
21. C. G. Overberger and E. B. Davidson, unpublished results.
22. J. Chatt and L. A. Duncanson, *J. Chem. Soc.*, **1953**, 2939.
23. D. Breslaw and N. R. Newberg, *J. Amer. Chem. Soc.*, **81**, 81 (1959).
24. A. K. Zefirove and A. E. Shilov, *Dokl. Akad. Nauk SSSR*, **136**, 599 (1961).
25. H. Freiser, M. E. Hobbs, and P. M. Gross, *J. Amer. Chem. Soc.*, **71**, 111 (1949).
26. J. D. Roberts, R. L. Webb, and E. A. McEchill, *J. Amer. Chem. Soc.*, **72**, 408 (1950).
27. K. S. Minsker, *Dokl. Akad. Nauk SSSR*, **147**, 636 (1962).

Received June 19, 1968

JOURNAL OF POLYMER SCIENCE: PART A-1 VOL. 7, 237–245 (1969)

Photo-oxidation of the 2,4-Dichloropentanes and PVC

KWEI-PING SHEN KWEI,*
Bell Telephone Laboratories, Incorporated,
Murray Hill, New Jersey 07974

Synopsis

The photo-oxidation of PVC and its model compounds, the *dl*- and *meso*-2,4-dichloropentanes, were studied by high-resolution NMR spectroscopy. The structure, $—CHCl—CH_2—CO—CH_2—$ was found to be present in PVC after photo-oxidation. Two peaks, which corresponded to the CHCl and CH_2 groups next to the carbonyl group, were observed in carbon disulfide–acetone-d_5 mixture, at 6.15 and 7.25τ, respectively. From the NMR spectra, the ratio of the CH_2 to CHCl protons in PVC and the model compounds were found to increase linearly with the time of photo-oxidation after induction periods. The initial rates of the model compounds were comparable with that of PVC; i.e., 1.6×10^{-2} hr^{-1}, at 30°C. Since similar gaseous products were also detected by mass spectrometry in the initial stage, their photo-oxidation probably assumed the same rate-determining step. According to the results that the *dl*-2,4-dichloropentane was photo-oxidized 1.5 times faster than the *meso*-compound, it would be likely that the syndiotactic sequences in PVC might be more easily photo-oxidized than the isotactic sequences.

INTRODUCTION

The stable conformers of the *dl*, and *meso*-2,4-dichloropentanes have been recognized as the models for the syndiotactic and isotactic structures of poly(vinyl chloride) (PVC). These conformations have been intensively studied by Shimanuchi,[1] Doskocilova et al.,[2] and Bovey[3] by using infrared and high-resolution NMR spectroscopy. The compounds were, therefore, used in this study as models for the photo-oxidation of PVC to see if steric effects were involved. From NMR spectra, the ratio of the CH_2 to CHCl protons can be derived to clarify which group is being oxidized.

In the previous work,[4] the photo-oxidation of PVC at 30°C was studied by infrared and mass spectrometry. The initial dissociation of chlorine atoms with ultraviolet light (2537 Å) was correlated with the presence of minute amounts of ozone. The β-chloroketones formed in the photo-oxidation of PVC were observed to decompose according to a Norrish type I reaction with evolution of gaseous products such as carbon dioxide, carbon monoxide, hydrogen, and methane. Hydrogen chloride was obtained only when PVC was heated. The dissociated chlorine atoms were highly reactive and probably reentered as radical sources in the chain reactions. From infrared spectra, the ratios of the CH_2 to $CHCl_5$ groups, which were

---

*Permanent Address: 197 Old Forge Rd., Millington, N.J. 07946.

determined from their characteristic bands, changed generally in the same manner as observed from the NMR spectra in this study during photo-oxidation, but became rather uncertain when the films were obscured by discoloration.

EXPERIMENTAL

The 2,4-dichloropentane was prepared as a mixture of stereoisomers by the Frinton Chemical Company, Vineland, New Jersey. The *dl*- (bp 139.5°C/760 mm) and *meso*-2,4-dichloropentane (bp 144.1°C/760 mm)[6] were separated by gas chromatography using the Aerograph Model A-700. A 20-ft column packed with 30% Carbowax 20M on Chromosorb was used satisfactorily at 63°C, with a flow rate of helium gas at 200 ml/min.

Photo-oxidation of the *dl*- and *meso*-2,4-dichloropentanes was carried out at 0 and 10°C under a 15-W GE germicidal lamp emitting at a wavelength of 2537 Å. A series of small quartz tubes were filled with 0.15 ml of the stereoisomers; oxygen was then introduced into the tubes after evacuating the frozen samples repeatedly. These tubes were placed on a platform at 3 in. below the lamp and immersed in a thermostatted water bath. Samples were removed for NMR studies after various periods of photo-oxidation. Photo-oxidation of PVC thin films (0.001 in. in thickness) were carried out in square cells at 30°C.

NMR spectra were obtained at 60 Mcps on a Varian HA-60 spectrometer. The spectra of the *dl*- and *meso*-2,4-dichloropentane were obtained by using 25–30% vol-% solutions in chlorobenzene at 0°C. Solutions in carbon disulfide–acetone-d_5 mixture (4:1 by volume) were used for the study of the downfield portion of the spectra.

The spectra of nonphoto-oxidized PVC were obtained by using 10 wt-% solutions in chlorobenzene at 100°C; and that of photo-oxidized PVC (5 wt-%) were run first at ambient temperature (40°C) for the study of thermally unstable products from photo-oxidation, then at 80°C or higher. Tetramethylsilane (2%) was used as the internal standard in all spectra. Only the representative spectra are presented here.

The ratio of $CH_2/CHCl$ protons were obtained by averaging ten integrations of the two quintets of PVC centered at 7.92 and 5.55τ; of *dl*-2,4-dichloropentane at 8.38 and 5.86τ;[2] and of *meso*-2,4-dichloropentane at 8.12 and 6.08τ.[2] Freshly prepared solutions were used in the measurements at 40°C for PVC and at 0°C for the 2,4-dichloropentanes because the products of photo-oxidation might decompose upon standing.

The gaseous products of the photo-oxidized samples were analyzed by mass spectrometry.

RESULTS AND DISCUSSION

NMR Spectra of 2,4-Dichloropentanes

The NMR spectrum of the racemic 2,4-dichloropentane in chlorobenzene showed a symmetrical sextet of the methyne (α-proton) resonance at

5.86τ, and a triplet with a split in the central peak of the methylene (β-proton) resonance at 8.38τ (Fig. 1*a*). The spectrum of the *meso* compound contained a symmetrical sextet of the α-protons at 6.08τ and a complex multiplet of 12 lines at 8.12 τ, which arose from the nonequivalent β-protons (Fig. 2*a*). The positions of these peaks agreed well with the values reported by Doskocilova et al.[2]

The slightly photo-oxidized diastereomers of 2,4-dichloropentane did not change shape in the peaks of α- and β-proton resonance (Fig. 2*b*). A

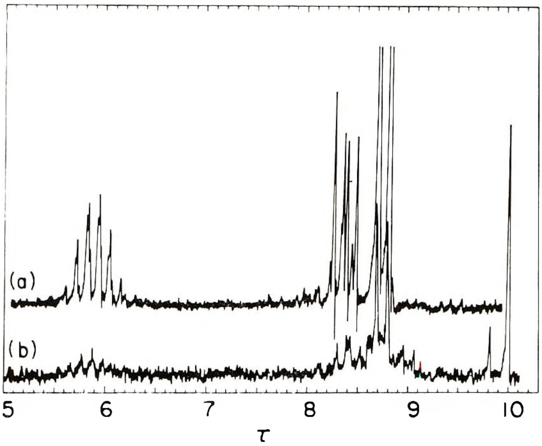

Fig. 1. NMR spectra of racemic 2,4-dichloropentane in chlorobenzene at 0°C: (*a*) nonirradiated, (*b*) photo-oxidized at 2537 Å, 10°C, for 209 hr.

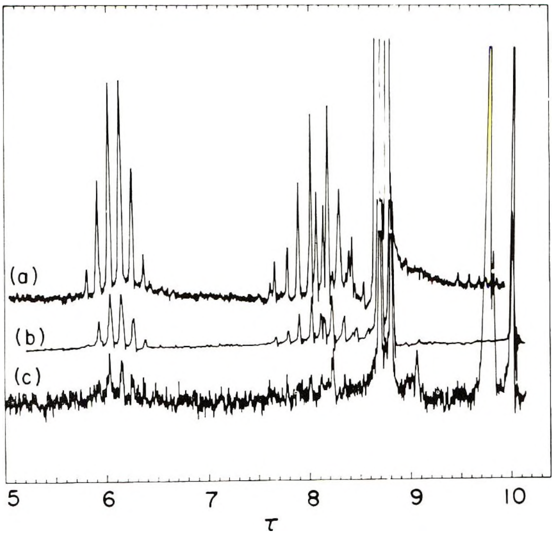

Fig. 2. NMR spectra of *meso*-2,4-dichloropentane in chlorobenzene at 0°C: (*a*) nonirradiated, (*b*) photo-oxidized at 2537 Å, 10°C, for 44 hr, (*c*) photo-oxidized at 2537 Å, 10°C, for 209 hr.

decrease in the area under the α-resonance, however, was noticed. No new peaks, which might arise from the products of photo-oxidation, were observed. According to the previous work,[4] the initial dissociation of the chlorine atoms was accelerated by a trace amount of ozone (1 ppm) which was formed under ultraviolet light at 2537 Å wavelength. The oxidation then resulted in the formation of a mixture of acetyl compounds. After photo-oxidation, the infrared spectra of the mixture showed an absorbance band at 1725 cm^{-1}, which arose from the carbonyl group between two methylene groups. It is possible that the products had decomposed during photo-oxidation since gaseous products consisting of carbon dioxide, carbon monoxide, hydrogen, and methane were detected by mass spectrometry. The highly reactive chlorine atoms probably reentered as radical sources. It is also possible that the new peaks have been masked under existing peaks. A mixture of several products was probably produced because, after prolonged photo-oxidation for 209 hr, some extra peaks were seen at the methyl resonance, and the peaks for the *meso*-methylene groups changed shape (Fig. 2*c*). In addition to these changes, methane was identified from the large peak at 9.78τ in the *meso* compound (Fig. 2*c*) and the small peak at 9.81τ in the racemic compound (Fig. 1*b*). The position of the peaks agreed well with the value for methane reported by Cavanaugh et al.[7]

NMR Spectra of PVC

The photo-oxidation of PVC was also studied by high-resolution NMR spectrometry, in addition to infrared[4] and mass spectrometry.[4] The NMR spectrum of the original PVC (Fig. 3*a*) in chlorobenzene contained two quintets, one symmetrical centered at 5.55τ and one less symmetrical at 7.92τ. The former peak is related to the methyne (α) protons and the latter peak to the methylene (β) protons. The position of these peaks agreed with the values reported by Johnsen[8] and Bovey.[3]

After being photo-oxidized slightly, the spectra of PVC (Fig. 3*b*) showed two quintets of essentially the same shape as the original PVC. However, there was a new peak at 6.44τ, which disappeared after 1 hr of measurements at 130°C. This indicated that the product was unstable at high temperatures. The area under the α-proton resonance had decreased relative to the area under the β-proton resonance.

After prolonged photo-oxidation, the spectrum of PVC in chlorobenzene showed a broadened α-proton resonance which shifted slightly to the left of 5.55τ and an unaltered quintet at 7.92τ (Fig. 3*c*). A further decrease in the area under the α-proton resonance was noticed as compared with the area under the β-proton resonance. In the solvent mixture of carbon disulfide and acetone-d_5 (4:1 by volume), the α-proton resonance showed at 5.54τ and the β-proton resonance shifted towards smaller τ values to 7.75τ. Two new peaks were observed at 7.25 and 6.14τ, (Fig. 3*d*) which corresponded to the peak at 6.44τ in chlorobenzene. The peak at 7.25τ

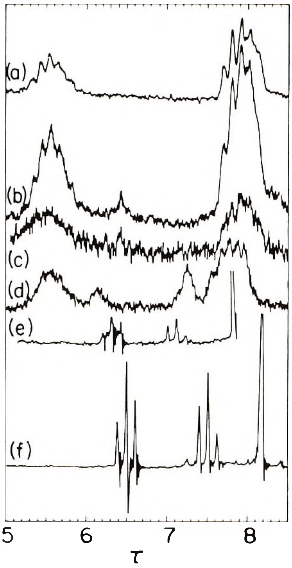

Fig. 3. NMR spectra of poly(vinyl chloride): (*a*) nonirradiated, measured in chlorobenzene at 100°C; (*b*) photo-oxidized at 40°C for 20 hr, measured in chlorobenzene at 130°C; (*c*) photo-oxidized at 30°C for 120 hr, measured in chlorobenzene at 80°C; (*d*) sample (*c*) measured in carbon disulfide–acetone-d_5 mixture at 40°C; (*e*) 4-chloro-2-butanone in carbon disulfide–acetone-d_5 mixture; (*f*) 4-chloro-2-butanone in chlorobenzene.

was probably shielded under the β-proton resonance when chlorobenzene was the solvent. The ratio of the areas under the two peaks at 7.25 and 6.15τ was approximately 2:1. No resonance due to unsaturated protons were observed between 3 and 5τ.

TABLE I
Chemical Shifts

Chain structure	τ in chlorobenzene (centered)	τ in carbon disulfide–acetone-d_6 (centered)[4]
PVC		
—CHCl—CH$_2$—	τ_A = 5.55	τ_A = 5.54
A B	τ_B = 7.92	τ_B = 7.75
Photo-oxidized PVC		
—CHCl—CH$_2$—CHCl—CH$_2$—$\underset{\underset{\text{O}}{\Vert}}{\text{C}}$—CH$_2$—	τ_C = 6.44	τ_C = 6.15
A B C D		τ_D = 7.25
4-Chloro-2-butanone		
CH$_2$Cl—CH$_2$—CO—CH$_3$	τ_A = 6.50	τ_A = 6.30
A B	τ_B = 7.52	τ_B = 7.12
1,3-Dichloroacetone		
CH$_2$Cl—CO—CH$_2$Cl	τ_A = 6.14	τ_A = 5.90
A		
1-Chloro-2-pentanone		
CH$_2$Cl—CO—CH$_2$—CH$_2$—CH$_3$	τ_A = 6.20	τ_A = 5.90
A B	τ_B = 7.70	τ_B = 7.45

The identification of the two new peaks was made with the aid of 4-chloro-2-butanone ($CH_3—CO—CH_2CH_2Cl$). Its chemical shifts in chlorobenzene and the solvent mixture (CS_2–acetone-d_5) are listed in Table I together with PVC and 1-chloro-2-pentanone. The two triplets for the CH_2 and CH_2Cl group next to the carbonyl group in 4-chloro-2-butanone appeared at 7.25 and 6.50τ (Fig. 1*f*), respectively, in chlorobenzene and at 7.12τ and 6.30τ (Fig. 1*e*), respectively, in carbon disulfide–acetone-d_5 mixture. The latter positions seemed to agree with the new peaks of PVC at 7.25 and 6.15τ in this solvent mixture, some shifts being allowed due to the polymeric media.

A study of the NMR spectra of 1,3-dichloroacetone ($CH_2Cl—CO—CH_2Cl$) and 1-chloro-2-pentanone ($CH_2Cl—CO—CH_2CH_2CH_3$) showed the resonance of CH_2Cl groups, neighboring the carbonyl group, at 6.14τ in chlorobenzene and at 5.90τ in carbon disulfide–acetone-d_5 mixture. Obviously, this position did not agree with photo-oxidized PVC. Therefore, the photo-oxidized PVC contained the structure, $—CH_2—CO—CH_2—CHCl—$, rather than $—CHCl—CO—CHCl$. The presence of this structure is also confirmed by our previous observation[7] of the absorbance band at 1725 cm^{-1} in the infrared spectra which arose from the carbonyl group next to the two methylene groups.

Ratio of CH_2 to CHCl Protons

Since the products resulting from the photo-oxidation of 2,4-dichloropentane and PVC might decompose upon standing, freshly prepared solutions in chlorobenzene were used in the measurements of integral curves for the CH_2 and CHCl protons. The ratios of CH_2 to CHCl protons for PVC (Fig. 4) and of the 2,4-dichloropentanes (Fig. 4), were found to increase linearly with the time of photo-oxidation, after short induction periods, and then increase slowly after 14 hr. This indicated that the α-protons (in the CHCl group) were being removed. PVC (Fig. 5) showed a long induction period of about 100 hr before the linear increase. Its presence was probably necessary to allow the formation of sufficient carbonyl groups in PVC to serve as photosensitizers.

The initial slopes from the above plots were 2.4 and 3.0×10^{-2} hr^{-1} for *meso*-2,4-dichloropentane at 0 and 10°C, respectively, and 3.43 and 4.78×10^{-2} hr^{-1} for *dl*-2-4-dichloropentane at 0 and 10°C, respectively. It is noticed here that the two sets of data at the two temperatures agreed well in that the slope of the *dl*-2,4-dichloropentane were approximately 1.5 times higher than those of the *meso*-compounds. After more than 14 hr of photo-oxidation, the ratio of CH_2 to CHCl protons increased rather slowly, due probably to partial decomposition of the products, or to the entering of β-protons into secondary reactions.

In Figure 5, the slope of the linear portion of the increasing ratios of CH_2/CHCl protons in PVC was 1.6×10^{-2} hr^{-1} at 30°C. In order to obtain the slopes of the dichloropentanes at 30°C which evaporated rapidly

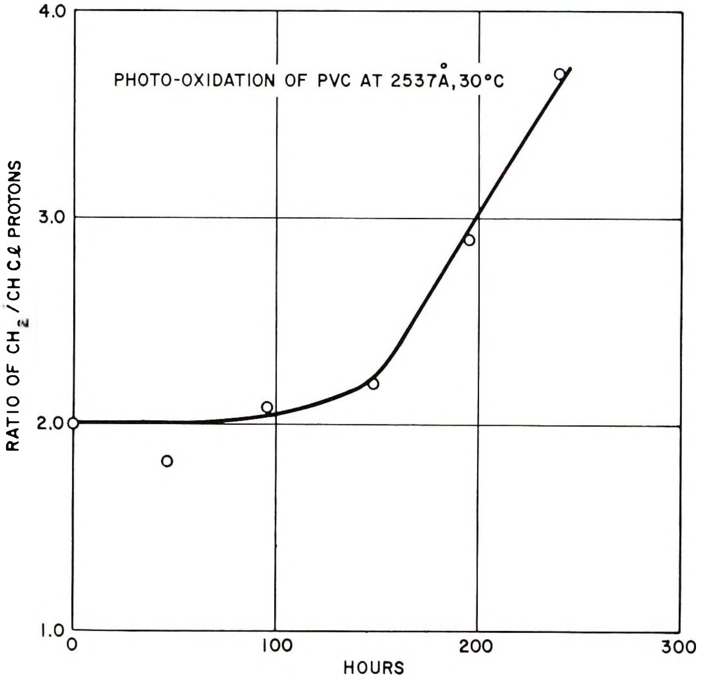

Fig. 4. Variations of ratios of CH_2 to CHCl protons in PVC during photo-oxidation at 2537 Å, 30°C.

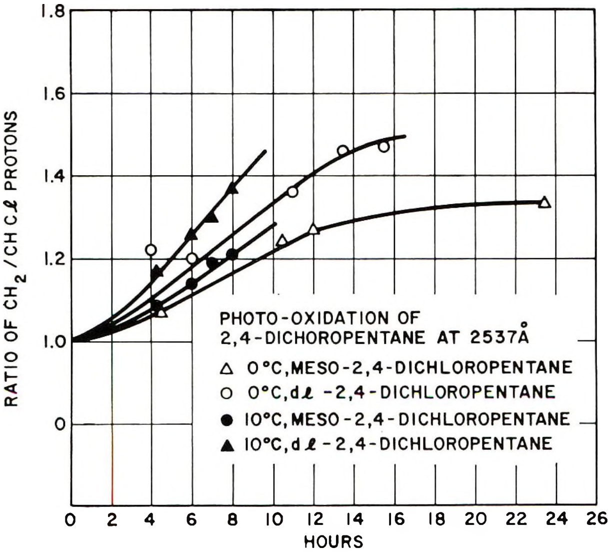

Fig. 5. Variations of ratios of CH_2 to CHCl protons in *dl*-and *meso*-2,4-dichloropentanes during photo-oxidation at 2537 Å, 10°C.

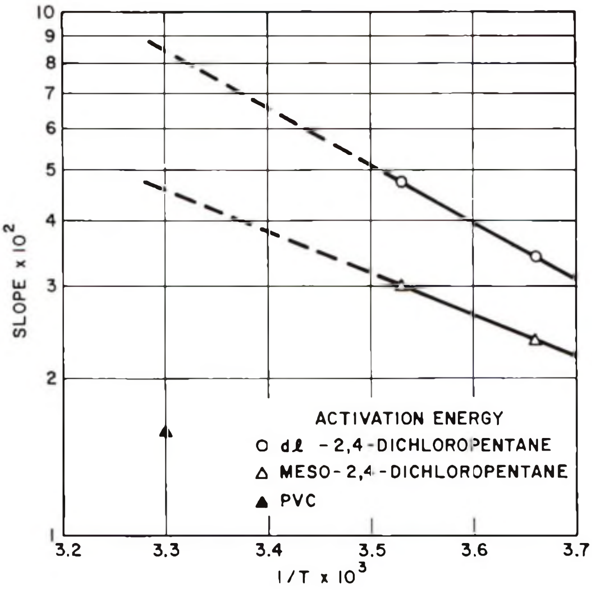

Fig. 6. Log (slope × 10^2) versus 1/T × 10^3

at this temperature, the logarithms of the slopes were plotted against 1/T°K in Figure 6. An extrapolation of the plots to 30°C gave 8.4×10^{-2} hr^{-1} for the *dl* compound and 4.6×10^{-2} hr^{-1} for the *meso* compound as the rates of increasing ratio of $CH_2/CHCl$ protons. Although the physical states of these compounds are different from PVC, these rates are comparable with that of PVC which was 1.6×10^{-2} hr^{-1} at 30°C This strongly suggests that the rate-determining step in the photo-oxidation of both PVC and 2,4-dichloropentane is the same. Furthermore similar major products were also detected in the gaseous phase by mass spectrometry. The products were carbon dioxide, carbon monoxide, hydrogen, and methane.[4] One may conclude, then, that the photo-oxidation of PVC very likely assumes the same mechanism as that of the 2,4-dichloropentanes.

It is interesting to find that the slopes of the increasing ratios of CH_2/-CHCl protons in the *dl*-2,4-dichloropentane was 1.5 times higher than that of the meso-2,4-dichloropentane at both 0 and 10°C. Although Billups[9] and Williams[10] have reported that the racemic compound was more stable than the meso-compound in an equilibrium mixture, the reactivity of the compound is not necessarily dependent upon the most stable conformation in the ground state. The conformations in their transition states, which can differ by a relatively large amount of energy, are important. A study of the space-filling models showed that the difference in the availability of α-protons for attack is indeed large between the planar zigzag conformation of the syndiotactic sequences and the 3_1-helical conformation in the isotactic sequences.

The α-proton (CHCl) resonance of PVC which centered at 5.55τ was fully described by Bovey et al.,[3] Satoh,[11] and Schneider et al.,[12] to consist of three quintets which were assigned to the syndiotactic units at 5.44τ, the heterotactic units at 5.55τ, and the isotactic units at the 5.77τ. Since the α-proton resonance of photo-oxidized PVC was broadened, it was difficult to distinguish whether the syndiotactic, or the isotactic peak vanished first. However, the shape and the values of the α-proton resonance were obviously influenced. In light of the above results from the 2,4-dichloropentanes, it is reasonable to assume that the syndiotactic sequences in PVC would, most likely, be photo-oxidized more easily then the isotactic sequences. Petersen and Rånby[13] have also reported recently that tacticity was involved in the chlorination of PVC.

The author would like to thank Dr. F. A. Bovey for his helpful suggestions and Dr. F. Heatley for his discussions.

References

1. T. Shimanouchi and M. Tasumi, *Spectrochim. Acta.*, **17**, 755 (1961).

2. D. Doskocilova, J. Stokr, B. Schndider, H. Pivcova, M. Kolinsky, J. Petranek, and E. Lím, in *International Symposium on Macromolecular Chemistry, Prague 1965*, (*J. Polym. Sci. C*, **16**), O. Wichterle and B. Sedlàček, Eds., Interscience, New York, 1967, p. 215.

3. F. A. Bovey, E. W. Anderson, D. C. Douglass, and J. A. Manson, *J. Chem. Phys.*, **39**, 1199 (1963).

4. K.-P. S. Kwei, *J. Polym. Sci.* Prod No. 5617.

5. O. Fredrickson and J. A. Crowo, *Makromol. Chem.*, **100**, 231 (1967).

6. D. Lím, M. Kolinsky, E. Votavova, M. Ryska, and J. Lucas, *J. Polym. Sci. B*, **4**, 573 (1966).

7. F. A. Bovey, *NMR Data Tables for Organic Compounds*, Vol. I, Interscience, New York, 1967, p. 10.

8. U. Johnsen, *J. Polym. Sci.*, **54**, 56 (1961).

9. W. E. Billups and A. N. Kurtz, *J. Amer. Chem. Soc.*, **90**, 1361 (1968).

10. A. D. Williams, J. I. Brauman, N. J. Nelson, and P. J. Flory, *J. Amer. Chem. Soc.*, **89**, 4807 (1967).

11. S. Satoh, *J. Polym. Sci. A*, **2**, 5221 (1964).

12. B. Schneider, J. Stokr, D. Doskocilova, M. Kolinsky, S. Sykora, and D. Lím, *International Symposium on Macromolecular Chemistry, Prague 1965*, (*J. Polym. Sci. C*, **16**), O. Wichterle and B. Sedlàček, Eds., Interscience, New York, 1967, p. 599.

13. J. Petersen and B. Ranby, *Makromol. Chem.*, **102**, 83 (1967).

Received June 4, 1968
Revised July 11, 1968

JOURNAL OF POLYMER SCIENCE: PART A-1 VOL. 7, 247-257 (1969)

Proton Magnetic Resonance Investigation of Structure of ω-Alkyl-α-Olefin/SO_2 Copolymers*

R. BACSKAI, L. P. LINDEMAN,
D. L. RANSLEY, and W. A. SWEENEY
Chevron Research Company,
Richmond, California

Synopsis

The 100 MHz proton magnetic resonance (PMR) spectra of free radical alternating ω-alkyl-α-olefin/SO_2 copolymers has been investigated. The data obtained from the quantitative evaluation of the spectra are consistent with a copolymer structure containing unrearranged olefinic monomer units. The 4-methyl-1-pentene/SO_2 copolymer shows a quadruplet resonance in the CH_3 proton region. This multiplicity, observed also in the analogous 1,2-dichloro-4-methylpentane and 1,2-dibromo-4-methylpentane, arises from the presence of magnetically nonequivalent CH_3 protons located in the vicinity of the asymmetric carbon atoms of the main chain. There is no detectable nonequivalency of CH_3 protons in the 5-methyl-1-hexene/SO_2 copolymer, probably because the center of asymmetry is further removed from the isopropyl group. In poly-4-methyl-1-pentene, prepared with Ziegler-Natta catalyst, the polymer structure around the main chain tertiary carbons is fairly symmetrical; and, as expected, the CH_3 protons of the isopropyl group are magnetically equivalent.

INTRODUCTION

Previous communications from this laboratory[1,2] presented evidence that the free-radical copolymerization of ω-alkyl-α-olefins with SO_2 proceeds without rearrangement, leading to products containing the incorporated olefin in 1,2-enchainment. For the copolymers of ω-(*sec*-butyl)-α-olefins, this evidence was based on the finding that optically active (+)-3-methyl-1-pentene, (−)-4-methyl-1-hexene, and (+)-5-methyl-1-heptene yield optically active copolymers with specific rotations similar to those of low molecular weight analogs. The formation of optically active copolymers indicates that the asymmetric carbon atom of the olefin monomers is not converted by rearrangement into a free radical during polymerization. In contrast, cationic homopolymers of the same olefins are either almost completely optically inactive, such as the polymers of (+)-3-methyl-1-pentene and (−)-4-methyl-1-hexene, or as in the case of (+)-5-methyl-1-heptene the polymers have a significant, however, lower than the expected,

---

* Presented at the National Meeting of the American Chemical Society, San Francisco, California, April 1968.

specific rotation. These results were interpreted as being consistent with a cationic polymerization mechanism in which the growing chains undergo intramolecular hydride shift, and the loss of optical activity is caused by the conversion of the asymmetric carbon atoms into stable carbonium ions.

For the free radical copolymers of ω-isopropyl-α-olefins and SO_2, evidence in favor of the unrearranged structure was based on the quantitative PMR analysis of a 4-methyl-1-pentene/SO_2 copolymer. However, when the PMR spectrum of this copolymer was examined in more detail, it was realized that it shows some unusual features which might be interpreted as being inconsistent with the proposed structure. The fact that the methyl resonance reported showed a broad singlet, with no evidence of splitting from the adjacent proton, was particularly disturbing. In order to clarify this and also some other apparent spectral anomalies, the 4-methyl-1-pentene/SO_2 copolymer spectrum was reexamined and the PMR analysis was extended to other ω-alkyl-α-olefin/SO_2 copolymers as well. The results of these investigations and a discussion of the causes that give rise to the unusual spectral features are the subject of this report.

EXPERIMENTAL

Materials

Polymers. The general method of free radical ω-alkyl-α-olefin/SO_2 copolymer preparation was described in a previous communication.[1] The purity of the olefins used in the polymerization reactions was higher than 99% (determined by vapor-phase chromatography). The copolymers were purified by reprecipitation from a $CHCl_3$ (solvent)-CH_3OH (precipitant) system. Elemental analyses and reduced specific viscosities (determined in $CHCl_3$ at 30°C and at 0.1 g/100 ml concentration) are given below.

ANAL. Calcd for alternating 3-methyl-1-butene/SO_2 copolymer: C, 44.75%; H, 7.51%; S, 23.89%. Found: C, 45.23%; H, 7.58; S, 24.13%.

Calcd for alternating 4-methyl-1-pentene/SO_2 copolymer: C, 48.62%; H, 8.16%; S, 21.63%. Found: C, 48.40%; H, 8.76%; S, 21.7%; η_{sp}/c = 1.36 dl/g.

Calcd for alternating 5-methyl-1-hexene/SO_2 copolymer: C, 51.82%; H, 8.70%; S, 19.76%. Found: C, 50.74%; H, 8.50%; S, 19.15%. η_{sp}/c = 0.74 dl/g.

Calcd for alternating 4-methyl-1-hexene/SO_2 copolymer: C, 51.82%; H, 8.70%; S, 19.76%. Found: C, 51.56%; H, 8.59%; S, 19.37%. η_{sp}/c = 0.53 dl/g.

Poly-4-methyl-1-pentene was prepared from 4-methyl-1-pentene with $AlEt_2Cl$–$TiCl_3$ catalyst; the polymer had $[\eta]$ = 2.6 dl/g (in decalin at 135°C).

Preparation of 1,2-Dichloro-4-methylpentane. Into a 2-liter jacketed turbomixer was placed 667 g (7.94 mole) 4-methyl-1-pentene, 1 liter carbon tetrachloride, and 79.4 g (0.3 mole) stannic chloride. A stream of chlorine containing 10% air (to inhibit radical chlorination reactions) was bubbled in the mixture at 675 ml/min. for 5 hr. The reaction temperature was maintained at 20°C by water cooling.

The reaction mixture was washed with two 500 ml portions of water, with 500 ml 5% sodium bicarbonate, and finally with water. It was dried over magnesium sulfate and distilled. The fraction boiling at 161–166°C represented a 68% yield of 1,2-dichloro-4-methylpentane. Redistillation gave a material that was 99% pure by VPC; boiling point: 161°C; $n_D^{20} = 1.4467$; $d_D^{20} = 1.0482$; Cl (theory): 45.7%; Cl (found): 46.7%.

The structure of the dichloride was confirmed by reconverting it into 4-methyl-1-pentene. This reaction was carried out in the following way. Into a three-necked flask was placed 8.2 g (0.338 mole) magnesium turnings and some anhydrous ether. To the refluxing mixture was added 5 g (0.02 mole) iodine over a 30-min period. Following that, 31 g (0.2 mole) of 1,2-dichloro-4-methylpentane in 40-ml ether was added over 1 hr. The mixture was refluxed for a further 3 hr. Additional ether (100 ml) was added to assist in washing the solid precipitate. Analysis by VPC indicated 50% conversion. Distillation through a 1 in. by 2 in. column packed with glass helices gave a dilute ether solution of the product. Comparison of the infrared spectrum of this solution with an ether solution of 4-methyl-1-pentene showed identical spectra including the major bands at 1820, 1630, 900, and 622 cm^{-1}. The retention time on a 20% Carbowax 20M or Chromosorb W (10 ft by $^1/_4$ in.) gas chromatographic column was shown to be identical for the product and authentic 4-methyl-1-pentene.

1,2-Dibromo Derivatives. 1,2-Dibromo-4-methylpentane and 1,2-dibromo-5-methylhexane were prepared by adding bromine dropwise to a dilute CCl$_4$ solution of the corresponding olefin. The resulting slightly yellow solutions were used for the PMR measurements.

PMR Measurements

The PMR spectra were recorded on a Varian HA-100 spectrometer. Chloroform was used as a solvent for the SO$_2$ copolymers at a temperature of 65°C; 1,3,5-trichlorobenzene at a temperature of 170°C was used for poly-4-methyl-1-pentene; and carbon tetrachloride with 5% benzene at a temperature of 35°C was used for the dihalogen compounds. The solvents provided the lock signal to stabilize the magnetic field. The chemical shifts reported in parts per million are downfield relative to hexamethyldisiloxane (HMDS) dissolved in the samples. Relative proton counts were calculated from the electronic integral.

RESULTS AND DISCUSSION

Possible general structures of alternating ω-alkyl-α-olefin/SO$_2$ copolymers, having different repeating units, are shown in structures I, II, III, and IV. Structures I and III represent the normal mode of addition; II and IV are rearranged polymers formed by hydrogen-atom migration. The possible reactions leading to such polymer structure were discussed earlier.[1]

ω-Isopropyl-α-olefin/SO_2 copolymers:

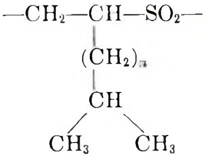

I

Unrearranged polymer

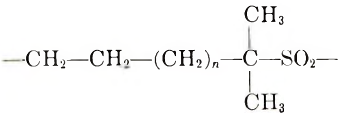

$$-CH_2-CH_2-(CH_2)_n-\overset{CH_3}{\underset{CH_3}{C}}-SO_2-$$

II

Rearranged polymer

ω-(*sec*-Butyl)-α-olefin/SO_2 Copolymers:

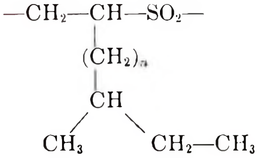

III

Unrearranged polymer

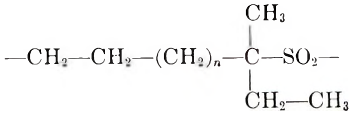

$$-CH_2-CH_2-(CH_2)_n-\overset{CH_3}{\underset{CH_2-CH_3}{C}}-SO_2-$$

IV

Rearranged polymer

In spite of the fact that there is no precedent for intramolecular hydrogen atom shifts in ordinary organic reactions,[3] such a rearrangement in the system discussed here would not be completely unexpected. The rearrangement of a propagating secondary radical into the tertiary radical is thermodynamically feasible, since the latter is more stable by several kcalories.[4] Also, one might expect that ionic resonance contributions to the transition state of the propagation step, as proposed by Walling,[5] would increase the propensity of the growing chain towards rearrangement.

The high-resolution 100 MHz PMR spectra of some typical representatives of these copolymers are presented in Figures 1, 2, and 3. (Due to insolubility the spectrum of the 3-methyl-1-butene/SO_2 copolymer could not be determined.) The peak assignments referring to structures A and C are indicated on the spectra. As expected, the $CH_2 + CH$ protons of the main chain, compared to the $CH_2 + CH$ protons of the side chain, are deshielded by the SO_2 group and appear at lower magnetic field. To improve resolution, these spectra were obtained at 65°C instead of 30°C as reported earlier for the 4-methyl-1-pentene/SO_2 copolymer. Under these conditions the methyl resonance, shown in Figure 1 and previously observed as a broad singlet,[1] appears as a poorly resolved quadruplet centered at 0.94 ppm. However, heating of the copolymers to higher temperature has the disadvantage of causing slight decomposition. Evidence for this can be seen in Figure 1, where the small peaks at 0.79 and 0.85 ppm coincide with the doublet of the CH_3 resonance of 4-methyl-1-pentene, the latter being formed probably by the thermal decomposition of the copolymer. By measuring the areas under the different resonances one can

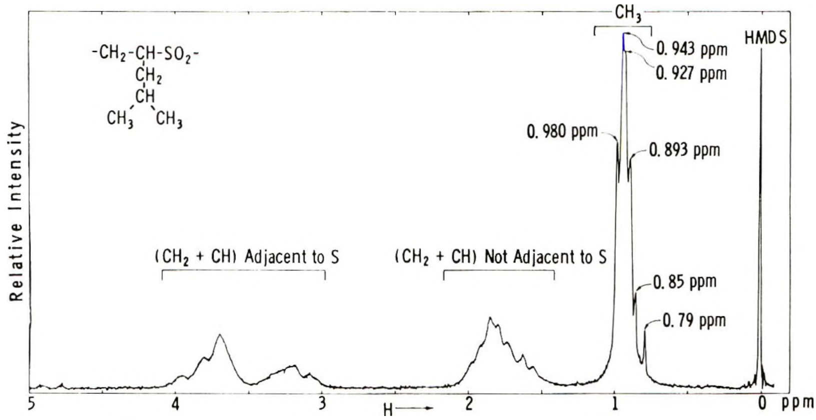

Fig. 1. 100 MHz PMR spectrum of 4-methyl-1-pentene/SO_2 copolymer (8 wt-% copolymer in $CHCl_3$, 65°C).

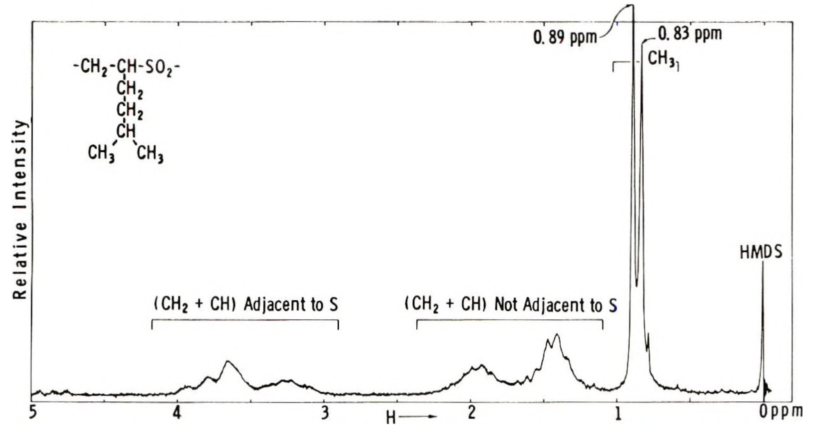

Fig. 2. 100 MHz PMR spectrum of 5-methyl-1-hexene/SO_2 copolymer (8 wt-% copolymer in $CHCl_3$, 65°C).

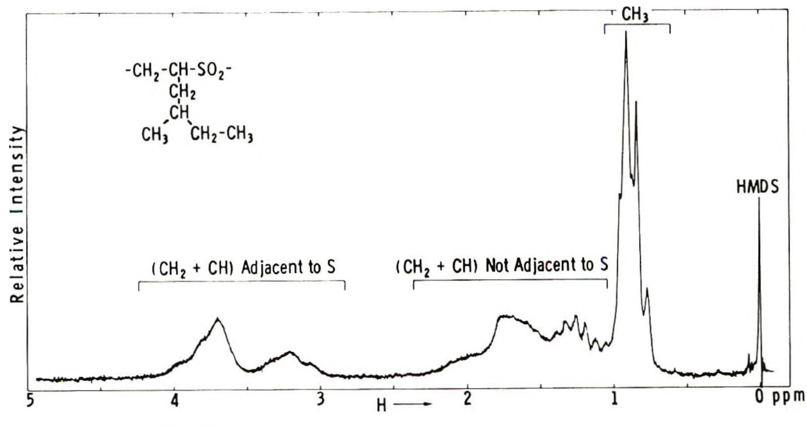

Fig. 3. 100 MHz PMR spectrum of 4-methyl-1-hexene/SO_2 copolymer (8 wt-% copolymer in $CHCl_3$, 65°C).

compare these values with the relative peak intensities expected for structures I, II, III, and IV. Such a comparison is shown in Table I.

The data show that the relative resonance intensities are in good agreement with the values expected for structures I and III. Since structures II and IV require a very different proton ratio, these results furnish good evidence that the free-radical copolymerization of ω-alkyl-α-olefins with SO_2 proceeds without rearrangement.

Although the quantitative analysis discussed above strongly supports the unrearranged polymer structure, some unusual aspects of the PMR spectra becloud this interpretation. Thus, previous workers[6–8] have found that cationic poly-ω-isopropyl-α-olefins exhibit a singlet CH_3 resonance characteristic of CH_3 groups attached to a quaternary carbon atom. However, polymers of the same olefins, prepared with Ziegler-Natta catalyst, show a doublet CH_3 resonance indicating spin-spin splitting caused by an adjacent tertiary hydrogen atom. These findings were interpreted as being evidence for rearranged and unrearranged polymer structure, respectively. Considering these results, the CH_3 resonance in the spectrum of unrearranged 4-methyl-1-pentene/SO_2 copolymer, such as I, would be expected to appear as a doublet, due to spin-spin splitting by the tertiary hydrogen of the isopropyl group. On the other hand in rearranged 4-methyl-1-pentene/SO_2 copolymer, such as II, where the CH_3 groups are attached to a quaternary carbon atom, the CH_3 resonance should be a singlet. In fact, this resonance appears to have four barely resolved lines (previously reported as a singlet[1]) centered at 0.94 ppm in Figure 1, which seems to be inconsistent with either structure. It was of interest, therefore, to investigate further this apparent anomaly.

In order to understand the unusual CH_3 resonance in 4-methyl-1-pentene/SO_2 copolymer, a comparison was made with the PMR spectra of analogous low molecular weight compounds, such as 1,2-dichloro-4-methylpentane and 1,2-dibromo-4-methylpentane. These compounds may be represented by the general formula V, in which the carbon atom with the asterisk is asymmetric and if X = —SO_2—, the formula corresponds to a

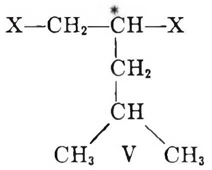

V

X = —Cl or —Br or —SO_2—

typical portion of the unrearranged 4-methyl-1-pentene/SO_2 copolymer. Although in V the CH_3 and CH_2 protons are apparently in similar environment, they can be magnetically nonequivalent and have different chemical shifts because of the proximity of an asymmetric carbon atom. For such compounds, the origin of magnetic nonequivalence is attributed to the so-called "asymmetry effect" and to differences of the residence times (and populations) of the molecule in each of the various rotational conformations [9,10].

TABLE I

Relative Resonance Intensities in the Proton Magnetic Resonance Spectra of ω-Alkyl-α-olefin/SO_2 Copolymers

	Relative intensity								
	4-Methyl-1-pentene/SO_2			5-Methyl-1-hexene/SO_2			4-Methyl-1-hexene/SO_2		
Proton	Found	Calculated for I $n = 1$	Calculated for II $n = 1$	Found	Calculated for I, $n = 2$	Calculated for II, $n = 2$	Found	Calculated for III, $n = 1$	Calculated for IV, $n = 1$
CH_3	2.1	2.0	3.0	2.0	2.0	3.0	2.0	2.0	3.0
(CH_2 + CH) high field[a]	1.0	1.0	2.0	1.8	1.66	3.0	2.0	1.66	3.0
(CH_2 + CH) low field[b]	1.0	1.0	1.0	1.0	1.0	1.0	1.0	1.0	1.0

[a] Protons not adjacent to S atoms.

[b] Protons adjacent to S atoms.

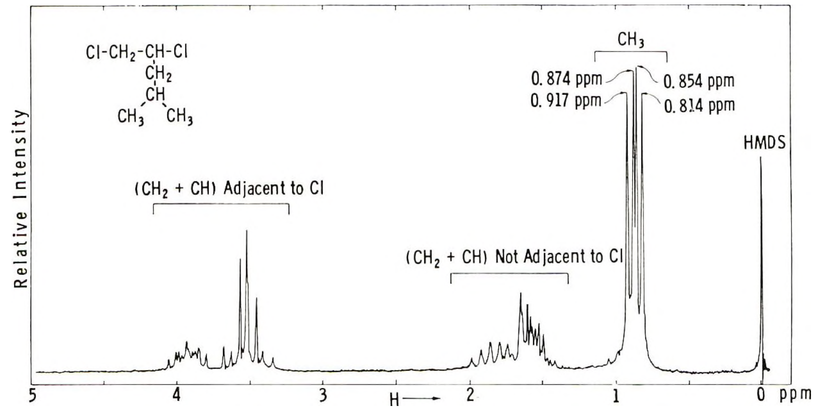

Fig. 4. 100 MHz PMR spectrum of 1,2-dichloro-4-methylpentane (solvent: 95% CCl_4 + 5% benzene, 35°C).

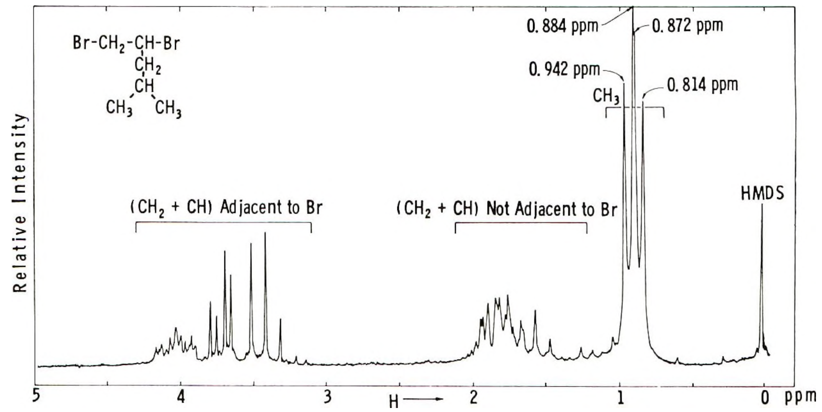

Fig. 5. 100 MHz PMR spectrum of 1,2-dibromo-4-methylpentane (solvent: 95% CCl_4 + 5% benzene, 35°C).

The 100 MHz high-resolution PMR spectra of 1,2-dichloro-4-methylpentane and 1,2-dibromo-4-methylpetane are presented in Figures 4 and 5. The peak assignments are indicated on the spectra. Due to magnetic nonequivalence of the CH_2 protons and spin-spin splitting, the spectra are very complex in both the CH_2 and CH proton regions. For this discussion the most significant portion of the spectra is the CH_3 proton region. In 1,2-dichloro-4-methylpentane (Fig. 4), the CH_2 resonance appears as a 1:1:1:1 quadrupelt centered at 0.86 ppm. corresponding to two sets of nonequivalent protons each of which is split into a doublet by the tertiary proton of the isopropyl group. In 1,2-dibromo-4-methylpentane (Fig. 5) the situation is similar, but the chemical shift difference of the nonequivalent methyl protons is such that the two inner peaks overlap and are just barely resolved. In effect, the resonance appears as a 1:2:1 triplet. It is significant, however, that those peaks which are separated by at least 2

2 cps are well resolved in both low molecular weight dihalogen compounds.

The PMR spectrum of the 4-methyl-1-pentene/SO_2 copolymer in the CH_3 proton region (Fig. 1) is similar to that of 1,2-dibromo-4-methylpentane. The protons of the two nonequivalent methyl groups are split into four peaks by the adjacent tertiary proton, but the two inner peaks overlap and the resonance resembles a triplet.* The apparently poor resolution of the polymer spectrum relative to the spectra of low molecular weight compounds (even for peaks separated by 3.7 cps) is due to constraints to chain motion which broaden the resonance and tend to obscure the finer details of the spectra.[12] A schematic representation of the methyl resonance of the compounds represented by the general formula V is shown in Figure 6. (The chemical shifts and coupling constants shown in this figure were confirmed by comparing spectra at both 60 and 100 MHz.)

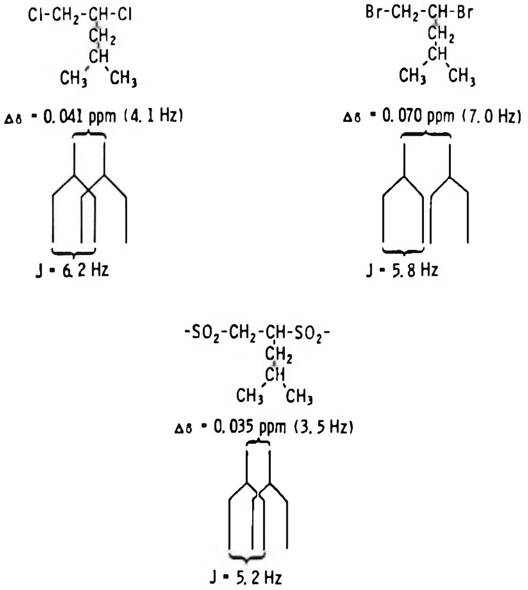

Fig. 6. Schematic representation of CH_3 resonance in 1,2-dichloro-4-methylpentane, 1,2-dibromo-4-methylpentane, and 4-methyl-1-pentene/SO_2 copolymer.

In the 5-methyl-1-hexene/SO_2 copolymer, where the center of asymmetry is further removed from the isopropyl group, the CH_3 protons are apparently magnetically equivalent. As expected, the resonance is split by the tertiary proton and the doublet separated by 6 cps is readily resolved (Fig. 2). Although in the spectrum of the analogous 1,2-dibromo-5-

---

* The magnetic nonequivalence of CH_2 protons in so-called racemic and meso diads or that of CH_3 protons in isotactic, syndiotactic, or heterotactic triads is a distinctly different phenomenon. In those cases, as it was first recognized by Bovey and Tiers;[11] nonequivalence results from the different relative configurations of two or three adjacent monomer units. In the examples discussed in this work, nonequivalence is independent of adjacent monomer units.

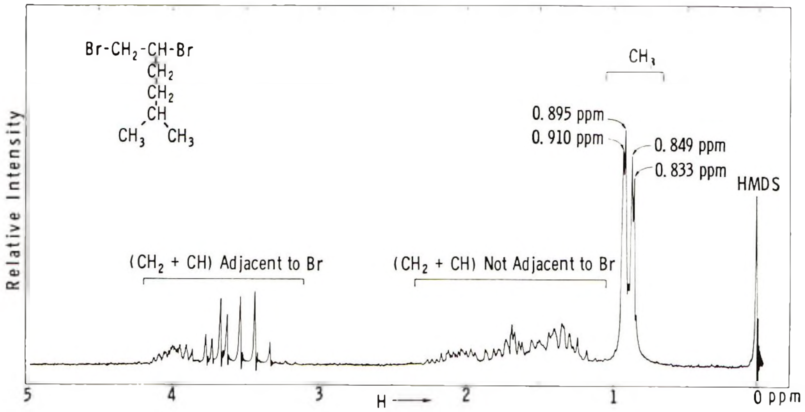

Fig. 7. 100 MHz PMR spectrum of 1,2-dibromo-5-methylhexane (solvent: 95% CCl_4 + 5% benzene, 35°C).

methylhexane (Fig. 7) the CH_3 protons of the isopropyl group are magnetically nonequivalent, the chemical shift difference is so small that the resulting pairs of split resonances are separated by only 1.5 cps. Such a small separation, even if it were present, could not be resolved in the copolymer because of line broadening.

In poly-4-methyl-1-pentene, prepared by Ziegler-Natta catalyst, the polymer structure around the main chain tertiary carbon atoms is symmetrical, and consequently the methyl protons are magnetically equivalent. As expected, the CH_3 resonance is split by the tertiary hydrogen; and the doublet separated by 6 cps is readily resolved. This is shown in Figure 8. The magnetic equivalence of the methyl groups in this polymer also indicates that the nonequivalency observed in the 4-methyl-1-pentene/SO_2 copolymer is not caused by "frozen" conformations associated with large rotational barriers, a fact also borne out of molecular model studies.

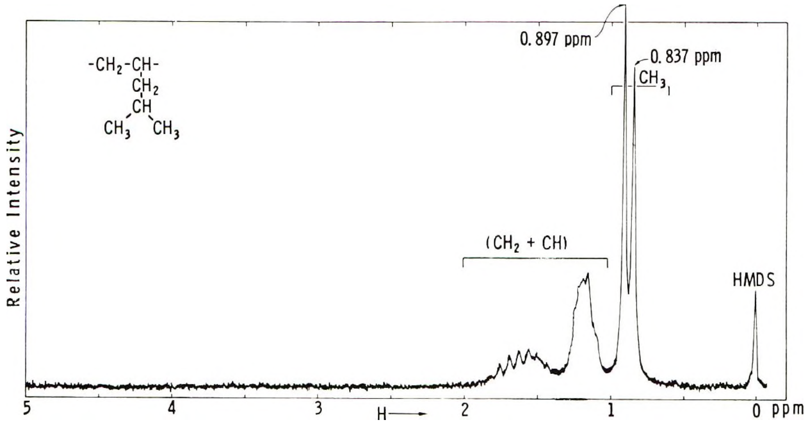

Fig. 8. 100 MHz PMR spectrum of poly-4-methyl-1-pentene (~4 wt-% copolymer in 1,3,5-trichlorobenzene, 170°C).

Another apparent anomaly in the PMR spectra of the SO_2 copolymers occurs at low magnetic field, between 3 and 4 ppm. Resonances in this region can be assigned to CH_2 and CH protons adjacent to a sulfur atom in the main chain of the copolymers. Normally, one would expect a CH_2 to CH proton ratio of 2:1, with the weaker CH resonance occurring at the lower magnetic field. However, in all three copolymers investigated in this work this intensity ratio appears to be reversed with the stronger resonance occurring at the lower magnetic field (Figs. 1, 2, and 3). This result can be explained by taking into account the nonequivalency of main chain CH_2 protons located close to a center of asymmetry. It is reasonable to assume that the resonance of one of the CH_2 protons is shifted to low field and it overlaps with the resonance of the CH proton. The comparison with analogous low molecular weight dihalogen compounds (Figs. 4 and 5) indicates that such an overlap is a distinct possibility.

As the result of these investigations it can be concluded that the PMR spectra of ω-alkyl-α-olefin/SO_2 copolymers are consistent with the unrearranged structure assigned to these compounds earlier, and the apparent spectral anomalies are readily explicable if the magnetic nonequivalence of protons located close to a center of asymmetry is considered.

References

1. R. Bacskai, *J. Polym. Sci. A-1*, **5**, 619 (1967).
2. R. Bacskai, paper presented at 150th Meeting, American Chemical Society, Atlantic City, September 1965.
3. C. Walling, in *Molecular Rearrangements, Part I*, P. De Mayo, Ed., Interscience, New York, 1963, p. 416.
4. J. Hine, *Physical Organic Chemistry*, McGraw-Hill, New York, 1962, p. 422.
5. C. Walling, *Free Radicals in Solution*, Wiley, New York, 1957, p. 224.
6. W. R. Edwards and N. F. Chamberlain, *J. Polym. Sci. A*, **1**, 2299 (1963).
7. J. P. Kennedy and A. W. Langer, Jr., *Fortschr. Hochpolymer Forsch.*, **3**, 523 (1964).
8. J. E. Goodrich and R. S. Porter, *J. Polym. Sci. B*, **2**, 353 (1964).
9. H. S. Gutowsky, *J. Chem. Phys.*, **37**, 2196 (1962).
10. P. M. Nair and J. D. Roberts, *J. Amer. Chem. Soc.*, **79**, 4565 (1957).
11. F. A. Bovey and G. V. D. Tiers, *J. Polym. Sci.*, **44**, 173 (1960).
12. D. W. McCall and W. P. Slichter, in *Newer Methods of Polymer Characterization*, B. Ke, Ed., Interscience, New York, 1964, p. 329.

Received June 10, 1968
Revised July 11, 1968

JOURNAL OF POLYMER SCIENCE: PART A-1 VOL. 7, 259-264 (1969)

Poly(vinyl 2-Furylacrylate), A New Photosensitive Polymer

MINORU TSUDA, *Government Chemical Industrial Research Institute, Tokyo, Hiratsuka, Kanagawa, Japan*

Synopsis

Poly(vinyl 2-furylacrylate), a new photosensitive polymer, was prepared, and its photosensitivity was investigated. The polymer cannot be synthesized by the usual procedure, condensation of poly(vinyl alcohol) and 2-furylacrylyl chloride in hot pyridine, but is easily prepared by the aqueous alkaline process, regardless of the degree of polymerization. Poly(vinyl 2-furylacrylate) is remarkably highly photosensitive and is spectrally sensitized by aromatic nitro compounds and aromatic carbonyl compounds. The mechanism of photochemical reaction is considered to involve the dimerization of the furylacrylyl group, and the quantum yield appears to be constant.

Introduction

Poly(vinyl 2-furylacrylate)(PVFA), a new photosensitive polymer, was prepared, and its photosensitivity was investigated in order to obtain a more photosensitive polymer than poly(vinyl cinnamate). PVFA cannot be synthesized by the ordinary procedure involving condensation of poly(vinyl alcohol) and 2-furylacrylyl chloride in hot pyridine, because PVFA is a thermosetting polymer and the product gels in the reaction vessel on heating. The polymer is easily prepared by the aqueous alkaline process[1] at a reaction temperature of −8 to −5°C, regardless of the degree of polymerization. PVFA has not been reported in the literature (Chemical Abstracts), possibly because of the difficulty of its synthesis.

PVFA is a remarkably photosensitive polymer, compared with poly(vinyl cinnamate), and is useful for many industrial purposes as a photosensitive resin. It forms a thick, lightly hardened film, and the film hardens by heating (burning-in); poly(vinyl cinnamate) also forms a thin lightly hardened film, but the burning-in is not effective.[2]

Synthesis

The synthesis was carried out by the reaction sequence (1).

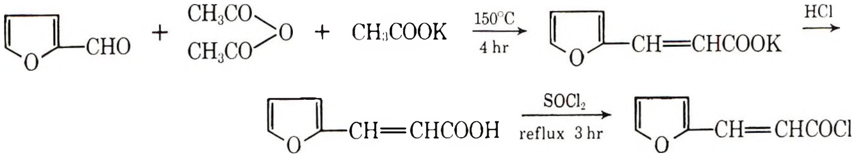

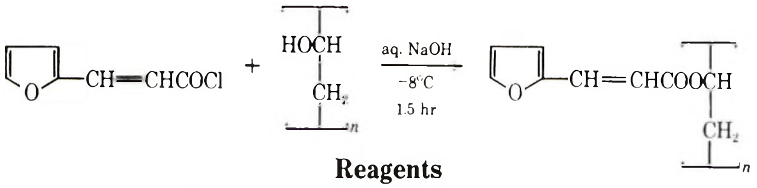

(1)

Reagents

2-Furylacrylic acid was prepared by the Perkin reaction,[3] mp 138–139°C.

To prepare 2-furylacrylyl chloride, 2-furylacrylic acid (138 g) was added to a benzene solution (500 ml) of thionyl chloride (230 g) at 70°C. The mixture was refluxed at 80°C for 3 hr. Benzene was distilled off, and furylacrylyl chloride was obtained from the residue at 90°C/2 mm Hg. The yield was 136 g (87%). The pale yellow crystals of the chloride were stored as methyl ethyl ketone solution.

Many kinds of poly(vinyl alcohol) were used. The average degree of polymerization was 500–2600 and the content of residual acetyl groups was 0–20 mole-%.

Procedure

Two solutions were prepared: solution A consisted of equal volumes of aqueous poly(vinyl alcohol)(PVA), 1 mole/l., aqueous sodium hydroxide, 4 mole/l., and methyl ethyl ketone; solution B consisted of 2-furylacrylyl chloride, 1.2 mole equivalents (to the hydroxyl group of PVA) and methyl ethyl ketone (1.4 volume). Solutions A and B were mixed and agitated for 90 min at −5 to −8°C. A few minutes later, the mixture separated into two layers; the product was contained in the upper layer. The solution of the upper layer could be used as a sensitizing solution. A pale yellow precipitate of PVFA formed in methanol. The yield was 75–80 wt-%. The reaction was not affected by the degree of polymerization and the residual acetyl group content.

Photosensitivity

The ultraviolet spectrum of PVFA film has a peak at about 297 mμ, extending to about 370 mμ.

PVFA shows photosensitivity. The mechanism of its photochemical reaction may be the same as that of poly(vinyl cinnamate), for the chemical structures of the two photosensitive groups are very similar.

The infrared spectra of PVFA before and after ultraviolet irradiation are

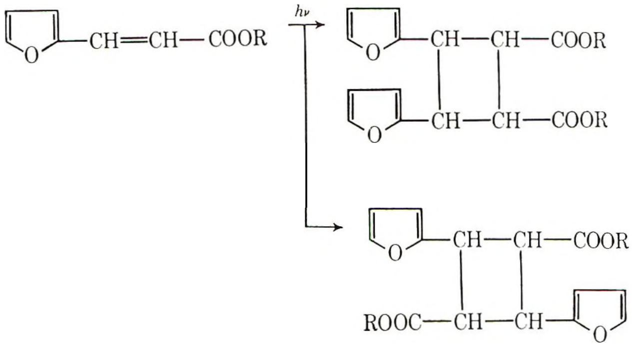

(2)

shown in Figure 1. After ultraviolet irradiation, conjugated double bonds (1640 cm^{-1}) decreased, and carbonyl groups of the ester of α,β-unsaturated carboxylic acid (1710 cm^{-1}) moved into the shorter wavelength region and approached that of saturated carboxylic acid. These phenomena are similar to those of ultraviolet irradiated poly(vinyl cinnamate). The change in the spectrum produced by ultraviolet irradiation is remarkable. The intensity of the absorptions becomes weak and the spectrum changes to a broad one; this may be attributable to the formation of crosslinks.

When we consider that the photochemical change in PVFA to be dimerization according to the eq. (2), the change on irradiation with light of energy dE may be proportional to the square of the number of photosensitive groups:[4]

$$dx/dE = K_1 (a - x)^2 \tag{3}$$

where x is the number of reacted photosensitive groups and a is the number of photosensitive groups at initiation. K_1 is a figure which is directly proportional to the quantum yield. The quantum yield is assumed to be constant in this case, and

$$dE = K_2 dt \tag{4}$$

where K_2 is a constant and t is the irradiation time. Integrating the equation obtained from eqs. (3) and (4), we obtain,

$$1/(a - x) - (1/a) = K_1 K_2 t \tag{5}$$

On the other hand, if Beer's law is satisfied at the absorption of 1640 cm^{-1},

$$K' (a - x + b) = -\log T \tag{6}$$

where b is the number of unpaired photosensitive groups which is known from the absorption spectrum at irradiation time $t \rightarrow \infty$. K' is the molecular extinction coefficient and T is the transmittance. Assuming $b = 0$ and combining eqs. (5) and (6) we obtain,

$$-(K_3/\log T) - 1 = K_4 t \tag{7}$$

where $K_3 = aK'$ and $K_4 = aK_1K_2$. The values of K_4 at various t are shown in Table I. K_4 is constant regardless of the change of t, and it may be

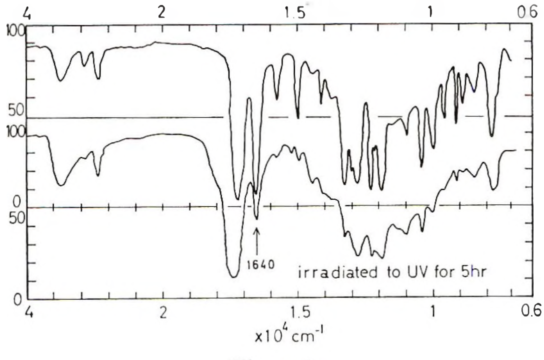

Figure 1.

TABLE I
Values of K_4

t, hr	$T \times 10^2$	K_4
0	8.7	
1	21.4	0.584
2	32.9	0.599
3	41.7	0.598
4	46.9	0.557
5	52.7	0.563
7	62.2	0.593
8	64.0	0.558
9	67.5	0.579
16	77.5	0.536

TABLE II
Sensitization of Poly(vinyl Cinnamate) and PVFA by Various Sensitizers

Polymer	Sensitizer	Relative sensitivity
Poly(vinyl cinnamate)[a]	None	0
	Picramide	400
	5-Nitroacenaphthene	1100
	N,*N*,*N*′,*N*′-Tetramethyl-4,4′-diaminobenzophenone	3200
	N,*N*,*N*′,*N*′-Tetraethyl-4,4′-diaminobenzophenone	3300
PVFA	None	4400
	Aromatic nitro compounds	
	4-Nitroaniline	9900
	2-Nitrofluorene	44550
	5-Nitroacenaphthene	29700
	2,6-Dichloro-*N*,*N*-dimethyl-4-nitroaniline	9900
	2,6-Dibromo-*N*,*N*-dimethyl-4-nitroaniline	14850
	4-Nitroacetanilide	14850
	N-Acetyl-4-nitro-1-naphthylamine	29700
	Aromatic carbonyl compounds	
	N,*N*,*N*′,*N*′-Tetramethyl-4,4′-diaminobenzophenone	89100
	N,*N*,*N*′,*N*′-Tetraethyl-4,4′-diaminobenzophenone	89100
	N,*N*-Dimethyl-4-aminobenzophenone	44550
	Anthraquinone	29700
	2-Methylanthraquinone	9900
	2-Ethylanthraquinone	44550
	2-Amylanthraquinone[b]	44550

[a] Prepared by the aqueous alkaline process.

[b] Mixture of *n*-amyl and isoamyl compounds.

concluded that the theoretical equation is in good agreement with the experimental data. The value of K_4 at $t = 16$ hr is rather small. This fact shows that b is not negligible when $a - x$ is small. Using the method of least squares, we obtain

$$b/(a + b) = 0.00995$$

since $a + b$ is the total number of photosensitive groups, b is about 1%. The value of T was determined by the baseline method.

Sensitization

PVFA is spectrally sensitized by aromatic nitro compounds and aromatic carbonyl compounds. Since the sensitizers of poly(vinyl cinnamate) are used for PVFA, the mechanism of sensitization is considered to be the same as that[5] of poly(vinyl cinnamate).

Sensitivity was measured by the gray scale method.[6] The light source was a super high-pressure mercury arc lamp (100 W), and poly(vinyl cinnamate) sensitized by picramide was used as a standard, for which the sensitivity was assumed to be 400. The concentration of sensitizer was 10 wt-% of the polymer. The measured values of the relative sensitivity are shown in Table II.

Appendix

From eqs. (4) and (5), the following equation is obtained:

$$\frac{\log T_0 \,[1 - (b/a + b)]}{\log T - \log T_0 \,(b/a + b)} = K_4 t + 1 \tag{8}$$

where

$$-\log T_0 = K' \,(a + b)$$

$b/(a + b)$ and K_4 are obtained by the method of least squares. We write

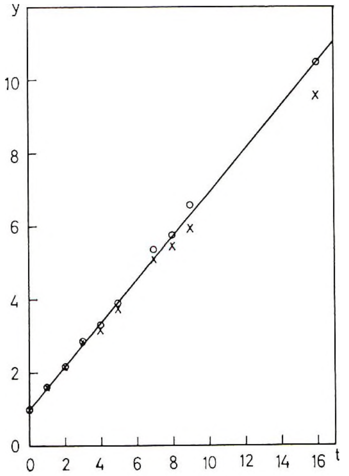

Figure 2.

here y for the left-hand side of the eq. (8), and the relationship between y and t is shown in Figure 2.

Mr. Y. Inukai communicated to the author their success in the synthesis of PVFA from PVA and chloride by the reaction in pyridine for 20 hr at 30°C only when the degree of polymerization was lower than 500; but they could not synthesize high molecular weight compounds. They also found the polymer had a higher photosensitivity than poly(vinyl cinnamate). The results were reported in the bulletin of their institute: Nagoyashi Kogyokenkyusho Kenkyuhokoku, No. 23,46 (1963).

References

1. M. Tsuda, *Makromol. Chem.*, **72,** 174, 183 (1964).
2. M. Tsuda, et al., *Nippon Shashin Gakkaishi,* **28,** 211 (1965).
3. *Organic Syntheses, Coll. Vol. III,* E. C. Horning, Ed., Wiley, New York, p. 426, 1962.
4. M. Tsuda, *J. Polym. Sci. A*, **2,** 2907 (1964).
5. M. Tsuda, *J. Polym. Sci. B,* **2,** 1143 (1964).
6. L. M. Minsk et al., *J. Appl. Polym. Sci.,* **2,** 302 (1959).

Received April 15, 1968

JOURNAL OF POLYMER SCIENCE: PART A-1 VOL. 7, 265–268 (1969)

Tri-o-tolylphosphine: A Rapid Photopolymerization Initiator

ROGER J. ELDRED, *General Motors Research Laboratories, Warren, Michigan 48090*

Synopsis

The rate of tri-*o*-tolyphosphine-initiated photopolymerization of methyl methacrylate was found to be significantly higher than that for the triphenylphosphine initiated polymerization. The mechanism was shown to be dependent upon the concentration of the initiator. At low concentrations (10^{-4} mole/l.), an activated complex is the initiating species, while at higher concentrations (above 10^{-2} mole/l.) homolytic cleavage of the phosphorus–carbon bond is the radical source. Steric inhibition of resonance is advanced as an explanation for the enhanced activity of tri-*o*-tolylphosphine over triphenylphosphine.

The use of triphenylphosphine as a photoinitiator for polymerization has been reported earlier.[1] It was shown that the polymerization was free-radical in nature and that the activity of the phosphine at low concentrations was restricted to acrylic monomers. The findings presented here are an extension of the previous investigation to the study of the tritolylphosphines, and specifically tri-*o*-tolylphosphine.

Experimental

The tritolylphosphines were obtained from Eastman Chemical Products, Inc. and purified by recrystallization from absolute ethanol. Methyl methacrylate was distilled from partially polymerized monomer immediately prior to use to ensure the absence of any inhibitor.[2]

The reaction mixtures were irradiated with light from a 450-W Hanovia medium-pressure lamp. The photopolymerization procedure has been described elsewhere.[1] Ultraviolet spectra were obtained on a Cary 14 recording spectrophotometer with cells having a 1 cm optical path.

Results

The results of the kinetic studies of methyl methacrylate polymerization photoinitiated by the three tritolylphosphines are given in Table I. The rates were corrected for the polymerization due to autocatalyzed reaction which amounted to 0.97×10^{-4} mole/l.-sec. It can be seen that the order of initiator effectiveness was *ortho* > *meta* > *para*. Because of the high autocatalyzed rate, the differences in the rates for the *meta*, *para*, and par-

TABLE I
Rate of Polymerization of Methyl Methacrylate

Initiator	Concentration × 10^4, mole/l.	Corrected rate × 10^4, mole/l.-sec
$(o\text{-}CH_3C_6H_4)_3P$	8	8.84
$(m\text{-}CH_3C_6H_4)_3P$	8	3.89
$(p\text{-}CH_3C_6H_4)_3P$	8	2.34
$(C_6H_5)_3P$	8	3.36

ent compound are not thought to be significant. However, it was thought that the unexpectedly high rate of polymerization caused by tri-*o*-tolylphosphine warranted further investigation of this compound.

The effect of tri-*o*-tolylphosphine concentration on the rate of photopolymerization of methacrylate was determined and is shown in Figure 1. The rate increased with increasing initiator concentration until a maximum was reached at 3 × 10^{-3} mole/l., whereupon the rate decreased with further increases in initiator. This behavior is similar to that observed with the parent compound, triphenylphosphine.[1] However, an increase in the concentration of tri-*o*-tolylphosphine above 2 × 10^{-2} mole/l. again was accompanied by an increase in rate. The upswing in the rate at these concentrations was also observed with triphenylphosphine.

Although tri-*o*-tolyl compound is much more reactive, there does not appear to be any difference in the slopes of the curves, thus indicating that the photoinitiating action of the two compounds is the same. Fur-

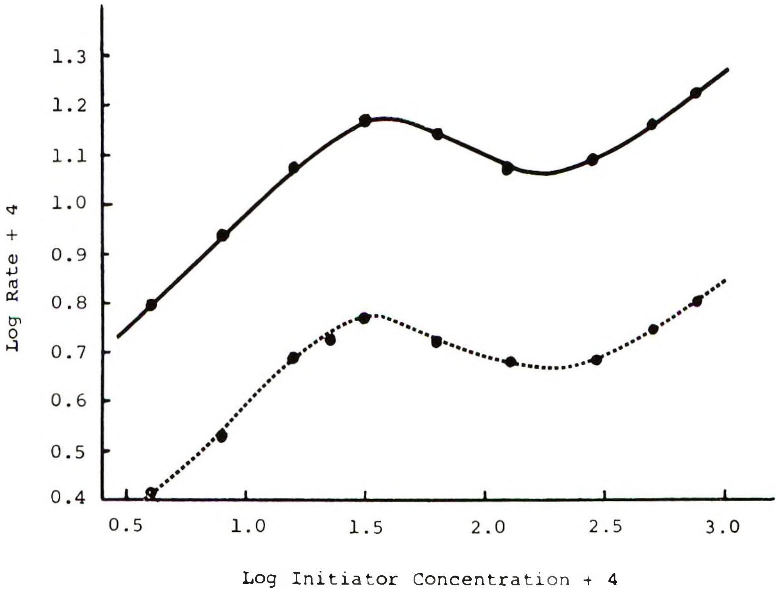

Fig. 1. Effect of initiator concentration on the rate of polymerization of methyl methacrylate: (——) $(o\text{-}CH_3C_6H_4)_3P$; (- - -) $(C_6H_5)_3P$.

TABLE II
Ultraviolet Spectra of Tolylphosphines in Methyl Methacrylate

Initiator	Concentration $\times 10^4$, mole/l.	λ_{max}, mμ	ϵ_{max}
$(o\text{-}CH_3C_6H_4)_3P$	1	292	8,100
$(m\text{-}CH_3C_6H_4)_3P$	1	292	4,900
$(p\text{-}CH_3C_6H_4)_3P$	1	292	5,100
$(C_6H_5)_3P$	1	292	7,300

ther evidence for this is afforded by the ultraviolet spectra of the three tolylphosphines in monomer, given in Table II. A complex peak at 292 mμ, the same wavelength previously reported for triphenylphosphine in methyl methacrylate, was observed in each case.

Discussion

The unusual effect of initiator concentration on the rate of polymerization can be explained on the basis of a dual mechanism. At lower concentrations, initiation occurred via interaction of light with the phosphine–monomer complex. At the maximum of the curve in Figure 1, a self-quenching of the excited complex similar to that reported for anthracene[3] became noticeable, and the rate decreased with increasing concentration. The subsequent increase in rate can be accounted for by polymerization initiated by free radicals from the photolytic homolysis of the phosphorus-carbon bond. That such free radicals are formed has been shown by Kaufman and Griffin[4] in their study of the ultraviolet irradiation of triphenylphosphine. As further evidence of homolysis at these concentrations, styrene was successfully photopolymerized with both tri-o-tolylphosphine and triphenylphosphine.

The difference in effectiveness between the two initiators can be explained by a combination of inductive and steric effects. In a re-evaluation of the work of Schindlbauer,[5] Halpern and Mislow[6] have shown that a torsional angle about the phosphorus–carbon bond exists in the tritolylphosphines. This angle is dependent upon the position of the methyl group. A bulky substituent would force the phenyl rings out of plane and destroy the resonance participation of the phosphorus electrons throughout the ring system.

In the mechanism operating at low initiator concentrations, the higher reactivity of tri-o-tolylphosphine can be explained by either the inductive effect of the methyl group or the steric effect on resonance. In either case, the resultant increase in electron density at the phosphorus atom probably aids in the stabilization of the excited complex providing a greater population in this state and therefore, more initiating radicals.

At concentrations above 2×10^{-2} mole/l., where homolysis is significant, the higher rate can be accounted for by a weaker phosphorus–carbon bond. In this case, the inductive effect should make the *ortho* methyl compound less reactive as evidenced by the work of Kaufman and Griffin,[4] in which it was shown that the *p*-tolyl group is more stable toward photolytic homolysis than the phenyl group. Therefore, the destruction of resonance in the out-of-plane conformation caused by the bulky methyl group must be sufficient to overcome the inductive effect and to significantly increase the ease of the homolysis.

References

1. T. J. Mao and R. J. Eldred, *J. Polym. Sci. A-1*, **5,** 1741 (1967).
2. P. D. Bartlett and K. Nozaki, *J. Amer. Chem. Soc.*, **68,** 2377 (1946).
3. R. G. W. Norrish and J. P. Simons, *Proc. Roy. Soc.* (London), **A251,** 4 (1959).
4. M. L. Kaufman and C. E. Griffin, *Tetrahedron Letters*, **1965,** 769.
5. H. Schindlbauer, *Monatsh. Chem.*, **96,** 1793 (1965).
6. E. J. Halpern and K. Mislow, *J. Amer. Chem. Soc.*, **89,** 5224 (1967).

Received February 20, 1968.
Revised July 8, 1968.

JOURNAL OF POLYMER SCIENCE: PART A-1 VOL. 7, 269-281 (1969)

Effects of Iron(III) Chloro Complexes on the Polymerization of Styrene

N. N. DASS and M. H. GEORGE, *Department of Chemistry, Imperial College, London, England*

Synopsis

The polymerization of styrene initiated by 2,2′-azobisisobutyronitrile has been studied in *N*,*N*-dimethylformamide solution at 60°C in the presence of hexakis(*N*,*N*-dimethylformamide) iron(III) tetrafluoroborate alone, and also in the presence of added lithium chloride. The presence of $Fe(DMF)_6^{3+}$ ions in the polymerizing systems caused retardation, but iron(III) chloro complexes produced well defined inhibition periods. Velocity constants at 60°C for polystyryl radicals towards $Fe(DMF)_6^{3+}$, $Fe(DMF)_5Cl^{2+}$, $Fe(DMF)_4Cl_2^{+}$, and $FeCl_4^{-}$ ions were calculated to be 847, 4.15×10^4, 6.55×10^4, and 3.14×10^4 l./mole-sec, respectively. Values of the initiator efficiency *f* for most systems investigated ranged from 0.59 to 0.62.

INTRODUCTION

In recent years there has been increasing interest in the kinetics of reactions between polyvinyl radicals and transition metal salts in nonaqueous solutions. Under appropriate conditions, ferric chloride in *N*,*N*-dimethylformamide (DMF) solution acts as an "ideal" retarder in the polymerization of styrene, since growing polystyryl radicals then react to give products incapable of further reaction.[1-3] In such circumstances kinetic analysis is simplified, and rates of initiation may be determined by the induction period technique or by measurements of the rate of formation of ferrous ions. Both techniques applied to styrene polymerization give results in good agreement.[4]

However, the precise nature of the polymer radical–substrate reaction has remained obscure, though it was realized that various complex ions of iron(III) might exist in monomer–DMF solution.[1,2,5] Recently, the complex ions produced when ferric chloride is dissolved in DMF and DMF–styrene solutions have been identified.[6] This paper reports the evaluation of the various kinetic constants at 60°C for the reaction of polystyryl radicals with individual iron(III) complex ions.

EXPERIMENTAL

Materials

The initiator 2,2′-azobisisobutyronitrile[7] (AIBN), *N*,*N*-dimethylformamide[8] (DMF), and styrene[9] were purified as described previously. The monomer and DMF were finally dried over calcium hydride, and the monomer was stored at −78°C under oxygen-free nitrogen until required.

The method of preparation and purification of hexakis(*N*,*N*-dimethylformamide) iron(III) tetrafluoroborate, $Fe(DMF)_6$–$(BF_4)_3$, A, has already been described.[6]

Laboratory reagent lithium chloride (B.D.H.) and anhydrous ferric chloride (Hopkin and Williams) were used directly in certain experiments. 1,10-Phenanthroline hydrate (Hopkin and Williams) was recrystallized from absolute AR ethyl alcohol and dried *in vacuo* before use in polymerization experiments, but was used as the monohydrate for estimating concentrations of ferrous ions in DMF–styrene mixtures spectrophotometrically. 1,10-Phenanthroline–ferrous perchlorate (Hopkin and Williams) was used to calibrate the spectrophotometric determination of iron(II) ions.

Procedure

Rates of polymerization were measured dilatometrically in the usual way,[7] care being taken to degas the reactants thoroughly before sealing off the dilatometers. In some experiments dilatometers with a bulb capacity of about 30 ml, and a capillary of 1.0 mm diameter were used to increase the accuracy of measuring reduced rates of polymerization.

Ultraviolet absorption spectra were recorded with a Unicam SP800 or SP500 spectrometer using matched quartz cells against DMF–styrene mixtures containing lithium chloride when appropriate.

Some determinations of iron(II) species produced in polymerizing styrene–DMF mixtures in the presence of AIBN and added iron(III) complexes were made by ceric titrations, after diluting the systems with excess DMF. However, the spectrophotometric determination, based on the formation of the tris(*o*-phenanthroline) complex of iron(II) was more successful. Polymerizations were then performed in small reaction tubes at 60°C, and at the end of a known time, a tube was cooled rapidly, cracked open and a 6:1 ratio of 1,10-phenanthroline based on the initial iron(III) concentration was added. Absorbancy readings for the solutions were measured at 518 mμ, at room temperature. The method was calibrated by using 1,10-phenanthroline ferrous perchlorate dissolved in similar DMF–styrene mixtures in the presence of lithium chloride.

Beer's law was obeyed up to a concentration of 1.8×10^{-4} mole/l. of ferrous ions with a molar absorptivity ϵ of 10,490 l./mole cm.

RESULTS AND DISCUSSION

Measurements with Ferric Chloride Alone

Some experiments were performed with the use of AIBN to initiate the polymerization of styrene in DMF at 60°C in the presence and absence of anhydrous ferric chloride.

Polystyryl radicals react with the species produced when ferric chloride is dissolved in DMF–styrene so readily that well defined induction periods are produced, at the end of which the rate rapidly attains that expected in the absence of ferric chloride. Typical results, in excellent agreement with those of Bamford et al.,[1] are shown in Figure 1.

A simple kinetic scheme has been used to explain the results,[1,10] assuming that ferric chloride exists as a single entity:

Initiation:

$$\mathrm{In} \rightarrow 2\mathrm{R}_c\cdot \tag{1a}$$

$$\mathrm{R}_c\cdot + M \rightarrow \mathrm{R}_1\cdot \tag{1b}$$

where the velocity constant of (1a) is k_d, and the rate of initiation is I.

Propagation:

$$R_r\cdot + \mathrm{M} \rightarrow \mathrm{R}_{r\cdot+1} \tag{2}$$

where the velocity constant is k_p.

Termination by Ferric Chloride:

$$\mathrm{R}_r\cdot + \mathrm{FeCl}_3 \rightarrow \mathrm{P}_r + \mathrm{FeCl}_2 \tag{3}$$

where the velocity constant is k_5.

Mutual Termination of Polystyryl Radicals:

$$\mathrm{R}_r\cdot + \mathrm{R}_s\cdot \rightarrow \mathrm{P}_{r+s} \tag{4}$$

where the velocity constant is $2k_t$.

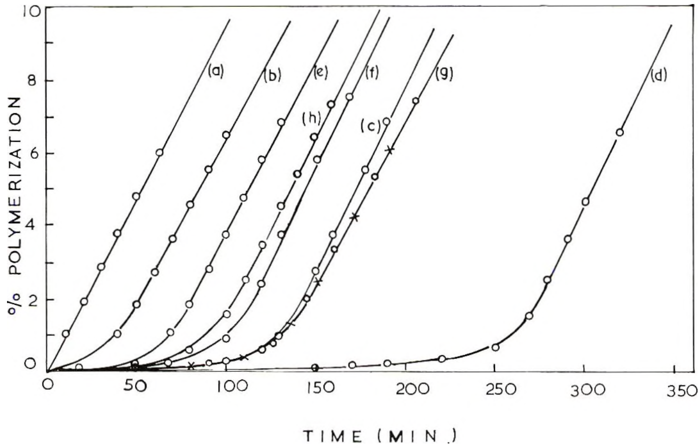

Fig. 1. Polymerization of styrene in DMF solution at 60°C initiated by AIBN in the presence of various iron(III) species: (*a*) no added iron(III) compound. (*b*) $[\mathrm{FeCl}_3]_0 = 2.62 \times 10^{-3}$ mole/l.; (*c*) $[\mathrm{FeCl}_3]_0 = 7.87 \times 10^{-3}$ mole/l.; (*d*) $[\mathrm{FeCl}_3]_0 = 1.58 \times 10^{-2}$ mole/l.; (*e*) molar ratio LiCl: A = 0.25:1, [A] = 7.87×10^{-3} mole/l.; (*f*) molar ratio LiCl: A = 1:1, [A] = 7.87×10^{-3} mole/l.; (*g*) (○) results for a molar ratio LiCl: A = 2:1; (×) results for a molar ratio of LiCl: A = 3:1, [A] = 7.87×10^{-3} mole/l.; (*h*) molar ratio LiCl: A = 10:1, [A] = 7.87×10^{-3} mole/l. At 60°C., [styrene] = 2.490 mole/l.; [DMF] = 8.792 mole/l.; [AIBN] = 7.72×10^{-2} mole/l.

In represents the initiator, AIBN, $R_c\cdot$ is a radical produced by direct decomposition of AIBN, $R_1\cdot$, $R_r\cdot$, and $R_s\cdot$ are all growing radicals, and M and P represent monomer and dead polymer molecules, respectively.

A stationary-state treatment leads to eq (5):

$$-(1/\phi_t) + \ln[(1 + \phi_t)/(1 - \phi_t)] = k_5[R\cdot]_s t + A^* \tag{5}$$

where ϕ_t is the reduced rate, equal to the ratio of the rate at any time t in the presence of ferric chloride to the final maximum rate, $[R\cdot]_s$ is the final maximum radical concentration when all of the ferric chloride has disappeared, and A^* is an integration constant.

Furthermore, if τ is defined as the time when the rate of polymerization has attained a value 0.648 of the final maximum value,

$$\tau = [FeCl_3]_0/I \tag{6}$$

where $(FeCl_3)_0$ is the initial concentration of ferric chloride at time $t = 0$. The rate of initiation I in any experiment may be expressed by the equation:

$$I = 2k_d f[\overline{In}] \tag{7}$$

where $[\overline{In}]$ is the mean initiator concentration and f is the initiator efficiency.

Further experiments with ferric chloride at 60°C indicated that with constant [M], [DMF], and $[FeCl_3]_0$, there was a linear relationship between τ^{-1} and $[\overline{In}]$. Again, for a series of experiments in which $[\overline{In}]_0$ was maintained constant but $[FeCl_3]_0$ was varied, there was a linear relationship between $(\overline{In})\ \tau$ and $[FeCl_3]_0$. Both these relationships may be predicted from eqs. (6) and (7); on assuming a value of k_d of 1.2×10^{-5} sec^{-1},[11,12] a mean value of f of 0.60 was obtained.

Expansion of the Kinetic Scheme

However, the above treatment is only approximate, since it has been shown[6] that when iron(III) chloride is dissolved at low concentrations in DMF–styrene mixtures at 60°C, the principal ionic species present are $Fe(DMF)_4Cl_2^+$ and $FeCl_4^-$.

A generalized kinetic scheme for systems containing arbitrary concentrations of iron(III) and chloride ions has, therefore, to include reactions of polymer radicals with $Fe(DMF)_6^{3+}$, $Fe(DMF)_5Cl^{2+}$, $Fe(DMF)_4Cl_2^+$, and $FeCl_4^-$, with corresponding velocity constants k_x, k_6, k_7, and k_8, respectively. For convenience in writing only, some of the ionic species have been represented as inner-sphere, rather than outer-sphere complexes.

The precise significance of the previous value of f is thus difficult to assess. For similar reasons, a detailed analysis of the ϕ_t–time t data by the method of Bamford et al.[1] was not made for the results obtained with ferric chloride alone.

It was confirmed spectroscopically that iron(II) species were produced, at least in part, by polystyryl radical attack on all of the iron(III) species studied. The value of k_x was determined by experiments involving the complex $Fe(DMF)_6-(BF_4)_3$, A, while k_6, k_7, and k_8 were evaluated by the study of polymerizing styrene systems containing A and added lithium chloride. Various ionic equilibria of the following type also have to be considered:[6,13]

$$Fe(DMF)_6^{3+} \rightleftharpoons Fe^{3+} + 6\ DMF \tag{8}$$

$$Fe(DMF)_6^{3+} + Cl^- \rightleftharpoons Fe(DMF)_5Cl^{2+} + DMF \tag{9}$$

$$Fe(DMF)_5Cl^{2+} + Cl^- \rightleftharpoons Fe(DMF)_4Cl_2^+ + DMF \tag{10}$$

$$Fe(DMF)_4Cl_2^+ + 2Cl^- \rightleftharpoons FeCl_4^- + 4\ DMF \tag{11}$$

It was checked that addition of lithium chloride alone, over the concentration range used in later experiments, produced no retardation or inhibition of the polymerization of styrene in DMF initiated by AIBN at 60°C.

Some rate measurements were also performed when 1,10-phenanthroline was added in varying amounts to the polymerizing styrene systems in the presence of anhydrous ferric chloride. Values of τ at 60°C were essentially identical to those observed in the absence of 1,10-phenanthroline. Since the latter functions predominantly by complexing with ferrous ions produced by iron(III)–radical interaction, it appears that a polystyryl radical is insufficiently electrophilic to accept an electron from an iron(II) species, and cause regeneration of an iron(III) ion:

$$Fe^{2+} + R_r\cdot \rightarrow Fe^{3+} + R_r:^- \tag{12}$$

Rate Measurements with Complex A; Evaluation of k_x

The tetrafluoroborate salt, A, $Fe(DMF)_6-(BF_4)_3$, was selected for study, since the BF_4^- ion shows little tendency to complex, and $Fe(DMF)_6^{3+}$ ions are formed in DMF–styrene mixtures.[6]

On polymerization of styrene at 60°C in the presence of AIBN, DMF, and A, retarded rates of polymerization were recorded dilatometrically. The rate results were analyzed by the method of Kice,[14,15] assuming that the equilibrium (8) was well over to the left-hand side. This kinetic scheme includes the steps of initiation, propagation, and mutual termination of polymer radicals and also the steps of eqs. (13)–(16), where Z· represents any species formed by reaction between a polymer radical and complex A, which, *a priori*, might be a radical.

Transfer:

$$R_r\cdot + A \rightarrow Z\cdot + P_r \tag{13}$$

where the velocity constant is k_x.

Copolymerization:

$$Z\cdot + M \rightarrow R\cdot \tag{14}$$

where the velocity constant is k_0.

Cross-termination:

$$Z\cdot + R_r\cdot \rightarrow \text{inert product} \tag{15}$$

where the velocity constant is k_c

Mutual Termination of Z· Radicals:

$$Z\cdot + Z\cdot \rightarrow \text{inert products} \tag{16}$$

where the velocity constant is $2k_z$.

If ϕ is defined as the ratio of the retarded rate of polymerization to the rate in the absence of retarder A, c is a constant equal to $(4k_tk_z/k_c^2)$, R_p is the fractional rate of polymerization, $-d(\ln[M])/dt$, in sec^{-1}, and experiments are conducted at constant [M] and [DMF], then

$$R_p\sqrt{1+\frac{c(1-\phi^2)}{\phi^2}} = \frac{k_pk_x}{2k_t}\,\frac{\phi^2[A]}{(1-\phi^2)}\left\{1+\sqrt{1+\frac{c(1-\phi^2)}{\phi^2}}\right\} - \frac{k_0k_p[M]}{k_c} \tag{17}$$

Thus a plot of the left hand side of eq. (17) against $\{\phi^2[A]/(1-\phi^2\}\{1+\sqrt{1+[c(1-\phi^2)/\phi^2]}\}$ at constant [M] should give a slope of $(k_pk_x/2k_t)$ and an intercept on the vertical axis of $-(k_0k_p/k_c)[M]$.

A value of c of 1×10^{-6} was chosen to give the least deviation of the experimental points from a straight line, and the results are collected in Table I and plotted in Figure 2.

The slope of the line in Figure 2 is 2.07×10^{-3} l./mole sec, and using values[16] of k_p and $2k_t$ equal to 176 and 7.2×10^7 l./mole-sec, respectively, k_x was 847 l./mole sec. From the intercept, (k_0/k_c) was 2.31×10^{-10} at 60°C.

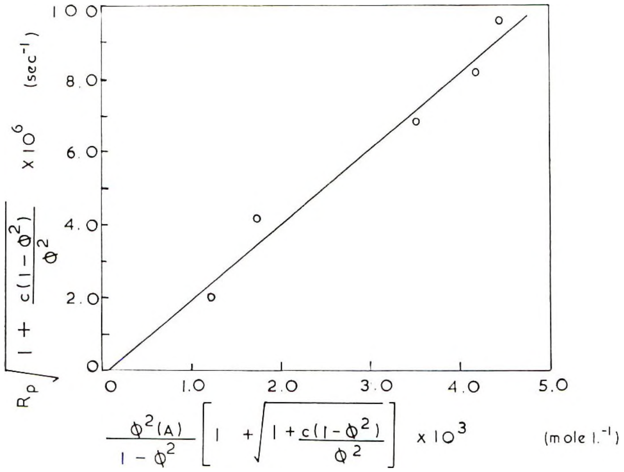

Fig. 2. Kice plot of retardation results with complex A alone. At 60°C., [styrene] = 2.490 mole/l.; [DMF] = 8.792 mole/l.; value of c chosen = 1.0×10^{-6}.

TABLE I

Effect of Complex A on the Polymerization of Styrene Initiated by AIBN in DMF Solution at 60°C[a]

[AIBN] $\times 10^2$, mole/l.	Rate of polymerization $\times 10^5$, mole/l. sec	Retarder concentration [A] $\times 10^3$, mole/l.	$\frac{\phi_2[A]}{1-\phi^2}\ 1+\left[\sqrt{1+\frac{c(1-\phi^2)}{\phi^2}}\right]$ $\times 10^3$, mole/l.	$R_p\sqrt{1+\frac{c(1-\phi^2)}{\phi^2}}$ $\times 10^6$, sec^{-1}
7.618	3.979	0.000	—	—
7.618	2.390	3.936	4.443	9.598
7.618	2.035	5.904	4.183	8.173
7.618	1.701	7.873	3.521	6.831
7.618	1.037	11.909	1.736	4.165
1.404	1.859	0.000	—	—
1.404	0.500	7.873	1.228	2.008

[a] [M] = 2.490 mole/l.; [DMF] = 8.792 mole/l.; value of c chosen = 1.0×10^6.

The low value of (k_0/k_c) indicates a low tendency of Z· species to attack monomer. The transfer constant for polystyryl radicals to DMF is only 4.0×10^{-4} at 60°C, and involves hydrogen atom abstraction from a CH_3 group.[9] Hence, unless the reactivity of a DMF molecule is greatly increased when it is a ligand in the complex ion, another type of radical–A reaction must also occur to explain the relatively high value of k_x. This might be as shown in eq. (18),

$$\sim CH_2\dot{C}HPh + Fe(DMF)_6^{3+} + 3BF_4^- \rightarrow \sim CH{=}CHPh + H^+BF_4^- + Fe(DMF)_6^{2+} + 2BF_4^- \quad (18)$$

for which the products are completely inert.

Effect of Adding LiCl to A on Rates of Polymerization

On progressively adding lithium chloride to mixtures of constant composition containing styrene, DMF, AIBN, and complex A, and measuring rates at 60°C, definite induction periods were observed, as indicated in Figure 1. A plot of τ, evaluated from individual rate curves, against concentration of lithium chloride added is shown in Figure 3, and this suggests that the various iron(III)–chloro complexes are all much more reactive towards polystyryl radicals than $Fe(DMF)_6^{3+}$ ions.

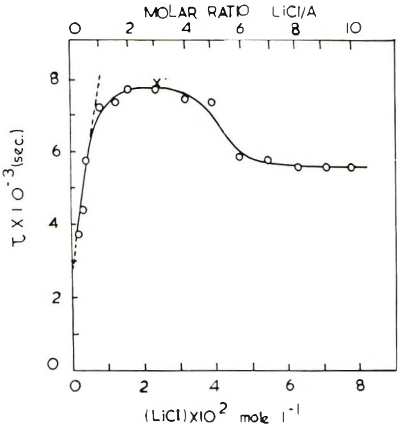

Fig. 3. Induction period τ as a function of added lithium chloride concentration. At 60°C., [styrene] = 2.490 mole/l.; [DMF] = 8.792 mole/l.; [A] = 7.87×10^{-3} mole/l.; [AIBN] = 7.62×10^{-2} mole/l.

The rate curves for molar ratios of LiCl to A of 2:1 and 3:1 were almost identical, but curve *g* of Figure 1 was not identical with that for ferric chloride at an equal concentration of iron(III), as might have been expected, although the τ values differed by only 3 min (Fig. 3).

Analysis of Results up to a Molar Ratio of [LiCl]/[A] of 1:1

Spectroscopic evidence[6] suggests that up to a 1:1 molar ratio of LiCl to A, $Fe(DMF)_5Cl^{2+}$ ions are progressively formed by the equilibrium reaction (9), which has a relatively high equilibrium constant. Since no chlorine could be found by microanalysis in low molecular weight polymers formed during induction periods, the predominant inhibition reaction may be written:

$$\sim\!\!\sim CH_2\dot{C}HPh + Fe(DMF)_5Cl^{2+} \rightarrow \sim\!\!\sim CH{=}CHPh + Fe(DMF)_6{}^{2+} + H^+Cl^- \quad (19)$$

and presumably the $Fe(DMF)_5{}^{2+}$ ion rapidly acquires another DMF molecule to become $Fe(DMF)_6{}^{2+}$.

In this case, the total τ value will depend on the initial equilibrium concentration of $Fe(DMF)_5Cl^{2+}$ ions and also on the concentration of $Fe(DMF)_5Cl^{2+}$ ions formed by equilibrium (9) as Cl^- ions are liberated in the reaction (19). If $[A]_0$ and $[Cl^-]_0$ are the initial concentrations of A and LiCl, and the equilibrium constant in (9) is high, the initial concentrations of $Fe(DMF)_6{}^{3+}$ and $Fe(DMF)_5Cl^{2+}$ are, $[A]_0 - [Cl^-]_0$ and $[Cl^-]_0$, respectively.

By analogy with eq (6),

$$\tau = \frac{k'\{[A]_0 - [Cl^-]_0\}}{I} + \frac{[Cl^-]_0}{I} = \frac{k'[A]_0}{I} + [Cl^-]_0\left(\frac{1}{I} - \frac{k'}{I}\right) \quad (20)$$

where the first term on the right-hand side of eq. (20) allows for the conversion of $Fe(DMF)_6{}^{3+}$ to $Fe(DMF)_5Cl^{2+}$, and k' is an arbitrary constant.

In accordance with this prediction, Figure 3 gave an initially linear plot of τ against $[Cl^-]_0$ up to a molar ratio of LiCl/A of 1:1. The slope was 5.748×10^5 sec-l./mole and intercept 2847.6 sec, and these values give a rate of initiation I equal to 1.07×10^{-6} mole/l.-sec. This is reasonable, since for $[\overline{In}]$ equal to 7.31×10^{-2} mole/l. over the range considered and k_d equal to 1.2×10^{-5} sec^{-1}, the initiator efficiency f is 0.62.

Again when both A and added LiCl have a concentration of 7.873×10^{-3} mole/l. at 60°C, the value of τ was 7,200 sec. Writing,

$$\tau = [Fe(DMF)_5Cl^{2+}]_0/I = [Cl^-]_0/I \quad (21)$$

and using the above-mentioned values of k_d and $(\overline{In})$, the value of f is 0.61. These values of f are in good agreement with other literature values,[17] although the dependence on the value of k_d used is clear.

A detailed analysis of the rate curve measured with a 1:1 molar ratio of LiCl/A was then made, and a plot of ϕ_t versus $k_6\,[R\cdot]_s t + A^*$ is shown in Figure 4, where it is assumed that only $Fe(DMF)_5Cl^{2+}$ ions are present, and k_6 refers to reaction (19). Agreement between the experimental and theoretical plot was reasonable when $k_6[R\cdot]_s$ was 4.00×10^{-3} sec^{-1}. Now,

$$k_6/k_p = k_6[R\cdot]_s[M]/R_{ps} \quad (22)$$

where R_{ps} represents the maximum rate of polymerization for the system. Using the experimental values of R_{ps} and $[M]$ of 4.23×10^{-5} mole/l. sec and 2.49 mole/l., respectively, and using k_p equal to 176 l./mole sec, we have for k_6 a value of 4.15×10^4 l./mole-sec at 60°C.

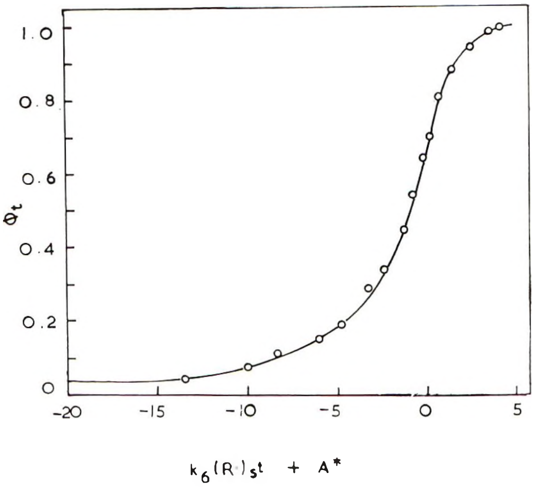

Fig. 4. Reduced rate ϕ_t as a function of reaction time t: (O) experimental points; (——) calculated curve. Molar ratio of LiCl: A = 1:1; at 60°C.; [styrene] = 2.490 mole/l.; [DMF] = 8.792 mole/l.; [AIBN] = 7.62×10^{-2} mole/l.; [A] = 7.87×10^{-3} mole/l.; [LiCl] = 7.87×10^{-3} mole/l.

Evaluation of k_7

Spectroscopic evidence[6] suggested that on adding lithium chloride to polymerizing systems in excess of a 1:1 molar ratio of LiCl:A, the equilibrium (10) is involved, and induction periods are possibly due to mechanisms (19) and (23), with the iron(II) complex becoming rapidly solvated with DMF.

$$\sim\!\!\sim CH_2\dot{C}HPh + Fe^{III}(DMF)_4Cl_2^+ \rightarrow \sim\!\!\sim CH{=}CHPh + Fe^{II}(DMF)_4Cl^+ + H^+Cl^- \quad (23)$$

The equilibrium constant in (10) is high,[6] so that for a 2:1 molar ratio of LiCl to A, all of the iron(III) ions exist as $Fe(DMF)_4Cl_2^+$. Hence,

$$\tau = [Fe(DMF)_4Cl_2^+]_0/I \quad (24)$$

The experimental τ value indicates a value of I of 1.03×10^{-6} mole/l.-sec and an f value of 0.59.

Analysis of the ϕ_t–time data by the method of Bamford et al.[1] gave k_7 equal to 6.55×10^4 l./mole sec at 60°C.

Evaluation of k_8

Spectroscopically, it was shown[6] that all iron(III) species from complex A with LiCl/A molar ratios in excess of about 6:1 exist as $FeCl_4^-$ ions in DMF–styrene mixtures at 60°C. Calculations indicated that the value of the equilibrium constant for eq. (11) was at least 10^8. In pure *N,N*-dimethylacetamide, a similar type of equilibrium is established[13] with an estimated equilibrium constant of at least 10^{10}.

Analysis of the ϕ_t–time t data was therefore performed for an experiment at 60°C with a LiCl/A molar ratio of 10:1, and the value of k_8 obtained was 3.14×10^4 l./mole-sec. The plot of ϕ_t against $k_8[\mathrm{R}\cdot]_s t + A^*$ is shown in Figure 5.

However, the measured values of τ for LiCl/A molar ratios greater than 6:1, although virtually constant with increase of (LiCl), seemed somewhat lower than suggested by the usual treatment[1] and gave values of f about 0.8. The rate of production of iron(II) species was therefore measured spectrophotometrically in a polymerization experiment with a LiCl/A molar ratio of 10:1. Iron(II) was determined as the trisphenanthroline complex. The results of an experiment are shown in Figure 6, and indicate a linear rate of production of iron(II) species of 1.11×10^{-7} mole/l. sec.

Assuming that each polystyryl radical is captured by one $\mathrm{FeCl_4^-}$ ion during the induction period, simple theory suggests that:

$$d[\mathrm{FeII}]/dt = I = 2k_d f[\overline{\mathrm{In}}] \qquad (25)$$

For an average value of $[\overline{\mathrm{In}}]$ equal to 7.52×10^{-3} mole/l. during the induction period, the corresponding value of f is 0.62, in good agreement with previous results.

A mechanism of radical scavenging by $\mathrm{FeCl_4^-}$ ions preserving a 1:1 radical-ion stoichiometry would be:

$$\sim\!\!\mathrm{CH_2\dot{C}HPh} + \mathrm{FeCl_4^-} \rightarrow \sim\!\!\mathrm{CH{=}CHPh} + \mathrm{H^+Cl^-} + \mathrm{FeCl_2} + \mathrm{Cl^-} \qquad (26)$$

The reason for the discrepancy between values of f calculated from τ measurements and those obtained by direct measurement of the rates of production of iron(II) species remains uncertain. However, the difference may be associated, in part, with the formation of other iron(III) chloro complexes such as $\mathrm{FeCl_5^{2-}}$ and $\mathrm{FeCl_6^{3-}}$ at very high chloride concentrations.[18]

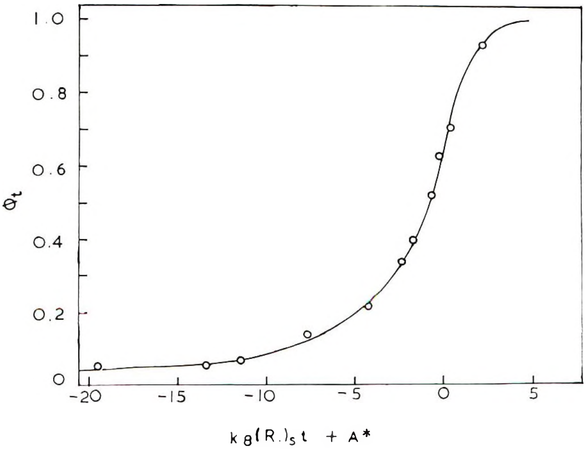

Fig. 5. Reduced rate ϕ_t as a function of reaction time t: (O) experimental points; (——) calculated curve. Molar ratio of LiCl:A = 10:1; at 60°C.; [styrene] = 2.490 mole/l.; [DMF] = 8.792 mole/l.; [AIBN] = 7.62×10^{-2} mole/l.; [A] = 7.87×10^{-3} mole/l.; [LiCl] = 7.87×10^{-2} mole/l.

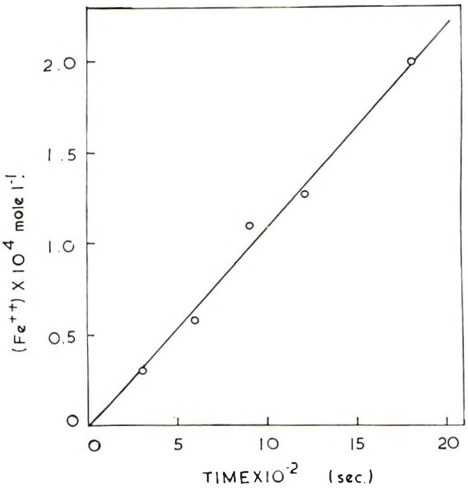

Fig. 6. Concentration of ferrous ions produced during an inhibition period as a function of time. At 60°C.; [styrene] = 2.490 mole/l.; [DMF] = 8.792 mole/l.; [AIBN] = 7.62×10^{-3} mole/l.; [A] = 4.40×10^{-4} mole/l.; [LiCl] = 4.40×10^{-3} mole/l.

Comparison of Velocity Constants

The velocity constant, k_x, for polystyryl attack on $Fe(DMF)_6^{3+}$, of 847 l./mole sec, is much less than the corresponding values for the iron(III) chloro complexes, $Fe(DMF)_5Cl^{2+}$, $Fe(DMF)_4Cl_2^+$ and $FeCl_4^-$ of 4.15×10^4, 6.55×10^4, and 3.14×10^4 l./mole sec, respectively. The presence of chloride ions in the complexes of iron(III), facilitates the electron transfer process in a way that is relatively unaffected by either the number of chloride ions present, even if a statistical correction is applied, by the net charge carried by the ion, or by the geometry of the complex, octahedral $\{Fe(DMF)_5Cl^{2+}$ and $Fe(DMF)_4Cl_2^+\}$ or tetrahedral $\{FeCl_4^-\}$.

The accelerative effect of chloride ions,[19] and other ions,[20] is well established for exchange reactions between iron(III) and iron(II) in aqueous solutions. The Cl^- ion might facilitate electron transfer by acting as a bridge between the two metal ions, or act as a "conductor" for the transfer of the electron. Precise mechanisms remain uncertain, however.[20]

For a few other polymer radical–iron(III) reactions, accelerative effects of ions within the complex have also been observed. Thus, velocity constants for termination of polyacrylamide radicals in aqueous solutions at 25°C with $Fe(H_2O)_6^{3+}$ and $Fe(H_2O)_5Cl^{2+}$ have values of 2.8×10^3 l./mole sec,[21] and 18.9×10^4 l./mole sec,[22] respectively. The high reactivity of the inner-sphere complex $Fe(H_2O)_4SO_4^+$ towards polyacrylamide radicals has also been noted.[21]

The authors express thanks to the Government of Assam, India, for the award of a Scholarship to N. N. Dass, and also acknowledge an equipment grant from the Science Research Council, London.

References

1. C. H. Bamford, A. D. Jenkins, and R. Johnston, *Proc. Roy. Soc.* (London), **A239,** 214 (1957).

2. C. H. Bamford, A. D. Jenkins, and R. Johnston, *J. Polym. Sci.*, **29,** 355 (1958).

3. J. Betts, F. S. Dainton, and K. J. Ivin, *Trans. Faraday Soc.*, **58,** 1203 (1962).

4. C. H. Bamford, A. D. Jenkins, and R. Johnston, *Trans. Faraday Soc.*, **55,** 1451 (1959).

5. E. R. Entwhistle, *Trans. Faraday Soc.*, **56,** 284 (1960).

6. N. N. Dass and M. H. George, *J. Polym. Sci. B*, **5,** 1119 (1967).

7. M. H. George and P. F. Onyon, *Trans. Faraday Soc.*, **59,** 1390 (1963).

8. M. H. George, *J. Polym. Sci. A*, **2,** 3169 (1964).

9. M. H. George, and P. F. Onyon, *Trans. Faraday Soc.*, **59,** 134 (1963).

10. C. H. Bamford, W. G. Barb, A. D. Jenkins, and P. F. Onyon, *Kinetics of Vinyl Polymerization by Radical Mechanisms*, Butterworths, London, 1958.

11. M. Talât-Erben and S. Bywater, *J. Amer. Chem. Soc.*, **77,** 3710 (1955).

12. J. C. Bevington, *Trans. Faraday Soc.*, **51,** 1392 (1955).

13. R. S. Drago, R. L. Carlson, and K. F. Purcell, *Inorg. Chem.*, **4,** 15 (1965).

14. J. L. Kice, *J. Amer. Chem. Soc.*, **76,** 6274 (1954).

15. J. L. Kice, *J. Polym. Sci.*, **19,** 123 (1956).

16. M. S. Matheson, E. E. Auer, E. B. Bevilacqua, and E. J. Hart, *J. Amer. Chem. Soc.*, **73,** 1700 (1951).

17. G. E. Ham, Ed., *Vinyl Polymerization, Part I.* Dekker, New York, 1967, Chapter 3.

18. E. Rabinowitch and W. H. Stockmayer, *J. Amer. Chem. Soc.*, **64,** 335 (1942).

19. J. Silverman and R. W. Dodson, *J. Phys. Chem.*, **56,** 846 (1952).

20. A. G. Sykes, *Kinetics of Inorganic Reactions*, Pergamon, New York–London, 1966.

21. E. Collinson, F. S. Dainton, B. Mile, S. Tazuke, and D. R. Smith, *Nature*, **198,** 26 (1963).

22. E. A. S. Cavell and I. T. Gilson, *J. Polym. Sci. A1*, **4,** 541 (1966).

Received April 17, 1968

JOURNAL OF POLYMER SCIENCE: PART A-1 VOL. 7, 283-296 (1969)

New High-Temperature Polymers. VIII. Ordered Benzoxazole- and Benzothiazole-Imide Copolymers

J. PRESTON, W. F. DEWINTER,* and W. B. BLACK, *Chemstrand Research Center, Inc., Durham, North Carolina 27702*

Synopsis

Ordered heterocycle copolymers of high thermal stability were prepared from aromatic dianhydrides reacted with aromatic diamines containing preformed benzoxazole or benzothiazole units. These ordered benzoxazole-imide and benzothiazole-imide copolymers were prepared in the form of their soluble precursor polyamic-acids, which, after fabrication to desired shapes, were converted to the thermally stable polymer. In general, these polymers are more resistant to air oxidation at elevated temperatures than are simple aromatic polyimides, and their thermoöxidative stability is equal to or greater than that reported for benzoxazole or benzothiazole homopolymers. Unlike the *o*-hydroxyamide precursors to simple polybenzoxazoles, the amic acid precursors to benzoxazole-imide ordered copolymers do not require temperatures above 300°C to complete ring closure nor inert atmospheres to prevent polymer degradation during ring formation. Excellent self-supporting films and film coatings for metals were prepared. Selected compositions were readily spun to excellent fiber.

INTRODUCTION

Previously[1,2] we have described the properties of some ordered heterocycle copolymers and the advantages provided by the ordered copolymer approach to the synthesis of thermally stable polymers. The chief virtue of such an approach is the ability to tailor polymers for specific needs by a judicious selection of two or more heterocycles and appropriate aromatic hydrocarbon units to make polymers having the desired balance of properties—thermal stability, tractability, crystallinity, modulus, glass transition temperature, drawability, etc.

Our earlier work has been extended to include benzoxazole and benzothiazole units, two heterocycle units which have been shown to possess very high thermal stability.[3-5] Techniques for preparing soluble precursors to the polybenzoxazoles have recently been reported,[3,4] but apparently no means have been found to date for fabricating high molecular weight aromatic polybenzothiazoles *per se* or via a tractable intermediate. Although the polybenzoxazoles can be prepared via soluble precursors, the conversion step employed is drastic, requiring a very high temperature and an inert atmosphere (or vacuum) for conversion.[4] By preforming benz-

---

* Present address: U. C. B. Central Research Laboratories, Drogenbos, Belgium.

TABLE I
Film Properties of Ordered Benzoxazole-imide Copolymers[a]

No.	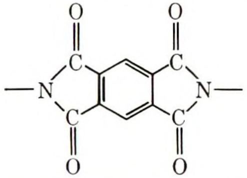 heterocycle derivative	Flexibility	
		Heated at 145°C[b]	Annealed at 300°C[c]
I	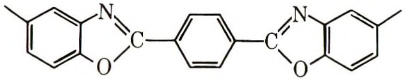	Brittle	Flexible
II	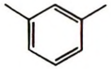	Brittle	Strong, flexible
III		Sl. brittle	Strong, flexible
IV	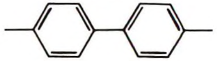	Very brittle	Brittle
V	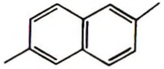	Brittle	Sl. brittle
VI	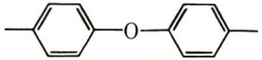	Flexible	Strong, flexible

VII	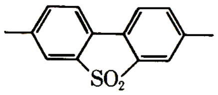	Very brittle	Very brittle
VIII	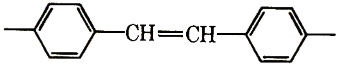	Brittle	Sl. brittle
IX	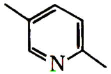	Brittle	Flexible
X	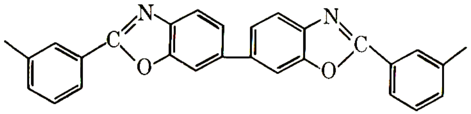	Sl. brittle	Strong, flexible
XI		Brittle	Strong, flexible
XII	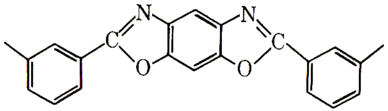	Brittle	Strong, flexible
XII′		Brittle	Strong, flexible
XII″	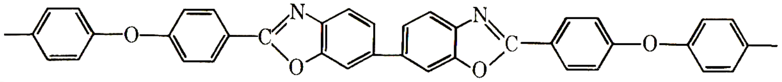	Strong, flexible	Strong, flexible

continued

TABLE I (*continued*)

No.	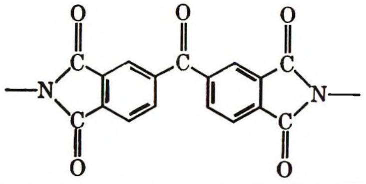 heterocycle derivative	Flexibility	
		Heated at 145°C[b]	Annealed at 300°C[c]
XIII	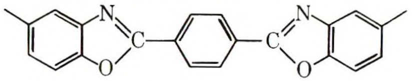	Flexible	Strong, flexible
XIV	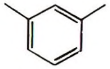	Strong, flexible	Strong, flexible
XV		Flexible	Strong, flexible
XVI	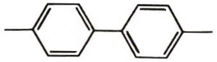	Strong, flexible	Strong, flexible
XVII	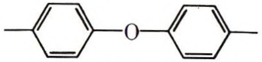	Strong, flexible	Strong, flexible
XVIII	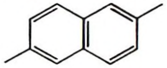	Brittle	Strong, flexible
XIX	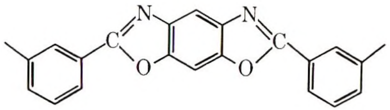	Flexible	Strong, flexible
XIX′		Flexible	Strong, flexible

---

[a] All of the films with the exception of XII″ (which was colorless) were of a light yellow color when freshly cast to film and freed of solvent.

[b] After the heat treatment at 145°C for 8–18 hrs., the films were slightly darker but still of a light yellow color.

[c] Heating at 300°C produced a film of yellow to yellow-brown or yellow-orange color.

oxazole or benzothiazole units in a difunctional block and then condensing with another thermostable monomer under conditions such that no rearrangement of bonds occurs, several of the problems encountered in the incorporation of benzoxazoles and benzothiazole units in homopolymers are circumvented. In this study, diamines containing preformed benzoxazole or benzothiazole units were prepared[6] and reacted with aromatic dianhydrides.

DISCUSSION AND RESULTS

Synthesis

The preparative route is illustrated in eq. (1), where Ar denotes the arylene radical and X may be —S— or —O—. The structures of the various polymers along with their film properties are given in Tables I and II; thermal properties of selected polymers are given in Table III.

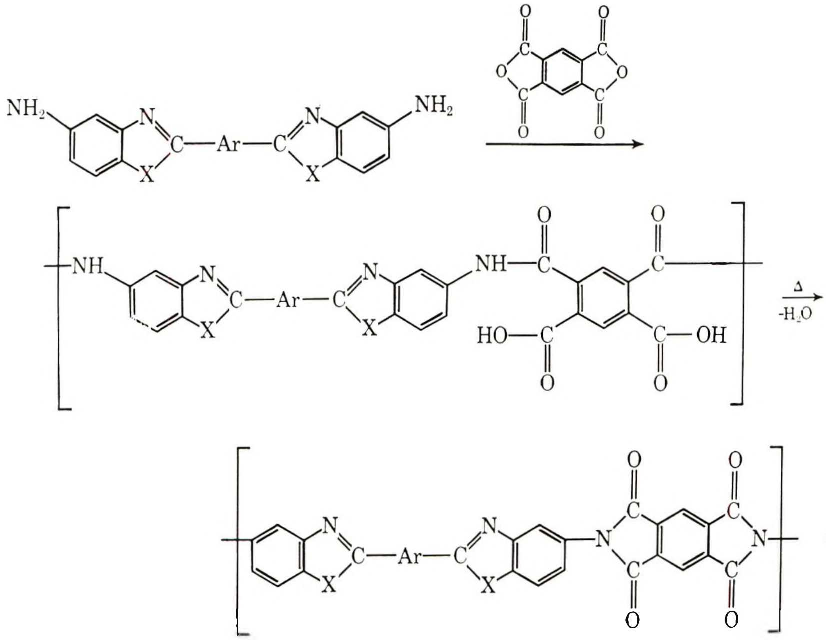

(1)

Solubility of Precursors

The polymers derived from pyromellitic dianhydride and from diamines containing a high portion of *para*-oriented rings tended to be insoluble at high solids content in solvents such as dimethylformamide (DMF) or dimethylacetamide (DMAc). *N*-Methylpyrrolidone (NMP) was a good solvent for all of the precursor polymers as was hexamethylphosphoric triamide (HPT), but the latter solvent was difficult to remove, causing some films to blacken when cured. Diamines containing "flex points," such as —O—, afforded precursors readily soluble in all of the solvents employed. Polymers derived from benzophenone dianhydride were also readily soluble even in DMF or DMAc.

TABLE II
Film Properties of Ordered Benzothiazole-imide Copolymers[a]

No.	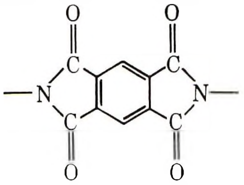 heterocycle derivative	Flexibility	
		Heated at 145°C[b]	Annealed at 300°C[c]
XX	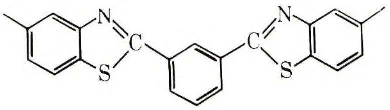	Sl. brittle	Strong, flexible
XXI	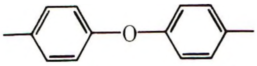	Flexible	Strong, flexible
XXII	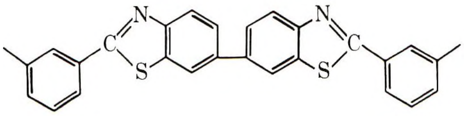	Sl. brittle	Strong, flexible
XXIII		Brittle	Strong, flexible
	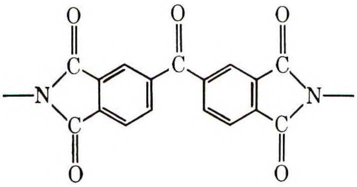 heterocycle derivative		
XXIV	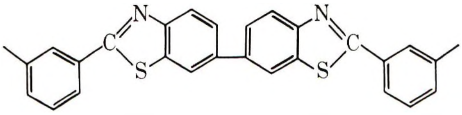	Flexible	Strong, flexible

[a] All of the films were of a light yellow color when freshly cast to film and freed of solvent.

[b] After the heat treatment at 145°C for 8–18 hrs., the films were slightly darker but still of a light yellow color.

[c] Heating at 300°C produced a film of yellow to yellow-brown or yellow-orange color.

The Curing Process and Film Flexibility

All of the curing operations on the ordered benzoxazole- and benzothiazole-amic acids to close the imide rings were carried out in air with good results; little or no oxidation occurred. This is in sharp contrast to the heating operations used to prepare polybenzoxazole and polybenzothiazole homopolymers; the curing of polybenzoxazole precursors must be carried out in inert atmospheres (or *in vacuo*) because of the sensitivity of the precursor polymers to oxidation.[4]

TABLE III
Thermal Properties of Ordered Benzoxazole- and Benzothiazole-imide Copolymers

Polymer	Melt transition temperature, °C[a]	Decomposition temperature, °C[b]
I	575	595
II	520	585
III	280[c]	—
V	—	570
VI	570	570 (550)
IX	570	570
X	580	565
XI	555	580
XII	590	575
XII′	625	625
XII″	280[c]	—
XIII	560	560
XIV	520	550
XV	280[c]	550
XVI	540	560
XVII	510	550
IXX	590	—
IXX′	610	625
XX	615	—
XXI	560	550
XXII	600	575 (565)

[a] Endothermic transition observed by differential analysis (DTA) in nitrogen, rate = 20°C/min. This transition is attributed to an incipient melting phenomenon; the polymers, with the exception of III, XII″, and XV, do not melt in the conventional sense.

[b] Decomposition temperature observed by thermogravimetric analysis (TGA) in nitrogen, rate = 15°C/min. The temperatures given are those at the inflection point in the TGA curve; these temperatures approximate those at which the weight loss is 10% of the original weight after correction for loss of absorbed water. Values given in parentheses were determined in air.

[c] Film was observed to undergo drastic softening when heated on a hot surface in air.

When first cast and freed of solvent, all films were flexible (flexibility was taken as a measure of the ability of the film to recover from a sharp creasing of the film). After partial cure by heating at 140–170°C, certain films were brittle and were easily broken during handling. Films from all of the polymers which contained flex points, however, were flexible at all points of cure and special care was not necessary to avoid fracturing them. As can be seen from an examination of Tables I and II, carbonyl groups in the chain and *meta*-oriented rings aid in improving the flexibility of the films at intermediate stages of cure. With few exceptions, even the very brittle partially cured films became quite tough and flexible after cure at 300°C.

The conversion of the film from the amic acid-heterocycle copolymer to the imide-heterocycle copolymer was followed by infrared spectroscopy. Thus, film of the precursor to the imide-benzoxazole VI prior to heating showed only a small absorption band at ~3500 cm^{-1}, whereas the film after heating at 145°C for 24 hr followed by annealing at 300°C for 30–180 min had two strong absorption bands at 1785 and 724 cm^{-1}, showing imide formation (Fig. 1).

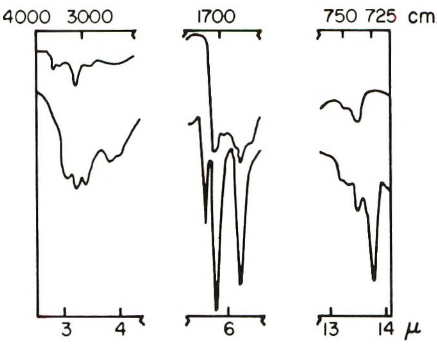

Fig. 1. Infrared spectra of the benzoxazole-imide VI (the upper trace was obtained for the precursor polymer).

Films after annealing were no longer soluble in the common organic solvents or even strong organic solvents employed for solution polycondensation such as DMAc, NMP, HPT; however, these films were soluble in sulfuric acid and in methanesulfonic acid. In sulfuric acid imide-benzoxazole VI degrades rapidly with a precipitate forming after several hours; in methanesulfonic acid the polymer degrades more slowly (Table IV).

TABLE IV
Degradation of An Ordered Benzoxazole-imide Copolymer in Methanesulfonic Acid[a]

Time, days	η_{inh}[b]
0	1.78
1	1.63
4	1.49
11	1.09
35	0.44

[a] Polymer VI.
[b] Determined on a 0.5% solution.

Coatings of imide-heterocycle copolymers were made by applying solutions of the amic acid-heterocycle precursor copolymers to sheet metal and heating to effect imide formation. The resultant coatings were tough and could not be stripped mechanically from the metal. Coatings of imide-benzoxazoles I and XIII were still tough and flexible after 8 hr at 425°C in air, showing excellent heat-aging performances.

Excellent fibers were readily spun from selected compositions; the tensile and thermal properties of these fibers will be reported in the near future.

Thermal Stability

With the exception of imide-benzoxazole polymers III and XV, which contain *ortho*-oriented phenylene units, all of the ordered heterocycle copolymers were very high-melting as indicated by differential thermal analysis (DTA) in nitrogen. All of the polymers were very thermally stable as shown by their retention of weight upon being heated to high temperatures [thermogravimetric analysis (TGA) in nitrogen]. DTA and TGA data for selected polymers from Tables I and II are given in Table III; selected DTA and TGA plots are given in Figures 2 and 3.

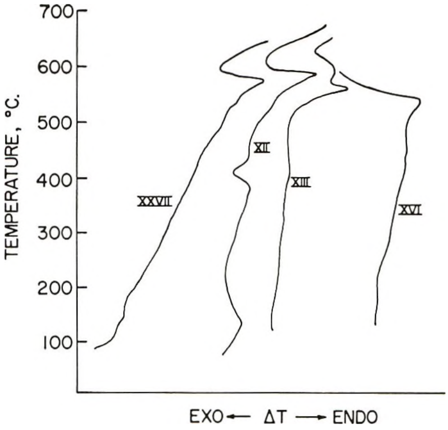

Fig. 2. Programmed DTA in nitrogen of some polymers containing heterocycles (rate = 20°C/min).

The DTA and TGA data suggest that the benzoxazole and benzothiazole units are of comparable thermal stability; however, studies of long-term oxidative stability at moderately elevated temperatures indicate that the benzoxazole ring is somewhat more thermoöxidatively stable. Both of these heterocyclic rings show considerably better thermoöxidative stability than the benzimidazole ring.[2] Of course, the oxidative thermal stability of the polymers is also dependent on the stability of the aromatic hydrocarbon rings; e.g., the *p*-phenylene ring appears to contribute more to thermal stability of the copolymer than the 4,4′-diphenyl ether moiety. The —CH═CH— linkage, because of conjugation with its flanking aromatic rings, is probably more oxidatively resistant than an isolated alkylene linkage.

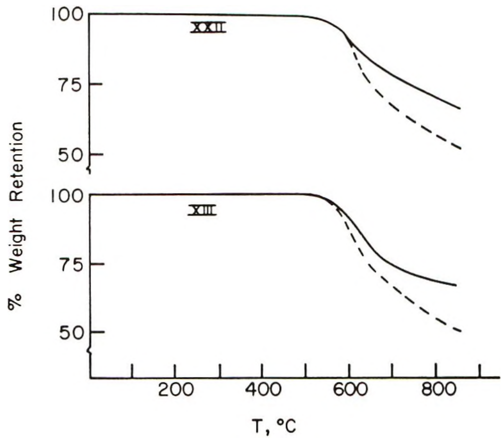

Fig. 3. Programmed TGA (rate = 15°C/min) of ordered benzoxazole- and benzothiazole copolymers XIII and XXII: (——) in nitrogen; (- - -) in air.

Of peripheral interest, this study indicates that the benzophenone-imide unit is more thermoöxidatively resistant than the pyromellitimide moiety.

Except for the benzoxazole-imide XII″ (Table I) and polymers containing *ortho*-oriented rings, the ordered benzoxazole- and benzothiazole-imide copolymers have melting points and decomposition temperatures remarkably alike, a fact observed earlier for ordered heterocycle copolymers in general.[2] The polymers derived from benzophenone dianhydride softened at temperatures slightly below those for corresponding polymers derived from pyromellitic dianhydride (Fig. 2); the lower softening points are undoubtedly accounted for by the greater flexibility of the polymer chains containing carbonyl linkages. The presence of two —O— groups per polymer repeat unit results in a polymer (XII″) of quite low softening point. It is interesting to note that even those copolymers which soften or melt at about 300°C do not degrade rapidly in air above their softening points. In great contrast, polyamides, even those which soften at 350–400°C, degrade very rapidly in air above their softening point.[7] Also, the decomposition behavior of the imide-heterocycle copolymers contrast sharply with that for aromatic ordered copolyamides where thermal stability increases as the proportion of *p*-phenylene units increases.[7]

In Table V the thermoöxidative stability of films of imide-benzoxazoles XIII and XVII, and that of the imide-benzothiazole XXII are compared with the thermoöxidative stability of film of two previously reported ordered oxadiazole-containing copolymers (XXV and XXVI),[2,8]

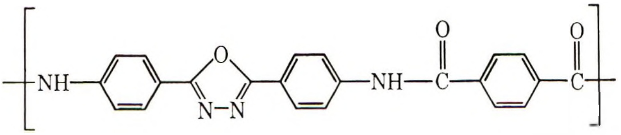

XXV

TABLE V
Heat-Aging of Films of Some Polyheterocycles in Air

Polymer	Temp, °C	Time, days	Color	Flexibility
XIII	300	100	Yellow	Flexible (no change)
XVII	300	100	Very slightly darker	Flexible (sl. change)
XXVII	300	100	Slightly darker	Flexible (little change)
XIII	300	114	Dark	Brittle
XVII	300	114	Dark	Very brittle
XXVII	300	114	Dark	Very brittle
XIII	350	1	Yellow	Flexible
XVII	350	1	Yellow	Flexible
XXII	350	1	Yellow	Flexible
XXV	350	1	Tan	Flexible
XXVII	350	1	Yellow	Flexible
XIII	350	2	Brown-yellow	Flexible
XVII	350	2	Brown-yellow	Flexible
XXII	350	2	Brown	Flexible
XXV	350	2	Brown	Flexible
XXVII	350	2	Brown-yellow	Flexible
XIII	350	5	Brown-yellow	Flexible
XVII	350	5	Brown-yellow	Flexible
XXII	350	5	Brown	Brittle
XXV	350	5	Black	Crumbled
XXVI	350	5	Brown	Losing flexibility
XXVII	350	5	Lt. brown	Flexible, losing strength
XIII	350	10	Brown-yellow	Flexible
XVII	350	10	Brown-yellow	Flexible
XXVI	350	10	Black	Sl. brittle
XXVII	350	10	Brown	Losing flexibility and strength
XIII	350	15	Lt. brown	Flexible
XVII	350	15	Yellow-brown	Flexible
XXVII	350	15	Brown	Brittle

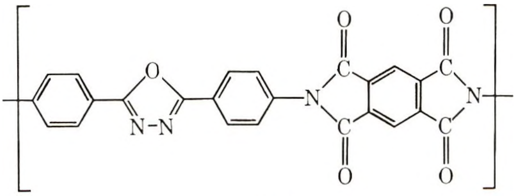

XXVI

and with that of film of the pyromellitimide of 4,4′-bis(*p*-aminophenyl) ether (XXVII, prepared by the method of Sroog et al.[9]).

After 14 weeks at 300°C the films of XXVI and XXVII as well as films of imide-benzoxazole XIII and imide-benzothiazole XXII were relatively unaffected, but after another two weeks all of the films began to fail rapidly. (Note: The ability of the films to be flexed after exposure was

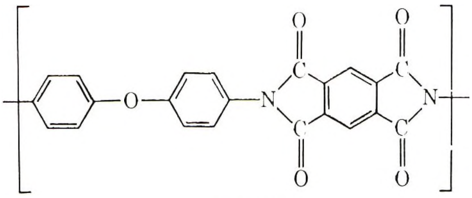

XXVII

taken as the primary measure of stability; darkening of the film correlated well with embrittlement.) It appears that there is an induction period, during which time little change occurs; after this period degradation takes place rapidly. Consequently, extrapolations based on short-term heat-aging to assess long-term heat-aging properties may be seriously questioned. The rapid degradation of the oxadiazole-amide XXV probably occurs because of the presence of 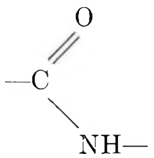 $-\mathrm{C}\begin{array}{l}{/\!\!/}\mathrm{O}\\ \backslash\mathrm{NH}-\end{array}$ linkages. (Compare also the heat-aging data for PBI, poly-2,2′-*m*-phenylene-5,5′-bibenzimidazole, which contains 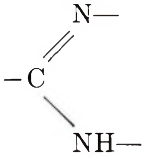 $-\mathrm{C}\begin{array}{l}{/\!\!/}\mathrm{N}-\\ \backslash\mathrm{NH}-\end{array}$ linkages.[2])

Heat-aging at 350°C in air, a much more severe test than heat-aging at 300°C, produced failure of the films in a much shorter period of time. In Figure 4 are compared the retention of weight of films of imide-benzoxazoles XIII and XVII, the imide-benzothiazole XXII, the oxadiazole-amide XXV, an oxadiazole-imide XXVI, and the polypyromellitimide of 4,4′-oxydianiline (XXVII) at 350°C in air. Here one clearly sees the thermoöxidative superiority of the benzothiazole- and benzoxazole-imide copolymers.

Although the benzoxazole- and benzothiazole-imide copolymers are not greatly superior in thermoöxidative stability to the previously reported oxadiazole-imides[2] at intermediate temperatures, their thermal and thermoöxidative stability at temperatures above 400°C is greatly superior. At temperatures above 500–525°C, the oxadiazole-imide has little stability even for short-term exposure, whereas a number of the benzothiazole- and benzoxazole-imides remain essentially in tact after such exposure for short periods of time. Thus, on balance, the benzothiazole- and benzoxazole-imides are the materials of choice in applications requiring both long-term oxidative thermal stability and short-term exposure to very high temperatures.

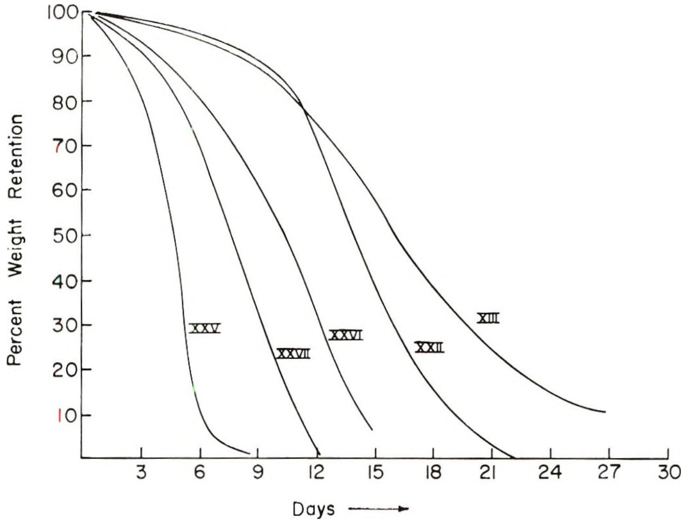

Fig. 4. Weight retention at 350°C in air for films of polymers containing heterocycles

EXPERIMENTAL

The preparation of the diamines were described elsewhere.[6] Commercial samples of dianhydrides were sublimed under reduced pressure. Solvents were dried over molecular sieves prior to use. Inherent viscosities were determined at 30°C for solutions of 0.5 g of polymer in 100 ml of DMAc.

Polymerization

The diamines were placed in DMF, DMAc, NMP, or HPT, cooled to 0°C, and equivalent amounts of dianhydride added. The solutions were stirred for 1–3 hr at 0°C, then for approximately 20 hr at room temperature.

In a typical polymerization a solution of 3.42 g. (0.01 mole) *m*-phenylene-2,2′-bis(5-aminobenzoxazole) in 40 ml pure dry DMAc was cooled to 0°C and 2.18 g of pyromellitic dianhydride was added. The mixture was stirred at 0°C until all of the diamine was dissolved (ca. 3 hr). Stirring at room temperature was continued for 20 hr; a viscous solution of polymer (η_{inh} = 1.5) was formed.

Films were cast from the clear viscous solutions onto a glass plate, leveled with a Gardner knife, and then baked at 100°C for 20 min. Preferably, the films were removed from the glass plate while still plasticized with solvent; otherwise, films were apt to adhere to the plate and could be removed only with great difficulty, especially if the films tended to be brittle (see Discussion and Results). The films were hung in an oven at 145°C for 20 hr; the somewhat brittle films were next heated at 300°C for 1 hr to yield the cured film, which, typically, was strong, flexible and of a light yellow color.

Heat-Aging Tests

The films were heated at elevated temperatures in air in a muffle furnace; the temperature of the furnace was carefully regulated, but no correction was made for the small temperature gradient which existed in the furnace. The films were suspended from a metal frame by means of small metal clamps in such a manner that they hung free in air, i.e., not under tension nor touching the frame or the surfaces of the furnace.

The authors wish to express their appreciation to Messrs. W. L. Hofferbert, Jr. and M. T. Bryant for their excellent technical assistance.

References

1. J. Preston and W. B. Black, *J. Polym. Sci. B*, **3**, 845 (1965).
2. J. Preston and W. B. Black, *J. Polym. Sci. A-1*, **5**, 2429 (1967).
3. T. Kubota and R. Nakanishi, *J. Polym. Sci. B*, **2**, 665 (1964).
4. T. Kubota, N. Yoda, and R. Nakanishi, *J. Polym. Sci. C*, in press.
5. P. M. Hergenrother, W. Wrasidlo, and H. H. Levine, *J. Polym. Sci. A*, **3**, 1665 (1965).
6. J. Preston, W. F. DeWinter, and W. L. Hofferbert, Jr., *J. Heterocyclic Chem.*, **5**, 269 (1968).
7. J. Preston, *J. Polym. Sci. A-1*, **4**, 529 (1966).
8. J. Preston and W. B. Black, *J. Polym. Sci. B*, **4**, 267 (1966).
9. C. E. Sroog, A. L. Endrey, S. V. Abramo, C. E. Berr, W. M. Edwards, and K. L. Oliver, *J. Polym. Sci. A*, **3**, 1373 (1965).

Received July 16, 1968

JOURNAL OF POLYMER SCIENCE: PART A-1 VOL. 7, 297-310 (1969)

Dielectric Properties of Stereoregular Poly(methyl Methacrylates)

HEISABURO SHINDO, ICHIRO MURAKAMI, and HITOSHI YAMAMURA, *Department of Chemistry, Faculty of Science, Hiroshima University, Hiroshima, Japan*

Synopsis

To obtain more useful information about the effect of the degree of stereoregularity on the motion of the polymer chain, the dielectric and dilatometric measurements were made for a series of stereoregular poly(methyl methacrylates) (PMMA). The α- and β-absorptions were observed in each sample, of which the dielectric behaviors of the α-process are discussed. The temperature dependence of the relaxation time of the α-process was sufficiently represented by the WLF equation and the resulting values of the parameters f_g and B in the modified WLF equation were found smaller for isotactic-rich PMMA than those values for syndiotactic PMMA. It may be deduced from these results that the chain mobility of the isotactic PMMA is larger than that of the syndiotactic. The dielectric increment of the α-process in the isotactic PMMA is much larger than that in the syndiotactic PMMA, increasing rapidly with temperature, and taking its maximum in the temperature range of 55 to 60°C. The dielectric transition was clearly observed in the case of isotactic-rich PMMA.

INTRODUCTION

It is known that for many atactic vinyl polymers there exist α- and β-processes in the dielectric relaxation, where the dielectric increment of the α-process is much greater than that of the β-process. However, for an atactic form of poly(methyl methacrylate) (PMMA), the increment of the α-process is much smaller than that of the β-process. Recently, several workers[1-6] showed that in the case of an isotactic PMMA the relation of the dielectric increment for the two processes mentioned above is quite the reverse of that in an atactic PMMA. Such an inversion of the dielectric increment is not well explained in relation to stereoregularity up to the present. Saito and Nakajima[7] pointed out for many crystallizable polymers that the dielectric increment of the α-process increases with temperature and assumes a maximum at a certain temperature above T_g. Later, many workers[8-10] discussed this problem in connection with what we call the order–disorder transition.

The fact that the temperature at which the α-absorption appears (which corresponds to the glass transition temperature) becomes lower as the isotacticity of PMMA is increased has also been studied.[5,6] Therefore, the internal chain mobility, which plays a major role in the appearance of the glass transition temperature, seems to be greater for the isotactic PMMA than for the syndiotactic.

To clarify these points, in the present study six different stereoregular PMMA's were prepared by a previously reported method,[11] and dielectric and dilatometric measurements were carried out for these samples. The effects of stereoregularity on the dielectric properties of the α-process were investigated. The parameters for the free volume were obtained by the application of the modified WLF equation to the relaxation times. The dependence of the internal chain mobility on the stereoregularity is discussed on the basis of the concept of free volume.

EXPERIMENTAL

Materials

A series of stereoregular PMMA's were prepared by anionic polymerization under the different conditions shown in Table I together with their tacticity. The crude products containing residual low molecular weight materials were purified by reprecipitation with chloroform and acetone as solvents and methanol and water as precipitants. The precipitated products were dried at 50°C *in vacuo* for several days. The dried samples were pressed into the plates at temperatures far above the glass transition point. The plates used for the dilatometric and dielectric measurements were about 1 mm in thickness. For the latter use, they were coated with silver as electrodes.

The stereoregularity (or tacticity) of the samples was determined from the NMR measurement according to the method of Bovey and Tiers.[12] NMR measurements were carried out in chloroform solution of the samples

TABLE I
Some Characteristics of Stereoregular Poly(methyl Methacrylates)

Sample	Initiator[a]	Polymerization conditions[b]	Triad analysis i, %	 h, %	 s, %
1	PhMgBr	Toluene soln at 0°C	100	0	0
2	$LiAlH_4$	Toluene soln at −70°C	86	11	3
3	n-BuMgBr	Toluene soln at −48°C	63	15	21
4	PhMgBr	Toluene soln at −35°C	49	19	32
5	—	Commercial grade	13	33	54
6	$LiAlH_4$	THF soln at −70°C	8	21	71

[a] Molar ratio of initiator to methyl methacrylate monomer was chosen in the range of 2–7%

[b] Concentration of monomer was in the range of 20–40 vol-%.

at a frequency of 100 MHz and at 80°C. Triad analysis is also given in Table I in terms of the percentage of isotactic (*i*), heterotactic (*h*), and syndiotactic (*s*). From the values of the tacticity listed in Table I, samples 1 and 2 are found to be isotactic-rich PMMA. Samples 3 and 4 are stereoblock PMMA, and samples 5 and 6 are syndiotactic-rich PMMA which are apparently atactic.

Procedures

The glass transition temperatures were determined by the usual dilatometric method. In all the cases, a low cooling (or heating) rate of 0.33°C/min was chosen to avoid the rate effects. Density measurements were carried out by the density gradient method. The gradient of the density was obtained by changing the concentration of an aqueous solution of lead nitrate.

An inductive-ratio-arm bridge[13] was employed for the measurement of the dielectric constant (ϵ') and the loss factor (ϵ'') in the frequency range of 10^6 to 30 Hz, while a resistive-ratio-arm bridge[14] was used in the range of 10 to 10^{-1} Hz. In the range of 10^{-2} to 10^{-4} Hz, the values of ϵ'' were determined by measuring the absorption current.[15] The temperature of the sample cell was held constant within ±0.1°C for several hours in a drybox submerged in an oil thermostat.

RESULTS

Diad analysis of the tacticity of the samples was made by using the results of the triad analysis; results are listed in Table II. The glass transition temperatures T_g for samples 3, 4, and 5 were determined from the volume–temperature diagrams in Figure 1. The plots for each sample can

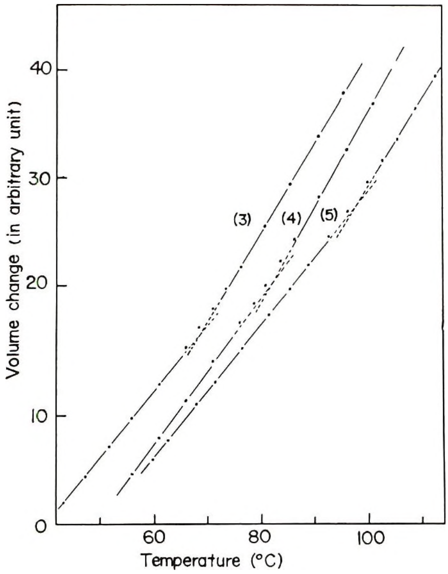

Fig. 1. Temperature dependence of the volume of samples 3, 4, and 5.

be represented by two straight lines, and the glass transition temperature is determined as the intersection point of these two lines. The glass temperature is found to decrease with increasing isotacticity as shown in Table II. The density of each sample is also given in Table II.

TABLE II
Some Characteristics of Stereoregular Poly(methyl Methacrylates)

Sample	T_g, °C	Density at 25°C, g/cc	Tacticity by diad analysis	
			i, %	s, %
1	47	1.228	100	0
2	55	1.225	91	9
3	68	1.220	71	29
4	82	1.208	58	42
5	97	1.185	30	70
6	116	1.190	19	81

The values of the dielectric loss factor ϵ'' for samples 1–6 at a fixed temperature are plotted against frequency in Figures 2 to 7. For all samples, two distinct absorptions are observed in the vicinity of T_g. The loss peak at the high-frequency side in each figure corresponds to the β-process. It should be noted, from Figures 4 and 5, that the β-absorption curve for stereoblock sample 3 has two peaks at 25.1, 34.4, and 44.8°C below T_g. On the other hand, the absorption curve for the other stereoblock sample (sample 4) has a single peak only.

The loss peak at the low-frequency side corresponds to the α-absorption, and the temperature at which the absorption begins becomes lower with increasing isotacticity. As shown in Figures 2 and 3, the loss maximum value of the α-process for an isotactic-rich PMMA is much higher than that

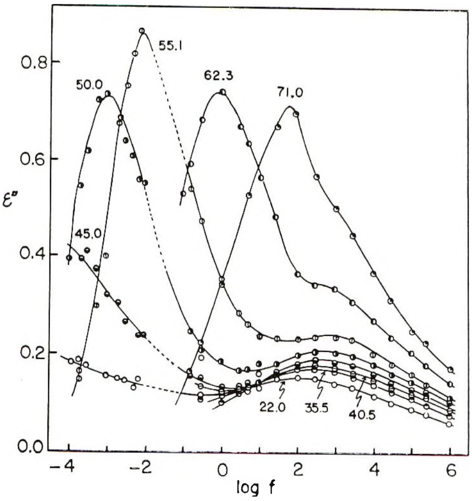

Fig. 2. Frequency dependence of ϵ'' at various fixed temperatures (°C) for sample 1.

of the β-process, and the β-loss peak becomes masked by the α-loss peak as the temperature is raised. However, these relationships between α- and β-absorptions are the reverse of those for a syndiotactic-rich PMMA.

In order to determine the dielectric increment $\Delta\epsilon$ for the α- and β-processes at the fixed temperatures, Cole's circular arc law[16] was applied to the values of the complex dielectric constant. Except for the temperature range where the α- and β-loss peaks are close together, the complex plots of the dielectric constants satisfied Cole's law for the α-process near and below T_g

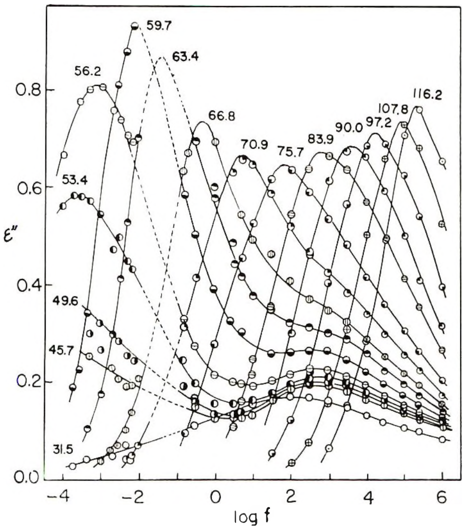

Fig. 3. Frequency dependence of ϵ'' at various fixed temperatures (°C) for sample 2.

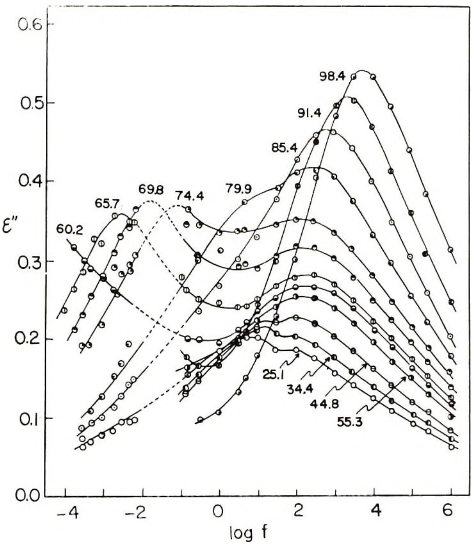

Fig. 4. Frequency dependence of ϵ'' at various fixed temperatures (°C) for sample 3.

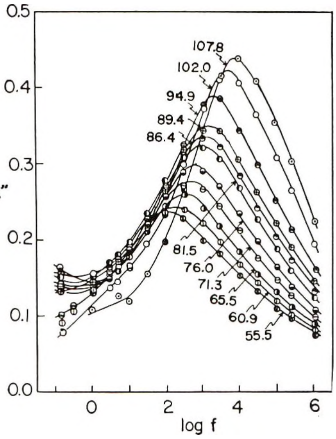

Fig. 5. Frequency dependence of ϵ'' at various fixed temperatures (°C) for sample 4.

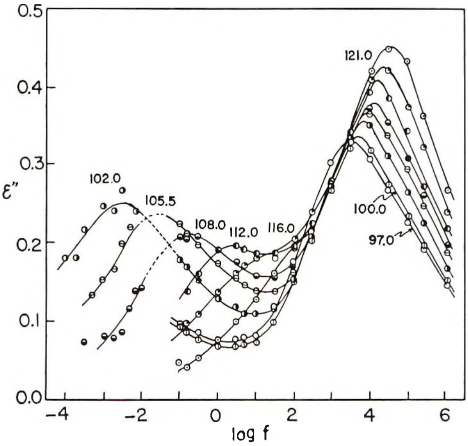

Fig. 6. Frequency dependence of ϵ'' at various fixed temperatures (°C) for sample 5.

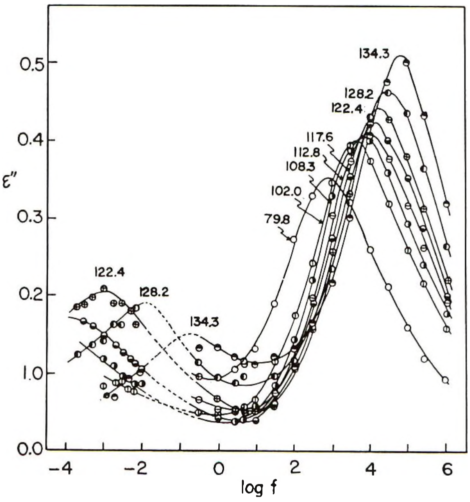

Fig. 7. Frequency dependence of ϵ'' at various fixed temperatures (°C) for sample 6.

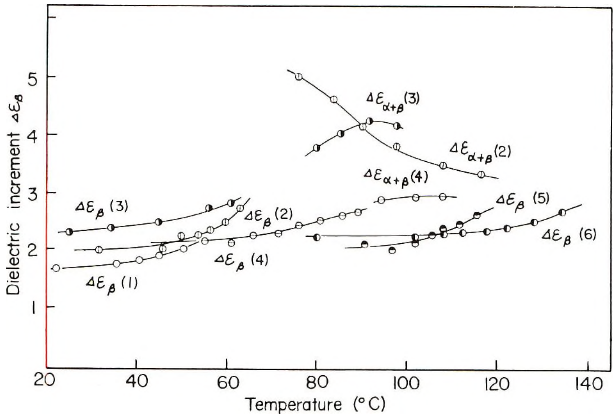

Fig. 8. Temperature dependence of the dielectric increment $\Delta\epsilon_\beta$ of the β-process for samples 1, 2, 3, 4, 5, and 6.

and for the ($\alpha + \beta$)-process far above T_g. From the intersection points of the curves, the dielectric increments $\Delta\epsilon_\beta$ and $\Delta\epsilon_{\alpha+\beta}$ were determined and are shown as a function of temperature in Figure 8. Here the dielectric increments far above T_g are denoted by $\Delta\epsilon_{\alpha+\beta}$. With increasing temperature, the dielectric increment for the β-process for each sample is nearly constant up to each glass transition interval; likewise, $\Delta\epsilon_{\alpha+\beta}$ is nearly constant in syndiotactic-rich PMMA, whereas it rapidly decreases in isotactic-rich PMMA. In the frequency range of 10^{-4} to 10^{-1} Hz, the dielectric increment for the α-loss curve was determined by two methods: first, by the method of integrating the area under the ϵ'' versus $\ln f$ curve:

$$\Delta\epsilon_\alpha = (2/\pi)\int_{-\infty}^{\infty} \epsilon''\ \mathrm{d}\ln f \qquad (1)$$

and secondly, by applying the theoretical formula of Kirkwood-Fuoss[17] to the α-process:

$$\Delta\epsilon_\alpha = 1.75\ \epsilon''_{\mathrm{max}}\Delta\log f \qquad (2)$$

where $\Delta\log f$ is the total half-width of the loss curve and $\epsilon''_{\mathrm{max}}$ is the maximum value of ϵ''. The dielectric increments obtained by both methods agree with each other within less than 5%. Values from the latter method are plotted against temperature in Figure 9. The dielectric increment for isotactic-rich PMMA samples 1 and 2 attained a maximum at 55 and 60°C, respectively. The relaxation time and its temperature dependence can be illustrated by plotting $\log f_{\mathrm{max}}$ against $1/T$, from which values of apparent activation energy can be evaluated. The plot shows an approximately straight line over the glass transition interval (Fig. 10). The values of apparent activation energy are determined from the line slope and are given in Table III, where ΔE_α and ΔE_β represent the values of the activation energy for the α- and β-processes, respectively. The activation energy for segmental motions of each sample is quoted from NMR measurement[11] and is compared with the dielectric data.

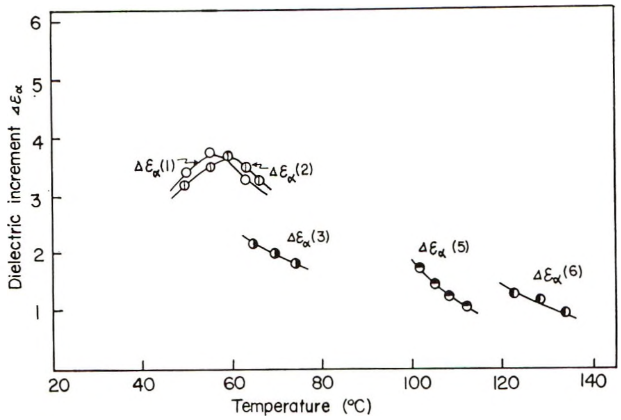

Fig. 9. Temperature dependence of the dielectric increment $\Delta\epsilon_\alpha$ of the α-process for samples 1, 2, 3, 5, and 6.

TABLE III
Activation Energy of Some Relaxational Modes for Poly(methyl Methacrylates) Obtained from the Dielectric and NMR Measurements

Sample	ΔE_α for the α-process, kcal/mole	ΔE_β for the β-process, kcal/mole	NMR measurement ΔE near T_g, kcal/mole[a]
1	120	9.7	12
2	130	13.4	—
3	132	15.7	—
4	—	20.9	—
5	147	22.5	16
6	151	21.2	15

[a] Data of Shindo et al.[11]

DISCUSSION

It has been shown by many workers,[10,18–21] that the α- and β-dielectric relaxation process in polymers of various methacrylic esters are attributable to the micro-Brownian motion of segmental chains and internal rotation or to micro-Brownian motion of ester side groups. In the case of stereoregular PMMA, the mechanisms of the α- and β-processes are considered to be the same as those of other polymethacrylic esters.

The activation energy for the α-process near T_g increases with decreasing isotacticity. From time dependence of the activation energy and the relaxation time on tacticity, it is derived that the chain segments of the isotactic PMMA are considered to have a higher degree of freedom[22] and a lower potential barrier, than those of the syndiotactic PMMA. Therefore, the isotactic PMMA is considered to have a greater internal chain mobility than the syndiotactic polymer. From the studies of dielectric and NMR measurements and of molecular weight dependence of T_g, the same conclusion has been derived for the polymers in solution[22] and in solid states.[5,6,11,23,24]

Now, let us consider the single absorption, denoted the ($\alpha + \beta$)-absorption, at temperatures far above T_g. It was shown in Figures 2 and 3 that for an isotactic-rich sample the β-absorption becomes masked by the α-absorption as the temperature is increased, and converse is true in the case of the syndiotactic sample. Mikhailov[25] interpolated the curve of $\log f_{\max}$ versus $1/T$ to determine whether the single absorption at high temperatures is to be attributed to the α- or to the β-absorption. Thus, we may derive from Figure 10 that the single absorption for the isotactic-rich samples at high temperatures should be attributed to the relaxational mode of the α-process and that the single absorption for the syndiotactic sample to the relaxational mode of the β-process.

It is well known that the temperature dependence of relaxation times can be described for many polymer systems by the WLF equation:[26]

$$\log \frac{f_{\max}(T_g)}{f_{\max}(T)} = -\frac{C_1(T - T_g)}{C_2 + T - T_g} \tag{3}$$

where $f_{\max}(T_g)$ and $f_{\max}(T)$ are loss maximum frequencies at T_g and T, respectively. C_1 and C_2 are constant. The value of $\log f_{\max}\ (T_g)$ was so chosen that the plots of $(T - T_g)/\{\log f_{\max}(T_g)/\log f_{\max}(T)\}$ versus $(T - T_g)$ could be represented by a straight line. It was found that the WLF

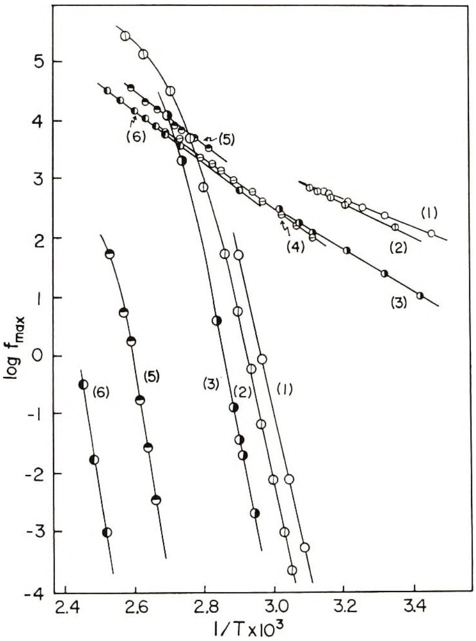

Fig. 10. Plots of the loss maximum frequency *log* $f_{\max}$ against the reciprocal of temperature $1/T$. Small circles and large circles correspond to the β-process and α-process, respectively; the numbers indicate the sample number.

TABLE IV

Some Parameters in Modified WLF Equation and Observed Physical Properties for Stereoregular Poly(methyl Methacrylates)

Sample	T_g, °C	$\Delta\alpha \times 10^{-4}$	C_1	C_2	C_1C_2	$\log f_{\max}(T_g)$	f_g	B
2	55	3.3	15.8	31.3	495	−4.75	0.0103	0.38
3	68	3.2	15.3	35.9	549	−3.00	0.0115	0.41
5	97	3.5	18.1	40.1	726	−4.60	0.0140	0.58

equation represents the data well for sample 2 over a wide range of temperature of 50 to 120°C. The values of C_1 and C_2 were obtained from the slope of the lines. They are listed, together with other parameters, in Table IV. On assuming that the fractional free volume f is in linear form with respect to temperature and that the free volume v_f is defined in the sense stated by Cohen and Turnbull,[27] the empirical WLF equation can be modified as follows,[28]

$$\log \frac{f_{\max}(T_g)}{f_{\max}(T)} = -\frac{\gamma v^*(T - T_g)}{\bar{v}_m(T - T_0)(T_0 - T_0)} \tag{4}$$

By comparing eq. (4) and eq. (3), we have

$$C_1 = \frac{\gamma v^*}{2.3\alpha_f \bar{v}_{\mathrm{m}}(T_g - T_0)} \tag{5}$$

$$B = \gamma v^*/\bar{v}_{\mathrm{m}}$$

$$C_2 = T_g - T_0 = f_g/\alpha_f \tag{6}$$

where v^* is the minimum free volume required for a motional unit to jump from one position to another, $\bar{v}_{\mathrm{m}}$ is the average volume of the motional unit of polymer, γ (having a numerical value between 1 and $^1/_2$) is a correcting factor for overlap of the free volume, T_0 is the temperature at which the free volume becomes zero, α_f is the thermal expansion coefficient of the free volume, and f_g is the fractional free volume at the glass transition temperature. If it is assumed that the expansion coefficient α_f is nearly equal to the difference $\Delta\alpha$ between the observed expansion coefficients in glassy and liquid states, the fractional free volume f_g and the numerical factor B could be estimated from the values of C_1 and C_2. The resulting values of f_g and B for samples 2, 3 and 5 are also listed in Table IV. Table IV shows the decrease of both values of f_g and B with increasing isotacticity. As a matter of course, this small value of f_g for an isotactic sample indicates that its free volume is smaller than that for syndiotactic PMMA at T_g. This is supported by the studies done on the permeability of gas into the polymer below the glass transition temperature.[29] The internal chain mobility may be explained in terms of the available degree of freedom and in terms of the potential barrier for the transition of the motional unit. The energy (strictly, free energy) necessary for the formation of a hole with a given size is considered not very different among the stereoregular PMMA's. The value of B in Table IV indicates the ratio between the volume of a motional unit and the minimum dimension of a hole to allow the transition. Therefore, the small value of B for an isotactic sample leads to the same conclusion regarding the internal chain mobility as stated above.

Dielectric Increment for the α-Process

For an isotactic-rich PMMA, the dielectric increment of the α-process increases near T_g, passes through its maximum at a certain temperature and then decreases as the temperature is increased. In the cases of crystallizable polymers, such a maximum was found to lie slightly above the glass transition temperature,[7] and was pointed out as direct evidence for the order–disorder transition.[8–10] The isotactic-rich PMMA is known to crystallize readily if treated with a fairly good solvent,[30] while the syndiotactic PMMA used here can not crystallize due to its substantially atactic form. Further, the isotactic chain has higher symmetry than the syndiotactic. Thus, it may be considered that the appearance of the maximum of the dielectric increment (i.e., dielectric transition) is associated with the symmetry of the polymer chain.

In general, it is very difficult to estimate the dielectric increment for amorphous polymers mainly because of their complex structure and also because of such factors as the dipole moment of the monomer unit, the dimension and microstructure of the motional unit, and the chain mobility. As mentioned in the previous section, the variation in the dielectric increment for the α-process owing to the change in tacticity of PMMA may arise from the difference of the microstructure of the motional unit. That is to say, the motional unit consisting of some monomer units possesses a greater effective dipole moment in isotactic PMMA than in a syndiotactic PMMA, due to the greater regularity of the isotactic PMMA in contrast to the random orientation of the dipoles of the syndiotactic PMMA. Therefore, it may be considered that the dielectric increment of the α-process is much larger for the isotactic PMMA than for the atactic.

As for sample 2, the dielectric increment of the ($\alpha + \beta$)-process, $\Delta\epsilon_{\alpha+\beta}$, does not seem to be inversely proportional to the absolute temperature as predicted in the Onsager's theory.[31] However the rapid decrease of $\Delta\epsilon_{\alpha+\beta}$ with increasing temperature appears to be the result of the decrease in the dimension of the motional unit.[8] At the highest temperature attained here, the dielectric increment $\Delta\epsilon_{\alpha+\beta}$ for all the samples does not differ greatly from each other (see Fig. 8). As the —C(O)O— dipoles are the same in all the samples, it may be expected that the motional unit has the same effective dipole moment at high temperatures. Therefore, the fact mentioned above may be considered to suggest a reduction of the dimension of the motional unit to the order of that of monomer unit in this temperature range, that is, the distribution of the repeating unit of the methyl methacrylate is statistical for all the samples used.

β-Process

As shown in Figure 8, the values of the dielectric increment $\Delta\epsilon_\beta$ for each sample, being little dependent on temperature below T_g, may be compared with one another at the temperature $T_g - 20°\text{C}$. They are plotted against the isotacticity of the samples in Figure 11. This curve seems to take its maximum near the isotacticity at 0.7. Such a maximum has been explained semiquantitatively by Yamafuji and Ishida.[3] Furthermore, the relaxation frequency of the β-process for isotactic PMMA shifts to a higher fre-

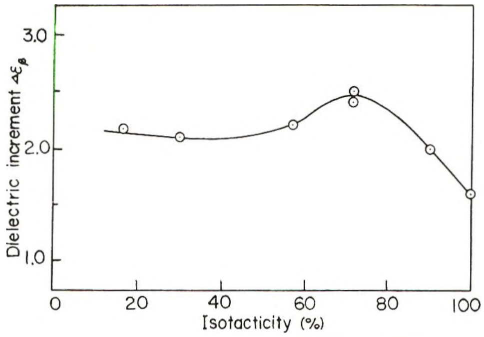

Fig. 11. Dependence of the dielectric increment $\Delta\epsilon_\beta$ for the β-process on the tacticity of the samples.

quency than that for syndiotactic polymer (see Fig. 10), and the activation energy of the β-process depends on the tacticity of the samples.

The dependence of the β-process on tacticity might contain many interesting problems and seems to be related to the length of the stereosequences of the polymer.[3] Further studies on the dielectric behavior of the β-process shall be reported in detail.

References

1. Y. Ishida, S. Togami, and K. Yamafuji, *J. Polym. Sci. B*, **5**, 745 (1967).
2. K. Matsumae, *Repts. Progr. Polym. Phys. Japan*, **10**, 421 (1967).
3. K. Yamafuji and Y. Ishida, *Repts. Progr. Polym. Phys. Japan*, **10**, 449 (1967).
4. S. Tomita, Y. Ishida and M. Takayanagi, paper presented at 17th Annual Meeting of Chemical Society of Japan, Kyoto, April 1964.
5. K. Matsumae and K. Yoda, paper presented at 15th Annual Meeting of Chemical Society of Japan, April 1962.
6. G. P. Mikhailov and T. I. Borisova, *Polymer Sci. USSR*, **2**, 387 (1961).
7. S. Saito and T. Nakajima, *J. Appl. Polym. Sci.*, **2**, 93 (1959).
8. W. Reddish, in *Transitions and Relaxations in Polymers* (*J. Polym. Sci. C*, **14**), R. F. Boyer, Ed., Interscience, New York, 1966, p. 123.
9. G. Williams, *Trans. Faraday Soc.*, **59**, 1387 (1962).
10. Y. Ishida and K. Yamafuji, *Kolloid-Z.*, **177**, 97 (1961).
11. H. Shindo, H. Ochiai, and H. Yamamura, *J. Sci. Hiroshima Univ. A-II*, **30**, 85 (1966).
12. F. Bovey and G. V. D. Tiers, *J. Polym. Sci.*, **44**, 173 (1960).
13. K. S. Cole and B. Gross, *Rev.Sci. Instr.*, **20**, 252 (1949).
14. S. Saito, *J. Polym. Sci.*, **31**, 423 (1958).
15. B. V. Hamon, *Progr. Inst. Elec. Engrs.*, **99**, IV, 151 (1952).
16. K. S. Cole and R. H. Cole, *J. Chem. Phys.*, **9**, 341 (1941).
17. R. M. Fuoss and J. G. Kirkwood, *J. Amer. Chem. Soc.*, **63**, 385 (1941).
18. G. P. Mikhailov, *J. Polym. Sci.*, **30**, 605 (1958).
19. L. Brouckere and G. Offergeld, *J. Polym. Sci.*, **30**, 105 (1958).
20. S. Strella and R. Zand, *J. Polym. Sci.*, **30**, 105, 197 (1958).
21. K. Deutsch, E. A. Hoff, and W. Reddish, *J. Polym. Sci.*, **13**, 565 (1954).
22. H. Pohl, T. Bacskai, and W. P. Purcell, *J. Phys. Chem.*, **64**, 1701 (1962).
23. A. Odajima, A. E. Woodward, and J. A. Sauer, *J. Polym. Sci.*, **55**, 181 (1962).
24. E. V. Thompson, *J. Polym. Sci. A*, **4**, 199 (1966).

25. G. P. Mikhailov and A. M. Lobanov, *Soviet Phys. Solid State*, **5**, 1933 (1964).
26. L. M. Williams, R. F. Landel, and J. D. Ferry, *J. Amer. Chem. Soc.*, **77**, 3701 (1955).
27. M. H. Cohen and D. Turnbull, *J. Chem. Phys.*, **31**, 1164 (1959).
28. S. Saito, *Kolloid-Z.*, **189**, 116 (1963).
29. Y. Kobouchi and R. Yamamoto, *Tech. Data, No.* **31**, Japan, 1952.
30. T. G. Fox, B. S. Garrett, W. E. Goode, J. F. Kincaid, A. Spell, and J. D. Stroupe, *J. Amer. Chem. Soc.*, **80**, 1768 (1958).
31. H. Fröhlich, *Theory of Dielectrics*, Oxford Univ. Press, 1950, Chap. II.

Received July 1, 1968

JOURNAL OF POLYMER SCIENCE: PART A-1 VOL. 7, 311-320 (1969)

Nature of the Active Component in the Catalytic System Prepared from Titanium(III) Chloride(AA), Ethylaluminum Dichloride, and Tetrakis(dimethylamino)silane, in the Polymerization of Propylene

KIICHIRO MATSUMURA, YUJI ATARASHI,*
and OSAMU FUKUMOTO,† *Central Research Laboratory,*
Toyo Rayon Company, Otsu, Japan

Synopsis

The chemistry of the titanium(III) chloride(AA)-ethylaluminum dichloride-tetrakis(dimethylamino)silane system for the polymerization of propylene was studied. A complex of ethylaluminum dichloride with tetrakis(dimethylamino)silane was isolated. It was shown that this complex contains ethylaluminum dichloride and tetrakis(dimethylamino)silane in the ratio of 2:1. This complex with titanium(III) chloride is responsible for the polymerization activity.

INTRODUCTION

Catalysts showing great stereospecificity in the polymerization of propylene to solid polymer are the crystalline halides of transition metals, especially titanium(III) chloride and an organometallic compound, such as the trialkylaluminum or dialkylaluminum halide compounds.[1,2] Alkylaluminum dihalides in combination with titanium(III) chloride are ineffective for the polymerization of propylene to solid polymer. However, highly stereospecific catalysts for the polymerization of propylene can be obtained by using a suitable amount of a third component in combination with alkylaluminum dihalide and violet titanium(III) chloride. Certain organic compounds containing phosphorus and/or nitrogen, such as hexaalkylphosphoric triamide, tertiary phosphine, tertiary amine, and tetrakis(dimethylamino)silane (TDSI) are especially effective as the third component.[3-8] The nature of the active species in these three-component systems has been investigated by several authors in recent years.

Natta and co-workers[8] postulated that alkylaluminum dihalides are

---

* Present address: Basic Research Laboratory, Toyo Rayon Co., Tebiro, Kamakura, Japan.

† Present address: Plastics Laboratory, Toyo Rayon Co., Showaku, Nagoya, Japan.

dismuted by the third components with the consequent formation of dialkylaluminum halide and that this compound participates in the formation of the active species. Zambelli and co-workers[9] also studied three-component systems comprising titanium(III) chloride, ethylaluminum dichloride, and a third component such as pyridine, dimethylformamide, hexamethylphosphoric triamide, triphenylphosphine, etc. They concluded that a dismutation reaction occurs when ethylaluminum dichloride is treated with one of these third components, and diethylaluminum chloride thus produced is responsible for promoting the polymerization of propylene.

The three-component systems were also investigated by McConnell and co-workers.[10] Their investigation demonstrated that a molecular complex is formed when ethylaluminum dichloride is treated at or below 100°C with a third component and that the dismutation reaction does not occur, at least at 100°C. These conclusions are not in agreement with those of Natta and Zambelli.

The present investigation was undertaken to elucidate the nature of active species in the $TiCl_3(AA)$–$C_2H_5AlCl_2$–TDSI system. The complex of ethylaluminum dichloride with TDSI, which is responsible for polymerization activity, was isolated, and this was submitted to analyses. This is the first isolation of the complex of ethylaluminum dichloride with the third component, which is capable of promoting the polymerization of propylene.

EXPERIMENTAL

Materials

Propylene was obtained from Mitsubishi Petro Chemical Co. Analytical results showed that it contains 99.8% propylene, 0.2% propane, 5–6 ppm oxygen, and 10–20 ppm water. It was used without further purification.

Benzene and heptane were obtained commercially. Both were shaken with sulfuric acid, washed with water, and dried by refluxing over sodium. They were carefully distilled at atmospheric pressure.

Ethylaluminum dichloride and diethylaluminum chloride were obtained from Ethyl Corp., and were distilled under reduced pressure; bp 70–72°C/9 mm Hg; $C_2H_5/Al = 1.01$, $Cl/Al = 2.01$, for ethylaluminum dichloride; bp 80°C/12 mm Hg for diethylaluminum chloride.

Titanium(III) chloride(AA) was obtained from Stauffer Chemical Co.

TDSI was obtained from Humphrey Wilkinson Co., and was distilled under nitrogen atmosphere *in vacuo*.

Aluminum chloride was obtained commercially and was purified by sublimation.

Polymerization Procedure

A typical polymerization was carried out as follows. Heptane, titanium(III) chloride, ethylaluminum dichloride, and TDSI were added into an autoclave under nitrogen atmosphere. The autoclave was closed and nitrogen was replaced with propylene. Stirring was started, and the temperature was raised to the desired temperature, then propylene was charged. The polymerization was carried out at a constant pressure of propylene and at constant temperature. Methanol was added to deactivate the catalyst and the reaction mixture was refluxed for several hours. The slurry thus obtained was cooled to room temperature, filtered, and then the polymer was dried at 60°C for 24 hr *in vacuo*.

Analyses of the Catalyst

Determination of Aluminum. A sample was dissolved in aqueous hydrochloric solution and the solution was heated with excess EDTA solution at pH 6 to form a complex. The excess EDTA was then titrated with standard iron solution by using salicylic acid as an indicator.

Determination of Chlorine. A sample was decomposed in aqueous sodium hydroxide. The solution was heated to dryness, and the residue was ignited. The ash thus obtained was dissolved in water and the solution was titrated with silver nitrate, potassium chromate being used as an indicator.

Determination of Ethyl Group. A sample was introduced by hypodermic syringe into a reactor containing a moist alundum shell suspended from the tip of a buret. Water vapor from the alundum shell decomposed the sample slowly with moderate evolution of ethane. Dilute hydrochloric acid was added through the buret to complete the reaction. The gas evolved was measured in calibrated burets, and the ethyl group content was calculated.

Determination of TDSI. TDSI can be determined by acid titration, since it contains four basic nitrogen atoms in its molecule. A sample was decomposed in aqueous hydrochloric acid, and the solution was titrated potentiometrically with sodium hydroxide.

RESULTS

Reactions of TDSI with Ethylaluminum Dichloride and Diethylaluminum Chloride

Reactions of TDSI with ethylaluminum dichloride were carried out in the following way. To a previously dried flask, under nitrogen atmosphere there were introduced ethylaluminum dichloride in heptane and TDSI. A white amorphous precipitate was obtained immediately with evolution of heat. The reaction mixture was then heated at 50°C for 60 min. After heating, the concentration of aluminum in the hydrocarbon phase was determined. The results are shown in Table I. The concentration of aluminum decreased with increasing amount of TDSI up to a molar ratio of TDSI/$C_2H_5AlCl_2$ of 0.5. For the ratio TDSI/$C_2H_5AlCl_2 > 0.5$, the concentration of aluminum was very low and remained constant. These results seem to indicate that one mole of TDSI reacts with nearly two moles of ethylaluminum dichloride to form a solid product which is hardly soluble in heptane.

TABLE I
Reaction of $C_2H_5AlCl_2$ with TDSI[a]

Vol. 2 mole/l. $C_2H_5AlCl_2$ in heptane, cc	TDSI, mmole	$\frac{\text{TDSI}}{C_2H_5AlCl_2}$	Al in liquid phase, wt-%
100	0	0	5.62
100	50	0.25	2.03
100	100	0.50	0.24
50	100	1.00	0.31
50	200	2.00	0.26

[a] Experimental conditions: 50°C, 60 min.

Reactions of TDSI with ethylaluminum dichloride were carried out in the same way as described above at 60°C for 5 min and 24 hr. The reaction product was filtered on a glass filter under nitrogen atmosphere. The solid product was washed repeatedly with heptane and finally dissolved in benzene. This solution was submitted to analyses. The analytical results are shown in Table II. It can be observed that the C_2H_5/Al ratio is nearly 1, $Cl/Al = 2$, and $TDSI/Al = 0.5$ in both runs.

TABLE II
Analyses of the Reaction Product of $C_2H_5AlCl_2$ with TDSI[a]

Reaction time at 60°C	Al, wt-%	C_2H_5, wt-%	Cl, wt-%	TDSI, wt-%	$\frac{C_2H_5}{Al}$	$\frac{Cl}{Al}$	$\frac{\text{TDSI}}{Al}$
24 hr	7.4	7.6	20.4	26.1			
	7.5	7.1	20.4				
Avg.	7.5	7.4	20.4	26.1	0.92	2.1	0.46
	6.8	7.5	18.4	22.9			
5 min.		7.4	18.4				
Avg.	6.8	7.5	18.4	22.9	1.0	2.1	0.44

[a] Experimental conditions; $TDSI/C_2H_5AlCl_2 = 0.5$, $C_2H_5AlCl_2 = 2$ mole/l. in heptane.

Diethylaluminum chloride and TDSI were mixed in heptane in the ratio of 2:1 and heated at 60°C for 24 hr, but neither a precipitate nor evolution of heat was observed.

These results suggest that no dismutation reaction occurs under these experimental conditions between ethylaluminum dichloride and TDSI, but some other reaction occurs, which precipitates the poorly soluble complex of those two components. The complex seems to contain both components in the ratio of nearly 1:2.

Reactions of Ethylaluminum Dichloride–TDSI Complex with Aluminum Chloride

It was shown above that ethylaluminum dichloride reacts with TDSI to form a complex poorly soluble in *n*-heptane having the empirical formula, TDSI·$(C_2H_5AlCl_2)_2$. The possibility that the above complex exists as a dismuted form, TDSI·$(C_2H_5)_2AlCl\cdot AlCl_3$, is small, because diethylaluminum chloride can not form a complex which is hardly soluble in *n*-heptane. The presence of aluminum chloride may affect the interaction between TDSI and diethylaluminum chloride, however, so there may be some possibility of the existence of the dismuted complex. Examination of ethylaluminum chloride released from the complex by the action of aluminum chloride would clarify whether the complex exists as dismuted form or not; that is, if the complex is in a dismuted form, then addition of aluminum chloride would release diethylaluminum chloride, while, on the contrary, if the complex is in non-dismuted form, then the released alkylaluminum chloride would be ethylaluminum dichloride. To clarify this point, the following experiments were carried out.

To a previously dried flask, under argon atmosphere, 22.75 cc of 2.17*M* heptane solution of ethylaluminum dichloride (49.4 mmole), and 21.65 cc of 1.14*M* heptane solution of TDSI (24.7 mmole) were added gradually, the temperature of flask being kept at 0°C by cooling it with ice. The temperature of the reaction mixture was then raised to 60°C and kept at that temperature for 3 hr. Then 2.398 g of anhydrous aluminum chloride (24.7 mmole), which was purified by sublimation, was added. After distillation of solvent at 100 mm Hg, the reaction product was distilled under 10^{-3} mm Hg. The temperature of the heating bath was kept below 100°C. The yield was 2.74 g. (This amount corresponds to 21.6 mmole of ethylaluminum dichloride, and this figure amounts to 87.5% of theoretical yield, in the case that the nondismuted complex is postulated.) The analytical results are shown in Table III. Table III indicates that the released alkylaluminum chloride is nearly pure ethylaluminum dichloride, and this shows that the complex does exist as nondismuted complex.

TABLE III
Analyses of the Released Alkylaluminum Chloride from TDSI·$2C_2H_5AlCl_2$ Complex by the Action of $AlCl_3$

	Al, wt-%	Cl, wt-%	C_2H_5, wt-%
Released product	21.1	52.6	24.8
$C_2H_5AlCl_2$ (measured)	21.2	53.0	25.1
$C_2H_5AlCl_2$ (calculated)	21.3	55.9	22.9
$(C_2H_5)_2AlCl$ (calculated)	22.4	29.4	48.2

Polymerization Runs

Some results of the polymerization with the $TiCl_3$–$C_2H_5AlCl_2$–TDSI system are shown in Figure 1. In the absence of TDSI, no solid polymer is

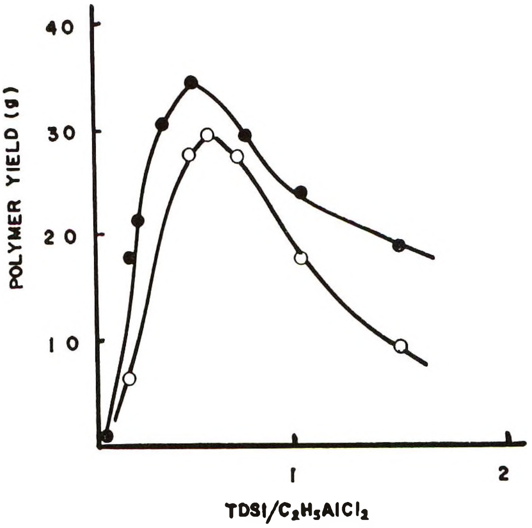

Fig. 1. Effect of molar ratio of catalyst components on polymerization activity: (●) 4 mmole $C_2H_5AlCl_2$; (○) 2 mmole $C_2H_5AlCl_2$ Heptane = 60 cc; $TiCl_3$ = 2 mmole; 50°C; pressure = 6 atm; 5 hr.

obtained, but with increasing amounts of TDSI, catalytic activity increases, reaching a maximum at a TDSI/$C_2H_5AlCl_2$ ratio of about 0.5, and then decreases gradually. That this system shows the maximum activity when the TDSI/$C_2H_5AlCl_2$ ratio is nearly 0.5, indicates that both components work as a 1:2 complex in the polymerization.

Reactions of ethylaluminum dichloride with TDSI in heptane resulted in the formation of an amorphous solid and a liquid phase, as described already. The polymerizations of propylene with the $TiCl_3$–amorphous solid

TABLE IV
Polymerization of Propylene with $TiCl_3$ and the Reaction Products of $C_2H_5AlCl_2$ with TDSI[a]

Metallorganic compound[b]	Solvent	Yield, g	[η] dl/g[c]
Component in liquid phase	heptane	3.4	13.03
Component in solid phase	benzene	13.4	10.83

[a] Polymerization conditions; $TiCl_3$(AA): 2 mmole, metallorganic compound: 2 mmole of Al (see note b); solvent = 60 cc; 60°C; 2 hr; pressure = 6 atm.

[b] A 100-cc portion of 2*M* heptane solution of ethyl-aluminum dichloride and 50 cc of 2*M* heptane solution of TDSI were reacted at 60°C for 3 hr, and the solid complex formed was separated from the liquid phase. The aluminum concentration in the liquid phase was determined. A suitable amount of this heptane solution, which contains 2 mmole of aluminum, was used for polymerization. The solid complex was dissolved in benzene, and aluminum concentration in benzene solution was determined. A suitable amount of this benzene solution, which contains 2 mmole of aluminum, was used for polymerization.

[c] Intrinsic viscosity was measured in tetralin at 135°C.

system, and the $TiCl_3$–liquid phase system were carried out. The results are shown in Table IV. The amorphous solid–$TiCl_3$ system has almost the same activity as the $TiCl_3$–$C_2H_5AlCl_2$–TDSI system (Fig. 1). (Actually, titanium (III) chloride seems to be activated by the dissolved species, though its concentration must be very small.) The liquid phase, on the contrary, when combined with $TiCl_3$ shows much lower activity. Hence, the amorphous solid, the complex of ethylaluminum dichloride with TDSI, is mainly responsible for the polymerization activity of $TiCl_3$–$C_2H_5AlCl_2$–TDSI system.

In Table V, some properties of the polypropylene obtained with the $TiCl_3$–$C_2H_5AlCl_2$–TDSI and $TiCl_3$–$(C_2H_5)_2AlCl$ systems are shown. The amount of heptane-insoluble material and the intrinsic viscosity of the polymer obtained with the three-component system are much higher than those of the polymer obtained with the other system. This is one of the evidences that the active species of the three-component system are different from those of the two-component system.

TABLE V
Some Properties of Polypropylene[a]

Catalyst system	Temp, °C	Heptane-insoluble material, %	[η] dl/g[b]
$TiCl_3(AA)$–$C_2H_5AlCl_2$–TDSI	65	98.2	11.1
	50	99.5	12.1
$TiCl_3(AA)$–$(C_2H_5)_2AlCl$	60	90.0	6.9

[a] Experimental conditions: pressure = 6 atm.
[b] Intrinsic viscosity was measured in tetralin at 135°C.

Heat Treatment of the Catalyst Components

Catalyst components were subjected to heat treatment at 100°C for 24 hr in heptane under a nitrogen atmosphere. The amount of gas evolved during the heat treatment was measured, and a color change in titanium(III) chloride was also observed. The results are reported in Table VI. Only a small amount of gas was evolved for the combinations TDSI–$C_2H_5AlCl_2$, $TiCl_3$–$C_2H_5AlCl_2$, and $C_2H_5AlCl_2$ only, but a large amount of gas was evolved when all three components, TDSI, $C_2H_5AlCl_2$, and $TiCl_3$, were heated together. Analyses by gas chromatography and mass spectroscopy indicated that the gas consists mainly of ethane. The best explanation of these results seems to be as follows. Ethylaluminum dichloride can alkylate titanium(III) chloride only when TDSI is present. Ethyltitanium dichloride thus formed decomposes to titanium dichloride and ethyl radical under the experimental conditions employed (100°C, 24 hr), since it (or at least some portion of it) is not stable, when exposed at a high temperature for a long time.[11] The color change of titanium(III)

TABLE VI
Heat Treatment of Catalyst Components[a]

No.	$TiCl_3$, mmole	$C_2H_5AlCl_2$, mmole	TDSI, mmole	Heptane, cc	Gas evolved, cc, at 20°C, 1 atm	Color of $TiCl_3$
1		80.8	40.4	50	0	
2	40.4	80.8		50	6	Reddish purple
3		80.8		50	7	
4	40.4	80.8	40.4	50	100	Black

[a] Conditions of heat treatment: 100°C, 24 hr.

chloride during the heat treatment also indicates formation of titanium dichloride. The ethyl radical is transformed to ethane and ethylene by disproportionation. The ethylene thus formed is readily polymerized to polyethylene.

DISCUSSION

The main reaction product of ethylaluminum dichloride with TDSI is the addition complex comprising these components in the ratio of 2:1. This complex is hardly soluble in heptane and is responsible for polymerization activity when used with titanium(III) chloride (AA). These results can best be explained as follows.

Ethylaluminum dichloride is a Lewis acid and TDSI is a Lewis base, hence the reaction of these two components proceeds by electrophilic addition of aluminum to lone pair of nitrogen of TDSI. TDSI can react with only two moles of ethylaluminum dichloride, in spite of having four nitrogen atoms in its molecule. The reason for this is not explicit, but there seem to be two explanations. First, there may be some steric hindrance when more than two moles of ethylaluminum dichloride react with one mole of TDSI. The second explanation would be that the aluminum in ethylaluminum dichloride may react with two nitrogen atoms in TDSI.

Wilson and co-workers,[12] and one of the present authors[11,13] indicated that the active center of the catalyst system consisting of titanium(III) chloride and trialkylaluminum or dialkylaluminum halide is alkyltitanium(III) dichloride which is produced by the alkylation of titanium(III) chloride with these alkylaluminum compounds. For the present system, $TiCl_3$–$C_2H_5AlCl_2$–TDSI, ethyltitanium dichloride is also responsible for the activity. Ethylaluminum dichloride can not alkylate titanium(III) chloride, hence titanium(III) chloride with ethylaluminum dichloride can not polymerize propylene. However, the $TiCl_3$–$C_2H_5AlCl_2$–TDSI system shows activity for the polymerization of propylene, since the addition product of ethylaluminum dichloride with TDSI can alkylate titanium(III) chloride for the following reason. Due to the electronegative character of the halogen atoms, the energy of the dative bond between the Lewis base (TDSI in this case) and the aluminum atom increases for the following compounds in the order: $AlR_3 < AlR_2X < AlRX_2 < AlX_3$, where R is the alkyl group and X is the halogen.

The complex of ethylaluminum dichloride with TDSI would be more stable when it exchanges an ethyl group for a chlorine atom with titanium(III) chloride to form an ethyltitanium dichloride. If the TDSI–$C_2H_5AlCl_2$ complex could exchange its ethyl group for chlorine with another TDSI–$C_2H_5AlCl_2$ complex, the dismutation reaction would occur. This is not the case for the $TiCl_3$–$C_2H_5Al_2$–TDSI system, however. The TDSI–$C_2H_5AlCl_2$ complex can only exchange its ethyl group for chlorine with titanium(III) chloride. (The exchange reaction seems to proceed through dissolved species, though the concentration must be low.) If some third component, for example pyridine, is used, the dismutation reaction between two moles of ethylaluminum dichloride may occur, and diethylaluminum chloride thus formed alkylate titanium(III) chloride.[9] The possible scheme of these reactions is as follows.

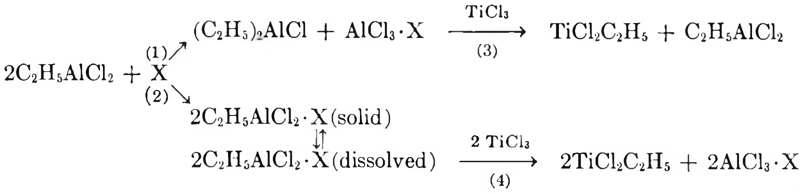

$$2C_2H_5AlCl_2 + X \xrightarrow{(1)} (C_2H_5)_2AlCl + AlCl_3\cdot X \xrightarrow[(3)]{TiCl_3} TiCl_2C_2H_5 + C_2H_5AlCl_2$$

$$2C_2H_5AlCl_2 + X \xrightarrow{(2)} 2C_2H_5AlCl_2\cdot X(\text{solid}) \rightleftarrows 2C_2H_5AlCl_2\cdot X(\text{dissolved}) \xrightarrow[(4)]{2\ TiCl_3} 2TiCl_2C_2H_5 + 2AlCl_3\cdot X$$

If X is TDSI, the reaction proceeds through reactions (2) and (4); on the other hand, if X is pyridine, the reaction proceeds through steps (1) and (3). It depends upon the nature of X whether the reaction proceeds through (2) and (4) or through (1) and (3), or, in other words, whether the dismutation reaction occurs or not.

Stereospecificity and intrinsic viscosity of the polymer formed with the $TiCl_3$–$C_2H_5AlCl_2$–TDSI system are much higher than those of the polymer formed with the $TiCl_3$–$(C_2H_5)_2AlCl$ system, as shown in Table V. These results indicate that the nature of active centers of these two systems must be different. The active centers must be formed by complicated reactions among ethyltitanium dichloride, alkylaluminum chloride, and other components present.

In summary, the $TiCl_3$(AA)–$C_2H_5AlCl_2$ system is an ineffective catalyst for the polymerization of propylene to solid polymer but the $TiCl_3$(AA)–$C_2H_5AlCl_2$–TDSI system is an effective one. In the latter system, an addition product of ethylaluminum dichloride with TDSI is first produced, and this complex with titanium(III) chloride is responsible for the polymerization activity. The dismutation reaction does not occur in the $TiCl_3$–$C_2H_5AlCl_2$–TDSI system.

The authors are grateful to Dr. H. Kobayashi and to K. Nukushina, the director of Central Research Laboratory, for their interest and encouragement.

References

1. G. Natta, P. Pino, and G. Mazzanti, Ital. Pat. 526,101 (Dec. 3, 1954).

2. G. Natta, *Angew. Chem.*, **68**, 393 (1956).

3. H. W. Coover, Jr., and F. B. Joyner, *J. Polym. Sci.*, **3**, 2407 (1965).

4. H. W. Coover, Jr., and F. B. Joyner (to Eastman Kodak Co.), U.S. Pats. 2,956,991 (1960), 2,969,345 (1961), 2,958,688 (1960).

5. A. Nicco (to Societe Normande de Matieres Plastiques), French Pat. 1,354,815 (1964).

6. Y. Atarashi and O. Fukumoto (to Toyo Rayon Co.), Brit. Pat. 1,017,708 (1966).

7. Firestone Tire and Rubber Co., Japan. Pat. 39-25293 (1964).

8. G. Natta, A. Zambelli, I. Pasquon, G. Gatti, and D. Deluca, *Makromol. Chem.*, **70**, 206 (1964).

9. A. Zambelli, J. Dipietro, and G. Gatti, *J. Polym. Sci. A*, **1**, 403 (1963).

10. R. L. McConnell, M. A. McCall, G. O. Cash, Jr., F. B. Joyner, and H. W. Coover, Jr., *J. Polym. Sci. A*, **3**, 2135 (1965).

11. Y. Atarashi, *Kobunshi Kagaku*, **21**, 409 (1964).

12. T. P. Wilson and G. F. Hurley, in *First Biannual American Chemical Society Polymer Symposium* (*J. Polym. Sci. C*), **1**, J. W. Starkweather, Jr., Ed., Interscience, New York, 1963, p. 281.

13. Y. Atarashi, *Kobunshi Kagaku*, **21**, 257 (1964).

Received April 25, 1967
Revised August 7, 1968

JOURNAL OF POLYMER SCIENCE: PART A-1 VOL. 7, 321-332 (1969)

Aromatic Polyimide-*co*-Amides. I

W. WRASIDLO and J. M. AUGL, *U. S. Naval Ordnance Laboratory, White Oak, Silver Spring, Maryland 20910*

Synopsis

A series of aromatic polyimide-co-amides of high thermal stability were synthesized. Low-temperature solution condensation involving aromatic diamines of varying basicity and bifunctional carboxylic acid chlorides containing preformed imide rings was employed. This approach offers several advantages over the conventional polyamic acid route. The final polymers obtained are linear, soluble, and of high molecular weight. Solution of the final polymers are stable in contrast to polyamic acid solutions, which depolymerize hydrolytically due to the neighboring-group effect. Tough, flexible films were cast from solution and required no heat cure. The properties of one polymer made by the preformed ring approach were compared to its structurally related amide and imide homologs.

INTRODUCTION

Aromatic polymers containing hetero rings in the chains have been described as being linear. However, there is a good chance that those made from monomers of more than two similarly reactive functional groups are at least slightly crosslinked. Examples of such polymers are the polyimides and the imide–amide copolymers. Conventionally these polymers are prepared through poly-*o*-carboxyamide intermediates, followed by thermal cyclization to form imide rings. Side reactions leading to crosslinked final products most likely occur during the cyclization step. This generally results in insoluble polymers with unusually high glass transition temperatures.

Poly-*o*-carboxyamides are hydrolytically unstable substances and require special storage and handling care. Their synthesis requires highly purified reagents and extremely anhydrous reaction conditions to achieve high molecular weights.[1,2]

One method of circumventing problems such as insolubility, high thermal cure, unstable intermediates, and stringent reaction conditions with these polymers is to synthesize them from monomers containing preformed imide rings. This approach has been applied with other hetero ring-containing aromatic polymers,[3-10] such as the polybenzimidazoles and polyoxadiazoles.

The present paper describes the synthesis and properties of linear aromatic polyimide-*co*-amides from monomers containing preformed imide rings.

EXPERIMENTAL

Preparation of Monomers

Oxy-bis[*N*-(4-phenylene)-4′-(chloroformyl)phthalimide]. A 2-liter round-bottomed flask, fitted with a mechanical stirrer, a thermometer, a reflux condenser, and a nitrogen inlet tube was charged with 100 g (0.50 mole) of 4,4′-oxydianiline and 400 ml of dimethylacetamide (DMAc). The flask was cooled to 0°C, and nitrogen was passed through the solution while 1.92 g (1.00 mole) of recrystallized trimellitic anhydride was added with stirring. The flask content was kept below 10°C during addition and stirred for an additional 6 hr at room temperature. Then 120 ml of acetic anhydride, followed by 30 ml of pyridine, was added; the clear solution was then heated by means of an oil bath to 150°C for 5 hr. A greenish precipitate which formed upon cooling was filtered, washed several times with acetone, recrystallized twice from dimethylacetamide, and finally washed with acetone to yield 195 g (74%) of the orange-colored diacid, mp 374°C.

The diacid (190 g, 0.35 mole) was then heated for 4 hr with 100 g (0.8 mole) of thionyl chloride and a few drops of dimethylformamide. The yellow colored product was filtered, washed with cyclohexane, and dried at 100°C under oil pump pressure. The yield was 200 g (99%), mp 238–239°C.

ANAL. Calcd for $C_{30}H_{14}N_2Cl_2O_7$: C, 61.55%; H, 2.41%; N, 4.78%; Cl, 12.11%. Found: C, 61.47%; H, 2.46%; N, 4.91%; Cl, 11.97%.

The phenyl ester was prepared from 5.85 g (0.100 mole) of acid chloride dissolved in 75 ml of dry nitrobenzene by adding 2.00 g (0.214 mole) of phenol dissolved in 20 ml of water containing 1.00 g (0.25 mole) of sodium hydroxide. The mixture was vigorously shaken for several minutes. The yield of white product was quantitative; mp 275–277°C.

ANAL. Calcd for $C_{42}H_{24}N_2O_9$: C, 72.06%; H, 3.46%; N, 4.00%. Found: C, 71.98%; H, 3.55%; N, 4.01%.

The ethyl ester was made by refluxing the acid chloride for 1 hr in absolute ethanol, followed by recrystallization from ethanol; mp 216–217°C.

Preparation of Sulfuryl[N-(4-phenylene)-4′-(chloroformyl)phthalimide]. This monomer was prepared by the reaction of 4,4′-diaminodiphenylsulfone and trimellitic acid anhydride under the same reaction conditions as used for the oxy derivative. On heating with sulfonyl chloride, a white crystalline diacid chloride was obtained in 71% overall yield; mp 301–302°C.

Preparation of Polymers

Condensation of Diamines with Diacid Chlorides. Several aromatic diamines were reacted with diacid chlorides following the general scheme (1).

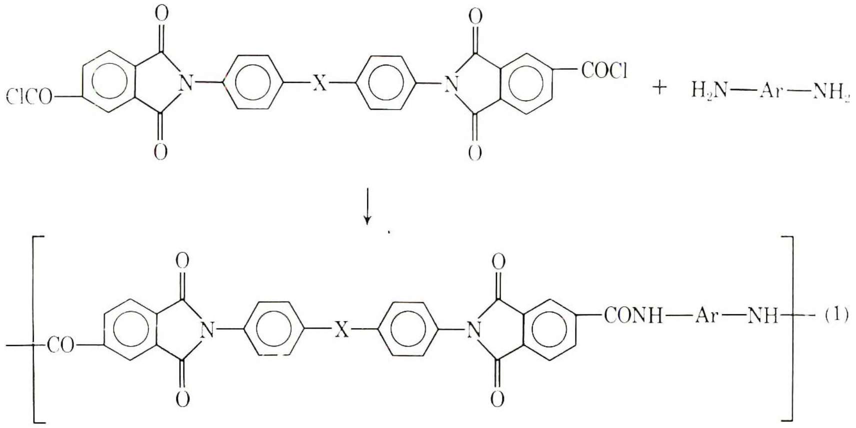

(1)

The diamines were recrystallized several times from ethyl acetate until white crystallites melting within 1°C were obtained. Dimethylacetamide was distilled over calcium hydride under reduced pressure and was stored over molecular sieves (water content $< 0.02\%$). A flamed-out three-necked flask fitted with stirrer and drying tube was flushed with nitrogen and charged with diamine and dimethylacetamide to obtain a 10–15% final solution of polymer. The flask was cooled below −15°C, and the diacid chloride (as a finely divided powder) added all at once with stirring. The flask content was kept below −10°C for 1 hr and then slowly raised to room temperature within 1/2 hr. The clear yellow, viscous solution was then neutralized with pyridine.

When *p*-phenylenediamine or benzidine were used, the product precipitated out of solution and it became necessary to add 5% lithium chloride and to heat on a steam bath in order to redissolve the polymer.

Condensation via Amic Acids. Two polymers were synthesized from trimellitic anhydride acid chloride and *p,p′*-oxydianiline.

The first polymer was made by adding a stoichiometric amount of trimellitic anhydride acid chloride to a solution of *p,p′*-oxydianiline in dimethylacetamide at −15°C. This gave the amine anhydride-terminated amide. Then the solution temperature was raised above 0°C. and the hydrochloric acid formed was neutralized with pyridine. A yellow, viscous solution formed and was stored in the cold until further use.

The second polymer was made by the same procedure using twice the stoichiometric amount of trimellitic anhydride acid chloride. In this way

TABLE I
Elemental Analysis of Imide-Amide Copolymers

Polymer structure	Abbreviation		Analysis C, %	 H, %	 N, %
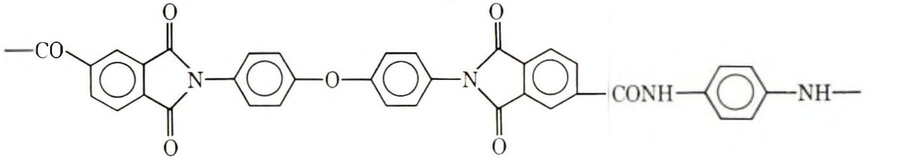	Polymer I	Calcd: Found:	69.67 68.06	3.24 3.64	9.02 8.86
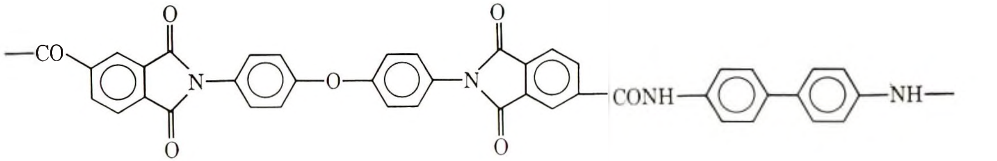	Polymer II	Calcd: Found:	72.41 72.35	3.47 3.54	8.04 7.96
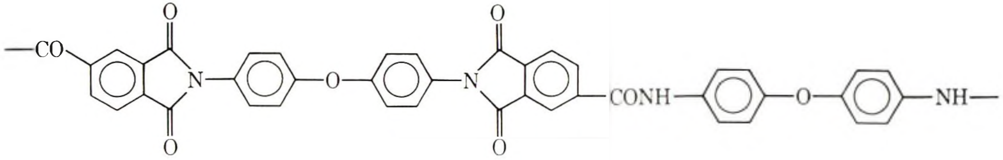	Polymer III	Calcd: Found:	70.78 70.63	3.39 3.33	7.86 7.77
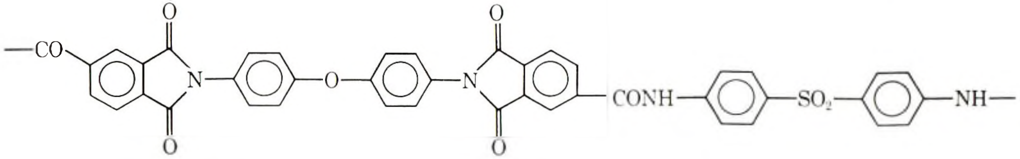	Polymer IV	Calcd: Found:	66.31 66.30	3.17 3.23	7.36 7.44

the dianhydride-terminated amide was formed which was then reacted with a stoichiometric amount of *p,p'*-oxydianiline by the conventional amic acid route.

Polymer Characterization

The polymers were characterized by infrared spectra and elemental analysis (Table I). The infrared spectra showed characteristic imide bands at 1785 cm^{-1} due to symmetrical carbonyl stretching vibrations, at 1730 cm^{-1} due to asymmetrical carbonyl stretching vibrations, and at 725 cm^{-1} possibly due to ring carbonyl deformations. The results from elemental analysis are in exceptional good agreement with the polymer structures assigned in Table I.

Properties of Polymers

Solution and thermal properties of polymers, whose structures are shown in Table I, were obtained and are summarized in Table II.

TABLE II
Properties of Imide-*co*-Amide Polymers

No.	R-group	Solubility in DMAc	Intrinsic viscosity $[\eta]$[a]	Glass transition temperature T_g, °C[b]	Thermal decomposition PDT, °C[c]	Isothermal weight loss at 325°C in air, %	
						After 120 hr	After 240 hr
I	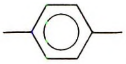	Ins[d]	0.7	—	455	9.8	11.5
II	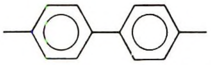	Ins[d]	0.9	315	520	10.1	10.1
III	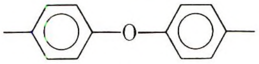	Sol[e]	2.0	290	460	14.8	19.5
IV	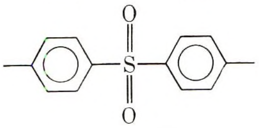	Sol[e]	1.6	275	475	7.4	7.4

[a] Determined in DMAc at 30°C.

[b] From dielectric loss measurements.

[c] By thermogravimetric analysis in vacuum at a heating rate of 5°C/min.

[d] Soluble in DMAc + 5–10% lithium chloride.

[e] In concentrations up to 30% solids.

Intrinsic viscosities were determined in DMAc at 30 ± 0.05°C in an Ubbelohe viscometer. The viscometer had a flow time of 180 sec for the

TABLE III
Mechanical Properties of Imide-*co*-Amide Polymer Films

Polymer	Tensile tear strength × 10^8, dyne-cm^2 [a]	Elongation, %	Coefficient of variation
Polymer III	5.90	5	0.06
Polymer IV	5.78	5	0.06
Polymer VI	4.65	6	0.04
Mylar	8.01	48	0.07

[a] Determined on dog-bone specimens cut from 1-mil thick films.

pure solvent. Glass transition temperatures were determined on films by means of dielectric loss measurements at a programed heating rate of 5°C/min. The thermal decomposition temperature of polymers was defined as the temperature of onset of weight loss, and it was obtained from thermogravimetric curves of powdered samples in vacuum at a heating rate of 5°C/min. Isothermal weight loss measurements were made in static air at the temperature indicated in Table II. Samples were heated in porcelain crucibles and periodically weighed. Films of polymers III and IV coated on aluminum cups were simultaneously heated and periodically checked for retention of creasability.

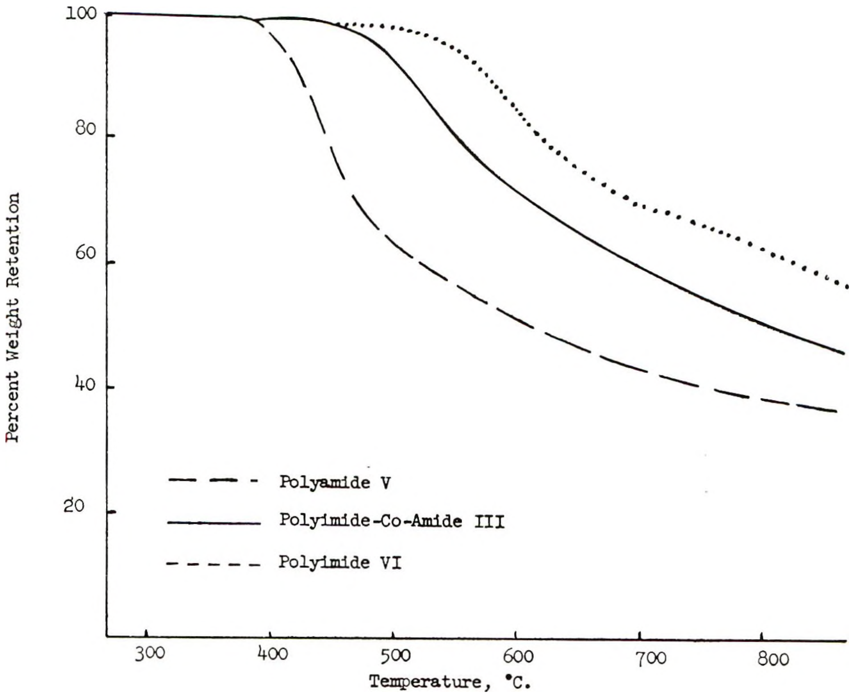

Fig. 1. Thermogravimetric analysis of structurally related polymers *in vacuo* (heating rate 5°C/min).

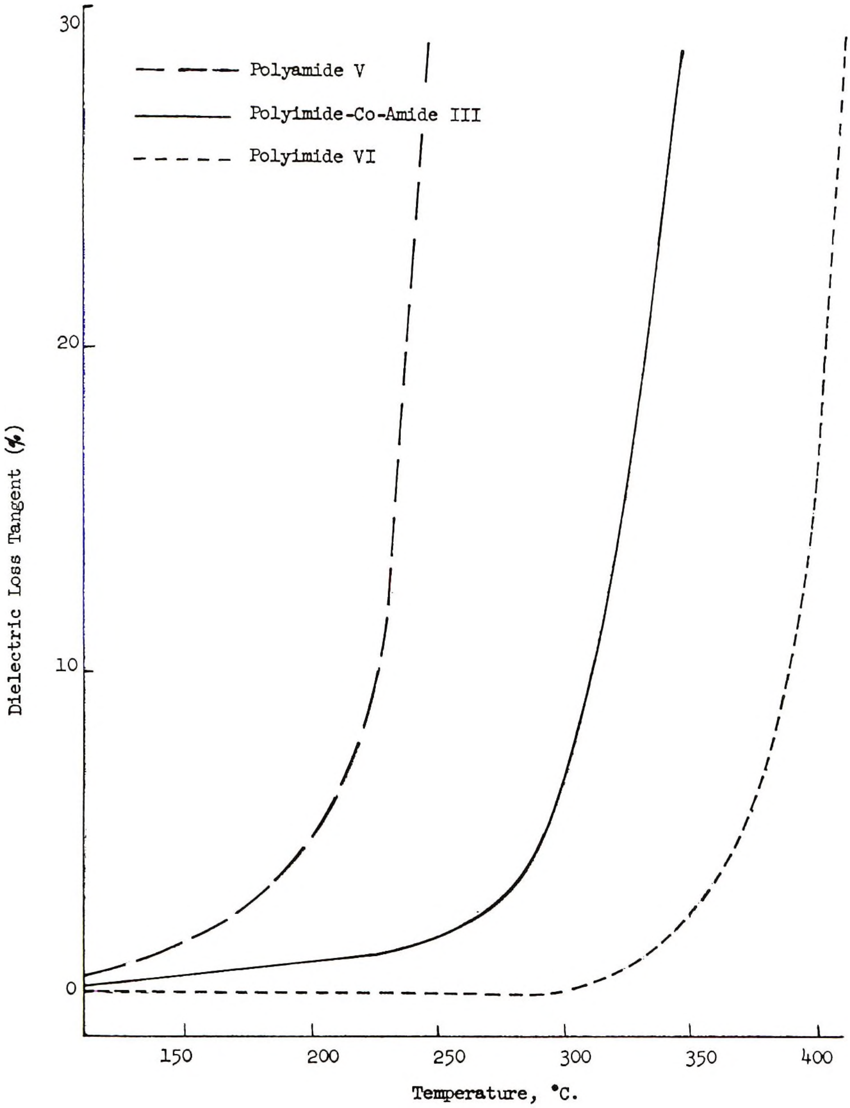

Fig. 2. Dielectric loss as a function of temperature (heating rate 5°C/min).

Films of polymers III and IV were tested for mechanical strength properties and break elongation. Mylar and a polyimide film were tested under identical conditions, and the results are included in Table III for comparison.

The films were prepared by casting 10% DMAc solutions on a glass plate by using a 10 mil spacer and evaporating the solvent under reduced pressure at 140°C. Films made from polyamic acid solutions were then baked for additional 2 hr at 260°C *in vacuo* to complete the thermal cyclization.

RESULTS AND DISCUSSION

Solution and Thermal Properties of Polyimide-*co*-Amides

Four new polyimide-*co*-amides have been synthesized by low temperature solution condensations of oxy-bis[*N*-(4′-phenylene)-4-(chloroformyl)-phthalimide] with various aromatic diamines (Table I). Polymers I and II containing the *p*-phenylene and *p,p*′-biphenylene moiety were insoluble, while III and IV were soluble in dimethylacetamide. This difference in solubility is presumably due to the higher degree of crystallinity arising from more chain regularity in polymers I and II. As a result of better solubility in the reaction solvent, polymers III and IV go to higher molecular weights, as indicated by higher intrinsic viscosities (Table II). Polymers I and II are readily soluble in dimethylacetamide containing 5–10% lithium chloride, and films can be cast from such solutions. However, the film properties are inferior to those made from polymers III and IV.

The glass transition temperatures varied from 275°C for polymer IV to

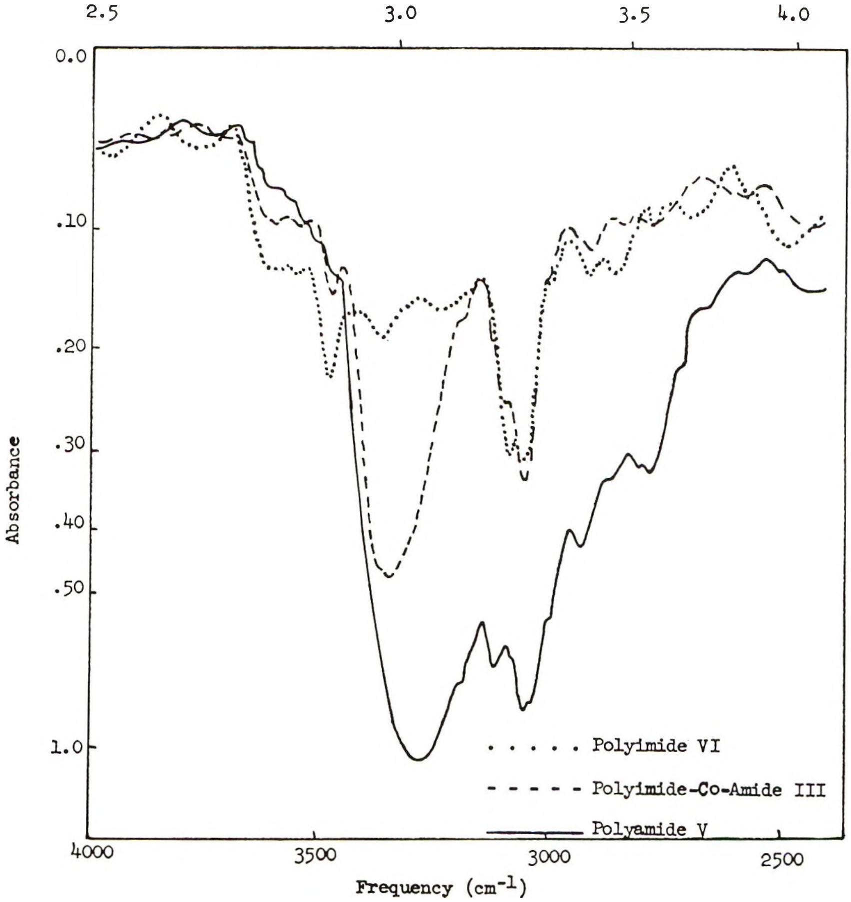

Fig. 3. Infrared spectra of structurally related polymers.

315°C for polymer II. From the results of thermogravimetric analysis the polymer decomposition temperatures were obtained (Table II, column 6) and were found to vary between 455°C for polymer I to 520°C for polymer II.

Isothermal aging of samples at 325°C in static air indicated excellent thermal-oxidation stability. Films of polymers III and IV remained clear and creasable when aged for 240 hr at this temperature. Polymer IV, containing the sulfone linkage, gave the lowest weight loss, and films from this polymer appeared to be least affected on thermal aging.

Mechanical testing of dog-bone film specimens was carried out on an Instron tester. Although this method of specimen preparation and testing does not yield pure tensile properties but rather mixed tensile tear strength; the relative values obtained are useful when compared to other standard film forming polymers such as Mylar. A polyimide film (polymer VI, a commercial product of du Pont known as H-film) was also tested and the results are included for comparison in Table III. The values obtained for these films were approximately 50% of the expected pure tensile strengths.

Effect of Imide Rings on Properties

As part of this study, the effect of imide rings in the polymer chain on the thermal properties has been investigated. The results are illustrated in Figures 1–4.

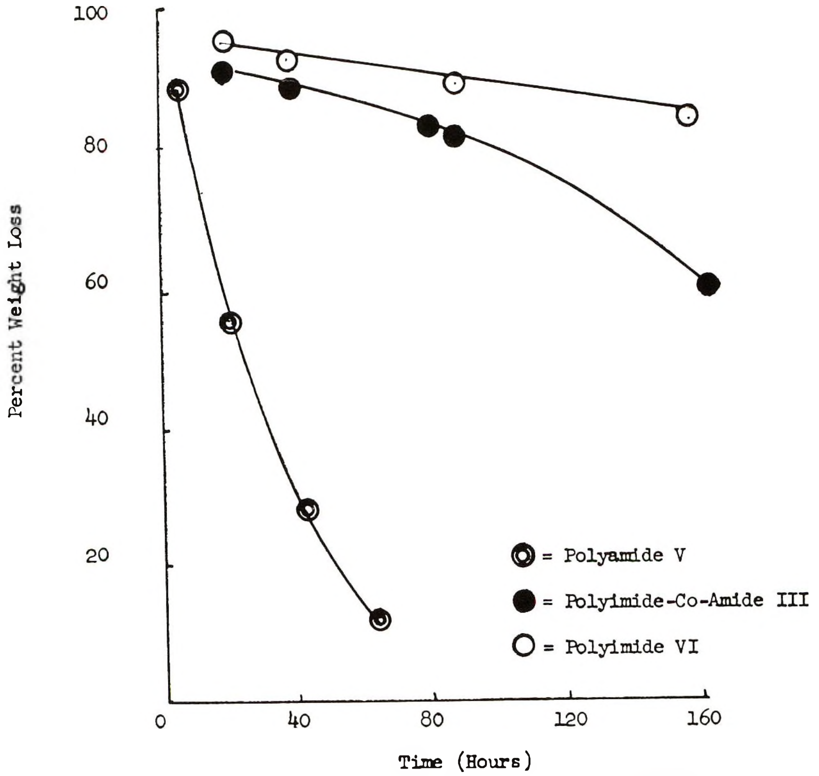

Fig. 4. Isothermal weight loss of structurally related polymers at 400°C in static air.

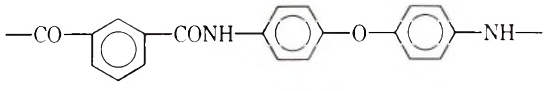

Polyamide V

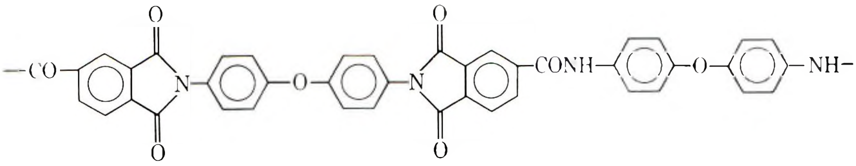

Polyimide-co-amide III

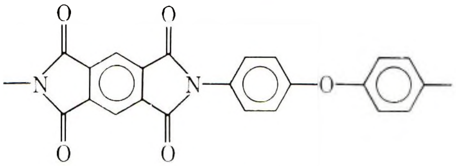

Polyimide VI

Repeat unit structures of the three polymers, polyamide V, polyimide-*co*-amide III, and polyimide VI, chosen for comparison are as shown.

Figure 1 shows TGA curves of the three polymers. The polyamide V gave a temperature of initial weight loss of 410°C, the amide-imide copolymer (III) showed a weight loss at 475°C, and polyimide (VI) at 545°C. A

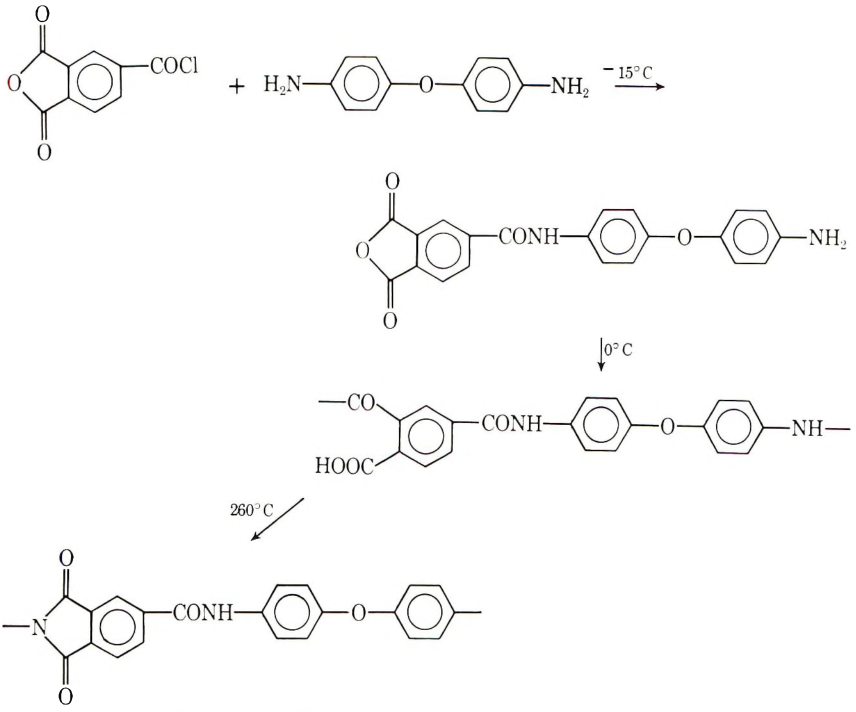

AB polymer (IIIa)

similar dependency on structure was observed from dielectric loss measurements (Fig. 2). From these measurements the relative glass transition temperatures obtained were 190°C for polymer V, 300°C for polymer III, and 365°C for polymer VI.

Infrared spectra between 2.5 and 4.0 μ of films (Fig. 3) shows the relative amide content by bands between 3300 and 3400 cm^{-1}. A weak band at 3350 cm^{-1} present in the polyimide VI is attributed to amide NH stretching vibrations. This band remained after heating the film to 300°C in vacuum and suggests that some crosslinking took place during thermal cyclization of this polymer.

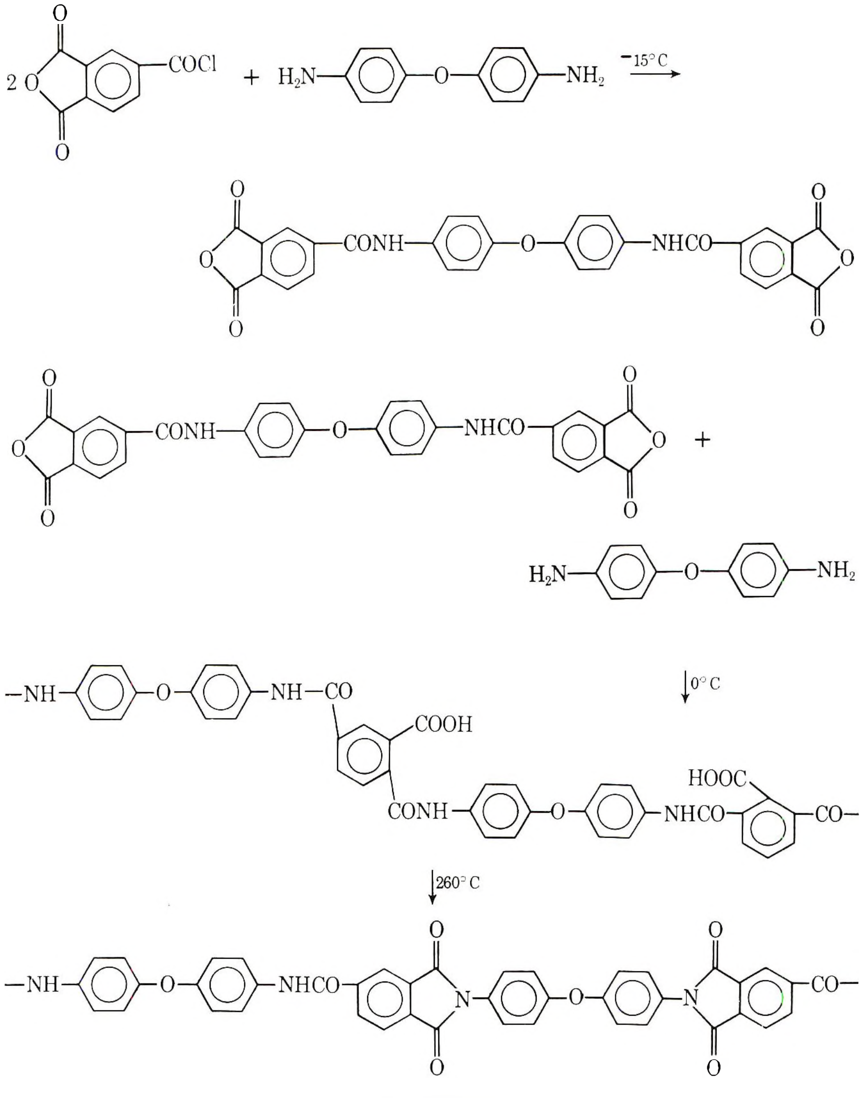

AA—BB polymer
(IIIb)

A pronounced effect of imide rings in the polymer chain on thermal stability was also observed from isothermal weight loss measurements at 400°C in air (Fig. 4). After 60 hr, the polyamide V lost 90%, while the polyimide-*co*-amide III lost only 10% and the polyimide VI lost 5% of the original weight.

Preparation via Polyamic Acids

Two polymers, structurally analogous to polymer III, have been synthesized by the polyamic acid route. The first polymer (IIIa) was made by reaction of trimellitic acid chloride and *p,p'*-oxydianiline at −15°C to form the amine-anhydride-terminated AB-monomer which was then allowed to polymerize in solution above 0°C to form the polyamic acid. Imidization was achieved by heating a polyamic acid film in vacuum at 260°C.

The second method consisted of reacting two moles of trimellitic acid chloride with one mole of *p,p'*-oxydianiline at −15°C to yield oxy-bis[(4-phenyl-4'-amido)-phthalic anhydride]. This intermediate was then reacted with an equal molar quantity of *p,p'*-oxydianiline without isolation to form the polyimide-*co*-amide.

By this method AA-BB polyimide-*co*-amides can also be made from different diamines via amic acid intermediates.

The thermal properties of polymers III, IIIa, and IIIb were very similar. However, solutions of the amic acids of polymers IIIa and IIIb were subject to hydrolytic degradation, as indicated by a decrease in intrinsic viscosity.

References

1. W. M. Edwards, Brit. Pat. 898,651, (1962).
2. M. L. Wallach, *J. Polym. Sci. A-1*, **5**, 653 (1967).
3. F. Robinson and J. Preston, *J. Polym. Sci. A-1*, **4**, 2093 (1966).
4. L. W. Frost, G. M. Bower, J. H. Freemann, H. A. Burgmann, E. C. Traynor, and C. R. Duffing, *J. Polym. Sci. A-1*, **6**, 215 (1968).
5. J. R. Caldwell, Fr. Pat. 1,450,704, (1965).
6. V. P. Sarzhevskaya, K. A. Kornev, S. E. Smirnova-Zamkova, S. Z. Levin, V. N. Kochinskii, and V. E. Griz. *Ukr. Khim. Zh.*, **30**, 83 (1964).
7. Y. Ywakura, Y. Iwakura, K. Uno, and Y. Imai, *Makromol. Chem.*, **77**, 33 (1964).
8. J. Preston, U.S. Pat. 3,354,120, (1967).
9. T. Shono, M. Saga, M. Obora, and K. Shinra, *Kogyo Kagaku Zasshi*, **70**, 1250 (1967).
10. H. Hopp and A. Krieger, *Makromol. Chem.*, **47**, 93 (1961).

Received July 12, 1968
Revised August 14, 1968

JOURNAL OF POLYMER SCIENCE: PART A-1 VOL. 7, 333-349 (1969)

Cationic Graft Copolymerization of Polystyrene onto Poly-2,6-dimethoxystyrene by the Termination Reaction

C. G. OVERBERGER* and C. M. BURNS,† *Department of Chemistry, Institute of Polymer Research, Polytechnic Institute of Brooklyn, Brooklyn, New York 11201*

Synopsis

Poly-2,6-dimethoxystyrene (P26) was used as the polymeric backbone and was obtained by a new synthetic route involving the Wittig reaction. The grafting reaction was studied by polymerizing styrene with stannic chloride as catalyst in the presence of various concentrations of preformed P26 in solution with carbon tetrachloride and nitrobenzene at 60, 45, 30, and 0°C. The product was fractionated with cyclohexane and the fractions were analyzed by ultraviolet absorption spectroscopy and density-gradient ultracentrifugation. The molecular termination constant of P26 at 30°C was 0.106 much larger than the value of 0.016 which had been obtained for poly-*p*-methoxystyrene at 0°C. The amount of grafting and grafting efficiency generally increased with increasing temperature, contrary to results using the cationic initiation reaction. Anomalous results were obtained at 0°C as the product was no longer completely soluble. The ratio of grafted to ungrafted polystyrene chains was proportional to the concentration of P26 and generally increased with temperature. The grafting reaction was competitive with the normal termination reaction, and the energy of activation of the grafting reaction was estimated to be larger by ca. 7 kcal/mole.

INTRODUCTION

Cationic methods for forming graft copolymers are an alternative to the more popular free-radical methods, such as high energy irradiation, mastication, free-radical catalysis or photoinitiation.[1] Graft copolymers could be formed either by using the polymeric chain to initiate the polymerization of a monomer for the grafted branch or by having a growing polymer chain graft itself to the polymeric main chain by a termination or transfer reaction.

In order to form graft copolymers cationically using the initiation reaction, several workers have studied the reactions of halogenated polymers with Friedel-Crafts catalysts in the presence of vinyl monomers. Plesch[2] has formed grafts of polystyrene and polyindene onto poly(vinyl chloride)

---

* Present address: Department of Chemistry, University of Michigan, Ann Arbor, Michigan 48104.

† Present address: Department of Chemical Engineering, University of Waterloo, Waterloo, Ontario, Canada.

and copolymers of vinyl chloride and vinylidene chloride. Degradation and discoloration of the graft copolymers were reduced by avoiding elevated temperatures and by using titanium tetrachloride as catalyst in place of aluminum chloride. Small amounts of polyisobutene were grafted onto chloromethylated and bromomethylated polystyrenes dissolved in carbon disulfide by Kocklebergh and Smets[3] by use of aluminum bromide as catalyst. The grafting of polystyrene onto a chlorinated copolymer of isoprene and isobutene was studied in detail by Minoura et al.[4] The amount of grafting and the efficiency (the ratio of the weight of polystyrene grafted to the total weight of polystyrene formed) were higher with stannic chloride than with titanium tetrachloride or boron trifluoride etherate. The amount of grafting and the grafting efficiency decreased with increasing temperature.

Less work has been done in cationic grafting by the transfer or termination reactions. Termination for the cationic homopolymerization of styrene may occur by spontaneous transfer with regeneration of catalyst, transfer with monomer,[5] and transfer with any solvent present.[6–9] A quantitative study of the attack of a cationically polymerizing polystyrene chain on various aromatic compounds of low molecular weight in a solution of carbon tetrachloride and nitrobenzene was performed by Overberger and Endres[10] at 0°C with stannic chloride as catalyst. The low molecular weight aromatic compounds were effective chain-transfer agents and decreased the molecular weight of the polystyrene formed. Electron-donating substituents, such as the methoxyl group in anisole, greatly increased the rate of the transfer reaction. The results indicated that the transfer reaction occurs by a Friedel-Crafts alkylation of the phenyl ring. This reaction occurred less readily when the monomer being polymerized was isobutene.[11] A growing polystyryl carbonium ion has a tendency to attack the aromatic groups of any polystyrene already formed, resulting in long chain branching when styrene was polymerized to high conversions.[12,13] When the phenyl rings of the preformed polystyrene have been substituted in the *para* position with a methoxyl group which possesses electron-donating characteristics, the ring reactivity is increased one hundred times.[14] Hass et al. have succeeded in obtaining graft copolymers using the cationic termination reaction by polymerizing styrene at 0°C in the presence of poly-*p*-methoxystyrene.[15]

The present study was undertaken to determine whether the grafting reaction could be enhanced by choosing a more suitable polymeric backbone and a more suitable temperature for the reaction.

EXPERIMENTAL

Synthesis and Polymerization of 2,6-Dimethoxystyrene

Since the methoxyl substituent is known to activate for electrophilic addition the ring positions *ortho* and *para* with respect to the substituent, it was decided to investigate the polymer of 2,6-dimethoxystyrene because the two substituents reinforce their activations of the 3- and 5- positions. Another advantage of such a main chain was expected to be the fact that the 3-, 4-, and 5- positions of the phenyl ring would be unsubstituted, and these positions should be the ones most sterically accessible to an attacking polymeric carbonium ion.

2,6-Dimethoxystyrene had been synthesized before by Shamshurin[16] as indicated in the reaction sequences (1) and (2) but no attempt was made to polymerize it. Korshak and Matveeva[17] followed Shamshurin's method in an attempt to prepare this monomer, but they failed to isolate any 2,6-dimethoxystyrene after repeated attempts. They did produce some poly-2,6-dimethoxystyrene of low molecular weight, however.

Use was made of Shamshurin's procedure in the initial attempt to synthesize 2,6-dimethoxystyrene. The starting material for this sequence of reactions was methylumbelliferone (β-methylbenzopyrone; 4-methyl-7-hydroxycoumarin) (I). In the presence of refluxing acetic anhydride, the

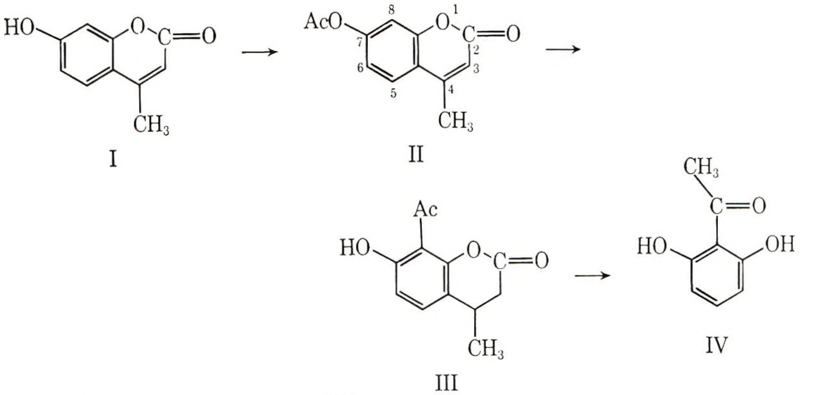

(1)

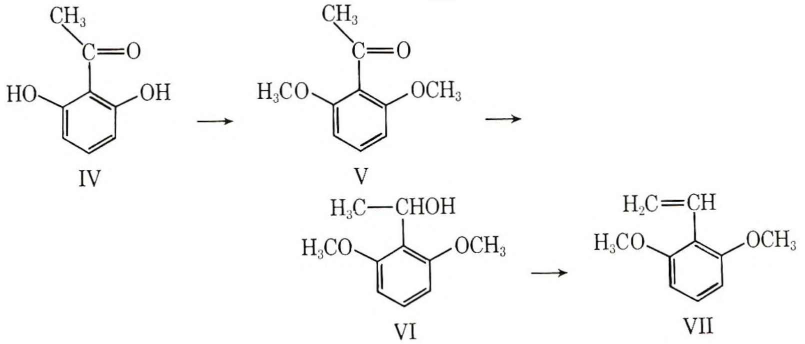

(2)

methylumbelliferone was acetylated in high yield to form 4-methyl-7-acetoxycoumarin (II).[18] Heating this acetoxy derivative with aluminum chloride brought about a Fries rearrangement to give 4-methyl-7-hydroxy-8-acetylcoumarin (III).[18] The heterocyclic ring was then cleaved by heating this 8-acetyl derivative with aqueous sodium hydroxide under nitrogen, resulting in the formation of 2,6-dihydroxyacetophenone (IV).[18]

2,6-Dimethoxyacetophenone (V). Methylation of both hydroxyl groups by treating the dihydroxyacetophenone with an excess of dimethyl sulfate according to the procedure of Cartwright et al.[19] proceeded with difficulty and a low yield was obtained, so that it was necessary to modify their procedure.

Under nitrogen 113.5 g (0.745 mole) of 2,6-dihydroxyacetophenone and 85 ml of distilled water were stirred together and 119 g (3.0 mole) of sodium hydroxide in 128 ml of water was added. The homogeneous mixture was heated to 95°C, the heating was stopped, and a small portion of dimethyl sulfate was added. When the mixture had cooled to 85°C it was heated again to 95°C, the heating was stopped, and another small portion of dimethyl sulfate was added. After four such additions, a small amount of yellow solid material was formed which was believed to be the monomethylated acetophenone. The addition of the remainder of the 273 g (1.55 mole) of the dimethyl sulfate was then performed continuously at a rate which maintained the temperature at 95°C without heating. The mixture was then heated at 95°C for 0.5 hr and 42.6 g (0.34 mole) of dimethyl sulfate was added, followed by sufficient 2*N* NaOH to keep the mixture alkaline. The solid material disappeared, and the temperature was maintained at 95°C for 0.5 hr. Upon cooling to room temperature, a solid material was formed, removed by filtration and washed with water. It was dried for 2 days in a vacuum oven (40°C, 120 mm pressure). The material was fractionally distilled under reduced pressure through a 12 in. helices-packed column, giving 85.4 g (63.5%) of 2,6-dimethoxyacetophenone, bp 135°C/4 mm, mp 69.5–70.0°C (from pentane) (lit.[19] bp 118°C/1.5 mm, mp 65–66°C). Vapor-phase chromatography of a solution of the dimethoxyacetophenone in dioxane with a Perkin-Elmer Vapor Fractometer equipped with a C column (silicone oil) at 189° gave a single peak at 13.0–13.3 min besides the solvent peak.

ANAL. Calcd for $C_{10}H_{12}O_3$: C, 66.65%; H, 6.71%. Found: C, 66.76, 66.77%; H, 6.69, 6.54%.

The reduction of the 2,6-dimethoxyacetophenone to 2,6-dimethoxyphenylmethylcarbinol (VI) had been carried out by Shamshurin by use of sodium in ethanol as the reducing agent. Korshak and Matveeva had attempted several times to follow exactly the conditions of this synthesis, but in no case had they been able to isolate any carbinol or any 2,6-dimethoxystyrene (VII). Using aluminum isopropoxide, they had obtained a dark brown polymeric residue which they had identified as poly-2,6-dimethoxystyrene with a molecular weight of about 3000.

Reductions of the dimethoxyacetophenone with lithium aluminum hydride in ether, lithium aluminum hydride in tetrahydrofuran, and sodium borohydride in methanol according to general procedures given by Gaylord[20] were unsuccessful, and only the acetophenone was recovered. Reductions with zinc dust and sodium hydroxide in ethanol[21] or purified magnesium powder and methanol[22] were also unsuccessful. When magnesium turnings were used in methanol, a brown polymeric residue was obtained which, from its intrinsic viscosity and elemental analysis, appeared to be poly-2,6-dimethoxystyrene of low molecular weight.

An alternate synthetic route to the carbinol was sought by way of the 2,6-dimethoxybenzaldehyde (X) [eq. (3)]. Bromobenzene was treated with lithium metal to form phenyllithium which then underwent an exchange reaction with dimethylresorcinol (VIII) to give 2,6-dimethoxyphenyllithium (IX), according to the procedure of Lambooy.[23] Addition of *N*-methylformanilide to the reaction mixture gave the desired benzaldehyde (X). The benzaldehyde was made also using commercially available 2,6-dimethoxyphenyllithium (Alfa Inorganics, Inc.). This benzaldehyde was reacted with methyl magnesium iodide in a Grignard reaction to form 2,6-dimethoxyphenylmethylcarbinol (VI).

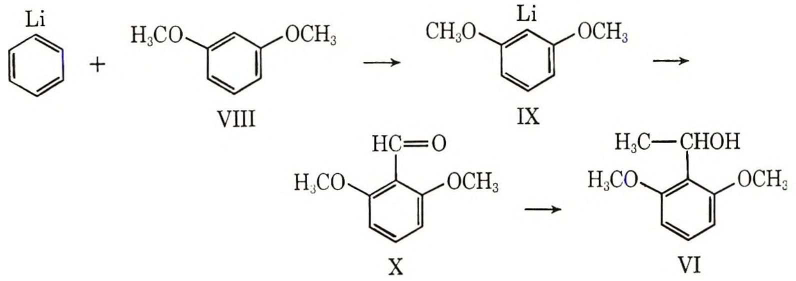

(3)

Dehydration of this carbinol was attempted by using fused potassium hydrogen sulfate as catalyst at 200°C as Shamshurin had done,[16] but only polymeric products were obtained despite precautions to prevent the polymerization of newly formed monomer.

The formation of 2,6-dimethoxystyrene (VII) directly from the benzaldehyde (X) was attempted by using the Wittig reaction.[24] Better results were obtained with methyllithium than with phenyllithium.

2,6-Dimethoxystyrene (VII). Tetrahydrofuran was stored over potassium hydroxide and before use was refluxed overnight over lithium aluminum hydride and then distilled. A mixture of 2 liters of freshly distilled tetrahydrofuran and 106.9 g (0.3 mole) of methyltriphenylphosphonium bromide was stirred under nitrogen and 0.3 mole of methyllithium in 180 ml of ether was added. After the mixture had become clear and yellowish, 49.5 g (0.28 mole) of 2,6-dimethoxybenzaldehyde in 2 liters of dry tetrahydrofuran was added. The adduct separated as a white solid. The mixture was refluxed for 1 hr at 65°C, during which time the mixture became clear and pale brown. The mixture was then extracted twice with a 10% aqueous solution of sodium chloride, twice with a saturated aqueous solution of sodium bisulfite and once more with the solution of sodium chloride. The nonaqueous layer was then dried overnight over anhydrous calcium sulfate. The tetrahydrofuran was removed at reduced pressure using a rotary evaporator. The residue solidified and was extracted repeatedly with pentane. The pentane extracts were combined and the pentane removed at reduced pressure on the rotary evaporator. The residue was fractionally distilled at reduced pressure in the presence of a small amount of *p-tert*-butylcatechol to give 22.4 g (45.8%) of 2,6-dimethoxystyrene, (bp 82–90°C/0.8–0.9 mm) (lit.[16] bp 92°C/16 mm). Vapor-phase chromatography on a C column at 172°C showed the major peak at 14.7 min, with a minor peak at 7.1 min, which was no longer observed after the monomer was redistilled at 70–75°C/0.2–0.45 mm; $n_D^{25} = 1.5663$, $d_{20}^{20} = 1.0836$ (lit.[16] 1.0145).

ANAL. Calcd for $C_{10}H_{12}O_2$: C, 73.14%; H, 7.37%. Found: C, 73.04, 72.96%; H, 7.47, 7.52%.

Poly-2,6-dimethoxystyrene. In a polymerization tube, 4.94 g (30 mmole) of 2,6-dimethoxystyrene was mixed with 0.0056 g (0.034 mmole) of azobisisobutyronitrile, and the mixture was repeatedly frozen and thawed under vacuum. Then the tube was sealed and placed in a constant temperature bath at 58°C with intermittent shaking. After 6.5 days the tube was opened and the product was repeatedly dissolved in methyl ethyl ketone, poured into methanol in which the polymer precipitated, removed by filtration and dried under vacuum. Conversion of monomer into polymer was 50% (2.47 g). The weight-average molecular weight determined by gel-permeation chromatography was 1.31×10^6.*

Compatibility in the System of Mixed Polymers

Polystyrene was chosen to be the grafted branch because little[11] or no[15,25] success had been achieved using other monomers for the transfer reaction. To indicate the compatibility of polystyrene (PS) and poly-2,6-dimethoxystyrene (P26), the two polymers ($[\eta]_{PS}$ was 0.15 dl/g in toluene at 25°C, and $[\eta]_{P26}$ was 0.16 dl/g in toluene at 25°C) were dissolved separately in approximately equal concentrations in methylene chloride. The two solutions were mixed and a portion of the combined solution was poured on a glass plate. Upon evaporation of the solvent a transparent film remained, indicating that the two polymers were compatible. Since compatibility is generally believed to be similar in all solvents,[26] PS and P26 were expected to be compatible in the polymerization medium.

Separation of Mixtures of PS and P26

In order to determine whether mixtures of PS, P26, and PS-P26 graft copolymer could be separated by differences in solubility, the solubilities of PS and P26 at room temperature were determined qualitatively in a large number of common solvents. The solubility behaviour of P26 in the solvents was quite similar to that of PS, with an exception in

---

* Gel permeation chromatography was performed on a Waters gel permeation chromatographic fractionator through the courtesy of Mr. Albert Wartman at the Central Research Department of Interchemical Corporation, Clifton, New Jersey. The polymers were dissolved in tetrahydrofuran. The 12 ft column had been calibrated with monodisperse fractions of polystyrene and poly (ethylene oxide).

TABLE I
Solvent-Precipitant Pairs Investigated Turbidimetrically

System no.	Solvent	Precipitant
1	Chloroform	Methanol
2	Toluene	Methanol
3	Methyl ethyl ketone	Methanol
4	Benzyl Alcohol	Methanol
5	Nitroethane	Nitromethane
6	Anisole	Methanol
7	Guiaicol	Methanol

the case of the cyclic hydrocarbons, cyclohexane, methylcyclohexane and decalin, which dissolved the PS but did not dissolve the P26.

Binary solvents which might have selectively dissolved the P26 without dissolving the PS were investigated by dissolving each polymer in a solvent and slowly adding a more polar precipitant. The solvent–precipitant pairs investigated are listed in Table I. The precipitation was monitored by measuring the amount of light scattered at 90° in a modified light scattering photometer.

With strong solvents (systems 1 and 2), precipitation of each polymer was observed to begin at almost identical ratios of the volume of precipitant to volume of solvent. With a poor solvent of higher polarity (system 3), a small difference in the volume ratios was observed, but this difference was insufficient for a complete separation of the polymers. With both a strongly hydrogen-bonding system (system 4) and a weakly hydrogen-bonding system (system 5), the values of the volume ratio at which precipitation occurred were very similar. With solvents of chemical structure similar to P26, the volume ratios at the point of precipitation showed little difference with anisole, but a larger difference with guiaicol, although only a small fraction of PS had precipitated at the concentration of methanol at which the P26 began to precipitate. Hence, none of the systems studied were suitable for precipitating effectively all of the PS while keeping the P26 in solution.

Density-gradient ultracentrifugation was also investigated as a technique for separating mixtures of PS and P26. When 15 mg of P26 and 18 mg of PS were dissolved in a mixture of 1.9 g of bromoform and 3.7 g of benzene and centrifuged for 32 hr at 47660 rpm. in a Beckman Spinco Model E analytical ultracentrifuge, two separate and distinct bands were formed showing that the mixed polymers had been separated. A graft copolymer would not have separated into two bands but would have formed a single band about some intermediate position.

Compositional Analysis of Mixtures of PS, P26, and PS-P26 Graft

In order to determine the relative amounts of PS and P26, the ultraviolet absorption spectra of solutions of the two polymers in methylene chloride

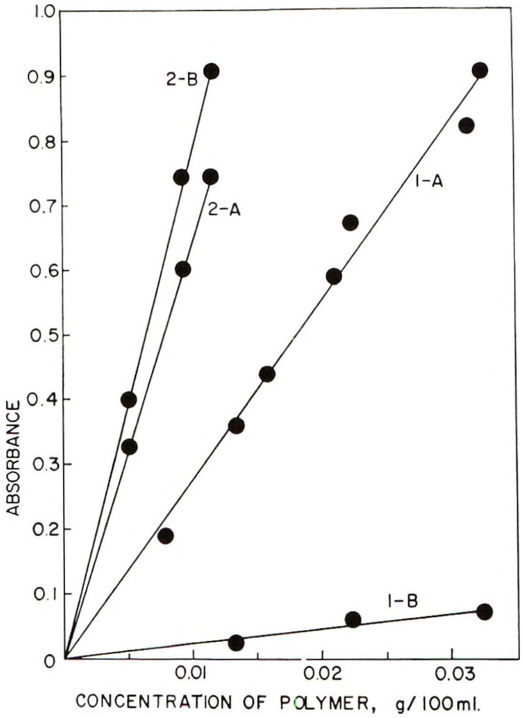

Fig. 1. Dependence on concentration of the absorbances of (*1*) PS and (*2*) P26 at (*A*) 262 mμ and (*B*) 278 mμ.

were measured on a Cary 14 Recording Spectrophotometer. The absorption spectra overlapped. The absorbances at 278 mμ were measured at various concentrations and were found to be linearly proportional to the concentrations of each polymer over the range of concentration studied (Fig. 1). From the slopes of the lines in Figure 1, an equation giving the relative amount of each polymer in mixtures was formulated.

$$\frac{C_{\mathrm{PS}}}{C_{\mathrm{P26}}} = \frac{(A_{262} \times 77.8) - (A_{278} \times 63.6)}{(A_{278} \times 27.35) - (A_{262} \times 1.76)}$$

where $C_{\mathrm{PS}}/C_{\mathrm{P26}}$ is the ratio of the weights of PS and P26, and A_{262} and A_{278} are the absorbances of the solution of the mixed polymers at 262 and 278 mμ, respectively.

Procedure for Graft Copolymerization

Graft copolymerization was to be attempted by polymerizing styrene cationically in the presence of P26 in solution. The conditions for polymerization were similar to those of Overberger and Endres.[10] For all polymerizations, the concentration of nitrobenzene was 40% by volume, the concentration of styrene was 22.5% by volume and the concentration of carbon tetrachloride was 37.5% by volume. The concentration of stannic chloride was maintained at 0.025 mole/l. The polymerization bottles were made by fitting 2 oz sample bottles with neoprene gaskets. The bottles, caps and gaskets were heated in an oven at 120°C for at least 10 hr before use. They were assembled in a dry box. The catalyst solution was made by adding the catalyst from a vial to an amount of carbon tetrachloride which had been calculated so that 1 ml of the final solution added to each polymerization bottle would give the desired catalyst concentration. Each polymerization bottle was weighed, and, after each component except catalyst was added, was weighed again.

The polymerization bottles and the catalyst solution were then thermostatted for a least 30 min. Polymerization was begun by removing 1 ml of catalyst solution with a syringe and injecting the solution into the polymerization bottle.

RESULTS AND DISCUSSION

Molecular Termination Constant for P26

A preliminary series of polymerizations was performed at 30°C. The weight of P26 was 4.7% of the weight of styrene monomer initially present. After 35–40 min, the mixtures were poured into cyclohexane and filtered, and the filtrate was poured into hexane. The hexane was decanted and the residual polymer was redissolved in methyl ethyl ketone and reprecipitated in methanol. The material which precipitated in cyclohexane was also redissolved in methyl ethyl ketone and reprecipitated in methanol. The composition of each fraction was determined by the uv composition equation. The cyclohexane-insoluble (CI) fractions were shown to have a considerable amount of PS present with the P26, while the cyclohexane-soluble (CS) fractions were shown to contain only a small proportion of the P26 together with the PS. Density-gradient centrifugation of each fraction at 42040 rpm. at 22°C showed for each CS fraction a very low, broad symmetrical peak intersecting the baseline at approximately the same position as previous samples of pure PS, while the CI fraction showed an unsymmetrical peak about the position previously observed for P26. The curve was flattened on the side of lower density (i.e. towards the position for pure PS). This flattening was interpreted to be due to the presence of some graft copolymer of PS and P26 together with ungrafted P26. The CS fraction was essentially ungrafted PS. Intrinsic viscosities were determined in benzene at 30°C for the PS from the control sample and the CS fraction of one graft copolymerization sample (Table II).

TABLE II
Intrinsic Viscosities of PS Fractions[a]

Sample no.	$[\eta]$, dl/g	$\bar{M}_n$[b]
3-1 (control)	0.239	14,100
3-3-CS	0.190	9,850

[a] Benzene, 30°C.

[b] Molecular weights were calculated from the intrinsic viscosities by using the equation of Pepper.[27]

The molecular termination constant, k_r/k_p, was calculated by using the usual chain transfer equation:

$$1/\bar{P}_n = (1/\bar{P}_{n0}) + (k_r[R]/k_p[M])$$

The number-average degrees of polymerization of the PS formed in the presence and absence of P26 are given by $\bar{P}_n$ and $\bar{P}_{n0}$, respectively. The molar concentration of styrene is given by $[M]$, and the equivalent molar concentration of repeating units of P26 is given by $[R]$. The ratio k_r/k_p is the ratio of the rate constants for termination by transfer and for propagation. The molecular termination constant for P26 was found to be 0.106, much larger than the value of 0.016 for poly-*p*-methoxystyrene at 0°C obtained by Hass et al.[14,15] Since the double substitution of methoxyl groups on the phenyl ring would simply be expected to double the value of the molecular termination constant, this greatly increased value must be attributed to the position of substitution and the increased temperature.

Dependence of Grafting on Concentration of P26 and on Temperature

Cationic graft copolymerization reactions were performed with various concentrations of P26 at 60, 45, 30, and 0°C. Each polymerizing mixture was poured into methanol to precipitate all the polymers and to terminate the polymerization. The solid polymer was removed by filtration with a fritted glass crucible, dried in a vacuum oven and weighed. The polymer was redissolved in a small amount of methyl ethyl ketone and the solution was filtered and poured into a large amount of methanol with stirring. The polymer was removed, dried and weighed. The polymer was again redissolved in methyl ethyl ketone and was subjected to the purification steps once more.

To effect the fractionation of the polymer, a sample of the polymerization product was then dissolved in a minimal amount of benzene and the solution was poured into well stirred cyclohexane. Despite the facts that a large amount of cyclohexane was used and that P26 had been purified by precipitation in cyclohexane, no precipitation was observed. The precipitation of solutions of P26 in various solvents by the addition of cyclohexane was then investigated turbidimetrically in order to find a better solvent for precipitation (Fig. 2). With benzene or dioxane, precipitation did not begin to occur until the volume of cyclohexane was about twice the volume of the solvent. As the amount of cyclohexane was increased further, the P26 precipitated very gradually. Using carbon tetrachloride as solvent, however, precipitation began when the amount of cyclohexane added was only one-half of the original volume of solution. Addition of more cyclohexane resulted in an abrupt precipitation of the P26 so that apparently precipitation was complete when the amount of cyclohexane was one and one-half times the original volume of the solution.

Accordingly the purified product from the copolymerization was dissolved in a minimal amount of carbon tetrachloride and then poured into a large amount of cyclohexane. The cyclohexane-insoluble (CI) fraction which precipitated was removed by filtration or by decantation of the liquid, followed by dissolving the polymer in methyl ethyl ketone, reprecipitating it in methanol and filtering. The cyclohexane filtrate was evaporated to dryness and the cyclohexane-soluble (CS) residue was redissolved in methyl ethyl ketone and reprecipitated in methanol. This fraction was then filtered and dried. The composition of each fraction was determined from the ultraviolet absorption spectrum in methylene chloride by using the ultraviolet composition equation.

The results at 60, 45, and 30°C are summarized in Table III. The per cent conversion of styrene was calculated from the total weight of polymer recovered, the weight of P26 added initially and the weight of styrene monomer initially present. The fraction of the total amount of PS formed which was present in the CI fraction was calculated. From this value and the fraction of the total amount of P26 which was present in fraction A, it was possible to calculate the total fraction of the polystyrene which would be expected to be grafted (viz., the grafting efficiency), assuming that any P26 in the CS fraction was grafted to the same extent as the P26 in the CI fraction.

It is seen that the rate of conversion decreased slightly in the presence of

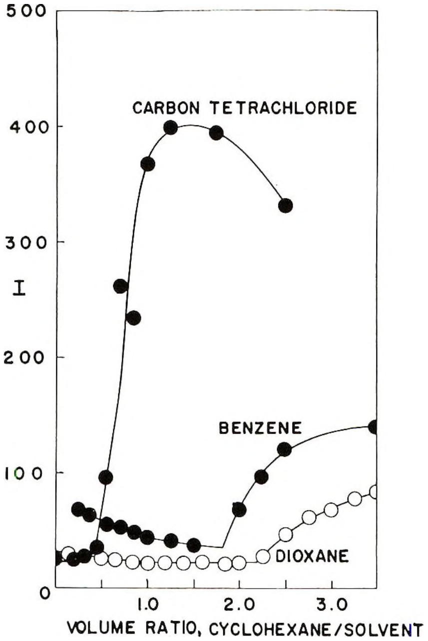

Fig. 2. Turbidimetric titration of P26 with cyclohexane in benzene, carbon tetrachloride, and dioxane. T = galvanometer reading × filter factor/concentration of polymer (mg/100 ml).

TABLE III

Results of Graft Copolymerization at 60, 45, and 30°C

No.	Temp, °C	Concn of P26, wt-%	Time, min	Conversion of styrene, %	PS in CI fraction, wt-%	P26 in CS fraction, wt-%	Fraction of PS in A	Grafting efficiency
4-1	60	0.000	10	4.33	—	—	—	—
4-2	60	0.199	25	10.96	61.2	3.9	0.085	0.136
4-3	60	0.393	40	22.02	71.0	7.7	0.135	0.312
4-4	60	0.855	50	32.9	68.3	12.2	0.174	0.442
4-5	60	1.603	100	35.6	64.1	19.1	0.242	0.561
4-6	60	0.000	10	4.18	—	—	—	—
5-3	45	0.309	60	22.3	64.2	5.5	0.114	0.208
5-4	45	0.763	60	24.2	59.3	5.7	0.204	0.275
5-5	45	1.578	60	17.2	49.1	9.7	0.356	0.424
5-6	45	0.000	45	18.1	—	—	—	—
6-1	30	0.000	90	35.3	—	—	—	—
6-2	30	0.152	120	43.7	75.7	4.5	0.058	0.197
6-3	30	0.389	120	40.3	69.8	2.2	0.094	0.141
6-4	30	0.763	120	36.9	62.9	1.1	0.180	0.196
6-5	30	1.582	123	28.0	51.8	5.7	0.321	0.354
6-6	30	0.000	90	35.6	—	—	—	—

P26 at the lower temperatures, but did not show any decrease at 60°C with the exception of the most concentrated sample.

The proportion of PS in the CI fraction was found to be sizable in all cases. This large amount of PS was an additional reason for the difficulty in precipitating this fraction in cyclohexane. At 30 and 45°C the proportion of PS decreased and the conversion of styrene decreased with increasing concentration of P26. At 60°C, however, the proportion of PS generally decreased with increasing concentration of P26 even as the conversion of styrene increased. Although the number of grafted branches would be expected to have been increasing with the conversion, the molecular weight of the chains would have been decreasing with increasing concentration of P26 and this effect of concentration apparently outweighed the effect of conversion.

P26 constituted only a small proportion of the CS fraction. Density-gradient centrifugation was performed on both fractions of sample 4-5. For the CI fraction only a single symmetrical band was observed at a position intermediate between the positions of P26 and PS. No band for pure P26 could be detected, so that it appears that all the chains of P26 had been grafted with PS. For the CS fraction, only a single broad band was observed, centered about the position for PS. Hence any P26 present must have been highly grafted and of low molecular weight.

The grafting efficiency was found to increase with the concentration of P26 and with the temperature of the reaction.

For the polymerizations conducted at 0°C, the product formed in the presence of P26 did not completely redissolve in methyl ethyl ketone, even when the mixture was agitated in a Waring Blendor. After filtering, the solid material did not dissolve in benzene either, so that its composition could not be determined directly from its ultraviolet absorption spectrum. The filtrate was reduced in volume and poured into methanol. The precipitate was soluble in cyclohexane. The composition of the CI fraction was calculated from the composition of the CS fraction and from the weights of materials before and after the reaction. The results are given in Table IV. These results do not follow the trend of decreasing grafting efficiency with decreasing temperature as was observed with the polymerizations at 60, 45, and 30°C, and in fact the efficiency was higher at 0°C than at 30°C. These results indicate that the reaction occurring at 0°C was not similar to the reaction at higher temperatures and possibly some heterogeneity may be occurring in the reaction medium at such a low temperature. The different experimental procedure necessary for the samples at 0°C may also account for some of the dissimilarity.

Kinetic Considerations

The weight of PS which had grafted onto P26 would be expected to be proportional to the rate of grafting:

$$\sim\!\sim C^{+} + \mathrm{P26} \xrightarrow{k_g} \text{graft}$$

TABLE IV
Results of Graft Copolymerization at 0°C

No.	Concn. of P26 % by wt-%	Time, min	Conversion of styrene, %	PS in CI fraction, wt-%	P26 in CS fraction, wt-%	Fraction of PS in A	Grafting efficiency
7-1	0.000	180	22.7	—	—	—	—
7-3	0.213	180	10.15	65.7	0.8	0.00706	0.0850
7-4	0.736	180	6.35	56.4	7.6	0.1360	0.2276
7-5	1.599	180	3.39	31.5	11.3	0.3523	0.3903
7-6	0.000	180	—	22.7	—	—	—

where the rate of grafting = $k_g[\mathrm{C}^+][\mathrm{P26}]$, where k_g is the rate constant for the grafting reaction; $[\mathrm{C}^+]$ is the concentration of polystyryl carbonium ions; and (P26) is the equivalent molar concentration of 2,6-dimethoxystyryl units in solution.

The weight of PS which had not been grafted onto P26 would be proportional to the rates of termination reactions other than grafting. The spontaneous termination reaction is usually considered to be the predominant mode of termination. Termination by transfer with monomer or solvent could also be considered and would not change the results since the monomer and solvent concentrations have been kept essentially constant throughout these experiments:

$$\sim\!\!\sim\mathrm{C}^+ \xrightarrow{k_t} \mathrm{PS}$$

where the rate of termination = $k_t[\mathrm{C}^+]$ and k_t is the rate constant for spontaneous termination. Thus

$$\frac{\text{Rate of grafting}}{\text{Rate of termination}} = \frac{k_g[\mathrm{C}^+][\mathrm{P26}]}{k_t[\mathrm{C}^+]}$$

$$= \frac{k_g[\mathrm{P26}]}{k_t}$$

$$= \frac{\text{wt. of PS grafted}}{\text{wt. of PS ungrafted}}$$

Thus the ratio of the weight of grafted and ungrafted PS (rather than the grafting efficiency) should be a linear function of the concentration of P26, with a slope equal to the ratio of the rate constants for grafting and spontaneous termination. The values of the ratios of the weights of ungrafted and grafted PS are plotted in Figure 3 as functions of the concentration of

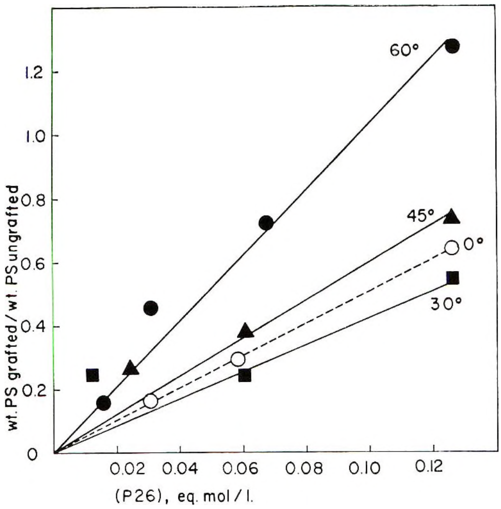

Fig. 3. Relative proportion of PS grafted at various concentrations of P26.

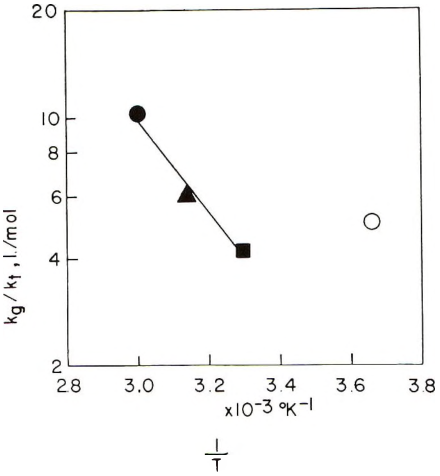

Fig. 4. Arrhenius plot of k_g/k_t.

P26 at the four temperatures studied. The ratio was found to be a linear function of the concentration of P26 and the slope increased with increasing temperature, with the exception of 0°C at which temperature inconsistent results were obtained. Thus in general the grafting reaction was preferred at higher temperatures. The logarithms of the slopes, $k\mathrm{I}/k_t$, were plotted as functions of $1/T$ in Figure 4. With the exception of the anomalous results at 0°, and approximately linear relationship was obtained. From the slope of the line was calculated a value of 6.94 kcal/mole which represents the difference in Arrhenius activation energies for the rate constants for the grafting and termination reactions.

The authors wish to gratefully acknowledge financial support for this research provided by the Petroleum Research Fund of the American Chemical Society, Charles Pfizer and Company, and the Pittsburgh Plate Glass Foundation.

This paper is taken from the dissertation submitted to the Faculty of the Polytechnic Institute of Brooklyn in partial fulfillment of the requirements for the degree of Doctor of Philosophy (Chemistry), 1967.

Elemental analyses were performed in the laboratory of Alfred Bernhardt, 433 Mülheim (Ruhr), Germany.

References

1. R. J. Ceresa, *Block and Graft Copolymers*, Butterworths, Washington, 1962.
2. P. H. Plesch, *Chem. Ind.* (London), **1958,** 954.
3. G. Kocklebergh and G. Smets, *J. Polym. Sci.*, **33,** 227 (1958).
4. Y. Minoura, T. Hanada, T. Kasabo, and Y. Ueno, *J. Polym. Sci. A-1*, **4,** 1665 (1966).
5. D. C. Pepper and P. J. Reilly, *Proc. Chem. Soc.*, **1961,** 460.
6. S. Okamura and T. Higashimura, *J. Polym. Sci.*, **21,** 289 (1956).
7. P. H. Plesch, *J. Chem. Soc.*, **1953,** 1659, 1662.
8. S. Okamura and T. Higashimura, *Kobunshi Kagaku*, **13,** 262 (1956).
9. T. Higashimura and S. Okamura, *Kobunshi Kagaku*, **13,** 338 (1956).
10. C. G. Overberger and G. F. Endres, *J. Amer. Chem. Soc.*, **75,** 6349 (1953); *J. Amer. Chem. Soc.*, **77,** 2201 (1955); *J. Polym. Sci.*, **16,** 283 (1955).
]

11. J. Penfold and P. H. Plesch, *Proc. Chem. Soc.*, **1961**, 311.

12. J. T. Atkins and F. W. Billmeyer, *J. Phys. Chem.*, **63**, 1966 (1959).

13. G. F. Endres, V. G. Kamath, and C. G. Overberger, *J. Amer. Chem. Soc.*, **84**, 4813 (1962).

14. P. M. Kamath and H. C. Hass, *J. Polym. Sci.*, **24**, 143 (1957).

15. H. C. Hass, P. M. Kamath, and N. W. Schuler, *J. Polym. Sci.*, **24**, 85 (1957).

16. A. A. Shamshurin, *Zh. Obshch. Khim.*, **16**, 99 (1946).

17. V. V. Korshak and N. G. Matveeva, *Byull. Akad. Nauk SSSR, Otd. Chim. Nauk* **1953**, 547.

18. A. Russell and J. R. Frye in *Organic Syntheses, Coll. Vol. III*, E. C. Horning, Ed., Wiley, New York, 1955, p. 282.

19. N. J. Cartwright, J. I. Jones, and D. Marmion, *J. Chem. Soc.*, **1952**, 3499.

20. N. G. Gaylord, *Reduction with Complex Metal Hydrides*, Interscience, New York, 1956.

21. F. Y. Wiselogle and H. Sonneborn, in *Organic Syntheses, Coll. Vol. I*, H. Gilman, Ed., Wiley, New York, 1941, p. 90.

22. L. Zechmeister and P. Rom, *Ann.*, **468**, 123 (1929); *Chem. Abstr.*, **23**, 2171 (1929).

23. J. B. Lambooy, *J. Amer. Chem. Soc.*, **76**, 113 (1954).

24. A. Maercker in *Organic Reactions*, Vol. XIV, A. C. Cope, Ed., Wiley, New York, 1965, p. 270.

25. V. G. Kamath, Ph.D. Dissertation, Polytechnic Institute of Brooklyn, Brooklyn, New York, 1962.

26. A. Dobry and F. Boyer-Kawenoki, *Ind. Plastiques*, **4**, 552 (1948).

27. D. C. Pepper, *Proc. Roy. Dublin Soc.*, **25**, 239 (1951); *J. Polym. Sci.*, **7**, 347 (1951).

Received May 3, 1968

JOURNAL OF POLYMER SCIENCE: PART A-1 VOL. 7, 351-362 (1969)

γ-Ray-Induced Terpolymerization of Carbon Monoxide, Aziridines, and Cyclic Ethers

TSUTOMU KAGIYA, MASATSUNE KONDO,* ISAO MARUTA,* and KENICHI FUKUI, *Faculty of Engineering, Kyoto University, Kyoto, Japan*

Synopsis

The terpolymerization of carbon monoxide, aziridines, and cyclic ethers was carried out by γ-irradiation. A partially crystalline solid copolymer was obtained. The infrared spectrum of the copolymer obtained indicated characteristic peaks due to the secondary amide and ester groups. The results of elementry analysis, infrared spectra, and x-ray diffraction of the copolymer showed that terpolymerization of carbon monoxide, aziridine, and cyclic ether took place by γ-irradiation. 2-Vinyl-1,3-dioxolane was polymerized in the system of carbon monoxide and ethylenimine to give a solid polymer. The infrared spectrum showed characteristics of the secondary amide and dioxolane ring, while no absorption due to carbonyl group of ester was observed. The infrared spectra and results of elementary analysis confirmed that the terpolymerization of carbon monoxide–ethylenimine–2-vinyl-1,3-dioxolane occurred.

INTRODUCTION

In a preliminary paper,[1] it has been reported that cyclic ethers, such as ethylene oxide, tetrahydrofuran, 1,3-dioxolane, and 1,4-dioxane, copolymerize with carbon monoxide an γ-irradiation to give polyesters. It has been also reported[2,3] that cyclic imines, such as ethylenimine, copolymerize with carbon monoxide on γ-irradiation to give polyamide. It has previously been shown that 2-vinyl-1,3-dioxolane polymerized with isomerization by α,α'-azobisisobutyronitrile or by γ-irradiation.[4]

As an extension of our previous works, the γ-ray-induced terpolymerization of carbon monoxide, aziridines, and cyclic ethers was studied.

EXPERIMENTAL

Materials and Procedure

Commercial ethylenimine was dried over KOH pellets and NaH and then fractionated at 55.5–56°C before use. *N*-Phenylethylenimine and *N*-methylethylenimine were prepared according to the methods of Heine[5] and Elderfield,[6] respectively. Ethylene oxide, tetrahydrofuran, 1,3-

---

* Present address: Central Research Laboratory, Sumitomo Chemical Co., Ltd., Tsukahara, Takatsuki, Japan.

dioxolane, and 1,4-dioxane obtained commercially were dried and distilled by the usual method.

The terpolymerization was carried out as follows. Measured amounts of ethylenimine and cyclic ether were charged into a stainless steel autoclave of 30 ml capacity. The vessel was evacuated twice under cooling with liquid nitrogen. Then, measured amounts of carbon monoxide were fed into the vessel from a reservoir. All irradiations were performed with γ-rays from a 5000 ci ^{60}Co source, and the reaction was carried out without stirring. After the reaction was stopped, the product was washed thoroughly with a large amount of diethyl ether, dried *in vacuo*, and weighed. The resulting polymer was extracted with chloroform at boiling point for 24 hr to remove any carbon monoxide–cyclic ether copolymer which was soluble in chloroform, and both the chloroform-soluble and insoluble parts were reserved for subsequent analysis.

Analysis of the Copolymers

The composition of the copolymer was determined from the contents of carbon, hydrogen, and nitrogen by elementary analysis. The infrared spectra were obtained by using KBr pellet techniques on a Shimadzu infrared spectrophotometer, Model IR-27, with NaCl prism. The x-ray diffraction diagram was recorded with a powder camera on a Shimadzu x-ray diffractometer, Model GX-3B, Ni-filtered CuKα radiation, standard techniques being used.

RESULTS AND DISCUSSION

Carbon Monoxide–Ethylenimine–Ethylene Oxide System

The results of the terpolymerization of carbon monoxide(CO)–ethylenimine(EI)–ethylene oxide(EO) system are shown in Table I. The table shows that the polymer yield increases with increasing feed of EI. From the results of the elementary analysis, it is found that the product consists of CO, EI, and EO components. The EI/CO molar ratio in the chloroform-insoluble part of the polymer approaches unity with the increase of EI in the feed. This fact suggests that the poly-β-alanine content in the product increases with increase of EI in the feed.

Infrared Spectra of the Copolymers. Figure 1 shows the infrared spectra of the copolymers obtained in this system. All the copolymers displayed major absorption peaks assignable to secondary amide at near 3300, 3080, 1635, and 1540 cm^{-1}. At 1735 cm^{-1} an absorption assignable to ester linkage appeared which increased with decreasing EI in the feed. The infrared spectra indicate that the main structure of the products is a secondary amide, and this fact shows that EI has a higher reactivity with CO than EO with CO. Figure 2 shows the infrared spectrum of the chloroform-soluble part of the product and that of the chloroform-insoluble part of the product having an EI/CO molar ratio of 2×10^{-2}. The spectra of

TABLE I

Copolymerization of Carbon Monoxide(CO)–Ethylenimine(EI)–Ethylene Oxide(EO) System by γ-Irradiation[a]

Expt no.	Feed (EI/CO) molar ratio	Yield, g	Elementary analysis				Polymer composition, molar ratio			
			C, %	H, %	N, %	Ash, %	CO	EI	EO	H_2O
1	2×10^{-3}	0.061	46.16	5.47	6.93	—	1.00	0.26	0.43	0.15
2	2×10^{-2}	0.195	47.56	6.30	12.22	—	1.00	1.04	0.82	0.70
		0.130[b]	48.39	6.62	13.04	2.77	1.00	0.73	0.34	0.07
3	1×10^{-1}	0.590	49.98	7.55	16.68	—	1.00	1.05	0.28	0.14
		0.540[b]	46.34	7.28	15.15	0.94	1.00	0.90	0.21	0.36
4	4×10^{-1}	1.988	49.93	8.03	16.12	—	1.00	1.28	0.47	0.24
		1.534[b]	44.31	7.22	14.43	—	1.00	1.03	0.31	0.41

[a] Reaction conditions: CO in feed, 3.0 g, EO, 4.5 g; dose rate, 3×10^5 rad/hr; total dose, 1.88×10^7 rad.;

[b] Chloroform-insoluble part.

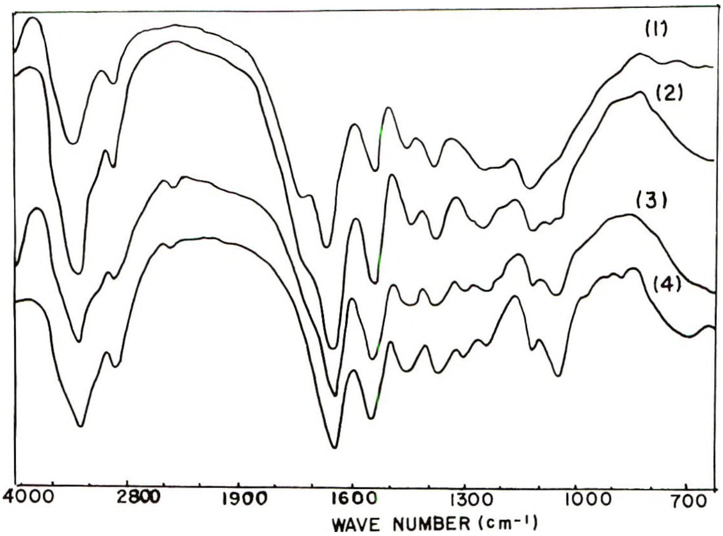

Fig. 1. Infrared spectra of the copolymer obtained in carbon monoxide(CO)–ethylenimine(EI)–ethyleneoxide(EO) system: (*1*) EI/CO molar ratio 2×10^{-3}; (*2*) EI/CO molar ratio 2×10^{-2}; (*3*) EI/CO molar ratio 1×10^{-1}; (*4*) EI/CO molar ratio 4×10^{-1}.

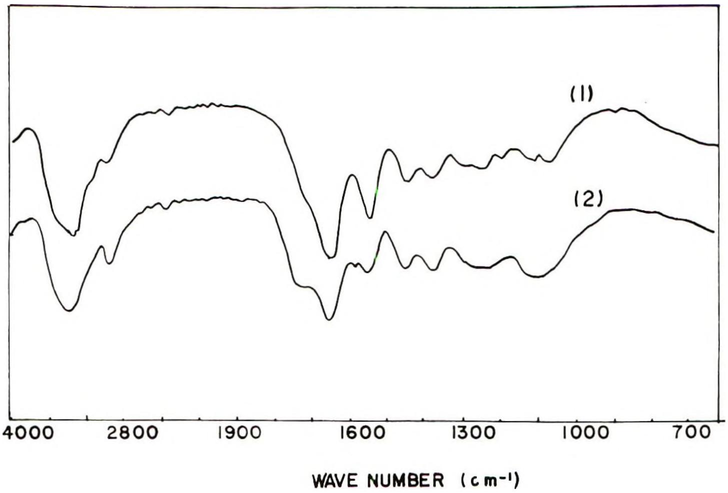

Fig. 2. Infrared spectra of the copolymer obtained in carbon monoxide–ethylenimine–ethylene oxide system: (*1*) chloroform-insoluble part; (*2*) chloroform-soluble part.

both parts of the polymer show the characteristic absorption of ester linkage at 1730 cm^{-1}. The spectrum of the insoluble polymer is almost the same as that of the crude polymer.

X-Ray Diffraction Diagrams of the Copolymers. Figure 3 shows the x-ray diffraction diagrams of the copolymers obtained in this system. It is evident from the figure that the half-width value of the peak at 23.6° decreases with increasing EI in the feed and that the diagrams become in-

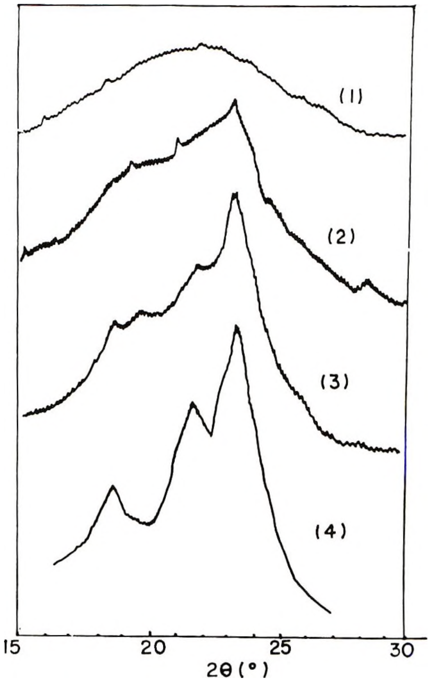

Fig. 3. X-ray diffraction diagrams of the copolymers obtained in carbon monoxide (CO)-ethylenimine(EI)-ethylene oxide(EO) system: (*1*) EI/CO molar ratio 2×10^{-2}; (*2*) EI/CO molar ratio 2×10^{-1}; (*3*) EI/CO molar ratio 4×10^{-1}; (*4*) poly-β-alanine obtained by the copolymerization of carbon monoxide and ethylenimine with γ-irradiation.

creasingly similar to that of poly-β-alanine with increasing EI feed. This tendency for the structure of the product to resemble that of poly-β-alanine with the increase of EI in the feed is in good accord with the trends noted the elementary analyses and the infrared spectra. From the results of x-ray diffraction diagrams, it is concluded that EO also takes part in the copolymerization and disturbs the crystallinity of the products.

The results of elementary analysis and the infrared spectra and x-ray diffraction diagrams lead to the conclusion that the terpolymer has mainly, poly-β-alanine structure and that ethylene oxide is contained in the terpolymer.

It has been reported by us[1] that CO and EO copolymerized by γ-irradiation give polymers having the structures I–IV.

$$—(CH_2—CH_2—O)—$$

I

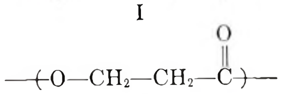

$$—(O—CH_2—CH_2—\overset{\overset{\displaystyle O}{\|}}{C})—$$

II

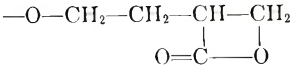

III

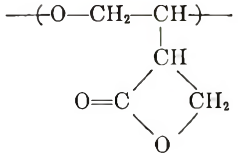

IV

In the CO–EI–EO system, infrared spectra support the existence of the structures I and II. The formic acid-insoluble products obtained in this system suggested that EI reacted with the β-lactone part of the structures III and IV to yield a crosslinked polymer with an amide structure.

Carbon Monoxide–*N*-Substituted Aziridine–Ethylene Oxide System

The copolymerization of carbon monoxide and *N*-alkyl- or *N*-aryl-substituted aziridines, which are considered to be less reactive to CO than EI because of their lower nucleophilicity, was carried out in the presence of ethylene oxide. The results for the CO–*N*-methylpropylenimine–EO and CO–*N*-phenylethylenimine–EO systems are shown in Table II. A yellowish white powdery polymer was obtained in each system. From the elementary analysis, it was found that the content of EO in these polymers was greater than that in polymers from the CO–EI–EO system. This shows the smaller reactivity of *N*-substituted aziridines than that of ethylenimine. This tendency was also shown from the infrared spectra (Fig. 4). The infrared spectra show the characteristic absorption peaks of tertiary amide at 1630 and 1650 cm^{-1}, respectively and both spectra show absorption at 1730 cm^{-1} due to ester linkage. The characteristic absorption of ester carbonyl in *N*-phenylethylenimine was stronger than with the use of ethylenimine.

TABLE II
Copolymerization of Carbon monoxide(CO)–*N*-Methylpropylenimine (NMPI)–Ethylene Oxide(EO) and Carbon Monoxide(CO)–*N*-Phenylethylenimine(NPEI)–Ethylene oxide(EO) Systems by γ-irradiation[a]

			Elementary analysis			Polymer composition, molar ratio			
Imine	Imine in feed, g	Yield, g	C, %	H, %	N, %	CO	Imine	EO	H_2O
NMPI	0.10	0.118[b]	54.80	7.33	5.76	1.00	0.36	0.77	—
NPEI	0.25	0.220	70.48	6.69	8.25	1.00	1.11	0.58	0.01
		0.146[c]	61.06	5.98	5.90	1.00	0.43	0.39	0.39

[a] Reaction conditions: in CO feed, 3.0 g; EO, 4.5 g.; dose rate, 2 × 10^5 rad/hr; total dose, 3.4 × 10^7 rad.; temperature, 10°C.

[b] Acetone-insoluble part.

[c] Chloroform-insoluble part.

The x-ray diffraction diagrams (Fig. 5) show no crystallinity in the CO–*N*-methylpropylenimine–EO system, while crystallinity in the CO–*N*-phenylethylenimine–EO system is almost the same as that of *N*-phenyl-

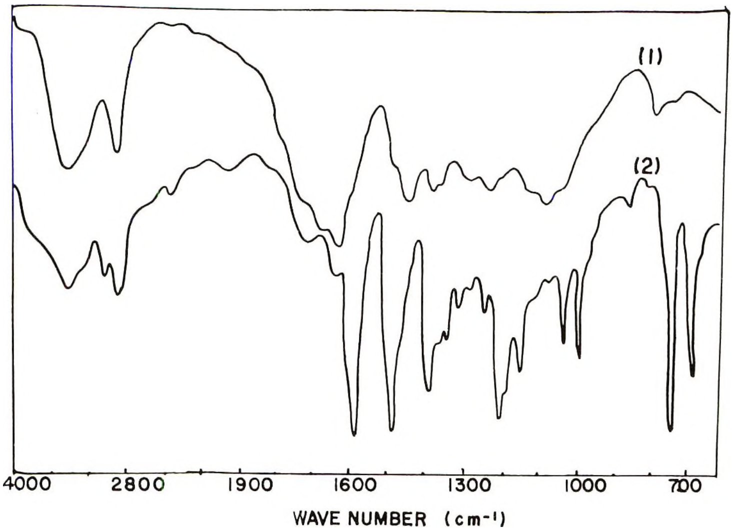

Fig. 4. Infrared spectra of the copolymer obtained in CO–EO–imine systems: (*1*) carbon monoxide–*N*-methylpropylenimine–ethyleneoxide; (*2*) carbon monoxide–*N*-phenylethylenimine–ethylene oxide.

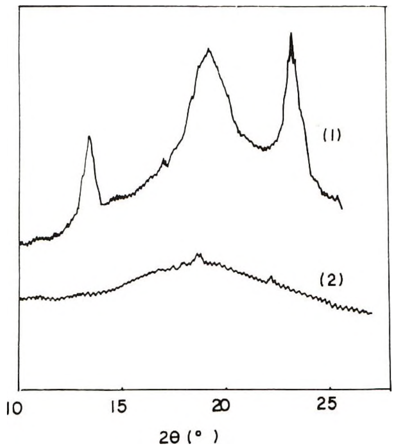

Fig. 5. X-ray diffraction diagrams of the copolymers obtained in CO–EO–imine systems: (*1*) carbon monoxide–*N*-phenylethylenimine–ethylene oxide; (*2*) carbon monoxide–*N*-methylethylenimine–ethylene oxide.

ethylenimine homopolymer. From these results, these reaction products are considered to be CO–*N*-methylpropylenimine–EO and CO–*N*-phenylethylenimine–EO terpolymers.

Carbon Monoxide–Ethylenimine–Cyclic Ether System

Table III shows the results of the terpolymerization of the CO–EI–cyclic ether system. The results of elementary analysis show that each product consists of CO, EI, and cyclic ether component.

TABLE III
Copolymerization of Carbon Monoxide(CO)–Ethylenimine(EI)–Tetrahydrofuran (THF), –1,3-Dioxolane(DOL), and –1,4-Dioxane (DOX) Systems

Cyclic ether	Amt Yield, g	Yield, g	Elementary analysis				Polymer composition, molar ratio			
			C, %	H, %	N, %	Ash, %	CO	EI	Ether	H_2O
THF	7.2	0.167	51.99	6.93	14.02	—	1.00	0.71	0.16	0.03
		0.110[b]	44.42	6.06	12.76	—	1.00	0.52	0.04	0.27
DOL	7.4	0.224	47.78	6.33	13.50	—	1.00	0.65	0.13	0.11
		0.140[b]	45.71	6.36	13.11	1.69	1.00	0.67	0.12	0.27
DOX	8.8	0.269	46.44	6.31	12.89	—	1.00	0.59	0.07	0.24
		0.233[b]	44.12	6.23	13.38	4.16	1.00	0.63	0.12	0.28

[a] Reaction conditions: Carbon monoxide, 3.0 g; EI/CO molar ratio, 2×10^{-2}; dose rate, 3×10^5 rad/hr; total dose, 2×10^7 rad; temperature, 10°C.

[b] Chloroform-insoluble part.

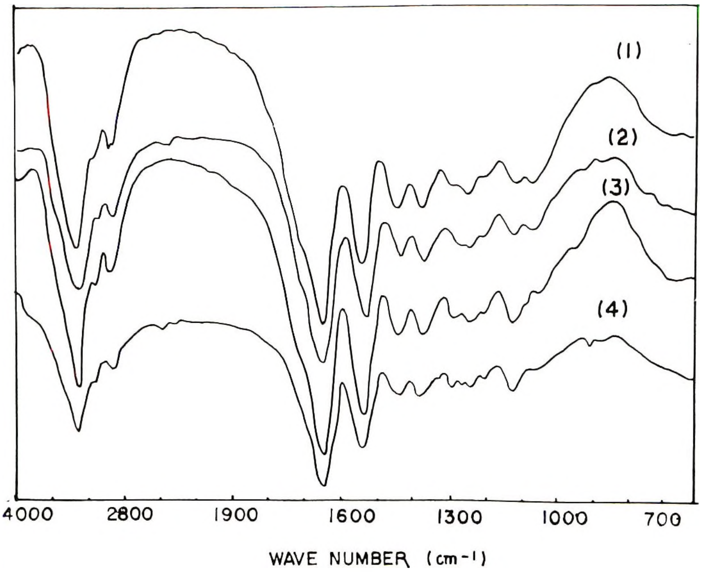

Fig. 6. Infrared spectra of the copolymers of carbon monoxide–ethylenimine–cyclic ethers with EI/CO molar ratio 2×10^{-2}: (*1*) ethylene oxide; (*2*) tetrahydrofuran; (*3*) 1,3-dioxolane; (*4*) 1,4-dioxane.

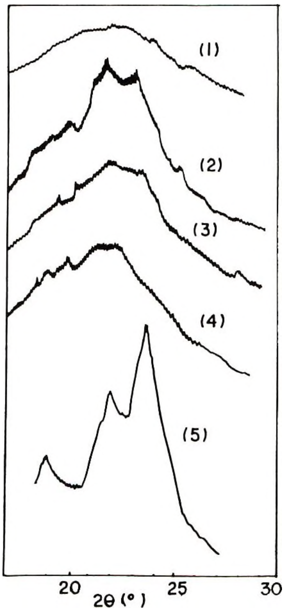

Fig. 7. X-ray diffraction diagrams of the copolymers of carbon monoxide–ethylenimine–cyclic ethers with EI/CO molar ratio 2×10^{-2}: (*1*) ethylene oxide; (*2*) tetrahydrofuran; (*3*) 1,3-dioxolane; (*4*) 1,4-dioxane; (*5*) poly-β-alanine obtained by copolymerization of CO and ethylenimine with γ-irradiation.

Figure 6 shows the infrared spectra of the products. It is obvious that characteristic absorptions of the secondary amide at 3300, 3100, 1640, and 1540 cm^{-1} were also observed as in the system of CO–EI–EO system. The infrared spectra show that the main structure of the product is secondary amide.

Figure 7 shows the x-ray diffraction diagrams of the reaction products. Apparently, each of them shows partial crystallinity, but their diffraction diagrams are not the same as that of poly-β-alanine. Based on the results of elementary analysis, infrared spectra, and x-ray diffraction diagrams, it may be concluded that terpolymerization occurred to give polyamide with some ester linkages in the CO–EI–cyclic ether system.

Carbon Monoxide–Ethylenimine–2-Vinyl-1,3-dioxolane System

A yellowish white powder was obtained by γ-irradiation of the CO–EI–2-vinyl-1,3-dioxolane system (Table IV).

TABLE IV
Copolymerization of Carbon Monoxide(CO)–Ethylenimine(EI)–2–Vinyl-1,3-dioxolane(VDOL) System by γ-Irradiation

Ether (VDOL), g	Yield, g	Elementary analysis			Polymer composition, molar ratio			
		C, %	H, %	N, %	CO	EI	VDOL	H_2O
4.8	0.332							
	0.200[b]	48.80	7.65	15.86	1.00	1.66	0.32	0.01

[a] Reaction conditions: CO in feed, 2.8 g; EI, 3.7 g; dose rate, 6 × 10^5 rad/hr; total dose, 1.2 × 10^7 rad; temperature, 60°C.

[b] Chloroform-insoluble part.

Figure 8 shows the infrared spectrum of the chloroform-insoluble portion of the product. There are characteristic secondary amide bands at

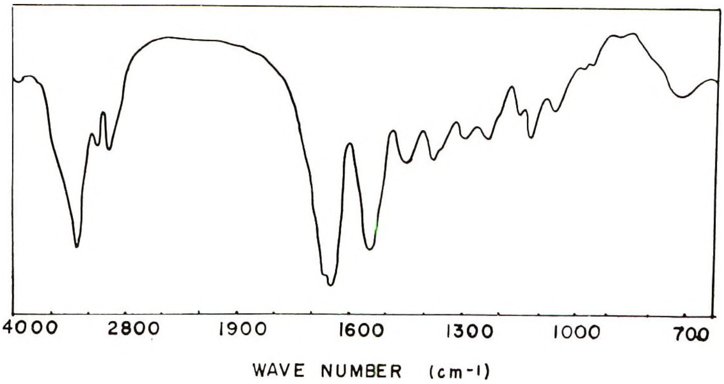

Fig. 8. Infrared spectrum of the copolymer of carbon monoxide–ethylenimine–2-vinyl-1,3-dioxolane.

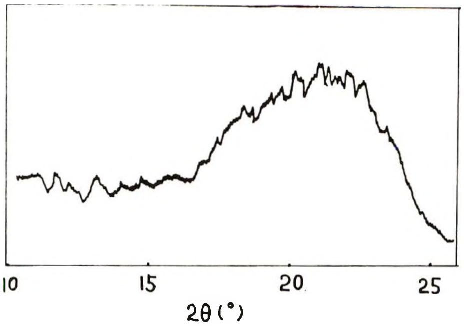

Fig. 9. X-ray diffraction diagram of the copolymer of carbon monoxide–ethylenimine–2-vinyl-1,3-dioxolane.

3100, 1650, and 1550 cm^{-1} and also a very weak absorption assignable to the dioxolane ring at 1130 cm^{-1}. Since no peak at 1730 cm^{-1} due to ester group was observed, isomerization polymerization which has been reported by us[4] does not occur in this system.

The x-ray diffraction diagram of the product (Fig. 9) is different from both that of CO–2-vinyl-1,3-dioxolane copolymer and that of CO–EI copolymer obtained by γ-irradiation. From these results and the result of the elementary analysis, it was concluded that copolymerization occurred in the CO–EI–2-vinyl-1,3-dioxolane system and that vinyl type polymerization occurred almost exclusively to give a product with polyamide and ketone structure.

Mechanism of the X-Ray-Induced Copolymerization of Carbon Monoxide and Aziridines in the Presence of Cyclic Ethers

Initiation. The same initiation mechanism was proposed for the γ-ray-induced copolymerization of carbon monoxide and aziridines in the presence of cyclic ethers as that in the copolymerization of carbon monoxide and aziridines or cyclic ethers. The initiation reaction involves the formation of carbonyl radicals by the reaction of carbon monoxide and radicals produced by the radiolysis of aziridine or cyclic ether as shown in eqs. (1).

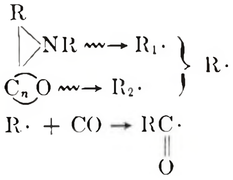

(1a)

(1b)

(1c)

The radical $R_2\cdot$ increases with the addition of cyclic ether, and the total of the radicals ($R_1\cdot + R_2\cdot$) initiates the copolymerization. As was described above, the main structure of the copolymer was poly-β-alanine. From the result, it is considered that the amount of radical $R_2\cdot$ formed in eq. (1b) is smaller than that of radical $R_1\cdot$ in eq. (1a).

Propagation. The main structure of the copolymers was poly-β-alanine, as described above. This may be attributable to the difference of the reactivity of aziridine and cyclic ether to the growing polymer radical. Since the carbonyl radical is highly electrophilic, aziridine having a higher nucleophilicity than cyclic ether, is considered to react exclusively with the carbonyl radical. The main propagation reaction is, therefore, proposed as shown in eqs. (2) and (3).

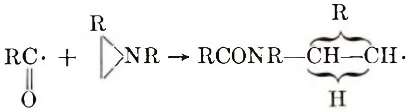

$$\underset{\underset{\mathrm{O}}{\|}}{\mathrm{RC}}\cdot + \overset{\mathrm{R}}{\triangleright}\mathrm{NR} \rightarrow \mathrm{RCONR{-}}\underbrace{\overbrace{\mathrm{CH{-}CH}}^{\mathrm{R}}}_{\mathrm{H}}\cdot \qquad (2)$$

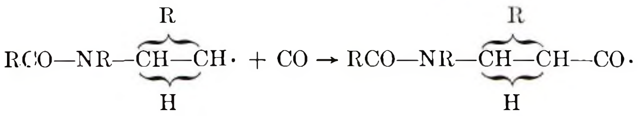

$$\mathrm{RCO{-}NR{-}}\underbrace{\overbrace{\mathrm{CH{-}CH}}^{\mathrm{R}}}_{\mathrm{H}}\cdot + \mathrm{CO} \rightarrow \mathrm{RCO{-}NR{-}}\underbrace{\overbrace{\mathrm{CH{-}CH}}^{\mathrm{R}}}_{\mathrm{H}}\mathrm{{-}CO}\cdot \qquad (3)$$

The alternate occurrence of two selective addition reactions (2) and (3) gives the poly-β-alanine. The fact that polyester structure was observed in the copolymers, shows that some addition of cyclic ether to the growing radical also takes place with at a slow rate to give the polyester, as shown in eq. (4).

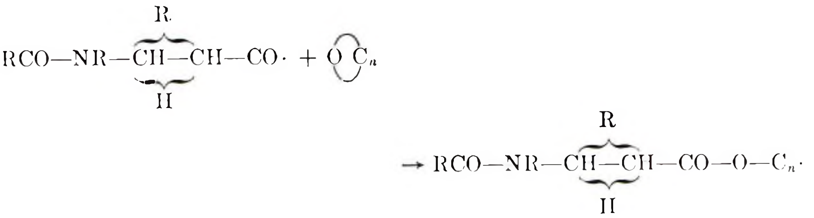

$$\mathrm{RCO{-}NR{-}}\underbrace{\overbrace{\mathrm{CH{-}CH}}^{\mathrm{R}}}_{\mathrm{H}}\mathrm{{-}CO}\cdot + \mathrm{O}\,\mathrm{C}_n \rightarrow \mathrm{RCO{-}NR{-}}\underbrace{\overbrace{\mathrm{CH{-}CH}}^{\mathrm{R}}}_{\mathrm{H}}\mathrm{{-}CO{-}O{-}C}_n\cdot \qquad (4)$$

The authors are appreciative of Sumitomo Atomic Energy Ind. Ltd. for supplying the irradiation equipment used in the experimental work.

References

1. T. Kagiya, M. Kondo, K. Fukui, and H. Yokota, *J. Polym. Sci.*, in press.
2. T. Kagiya, S. Narisawa, T. Ichida, and K. Fukui, H. Yokota, and M. Kondo, *J. Polym. Sci. A-1*, **4**, 293 (1966).
3. T. Kagiya, T. Ichida, S. Narisawa, and K. Fukui, *J. Polym. Sci. A-1*, **5**, 2031 (1967).
4. T. Kagiya, T. Nakayama, Y. Nakai, and K. Fukui, *J. Polym. Sci. A-1*, **5**, 2351 (1967).
5. H. W. Heine, B. L. Kaupur, and C. S. Mitch, *J. Amer. Chem. Soc.*, **76**, 1173 (1954).
6. R. C. Elderfield, *J. Amer. Chem. Soc.*, **81**, 4689 (1959).

Received April 19, 1968
Revised August 14, 1968

JOURNAL OF POLYMER SCIENCE: PART A-1 VOL. 7, 363-377 (1969)

The High-Temperature Degradation of Poly(2,6-dimethyl-1,4-phenylene Ether)

A. FACTOR, *General Electric Research and Development Center, Schenectady, New York 12301*

Synopsis

The thermal degradation of poly(2,6-dimethyl-1,4-phenylene ether) has been investigated to 1000°C in an inert atmosphere. X-ray diffraction, thermogravimetric analysis, and differential scanning calorimetry were employed to study the physical changes in the polymer, and vapor-phase chromatography, infrared spectroscopy, and mass spectrometric thermal analysis were used to elucidate the chemical aspects of the degradation process. It was found that degradation occurs in two steps: (*1*) a rapid exothermic process occurs between 430 and 500°C, leading to the evolution of phenolic products, water, and a black, highly crosslinked residue, and (*2*) a slower, char-forming process occurs above 500°C, characterized by the evolution of methane, carbon monoxide, and hydrogen. The chars formed in process 2 were found by x-ray analysis to be amorphous. The infrared spectrum of a sample heated to 510°C is nearly identical with that of the starting polymer, indicating that oxidative reactions are not important in the first process. The data for the low-temperature process are consistent with a thermal degradation scheme based on the radical-redistribution reaction of polyphenylene ethers and/or the degradation of *o*-benzylphenols formed by the thermal rearrangement of *o*-methyl diphenyl ethers. The char-forming process is best explained by simultaneous operation of the Szwarc mechanism of toluene pyrolysis, producing hydrogen and methane and reactions that cleave the aromatic rings and produce carbon monoxide.

INTRODUCTION

The ether linkage of aryl ethers is one of the most stable chemical bonds. This accounts for the high decomposition temperatures of polyphenyl ethers, which has made them important heat-exchange fluids and high-temperature lubricants.[1,2] Little work bearing on the mechanism of the thermal decomposition of this class of compounds has been published. The decomposition of poly(2,6-dimethyl-1,4-phenylene ether), or PPO (registered trademark of General Electric Company), was studied in this laboratory to determine its mode of breakdown. Although the study was restricted to this compound, the results should be generally applicable to other polyphenylene ethers.

Since polymer degradation is often complex, it was felt that the mechanism of degradation could best be found by correlating the information from a variety of analytical techniques. In this work x-ray diffraction, thermogravimetric analysis, and differential scanning calorimetry were employed to study the physical changes in the polymer during degradation, and vapor-phase chromatography, infrared spectroscopy, and mass-spectrometric thermal analysis were used to study the chemical aspects of the degradation process.

EXPERIMENTAL

Polymer Sample

The resin used in this study was obtained from the General Electric Company and had been produced by the Hay process,[3] eq. (1). The polymer had an intrinsic viscosity of 0.50 dl/g in chloroform at 25°C, a $\bar{M}_n$ of 18,500 g/mol, and a $\bar{M}_w$ of 37,200 g/mol. Prior to use the resin was dried overnight at 60°C in a vacuum.

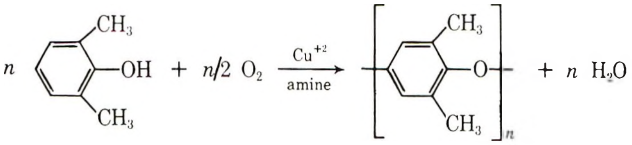

(1)

Instrumentation

Infrared spectra were measured with a Perkin-Elmer Model 521 Spectrophotometer, thermogravimetric analyses (TGA) were performed with a Chevenard thermobalance, and differential scanning calorimetry (DSC) were made with a Perkin-Elmer Model DSC-1 Differential Scanning Calorimeter.

Mass Spectrometric Thermal Analysis

Mass spectrometric thermal anyalsis (MTA) has recently been employed in studying the thermal decomposition of polymers.[4–6] By the MTA technique, decomposition gases are continually analyzed with a time-of-flight mass spectrometer during linear-programmed heating of samples. Shulman[4] has shown that, because the pyrolysis occurs in a rapidly pumped system, the pressure in the vicinity of the ionizing filament depends on the rate of production of effusing gases. The peak height is therefore proportional to the rate of production of a given species at each temperature. Given this relationship, a semilogarithmic plot of peak intensity versus reciprocal absolute temperature (Arrhenius plot) will give a straight line of slope E_a/R in the early stages of decomposition when the amount of the chemical source responsible for a particular peak has not changed significantly. Thus, by the MTA method one is able both to identify the products of thermal decomposition of polymers and to measure their rates of production as a function of temperature.

The MTA results for poly(2,6-dimethyl-1,4-phenylene ether) were obtained by Dr. H. L. Friedman (General Electric Company, Space Sciences

Laboratories, King-of-Prussia, Pennsylvania) and his co-workers with apparatus that is described elsewhere.[6] In a typical run the polymer, contained in a porcelain boat in an evacuated quartz tube situated about 1 m from the inlet leak of a Bendix "time-of-flight" mass spectrometer, was heated at a linear-programmed rate. The ion intensities of masses 1, 2, 12 to 18, 22, and 24 to 212 were read once a minute by using a 200-position rotary reed switch in conjunction with 200 wire-wound potentiometers, which sequentially varied the gate voltage. The mass, temperature, and intensity were recorded for each peak on punched tape. By means of a computer these data were automatically displayed as graphs of intensity versus temperature for each of the 200 mass units. Currently the apparatus is in a state of evolution, and the data acquired may contain errors of approximately 25% because of erroneous gate voltage settings. Nonetheless, the data obtained yield an excellent qualitative picture of the thermal decompositions of this polymer. The products identified by the MTA technique were verified by vapor-phase chromatography of products of replicate polymer decompositions.

RESULTS AND DISCUSSIONS

Thermogravimetric Analysis (TGA)

Previous studies[7-9] of the thermal properties of poly(2,6-dimethyl-1,4-phenylene ether) have shown that in an inert atmosphere the polymer decomposes above 400°C. The TGA curve of its pyrolysis in nitrogen (Fig. 1) closely agrees with that published by Hoyt et al.[8] There was no

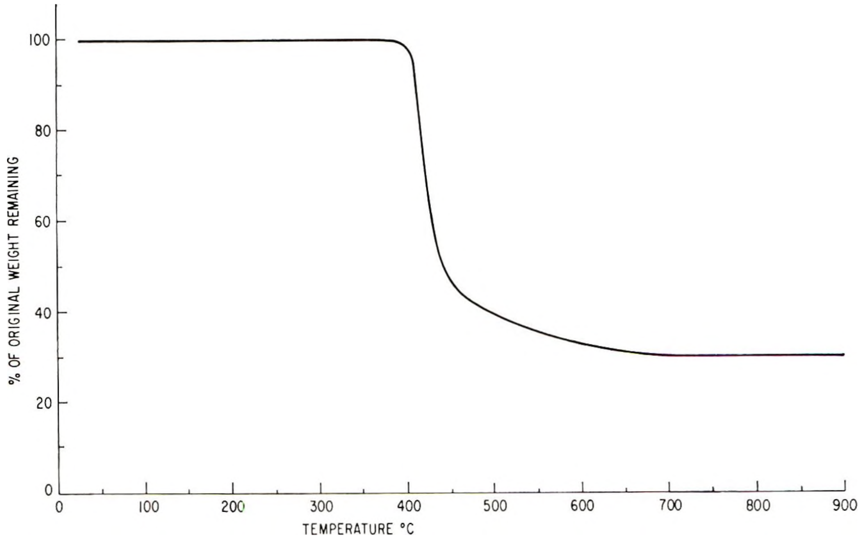

Fig. 1. TGA curve for poly(2,6-dimethyl-1,4-phenylene ether) in nitrogen: heating rate 100 C°/hr, sample weight 0.100 g, gas flow 275 ml/min.

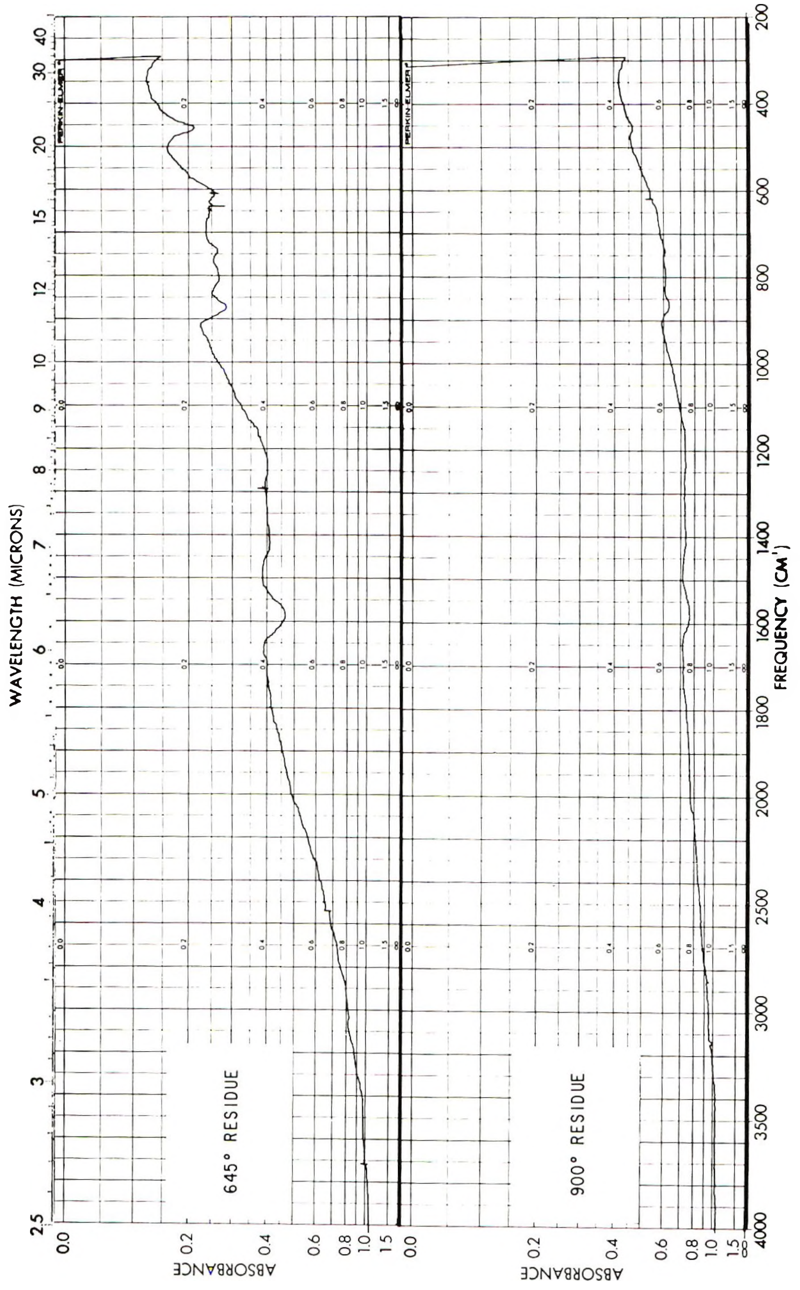
WAVELENGTH (MICRONS)
2.5
3
4
5
6
7
8
9
10
12
15
20
30
40
FREQUENCY (CM⁻¹)
4000
3500
3000
2500
2000
1800
1600
1400
1200
1000
800
600
400
200
ABSORBANCE
0.0
0.2
0.4
0.6
0.8
1.0
1.5
∞
645° RESIDUE
900° RESIDUE
PERKIN-ELMER

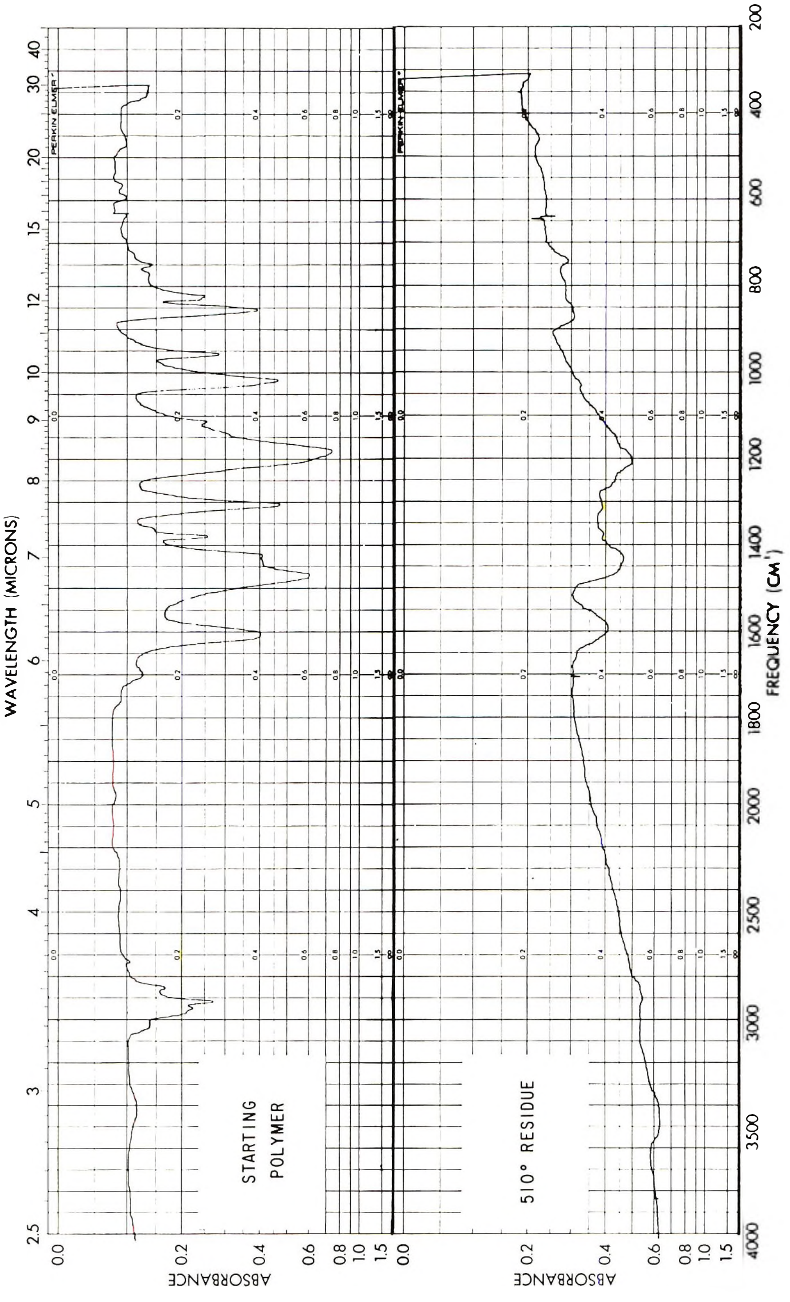

Fig 2. Effect of pyrolysis on infrared spectrum of poly(2,6-dimethyl-1,4-phenylene ether.

weight change up to 400°C, but between 400 and 500°C the polymer rapidly lost 60% of its weight. The gaseous products of this experiment were not investigated directly; however, analysis was made of the volatile products (2% yield) from the pyrolysis of a sample of polymer that was heated for 4 hr at 350°C in a sealed, evacuated tube. Mass-spectrometric analysis of the noncondensable portion shows the presence of hydrogen, methane, and carbon monoxide in the ratio of 94:2:1, and vapor-phase chromatography on a silicon gum rubber (SE 30) column indicates the presence of at least twenty components in the condensable fraction. The approximate yields of the major products were toluene (0.5%), 2,6-xylenol (0.5%), *o*-, *m*-, and *p*-cresols (0.3%), and 2,4,6-mesitol (0.1%). The other components had molecular weights corresponding to dimeric and trimeric polymer units.

Analysis of Polymer Residues

The residues of several TGA runs, terminated at different temperatures, were analyzed for carbon and hydrogen (Table I). All the residues had a carbonized appearance. The analyses show that at higher pyrolysis temperatures the percentage of carbon in the residue increased at the expense of those of hydrogen and oxygen. It is interesting to note how little the analysis of the 510°C residue differs from that of the original polymer, since only 40% of the original mass remains after pyrolysis.

TABLE I
Analysis of TGA Residues[a]

Highest temp., °C	Analysis, %		
	C	H	O[b]
Starting polymer	80.0[c]	6.7[c]	13.3[c]
510	84.7	4.4	10.9
645	91.3	2.8	5.9
900	96.9	1.9	1.2

[a] TGA run in a nitrogen atmosphere at 150°C/hr.
[b] Calculated by difference.
[c] Calculated analysis for $[C_8H_8O]_n$.

During the high-temperature degradation of phenol formaldehyde resin, Jackson and Conley[10] observed the appearance of carbonyl bands in the infrared spectra of the polymer residues even when the pyrolysis was conducted in the absence of oxygen. They were also able to detect a "graphite-like" line in the x-ray diffraction patterns of chars formed above 600°C. By contrast, the infrared spectra of the residues listed in Table I and illustrated in Figure 2 show no carbonyl bands and have the same general features as the spectrum of the starting polymer, except for band-broadening, which increased with pyrolysis temperature. A new band at 460 cm^{-1} was seen in the 645°C residue; however, its significance is not known.

The spectrum of the 900°C residue no longer showed any discrete bands but only a continuous absorption. X-ray analysis of these residues indicate that, unlike the chars from phenol formaldehyde resin, they were completely amorphous.

Differential Scanning Calorimetry (DSC)

The DSC curve for poly(2,6-dimethyl-1,4-phenylene ether), Figure 3, shows a small endotherm of 4 cal/g between 240 and 275°C, corresponding to crystal melting,[7] and a large exotherm of 86.8 cal/g (10.4 kcal/mol-monomer) between 430 and 500°C. Comparison of the DSC and TGA curves indicates that the degradative weight loss observed between 400 and 500°C is a strongly exothermic process. A higher decomposition threshold temperature, 430°C, was observed by the DSC method, because a faster temperature program was utilized.

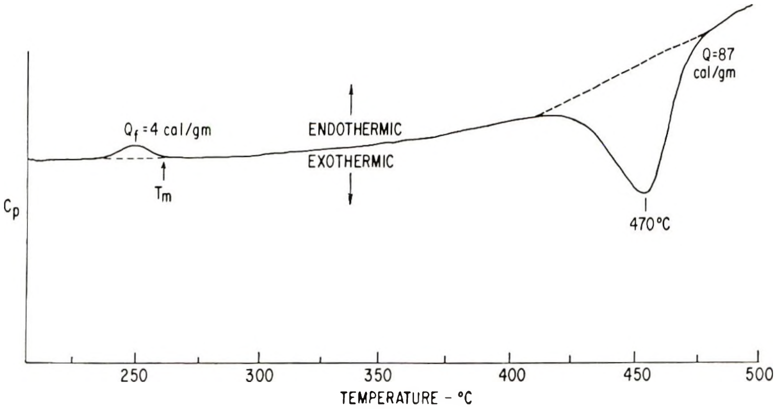

Fig. 3. DSC curve for poly(2,6-dimethyl-1,4-phenylene ether): heating rate 40 C°/min, sample weight 0.0047 g, nitrogen atmosphere.

Mass Thermal Analysis (MTA)

A 5 mg sample of finely ground polymer contained in a porcelain boat was heated in the evacuated quartz inlet tube of the MTA apparatus at the rate of 10°C/min from ambient temperature to 1,000°C. The mass, temperature, and ion intensity of each mass peak was recorded automatically every minute. The data were then processed by computer and produced plots of relative ion intensity versus temperature for each mass. The identities of the major pyrolysis products were determined by a comparison of these curves with known mass spectra and from results previously obtained by vapor-phase chromatography. The products are listed in Table II with the temperatures at which their rates of formation are at a maximum, their activation energies, and their characteristic mass numbers, ions, and interfering fragments. Figures 4 and 5 show the graphs of the uncorrected relative intensity versus temperature for the major products; Figure 6 shows the Arrhenius plot for these products.

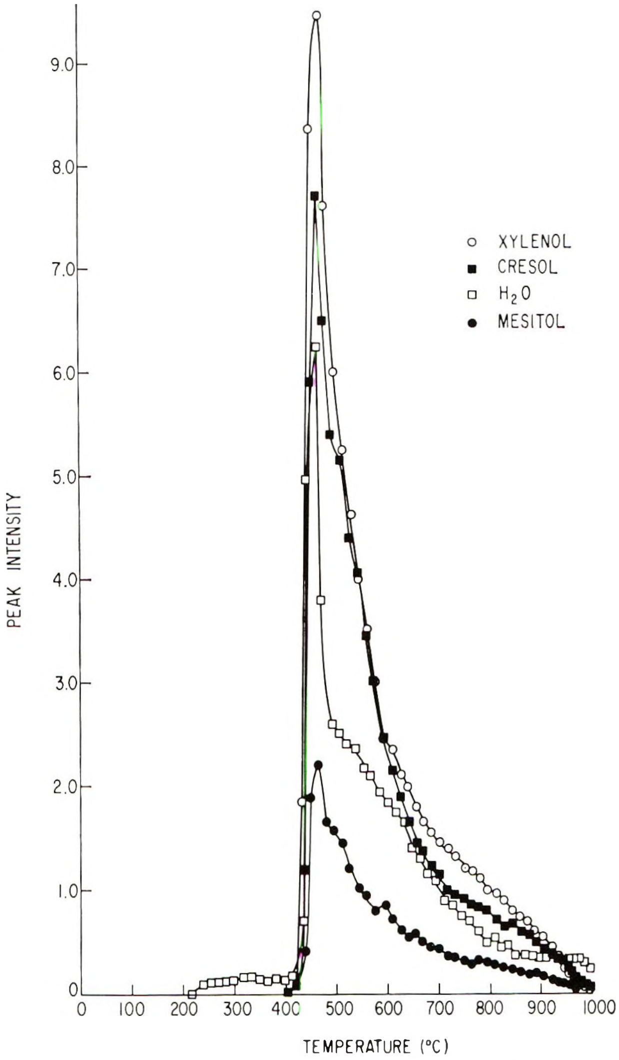

Fig. 4. Effect of temperature on product distribution from pyrolysis of poly(2,6-dimethyl-1,4-phenylene ether).

A study of these figures reveals the occurrence of two separate processes: (*1*) a general, rapid degradation with a maximum rate at 456°C, leading to the evolution of phenolic products, water, and residue corresponding to the exothermic process seen by DSC and TGA, and (*2*) a slower process characterized by the evolution of methane, carbon monoxide, and hydrogen in the temperature range 500 to 800°C, corresponding to char-forming reactions in the polymer. A second maximum in the rate of carbon monoxide formation (Fig. 5) may indicate that another char-forming process is occurring above 900°C, but machine error at these high temperatures makes this uncertain.

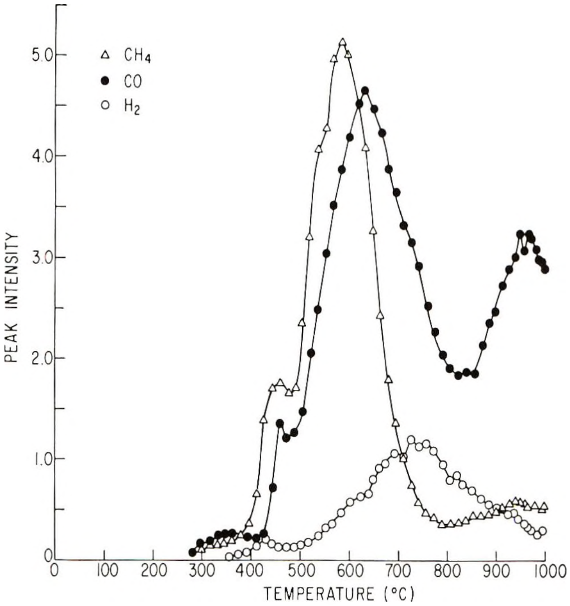

Fig. 5. Effect of temperature on product distribution from pyrolysis of poly(2,6-dimethyl-1,4-phenylene ether).

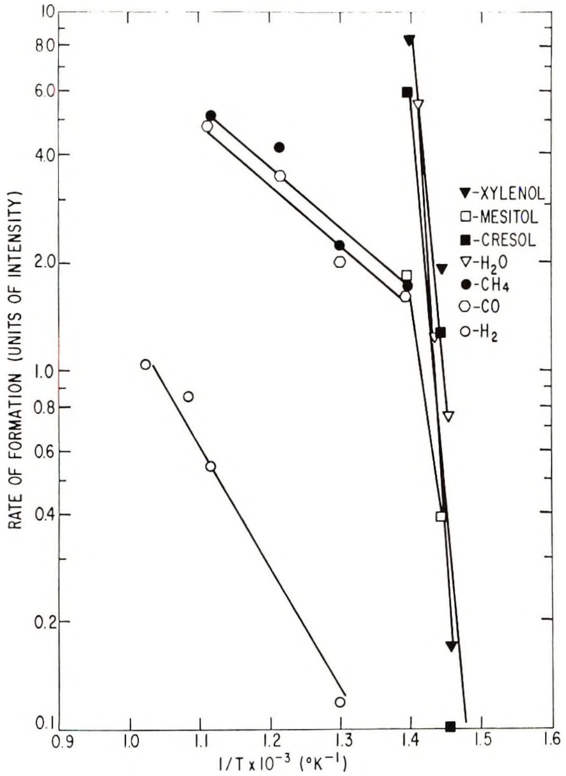

Fig. 6. Temperature dependence of poly(2,6-dimethyl-1,4-phenylene ether) pyrolysis.

TABLE II
Characteristics of the Pyrolysis Products
of Poly(2,6-dimethyl-1,4-phenylene ether)

Species	Temp. of max. rate, °C	Activation energy, kcal/mol	Mass no.	Ion	Interfering fragment (source)
H_2	725	16	2	H_2^+	none
CH_4	590	10	16	CH_4^+	O^+ (H_2O, CO)
H_2O	456	57	18	H_2O^+	none
CO	630/950	9	28	CO^+	CO^+ (phenol, cresol, xylenol, mesitol)
Phenol	456	—	94	$C_6H_6O^+$	none
Xylene	540	—	106	$C_8H_{10}^+$	none
Cresol	456	78	108	$C_7H_8O^+$	$C_7H_8O^+$ (xylenol, mesitol)
Xylenol	456	72	122	$C_8H_{10}O^+$	$C_8H_{10}O^+$ (mesitol)
Mesitol	456	76	136	$C_9H_{12}O^+$	none

At 456°C, the temperature at which the rate of degradation is a maximum, a semiquantitative estimate was made for each product by correcting its characteristic peak for contributions due to fragments of higher molecular products. In this way it was possible to eliminate as major pyrolysis products, compounds such as carbon dioxide, toluene, and benzene. For this estimation the fracture patterns of 2,4,6-trimethylphenol, 2,6-xylenol, and *o*-cresol were used, although other isomers may very well be products of the pyrolysis. In theory it should be possible to differentiate between

TABLE III
Analysis of Gaseous Products at 456°C in the Vacuum
Pyrolysis of Poly(2,6-dimethyl-1,4-phenylene ether)

Species	Yield, mol-%	$-H_f^\circ$ at 25°C (kcal/mol)	(state)	Ref.
Xylenol	41	38.7	(gas)	12
Cresol	31	30.7	(gas)	12
H_2O	11	57.8	(gas)	13
Mesitol	10	46.8	(gas)	Calcd. by method of Cox (14)
Phenol	2	23.1	(gas)	12
Xylene	2	−4.0	(gas)	Calcd by method of Cox (14)
CO	0	—		
CH_4	2	17.9	(gas)	13
H_2	1	0	(gas)	definition
PPO	—	31.9[a]	(solid)	15

[a] Per mole of monomer.

isomers by mass spectral methods; however, the results of this experiment are too crude for such a determination. Nonetheless, since most isomers of these compounds have approximately the same characteristic fracture pattern, a good estimate of the total isomer content can be made. In these calculations it was assumed that all phenols had the same sensitivity constants. The data of Aczel and Lumpkin[11] indicate that this is a fairly good assumption, especially for isomeric phenols. The results of this analysis are shown in Table III.

Using this analysis, one can calculate a carbon, hydrogen, and oxygen composition for the volatile products of 76.92, 8.11, and 14.96%, respectively. By noting that the TGA (Fig. 1) indicates that 60% of the polymer volatilized at 510°C one can calculate the composition of the residue by subtracting 60% of these percentages from the composition of the original polymer, which yields, when normalized, a composition of 84.62, 4.57, and 10.80%. These values agree quite well with the actual analysis of the 510°C residue shown in Table I and explains why this residue analysis differed so little from that of the original polymer.

Heat of Reaction

The exothermic character of the thermal decomposition of poly(2,6-dimethyl-1,4-phenylene ether) was initially surprising, since most polymers degrade endothermically. However, a study of the heats of formation (ΔH_f°) of the major volatile pyrolysis products, shown in Table III, revealed that they are generally more negative than that of the starting polymer, and therefore one should expect this reaction to be exothermic.

Mechanisms

In many ways the results of this study are analogous to the results found previously for the pyrolysis of phenol formaldehyde resin. The MTA of phenol formaldehyde resin made by Shulman and Lochte[5] indicates that, like the pyrolysis of poly(2,6-dimethyl-1,4-phenylene ether), a rapid evolution of phenolic compounds occurs above 400°C in a process with a high activation energy (70 kcal/mol), followed at higher temperatures by the slower evolution of methane and hydrogen. Unlike the pyrolysis of the phenylene ether, water and formaldehyde are formed below 400°C because of a "post-curing" reaction in the polymer. In addition, above 400°C carbon dioxide, carbon monoxide, and water are important products of phenol formaldehyde degradation, indicating the importance of oxidative pathways in the degradation of phenol formaldehyde.[10] In the case of the thermal degradation of poly(2,6-dimethyl-1,4-phenylene ether) no evidence of an oxidative decomposition process has been detected either in infrared studies of degraded polymer or from the formation of volatile oxidation products. Therefore, only thermal degradation reactions can account for the products of this pyrolysis.

A reaction scheme that rationalizes the products found may be written by utilizing the established reaction of aryl ethers. In the formulation of this scheme an effort was made to avoid using direct bond-scission reactions as much as possible because of the high activation energies required in this type of reaction.

Hydrogen and methane are produced early in the pyrolysis, although their yields become substantial only at higher temperatures. The source of these gases is probably through a series of reactions analogous to the scheme demonstrated for the pyrolysis of toluene.[16] The initial step, eq. (2), has a high activation energy (78 kcal/mol) and therefore would

$$\mathrm{ArCH_3} \xrightarrow{\text{catalyst (?)}} \mathrm{ArCH_2\cdot} + \mathrm{H\cdot} \tag{2}$$

$$\mathrm{H\cdot} + \mathrm{ArCH_3} \rightarrow \mathrm{ArH} + \mathrm{CH_3\cdot} \tag{3}$$

$$\mathrm{H\cdot} + \mathrm{ArCH_3} \rightarrow \mathrm{ArCH_2\cdot} + \mathrm{H_2} \tag{4}$$

$$\mathrm{CH_3\cdot} + \mathrm{ArCH_3} \rightarrow \mathrm{ArCH_2\cdot} + \mathrm{CH_4} \tag{5}$$

not be expected to proceed rapidly at temperatures below 600°C unless catalyzed by impurities in the polymer, such as copper remaining from the polymerization catalyst.[3] The benzyl radicals formed in these reactions probably lead to extensive crosslinking of the polymer.

The redistribution of phenol ethers has been shown to occur readily at moderate temperatures in a chain reaction, probably involving a quinone ketal intermediate;[17] see eq. (6).

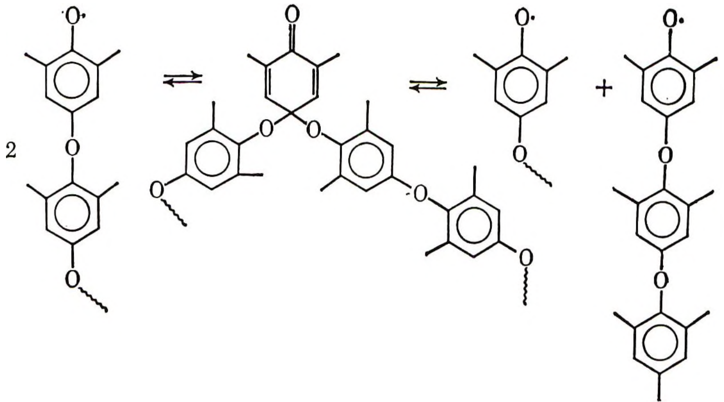

(6)

Analogously, the general degradation found between 400 and 500°C could proceed by redistribution reactions initiated by attack on the polymer of hydrogen atoms and methyl radicals formed in eqs. (2) and (3); for example,

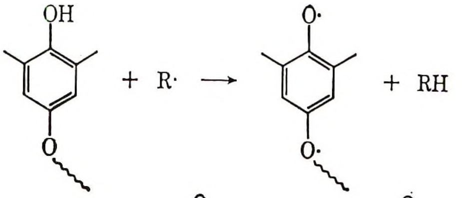

(7)

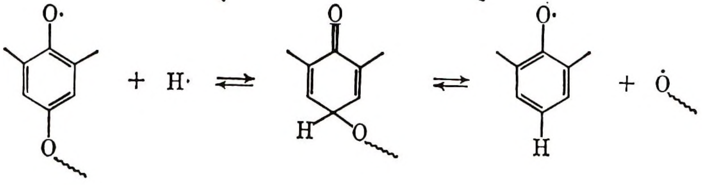

(8)

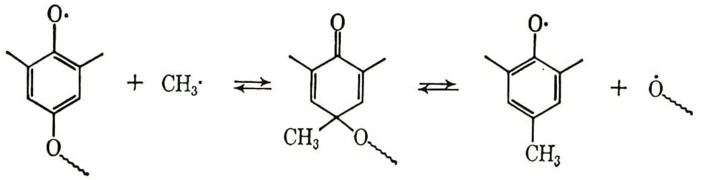

(9)

These reactions would account for the formation of xylenol and mesitol. In addition, cresol would be produced in eq. (8), if one of the *o*-methyl groups in the substrate had already been displaced by a hydrogen atom, as in eq. (3). The "end nibbling" process shown in eqs. (7), (8), and (9) would account for the fact that no dimeric products were detected in the MTA of the polymer, only simple phenols. The 40% of polymer residue probably did not degrade to simple phenols, because it was extensively crosslinked.

Another scheme for the formation of mesitol and cresol must be considered. It has been discovered[18] that when *o*-methyl diaryl ethers are heated to above 350°C they rearrange nearly quantitatively to *o*-benzyl phenols; see eq. (10). At 450°C this reaction will be extremely rapid and

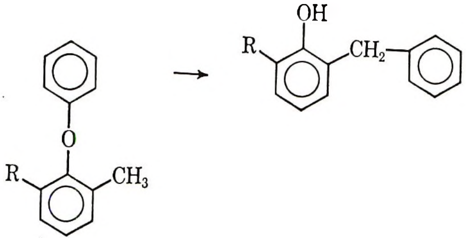

(10)

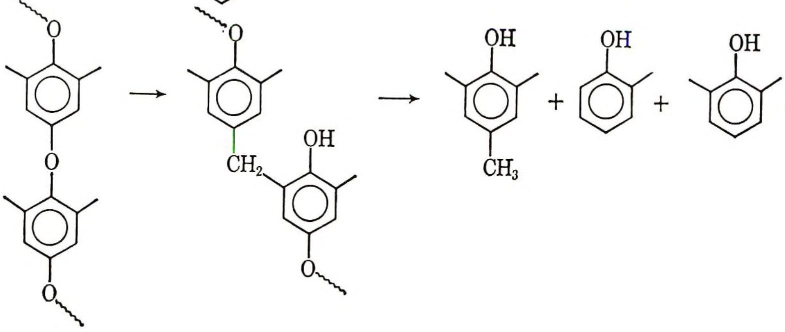

(11)

therefore constitutes an important degradation pathway; see. eq. (11). Fracture of rearranged segments either by direct cleavage or by a redistribution-like reaction would be expected to yield xylenol, cresol, and mesitol.

The formation of water is best rationalized as arising from an hydroxyl radical formed from a phenol by displacement or direct cleavage; see eqs. (12) and (13).

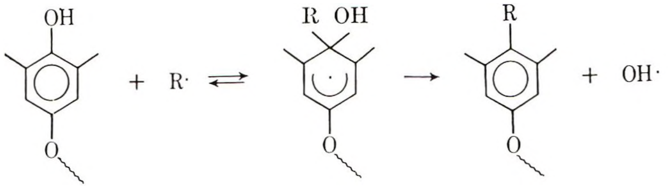

(12)

$$OH\cdot + RH \rightarrow H_2O + R\cdot \qquad (13)$$

The high-temperature, char-forming reaction is accompanied by the formation of hydrogen, methane, and carbon monoxide. The evidence indicates that the remaining char has no gross structure. The formation of hydrogen and methane again probably arises from eqs. (2) to (5). This degradation presumably involves the decomposition of polymer that was unable to redistribute to low molecular weight products because of extensive crosslinking. The production of carbon monoxide, however, can only be derived by ring cleavage at these elevated temperatures. The mechanism of this process is unclear; however, it is not surprising that carbon monoxide is a major pyrolysis product at these high temperatures. Other high-energy reactions, such as fragmentation in mass spectrometry,[19] indicate that the loss of carbon monoxide is an important pathway in the decomposition of phenols and diphenyl ethers.

The author would like to express his indebtedness to H. L. Friedman, G. A. Griffith, and J. E. Brown for the mass spectra discussed in this work and for helpful suggestions, to R. A. Kluge for differential scanning calorimetry, to Miss D. V. McClung for recording infrared spectra, to L. B. Bronk for thermogravimetric analyses, and to D. M. White for vapor-phase chromatographic runs.

References

1. C. L. Mahoney and E. R. Barnum, in *Synthetic Lubricants*, Gunderson and Hart, Eds., Reinhold, New York, 1962, Ch. 11.
2. W. L. Archer and K. B. Bozer, *Ind. Eng. Chem. Prod. Res. Develop.*, **5**, 145 (1966).
3. A. S. Hay, H. S. Blanchard, G. F. Endres, and J. W. Eustance, *J. Am. Chem. Soc.*, **81**, 6335 (1959).
4. G. P. Shulman, *J. Polym. Sci.*, B **3**, 911 (1963).
5. G. P. Shulman and H. W. Lochte, *J. Appl. Polym. Sci.*, **10**, 619 (1966).
6. H. L. Friedman and G. A. Griffith, *Proc. First Intern. Thermal Analysis Conf.*, 1965, J. P. Redfern, Ed., Macmillan, London, 1965, p. 22.
7. F. E. Karasz and J. M. O'Reilly, *J. Polym. Sci. B*, **3**, 561 (1965).
8. H. E. Hoyt, B. D. Halpern, K. C. Tsou, M. Bodnar, and W. Tannar, *J. Appl. Polym. Sci.*, **8**, 1633 (1964).
9. R. T. Conley and W. M. Alvino, *Org. Coatings Plastics Chem. Preprints*, **25**, No. 2, 149 (1965).

10. W. M. Jackson and R. T. Conley, *J. Appl. Polym. Sci.*, **8,** 2163 (1964).

11. T. Aczel and H. E. Lumpkin, *Anal. Chem.*, **32,** 1819 (1960).

12. R. J. L. Andon, D. P. Biddiscombe, J. D. Cox, R. Handley, D. Harrop, E. F. G. Herington, and J. F. Martin, *J. Chem. Soc.*, **1960,** 5246.

13. "Selected Values of Chemical Thermodynamic Properties," *Natl. Bur. Std. (U.S.)*, *Circular 500*, Washington, D.C. (1952).

14. J. D. Cox, *Tetrahedron*, **18,** 1337 (1962).

15. M. Joshi and B. J. Zwolinski, *Abstr. 152nd Am. Chem. Soc. Meeting, September, 1966.*

16. M. Szwarc, *J. Chem. Phys.*, **16,** 128 (1948); A. Blades and E. W. R. Stacie, *Can. J. Chem.*, **32,** *298 (1954)*.

17. (a) H. L. Finkbeiner, G. F. Endres, H. S. Blanchard, and J. W. Eustace, Am. Chem. Soc. Div. Polymer Chem. Preprint Booklet No. 2, Washington, D.C., Sept. 1961, p. 340. (b) G. D. Cooper, H. S. Blanchard, G. F. Endres, and H. Finkbeiner, *J. Am. Chem. Soc.*, **87,** 3996 (1965). (c) G. D. Cooper, A. R. Gilbert, and H. Finkbeiner, *Polymer Preprints of Phoenix Meeting of American Chemical Society*, Washington, D.C., 1966, p. 166. (d) D. A. Bolon, *J. Org. Chem.*, **32,** 1984 (1967). (e) E. McNellis, *J. Org. Chem.*, **31,** 1255 (1966).

18. A. Factor, H. L. Finkbeiner, R. A. Jerussi, and D. M. White, *J. Org. Chem.*, in press.

19. H. Budzikiewicz, C. Djerassi, and D. H. Williams, *Mass Spectra of Organic Compounds*, Holden-Day, 1967, pp. 116, 249.

Received December 6, 1967
Revised March 26, 1968

JOURNAL OF POLYMER SCIENCE: PART A-1 VOL. 7, 379-385 (1969)

The Cupric Sulfate–Hydrazine System as an Initiator of Vinyl Polymerization. I. The Polymerization of Methyl Methacrylate in Aqueous Solution in the Presence of Oxygen

JOAN BOND* and P. I. LEE, *The University of Salford,*†
Salford 5, Lancashire, England

Synopsis

The cupric sulfate–hydrazine system has been used to initiate the aqueous solution polymerization of methyl methacrylate at pH 9.25 in the presence of oxygen. At cupric sulfate concentrations greater than the saturation solubility of cupric hydroxide, hydrazine is adsorbed on, and decomposes on, the surface of the hydroxide. The kinetics of the decomposition are zero-order both in the absence and the presence of monomer. The initiation of the polymerization occurs both at the surface of the cupric hydroxide onto which some monomer is adsorbed and also in solution. Below the saturation solubility of cupric hydroxide, the initiation reaction between cupric ions and hydrazine occurs in solution.

The decomposition of hydrazine in the presence of metallic ions has been reported[1-3] to result in the production of the hydrazyl radical, N_2H_3. Menon and Kapur[4] have postulated that this radical is capable of initiating the aqueous solution polymerization of methyl methacrylate.

Parravano[5] has polymerized methyl methacrylate in aqueous solution using hydrazine, catalytically decomposed at a palladium surface, as the initiator. Since the experiments of Menon and Kapur were carried out in alkaline solution in which insoluble cupric hydroxide was probably present, the object of the work reported in this paper was to ascertain whether, (*a*) the decomposition of hydrazine in alkaline solutions of cupric sulfate is also a surface reaction and (*b*) if any other reaction is of importance in the initiation of the polymerization of methyl methacrylate, e.g., that between cupric ions and the hydrogen peroxide produced in the oxidation of hydrazine.

EXPERIMENTAL

Preparation and Purification of Materials

Methyl Methacrylate. Stabilized methyl methacrylate was distilled under reduced pressure in an atmosphere of nitrogen and used immediately.

---

* Present address: Headmistress, Westholme School, Blackburn, Lancashire, England.

†Formerly the Royal College of Advanced Technology.

Hydrazine Hydrate. The concentration of each freshly prepared solution of hydrazine hydrate was estimated by titrating 5 ml of the solution with 0.25*N* potassium iodate solution in the presence of 5 ml 12*N* hydrochloric acid and 2 ml chloroform. The solution was used immediately after preparation.

Cupric Sulfate. Analytical reagent grade cupric sulfate was used and, on analysis, was found to be 99.5% pure, containing less than 0.02% ferric ion.

Hydrogen Peroxide. Analytical reagent grade, hydrogen peroxide (stabilizer free) was used and was found to contain 30.5% weight for volume hydrogen peroxide.

Method

The apparatus consisted of eight tubes immersed in a constant temperature bath which was maintained at 30°C. Each tube was fitted with a condenser and a gas inlet tube. Oxygen was supplied to the tubes from a cylinder with the aid of an eight piece manifold. The reaction mixture was used as follows: x ml 0.125 mole/l methyl methacrylate solution, y ml 1 mole/l hydrazine hydrate solution, z ml 1×10^{-3} mole/l cupric sulfate solution, $50 - (x + y + z)$ ml deionized water.

By suitable variation of x, y, and z, the whole range of concentrations used was obtained. The water and the cupric sulfate solution were added to each tube and a stream of oxygen was passed through the solution for 1 hr after which time the flow rate was reduced to about two bubbles per second and this rate maintained throughout the polymerization; the monomer solution was then added. Polymerization was started by the addition of the hydrazine solution. Complete mixing was achieved by increasing the rate of oxygen flow for several seconds after which it was again reduced to two bubbles per second.

The polymerization in a particular tube was stopped after a given period of time by the addition of 5 ml 4*N* hydrochloric acid to the reaction mixture. One hour was allowed for complete coagulation and the polymer was then filtered through a preweighed glass sintered crucible and dried to constant weight in an air oven at 70°C and cooled in a desiccator which contained silica gel. The reaction mixtures in the other tubes were similarly treated after polymerization had continued for different periods of time. The rates of polymerization were reproducible to ±1%. The amount of hydrazine remaining was determined by titrating 5 ml of the filtrate with 0.25*N* potassium iodate solution in the presence of 5 ml 12*N* hydrochloric acid and 2 ml chloroform. Methyl methacrylate did not interfere with the endpoint of the titration. The amount of hydrazine was determined to an accuracy of ±0.1%.

Results

For convenience and brevity, the results are expressed in graphical form (Figs. 1–5).

DISCUSSION

Figure 1 shows the variation of the rate of polymerization of methyl methacrylate with cupric sulfate concentration. The rate is directly proportional to the concentration of cupric sulfate below 9×10^{-6} mole/l while above this concentration, the rate of polymerization decreases rapidly. In the absence of cupric sulfate no polymerization occurs. At the pH of the reaction mixture, (9.5), cupric hydroxide, whose saturation solubility is reported in the literature[6,7] to be 10^{-5} to 10^{-6} mole/l at 30°C, is formed by the hydroxylation of the cupric ions. Visible precipitation of the hydroxide does not occur until the cupric sulfate concentration is around 10^{-4} mole/l so that at concentrations between 10^{-5} and 10^{-4} mole/l, the hydroxide is in the form of a sol. Figure 2 shows that the rate of decomposition of hydrazine increases slowly with increasing concentration of cupric sulfate until at a concentration of about 10^{-3} mole/l the rate of decomposition of the hydrazine becomes very rapid. The decomposition of hydrazine in the presence of 5×10^{-5} mole/l cupric sulfate is zero-order both in the absence and the presence of monomer, (Fig. 3).

When hydrazine is added to a solution of monomer and cupric sulfate at a concentration greater than 10^{-5} mole/l, there is an extremely rapid decrease in its concentration in solution. On the addition of less than 0.002 mole/l of hydrazine to a reaction mixture containing 5×10^{-5} mole/l cupric sulfate, hydrazine cannot be detected in the solution, 15 sec after its addition. Solutions of higher concentrations of hydrazine

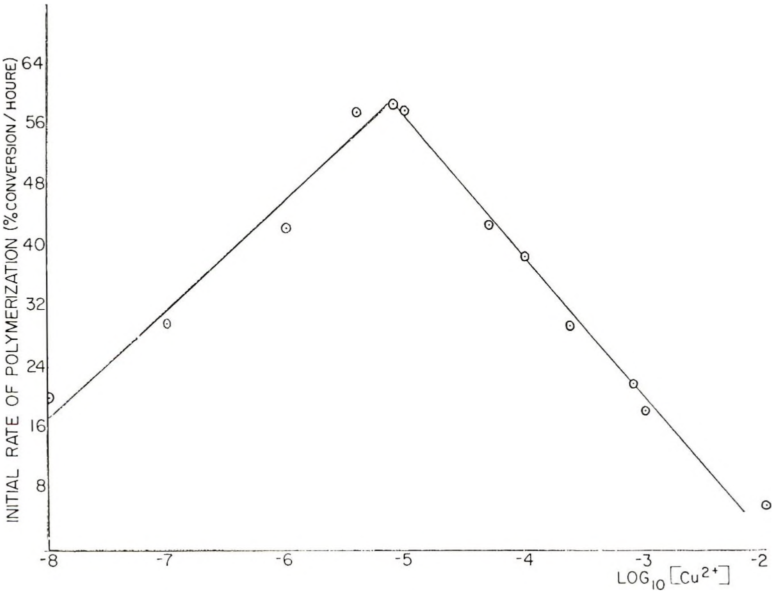

Fig. 1. The dependence of the initial rate of polymerization on the concentration of cupric sulfate. (0.08 mole/l hydrazine hydrate, 0.02 mole/l methyl methacrylate).

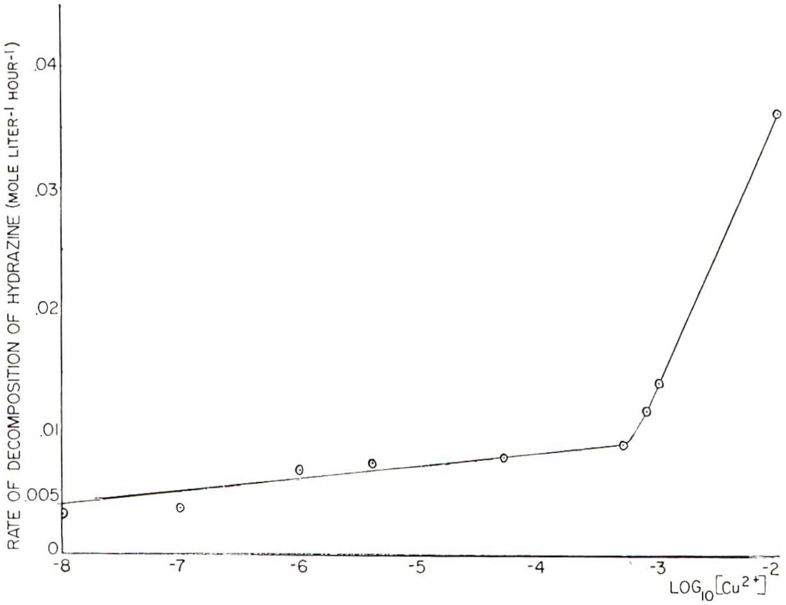

Fig. 2. The dependence of the rate of decomposition of hydrazine on the concentration of cupric sulfate. (0.08 mole/l hydrazine hydrate, 0.02 mole/l methyl methacrylate).

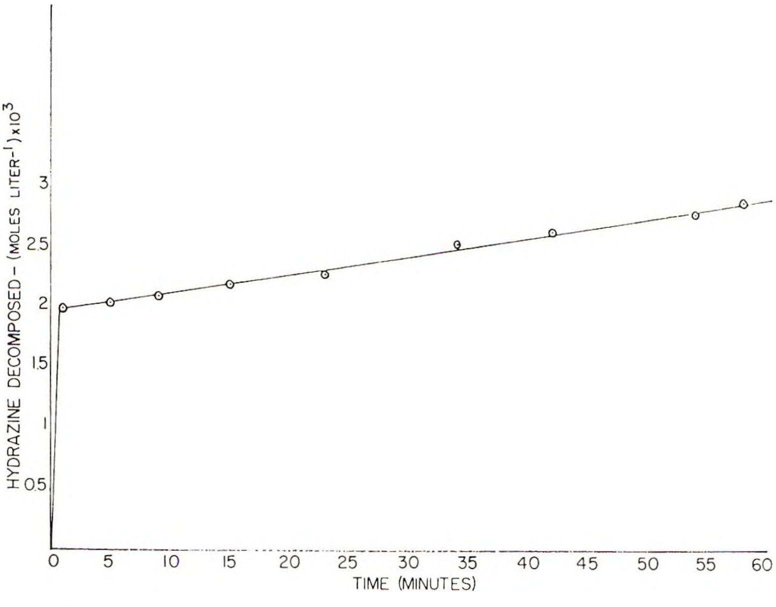

Fig. 3. The zero-order rate curve of the decomposition of hydrazine at a cupric sulfate concentration of 5×10^{-5} mole/l. (0.008 mole/l hydrazine hydrate, 0.02 mole/l methyl methacrylate).

show an immediate decrease of 0.002 mole/l. A similar result is obtained with a cupric sulfate concentration of 1×10^{-2} mole/l when the critical concentration of hydrazine is 0.003 mole/l.

At initial concentrations of hydrazine greater than 0.003 mole/l, the concentration of hydrazine removed from the solution after 30 min reaction time is 0.0024 mole/l and this is independent of the initial concentration of hydrazine (Fig. 4). The rate of polymerization increases with increasing initial hydrazine concentration and attains a constant value at about 0.007 mole/l hydrazine.

These results suggest that when cupric hydroxide is precipitated there is decomposition of hydrazine on the surface of the precipitate. While the decomposition of the hydrazine increases as the total surface area increases, there is a decrease in the rate of polymerization after the formation of the hydroxide sol (Fig. 1). This decrease in rate can be attributed to the adsorption and recombination of the primary radicals at the surface of the precipitate. The recombination of radicals on the surface of a finely divided solid is a common feature of free-radical chain reactions.[8] At concentrations below the saturation solubility of the cupric hydroxide there is no instantaneous decrease in the hydrazine concentration and the rates of both the decomposition of hydrazine and of the polymerization are directly proportional to the concentration of cupric ions. Cuprous ions produced in the cupric ion–hydrazine reaction are oxidized to cupric ions by the oxygen present in the system, the initiating reaction occurring in solution.

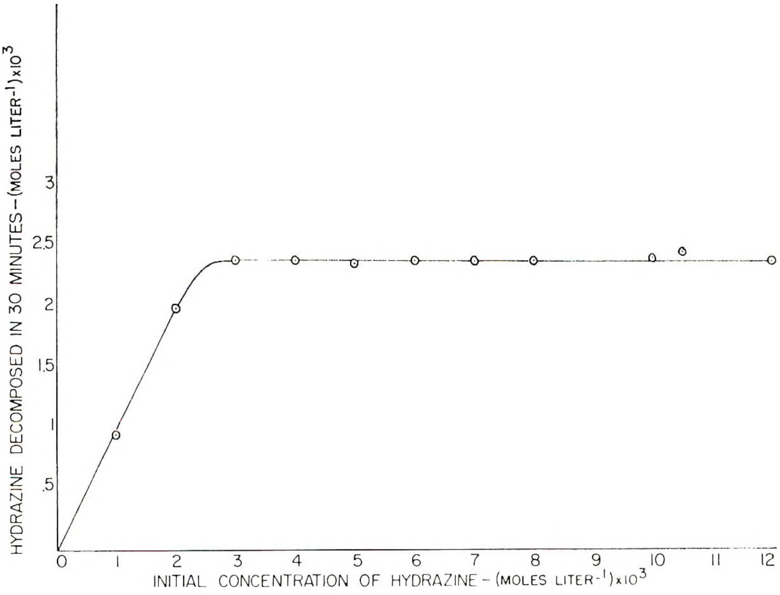

Fig. 4. The variation of the amount of hydrazine decomposed in 30 min with varying initial hydrazine concentrations. (5×10^{-5} mole/l cupric sulfate, 0.02 mole/l methyl methacrylate).

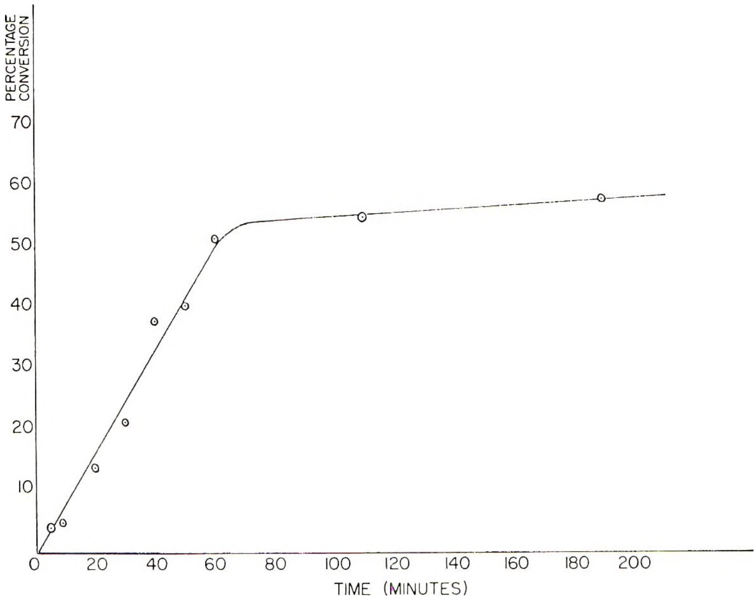

Fig. 5. The rate curve for the polymerization of methyl methacrylate. (0.08 moles/l hydrazine, 4 × 10^{-6} mole/l cupric sulfate, 0.02 mole/l methyl methacrylate).

The rates of decomposition of hydrazine and of the polymerization increase with increasing alkalinity to reach a maximum at pH 9.5. This effect will be due to the decreasing dissociation of the hydrazine hydrate with increasing pH, the hydrazine hydrate molecule being the active species,[9] and to its increasing adsorption on the surface of the precipitating cupric hydroxide. Above pH 9.5, the rate decreases because of changes in the conditions of hydration and association of the hydrazine.[10]

At constant cupric sulfate concentration (5 × 10^{-5} mole/l), the rate of the hydrazine decomposition is independent of the initial monomer concentration. The rate of polymerization shows an order of 0.4 with respect to monomer at concentrations from 0.02 to 0.1 mole/l and is not first-order as reported by Menon and Kapur.[4] This suggests that some monomer is also adsorbed onto the surface of the solid and that initiation of polymerization does not proceed entirely in solution. To demonstrate that methyl methacrylate can be adsorbed, a known amount of the monomer was shaken with cupric sulfate solution (10^{-2} mole/l, pH 9) and the precipitate was filtered from the solution and washed with water of pH 9. The filtrate was analyzed for monomer by the standard technique of bromination and there was some 30% reduction in the concentration of methyl methacrylate in solution.

At cupric sulfate concentrations below the saturation solubility, the rate of hydrazine decomposition is again independent of the initial monomer concentration but the rate of polymerization is proportional to the monomer concentration up to 0.04 mole/l after which deviations occur.

Figure 5 shows a typical graph of "percentage conversion of monomer" against "time," the same shape of curve being obtained at all cupric sulfate concentrations. A decrease in the rate of polymerization at high conversions (>55%) is again noted and this can be attributed to the adsorption of radicals on the precipitated polymer. This was shown experimentally by the addition of a suspension of poly(methyl methacrylate) to the original reaction mixture when an overall decrease in the rate of polymerization was observed.

In the absence of cupric sulfate, hydrazine is oxidized in alkaline solution to form hydrogen peroxide.[11] It would, therefore, be expected that the cupric ion–hydrogen peroxide system would initiate solution polymerization since it has been reported as an initiator for emulsion polymerization.[2] It was found that this system will not initiate polymerization in solution and so can be discounted in the cupric sulfate–hydrazine kinetic scheme.

Differences between the present work and that reported by Menon and Kapur[4] are due to the narrow concentration ranges of reactants which they used. Also, as they did not pass oxygen into the reaction mixture it would soon have become depleted in oxygen. This would result in progressive changes in the kinetics of the initiating system and, hence, in the kinetics of the polymerization.

The authors wish to thank Geigy (U.K.) Ltd., Manchester 22, England, for a grant to one of us (P. I. L.) which allowed this work to be carried out.

References

1. E. J. Cuy, *J. Amer. Chem. Soc.*, **46,** 1810 (1924).
2. E. J. Cuy, M. E. Rosenberg, and W. C. Bray, *J. Amer. Chem. Soc.*, **46,** 1796, (1924).
3. W. C. E. Higginson and P. Wright, *J. Chem. Soc.*, **1955,** 1551.
4. C. C. Menon and S. L. Kapur, *J. Polym. Sci.*, **54,** 45, (1961).
5. G. Parravano, *J. Amer. Chem. Soc.*, **72,** 3856 (1950).
6. H. Stephen and P. Stephen, Eds., *Solubilities of Inorganic and Organic Compounds*, Vol. 1, Part 1, Pergamon Press, 1963, p. 14.
7. W. F. Linke, *Solubilities of Inorganic and Metal–Organic Compounds*, Vol. 1, 4th ed., D. van Nostrand, Princeton, 1958, p. 959.
8. F. S. Dainton, *Chain Reactions—An Introduction*, Methuen, London, 1956, p. 69.
9. E. C. Gilbert, *J. Amer. Chem. Soc.*, **51,** 2744 (1929).
10. L. F. Audrieth and B. A. Ogg, *The Chemistry of Hydrazine*, 1951, p. 144.
11. M. Gordon, in *3rd. Symposium on Combustion, Flame and Explosion Phenomena*, University of Wisconsin, 1948, p. 483.
12. J. Bond and D. B. Hobson, *J. Polym. Sci. A*, **1,** 2185 (1963).

Received November 10, 1967

JOURNAL OF POLYMER SCIENCE: PART A-1 VOL. 7, 387–394 (1969)

Metal-Containing Initiator Systems. VI. Polymerization of Butadiene with Metal–Organic Halide Systems

TAKAYUKI OTSU and MASAMI YAMAGUCHI, *Department of Applied Chemistry, Faculty of Engineering, Osaka City University, Sugimotocho, Sumiyoshi-ku, Osaka, Japan*

Synopsis

The polymerization of butadiene with binary initiator systems consisting of some activated metals and organic halides was investigated at 60°C. From the results obtained, it was found that systems of reduced nickel and methyltrichlorosilane or dimethyldichlorosilane were most effective for the polymerization, and those of reduced nickel and carbon tetrachloride, benzyl chloride, benzyl bromide and benzoyl chloride, showed moderate activity. The polybutadienes obtained with these systems were observed to contain product of more than 80% *cis*-1,4 microstructure. From detailed studies on the reduced nickel-methyltrichlorosilane system, these polymerization mechanisms were explained by the hypothesis that the initiation occurred through the reaction of the dissociated transition state complex with the monomer or with a trace amount of water, and then the propagation proceeded via a coordinated cationic mechanism. These systems did not show a good activity for the *cis*-1,4 polymerization of isoprene.

INTRODUCTION

A great number of studies on the stereospecific polymerization of butadiene with catalyst systems containing zero-valent nickel have been published recently. Ueda and co-workers[1] have stated that the systems of reduced nickel and some Lewis acids can induce stereospecific polymerization of butadiene to give high polymers which consist of about 95% *cis*-1,4 content. Similar observations have been reported on the polymerization of butadiene with the systems nickel carbonyl–molybdenum pentachloride,[2] olefinic nickel(0) complexes–Lewis acids,[3] and allylic nickel(0) complexes–Lewis acids.[4]

Recently, we have found that systems of activated nickel and some organic halides can initiate the radical polymerization of some vinyl monomers.[5–8] From more extensive studies on these initiator systems,[9] it was observed that the systems of reduced nickel and methylchlorosilanes also induced both radical polymerization of methyl methacrylate and cationic polymerizations of styrene and isobutyl vinyl ether. For the selective initiation with these systems, a possible reaction mechanism has been proposed and discussed in the previous paper.[9]

The present paper deals with the results of polymerization of butadiene by use of systems of some metals and various organic halides, and the results obtained are compared with the brief results obtained from isoprene polymerization.

EXPERIMENTAL

Materials

The kinds of metals used and their activation treatments were the same as described in the previous papers.[8,9]

Organic halides were commercially available reagents which were distilled before use. Butadiene and isoprene were purified by usual methods and distilled before use. The other reagents were used after purification.

Polymerization Procedure

Polymerizations and copolymerizations were carried out in a sealed glass tube under shaking in a thermostat maintained at 60°C. After polymerization for a given time, a small amount of dilute methanol solution of phenyl-β-naphthylamine and then a large amount of benzene were added successively to the polymerized mixture. After the precipitated initiator residue was separated by centrifugation from the polymerized mixture, the resulting polymer was isolated by the addition of a large amount of methanol, washed with methanol, and then dried under vaccum.

Analysis of the Polymers

The intrinsic viscosity $[\eta]$ of the resulting polybutadienes was determined in toluene at 30°C.

The microstructure of the resulting polymers was determined from their infrared spectra, by using the absorbancy indexes reported by Morero et al.[10] for polybutadiene and those of Binder et al.[11] for polyisoprene.

The composition of the compolymers of butadiene with styrene was determined on thin films from the refractive index obtained with an Abbé refractometer.[12]

RESULTS AND DISCUSSION

Effect of Metals on Butadiene Polymerization

Table I shows the results of polymerization of butadiene with binary systems of various types of metals and benzyl bromide at 60°C. These metals used did not show any activity for initiation in the absence of benzyl bromide.

As can be seen from Table I, the systems containing metals other than reduced nickel did not show good activity as initiator. Although Raney metals were effective for the radical polymerizations of styrene[7] and methyl methacrylate[8] in the presence of carbon tetrachloride, they were inactive

TABLE I
Polymerization of Butadiene by the Systems of Metals and Benzyl Bromide at 60°C[a]

Metals	Yield, %	Microstructure, %		
		cis-1,4	*trans*-1,4	1,2
Raney Ni	3.2	25.2	54.2	20.6
Reduced Ni	35.0[b]	75.6	20.0	4.4
Commercial Ni	0.4	15.5	59.0	25.5
Raney Co	2.5	14.4	60.7	24.9
Commercial Co	0.1	22.3	50.1	27.6
Raney Fe	2.3	31.9	49.8	18.3
Commercial Fe	1.1	17.3	42.3	40.4
Raney Cu	4.7	27.6	53.1	19.3
Commercial Cu	Trace	—	—	—
Rd on charcoal	Trace	—	—	—
Rh on charcoal	Trace	—	—	—
Commercial Ti	0.2	16.7	56.5	26.8
Commercial Mn	0.2	10.8	64.6	24.6
Commercial Cr	0.2	14.6	60.3	13.6
Commercial Sn	1.4	37.4	39.3	23.3
None	0.1	7.1	66.9	26.0
AIBN	18.3[c]	11.6	63.3	25.1

[a] Time 1 hr (unless otherwise noted); [Metal] = 0.43 g-atom/l; [Halide] = 0.1 mol/l; [M] = 5.8 mol/l; in benzene.

[b] Polymerized for 30 hr.

[c] Polymerized with azobisisobutyronitrile (0.03 mol/l).

for butadiene polymerization. The other hydrogenation metal catalysts and commercial metal powders were also ineffective. These results might be understandable from the consideration that the initiating activities of these systems were markedly dependent on the surface nature of the metals (purity and area), as stated in the previous paper.[8]

It was noted that the microstructure of the resulting polybutadienes changed somewhat from that of ordinary radical polymer with the nature of the metals used. Especially, the system of reduced nickel and benzyl bromide was found to produce a polybutadiene which is high in *cis*-1,4 content.

Effect of Halides on Butadiene Polymerization

The results of polymerization of butadiene with systems of reduced nickel and various types of organic halides are shown in Table II.

The systems of reduced nickel and various halides, except for chloroform and di-*n*-butylchloroamine, initiated the polymerization of butadiene to give solid polymers which are high in *cis*-1,4 content. However, viscous liquid polymers which consisted of almost the same microstructure were obtained by using both azobisisobutyronitrile and the systems of Raney nickel and carbon tetrachloride or di-*n*-butylchloroamine at 60°C. The results indicate that these systems induce the ordinary radical polymerization of butadiene.

TABLE II
Polymerization of Butadiene by the Systems of Reduced Nickel and Organic Halides at 60°C[a]

				Microstructure, %		
Halide	Time, hr	Yield, %	[η], dl/g	*cis*-1,4	*trans*-1,4	1,2
CCl_4	24	24.7	0.28	79.0	16.3	4.7
$CHCl_3$	48	1.5	—	28.7	52.4	18.9
$C_6H_5CH_2Cl$	24	27.1	0.28	76.1	19.1	4.8
$C_6H_5CH_2Br$	30	35.0	0.25	75.6	20.0	4.4
C_6H_5COCl	24	28.0	0.48	82.6	12.8	4.6
$C_6H_5SO_2Cl$	48	4.2	0.32	34.5	45.0	20.5
tert-C_4H_9OCl	48	14.3	0.40	64.9	25.5	9.6
(*n*-$C_4H_9)_2NCl$	48	7.4	—	14.0	61.0	25.0
CH_3SiCl_3	5	20.2	0.67	90.4	7.6	2.0
$(CH_3)_2SiCl_2$	5	27.4	0.61	82.7	13.8	3.5
None	48	1.5	—	60.3	26.1	13.6

[a] [Ni] = 0.43 g-atom/l; [Halide] = 0.1 mol/l; [M] = 5.8 mol/l; in benzene.

In the previous paper,[8] it was pointed out that the initiating activity of the organic halides to the activated nickel in radical polymerization of methyl methacrylate was dependent on the bond-dissociation energy and the polarization of the carbon–halogen bonds involved,[9] and on the reactivity of the resulting radical toward the monomer. However, the results of Table II may suggest that the *cis*-1,4 polymerization proceeds by a nonradical mechanism.

It is interesting to note (Table II) that the systems of reduced nickel and methyltrichlorosilane or dimethyldichlorosilane show the highest activity for *cis*-1,4-polymerization of butadiene, and the intrinsic viscosity of the resulting polymers is relatively high.

Figure 1 shows the infrared spectra of the polybutadienes obtained with azobisisobutyronitrile and reduced nickel–methyltrichlorosilane at 60°C.

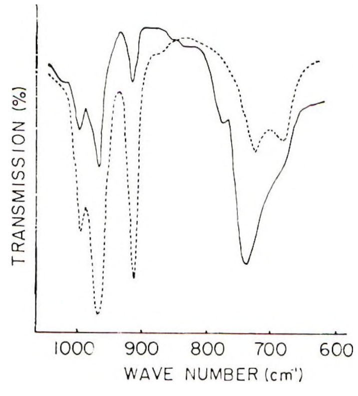

Fig. 1. Infrared spectra of the polybutadienes obtained by (- - -) azobisisobutyronitrile and (——) the reduced nickel–methyl trichlorosilane system at 60°C.

Polymerization with Reduced Nickel–Methyltrichlorosilane System

The effect of the concentration of methyltrichlorosilane on the polymerization of butadiene with the system consisting of reduced nickel at 60°C. was investigated. The results are shown in Table III.

TABLE III
Effect of the Concentration of Methyltrichlorosilane on Butadiene Polymerization in the Presence of Reduced Nickel at 60°C[a]

$[CH_3SiCl_3]$, mol/l	Time, hr	Yield, %	R_p, %/hr	$[\eta]$, dl/g
0	48	1.5	0.03	—
0.005	20	6.2	0.31	—
0.01	20	17.1	0.86	0.71
0.05	5	24.2	4.84	0.63
0.1	5	20.2	4.01	0.67

[a] [Ni] = 0.43 g-atom/l; [M] = 5.8 mol/l; in benzene.

It was observed that the rate of polymerization increased approximately with the 1.2 power of the concentration of methyltrichlorosilane at concentrations lower than 10^{-2} mole/l., but the intrinsic viscosity of the resulting polymers remained almost constant. These observations might also suggest that this polymerization proceeded via a nonradical mechanism.

Copolymerization with Styrene with Systems of Reduced Nickel and Halides

In order to elucidate further the polymerization mechanism with the systems of reduced nickel and benzyl chloride or methyltrichlorosilane, the copolymerization of butadiene (M_2) with styrene (M_1) was carried out at 60°C. The results are shown in Table IV. The copolymer compositions obtained from refractive index were in agreement with those from infrared spectrum data of the copolymers.

From Table IV, the copolymer composition curves were obtained as is seen in Figure 2. The monomer reactivity ratios with both initiator systems were calculated as follows: $r_1 = 0.66$, $r_2 = 2.25$. These values were somewhat different from those reported[13] with benzoyl peroxide initiator ($r_1 = 0.78$, $r_2 = 1.39$) but quite different from those obtained[14] with butyllithium ($r_1 = 0.05$, $r_2 = 20$).

Since the polymerization with these systems was greatly dependent on the nature of the monomers used,[9] the results of copolymerization with styrene might not always coincide with those of the homopolymerization of butadiene. Indeed, the copolymers obtained were only a viscous liquid, contrary to the observation that the butadiene polymers were solid and of high *cis*-1,4 content (Table II). Accordingly it may be concluded that the homopolymerization of butadiene proceeds via a different mechanism from the copolymerization with styrene with these systems.

TABLE IV
Copolymerization of Butadiene (M_2) and Styrene (M_1) with the Systems of Reduced Nickel and Benzyl Chloride or Methyltrichlorosilane at 60°C[a]

Halide	$[M_1]$ in feed monomer, mol-%	Time, hr	Yield, %	Refractive index at 25°C	$[M_1]$ in copolymer, mol-%
$C_6H_5CH_2Cl$	19.48	10	4.4	1.5327	12.33
	39.97	10	6.3	1.5487	25.12
	49.96	10	4.2	1.5604	35.29
	59.48	2	1.4	1.5707	44.71
	80.36	2	1.6	1.5940	67.91
CH_3SiCl_3	19.97	3	5.8	1.5320	10.45
	38.68	3	10.8	1.5470	23.70
	50.81	3	14.1	1.5630	37.64
	62.57	1	10.0	1.5732	47.16
	77.41	0.4	3.5	1.5922	66.07

[a] [Ni] = 0.43 g-atom/l; [Halide] = 0.1 mol/l; ($[M_1]$ + $[M_2]$) = 7.0 mol/l; in benzene.

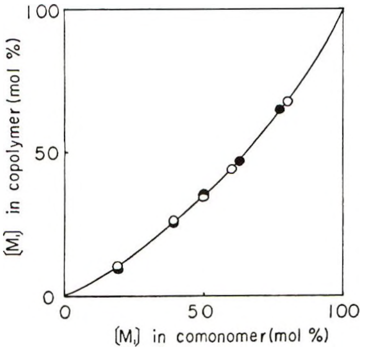

Fig. 2. Copolymer composition curves for the copolymerization of styrene (M_1) and butadiene (M_2) by the systems of reduced nickel and benzyl chloride (-○-) or methyltrichlorosilane (-●-) at 60°C.

Mechanism of Butadiene Polymerization

From the results of Table II, it was found that the systems of reduced nickel and methyltrichlorosilanes, benzyl halides, benzoyl chloride, and carbon tetrachloride were effective initiator for *cis*-1,4-polymerization of butadiene. The considerations above mentioned might suggest that the *cis*-1,4-polymerization with these systems proceeded via a coordinated cationic mechanism. Such a mechanism was first proposed by Otsuka et al.[2] for the *cis*-1,4-polymerization of butadiene with nickel carbonyl–molybdenum pentachloride system.

In the previous paper,[9] it was stated that reduced nickel and methylchlorosilanes could induce the cationic polymerizations of styrene and isobutyl vinyl ether, and proposed a possible initiation mechanism as follows:

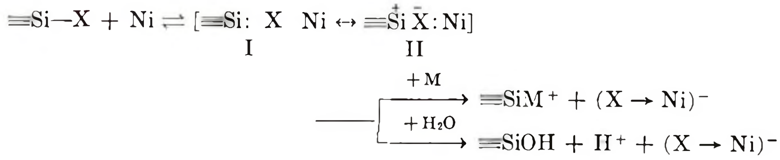

$$\equiv\!Si{-}X + Ni \rightleftharpoons [\underset{I}{\equiv\!Si\!:\;X\;\;Ni} \leftrightarrow \underset{II}{\equiv\!\overset{+}{Si}\,\overset{-}{X}\!:\!Ni}]$$

$$\longrightarrow \begin{cases} \xrightarrow{+M} \equiv\!SiM^{+} + (X \rightarrow Ni)^{-} \\ \xrightarrow{+H_2O} \equiv\!SiOH + H^{+} + (X \rightarrow Ni)^{-} \end{cases}$$

Here the structures I and II show the transition state complex structure in the dissociation, and the electron-donating monomers such as styrene and vinyl ether, or the trace water as a nucleophile react with this complex to give an initiating cation. In this case, no oxidation of the zero valent nickel atom occurred.

The fact that the high molecular weight poly(isobutyl vinyl ether) is produced from these systems may be explained as follows:[9] the resulting chloride counterion is adsorbed on the surface of the solid nickel atom, and hence the reacting butadiene monomer in the propagation step may react with insertion between the growing cation and the zero valent nickel existed as a counterion.

In the cases of some organic halides which have the carbon–halogen bond, a similar polymerization mechanism may be considered, and the *S*ɴ 1 mechanism involving the dissociation of the carbon–halogen bond in halides for initiation may also be possible.

Polymerization of Isoprene with These Systems

The results of the polymerization of isoprene with these systems are shown in Table V.

TABLE V

Polymerization of Isoprene with Activated Metals and Halides at 60°C[a]

Initiator system			Microstructure, %			
Metal	Halide	Yield, %	*cis*-1,4	*trans*-1,4	1,2	3,4
Reduced Ni	CCl_4	7.8	6.0	80.1	7.4	6.5
"	$C_6H_5CH_2Cl$	2.9	4.1	86.7	3.0	6.2
"	$C_6H_5SO_2Cl$	9.4	5.8	78.0	6.0	8.2
"	*tert*-C_4H_9OCl	9.2	2.0	82.1	7.3	8.6
"	$(n\text{-}C_4H_9)_2NCl$	5.5	4.7	81.3	8.0	6.0
"	CH_3SiCl_3	6.7	6.6	78.9	5.4	9.1
"	$(CH_3)_2SiCl_2$	9.4	6.5	78.4	9.0	6.1
Raney Ni	CCl_4	3.5	3.1	82.7	7.2	7.0
Raney Co	"	4.6	7.4	77.5	8.0	7.1
Raney Cu	"	8.6	4.0	81.7	8.0	6.3
Raney Fe	"	7.8	3.2	82.0	8.1	9.7
Reduced Ni	—	0.5	—	—	—	—
—	CH_3SiCl_3	1.6	—	—	—	—
AIBN		15.7	9.3	73.3	7.9	9.5

[a] Time, 72 hr; [Metal] = 0.43 g-atom/l, [Halide] = 0.1 mol/l, [M] = 5.0 mol/l in benzene.

It was observed that isoprene was hardly polymerized with the initiator systems and the resulting polymers were viscous liquids and consisted of mainly *trans*-1,4 microstructure. These results may coincide with the reported observation which the catalytic systems consisting a zero-valent nickel did not induce *cis*-1,4-polymerization of isoprene.

References

1. K. Ueda, A. Onishi, T. Yoshimoto, J. Hosono, K. Maeda, and T. Matsumoto, *Kogyo Kagaku Zasshi*, **66**, 1103 (1963).
2. S. Otsuka and M. Kawakami, *Kogyo Kagakv Zasshi*, **68**, 874 (1965).
3. F. Dawans and P. Teyssie, *J. Polym. Sci. B*, **3**, 1045 (1965).
4. L. Porri, G. Natta, and M. C. Gallazzi, paper presented at the International Symposium on Macromolecular Chemistry, Prague, 1965; in *International Symposium on Macromolecular Chemistry* (*J. Polym. Sci. C*, **16**), O. Wichterle and B. Sedláček, Eds., Interscience, New York, 1967, p. 2525.
5. T. Otsu, M. Yamaguchi, Y. Takemura, Y. Kusuki, and S. Aoki, *J. Polym. Sci. B*, **5**, 697 (1967).
6. T. Otsu, S. Aoki, M. Nishimura, M. Yamaguchi, and Y. Kusuki, *J. Polym. Sci. B*, **5**, 835 (1967).
7. T. Otsu and M. Yamaguchi, *Bull. Chem. Soc. Japan*, in press.
8. T. Otsu and M. Yamaguchi, *J. Polym. Sci. A-1*, **6**, 3075 (1968).
9. T. Otsu, S. Aoki, M. Nishimura, M. Yamaguchi, and Y. Kusuki, *J. Polym. Sci.* in press.
10. D. Morero, A. Santambrogio, L. Porri, and F. Ciampelli, *Chim. Ind.* (Milan), **41**, 758 (1959).
11. J. L. Binder and H. C. Ransaw, *Anal. Chem.*, **29**, 503 (1957).
12. G. S. Whitby, *Synthetic Rubber*, Wiley, New York, 1954, p. 328; ASTM D1416-58a T (1958).
13. F. M. Lewis, C. Walling, W. Cummings, E. R. Briggs, and W. J. Wenisch, *J. Amer. Chem. Soc.*, **70**, 1527 (1948).
14. A. A. Korotkov and N. N. Chesnokova, *Vysokomol. Soedin.*, **2**, 365 (1960).

Received January 4, 1968
Revised March 19, 1968

JOURNAL OF POLYMER SCIENCE: PART A-1 VOL. 7, 395–407 (1969)

Polycondensation Rate of Poly(ethylene Terephthalate). II. Antimony Trioxide–Catalyzed Polycondensation in Static Thin Films on Metal Surfaces*

ROBERT W. STEVENSON, *Mobil Chemical Company, Research and Development Laboratories, Edison, New Jersey 08817*

Synopsis

In the catalyzed polycondensation reaction of poly(ethylene terephthalate), defined by

$$2 \sim\!\sim\mathrm{COOCH_2CH_2OH} \xrightarrow{k_p} \sim\!\sim\mathrm{COOCH_2CH_2OOC}\sim\!\sim + \mathrm{HOCH_2CH_2OH}$$

rates of polymerization in thin films under vacuum are orders of magnitude greater than those observed in an equilibrating system. Such behavior is consistent with a mechanism in which a volatile component of the reaction mixture reacts reversibly with the catalyst to render it unreactive in polycondensation; removal of this component is facilitated as polymerizing melt thickness is decreased. In accord with such a mechanism polycondensation rates for polymerizations carried out on metal surfaces at thicknesses of 1 to 5 mils of polymerizing melt are observed to increase with decreasing thickness, provided a catalyst is present. In the absence of a catalyst there is no tendency of rate to increase with decreasing thickness. A number of metal surfaces were found to dissolve in the polymerizing melt. On rhodium and silver, which were found to be inert to such dissolution, uncatalyzed polycondensation rate constants k_p of 0.03 and 0.04 liter mol^{-1} min^{-1} were found. These values of k_p are low and identical within experimental error. This behavior is in accord with the assumption that no catalysis occurs at the interface of the polymerizing melt and the metal surface. A typical value for the catalyzed rate constant k_p (uncorrected for catalyst concentration) was 0.6 liter mol^{-1} min^{-1} in a 1-mil thickness of polymerizing melt at 275°C and in the presence of 0.025 wt-% antimony trioxide. The activation energy for the antimony trioxide–catalyzed polycondensation was found to be 14 kcal; for the uncatalyzed polycondensation it was 45 kcal.

INTRODUCTION

Differences of orders of magnitude can be observed in the polycondensation (polymerization) rate in the synthesis of poly(ethylene terephthalate) by different techniques. Differences are so large that differences in reaction order or differences in type or concentration of catalyst are inadequate to

---

* Presented in part at the 155th Meeting of the American Chemical Society, San Francisco, April, 1968.

explain them. In a previous paper the rate constant k_p for the reaction

$$2 \sim\mathrm{COOCH_2CH_2OH} \underset{k'}{\overset{k_p}{\rightleftharpoons}} \sim\mathrm{COOCH_2CH_2OOC}\sim + \mathrm{HOCH_2CH_2OH}$$

was estimated to be 0.02 liter mol^{-1} min^{-1} at 280°C in the presence of 0.025% by weight $\mathrm{Sb_2O_3}$.[1] Catalyst concentration was included in k_p. The technique employed took complete account of the reverse reaction. Nevertheless, the observed rate was considerably less than rates derivable from data on polycondensation reactions in which the reverse reaction was only partially suppressed and for which the residual reverse reaction was ignored in the rate calculation.

An even wider divergence is apparent when data from the patent literature are taken into account.[2] Values of k_p as high as 9.1 liter mol^{-1} min^{-1} at 275°C may be calculated from the polymerization of poly(ethylene terephthalate) in the form of a 0.1-mil film on a stainless-steel surface. It is the purpose of this paper to attempt to resolve this discrepancy and to provide data supporting the hypothesis set forth in the preceding paper.[1]

Disregard for the slow-catalysis rates exhibited in the polycondensation reaction in the presence of the reverse reaction permits one to suggest that the observation of extremely high rates in polymerizing thin films is due to complete suppression of the reverse reaction. Implicit in this suggestion is the assumption that the reverse reaction is much faster than the forward polycondensation reaction. This, however, cannot be true, since the ratio of forward to reverse rates is $K = k_p/k' = 0.36$; that is, the reverse reaction is no more than three times as fast as the forward reaction.[1]

Another proposed explanation of high rates in thin films, according to Turner,[2] is catalysis of the polycondensation reaction by the metallic surface. Thus, Turner teaches that a stainless-steel surface exhibits a marked catalytic effect on the polycondensation reaction. He does not, however, indicate the nature of catalysis by the metal surface. Such catalysis could result from dissolution of some of the surface into the polymerizing melt; concurrently or alternately, catalysis could occur at the melt–metal interface. Catalysis by dissolved metals is certainly a possibility; many metal salts are known to catalyze polycondensation reactions.[3] However, since the solubility of metal salts in poly(ethylene terephthalate) is extremely limited,[4] the increase in observed rate would also necessarily be limited. Catalysis by surface *as such* at the melt–metal interface could account for the observation that polycondensation rates in thinner films on the same surface are higher than in thicker films. Experimental evidence is necessary before catalysis at the melt–metal interface can either be admitted or excluded under conditions employed in this work.

If catalysis at the interface of the polymerizing melt with the metal surface can be excluded, an alternate explanation of the apparent discrepancy between rates measured in the presence of the reverse reaction and rates observed in polymerizing thin films under vacuum is required. Such an explanation has been suggested in a previous paper.[1] The hypothesis suggested states that the vast difference observed between k_p measured in equilibrium systems and k_p measured in polymerizing thin films under vacuum cannot be accounted for on the basis of suppression of reverse reaction. Therefore, the rate differences observed are attributed to reversible interaction of a difficultly volatile species with the catalyst present in such a way as to inactivate it. The mechanism is a reasonable one, since the catalyst is present in low concentration, and therefore large amounts of the "poisoning" species are not necessary. Under such circumstances the volatility of the inactivating compound need not be too limited. The lowest "oligomer" of poly(ethylene terephthalate), namely bishydroxyethyl terephthalate, was nominated as the probable "poisoning" species in the previous paper.[1]

Experimental work reported in this paper explores the polycondensation reaction at constant film thickness and on various metal surfaces, in order to clarify the situation with respect to the suggested catalysis by surface. The effect on rate of various thicknesses of polymerizing melt on several surfaces under various conditions is also investigated. The polycondensation is examined in the presence of catalyst, in the presence of typical levels of metallic impurities, and in the substantial absence of catalyst and metallic impurities. The effect of polycondensation temperature on rate is examined both in the presence and in the absence of catalyst. Such determinations permit conclusions to be drawn relative to the hypothesis set forth in the preceding paragraph.

EXPERIMENTAL

Shallow circular polymerization dishes were constructed of metal foil bent to shape or machined from 304 stainless-steel stock. The dishes were of known cross section, so that polymerizing melt thickness could be estimated from prepolymer weight and the assumed specific volume, 0.86 ml/g. A typical polymerization dish is shown in Figure 1.

The polymerizations were carried out with the dishes supported on an aluminum foil plug in the bottom of a polymerization flask assembly, as shown in Figure 2. The assembly was evacuated before immersion in the oil bath used for heating. The most satisfactory temperature-control technique (of several attempted) employed internal contact of a thermocouple wire with a small amount of material identical with that used for the polymerization dish. The material contacted by the thermocouple was immediately adjacent to the polymerization dish. The temperature indication obtained was shown by calibration to be identical with that on the surface of the polymerization dish.

The usual polymerization temperature was 275°C; temperature effects were measured in the range 265 to 285°C. Pressures were ordinarily 0.025 mm, attained by means of a Hyvac 7 two-stage pump. Polymerization times were measured from the time the desired internal temperature was reached; the final time was the time the oil bath was removed.

Fig. 1. Polymerization dish in place in polymerization apparatus.

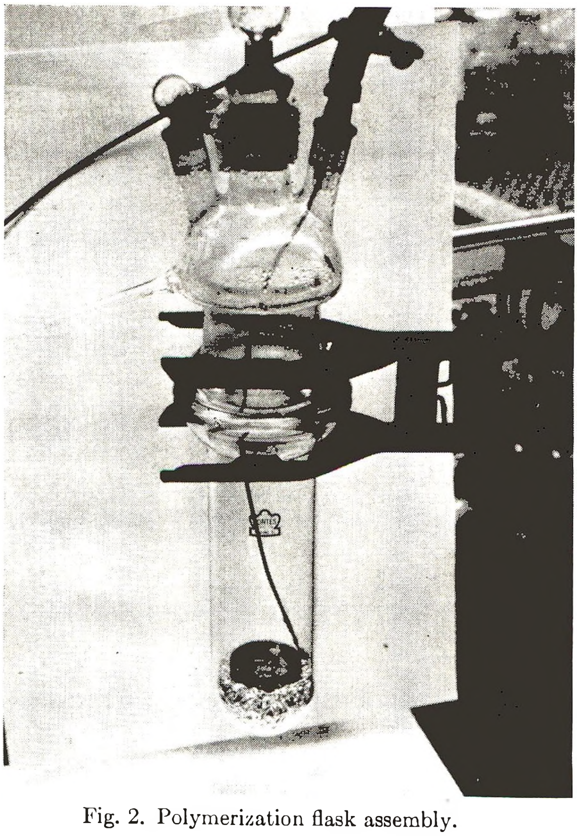

Fig. 2. Polymerization flask assembly.

Solution viscosities were used to estimate molecular weight, from which hydroxyl endgroup (B') concentration was estimated in turn. Polymer samples generated in this work were usually sufficient for measurement of solution viscosity at only one concentration in 50:50 tetrachloroethane–phenol. The reduced specific viscosity (RSV) so determined was converted to intrinsic viscosity graphically, according to the equation

$$[\eta] = (1/c)\,(\eta_{\mathrm{sp}} - \ln \eta_{\mathrm{rel}})^{1/2}/K^{1/2}$$

The value of K had been determined by experiment to be 0.507; $\eta_{\mathrm{sp}} = \mathrm{RSV}(c)$ and $\eta_{\mathrm{rel}} = \eta_{\mathrm{sp}} + 1$.

The intrinsic viscosity $[\eta]$ so obtained was graphically converted to M_n by the equation of Conix;[5] that is,

$$[\eta] = (2.1 \times 10^{-4}) M_n^{0.82}$$

The reciprocal endgroup concentration is then given by

$$1/B' = (4.3 \times 10^{-4}) M_n$$

on the assumption of a specific volume of 0.86 l/kg. A plot of $1/B'$ versus polycondensation time should yield a straight line of slope $2k_p$ if, as is assumed, the polycondensation reaction is second order in endgroups.

Three prepolymers, varying in content of impurities, catalyst, and initial glycol and bishydroxyethyl terephthalate content, were used. The compositions of these prepolymers are given in Table I.

TABLE I
Characteristics of Prepolymers Employed for Study of Polycondensation in Static Thin Films on Metal Surfaces

Pre-polymer	Content, ppm			Content, wt-%		Added
no.	Fe	Cr	Ni	Glycol	bis-HET	catalyst
1	6.7	1.1	3.2	0.38	1.36	none
2	6.7	1.1	3.2	1.03	3.66	0.025 wt-% Sb_2O_3
3	1.2	—	—	0.78	4.67	none

RESULTS AND DISCUSSION

Investigation of Catalytic Effects of Various Metal Surfaces

The assumption that there is no catalysis of the polycondensation reaction at the melt–metal interface would be supported by the discovery of two or more surfaces on which polycondensation rates are low and essentially the same. Such metal surfaces should be inert to dissolution in the polymerizing melt; otherwise, contribution to catalysis due to dissolved metal could occur. Polymerizations were carried out on eighteen different surfaces. Some surfaces were extremely resistant to wetting by molten prepolymer, even after roughening. Because of purity considerations no attempt was made to employ wetting agents. It was noted, however, that

TABLE II
Investigation of Catalytic Effects of Various Metal Surfaces at 275°C

	Wettab.[a]	Metal,[b] ppm	Asymptotic loss,[c] wt-%		$2k_p$,[c] liter mol^{-1} min^{-1}	
			Prep. 1	Prep. 3	Prep. 1	Prep. 3
Aluminum	G	≈30 Al	—	18	0.18	0.164
Brass	G	80 Cu, 380 Zn	13	—	0.364	—
Cobalt	G	950 Co	16	—	0.239	—
Copper	G	520 Cu	20	—	0.079	—
Gold	P	none	—	18.5	—	0.036
Iron	G	580 Fe	17.7	15	0.375	0.396
Lead	G	>1500 Pb	12.7	—	0.209	—
Molybdenum	F	none	17.7	17.4	0.138	0.114
Nickel	very P	5 Ni	20	—	0.088	—
Platinum	P	none	—	—	—	—
Rhodium	G	none	25.2	18.5	0.114	0.058
Silver	F	none	18	19	0.252	0.075
304 S.S.	G	13 Fe, 2 Ni	16	—	0.41	—
Pass. 304 S.S.	G	130 Fe, 18 Ni	—	18.2	—	0.106
Pass. 316 S.S.	G	210 Fe, 24 Ni	—	17.8	—	0.117
Tantalum	G	10–100 Ta	20	19	0.123	0.078
Titanium	G	50 Ti	16.4	—	0.194	—
Zinc	G	high Zn	20	—	0.286	—
Zirconium	G	160 Zr	25.4	—	0.667	—

[a] Good, fair, and poor.

[b] Dissolved from surface at 0.029 cm thickness of polymerizing melt.

[c] Prepolymers 1 and 3, thickness 0.007 cm.

dissolved catalyst or iron impurity markedly improved the wetting of metal surfaces by molten prepolymer.

The data shown in Table II were taken with two poly(ethylene terephthalate) prepolymers. The principal difference between these two prepolymers, as shown in Table I, was in their content of impurities. The first column of Table II indicates the observed wettability for each metal surface examined. Metals being poorly wettable by prepolymer were not suitable for further study, because the thickness of polymerizing melt could not be readily calculated; nevertheless, rate "constants" were calculated for these surfaces, although actual polymerizing melt thicknesses must have been much greater than indicated. The second column of Table II gives the tendency of various surfaces to dissolve in the polymerizing melt. All but gold, molybdenum, platinum, rhodium, and silver are detected by x-ray fluorescence spectroscopy in poly(ethylene terephthalate) prepared on the various surfaces. Of these materials gold and platinum must be excluded from consideration, because they are not well wetted, and hence, if polymerization rate is a function of thickness, one could not expect to observe comparable polymerization rates thereon. Passivated 304 stainless steel apparently contributes more iron to the polymerizing melt than does untreated 304 stainless steel. This is felt to be an artifact; however, it is probable that in the case of the passivated steel, part of the inert oxide surface was stripped away with the polymer film when it was removed for analysis. Moreover, polymerization rates on passivated stainless steel are low, although dissolved iron is known to be an efficient polycondensation catalyst. On this basis passivated 304 stainless steel is considered to be inert to dissolution. Similarly, tantalum is known to be brittle, and the observed tantalum content can be rationalized on the basis of adherence of some of the tantalum to the polymer film when it is stripped.

Because of excessive tendency to dissolve in polymerizing melt, brass, cobalt, copper, lead, zinc, and zirconium were excluded from further consideration. Titanium was excluded because it apparently gave rise to molecular weight degradation for longer polymerization times. Some further study was carried out on aluminum, since the tendency to dissolve was not excessive and, although Al_2O_3 is a known polymerization catalyst,[6] it is not an extremely efficient one.

Surfaces deemed inert to dissolution and also readily wetted by prepolymer thus include molybdenum, rhodium, silver, passivated stainless steel, and tantalum. Such surfaces, therefore, should be capable of yielding polycondensation rates essentially free of catalytic influences due to dissolved material. With starting prepolymer essentially free of catalyst nearly identical rates were obtained on rhodium and silver. Observed values of $2k_p$ were 0.058 and 0.075, respectively (Table II, last column). Similarly, low values of $2k_p$ were also observed on tantalum (0.078), molybdenum (0.114), and passivated 304 stainless steel (0.106).

The data are in accord with the assumption of no polycondensation catalyzing by the metal surface at the interface between the polymerizing melt and the metal surface. The slight differences in rate that have been observed with change of surface could be due to contribution to polycondensation catalysis by traces of material dissolved from the surface. Data for polymerization on rhodium and silver require no equivocation: polymerization rates are low and identical within experimental error, and no evidence of dissolution of either of these two surfaces could be obtained.

Effect of Thickness of Polymerizing Melt: Catalyst Present

The effect of various thicknesses of polymerizing melt was investigated on surfaces of aluminum, untreated 304 stainless steel, and silver. The derived values of $2k_p$ for the different thicknesses at 275°C are listed in Table III. Plots of $1/k_p$ versus thickness are given in Figure 3.

Plots of $1/k_p$ versus thickness of polymerizing melt on an aluminum surface scatter about two straight lines. The lower line is for prepolymer 2 (Sb_2O_3 catalyst plus metal impurities) and the upper line for prepolymer 1 (metal impurities only). Scatter is attributed to variable dissolution of Al_2O_3 from the surface and subsequent contribution to polycondensation catalysis.

Plots of $1/k_p$ versus thickness of polymerizing melt for polymerizations carried out on a silver surface fall on straight lines with little scatter. The extrapolation of these lines to $1/k_p = 0$ gives a finite value of polymerizing film thickness for $k_p = \infty$, an obviously impossible situation. The discrepancy can be explained, at least in part, by deviation of the actual from the nominal film thickness. Loss of weight due to removal of glycol and other volatiles will alter the thickness; the marginal wettability of silver surface with prepolymer could cause a further departure from ideality in estimation of polymerizing film thickness. Alternatively, the possibility that the slope of $1/k_p$ versus thickness decreases with approach to the origin cannot be excluded.

Roughened 304 stainless-steel surfaces were wettable by prepolymer to

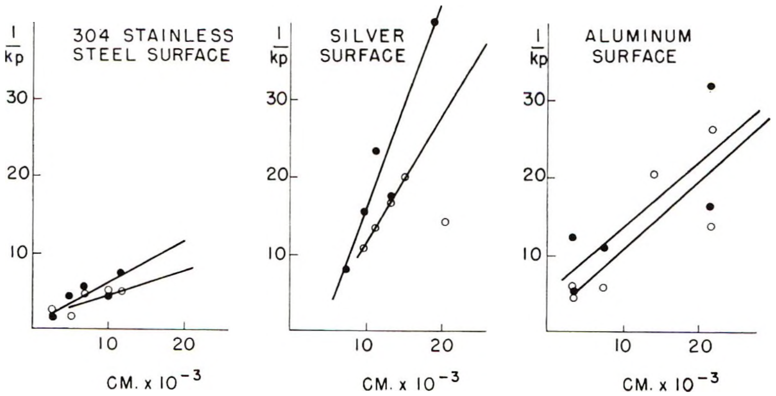

Fig. 3. Polycondensation rate in the presence of catalyst, as a function of thickness of polymerizing melt on metal surfaces: (●) prepolymer 1; (○) prepolymer 2.

TABLE III
Second Order Rates As A Function Of Polymerizing Melt Thickness On Aluminum, Silver and 304 Stainless Steel At 275°C

Melt thickness, cm ($\times 10^{-3}$)	$2k_p$, liter mol^{-1} min^{-1}	Prepolymer (Table I)	Remarks
Silver:			
7.4	0.252	1	Marginal wetting at lowest thickness
9.3	0.128	1	
11.1	0.086	1	
12.9	0.113	1	
14.8	0.069	1	
18.5	0.049	1	
9.3	0.187	2	
11.1	0.148	2	
12.9	0.119	2	
14.8	0.098	2	
18.5	0.119	2	
304 S.S.:			
2.3	1.56	1	More scatter of data for lower thicknesses
4.7	0.47	1	
7.0	0.38	1	
9.3	0.49	1	
11.7	0.26	1	
2.3	0.86	2	Much less scatter than in absence of Sb_2O_3
4.7	1.22	2	
7.0	0.44	2	
9.3	0.46	2	
11.7	0.41	2	
Aluminum:			
3.7	0.16	1	Lack of reproducibility attributable to variability in dissolved Al_2O_3
3.7	0.42	1	
7.4	0.18	1	
21.6	0.12	1	
21.6	0.065	1	
3.7	0.33	2	
3.7	0.44	2	
7.4	0.33	2	
14.8	0.098	2	
21.6	0.075	2	
21.6	0.148	2	
Passiv. 304 S.S.:			
2.3	0.130	3	
4.7	0.106	3	
7.0	0.109	3	
9.3	0.186	3	
11.7	0.196	3	

smaller thicknesses of polymerizing melt. The slope of $1/k_p$ versus thickness for the range of thicknesses examined is smaller than that observed on silver for a higher thickness range. This could be indicative of a diminution in slope with approach to the origin. The data scatter is more severe than on silver. The scatter is probably due in part to amplification of sources of error with reduction in the amount of material polymerized as polymerizing film thickness is decreased.

On all three surfaces (aluminum, silver, and 304 stainless steel), despite variable scatter and different thickness ranges examined, a tendency of k_p to increase with decreasing thickness of polymerizing melt was observed. Values of k_p were higher in the presence of antimony trioxide than in its absence. It is assumed that in the absence of antimony trioxide (prepolymer 1) the metallic impurities present function as catalyst. Thus, the essential difference between runs carried out with prepolymer 1 and prepolymer 2 is a difference in catalyst concentration.

The results are thus in agreement with the hypothesis that a volatile component of the reaction mixture inactivates a portion of the catalyst, whether antimony trioxide or traces of iron, chromium, and nickel, the impurities present in prepolymer 1.

Effect of Thickness of Polymerizing Melt: Catalyst Absent

The hypothesis that the increase in polymerization rate observed with decrease in polymerizing melt thickness is due to improved removal of a volatile component of the reaction mixture, which inactivates the catalyst, requires the following: in the complete absence of catalyst or catalyzing impurities low rates should be observed, and no increase in rate should be observed on decreasing the thickness of polymerizing melt.

Such results are indeed obtained for a very pure prepolymer (prepolymer 3) for runs carried out on passivated stainless steel. A plot of $1/k_p$ versus polymerizing melt thickness (Fig. 4) scatters about a horizontal line. Five different thicknesses of polymerizing melt give rates that vary at random

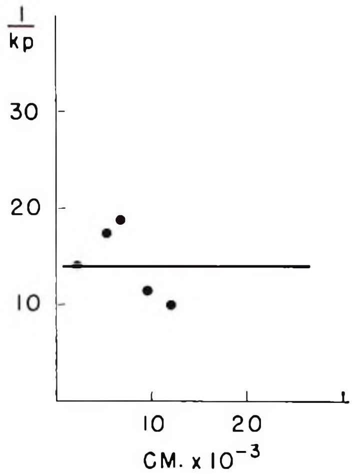

Fig. 4. Polycondensation rate in the absence of catalyst or catalyzing impurities, as a function of thickness of polymerizing melt on passivated 304 stainless steel.

from 0.11 to 0.2 liter mol^{-1} min^{-1}, with no tendency to increase with decreasing melt thickness.

The data are interpreted to mean that within experimental error polymerization rate does not vary with polymerizing melt thickness in the essential absence of catalyst. The rates observed are low compared with others given in this paper (see the preceding section).

Effect of Temperature on Polymerization Rate for Polymerizing Melt 3 mils Thick

Under conditions in which the reverse reaction to polycondensation (glycolysis) is essentially absent, an activation energy for the polymerization of poly(ethylene terephthalate) may be estimated. Results of the preceding sections are in accord with the assumption that glycol removal is essentially complete under the experimental conditions employed in this work. If it were not, the observation of no rate increase in a catalyst-free system on decreasing polymerizing melt thickness could not have been made. Data given in Table IV and Figure 5 indicate the effect of temperature on polymerization rate for prepolymers 2 and 3 on 304 stainless steel.

In the presence of added catalyst the contribution to catalysis by materials dissolved from surface is assumed negligible. An estimation of the activation energy for Sb_2O_3-catalyzed polycondensation on this basis (Fig. 5) is 14 kcal. The estimated activation energy for polymerization of a catalyst-free prepolymer on a passivated stainless-steel surface is, by contrast, quite large, namely 45 kcal.

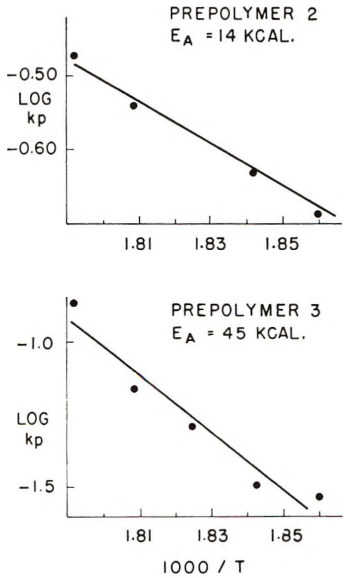

Fig. 5. Activation energy for catalyzed and uncatalyzed polycondensation of poly(ethylene terephthalate): 3-mil thickness on 304 stainless steel.

TABLE IV
Second-Order Rate Constants for Polymerization as a Function of Temperature at a 3-mil Thickness on 304 Stainless Steel

Prepolymer no. (cf. Table I)	Temp., °C	$2k_p$, liter mol^{-1} min^{-1}	Remarks
2	265	0.415	
2	270	0.490	
2	280	0.579	
2	285	0.675	
3	265	0.0585	surface passivated
3	270	0.0670	
3	275	0.106	
3	280	0.139	
3	285	0.271	

The lower value for the activation energy in the presence of antimony trioxide is considered to be that for the following reaction:

$$\text{—EB}'\text{C} + \text{—EB}' \rightarrow \text{—EE—} + \text{BB}\uparrow + \text{C}$$

wherein E is $\text{—C}_3\text{H}_2\text{COOCH}_2\text{—}$, an ester equivalent or one half of a poly(ethylene terephthalate) repeating unit, $\text{—}B'$ is $\text{—CH}_2\text{OH}$, a glycol equivalent attached to an E unit, C is a catalyst moiety, and B is $\text{—CH}_2\text{OH}$, a glycol equivalent in free glycol. The higher value of the activation energy, based on the low rates observed on polycondensation of a catalyst-free prepolymer (prepolymer 3) on a passivated stainless-steel surface, is considered to be that for uncatalyzed polycondensation, namely

$$\text{—EB}' + \text{—EB}' \rightarrow \text{—EE—} + \text{BB}\uparrow$$

CONCLUSIONS

In the region of 1 to 5 mils in thickness of polymerizing melt the polycondensation of poly(ethylene terephthalate) catalyzed by antimony trioxide or by dissolved iron exhibits markedly increased rates as the thickness of polymerizing melt is decreased. In the essential absence of catalyst there is no tendency of polymerization rate to increase with decreasing polymerizing melt thickness. On surfaces inert to dissolution in the polymerizing melt (rhodium, silver) virtually identical low rates support the supposition that there is no contribution to catalysis at the melt–metal interface. All these observations support the hypothesis that the principal cause of increased rates with diminished thickness of polymerizing melt is a reversible interaction of the catalyst with a volatile component of the reaction mixture, inactivating it. Improved efficiency of removal of this volatile component (e.g., decreasing thickness of polymerizing melt) improves availability of the catalyst to the polycondensation reaction and thus increases the observed rate.

I should like to thank W. H. McCarty for many interesting discussions during which the approach to this work was suggested. Thanks are also due Robert J. Carls for x-ray fluorescence spectroscopy, T. Singleton for solution viscosity measurements, and F. G. Haliczky, J. A. Kocsis, and H. U. Yourison for carrying out most of the experimental work.

References

1. R. W. Stevenson and H. R. Nettleton, *J. Polym. Sci.* A-1, **6**, 889 (1968).
2. G. M. Turner (to E.I. du Pont de Nemours & Co.), U. S. Pat. 3,161,710 (Dec. 15, 1964).
3. H. Zimmerman, *Faserforsch. Textiltech.*, **13**, 481 (1962).
4. W. Griehl and G. Schnock, *J. Polym. Sci.*, **30**, 413 (1958).
5. A. Conix, *Makromol. Chem.* **26**, 226 (1958).
6. V. V. Korshak, N. I. Bekasova, and V. A. Zamiatina, *Bull. Acad. Sci. USSR Div. Chem. Sci., Engl. transl.*, 463 (1958).

Received March 11, 1968

NOTE

Synthesis of Isoalloxazine Polymer (Vitamin B_2 Polymer)

A vast number of redox polymers are found in living systems. In fact, it may be safely stated that all living organisms, animal and plant, function by virtue of polymeric redox systems.

Among these systems are the host of oxidases and reductases, and other enzymes that carry out reactions in which electrons are removed or introduced into reagent and product molecules.

Some attempts to synthesize such enzymes themselves or their model polymers have been made. Thus, Okawara et al.[1] and Lloyd and Durocher[2] prepared pyridinium salts having redox properties by quaternizing nicotinamide with the chloromethylated polystyrene. This polymer was also prepared by the homopolymerization and copolymerization of the corresponding monomer.[3]

In a search for a novel redox polymer which not only follows normal redox reactions, but also indicates some interesting characteristics such as emission of fluorescence and biochemical peculiarities, a linear vinyl polymer containing the isoalloxazine nucleus as a side chain in the molecule has been prepared.

Isoalloxazine is noted as the redox component of riboflavin, which constitutes the prosthetic group of dehydrogenase flavoprotein, the yellow enzyme of yeast, and is also responsible for the physiological action of vitamin B_2. The reduction of this grouping involves 1,4-addition of hydrogen to the conjugated system[4]

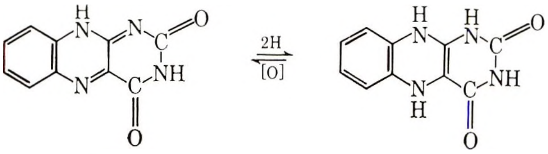

Isoalloxazine
(yellow)

Leucocompound
(colorless)

The isoalloxazine polymers were prepared by the condensation reaction of the *N*-hydroxymethylacrylamide group in polymer with riboflavin-5′-phosphate in aqueous solutions, making use of the well-known acid-catalyzed condensation reaction of *N*-hydroxymethylamide group with alcohols.[5]

This reaction is particularly advantageous for the formation of ether linkage under very mild conditions. A typical procedure is as follows.

To a 5% aqueous solution of polyacrylamide (intrinsic viscosity $[\eta]_{H_2O}^{30°C} = 1.2$) made basic with a small amount of potassium hydroxide to pH 11 was added approximately a twofold excess of paraformaldehyde, the mixture being kept stirring 1 hr at room temperature, during which time paraformaldehyde was gradually dissolved and reacted to yield a transparent solution. The resulting solution was precipitated into a large quantity of acetone, and then twice dissolved in water and subsequently precipitated into acetone. The methylolated polyacrylamide thus obtained was dissolved in water, equivalent riboflavin-5′-phosphate monosodium salt was added, and the solution was made weakly acidic (ca. pH 4) with a small amount of *p*-toluene sulfonic acid. The solution was then kept at 50°C for 8 hr with stirring in the absence of light. The reaction product was neutralized with aqueous ammonia and precipitated into ethanol, followed by centrifugation. The polymer was then dissolved in water and reprecipitated into ethanol. This operation was reiterated at least twice and the polymer thus purified was freeze-dried from water to yield a fluffy yellow material (extent of reaction by redox titration, 87.5% of theory).

The electronic spectra of this polymer in aqueous solutions are shown in Figures 1 and 2. These spectra might indicate that the functional group isoalloxazine was kept completely intact during this procedure.

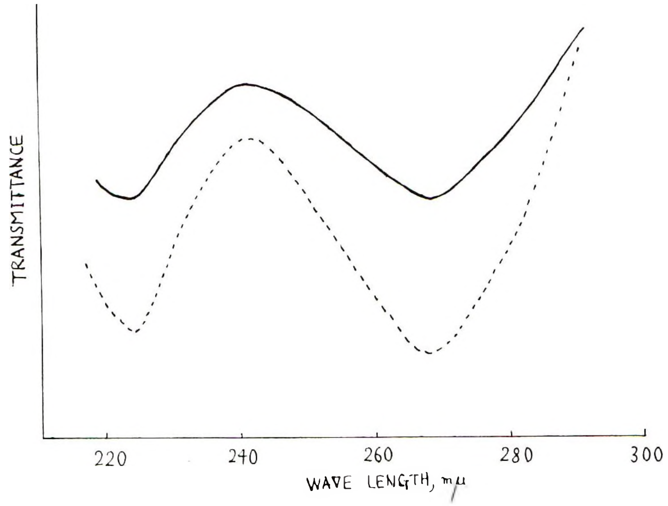

Fig. 1. Ultraviolet absorption spectrum for the isoalloxazine polymer in aqueous solution: (——) isoalloxazine polymer; (- -) riboflavin-5′-phosphate monosodium salt.

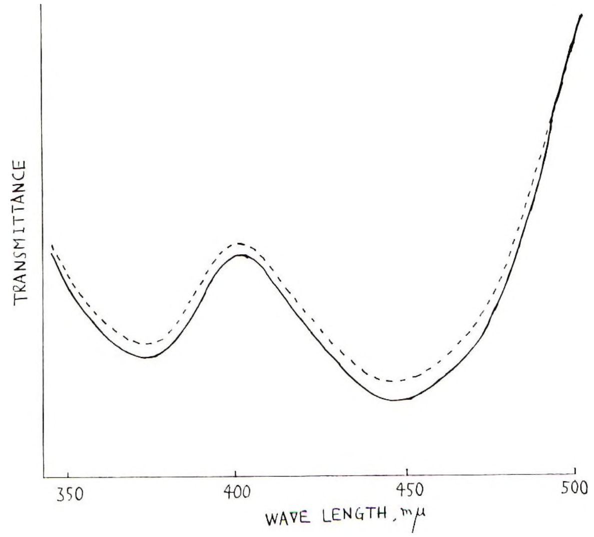

Fig. 2. Visible absorption spectrum for the isoalloxazine polymer in aqueous solution: (——) isoalloxazine polymer; (- -) riboflavin-5-phosphate monosodium salt.

In Figure 3 is shown the reductive titration curve of an aqueous solution of the isoalloxazine polymer with titanous chloride solution. It is recognized from this that this redox system is of the two-electron transfer type and that normal redox potential $E^{20°C}_{0}$ for the polymer (+0.202 V against a saturated calomel electrode) is approximately equal to that for sodium riboflavin-5′-phosphate (+0.193 V). With progress of reduction, the initial yellow color of the polymer solution changes to greenish yellow and finally to light brown at the equivalence point without appearance of any precipitates, whereas, in sodium riboflavin-5′-phosphate, a cloudy precipitates appeared immediately.

The polarogram of this polymer in an aqueous buffer solution (pH 5) also indicates a single-step reduction curve, the half-wave potential of which is −0.44 V (−0.60V for riboflavin-5′-phosphate), as shown in Figure 4.

Another feature of this polymer is the emission of a strong green fluorescence, as indicated in Fig. 5. The optimum exciting wavelength from a xenon lamp is a little higher in the case of the polymer (479 mμ) as compared with riboflavin-5′-phosphate (468 mμ). The shape of the emission spectrum for the polymer is, however, almost the same as that for the low molecular weight compound.

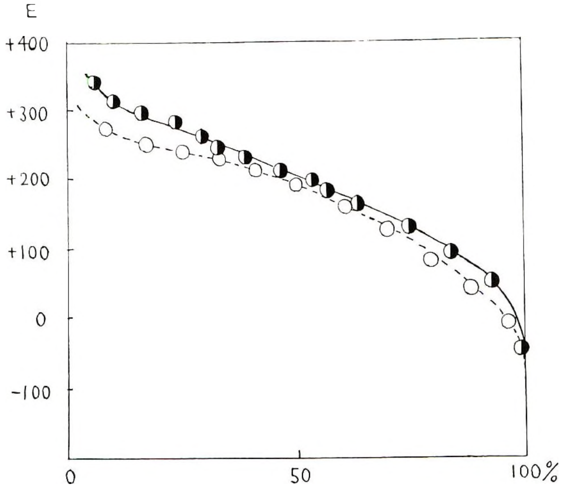

Fig. 3. Reductive titration curve of aqueous solution of the isoalloxazine polymer with titanous chloride (0.0706N) at 20°C. Concentrations of the polymer (–◐–) and riboflavin-5′-phosphate monosidum salt (--○--) are 32.9 and 31.7 mg/100 ml, respectively. E on the calomel scale in millivolts is plotted against per cent reduction.

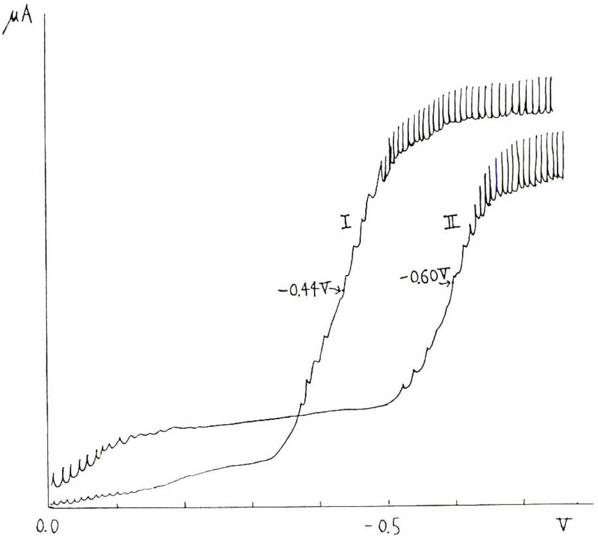

Fig. 4. Polarogram of the isoalloxazine polymer with the dropping mercury electrode in aqueous buffer solution (0.1N sodium acetate + acetic acid; pH 5): (*I*) isoalloxazine polymer; (*II*) riboflavin-5′-phosphate.

The infrared spectrum of this polymer indicates an absorption at 1110 cm^{-1} which is absent in both the substrate polymer and riboflavin-5′-phosphate and which is attributable to the ether linkage.

All these results might induce us to allot the chemical structure for the isoalloxazine polymer given in eq. (1),

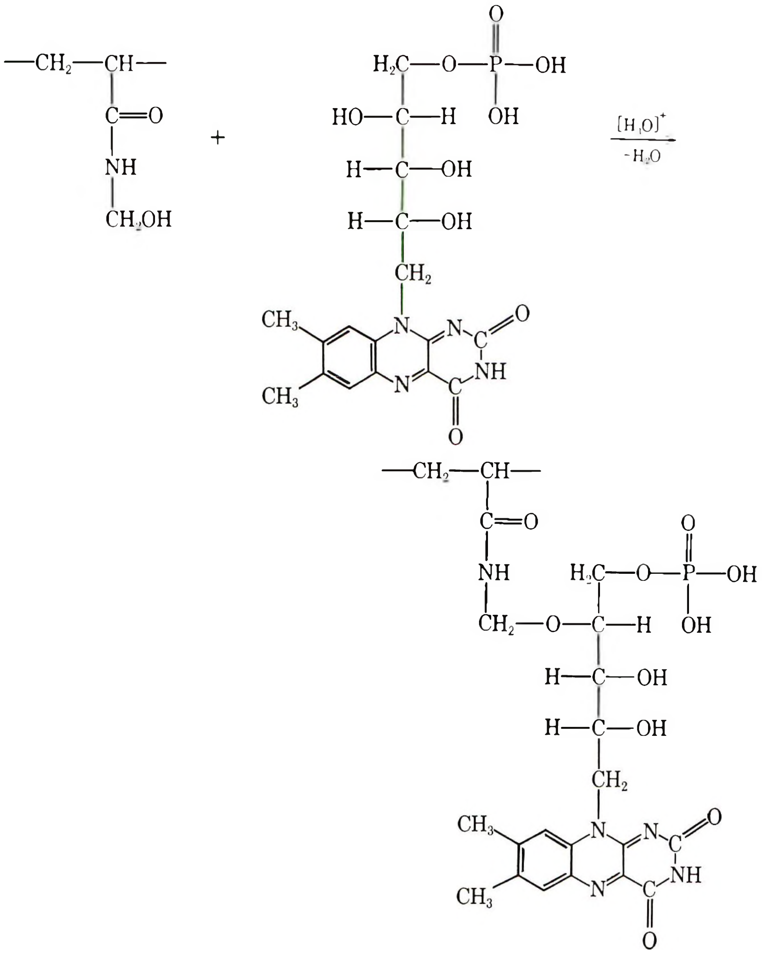

(1)

where however, all alcoholic hydroxyl groups in the riboflavin molecule are equivalent for the etherification.

Since the ether linkage between the polymer substrate and the riboflavin portion is of a hemiacetal nature, this polymer is expected to liberate riboflavin gradually by hydrolysis in acid media, as in the human stomach.

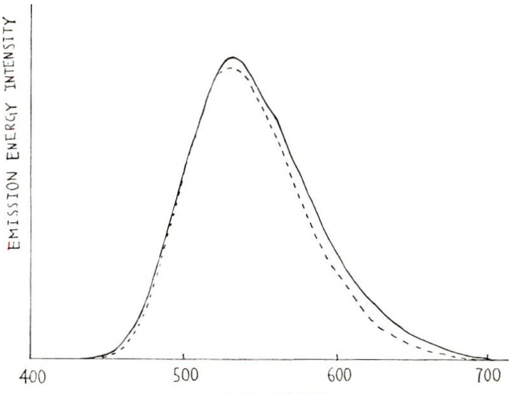

Fig. 5. Fluorescence emitted from the isoalloxazine polymer in aqueous solution: (——) isoalloxazine polymer, excited by radiation of wavelength 479 mμ (maximum intensity); (- -) riboflavin-5′-phosphate, excited by radiation of wavelength 468 mμ (maximum intensity).

References

1. M. Okawara, Y. Oiji, and E. Imoto, *Kogyo Kagaku Zasshi,* **65,** 1658 (1962).
2. W. G. Lloyd and T. E. Durocher, *J. Appl. Polym. Sci.,* **7,** 2025 (1963).
3. H. G. Cassidy and K. A. Kun, *Oxidation-Reduction Polymers,* Wiley, New York, 1965, p. 47.
4. L. F. Fieser and M. Fieser, *Advanced Organic Chemistry,* Reinhold, New York, 1961, p. 1067.
5. E. Müller, K. Dinges, and W. Graulich, *Makromol. Chem.,* **57,** 27 (1952).

Hiroyoshi Kamogawa

Textile Research Institute
4 Sawatari, Kanagawa
Yokohama, Japan

Received December 11, 1967
Revised April 30, 1968

INFORMATION FOR CONTRIBUTORS

This *Journal* Does Not Carry a Page Charge for Contributions

1. Manuscripts should be submitted to H. Mark, Polytechnic Institute of Brooklyn, 333 Jay Street, Brooklyn, New York 11201, or for Part A-1 (Polymer Chemistry) to C. G. Overberger, Department of Chemistry, University of Michigan, Ann Arbor, Michigan 48104, or for Part A-2 (Polymer Physics) to T. G. Fox, Mellon Institute, Pittsburgh, Pennsylvania 15213. Address all other correspondence to Periodicals Division, Interscience Publishers, John Wiley & Sons, Inc., 605 Third Avenue, New York, New York 10016.

2. It is the preference of the Editors that papers be published in the English language. However, if the author desires that his paper be published in French or German, it is necessary that a particularly complete and comprehensive English synopsis be furnished.

3. Manuscripts should be submitted in triplicate (one *original*, two carbon copies), typed *double space* throughout and on one side of each sheet only, on a *heavy* grade of paper with margins of at least one inch on all sides.

4. A short synopsis (maximum length 200 words) is required for papers in Parts A-1 and A-2. No synopsis is published for Part B or for "Notes" in Parts A. This synopsis should be carefully prepared, for it is automatically the source of most abstracts. The Synopsis should be a summary of the entire paper; not the conclusions alone.

5. The paper should be reasonably subdivided into sections and, if necessary, subsections. Please refer to any issue of this *Journal* for examples.

6. The references should be numbered consecutively in the order of their appearance and should be complete, including authors' initials and—for unpublished lectures or symposia—the title of the paper, the date, and the name of the sponsoring society. Please compile references on a separate sheet at the end of the manuscript. Abbreviations of journal titles should conform to the practices of *Chemical Abstracts*.

7. Please supply numbers and titles for all tables. All table columns should have an explanatory heading.

8. It is particularly important that all figures be submitted in a form suitable for reproduction. Good glossy photographs are required for halftone reproductions. For line drawings (graphs, etc.), the figures must be drawn clearly with India ink on heavy white paper, Bristol board, drawing linen, or coordinate paper with a very light blue background. The India ink lettering of graphs must be large, clear, and "open" so that letters and numbers do not fill in when reduced for publication. It is the usual practice to submit drawings that are twice the size of the final engravings; the maximum final size of figures for this *Journal* is $4^1/_2 \times 7^1/_2$ inches.

It is the author's responsibility to obtain written permission to reproduce material which has appeared in another publication.

If in doubt about the preparation of illustrations suitable for reproduction, please consult the publisher at the address given above in paragraph *1* and ask for a sample drawing.

9. Please supply legends for all figures and compile these on a separate sheet.

10. Authors are cautioned to type—wherever possible—all mathematical and chemical symbols, equations, and formulas. If these must be handwritten, please print clearly and leave ample space above and below for printer's marks; please use only ink. All Greek or unusual symbols should be identified in the margin the first time they are used. Please distinguish in the margins of the manuscript between capital and small letters of the alphabet wherever confusion may arise (e.g., k, K, κ). Please underline with a wavy line all vector quantities. Use fractional exponents to avoid root signs.

The nomenclature sponsored by the International Union of Chemistry is requested for chemical compounds. Abbreviations should follow the American Chemical Society *Handbook for Authors*. Chemical bonds should be correctly placed, and double bonds clearly indicated. Valence is to be indicated by superscript plus and minus signs.

11. Authors will receive 50 reprints of their articles without charge. Additional reprints can be ordered and purchased by filling out the form attached to the galley proof. Page proofs will not be supplied.

12. No manuscript will be returned following publication unless a request for return is made when the manuscript is originally submitted.

Manuscripts and illustrations not conforming to the style of the *Journal* will be returned to the author for reworking, thus delaying their appearance.